

THE STRUCTURE AND FUNCTION OF ENTHESES AND ENTHESIS ORGANS

A Thesis submitted to the University of Wales for the degree of Doctor of Philosophy.

By

Hannah Margaret Shaw B.Sc. (Hon.)

Cardiff School of Biosciences,
University of Wales, Cardiff.

September 2007

UMI Number: U236422

All rights reserved

INFORMATION TO ALL USERS

The quality of this reproduction is dependent upon the quality of the copy submitted.

In the unlikely event that the author did not send a complete manuscript and there are missing pages, these will be noted. Also, if material had to be removed, a note will indicate the deletion.



UMI U236422

Published by ProQuest LLC 2013. Copyright in the Dissertation held by the Author.
Microform Edition © ProQuest LLC.

All rights reserved. This work is protected against
unauthorized copying under Title 17, United States Code.



ProQuest LLC
789 East Eisenhower Parkway
P.O. Box 1346
Ann Arbor, MI 48106-1346

Declaration

This work has not previously been accepted in substance for any degree and is not being concurrently submitted in candidature for any degree.

Signed.....HAUS.....(Candidate)
Date.....19/9/07.....

Statement 1

This thesis is being submitted in partial fulfilment of the requirement for the degree of PhD

Signed.....HAUS.....(Candidate)
Date.....19/9/07.....

Statement 2

This thesis is the result of my own independent investigation, except where otherwise stated. Other sources are acknowledged by footnotes giving explicit references.

Signed.....HAUS.....(Candidate)
Date.....19/9/07.....

Statement 3

I hereby give consent for my thesis, if accepted, to be available for photocopying and for inter-library loan, and for the title and summary to be made available to outside organisations.

Signed.....HAUS.....(Candidate)
Date.....19/9/07.....

SUMMARY

The attachments of tendons, ligaments and muscles to bone are known as entheses. These musculoskeletal links are believed to be highly innervated and may therefore have an important role in proprioception. Pathologies associated with entheses are also described as particularly painful; however, the aetiology of these conditions is not fully understood. This thesis deals with the structure and innervation of 3 different types of attachments - the fibrous enthesis of the medial collateral ligament, the muscular attachment of the tibialis anterior onto the tibia, and the fibrocartilaginous enthesis organ of the Achilles tendon. Particular attention was paid to the latter and it was shown that in rats at all ages (neonate, 4 week, 4 month, and 2 month) only the retromalleolar fat pad of the enthesis organ was innervated. In the light of these findings, the fat was studied in further detail and an *in vitro* investigation determined whether nerve fibres are specifically attracted to the adipose tissue. In man, it was confirmed that the equivalent fat pad (Kager's fat pad) was also innervated and a number of anatomical and histopathological observations associated with this tissue in elderly dissecting room cadavers were described. The relationship between weight, height and foot length with fat pad structure in human cadaveric tissue was investigated, and the effect of the appetite-inducing hormone, ghrelin on the size of the fat pad in the rat was also explored. As entheses are the primary target organs in the seronegative spondyloarthropathies (autoinflammatory rheumatic conditions), the presence of resident and inflammatory macrophages and neutrophils in the rat Achilles tendon enthesis organ was investigated at a variety of ages. Overall, it was concluded that adipose tissue associated with entheses may play a role in proprioception and be a source of pain in enthesopathies.

ACKNOWLEDGEMENTS

I would like to thank my supervisors, Professor Mike Benjamin, Dr. Rob Santer and Dr. Alan Watson for their eternal patience and support throughout the course of my PhD.

I would also like to thank Derek Scarborough for his help with histological processing, Dr Hann and Guy Pitt for their help with electron microscopy, Dr. Stefan Milz (AO Research Institute, Davos) for his assistance with the human work, Professor Alun Davies and Dr. Gerard O’Keefe for their help with the *in vitro* nerve growth study, Dr Tim Wells and Dr. Jeff Davies for their help with the Ghrelin work, Professor Tsukasa Kumai (Nara Medical University, Japan) for supplying human pathological samples, Dr. Andy Bathe (Rosssdales Equine Hospital, Newmarket) for supplying and helping with the equine specimens, Professor Graeme Bydder (University of California San Diego - Radiology) for supplying MRI images of the hindfoot, and finally Dr. Daisuke Suzuki and Dr. Koji Hayashi for their help with routine histology and allowing me to examine histological material that they have cut.

Thanks also to the Anatomical Society of Great Britain and Ireland for their funding.

I would also like to thank the many people who helped and supported me during the course of my PhD in Cardiff: Laura, Paula, Kirsty, Becky, Samantha, Ilyas, Rhiannon, Hechmi, Sarah, and Helen.

Finally I would like to thank my family - Mum, Dad, and Vic, my ‘extended’ family – Ray, Dan, Sam, Julie and Lindsey for all there support, but most of all, I would like to thank Josh for his continued support and motivation.

LIST OF CONTENTS

	Page
TITLE.....	i
DECLARATION.....	ii
SUMMARY.....	iii
ACKNOWLEDGEMENTS.....	iv
LIST OF CONTENTS.....	v
LIST OF FIGURES.....	ix
LIST OF TABLES.....	xv
ABBREVIATIONS.....	xvi
Chapter 1: GENERAL INTRODUCTION.....	1
1.1. JOINT AND CONNECTIVE TISSUE INNERVATION.....	2
Nerve Fibre Classification.....	2
Joint Receptors.....	4
1.2. ENTHESES.....	8
What are entheses and why are they important.....	8
A historical note on terminology.....	11
1.2.1. ENTHESIS STRUCTURE.....	12
MACROSCOPIC STRUCTURE.....	12
MICROSCOPIC STRUCTURE.....	13
The classification of entheses.....	13
Fibrocartilaginous Entheses.....	16
Fibrous Entheses.....	24
Muscular Entheses.....	26
1.2.2. THE ENTHESIS ORGAN CONCEPT.....	26
1.2.3. ENTHESOPATHIES.....	28
Iliotibial Band Syndrome.....	30
Bony Spurs (Enthesophytes).....	30
Spondyloarthropathies.....	31
1.3. TENDON.....	32
MACROSCOPIC STRUCTURE.....	32

MICROSCOPIC STRUCTURE.....	33
MOLECULAR STRUCTURE.....	35
VASCULARISATION.....	36
INNERVATION.....	38
1.4. SUMMARY OF THE OVERALL AIMS OF THE THESIS.....	39
Chapter 2: GENERAL MATERIALS AND METHODS.....	41
2.1. ROUTINE HISTOLOGY.....	41
Fixation and Paraffin Embedding.....	41
Sectioning.....	41
Staining.....	41
Microscopy.....	42
2.2. IMMUNOHISTOCHEMISTRY.....	42
Sectioning.....	42
2.2.1. Immunofluorescence.....	42
Controls.....	43
Microscopy.....	43
2.2.2. Peroxidase Labelling.....	43
Control.....	44
Microscopy.....	44
Chapter 3: INNERVATION OF THE RAT ACHILLES TENDON ENTESIS ORGAN	47
3.1. INTRODUCTION.....	47
3.2. MATERIALS AND METHODS.....	51
3.3. RESULTS.....	52
3.4. FIGURES.....	60
3.5. DISCUSSION.....	71
Chapter 4: ANATOMY AND INNERVATION OF KAGER'S FAT PAD.....	80
4.1. INTRODUCTION.....	80
4.2. MATERIALS AND METHODS.....	83
4.3. RESULTS.....	86
4.4. FIGURES.....	92
4.5. DISCUSSION.....	112

Chapter 5: ULTRASTRUCTURE OF THE RETROMALLEOLAR FAT PAD.....	118
5.1. INTRODUCTION.....	118
5.2. MATERIALS AND METHODS.....	123
5.3. RESULTS.....	128
5.4. FIGURES.....	134
5.5. DISCUSSION.....	143
Chapter 6: CELL INTERACTIONS AND CELL COMPOSITION OF THE RETROMALLEOLAR FAT PAD.....	148
6.1. INTRODUCTION	148
6.2. MATERIALS AND METHODS.....	155
6.3. RESULTS.....	156
6.4. FIGURES.....	160
6.5. DISCUSSION.....	168
Chapter 7: DEVELOPMENT OF KAGER'S FAT PAD.....	173
7.1. INTRODUCTION.....	173
7.2. MATERIALS AND METHODS.....	175
7.3. RESULTS.....	176
7.4. FIGURES.....	179
7.5. DISCUSSION.....	185
Chapter 8: THE STRUCTURE AND INNERVATION OF OTHER ENTHESES.....	189
8.1. INTRODUCTION.....	189
8.2. MATERIALS AND METHODS.....	201
8.3. RESULTS.....	202
8.4. FIGURES.....	207
8.5. DISCUSSION.....	228
Chapter 9: THE EFFECT OF GHRELIN ON THE RAT ACHILLES TENDON ENTHESIS ORGAN.....	235
9.1.1. INTRODUCTION.....	235
9.2. MATERIALS AND METHODS.....	238

9.3.	RESULTS.....	240
9.4.	FIGURES.....	241
9.5.	DISCUSSION.....	245
Chapter 10: <i>IN VITRO</i> STUDY OF TARGET DERIVED NERVE GROWTH.....		246
10.1.	INTRODUCTION.....	246
10.2.	MATERIALS AND METHODS.....	250
10.3.	RESULTS.....	253
10.4.	FIGURES.....	257
10.5.	DISCUSSION.....	265
Chapter 11: GENERAL DISCUSSION.....		270
List of References.....		277
Appendices.....		303
Publications arising from this work.....		308

LIST OF FIGURES

CHAPTER 1	Page
Figure 1.1: The direct fibrous enthesis of pronator teres.....	14
Figure 1.2: The indirect fibrous enthesis of the suspensory ligament in the equine limb.....	14
Figure 1.3: Low power view of the Achilles tendon enthesis organ.....	15
Figure 1.4: The fibrocartilaginous enthesis of the Achilles tendon.....	15
Figure 1.5: Grommet analogy.....	17
Figure 1.6: Schematic illustration of fibrous enthesis migration during development.....	25
Figure 1.7: Schematic illustration of a tendon cut longitudinally (A) and transversely (B).....	34
Figure 1.8: Schematic illustration of the hierarchy in the Achilles tendon.....	35
CHAPTER 3	
Figure 3.3.1.A-F: Routine histology of the rat Achilles tendon enthesis organ.....	60
Figure 3.3.2.A-F: Routine histology of the rat Achilles tendon enthesis organ.....	62
Figure 3.3.3.A-F: Routine histology of the rat Achilles tendon enthesis organ.....	63
Figure 3.3.4.A-F: Routine histology of the rat Achilles tendon enthesis organ.....	64
Figure 3.3.5.A-F: Rat Achilles tendon enthesis organ immunolabelled with protein gene product 9.5.....	65
Figure 3.3.6.A-F: Rat Achilles tendon enthesis organ immunolabelled with calcitonin gene related peptide.....	66
Figure 3.3.7.A-G: Rat Achilles tendon enthesis organ immunolabelled with Substance P.....	68
Figure 3.3.8.A-F: Rat Achilles tendon enthesis organ immunolabelled with neurofilament 200.....	69
Figure 3.3.9.A-F: Rat Achilles tendon enthesis organ negative control sections.....	70
Figure 3.4.1: Diagram illustrating the how peripheral sensitization of the peptidergic nerve fibres in the fat pad may occur.....	78
Figure 3.4.2: Diagram illustrating the process of neurogenic inflammation.....	79
CHAPTER 4	
Figure 4.1.1: Schematic representation of Kager's triangle in man.....	81
Figure 4.1.2: MRI images of Kager's fat pad in man.....	81
Figure 4.2.1: Dissection of the tip of Kager's fat pad	84

Figure 4.3.1.A-E: Gross anatomy of the Achilles tendon enthesis organ in man.....	92
Figure 4.3.2.A-E: Gross anatomy of the tip of Kager’s fat pad.....	93
Figure 4.3.3: Low-power, sagittal section through the Achilles tendon enthesis organ in man	94
Figure 4.3.4.A-H: Sagittal histological sections through Kager’s fat pad.....	96
Figure 4.3.5.A-D: Sagittal histological sections through Kager’s fat pad	98
Figure 4.3.6.A-E: Sagittal histological sections through Kager’s fat pad	99
Figure 4.3.7.A-E: Sagittal histological sections through the Achilles tendon enthesis organ in man	100
Figure 4.3.8.A-C: Sagittal histological sections of Kager’s fat pad taken from patients with Haglund’s deformity who had symptoms of retrocalcaneal bursitis.....	101
Figure 4.3.9.A-D: 3D reconstructions composed from serial MRI images of the adult hindfoot in plantar and dorsiflexion	102
Figure 4.3.10: Sagittal MRI images of the adult hindfoot through 50° of plantarflexion.....	103
Figure 4.3.11.A-F: Surface anatomy of the hindfoot in man	104
Figure 4.3.12.A: Histograms comparing the weight of Kager’s fat pad between male and female dissecting room cadavers.....	105
Figure 4.3.13.B: Histograms comparing the weight of Kager’s fat pad between three different weight categories in dissecting room cadavers.....	106
Figure 4.3.14.A-E: Kager’s fat pad labelled with protein gene product 9.5.....	107
Figure 4.3.15.A-F: Kager’s fat pad labelled with neurofilament 200.....	108
Figure 4.3.16.A-B: Kager’s fat pad labelled with substance P.....	110
Figure 4.3.16.C-D: Kager’s fat pad labelled with calcitonin gene related peptide.....	110
Figure 4.3.16.E-G: Negative control sections of Kager’s fat pad	110
Figure 4.3.17: Stills taken from a 3D movie of a schematic representation of the relationship between adipocytes and nerve fibres in Kager’s fat pad.....	111

CHAPTER 5

Figure 5.1.1: Immunoperoxidase labelled nerve fibres in the retromalleolar fat pad in man and rat illustrating how they weave between adjacent adipocytes.....	118
Figure 5.1.2: Schematic illustration of brown and white adipocytes.....	119
Figure 5.2.1.1: Gross anatomy of the retromalleolar fat pad in the rat illustrating the peroneal anastomotic branch of the sural nerve supplying the fat pad.....	123
Figure 5.2.4.1: Illustration of nerve fibre counting.....	125

Figure 5.3.1.A-H: Toluidine blue stained, semi-thin sections of the rat retromalleolar fat pad.....134

Figure 5.3.2.A-B: Toluidine blue stained, semi-thin sections of the nerve supplying the retromalleolar fat pad.....135

Figure 5.3.3.A-F: Ultrathin sections of the rat retromalleolar fat pad.....136

Figure 5.3.4.A-F: Ultrathin sections of the rat retromalleolar fat pad.....137

Figure 5.3.5.A-F: Ultrathin sections of the nerve supplying the rat retromalleolar fat pad.....138

Figure 5.3.6.A-D: Ultrathin sections of the nerve supplying the retromalleolar fat pad immunogold labelled for calcitonin gene related peptide using the detergent method.....139

Figure 5.3.6.E-F: Ultrathin sections of the dorsal horn from the spinal cord immunogold labelled for calcitonin gene related peptide using the detergent method.....139

Figure 5.3.7.A and B: Representative ultrathin sections through the nerve supplying the retromalleolar fat pad in the rat used for morphometric analysis.....140

Figure 5.3.8.A: Histograms illustrating the number of nerve fibres per $1,552\mu\text{m}^2$ of the nerve supplying the retromalleolar fat pad in the 4 and 24 month rat.....141

Figure 5.3.7.B: Histogram representing the number of unmyelinated axons in $1,552\mu\text{m}^2$ of the nerve supplying the retromalleolar fat pad in the 4 and 24 month rat.....141

Figure 5.3.7.C: Graph representing the thickness of the myelin sheath in $1,552\mu\text{m}^2$ of the nerve supplying the retromalleolar fat pad in the 4 and 24 month rat.....141

Figure 5.3.8.A: Histogram illustrating the distribution of myelinated nerve fibre area (μm^2) in the 4 and 24 month rat.....142

CHAPTER 6

Figure 6.1.1.: Cell-cell and cell-matrix interactions.....149

Figure 6.3.1.A: The retromalleolar fat pad immunolabelled with connexin 32.....160

Figure 6.3.1.B: The retromalleolar fat pad immunolabelled with Alexa488 conjugated Phalloidin.....160

Figure 6.3.1.C: The retromalleolar fat pad immunolabelled with vinculin.....160

Figure 6.3.1.D: The retromalleolar fat pad immunolabelled with N-cadherin.....160

Figure 6.3.2.A-C: Negative control sections of the rat Achilles tendon enthesis organ.....161

Figure 6.3.3.A-F: The rat Achilles tendon enthesis organ at various ages immunolabelled with CD68.....162

Figure 6.3.4.A-F: The rat Achilles tendon enthesis organ at various ages immunolabelled with CD68.....163

Figure 6.3.5.A-F: The rat Achilles tendon enthesis organ at various ages immunolabelled with CD68.....	164
Figure 6.3.6.A-F: The rat Achilles tendon enthesis organ at various ages immunolabelled with MRP14.....	165
Figure 6.3.7.A-F: The rat Achilles tendon enthesis organ at various ages immunolabelled with MRP14.....	166
Figure 6.3.8.A-F: Positive and negative control sections of the rat Achilles tendon enthesis organ	167

CHAPTER 7

Figure 7.3.1.A-E: Sagittal histological sections through the Achilles tendon enthesis organ in the 45mm foetus.....	179
Figure 7.3.2.A and B: Sagittal histological sections through the Achilles tendon enthesis organ in the 53mm foetus.....	180
Figure 7.3.3.A: Sagittal histological sections through the Achilles tendon enthesis organ in the 57mm foetus.....	181
Figure 7.3.4.A-E: Sagittal histological sections through the Achilles tendon enthesis organ in the 110mm foetus.....	182
Figure 7.3.5.A-F: Sagittal histological sections through the Achilles tendon enthesis organ in the 177mm foetus.....	183
Figure 7.3.6.A-E: Sagittal histological sections through the Achilles tendon enthesis organ in the 332mm foetus.....	184

CHAPTER 8

Figure 8.1.1.1: Gross anatomy of the rat medial collateral ligament.....	190
Figure 8.1.2.1: Gross anatomy of the rat tibialis anterior muscle	195
Figure 8.1.2.2: Anatomy of the rat tibia and fibula.....	196
Figure 8.1.3.1: Gross anatomy of the attachment of the suspensory ligament to the 3 rd metatarsal bone.....	199
Figure 8.3.1.A-C: Routine histology of the fibrous enthesis of the medial collateral ligament.....	207
Figure 8.3.2.A-D: Routine histology of the muscular enthesis of tibialis anterior.....	208

Figure 8.3.3.A-E: Routine histology sections of the origin of the suspensory ligament on the 3 rd metatarsal bone (Foal).....	209
Figure 8.3.4.A-H: Routine histology sections of the origin of the suspensory ligament on the 3 rd metatarsal bone (Adult).....	211
Figure 8.3.5.A-D: Routine histology sections of the origin of the suspensory ligament on the 3 rd metatarsal bone (Pathological).....	212
Figure 8.3.6.A-F: Fibrous enthesis of the medial collateral ligament immuolabelled with PGP9.5.....	213
Figure 8.3.7.A-E: Fibrous enthesis of the medial collateral ligament immuolabelled with neurofilament 200.....	214
Figure 8.3.8.A-G: Fibrous enthesis of the medial collateral ligament immuolabelled with Substance P or calcitonin gene related peptide.....	216
Figure 8.3.9.C-D: Negative control sections of the fibrous enthesis of the medial collateral ligament.....	217
Figure 8.3.10.A-H: Muscular enthesis of tibialis anterior immunlabelled with PGP9.5.....	219
Figure 8.3.11.A-F: Muscular enthesis of tibialis anterior immuolabelled with neurofilament200.....	220
Figure 8.3.12.A-F: Muscular enthesis of tibialis anterior immuolabelled with substance P or calcitonin gene related peptide.....	221
Figure 8.3.13.A-D: Muscular enthesis of tibialis anterior immuolabelled with actin or vinculin.....	222
Figure 8.3.14.A-C: Negative control sections of the muscular enthesis of tibialis anterior.....	223
Figure 8.3.15.A-E: Origin of the suspensory ligament immunolabelled with PGP 9.5 (foal).....	224
Figure 8.3.16A-E: Origin of the suspensory ligament immunolabelled with PGP 9.5 (adult).....	225
Figure 8.3.17.A-C: Origin of the suspensory ligament immunolabelled with PGP 9.5 (pathological).....	226
Figure 8.3.18.A-C: Negative control sections of the origin of the suspensory ligament (adult).....	227
Figure 8.4.2.1: Schematic diagram of the muscle pull on the muscular enthesis of tibialis anterior.....	231

CHAPTER 9

Figure 9.3.1.A-E: Routine histology of ghrelin treated rats241
Figure 9.3.2.A-E: Nerve immunolabelling of ghrelin treated rats242
Figure 9.3.3.A-F: BrdU immunolabelling of treated rats.....243
Figure 9.3.4.A-D: Negative control sections of treated rats.....244

CHAPTER 10

Figure 10.2.2.1: Sterile setup for removal of explants.....250
Figure 10.2.3.1: Experimental setup of tissue explants.....251
Figure 10.3.1.A-G: First 6 days in target derived nerve growth (neonatal target).....257
Figure 10.3.2.A-F: Day 13 target derived nerve growth (neonatal target).....258
Figure 10.3.3.A-F: Day 13 target derived nerve growth (neonatal target).....259
Figure 10.3.4.A-H: Oil red – O stained day 13 in target derived nerve growth (neonatal target).....261
Figure 10.3.5.A-F: First 6 days in target derived nerve growth (adult targets).....262
Figure 10.3.6.A-F: Day 13 target derived nerve growth (adult targets).....263
Figure 10.3.7.A-F: Control cultures of target derived nerve growth264
Figure 10.4.1: Proposed mechanism for the temporal regulation of the innervation of the retromalleolar fat pad267

LIST OF TABLES

CHAPTER 1	Page
Table 1.1: Classification system of primary afferent axons.....	3
CHAPTER 2	
Table 2.1: Primary antibodies.....	45
Table 2.2: Secondary antibodies.....	46
CHAPTER 3	
Table 3.3.1: Summary of results from nerve fibre immunolabelling of the rat Achilles tendon enthesis organ	58
CHAPTER 4	
Table 4.3.1: Anthropometric measurements taken from dissecting room cadavers for anthropometric evaluation.....	90
CHAPTER 6	
Table 6.3.1: Summary of results from immunolabelling the Achilles tendon enthesis organ with CD68 and MRP14.....	159
CHAPTER 7	
Table 7.3.1: Summary of results from development of the Achilles tendon enthesis organ in man.....	178
CHAPTER 10	
Table 10.3.2.1: The number and form of co-cultures used for <i>in vitro</i> study of target derived nerve growth.....	252

ABBREVIATIONS

3D	– Three Dimensional
ACAM	- Adipocyte Adhesion Molecule
ACL	– Anterior Cruciate Ligament
ATP	- Adenosine Triphosphate
BAT	– Brown Adipose Tissue
BDNF	– Brain Derived Neurotrophic Factor
BMP	– Bone Morphogenic Protein
BrDU	- Bromodeoxyuridine
BSA	–Bovine Serum Albumin
CFC	– Calcified Fibrocartilage
CGRP	– Calcitonin Gene Related Peptide
ChM-I	–Chondromodulin I
CNS	–Central Nervous System
CO ₂	– Carbon Dioxide
CRL	– Crown-Rump Length
CS	– Chondroitin Sulphate
Cxn	–Connexin
DAB	- 3,3'Diaminobenzidine
DFCT	– Dense Fibrous Connective Tissue
DISH	- Diffuse Idiopathic Skeletal Hyperostosis
DRG	–Dorsal Root Ganglion
ECM	– Extracellular Matrix
EDTA	-Ethylenediaminetetraacetic Acid
EF	– Enthesis Fibrocartilage
FACIT	- Fibril-Associated Collagens with Interrupted Triple helices
FHL	– Flexor Hallucis Longus
FP	–Fat Pad
GAG	– Glycosaminoglycan
GDNF	- Glial Cell line-derived Neurotrophic Factor
GH	– Growth Hormone
GHS-R	– Growth Hormone Secretagogue Receptor
H & E	- Haematoxylin and Eosin
IgG	– Immunoglobulins
IP ₃	– Inositol Triphosphate

ITB – Illiotibial Band
IVD – Intervertebral Disc
MCL – Medial Collateral Ligament
MCP1 – Monocyte Chemoattractant Protein
MHC – Major Histocompatibility Complex
MMP – Matrix Metalloproteinases
MRI – Magnetic Resonance Imaging
MRP – Myeloid Related Protein
MTJ – Myotendinous Junction
MT-MMP - Membrane Bound Matrix Metalloproteinases
NA – Noradrenaline
NF200 – Neurofilament 200
NGF – Nerve Growth Factor
NPY – Neuropeptide Y
NT – Neurotrophin
OsO₄ – Osmium Tetroxide
PB – Phosphate Buffer
PF – Periosteal Fibrocartilage
PG – Proteoglycans
PGP9.5 – Protein Gene Product 9.5
PNS – Peripheral Nervous System
PsA – Psoriatic Arthritis
PTHrP – Parathyroid Related Protein
RA – Rheumatoid Arthritis
RB – Retrocalcaneal Bursa
SEM – Scanning Electron Microscopy
Sema3A – Semaphorin 3A
SF – Sesamoid Fibrocartilage
SP – Substance P
SpA – Seronegative Spondyloarthropathies
TA – Tibialis Anterior
TB – Tris Buffer
TeM – Tenomodulin
TEM - Transmission Electron Microscopy
TL – Tendon or Ligament
TNF- α – Tumor Necrosis Factor – alpha
Trk - Tyrosine kinase receptor

US – Ultrasonography
VIP – Vasoactive Intestinal Peptide
WAT – White Adipose Tissue

1. GENERAL INTRODUCTION

The awareness of the position of the body in space is known as proprioception and it plays a key role in controlling movement and balance (Bear et al., 2006). Sensory receptors located in tendons, ligaments, joint capsules, muscles, and the skin signal to the central nervous system (CNS) where this information is co-ordinated with motor functions. The majority of interest regarding proprioception has focussed on the muscle spindles and Golgi tendon organs. However, information on the sensory innervation of joints and associated connective tissues including tendons, ligaments, and joint capsules is more limited (Freeman and Wyke, 1967c; Kellgren and Samuel, 1950; McDougall et al., 1997; Samuel, 1952; Zimny, 1988). Furthermore, in contrast to myotendinous junctions, there is a significant lack of literature describing the innervation of the bony attachments ('entheses') of tendons, ligaments, joint capsules and muscles. Despite this, many textbooks and reviews state that entheses are highly innervated (Benjamin and McGonagle, 2001; Benjamin and Ralphs, 1997; Khan et al., 2000; Klippel and Diepp, 1998; Niepel et al., 1966; Palesy, 1997; Resnick and Niwayama, 1983). It is therefore one of the principal aims of this thesis to describe the innervation of 3 classical forms of entheses. The structure of the entheses is described in section 1.2.

Entheses are essential links in the musculoskeletal system and the innervation of these regions may contribute to proprioception through monitoring the movement of tendons or ligaments relative to bone. Understanding the innervation of entheses is also particularly significant as they are frequently affected by overuse injuries (Jozsa and Kannus, 1997) and inflammation in autoimmune diseases such as the seronegative spondyloarthropathies (SpA) (Borman et al., 2006; D'Agostino and Olivieri, 2006). Both types of conditions are reported by patients to be particularly painful. There is currently a lack of understanding of the pathobiology of overuse injuries and SpA - there is continuing debate as to the role of inflammation in overuse injuries (Khan et al., 1999a) and the exact cause of SpA is still unknown. Aging is also known to have a profound effect on proprioceptive function. Research indicates that with increasing age, there is both a reduction in the number, and a change in the morphology of sensory receptors located in joints and their associated

structures. This is believed to contribute to falls in the elderly (Shaffer and Harrison, 2007). It is therefore also important to understand changes in the innervation of entheses with age.

1.1 JOINT AND CONNECTIVE TISSUE INNERVATION

The following section presents an account of the basic structure and function of the sensory innervation of joints and associated connective tissues with particular reference to pain and proprioception.

NERVE FIBRE CLASSIFICATION

The primary afferent axons that carry sensory information to the CNS vary considerably in diameter and are described using two classification schemes that are illustrated in Table 1.1. Those axons from skin receptors are usually designated $A\alpha$, $A\beta$, $A\delta$ and C, while those axons innervating muscles and tendons are classed into groups I, II, III, and IV. The group in which sensory axons are classed depends on their diameter and conduction velocity. The size of the axon also reflects the type of sensory receptor with which it is associated (Bear et al., 2006; Willis and Coggeshall, 1991).

Axons from skin	A α	A β	A δ	C
Axons from muscles	Group I	II	III	IV
				
Diameter (μm)	13-20	6-12	1-5	0.2-1.5
Speed of conduction (m/sec)	80-120	35-75	5-30	0.5-2
Sensory receptors	Proprioceptors of skeletal muscle and tendons	Mechanoreceptors	Fast pain, temperature	Temperature, slow pain, itch
Marker	NF200	NF200		SP, CGRP

Table 1.1: Primary afferent axon classification system (Bear et al., 2007)

Very large myelinated axons are classed in group I which convey information from specialised sensory receptors which monitor stretch in skeletal muscle - known as muscle spindles (classed as group Ia), and also from Golgi tendon organs (classed as group Ib (Lloyd, 1943). Myelinated nerve fibres from group II convey information from a large number of specialised receptors with different morphological characteristics (see below) which are capable of sensing mechanical deformation and transducing it into an impulse (Willis and Coggeshall, 1991). These large and small myelinated nerve fibres can be identified in the rat by the use of antibodies against phosphorylated and non-phosphorylated neurofilament 200 proteins (Perry et al., 1991). The different types of

receptors located in joints and associated connective tissues are described in the following section using the terminology proposed by Freeman and Wyke (1967c).

JOINT RECEPTORS

A number of different types of receptors have been identified within joint connective tissues, and are adapted to respond to a variety of different proprioceptive stimuli. These receptors are all classed as mechanoreceptors as they respond to tissue deformation. Physical stimulation is transduced by the receptor into an electrical signal (receptor potential) through activation of ion channels sensitive to stretching and tension of the peripheral segment of axonal membrane lacking voltage dependent ion channels. The intensity and duration of the receptor potential depends largely on the intensity and duration of the stimulus, however some receptors are adapted only to generate action potentials in response to low or high intensity stimuli (Bear et al., 2006; Willis and Coggeshall, 1991). In addition, receptors themselves show adaptations during maintained stimulation and can therefore be classed into two groups depending on the speed of this adaptation: (i) slowly adapting and (ii) rapidly adapting receptors. Stimulation of slowly adapting receptors results in prolonged firing of action potentials during the period of stimulation and are therefore suited to collecting information on static positions (Bear et al., 2006; Willis and Coggeshall, 1991). In contrast, rapidly adapting receptors signal motion. When a rapidly adapting receptor is stimulated an action potential is evoked, but unlike slowly adapting receptors, the receptor potential decreases during the duration of the stimulus and action potentials are not evoked following the initial stimulation. This rapid adaptation allows the receptor to signal information on changing and moving stimuli (Bear et al., 2006; Willis and Coggeshall, 1991).

Receptor endings can be broadly divided into two groups; encapsulated and non-encapsulated receptors, depending whether the nerve ending is surrounded by a connective tissue capsule. A vast number of encapsulated receptors have been described in association with joints, but most are merely variations on two themes – those with layered capsules and those with thin capsules. The function of the capsule is unknown in a number of these receptors but in some cases it is believed that the capsule functions as a mechanical filter,

which modifies the mechanical stimuli before it reaches the nerve terminal (Bear et al., 2006). In the light of the confusion associated with the numerous different names given to encapsulated nerve endings with the same or similar structures, Freeman and Wyke (1967c) re-classified the receptors associated with joints into 4 categories depending on their basic structure.

Encapsulated Nerve Endings

Type I Endings

Slowly adapting, low threshold type I endings - classically known as Ruffini endings - are ovoid or globular encapsulated corpuscles (Freeman and Wyke, 1967c). In the centre of the capsule is a collection of coiled un-myelinated fibres and these are surrounded by one or two layers of fibrous connective tissue. Such corpuscular endings have been identified within the joint capsule, ligaments, tendons, and menisci (Mine et al., 2000; Stilwell, 1957; Zimny, 1988). Type I endings have also been identified in the periosteum adjacent to the joint. Interestingly in the knee, type I endings are more densely arranged in the anterior and posterior regions of the joint capsule when compared to the medial and lateral regions (Zimny, 1988). These receptors were initially believed to respond to a range of joint movements and were therefore believed to signal joint position; however it was subsequently demonstrated that type I receptors are rarely active in intermediate joint positions, but respond primarily to the extremes of angular joint movement (Willis and Coggeshall, 1991). This explains their predominant location in the anterior and posterior regions of the joint capsule of the knee. Type I articular nerve endings have also been described as Golgi-Mazzoni endings, spray type endings and Meissner corpuscles (Freeman and Wyke, 1967c).

Type II Endings

Type II endings have been classically described as Pacinian-like receptors. These specialised nerve endings are low threshold, rapidly adapting receptors which have been identified in the joint capsule and the periosteum adjacent to the attachment of the joint capsule (Freeman and Wyke, 1967c; Zimny, 1988). Type II endings, have similar structures to 'true' Pacinian corpuscles which are composed of an unmyelinated axon

terminal covered by layers of concentric non-neuronal lamellae of squamous epithelial cells and condensed connective tissue (Bell, 1994). However, Freeman and Wyke (1967c) consider that 'true' Pacinian corpuscles are only present in extra-articular tissue.

It is understood that the capsule is responsible for the rapidly adapting nature of this receptor. Compression of the external capsule, leads to deformation of the terminal axon and opening of mechanosensitive ion channels that generates a receptor potential. If this receptor potential exceeds a certain threshold, the axon will initiate an action potential. However, when compression is maintained, the receptor potential rapidly dissipates due to the elasticity of the capsule, and no action potential is evoked. Experiments in which the capsule is removed from the nerve demonstrated that it is the capsule which makes the Pacinian corpuscle particularly sensitive to vibration rather than steady pressure (Bear et al., 2006; Nolte, 2002)

Type III Endings

Type III endings are also known as Golgi tendon organs. These receptors are also slowly adapting structures, although they have higher thresholds than type I endings. They are fusiform shaped corpuscles located within the fibrous connective tissue between the muscle and the tendon proper i.e. at the myotendinous junction, where these receptors monitor active and passive muscle stretch (Schoultz and Swett, 1974). Morphologically, type III receptors are composed of several longitudinally arranged compartments which contain either densely or loosely packed collagen fibres. A large myelinated axon enters the capsule and branches within the receptor, interweaving between the collagen fibres. It is proposed that when the muscle fibres associated with the tendon organ contract, the collagen fibres within the corpuscle will become taut, leading to contraction of the axonal branches present between them; inducing an action potential (Schoultz and Swett, 1974). Type III receptors with similar structures have also been identified within ligaments (Freeman and Wyke, 1967c) where they are also believed to monitor stretch.

Non-encapsulated nerve endings associated with joints are usually seen as free nerve endings rather than endings associated with accessory structures which are common in the

skin, ear and eye (Bear et al., 2006). Free nerve endings are branching terminations of sensory nerves which have no obvious specialised structure surrounding them. These endings are commonly nociceptors, gathering information on damaging stimuli (Bear et al., 2006; Willis and Coggeshall, 1991) but some non-encapsulated nerve fibres such as those in the peridonal ligament are believed to have a mechanoreceptive functions, that may be analogous to non-encapsulated stretch receptors in blood vessels (Byers, 1985).

Non-encapsulated Nerve Endings

Type IV Nerve Endings

Free nerve endings have very high thresholds and therefore collect information on mechanical and damaging stimuli (nociceptive) (Freeman and Wyke, 1967c). The majority of these receptors do not have any distinguishing morphological characteristics to define them, however ultrastructural analysis has demonstrated that the nerve endings are frequently branched and have a beaded appearance (Heppelmann et al., 1990; Heppelmann et al., 1989). Type IV nerve endings are the most abundantly distributed nerve endings associated with joints, and are located within most tissues including joint capsules, ligaments, tendons, and adjacent periosteum (Freeman and Wyke, 1967c). It is these nerve endings which are primarily responsible for nociceptive signalling in joint and connective tissue pathology (Heppelmann, 1997; Schaible and Schmidt, 1985). Unlike the aforementioned receptors, free nerve endings branch from either thinly myelinated or unmyelinated nerve fibres (i.e group III or IV fibres). Useful markers for group IV, nociceptive fibres are the neuropeptides substance P (SP) and calcitonin gene related peptide (CGRP), which are known to be co-localised. However, it has been demonstrated that some nociceptive nerve fibres do not contain neuropeptides (Hanesch et al., 1991). The occurrence of these peptidergic nerve fibres within joints and associated connective tissues is well known (Ackermann et al., 1999; Kido et al., 1993; Marshall et al., 1994; McDougall et al., 1997; Wojtys et al., 1990). However, these neuropeptides are not only involved in conveying nociceptive information centrally; SP and CGRP can also be released from the free nerve endings (Holzer, 1988; Yaksh, 1988). In the periphery, SP and CGRP have a number of functions on the surrounding tissue causing sensitisation of other nociceptive nerve fibres in the area, therefore lowering the threshold at which the nerve

fibres can be stimulated resulting in hyperalgesia (Nakamura-Craig and Gill, 1991). The release of these peptides can, however, also result in the dilation of arterioles and leakage of plasma from venules (i.e. redness and swelling) (Holzer, 1988; Kenins, 1981; Kenins et al., 1984), but substance P is also able to stimulate phagocytes and attract other inflammatory cells to the damaged area (as reviewed by - Schaffer et al., 1998). Such symptoms are frequently associated with joint pathology and as a result SP and CGRP have been heavily implicated in conditions such as rheumatoid arthritis (Pereira da Silva and Carmo-Fonseca, 1990; Weihe et al., 1988) and tendinopathies (Ackermann et al., 1999; Ackermann et al., 2003). It is therefore of particular importance to describe the distribution of SP and CGRP containing nerve fibres at entheses.

1.2 ENTHESES

What are Entheses and why are they Important? An enthesis is the attachment of a tendon, ligament (TL), or joint capsule to bone. It is also called an insertion site, osteotendinous or osteoligamentous junction. Benjamin & McGonagle (2001) have coined the term 'enthesis organ' to define a collection of structures adjacent to, and associated with, the enthesis itself, that help to reduce stress concentration at the attachment site (Benjamin and McGonagle, 2001). They have also introduced the term 'functional enthesis' to describe the wrap-around regions of tendons or ligaments, where the TL change direction by passing around bony or fibrous pulleys (Vogel and Koob, 1989). This highlights the parallels between such regions and 'true' entheses.

Functionally, entheses provide strong and stable anchorages that promote musculoskeletal movement with concomitant joint integrity. However, they must serve as more than simple anchors, for in linking soft to hard tissue, entheses also need to minimise the risk of damage in the face of high levels of mechanical loading, by allowing the smooth transfer of force between soft and hard tissue (Benjamin et al., 2002; Benjamin et al., 2006). The bony attachment site is thus a key link in any muscle-TL-bone unit and one which may experience considerably more stress than the TL itself. Curiously however, at some animal sites at least, not all of the force generated by a muscle is transferred to bone via its

connecting tendon. Rijkelijkhuzen et al., (2005) have shown that force can be transferred from muscle to bone, even when the tendon is severed - if the connection between the epimysium and the epitendinous tissue is substantial and intact (Rijkelijkhuzen et al., 2005). This is in line with the principle of myofascial continuity, which suggests that closely associated muscles can transmit force between each other via fascial connections (Myers, 2001). These observations correlate with early literature which likened the fascia of the lower limb to an ectoskeleton, to which muscles form extensive attachments (Jones, 1982). This allows the muscles to function as a rigid column and perform powerful movements; such fascial connections are not observed in the upper limb where discrete intricate movements are required (Jones, 1982).

Despite the stress concentration at entheses, they are less likely to fail than other parts of the musculoskeletal chain because of their ability to withstand high mechanical loads. Entheses are nonetheless vulnerable to overuse injuries and these present as a number of poorly-understood, pathological changes that are collectively referred to as enthesopathies. Any such injury can have a significant impact on the lifestyle of the general population and on the ability of athletes to pursue their sport. Pathologies such as the epicondyloses (tennis elbow), proximal patellar tendinopathy (jumper's knee), a variety of Achilles insertional disorders and plantar fasciosis ('fasciitis') are well known (Khan et al., 1996; Niepel et al., 1966; Niepel and Sit'aj, 1979; Resnick and Niwayama, 1983).

However, entheses are also targeted in the seronegative spondyloarthropathies (Benjamin and McGonagle, 2001). These are a diverse collection of chronic, autoimmune joint diseases that are among the most prevalent of rheumatic conditions. They include ankylosing spondylitis, reactive arthritis, psoriatic arthritis, arthritis associated with inflammatory bowel disease and undifferentiated spondyloarthropathies (Peloso and Braun, 2004). Similarly, DISH (Diffuse Idiopathic Skeletal Hyperostosis - formerly known as Forestier's disease), is also characterised by excessive bone deposition at entheses that leads to the formation of bony spurs, as reviewed by Childs et al., (2004).

Entheses are of particular concern to orthopaedic surgeons because of the need to re-attach TL to bone – e.g. during the reconstruction of an anterior cruciate ligament. It is uniquely challenging to recreate the natural smooth transfer of load from TL to bone that typifies the healthy, original attachment site (Pendegrass et al., 2004). A variety of techniques have been pioneered surgically that attempt to do so, but most simply involve stapling the TL to the bone. More recently however, various materials with viscous properties (e.g. hydroxyapatite) have been coated on the attachment site of the implanted TL (Pendegrass et al., 2004).

Skeletal attachment sites have also long been of interest to archaeologists in relation to physical activity. Their focus has been exclusively on the characteristic markings left by entheses following maceration of the skeleton. The premise is that the markings left by TL on dried bones convey useful information about the lifestyle of ancient populations (Galera and Garralda, 1993). Greater physical activity (e.g. between males and females) is reflected by different entheses markings. The constant stressing of a muscle from daily repetitive tasks of various types, gives the archaeologist a skeletal record of habitual activity patterns and this has contributed to understanding a wide range of issues relating to ancient populations (social, cultural, labour, the development and use of tools etc.) (Galera and Garralda, 1993). Although the link between physical activity and osteological characteristics seems plausible, comparison of the findings of different authors is hampered by a lack of objectivity in evaluating entheses footprints. It is thus worth noting that Zumwalt (2005) has developed a method of quantifying the 3D topography of attachment sites by a fractal analysis of insertions photographed with a 3D laser scanner. One of her principal findings was that the markings left at the periphery of entheses are particularly complex and suggestive of highly-varied load (Zumwalt, 2005). Histologically, it is understood that the structure of many entheses varies, in that parts of the peripheral regions are fibrous; whereas the inner regions (often the joint side) are fibrocartilaginous (see below). Therefore, it may well be that some areas of insertions sites are more heavily loaded than others (Maganaris et al., 2004).

Finally, the specialised adaptations of TL entheses that stem from their interface location are paralleled elsewhere. Nature has adapted a vast number of structures throughout the animal kingdom in order to overcome the difficult task of linking hard and soft tissues, usually through the use of an intermediate form of tissue. Examples include the attachment of the underlying soft tissues to the hard jaw of the marine polychaete worm, and the byssus threads (effectively extracorporeal tendons) by which mussels anchor themselves to rocky shores (Benjamin et al., 2006; Waite et al., 2004). A comparative survey of anchorage sites is largely uncharted territory, but likely to highlight the most important of basic constructional principles that apply to TL.

An Historical Note on Terminology: The earliest origins of the word ‘enthesis’ are unclear. It is possible that they have a mythological background. The nymph *Thetis* (mother of Achilles), is said to have dipped Achilles into the river Styx. This made him invulnerable, except for the heel by which she held him. However, Khan (2002a) has presented an alternative view on the origin of *enthesis*. He considers that the word is derived from the adjective *enthetic*. According to its Greek roots, this means ‘fit for implanting’. Khan (2002a) states that *enthetic* was originally used in the C19th to refer to diseases which had been inoculated or implanted into a body from an external source - particularly infections. In the C20th, the use of the adjective diminished, and the noun *enthesis* was used to describe the use of artificial materials for repairing a defect. Certainly, what is clear is that it is only much more recently that an *enthesis* has come to mean the site where a tendon or ligament attaches to bone. Such a meaning started in rheumatology, but the usage is now common and has spread to many other branches of medicine and science.

One of the most influential early descriptions of TL insertional structure was that of Dolgo-Saburoff (1929). He clearly described the anatomy of the cat patellar ligament and its multilayered appearance. Following these studies, further work reported in the German literature (see Knese and Biermann (1958) for further details) lead to the detailed description of the attachments of a large number of human entheses. However, it was not until the late 1960s, that the pathology of attachment sites attracted significant attention via

the seminal work of Niepel and colleagues (1966). They introduced the word *enthesopathy* – a term which is still in use today to refer to any pathological disorder of an enthesis.

1.1.1. ENTHESIS STRUCTURE

MACROSCOPIC STRUCTURE

As TL approach bone, they flare out in order to increase the surface area of the attachment. A good example of this is the combined insertion of the tendons of sartorius, gracilis and semitendinosus onto the tibia. These 3 tendons constitute the *pes anserinus* or ‘duck’s foot’ because of their highly flared appearance. The *pes anserinus* is also illustrative of the general principle that neighbouring entheses often merge with each other on the skeleton to form stronger and more stable attachments. Indeed, this may be reflected in their development - as with the Achilles tendon and the plantar fascia. In the foetus, the Achilles tendon and plantar fascia are continuous over the posteroinferior aspect of the calcaneus, because both structures initially attach to the perichondrium, rather than to the cartilaginous anlagen itself (Snow et al., 1995). With growth, this continuity is reduced, but according to Milz et al (2002), may still be evident in adulthood – though Snow et al., (1995) disagree. The direct continuity of one enthesis with another has also been observed between the insertion of the quadriceps tendon and origin of the patellar ligament. Fibres from the former pass over the anterior surface of the patella to become directly continuous with the patellar ligament at its enthesis (Toumi et al., 2006). The convergence of entheses and the blending of attachment sites to adjacent fasciae is an adaptation for dissipating stress between one TL and another and thus reducing the risk of local failure. On the other hand, there is a need to ensure that certain tendons attach to bone discreetly in order to promote precise and highly intricate movements. This almost certainly relates to the greater propensity of tendons with small areas of bony attachment (relative to the size of the whole musculoskeletal unit) for avulsion. However, it should be recognised that load may be reduced at a given attachment site (thus reducing the risk of avulsion) by dissipating the action of a single muscle belly over more than one tendon – e.g. as with the digital tendons. In other regions of the body, stress dissipation is promoted by a single tendon attaching to a number of bones. Thus, peroneus longus attaches to both the medial cuneiform and the 1st

metatarsal and tibialis posterior sends tendinous slips to every tarsal bone except the talus (Standring, 2004).

MICROSCOPIC STRUCTURE

The Classification of Enteses

Because the pioneering histological descriptions of enteses were largely published in German, enteses were classified by Knese and Biermann (1958) as *die diaphysären-periostalen Ansätze* (which translates as ‘diaphysial-periosteal attachments’) or *die chondralen-apophysären Ansätze* (chondral-apophyseal attachments). Unfortunately, these terms only refer to the attachments of TL to long bones and cannot be easily applied to other parts of the skeleton. Thus, more recently, broader terminologies have been devised to encompass the entire musculoskeletal system. Benjamin et al., (1986) have regarded enteses as being either fibrous or fibrocartilaginous, depending on the character of the tissue at the TL-bone interface (Fig 1.1-4). Fibrous enteses are usually present where TL attach to the diaphysis or metaphysis of a bone – e.g. the tibial attachment of the medial collateral ligament (MCL) of the knee. They equate to the diaphysial-periosteal attachments of Knese and Biermann (1958), which these authors have in turn sub-classified as either ‘areal’ or ‘circumscribed’ enteses. The distinction relates to the surface area (i.e. the footprint) of the attachment; the former flaring its fibres over a larger area than the latter. Fibrous enteses can also be further classified as either ‘bony’ or ‘periosteal’ fibrous attachments (Hems and Tillmann, 2000) to indicate whether the tendon inserts directly into the bone (Fig. 1.1) or indirectly to it via the periosteum (Fig. 1.2). It should be recognised however, that as development proceeds, periosteal enteses can become bony ones (Gao et al., 1996).

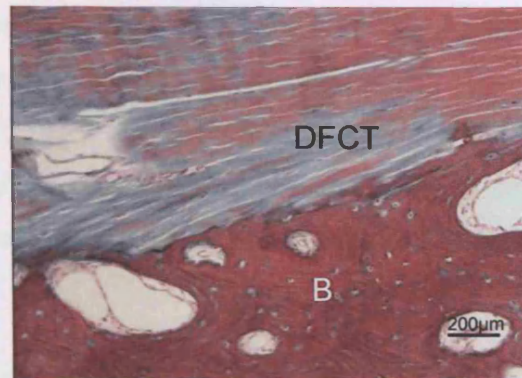


Figure 1.1: The direct fibrous enthesis of pronator teres. Note the direct attachment of the dense fibrous connective tissue (DFCT) of the tendon to the underlying bone (B). (Specimen acquired and processed by Dr Koji Hayashi)

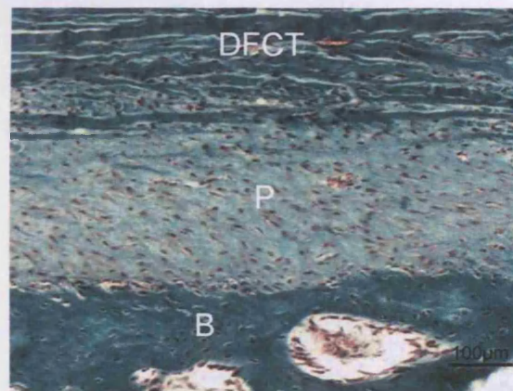


Figure 1.2: The indirect fibrous enthesis of the suspensory ligament of the equine limb. The dense fibrous connective tissue (DFCT) of the ligament is attached to the underlying bone (B) via the periosteum (P).

Fibrocartilaginous entheses are more common than fibrous entheses and predominate at epiphyses and apophyses (Benjamin et al., 1986; Knese and Biermann, 1958). The archetypal fibrocartilaginous attachment is exemplified by that of the Achilles tendon on the calcaneus (Fig. 1.3). It should be noted however that the structure of a given enthesis can vary greatly from region to region. Hems and Tillmann (2000) emphasised this in their study of the attachments of the masticatory muscles and Benjamin et al., (1986) have pointed out that what are termed fibrocartilaginous entheses are not cartilaginous in all regions. For example, at the Achilles tendon insertion, the most superficial part of the attachment is purely fibrous (Benjamin et al., 2002). The significance of this is in understanding the differential load transfer across the footprint of an enthesis which has yet to be thoroughly explored, though this is recognised by Maganaris et al. (2004).

It is also important to recognise that some muscles have fleshy attachments to bone and thus lack a tendinous link to the skeleton – though usually at one end only. Even at such attachment sites, muscle fibres do not anchor directly to the underlying periosteum, but attach via a small amount of connective tissue associated with the muscle fibres (Suzuki et al., 2002). These entheses correspond to the muscular or ‘fleshy’ attachment sites of Knese and Biermann (1958).

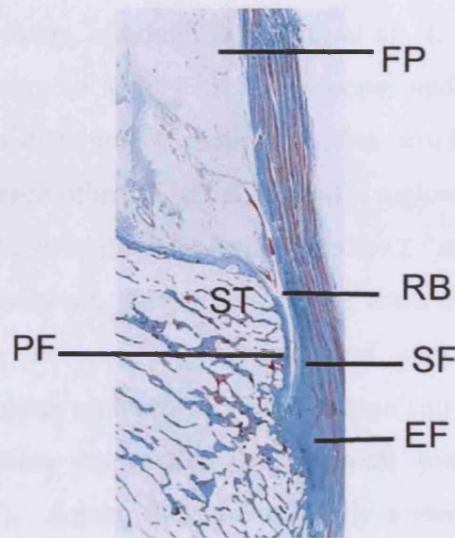


Figure 1.3: A low power view of the enthesis organ associated with the human Achilles tendon. The enthesis organ comprises the enthesis itself (EF), sesamoid (SF) and periosteal (PF) fibrocartilages, the retrocalcaneal bursa (RB) and the tip of Kager's fat pad (FP). Note the virtual absence of compact bone at the enthesis.

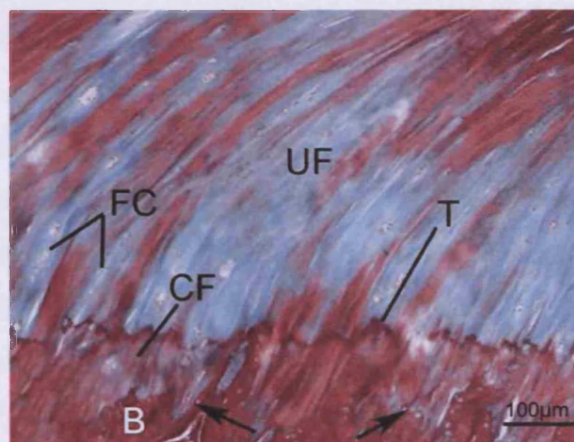


Figure 1.4: The fibrocartilaginous enthesis of the human Achilles tendon. Zones of calcified (CF) and uncalcified fibrocartilage (UF) are readily visible and large rounded fibrocartilage cells (FC) are conspicuous in the former. Note that a calcification front (the tidemark - T) separates hard from soft tissue, but that this is

subtly different from the tissue boundary between tendon and bone (B). This boundary is marked by an irregular cement line (arrows).

Fibrocartilaginous Entheses

Dolgo-Saburoff (1929) described a multilayered bony attachment of the cat patellar ligament in which he could distinguish 4 zones of tissue - the ligament itself, uncalcified fibrocartilage, calcified fibrocartilage and bone (Fig 1.4). The zonal concept remains the foundation of descriptions today, although Benjamin et al., (2007b) have pointed out that one or more of the zones may be locally absent. Cooper and Misol (1970) later showed that each of the zones has different characteristics, but emphasised how the layers can blend imperceptively with each other. Typically, the TL region (i.e. furthest away from the bone) is characterised by the presence of parallel bundles of collagen fibres, with rows of elongate fibroblasts lying between them. Within the zone of uncalcified fibrocartilage, these collagen fibres may become less obvious and assume a more 'basketweave' appearance, with the fibroblasts replaced by fibrocartilage cells. The latter cells are more rounded and lie in lacunae, surrounded by a small amount of proteoglycan-rich extracellular matrix (ECM). Again, they are typically arranged in longitudinal rows – reflecting their metaplastic origin from TL fibroblasts during development (Cooper and Misol, 1970; Rufai et al., 1992). The basketweave arrangement of collagen fibres is believed to help dissipate the load of the TL (Knese and Biermann, 1958).

Functional Significance of Uncalcified Enthesis Fibrocartilage: The uncalcified fibrocartilage at an enthesis promotes a gradual change of elastic modulus, which encourages the smooth transfer of load across the soft-hard tissue interface (Hems and Tillmann, 2000). It allows the gradual bending of TL collagen fibres as they approach the bone, in much the same way that a grommet on an electrical plug controls the bending of the lead which enters it (Fig 1.5.) (Schneider, 1956). The 'bending-control' function is supported by the correlation which exists between the quantity of uncalcified fibrocartilage at different entheses, and the range of insertional angle change that occurs with joint movement – the greater the angle change, the more fibrocartilage is present (Benjamin and Ralphs, 1998; Frowen and Benjamin, 1995). Fibrocartilage is thus a tissue designed for

resisting compression and/or shear (Benjamin and Ralphs, 1998). It may also act as a stretching brake for tendons during muscular contraction (Benjamin et al., 1986; Knese and Biermann, 1958). In other words, it may prevent a tendon from narrowing as it elongates; any significant attempt at narrowing too close to a bony interface may weaken the tendon attachment.

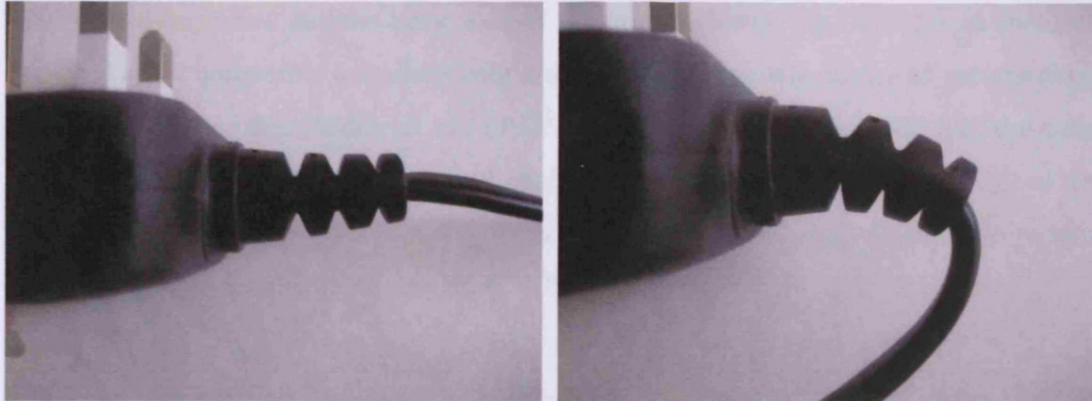


Figure 1.5: The uncalcified fibrocartilage at the insertion of a fibrocartilaginous enthesis is analogous to the grommet on an electrical plug, facilitating gradual bending of the cord (tendon) to prevent wear and tear.

Knese and Biermann (1958) highlighted the specialised nature of fibrocartilage cells and this issue has been addressed in much further detail by Benjamin and Ralphs (2004). Benjamin and colleagues have highlighted the transitional character of fibrocartilage and emphasised that the term includes a wide spectrum of tissues with properties intermediate between those of dense fibrous connective tissue and hyaline cartilage. However, it is the cartilage-like molecules in the ECM of fibrocartilage which are of particular interest in providing a TL with the ability to withstand compression. Such loading is an inevitable consequence of the changing insertional angle of a TL that accompanies joint movement (Benjamin et al., 1986; Milz et al., 2005). More recently, the orientation of collagen fibres at the insertion site has attracted attention in relation to mechanisms for reducing stress concentration. Thomopoulos et al., (2006) demonstrated that the changing orientation of the collagen fibres from tendon to bone results in changes to the predicted stress concentrations; this may therefore influence the cell phenotype and matrix production at the insertion (Thomopoulos et al., 2006).

Tidemarks: The layers of calcified and uncalcified fibrocartilage are separated by a calcification front which is most commonly called the tidemark (Fig. 1.3), but which in the older German literature was called *die Grenzlinie* (Knese, 1957; Knese and Biermann, 1958). Although, a tidemark separates the zones of calcified and uncalcified fibrocartilage, collagen fibres from the latter are continuous with those in the former, but become obscured by the mineralised matrix and lose evidence of crimp (Clark and Stechschulte, 1998). Although few authors have studied the importance of the tidemark at entheses, the presence of a comparable boundary within articular cartilage has attracted greater attention. It is worth noting that Redler et al., (1975) have raised the possibility that the tidemark tethers the perpendicularly-orientated, collagen fibres in articular cartilage to reduce shearing stresses. It has also been suggested that it prevents blood vessels from penetrating uncalcified cartilage (Havelka and Horn, 1999).

The exact structure of the tidemark is difficult to define. Havelka and Horn (1999) have described a wide spectrum of appearances – from fibrillated to granular and pointed out that the tidemark may be ill-defined (particularly if the tissue is pathological), vary with age and change with the degree of loading (Havelka and Horn, 1999). Lyons et al., (2005) believe that the tidemark in articular cartilage is formed by two juxtaposed laminae with differing biochemical characteristics. They suggest that, the tidemark serves to inhibit hydroxyapatite crystal formation and growth after musculoskeletal maturity. In this way, the cartilage is protected from progressive mineralization. Clearly, this could apply to entheses as well. It may help to bear this in mind when considering the significance of multiple tidemarks that may appear in degenerative insertional tendinopathies. The original tidemark remains as an indicator of a previous wave of calcification (Lyons et al., 2005). In articular cartilage, Lyons et al.,(2006) suggest that the tidemark may fail to migrate in local regions, so that a region of uncalcified cartilage reaches the subchondral bone directly. This may provide a pathway for nutrients required by the chondrocytes. The cells within the calcified (fibro)cartilage that lies immediately deep to the tidemark, have similar characteristics to those of the uncalcified (fibro)cartilage, but are surrounded by a mineralised matrix. Their viability has been confirmed by a number of authors, as reviewed in articular cartilage by Havelka and Horn (1999).

Subchondral Bone Plate: Although the tidemark is the mechanical boundary of an enthesis, it is subtly distinct from the tissue boundary – i.e. the interface between TL and bone. This is represented by a cement line (Fig. 1.3) (Hems and Tillmann, 2000). In sharp contrast to the straightness of the tidemark, the cement line is highly convoluted and the increased surface area it creates between TL and bone, promotes firm anchorage and resistance to shear (Schneider, 1956). Whether or not there is significant continuity of collagen fibres across the cement line (i.e. from TL to bone) at a fibrocartilaginous enthesis is debatable. The traditional view is that TL attach to bone via ‘Sharpey’s fibres’ and indeed, such fibres are obviously present at certain fibrous entheses (Hems and Tillmann, 2000). However, Benjamin et al. (2007b) point out that compact bone may be virtually absent at even the largest of fibrocartilaginous entheses and that the cortical shell is often no more than a continuum of spongy bone trabeculae. Thus, there would seem to be insufficient cortical bone at the attachment site itself, to accommodate many/any perforating fibres of Sharpey. This even applies to a tendon as large as the Achilles where the absence of a substantial cortical shell is conspicuous (Fig. 1.3). It is worth noting however that Haines and Mohuiddin (1968) suggest that the fibres which cross the tidemark between uncalcified and calcified fibrocartilage at fibrocartilaginous entheses should be considered as equivalent to Sharpey’s fibres, because calcified fibrocartilage can be viewed as a form of ‘metaplastic’ bone. Although such considerations are valid, Milz et al.,(2002) suggest that it is the highly interdigitating nature of the calcified fibrocartilage zone of the inserting TL and underlying bone, which is of fundamental importance in promoting attachment.

Why is there so Little Compact Bone at Fibrocartilaginous Enteses? One possibility is that the dominance of spongy rather than compact bone, contributes to stress dissipation by allowing slight deformation of the bone during loading of the TL (Benjamin et al., 2007b; Currey, 1984). In other words, stress dissipation is not the sole prerogative of the soft tissue side of an enthesis, but continues within the bone itself (Benjamin et al., 2007b). This may relate to the patterns of bone oedema that may be seen at certain entheses in patients with SpA and be reflected in the anisotropic arrangement of trabeculae at

attachment sites (Benjamin et al., 2007b; Toumi et al., 2006). In addition, the absence of compact bone may also be an adaptation to promote access of the soft tissue to marrow blood vessels, for there are local areas at the enthesis where both the subchondral bone and calcified fibrocartilage are completely missing (Benjamin et al., 2007b). Such 'holes' may also provide access to immunocompetent cells and stem cells in the underlying bone marrow. Similar defects have been reported in the subchondral bone plate that supports articular cartilage (Shibakawa et al., 2005). It has been suggested that these could be involved in bone resorption and remodelling, and that they may also trigger proteoglycan degradation in the adjacent articular cartilage (Shibakawa et al., 2005). This could occur via the expression of matrix metalloproteinases (MMPs) by osteoclasts within the pit. Although such a potential for remodelling may be construed as beneficial, the formation of local defects in any subchondral plate (i.e. either that which supports articular cartilage or a TL enthesis) might equally create an imbalance in stress transduction within the overlying (fibro)cartilage. Clearly this could promote local degeneration (Shibakawa et al., 2005). In the light of the above considerations, it is interesting to note that damage to the subchondral bone (fractures) can lead to lesions in the overlying articular cartilage (Lahm et al., 2004). The authors have suggested that the healed bone is harder than the original, so that load transfer is altered and degeneration of articular cartilage ensues (Johnson et al., 1998; Lahm et al., 1998). Intriguingly, when alendronate (an inhibitor of bone resorption) was given to rats with subchondral bone fractures, remodelling of the subchondral plate was suppressed and the formation of cartilage lesions prevented (Hayami et al., 2004). Whether similar findings could apply to the enthesis is unknown.

Molecular Composition of Enthesis Fibrocartilage: The ECM molecules in enthesis fibrocartilage play an important role in transferring the complex, multi-directional forces that act at the attachment site (Thomopoulos et al., 2003). The type of molecule present is directly related to the mechanical demands at the interface and this is why cartilage-related molecules are typical. The expression of the glycosaminoglycans (GAGs), chondroitin - 4 and 6 – sulphate is elevated at fibrocartilaginous entheses (as at functional entheses (Benjamin and Ralphs, 1998; Milz et al., 2005). These GAGs are usually associated with aggrecan - a large, aggregating proteoglycan that is a major constituent of the ECM in

hyaline articular cartilage. Aggrecan is a hydrophilic molecule that imbibes water and thus allows the tissue to withstand compression (Kiani et al., 2002).

It is undoubtedly the aggrecan content of entheses that accounts for the ability of the uncalcified fibrocartilage to dissipate collagen fibre bending and prevent TL narrowing under load. Other small, leucine-rich, proteoglycans such as decorin, fibromodulin and lumican, have also been detected immunohistochemically in enthesis fibrocartilage. They may have an important role in regulating collagen fibril formation and thus determining the tensile strength of the TL (Milz et al., 2005). The importance of cartilage-like molecules in tendons has been highlighted by Corps et al., (2006, 2004). They demonstrate that levels of aggrecan and biglycan in painful tendinopathy are increased and may reflect the change in mechanical loading at the site of the lesion, leading to a more cartilage-like phenotype of the tissue (Corps et al., 2006). Such an increased expression of these proteoglycans would also be expected to occur at entheses, as changes in mechanical loading are also experienced here in injured tendons. These changes may in turn cause a further alteration in the mechanical loading and consequently trigger a vicious cycle of increased pathology (Maffulli et al., 2006).

While type I collagen generally predominates in the mid-substance of a TL, and in bone, type II collagen (the typical collagen of cartilage) is only characteristic of the fibrocartilage zones (Milz et al., 2005). Although types III and VI collagen show no significant regional variations across the TL-bone unit, the expression of the latter does vary between the mid-substance of the TL and the fibrocartilage zones. In the TL itself, type VI collagen is found throughout the ECM, while in the fibrocartilaginous regions it has a more restricted and pericellular distribution, suggesting that type VI collagen has different matrix binding functions in these regions (Waggett et al., 1998). Type III collagen has the ability to form heterotypic fibrils with types I and V collagen and is believed to play a role in controlling fibril diameter (Birk and Mayne, 1997; Waggett et al., 1998). Type X collagen has also been identified at entheses (within the zone of calcified fibrocartilage) and is important in controlling calcification (Fujioka et al., 1997). Interestingly, Kruzynska-Frejtag et al., (2004) have demonstrated the presence of a cell-adhesion molecule called “periostin” at the

periodontal ligament enthesis, that may also be involved in controlling mineralisation. They suggest that high levels of periostin present at hard-soft tissue interfaces may prevent ligament cells near the soft-hard tissue boundary, from differentiating into an osteogenic phenotype (Kruzynska-Frejtag et al., 2004). In other words, the molecule helps to maintain the ligament as a non-mineralised tissue. It would thus be of interest to know whether periostin is expressed at other entheses and whether a reduction in its expression is associated with the spread of mineralization into soft tissues. Finally, it must be acknowledged that we know little about the turnover of any enthesis ECM molecules, but in the rest of the TL, it seems that men have elevated levels of collagen synthesis following exercise compared with women (Miller et al., 2006). This has been related to the greater incidence of exercise-related musculoskeletal injuries in women (Miller et al., 2006).

Non-Invasive Imaging of Fibrocartilaginous Entheses: A number of methods have been used to determine the structure of entheses. The most widely used and effective is routine histology and immunohistochemistry. However, such invasive methods are not suitable for identification of pathological changes in the living. Non-invasive imaging is a practical alternative to identifying the structure and pathology of entheses. Conventional Magnetic Resonance Imaging (MRI) has proved relatively successful in identifying pathological changes, however, the normal structure of fibrocartilage, tendons and ligaments, along with many other structures are difficult to identify because these structures have very short transverse relaxation times (T_2), this means that the magnetization induced in them through MR imaging decays very quickly and cannot be imaged. Recent technological advances in MR imaging have allowed the visualisation of those tissues at entheses such as fibrocartilage which have been previously almost impossible to distinguish. The recent development of ultrashort echo time and magic angle imaging has however, improved imaging of entheses, allowing differentiation of various tissues at the attachment site. Ultrashort echo time works by shortening the time to the beginning of the data reception by a factor of 20-200, and by using techniques which can spatially encode data as soon as the gradient system is enabled, it is possible to detect signals from tissues with short T_2 . Radiofrequency pulses can then be used to manipulate this signal (Robson et al., 2004). The second method that can be used to distinguish entheses is magic angle imaging. This

works by highlighting differences between fibre organisations through altering the orientation of the collagen fibres in relation to the static magnetic field of the system. The different organisation of the collagen fibres results in different signal intensities therefore allowing differentiation of the different tissues found at entheses (Gatehouse and Bydder, 2003). Such advances in MRI imaging may prove particularly useful in identifying pathological changes associated with specific structures of the enthesis (Robson et al., 2004) and also preventing misdiagnoses. Recent studies have also reported the importance of adipose tissue at entheses (Benjamin et al., 2004b). Unlike the other tissues of the enthesis, adipose tissue provides a high signal and it is therefore very easy to visualise with the use of MRI. However, it is possible to suppress this high signal. These modifications in MRI pulse sequence parameters also allows the detection of fluids used in bursographies and arthrographies; techniques which are particularly useful in highlighting the structure of bursae associated with TL attachment sites and various pathologies associated with these structures (Pfirrmann et al., 2001; Steinbach et al., 2002).

Ultrasonography is another useful method which can be used to view the structure of entheses. Morel et al., (2005) used normal and contrast ultrasonography along with microscopic and macroscopic observations to determine the vascularisation of the normal Achilles enthesis. Macroscopically a network of blood vessels were found in the most superficial (fibrous) region of the Achilles enthesis, however, these vessels could not be seen in with the use of normal or contrast US. This technique did however; highlight the highly vascular network of blood vessels within Kager's triangle (Morel et al., 2005). Kamel et al., (2003) compared the use of MRI and ultrasound in identifying early enthesopathic changes associated in SpA. According to Kamel (2003) ultrasonography is preferential in identifying early pathological changes at entheses, by detecting fatty degeneration and early signs of calcification at the enthesis earlier than MRI. Ultrasound elastography, a novel form of non-invasive imaging, has recently been used to demonstrate the high levels of strain exerted at the insertion sites of the anterior cruciate ligament (ACL). This technique also demonstrated that the degree of deformation experienced in the tendon proper decreased towards bone. This reflects the increased stiffness of the

interface with an alteration in the matrix organisation at the tendon-bone interface (Spalazzi et al., 2006).

Fibrous Entheses

Fibrous entheses have attracted far less interest than fibrocartilaginous attachments, probably because they are less frequently involved in enthesopathies. Nevertheless, a number of large and powerful muscles (e.g. deltoid, pectoralis major and latissimus dorsi - Benjamin et al., (1986) and important ligaments (e.g. the knee joint medial collateral ligament (MCL) (Matyas et al., 1990; Wei and Messner, 1996) have fibrous entheses. The footprint of fibrous entheses is generally broad (hence the term 'areal' used by Biermann (1957) and Knese and Biermann (1958) and this helps to dissipate the stress over a broad area and minimise stretching of the fibres within the TL. Typically, tendons with fibrous entheses tend to be relatively short.

As outlined earlier, there are two forms of fibrous entheses - those which attach directly to cortical bone and those which attach indirectly to it via the periosteum (Fig. 1.2 and 1.3). Following closure of the growth plate, a 'periosteal' fibrous enthesis can become a bony one, although some TL attach to the periosteum throughout life (Hems and Tillmann, 2000). It is important to recognise that the initial attachment of a metaphyseal TL to the periosteum of a long bone (rather than to the bone itself), allows the TL to migrate as the bone lengthens, so that the relative position of the ligament remains unchanged (Fig 1.6). This is because the periosteum can grow interstitially, but the bone itself cannot – it can only grow by appositional means (Dorfl, 1980a, b). A periosteal, fibrous enthesis is inevitably weaker than a bony one.

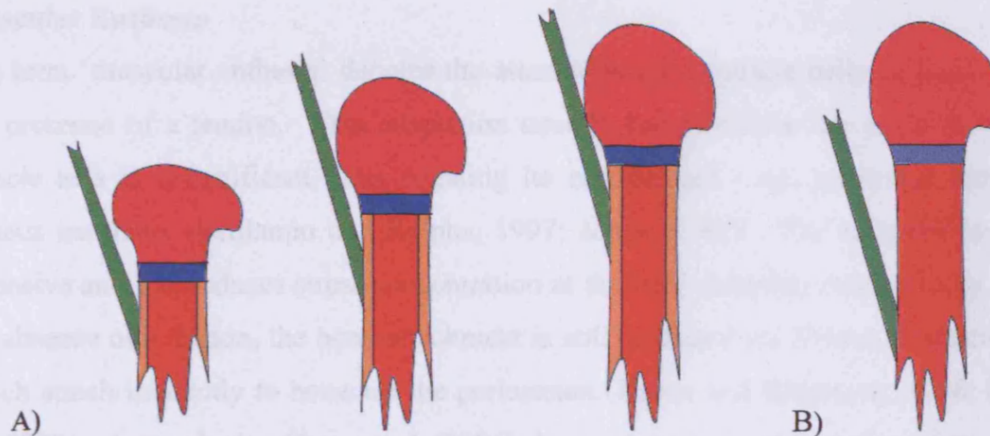


Figure 1.6: Schematic representation of the migration of a metaphyseal fibrous enthesis during growth of a long bone. (A) The indirect attachment of a tendon or ligament to the periosteum (rather than to the underlying bone) allows migration of the attachment during growth and ensures that the attachment site remains in the same relative location with respect to the position of the growth plate (shown as a blue band). (B) If the tendon or ligament attached directly to bone, the attachment would not be able to migrate during elongation of the bone.

The tibial attachment of the knee joint MCL has been the focus of most interest in fibrous entheses, because of the involvement of this ligament in traumatic knee injuries (Dorfl, 1980a, b; Gao et al., 1996). Its structure has been described in detail by Matyas et al., (1990) in the rabbit MCL. They distinguished 5 layers. Layer I is formed by a delicate connective tissue on the surface of the ligament, which becomes continuous distally with the superficial layer of periosteum. Layer II is composed of the densely packed collagen fibres of the ligament itself, which merge with the fibrous layer of the periosteum. Layer III is formed by the loose connective tissue covering the deep surface of the ligament. This blends with the osteogenic layer of the periosteum at the insertion site. Layers II and III are however lost during maturity - mineralization of these ligament layers forms layer IV, which may equate to the specialised form of bone, known as 'fibre bone' or 'insertion bone' as described by Petersen (1930). Finally, layer V is the underlying cortical bone (Matyas et al., 1990).

Muscular Entheses

The term ‘muscular enthesis’ denotes the attachment of a muscle belly to bone - without the presence of a tendon. This adaptation usually occurs where the angle at which the muscle acts is insignificant, thus negating its requirement - eg. quadratus femoris and gluteus maximus (Benjamin and Ralphs, 1997; Jones, 1982). The footprint is typically extensive and this reduces stress concentration at the bony interface substantially. Despite the absence of a tendon, the bony attachment is still mediated via fibrous connective tissue which attach indirectly to bone via the periosteum (Knese and Biermann, 1958; Suzuki et al., 2002). Intriguingly, Chen et al.,(2006) demonstrated the expression of parathyroid-hormone related protein (PTHrP) at muscular entheses – a molecule which has also been identified in the periosteum at fibrous entheses, however its role in this location is still unknown (Chen et al., 2006).

1.1.2. THE ENTHESES ORGAN CONCEPT

Benjamin and McGonagle (2001) coined the term ‘enthesis organ’ to denote a collection of structures adjacent to the attachment site itself, which are functionally associated with the enthesis and which also play an important part in reducing stress concentration at the soft-hard tissue interface. The concept of an enthesis organ explains why patients may present with symptoms adjacent to an enthesis as well as at the enthesis itself (Olivieri et al., 1998). Curiously, the idea that there is more to an enthesis than just the attachment site itself was considered by Niepel and Sit’aj (1979) over quarter of a century ago, but ignored at that time.

The archetypal enthesis organ is that of the Achilles tendon (Fig. 1.3), which Canoso described as the “première enthesis” (Canoso, 1998). Canoso had long been aware of the contribution of neighbouring structures to the role of the enthesis itself and had made particularly pertinent observations on the functions of Kager’s fat pad which protrudes into the retrocalcaneal bursa (Canoso et al., 1988). The triangular tip of this fat pad, the retrocalcaneal bursa itself and the fibrocartilages which form its walls collectively constitute the enthesis organ of the Achilles tendon (Fig. 1.3). The two fibrocartilages in

the bursal walls comprise a variably-thick, periosteal fibrocartilage on the superior tuberosity of the calcaneus, and a sesamoid fibrocartilage within the deep surface of the opposing tendon. They are an adaptation to resist compression and/or shear when the foot is dorsiflexed and the tendon is brought in contact with the calcaneal tuberosity. The fluid-filled bursa facilitates a change in insertional angle between the tendon and the bone during foot movements. By analogy with synovial joints, the presence of hyaluronan within the bursa might be expected to reduce the coefficient of friction substantially and thus prevent the build up of heat. Bursal fluid may also be important as a source of nutrients and oxygen for the avascular fibrocartilages (Mason et al., 1999).

In understanding the concept of an enthesis organ, the reader should note that the bone immediately adjacent to the Achilles tendon enthesis (i.e. the tuberosity) acts as a mini pulley for the tendon and that contact between the two reduces stress concentration at the enthesis itself – albeit at the expense of increasing wear and tear in the contact zone (Benjamin et al., 2007a). Evidence of this is common in the walls of the retrocalcaneal bursa of elderly individuals (Rufai et al., 1995). It should be noted that as the foot is dorsiflexed, the Achilles tendon presses against the tuberosity, so that the insertional angle of the tendon is not altered with further dorsiflexion.

In generalising from the specific features of the Achilles tendon enthesis organ to concepts which apply elsewhere in the body, it is important to recognise that TL often attach to bone near tuberosities or are sunken into pits. The former are exemplified by the insertion of biceps brachii and the patellar tendon, and the latter by the attachment of the tendon of popliteus and the collateral ligaments of the interphalangeal joints. Wherever a TL sinks into a pit at its attachment, the adjacent bone surface is higher and can thus act as a pulley, dissipating stress away from the attachment site itself (Benjamin et al., 2006).

Adipose Tissue at Entheses

The presence of adipose tissue at other entheses is also common. However, its significance is often misinterpreted and many authors merely equate it with TL degeneration (Jozsa and Kannus, 1997). Although Benjamin et al. (2004b) agree that fat in TL may be pathological,

they argue for a variety of normal functions of fat at or near entheses. They have shown that adipose tissue is present not only at the insertional angle of many entheses, but also in the epitendon and endotenon near the attachment site (Benjamin et al., 2004b). Endotenon fat is particularly characteristic of certain entheses where the TL flares out (e.g. peroneus longus insertion and the tibial attachment of the ACL) and may thus contribute as a space filler and/or promote the independent movement of fascicles (Benjamin et al., 2004b). In light of these observations it is clear that the presence of adipose tissue at entheses needs further investigation. This study will therefore also describe the structure of the retromalleolar fat pad associated with the Achilles tendon enthesis.

1.1.3. ENTHESOPATHIES

Despite the adaptations which occur at entheses for preventing wear and tear, they are still prone to pathological changes, overuse injuries in particular are common. They are best termed ‘enthesopathies’ (a term which embraces both tendons and ligaments), but have also been called ‘enthesiopathies’, ‘insertional tendinopathies’ or ‘insertional tendinoses’ – though the last two can only be applied to tendons. It should be noted that some authors use a more general pathological term, which applies to a whole tendon or ligament, when discussing enthesopathies. ‘Achillodynia’ (painful Achilles) for example, covers the whole spectrum of Achilles tendon problems and may disguise the fact that an author is at least partly considering enthesopathies. The term ‘enthesitis’ may be appropriate for some enthesopathies (particularly in patients with spondyloarthropathies (Francois et al., 2001), but carries with it the implication that the attachment site is inflamed. The reader should note therefore that the current consensus view is that most overuse injuries at entheses are degenerative rather than inflammatory (Khan et al., 1999a; Lemont et al., 2003). Where inflammation does occur, it may be a secondary change related to tissue repair (Khan et al., 1999a).

Enthesopathies can affect a wide variety of different TL and among the most common are the Achilles tendon, patellar tendon (both ends), quadriceps tendon, supraspinatus, and the common extensor and flexor tendons of the forearm (Khan et al., 1999a). The aetiology of

enthesopathies is often unclear, though as with tendinopathies in general, both intrinsic and extrinsic factors are involved. Maganaris et al. (2004) have made the interesting suggestion that parts of entheses may be stress-shielded, so that when increased loading occurs, that particular region of the attachment site is unable to adapt sufficiently. They point out that the stress-shielded site is often subject to greater compressive (rather than tensile) loading than the rest of the enthesis. Such regions are characterised by fibrocartilage (Benjamin and Ralphs, 1998) – a tissue which can show a variety of pathological changes at the certain entheses – e.g. that of the Achilles tendon (Rufai et al., 1995). Maganaris et al (2004) have thus argued that some enthesopathies that are traditionally viewed as overuse injuries could be better viewed as ‘underuse injuries’ – a contention that has also been applied more broadly to other musculoskeletal injuries in athletes (Stovitz and Johnson, 2006). Maganaris et al (2004) suggest that tensile loading at entheses is non-uniform and it is the less heavily loaded regions that are most vulnerable. Commonly, these are on the joint side of an attachment site – e.g. in rotator cuff problems, jumper’s knee and Achilles insertional disorders (Maganaris et al., 2004). Certainly, so-called ‘fibrocartilaginous entheses’ are of non-uniform composition and are purely fibrous in some parts of the enthesis (Benjamin et al., 1986; Woo and Buckwalter, 1988). This is likely to reflect regional differences in tensile loading. It must be remembered however that an increase in compressive/tensile loading in what is regarded as a ‘stress-shielded’ site of an enthesis, may lead to degenerative changes which parallel those in osteoarthritic articular cartilage. These may contribute to the histopathological basis of overuse injuries. It should also be noted that Toumi et al (2006) highlight regional differences in trabecular architecture at the patellar enthesis of the patellar tendon. Their results suggest that the medial region is subject to greater tensile loading than the lateral – yet it is the medial part of the enthesis that is most typically associated with jumper’s knee.

Finally, it is important to remember that other components of an enthesis organ may be subject to pathological change in addition to the enthesis itself. Thus, degenerative changes have been documented in the periosteal and sesamoid fibrocartilages of the Achilles tendon enthesis organ, in addition to the attachment site (Rufai et al., 1995). These changes include fissuring, fragmentation, partial delamination, cell clustering and calcification.

They serve as a reminder that the clinical symptoms of an enthesopathy need not necessarily affect only the enthesis (Rufai et al., 1995).

Iliotibial Band (ITB) Syndrome

Iliotibial band (ITB) syndrome is characterised by pain and tenderness over the lateral epicondyle of the femur, particularly at 30° of flexion. The band itself is a lateral thickening of the dense fibrous connective tissue of the fascia lata of the thigh which attaches to Gerdy's tubercle on the anterolateral aspect of the tibia after passing over the lateral femoral epicondyle. ITB syndrome is a well recognised overuse injury common in runners and cyclists but has also been noted in other sports including skiing and weightlifting. It is traditionally believed that the condition is caused by repetitive friction between the ITB and the lateral epicondyle of the femur, when the band 'rolls over' it during knee movement. However, recent investigation into this condition by Fairclough et al., (2006, 2007) has brought to light novel anatomical information which has not previously been recognised. They contest that the ITB does not actually move in an anterior-posterior direction, this is an illusion created but the sequential shifting of tensile load from the anterior fibres of the ITB to the posterior fibres during knee flexion. They also demonstrate the presence of fibrous strands anchoring the ITB to the distal part of the femur, penetrating the periosteum and the presence of adipose tissue between the band and the lateral epicondyle, therefore resembling a bony enthesis (as above). In addition to these histological findings, MRI data has demonstrated that the ITB moves in a medial to lateral direction during knee flexion i.e. a change in the insertional angle of the attachment. The correlations between this structure and entheses suggest that ITB syndrome could be classified as an enthesopathy (Fairclough et al., 2006, 2007).

Bony Spurs (Enthesophytes)

Particular mention is made of bony spurs (enthesophytes) as they are commonly found in athletes – especially at the attachment of the Achilles tendon, common extensor origin and plantar fascia. Some spurs may exceed 1 cm in length (Maffulli et al., 2004), but some may not be symptomatic (Williams, 1987). However, they may be associated histologically with evidence of degenerative change elsewhere at the enthesis (Rufai et al.,

1995). We would raise the possibility that spur formation is not necessarily pathological. Some spurs may represent an adaptive mechanism to increase the surface area of contact between tendon and bone at an enthesis and thus maintain the tendon-bone unit at maximum efficiency, in the face of increased mechanical loading (Galtes et al., 2006). Perhaps this is why some bony spurs re-form after they have been surgically removed?

An enthesophyte must be distinguished from what is simply a region of soft tissue calcification that has developed at an enthesis. The term implies specifically that ossification has extended from the bone into the TL at the attachment site, whereas soft tissue calcification merely means the deposition of calcium salts. It is commonly reported in tendons as calcifying tendonitis or tendinopathy (Uthoff et al., 1976). Calcification obviously accompanies ossification, but can occur in its absence and this is a point of common confusion among those new to the field. The distinction between soft tissue calcification at an enthesis and bony spur formation can easily be made in histological sections, but may also be made radiologically (Rufai et al., 1995). The molecular pathways which leads to spur formation, have not yet been clearly elucidated, though it has recently been suggested that loss of *noggin* - an antagonist of bone morphogenic protein (BMP) expression, can induce ectopic bone formation in ankylosis (Lories et al., 2006).

Seronegative Spondyloarthropathies (SpA)

The spondyloarthropathies are a collection of related inflammatory disorders, including ankylosing spondylitis, reactive arthritis, psoriatic arthritis (PsA), undifferentiated spondyloarthropathy and inflammatory bowel-disease associated arthritis. Inflammation at entheses - 'enthesitis' – is a characteristic feature of this collection of diseases and has been demonstrated (with the use of MR imaging) to be a unifying feature between them (Benjamin and McGonagle, 2001). Inflammation of other parts of the body including joints and some non-articular structures such as the skin, eye, gut and aortic valve also occur in these conditions. Although, many groups have studied these diseases, the aetiology of SpA is still widely debated. Some suggest there is a microbial background to the condition which induces an immune-mediated pathogenesis; however, no organisms have been cultured successfully from joints inflamed by SpA (McGonagle et al., 2002).

There has also been determined a strong genetic contribution to SpA with HLA-B27, (human leukocyte antigen B27) an allele of the major histocompatibility complex (MHC). However, there is a degree of variation in its involvement between different forms of SpA and this is also demonstrated to differ greatly between ethnic groups. Therefore testing for HLA-B27 is not considered clinically helpful, as SpA can occur without the presence of the allele (as reviewed by - Khan, 2002b). It has also been proposed that the breakdown of aggrecan and type II collagen molecules of the fibrocartilaginous enthesis - in response to mechanical loading - may initiate an autoimmune response to these molecules in a similar manner to animal models, injected with aggrecan or versican (as reviewed by - Zhang et al., 2002). However, Benjamin and McGonagle (2001) proposed that the diverse localisation of lesions identified in SpA may be related to the high levels of mechanical stress experienced at these various anatomical sites, resulting in large amounts of tissue microtrauma leading to the liberation of inflammatory factors, and deposition of microbes at the site in response to healing. These co-stimulatory factors in susceptible individuals with the HLA-B27 gene, may all contribute to the formation of the lesion and development of the disease (McGonagle and Emery, 2000).

1.2. TENDON

MACROSCOPIC STRUCTURE

Tendons are dense regular connective tissue structures which serve to transmit the force generated by muscle to bone to facilitate joint movement. However, the biology and structural anatomy of the tendon allows it to perform a number of other functions associated with this principal role of joint movement (as reviewed by - Benjamin and Ralphs, 1997): (a) Long tendons allow the muscle to work at a distance from its site of insertion such as in the hand or foot. This arrangement prevents the bulk of the muscle compromising dextrous movements. Furthermore, en route to their site of action tendons are able to (b) wrap around fibrous or bony pulleys, therefore permitting a change in the direction of muscle pull and (c) pass through confined spaces. In these locations, tendons are usually surrounded by specialised synovial tendon sheaths, which consist of two layers, which are filled with synovial fluid to reduce friction during movement (Lovell and

Tanner, 1908). In addition, tendons are able to support synovial joints such as those in the finger or knee by forming part of the joint capsule. There is a whole host of anatomical variations among tendons. Structurally, tendons can form broad, flat aponeuroses to oval, or round thin, cord-like structures. Furthermore, numerous tendons can arise from a single muscle to distribute the force exerted from the muscle. In some cases such, as the extensors of the hand, tendinous slips, known as juncturae tendinum, are present to connect these adjacent tendons together – although there is a large variation in their shape and occurrence between individuals (von Schroeder et al., 1990). Functionally, juncturae tendinum are believed to further distribute muscle force, but also ensure coupled movement of the fingers (von Schroeder and Botte, 1993).

Although, most tendons experience tensional forces in regions where the tendon passes around bony pulleys, the tendon is also subjected to compressional and frictional forces. In these regions it has been well documented that fibrocartilage formation occurs which allows the tissue to resist compressive stress (Benjamin et al., 1995; Vogel and Koob, 1989).

MICROSCOPIC STRUCTURE

In the adult, the midsubstance of a tendon is composed of a collagenous ECM and a relatively small number of tendon fibroblasts. The collagenous ECM primarily contains type I collagen fibre bundles that lie in a parallel organisation to form a dense regular connective tissue synthesised by the resident tendon fibroblasts, which lie in parallel rows between the bundles of collagen fibres (Fig 1.7.A) (Kannus, 2000; Stevens and Lowe, 2001). When examined in cross section, the inactive tendon fibroblasts have a spindle, or stellate appearance and possess long thin, cell processes that allow adjacent cells to interact with one another (Fig 1.7.B)(McNeilly et al., 1996). At these sites of cell interactions, cell-cell junctions are located which are understood to allow communication between cells, and can therefore allow the cells to act as an integrated cell population (McNeilly et al., 1996). However, they have also been shown to have an important role in early development of the tendon from mesenchymal condensations (Fish, 2006).

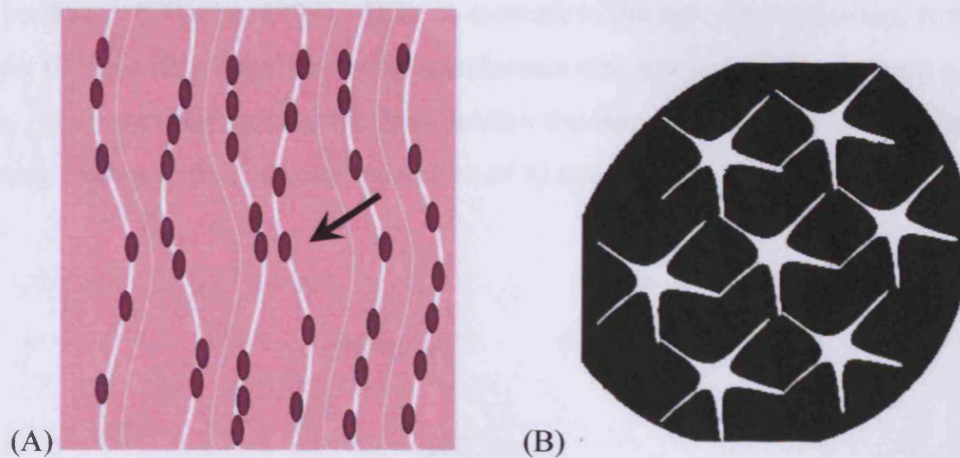


Figure 1.7: (A) Schematic representation of a longitudinal section through an adult tendon. Arrow indicates longitudinally running tendon fibroblasts and their characteristic elongated nuclei (Stevens and Lowe, 2001). (B) Schematic representation of a cross section through an adult tendon. Stellate shaped tendon fibroblasts (white) send out elongated lateral processes to form a cell network within the highly collagenous tissue (black)(McNeilly et al., 1996).

Tendons are made up of an ascending hierarchy of collagen bundles that generates an organised fascicular structure (Fig 1.8). Several collagen molecules combine to form a microfibril, which when combined with 4 or more other microfibrils forms a fibril. When several fibrils combine, these are known as fibres. The fibres run the entire length of the tendon and are arranged along the long axis of the tendon (Kannus, 2000). Scanning electron microscopy (SEM) has demonstrated that the collagen fibres do not always lie in a parallel fashion, some fibres crossing over each other and form pleats. This 3D structure provides the tissue with a greater ability to withstand transverse and rotational forces which are frequently experienced by tendons (Jozsa et al., 1991; Jozsa and Kannus, 1997). A collection of fibres (primary and secondary fibre bundles), surrounded by endotenon, is known as a fascicle. Endotenon is a loose reticular network of connective tissue that facilitates movement of the fascicles and provides a supportive passage for neurovascular bundles and lymphatics to run deep into the tendon (Edwards, 1946). A group of fascicles, constituting the tendon proper, is enclosed by the epitenon which is structurally similar to the endotenon with a characteristic criss-cross pattern of crimped collagen fibres that act to dissipate stress between the fascicles and hold them together (Rowe, 1985). Covering this

is the paratenon (O'Brien, 1997). This, in contrast to the epi- and endotenon, contains fine collagen fibrils within a series of thin membranes that run parallel to the long axis of the tendon. The paratenon reduces friction between the tendon and surrounding tissue, thereby enhancing tendon gliding, through secretion of synovial fluid from its inner surface (Rowe, 1985).

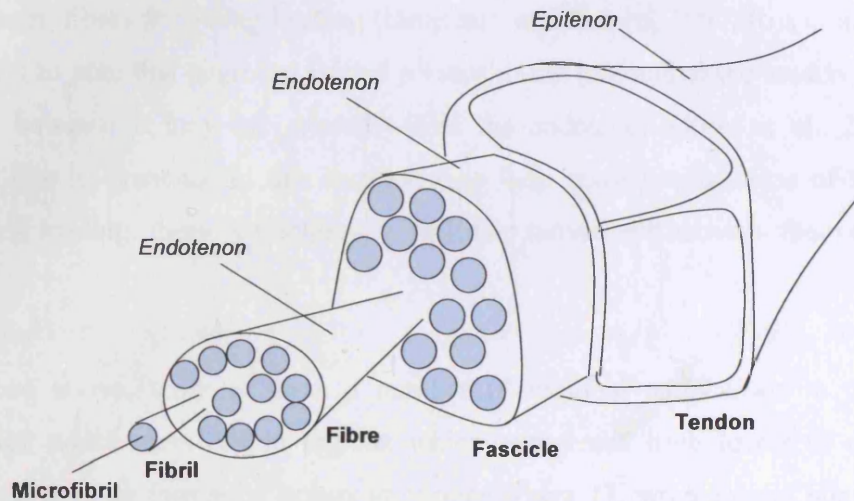


Figure 1.8: Simplified schematic drawing of the ascending hierarchical structure of the Achilles tendon (Modified from - Kannus, 2000).

MOLECULAR STRUCTURE

In addition to type I (and III collagen), which provide the tendon with high tensile strength, collagen types V and VI are also present in small quantities within tendons (Carvalho et al., 2006; Vogel and Meyers, 1999; Waggett et al., 1998). These fibrillar collagens are associated with type I collagen molecules and regulate fibril diameter and ECM organisation within the tendon (Birk et al., 1990; Birk and Mayne, 1997; Bonaldo et al., 1990). Furthermore, the small-leucine rich proteoglycans (SLRPs) decorin, fibromodulin, and lumican are present in the tendon midsubstance (Svensson et al., 1999; Waggett et al., 1998). Decorin is understood to play an important role in controlling fibril orientation and deposition during tendon development (Scott, 1996) as are the other aforementioned SLRPs (Svensson et al., 1999), although at different developmental periods (Ezura et al., 2000). Biglycan, another SLRP, was also identified in the tendon midsubstance (Vogel and Meyers, 1999; Waggett et al., 1998). The function of biglycan is however less well

understood. It is suggested that biglycan may have a role in binding transforming growth factor (TGF) – β which may result in upregulation of aggrecan expression and fibrocartilage formation under conditions of compression (Robbins et al., 1997). Although tendons are known to have limited elastic ability, elastic fibres are present within the tendon. These fibres are understood to play an important role in restoring the natural crimp to the collagen fibres following loading (Benjamin and Ralphs, 1997; Ros et al., 1995). It is interesting to note that aggrecan is also present in the mid-substance tendon (Waggett et al., 1998); however it may be isolated within the endotenon (Rees et al., 2007). It is speculated that its presence in this location may help resist compression of the collagen fibres during loading, therefore helping to facilitate movement between them (Rees et al., 2007).

As described above, tendons show a number of regional adaptations in the form of fibrocartilage which develops in regions which experience high levels of compressive stress. Fibrocartilage formation occurs at regions where TL wrap around bony or fibrous pulleys, in addition to bony attachment sites. These wrap-around regions have also been termed ‘functional entheses’ by (Benjamin and McGonagle, 2001), due to their structural and functional similarities to true entheses. Fibrocartilage in tendon wrap around regions, like entheses, is characterised by metaplasia of tendon fibroblasts into rounded, fibrocartilage-cells, resulting in the expression of type II collagen, and the up-regulation of aggrecan in addition to the normal ECM molecules described above in tendon due to their metaplastic origin (Vogel, 2004; Vogel et al., 1986; Vogel and Koob, 1989). Aggrecan and type II collagen molecules work together to form a stable compression resistant matrix, which will prevent excess wear and tear to the region during skeletal movement in a similar manner to articular cartilage (Buckwalter and Mankin, 1998). Under conditions of pathology or repair, the midsubstance of the Achilles tendon can also contain fibrocartilage formations which are able to ossify into bony nodules (Rooney et al., 1993).

VASCULARISATION

Tendons receive their blood supply from the vessels that surround them and provide the peri- and intra-tendinous tissue with a network of blood vessels (Ahmed et al., 1998; Zantop et al., 2003). These vessels are organised in a uniform fashion throughout the

tissue, via a series of longitudinal channels running within the endotenon, with transverse anastomoses linking the longitudinally running vessels at regular intervals. Capillaries branch from these arterial beds within the endotenon but have not been shown to penetrate the collagen bundles (Edwards, 1946). The tissue itself is therefore considered to be a relatively avascular structure primarily due to the low metabolic requirements of a predominately extracellular tissue. Pathologically, tendon vascularisation has been a source of debate. Numerous studies have described regions in certain tendons (such as the human Achilles tendon) which have particularly low levels of vascularisation. These regions are prone to degenerative changes and subsequent rupture (Peacock, 1959); however variations between studies have provided no conclusive proof that hypovascularisation of these regions is the primary cause of these changes (as reviewed by - Theobald et al., 2005). In contrast, hypervascularisation is frequently observed in pathology (Astrom and Rausing, 1995); however its role in healing is unclear (as reviewed by Fenwick et al., 2002).

Regions of fibrocartilage in tendon are particularly avascular (Kraus et al., 1995; Tillmann and Koch, 1995). Studies have demonstrated that blood vessel formation (angiogenesis) is inhibited in avascular tissues through one of two ways: either expression of inhibitory factors, or the intrinsic insufficiency of resident cells to express stimulatory peptides. It has recently been reported that VEGF (vascular endothelial growth factor), which promotes angiogenesis, is present in the developing tendon until the induction of intrauterine movement. However, in regions which are designated to become fibrocartilaginous (and avascular), VEGF is continually absent, suggesting that these cells are incapable of expressing such stimulatory peptides, therefore preventing its vascularisation (Petersen et al., 2002). Within the adult tendon VEGF is down-regulated, so it is possible that the continued absence of the blood vessels within adult fibrocartilage is maintained by inhibitory peptides. Pufe et al., (2003) therefore tested the role of endostatin, a potent inhibitor of endothelial proliferation and therefore angiogenesis. High levels of endostatin were subsequently determined in the developing tendon. Why both stimulatory and inhibitory factors are present in the developing tendon is unknown, although it is postulated that, inhibitory factors may either play a role to inhibit vascular overgrowth in the

developing tendon which may be the result of high levels of VEGF (Petersen et al., 2002; Pufe et al., 2003).

Fibrocartilage formation in tendon is induced by shear and compressive forces (Vogel and Koob, 1989), as a result, it is suggested that the expression of VEGF and endostatin are mechanically regulated. This hypothesis was tested with rat tendon fibroblasts exposed to intermittent hydrostatic pressure in vitro (Petersen et al., 2002). Levels of VEGF are increased under continuous mechanical loading and this can be considered to have both favourable, by increasing regenerative potential, and unfavourable effects, by weakening the tissue through endothelial growth (Petersen et al., 2004). Within adult tissues, levels of endostatin were retained in fibrocartilage wrap around regions, but down-regulated in normal tendon, suggesting that the expression of endostatin is essential in retaining the avascular nature of this tissue. It was also demonstrated that mechanical factors such as compression and shear, the same factors which induce the formation of fibrocartilage in tendon, regulate the expression of secreted factors which act as inhibitors to angiogenesis (Pufe et al., 2003). The same principle of angiogenesis inhibition could therefore be applied to fibrocartilage of the Achilles tendon insertion. More recently another inhibitor of angiogenesis has been discovered in tendons and ligaments. It is a novel type II transmembrane protein, named tenomodulin (TeM) which has a domain homologous to the cartilage specific angiogenic inhibitor chondromodulin I (ChM-I) (Shukunami et al., 2005).

INNERVATION

Tendon innervation was first studied by Stilwell (1957), who described that these structures are innervated primarily by nerve fibres from surrounding structures. More recently Ackermann et al., (2001) described the innervation of the mid-substance of the rat Achilles tendon in detail. This latter study established that the tendon itself has a relatively poor nerve supply, and like its vascularisation, the majority of nerve fibres are present within the supportive connective tissues (i.e. the paratenon and endotenon). These nerve fibres were described as either “free” nerve endings or blood vessel associated. The vessel-associated nerve fibres were identified as autonomic by the presence of the neurotransmitters, neuropeptide Y (NPY) and noradrenaline (NA) - which have

vasoconstrictive properties, and vasoactive intestinal peptide (VIP) - a vasodilatory factor. These autonomic fibres are therefore believed to play a major role in the regulation of blood flow within the Achilles tendon (Ackermann, 2001). The “free” nerve fibres within the endotenon contained the neuropeptides SP and CGRP indicating that they collect sensory and nociceptive information and conduct this information to the CNS (Ackermann, 2001). A similar study has also been carried out in man by Bjur et al., (2005). It was found that the human Achilles tendon is also primarily supplied by sensory nerves travelling within the connective tissue sheaths of the tendon (Bjur et al., 2005). By comparing the innervation of the Achilles tendon and a number of ligaments, Ackermann (1999) identified that there was a predominance of SP and CGRP in the Achilles tendon over the tested ligaments. It is hypothesized that this difference may reflect different levels of vulnerability to repetitive mechanical loading between the two dense fibrous connective tissue structures (Ackermann et al., 1999). Several opioids (pain modulating neuropeptides) have also been identified within the peritendinous tissue of the Achilles tendon. It can therefore be assumed that the Achilles tendon may have an inherent, active system that may be used to reduce signalling from nociceptive nerve fibres (Ackermann, 2001).

A study into exercise-induced Achilles tendon disorders in the rat (which resemble that of tendinosis or paratendinosis in man), showed an increase in the number of nerve fibres and hypervascularisation in the tendon. The increased numbers of nerve fibres may therefore indicate where pain associated with these conditions originates from (Messner et al., 1999). A similar increase in nerve fibres in tendonosis has also been identified in man (Schubert et al., 2005).

1.4 SUMMARY OF THE OVERALL AIMS OF THE THESIS

1. Due to the potential importance of enthesial innervation in health and disease, this thesis aims to describe the innervation of the 3 different types of entheses:

- ❖ The rat Achilles tendon enthesis organ and changes in its structure and innervation with the age of the animal from neonate to 24 months of age.

- ❖ The fibrous enthesis of the medial collateral ligament in the rat.
- ❖ The muscular enthesis of tibialis anterior in the rat.

In addition, the structure and innervation of the proximal attachment of the suspensory ligament in the equine hindlimb is described in normal and pathological samples.

2. In light of the recent interest in adipose tissue at entheses, the retromalleolar fat pad associated with the Achilles tendon enthesis organ will also be studied in detail, including:

- ❖ Routine structure of the fat pad and changes with the age of the rat.
- ❖ The ultrastructure of the fat pad in the rat.
- ❖ The presence of macrophages and inflammatory cells in the fat pad and changes in their number and distribution with the age of the rat.
- ❖ The effect of appetite inducing hormones on the size of the fat pad in the rat.
- ❖ Anatomical variations and the effect of weight on the size of the fat pad in cadaveric specimens.
- ❖ The development of the fat pad in the human foetus.

3. Finally, this study aims to understand the mechanisms controlling the innervation of the rat Achilles tendon enthesis organ in the adult and newborn rat with the use of a competitive *in vitro* nerve growth study.

NOTE

This Chapter forms the basis of a review article published in the Scandinavian Journal of Medicine and Science in Sports. See page 308.

2. GENERAL MATERIALS AND METHODS

2.1. ROUTINE HISTOLOGY

Fixation and Paraffin Embedding

Specimens were fixed in 10% neutral buffered formalin solution or 4% paraformaldehyde in 0.1M phosphate buffer (PB) (see appendix I) for 1 week and decalcified in 5% nitric acid or 10% ethylenediaminetetraacetic acid (EDTA) disodium salt solution (see appendix I). Samples were subsequently washed in 0.1M PB (see appendix I) and dehydrated in graded alcohols (70%, 95%, and 100% with two changes of 20 minutes each), cleared in xylene (two changes of 20 minutes) and embedded in 58°C paraffin wax.

Sectioning

Following paraffin embedding, serial sagittal sections were cut at 8µm throughout each block on a Leitz microtome (Leitz, Wetzlar, Germany). Sections were collected from a water bath (45-50°C; RA Lamb Medical Supplies, Eastbourne, UK) and mounted on glass slides (RA Lamb Medical Supplies, Eastbourne, UK). The slides were air dried for approximately 1h on a heated rack and dried overnight in an incubator (B and T, Unitemp, High Wycombe, UK) at 45°C.

Staining

Sections were dewaxed in xylene (two changes of 5 minutes), and re-hydrated in a descending series of alcohols: two changes of 100% - 2 minutes each, one change of 95% and 70% (2 minutes each) and subsequently washed in running tap water. The sections were stained with toluidine blue, Haematoxylin and Eosin (H & E), Masson's trichrome, or van Gieson's elastic stain (see appendix I). Following staining (except toluidine blue), sections were dehydrated in graded alcohols (one change of 95% for 1 minute, two changes of 100% - 2 minutes each), cleared in xylene (two changes of 5 minutes each; see appendix I). Sections were then mounted under coverslips using DPX (Distyrene, Plasticizer, and Xylene - RA Lamb Medical Supplies, Eastbourne, UK). Slides stained with toluidine blue were, air dried, cleared in xylene (two changes of 5 minutes) and mounted under coverslips using DPX.

Microscopy

Slides were viewed with a Leitz DMRB Leica (Leitz, Wetzlar, Germany) light microscope and images captured using either a 3-CCD color video camera (JVC KY-F55B; JVC Wayne, NY), or moticam 2000 (Motic China Group Co Ltd.) and subsequently processed digitally using Adobe Photoshop (version 6).

2.2. IMMUNOHISTOCHEMISTRY

Sectioning

Following fixation, specimens were soaked in 10% sucrose solution in 0.1M PB (see appendix I) overnight at 4°C prior to cryosectioning. This reduces damage caused by ice crystals within the tissue during freezing. Material was frozen at -80°C in Serotec cryoprotectant (RA Lamb, Eastbourne, UK) onto a cryostat chuck. Sections were cut at 12µm on a cryostat (Bright OFT 5000, Huntingdon, UK) collected on Histobond microscope slides (RA Lamb Medical Supplies, Eastbourne, UK) and stored at -20°C for subsequent immunolabelling.

2.2.1. Immunofluorescence

Indirect immunofluorescence was carried out in a light-proof, humidified chamber. Slides were removed from the freezer and allowed to adjust to ambient room temperature. A ring was drawn around the specimens with a waterproof pen (Zymed® Laboratories, San Francisco, US) to retain solutions on the slide. The samples were re-hydrated in 0.1M PB containing 0.1% Triton X (Sigma-Aldrich Company Ltd, Gillingham, UK; see appendix I), a wetting agent which increases permeability of the antibody. Twenty percent normal goat or swine serum (Dako UK, Ely, Cambridgeshire, UK) - appropriate to the species in which the secondary antibody was raised - was then applied to the sections for 1h. The blocking serum binds epitopes within the tissue to which the secondary antibody may bind non-specifically. The blocking serum was gently poured off the slide and the primary antibodies applied (see Table 2.1) directly without washing. The antibody-treated sections were incubated in the dark overnight at 4°C. Following incubation, the slides were washed 3 times for 5min in 0.1M PB. The sections (except those labelled directly for actin) were incubated for 1h with the secondary antibody swine anti-rabbit FITC (Dako UK, Ely, Cambridgeshire, UK) or goat anti-mouse FITC (Dako UK, Ely, Cambridgeshire, UK) following pre-incubation with 1% normal rat serum (Invitrogen, Paisley, UK) for 1h at 4°C. Following several washes the slides were mounted under a 22mm x 50mm coverslips (RA

Lamb Medical Supplies, Eastbourne, UK) using Vectorshield containing DAPI (Vector Labs, Peterborough, UK).

Controls

The Achilles tendon acted as a positive internal control for the actin, vinculin, N-cadherin antibodies (Ralphs et al., 2002), and the base of the rat bladder was used as a positive control for the neuronal antibodies (Khan et al., 1999b; Wakabayashi et al., 1998; Yokokawa et al., 1985; Yokokawa et al., 1986). Negative control sections were incubated with 0.1M PB, Mouse Immunoglobulins(IgG1; Dako, Cambridgeshire, UK), Mouse IgG2a (Dako, Cambridgeshire, UK), or non-immune rabbit IgGs (Dako, Cambridgeshire, UK) in place of the primary antibody.

Microscopy

Sections were examined by epifluorescence microscopy using either an Olympus BX-61 (Olympus UK Ltd, London, UK) captured using AnalySIS or AxioVision software using a Leitz DMRB (Leica Microsystems Ltd; Milton Keynes, UK), and processed using Adobe Photoshop (Version 6) or AxioVision LE Application Rel. 4.2.

2.2.2. Peroxidase Labelling

Peroxidase labelling was carried out as above in a light-proof, humidified chamber. The slides were allowed to adjust to room temperature, and a waterproof ring was drawn around the specimens. Sections were rehydrated with 0.1M PB and where necessary, antigen-retrieval procedures were performed (Table 2.1). Endogenous peroxidase activity was blocked with 3% hydrogen peroxide in distilled H₂O for 10min. Following washing, 20% normal goat or horse serum (Dako UK, Ely, Cambridgeshire, UK) - appropriate to the species in which the secondary antibody was raised - diluted in 0.1M PB Triton X, was applied to the sections for 1h. Sections were then incubated overnight at 4°C with primary antibodies (Table 2.1) diluted with 0.1M PB Triton X. Following washing, either horse anti-mouse, or goat anti-rabbit biotinylated secondary antibody (Table 2.2) was applied for 1h at room temperature (following pre-incubation with 1% normal rat serum for 1h at 4°C). An avidin-biotin complex (Vector Labs, Peterborough, UK) was then applied for 30min, following further washes in 0.1M PB. Sections were washed yet again and developed either with NovaRED or 3,3'-Diaminobenzidine (DAB) substrate kits (Vector Laboratories, Peterborough, UK). Slides were subsequently immersed in filtered Mayer's Haematoxylin

(RA Lamb) for 15s and washed for 10min until blue. The slides were then de-hydrated in graded alcohols (see appendix I), cleared in xylene and mounted in DPX.

Controls

The greater omentum of 4 month rats was used as a positive control for CD68, and myeloid related protein 14 antibodies (Biewenga et al., 1995; Lagasse and Weissman, 1992). Negative control sections were incubated with 0.1M PB, Rabbit IgGs, Mouse IgG1 (Dako, Cambridgeshire, UK), or Mouse IgG2a (Dako, Cambridgeshire, UK) in place of the primary antibody.

Microscopy

Slides were viewed with a Leitz DMRB Leica (Leitz, Wetzlar, Germany) light microscope and images captured using either a 3-CCD color video camera (JVC KY-F55B; JVC Wayne, NY), or moticam 2000 (Motic China Group Co Ltd.) and subsequently processed using Adobe Photoshop (version 6).

Primary Antibody	M/P	Un-masking treatment	Dilution/Concentration	Source	Reference	
Rabbit anti-9.5	PGP	P	None	1:400	Ultraclone, Isle of Wight, UK.	(Doran et al., 1983)
Rabbit anti-substance P	P	P	None	1:2000	Biomol, Exeter, UK	(Hoyle et al., 1998)
Rabbit anti-calcitonin gene related peptide (ARP296/1)	P	P	None	1:500	Biomol Exeter, UK	(Hoyle et al., 1998)
Rabbit anti-neurofilament 200	P	P	None	1:2000	Sigma-Aldrich, Gillingham, UK	(Lawlor et al., 1999)
Mouse anti-hVin1 (binds to vinculin)	M	M	None	10µg/ml	Gift from Dr. J Ralphs (Sigma - Aldrich, Gillingham, UK)	(Goncharova et al., 1992)
Mouse anti-ACAM (binds to N-cadherin)	M	M	None	10µg/ml	Gift from Dr J. Ralphs (Sigma - Aldrich, Gillingham, UK)	(Volk and Geiger, 1984)
Alexa-488 conjugated phalloidin (for filamentous actin)	N/A	N/A	None	1U/ml	Gift from Dr J. Ralphs (Molecular Probes; Invitrogen, Paisley, UK)	
Mouse anti-CXN32 (for connexin 32)	M	M	None	10µg/ml	Gift from Dr J. Ralphs (Chemicon, Millipore, Chancellors Ford, Hampshire, UK)	(Goodenough et al., 1988)
Mouse anti-COL-1 (for collagen I)	M	M	1.5U/ml Hyaluronidase 30min at 37°C	1:2000	Gift from Prof. C Archer (Sigma-Aldrich, Gillingham, UK)	(Mayne, 1988)
Mouse anti-CD68 (macrophage marker for lysosome-associated antigens)	M	M	None	1:400	AbD Serotec, Oxford, UK	(Damoiseaux et al., 1994)
Mouse anti-S100A9 (IC10) - for myeloid-related protein 14 (monocyte and local inflammation marker)	M	M	None	1:200	Abnova; Stratech, Newmarket, UK	-
Mouse anti-BrdU	M	M	2N HCl (30 min) and 0.25% trypsin (20 min) at 37°C	1:500	Sigma-Aldrich, Gillingham, UK	(Gratzner, 1982)
Rabbit IgG Normal Fraction. Negative control	N/A	N/A	None	5µg/ml	Dako, Ely, Cambridgeshire, UK	
Mouse IgG1 Negative control	N/A	N/A	None	5µg/ml	Dako, Ely, Cambridgeshire, UK	
Mouse IgG2a Negative control	N/A	N/A	None	5µg/ml	Dako, Ely, Cambridgeshire, UK	

Table 2.1: Primary antibodies used to detect nerves, extracellular matrix components and inflammatory cells. Negative control sera are also included in this table. M - Monoclonal, P - Polyclonal, N/A - Non-applicable.

Secondary Antibodies	Dilution	Source
Swine anti- Rabbit FITC	10 μ l/ml	Dako UK, Ely, Cambridgeshire, UK
Goat anti-mouse FITC	10 μ l/ml	Dako UK, Ely, Cambridgeshire, UK
Horse anti-mouse biotinylated secondary antibody	5 μ l/ml	Vector Labs, Peterborough, UK
Goat anti-rabbit biotinylated secondary antibody	5 μ l/ml	Vector Labs, Peterborough, UK

Table 2.2: Secondary antibodies used to detect primary antibodies.

3. INNERVATION OF THE RAT ACHILLES TENDON ENTHESIS ORGAN

3.1. INTRODUCTION

Despite common textbook/review statements that entheses are highly innervated (Benjamin and McGonagle, 2001; Benjamin and Ralphs, 1997; Khan et al., 2000; Klippel and Diepp, 1998; Niepel et al., 1966; Palesy, 1997; Resnick and Niwayama, 1983), there are no original research articles which deal extensively with the nerve supply of tendon/ligament or muscle attachment sites. It is therefore the aim of this study to describe the innervation of the Achilles tendon enthesis organ in the rat with the use of immunofluorescence.

The attachment of the Achilles tendon has been described as the “premiere enthesis”, due to its highly differentiated character – which in turn relates to the high levels of mechanical loading to which it is subject (Canoso, 1998). As in man, the rat Achilles tendon enthesis organ is composed of three fibrocartilages (the enthesis, sesamoid and periosteal fibrocartilages), a fluid-filled bursa between the superior tuberosity of the calcaneus and the tendon, and a retromalleolar fat pad protruding into the bursa (Rufai et al., 1992; Rufai et al., 1996). These structures work together, to dissipate stress away from the attachment of the tendon to bone. The purpose of the current study therefore, is not simply focus on the sensory innervation of the enthesis itself, but to consider the entire enthesis organ.

Brief Review

Anatomy of the Rat Achilles Tendon

The rat Achilles tendon is formed from the conjoined tendons of triceps surae which consists of the muscles gastrocnemius and soleus. M. gastrocnemius is bipennate with two heads, lateral and medial. The lateral head originates from the head of the fibula and the lateral epicondyle (external condylar ridge) of the femur, while the medial head of gastrocnemius arises from the medial epicondyle (internal condylar ridge) of the femur (Greene, 1935). Within the muscular origins of gastrocnemius is a small sesamoid bone named the fabella which have well defined articular surfaces that develop just proximal to the condyles of the femur. Fabellae are variably present in man and are often associated with posterolateral knee pain (Chihlas et al., 1993; Robertson et al., 2004). The aponeurotic tendon of gastrocnemius inserts into the posterior part of the tuber calcaneus as part of the common calcaneal or Achilles tendon, acting on this to plantarflex the ankle

joint. In contrast, the unipennate muscle soleus arises via a long, slender tendon from the head of the fibula and inserts onto the calcaneus by merging with the tendon of gastrocnemius (Greene, 1935; Hebel and Stromberg, 1986).

In the rat, plantaris originates from the lateral epicondyle of the femur, the lateral fabella of gastrocnemius, and the medial border of the head of the fibula; while its insertional tendon emerges from the lateral side of gastrocnemius, overlays the Achilles tendon and rotates around to the medial side where it forms a cap over the tuber calcaneus. The tendon subsequently becomes continuous with flexor digitorum brevis which arises as three delicate muscles. The long tendons of these muscles divide into two at the base of the first phalanx to pass around the tendon of flexor hallucis longus and insert into the proximal part of the second phalanx on the second, third, and fourth digits. The function of flexor digitorum brevis is to extend the tarsal joint and flex digits 2-4 (Greene, 1935; Hebel and Stromberg, 1986). In man, the tendon fibres of gastrocnemius rotate around those of soleus and come to attach laterally onto the calcaneus and the fibres of soleus rotate but insert medially onto the calcaneus (Banks et al., 2001; Barfred, 1973; Schmidt-Rohlfing et al., 1992). It is suggested that this twisting reduces fibre bulking in the lax tendon and deformation in the taught tendon (Banks et al., 2001; Barfred, 1973). It is also proposed that twisting of the fibres increases the tensile strength of the tendon itself, by spreading the load experienced in a multitude of directions, rather than solely longitudinally. This fibre twisting occurs not only at a gross macroscopic level, but also at a molecular level, where collagen peptides twist around each other to form a triple-helical collagen molecule (Fietzek and Kuhn, 1976). No comparative study of collagen fibre twisting has been carried out in the rat Achilles tendon; however it is possible that the rotation of the tendon of plantaris around the Achilles tendon may act in a similar fashion and produce the same benefits. In contrast to the rat, plantaris in man remains deep to gastrocnemius after arising superior to the condyle of the femur, and its tendon inserts into the calcaneus as part of the Achilles (Tortora and Grabowski, 1996; Standring, 2007)

Blood Supply of the Rat Hind Limb

The rat pelvic limb is primarily supplied by a branch of the external iliac artery; the femoral artery which extends down the medial side of the thigh, to become the popliteal artery, after passing into the popliteal fossa (Greene, 1935). The femoral artery has six branches namely, the superficial circumflex iliac, muscular superficial epigastric, highest

genicular, great saphenous and profunda femoris. The majority of these branches supply the muscles of the thigh. However, the largest branch is the saphenous artery which runs superficially and medially with the saphenous nerve to the ankle. At the posterior border of semitendinosus the saphenous artery divides into two and then into five terminal branches. The medial tarsal branch runs to the extensor surface of the foot with the saphenous nerve, a communicating branch also runs with the saphenous nerve between tibialis posterior and the tibia. The final 3 branches pass posterior to the medial malleolus in order to supply the flexor surface of the foot via the lateral plantar artery and the superficial and deep branches of the medial plantar artery. The popliteal artery is relatively short and bifurcates at the anterior margin of the m. popliteus. The popliteal artery gives rise to 7 branches. The superior muscular artery is the largest and runs along the surface of gastrocnemius (Greene, 1935; Hebel and Stromberg, 1986).

Nerve Supply of the Rat Hind Limb

The lower part of the rat hind limb is innervated by the sacral plexus formed by part of the fourth, the fifth and part of the sixth lumbar nerves (Greene, 1935). These integrate to form the lumbosacral trunk which becomes the sciatic nerve. The sciatic nerve separates at the level of the popliteal fossa into the two terminal components, the tibial and common peroneal nerves. The common peroneal nerve runs down the lateral side of the leg while the tibial nerve runs more medially. An articular branch from the common peroneal nerve supplies the knee joint while the sural nerve supplies the skin to the lower part of the leg after passing between biceps femoris and the lateral head of gastrocnemius. Beyond this point it becomes superficial and sends a peroneal anastomatic branch beneath the Achilles tendon to the lateral plantar nerve to the lateral side of the fifth digit, where it passes posterior to the lateral malleolus to end in the skin and fascia of the ankle and heel. The origin of the sural nerve in the rat is very different from that in the man. In man, it is formed by the medial sural branch of the tibial nerve and an anastomatic branch from the common peroneal, although the pattern in the rat can be seen as a variation in man (Greene, 1935).

The tibial nerve runs with the common peroneal nerve. However, at the popliteal fossa, it runs obliquely to enter the lower leg and run deep between the two heads of gastrocnemius, where it gives off three muscular branches (Greene, 1935). The first supplies plantaris, soleus and the lateral head of gastrocnemius, the second supplies the medial head of

gastrocnemius and the third supplies flexor hallucis longus, tibialis posterior and flexor digitorum longus. More recently studies have been extended to demonstrate that the muscles of the rat hindlimb are composed of smaller entities, or neuromuscular compartments. These compartments are regions of muscle innervated by a single, naturally occurring primary muscle nerve branch (Donahue and English, 1989). The tibial nerve continues between plantaris and the medial head of gastrocnemius and divides in the medial and lateral plantar nerves just proximal to the ankle. The lateral plantar nerve runs across the medial aspect of the calcaneus to the plantar surface of the foot. The peroneal anastomotic branch of the sural nerve runs under the tendons of soleus and gastrocnemius to reach the lateral plantar nerve just above the heel and the medial plantar nerve supplies the digits (Greene, 1935). As with other structures such as joints, the Achilles tendon itself is supplied by the nerves which supply the surrounding structures. It is therefore possible that the Achilles tendon is supplied by branches of the tibial and sural nerves (Tortora and Grabowski, 1996).

3.2. MATERIALS AND METHODS

3.2.1. Source of Material

White male Wistar rats aged 1 day, 1 month, 4 months, and 24 months (3 from each age group) were used in this study. 4 month rats and pregnant female rats were obtained from accredited commercial suppliers. Following parturition the offspring were maintained at Cardiff University until the appropriate age.

3.2.2. Dissection Procedure

Adult rats were killed with an overdose of carbon dioxide followed by cervical dislocation. Neonates were stunned and then killed by cervical dislocation. The hind-limbs from adult rats were skinned and amputated. The ankle region was removed from the limb by cutting through the tibia and fibula midway down the leg. The forefoot was removed from the ankle by cutting through the proximal part of the metatarsus leaving the Achilles tendon intact and attached to the calcaneus. The whole hind-limbs were removed and used from neonatal rats. Tissues were kept moist at all stages during dissection with 0.1M PB.

3.2.3. Routine Histology

Routine histology was carried out as described in chapter 2.

3.2.4. Immunohistochemistry

Immunofluorescence and immunoperoxidase labelling was carried out as described in chapter 2 using the antibodies against, PGP 9.5, Neurofilament 200, CGRP, and Substance P (see Table 2.1).

3.3. RESULTS

In order to explain the innervation of the enthesis organ of the rat Achilles tendon fully, it is first necessary to describe its routine histological structure.

3.3.1. Routine Histology

Anatomy of the Achilles Tendon Insertion

The rat Achilles tendon insertion was associated with 3 different fibrocartilages – enthesis fibrocartilage at the attachment zone itself, sesamoid fibrocartilage near the deep surface of the tendon, and periosteal fibrocartilage covering superior tuberosity of the calcaneus. Between the periosteal and sesamoid fibrocartilages was the retrocalcaneal bursa, into which protrudes a tip of the synovial covered fat pad (Fig.3.3.1.A.). This filled the triangular space, superior to the calcaneus, anterior to the Achilles tendon, and posterior to the tendon of flexor hallucis longus.

The Relationship of the Achilles Tendon to Plantaris

The Achilles tendon approached its bony insertion site on the calcaneus at an oblique angle. In H & E sections, the darkly stained nuclei of elongated tendon fibroblasts were evident and the cells were arranged in longitudinal rows between parallel collagen fibres (Fig. 3.3.1.B.). Toluidine blue staining was stronger away from the superficial ‘non-compressional’ region of the tendon, towards the deep surface of the Achilles tendon (Fig. 3.3.1.C.). When stained with Masson’s trichrome, the tendon was deep red, becoming green towards the deep surface of the tendon (Fig. 3.3.1.D). Small blood vessels could be seen running along the surface of the Achilles tendon within the paratenon (inset of Fig. 3.3.1.E.). This figure also illustrates the position of the tendon of plantaris and the green staining at the deep surface of this tendon, where it opposes the superficial surface of the Achilles tendon. The plantaris tendon (especially in older animals) was also strongly stained towards its deep surface with toluidine blue (Figure 3.3.1.F.).

In some older animals, the central part of the Achilles tendon itself was fibrocartilaginous. These areas were green in Masson’s trichrome as illustrated (Fig 3.3.2.A.). The normally elongated tendon fibroblasts were round; i.e. the cells were similar in appearance to those seen in the fibrocartilage of the insertional region.

Enthesis Fibrocartilage

There were 4 distinct zones of tissue visible at the enthesis itself; tendon, UF, CF and bone (Figure 3.3.2.B). The cells of UF lay in rows between collagen fibres as in the midsubstance of the tendon. However, the cells were larger, more rounded and lay in a strong toluidine blue-stained, pericellular matrix than those of the tendon proper (Fig. 3.3.2.C.). Aged rats (24 months) showed very little difference when compared to sexually mature adults (4 months). The quantity of UF across the insertion was not uniform - it was most conspicuous closest to the retrocalcaneal bursa (Fig. 3.3.1.D and 3.3.2.B). The boundary between UF and CF was defined by a basophilic line known as the tidemark, however in these sections the tidemark was not particularly prominent (Fig. 3.3.2.B and C). CF lay between the tidemark and the underlying subchondral bone. The characteristics of these fibrocartilage cells were the same as those described for UF, although the nuclei appeared to be slightly shrunken (arrow) and the cell population reduced (Fig. 3.3.2.C). The collagen fibres of the tendon, UF, and CF were continuous to the point at which they attach to the subchondral bone. The subchondral bone of the calcaneus illustrated typical Haversian systems of compact bone (Fig. 3.3.2.B.) and this region was much thicker than described in human samples. The highly irregular border of the CF and subchondral bone was also evident (Fig. 3.3.2.B and C).

Sesamoid and Periosteal Fibrocartilage

Other regions of the Achilles insertion also demonstrated the presence of fibrocartilage (Fig. 3.3.2.D – F and 3.3.3.A). Thus, all specimens had fibrocartilage lining the walls of the retrocalcaneal bursa; overlying the calcaneus ('periosteal fibrocartilage'), and within the deep surface of the adjacent Achilles tendon ('sesamoid fibrocartilage'). This was evident in sections stained with toluidine blue by very strong staining (Fig. 3.3.2.E.). The periosteal fibrocartilage was more darkly stained than the adjacent sesamoid fibrocartilage (Fig. 3.3.1.C and 3.3.2.E.). Cells of both these fibrocartilages had a similar shape to those in the enthesis fibrocartilage. The majority of cells were rounded, although some had a more irregular shape and a strongly-staining, pericellular matrix (Fig. 3.3.2.D and 3.3.3.A.). At the insertional angle (i.e. the angle between the tendon and the bone) the periosteal, sesamoid and enthesis fibrocartilages were continuous with each other, and no distinct boundaries were present between them (Fig. 3.3.1.C-D.). Also evident, was a thin acellular layer which lines the insertional angle. This was obvious in sections stained with toluidine blue, but was not clear with Masson's trichrome (Fig. 3.3.1.D and E).

Retrocalcaneal Bursa and Retromalleolar Fat Pad

The retrocalcaneal bursa was lined by the periosteal and sesamoid fibrocartilages, as described above. Proximal to the insertional angle was a large synovial-covered fat pad. The pad extended from the inferior border of triceps surae, filling the space created by the extended length of the calcaneus. The pad invaginated a small way into the retrocalcaneal bursa as a synovial-covered, tongue-like protrusion (Fig. 3.3.1.A and 3.3.3.D.). The majority of the fat pad cells had a characteristic 'honeycomb' appearance, with thin peripheral seams of cytoplasm and small, flattened peripherally-located nuclei (Fig. 3.3.3.B). Some fibrous strands were also present running through the fat pad (Fig. 3.3.3.C). The part of the pad that protruded distally into the retrocalcaneal bursa had a considerably more fibrous appearance than that which was more proximal and in older animals the tip was especially fibrous (Fig. 3.3.3.D and E). However, one specimen at 4 months of age had a region of fibrocartilage with a bony core near the tip of the pad (Fig. 3.3.3.F and 3.3.4.A). The cells within this region resembled those of the insertional fibrocartilages, with rounded cells and a strongly-staining, pericellular matrix. The pad was covered by a synovial membrane which folds back on itself to line the most proximal part of the retrocalcaneal bursa (Fig. 3.3.4.B.). However, the most proximal part of the fat pad had a more fibrous lining (Fig. 3.3.4.C). Just beneath both the synovial membrane and the fibrous lining is a highly vascular region. This contained a large population of mast cells (Fig. 3.3.4.D.). The pad also contained a number of large blood vessels, often associated with the fibrous strands and small capillaries branched throughout the pad. Several large nerve branches were also present, usually running in association with blood vessels (Fig. 3.3.4.C.). The tip of the pad was devoid of large blood vessels and large nerve branches although some small capillaries were seen (Fig. 3.3.3.D.). No encapsulated nerve endings were identified.

Staining with toluidine blue highlighted the abundant mast cells within the fat pad. The cells were most frequently identified in close association with the synovial and fibrous membrane of the fat pad, and the capillary layer just beneath its lining (Fig. 3.3.4.D.). Mast cells were also seen within some large nerve branches (Fig. 3.3.4.E.). Their location was not restricted to a specific region of the pad.

3.3.2. Immunohistochemistry

Innervation of the Rat Achilles Tendon Enthsis Organ

The results are summarised in Table 3.3.1.

Enthesis Fibrocartilages

Immunohistochemical labelling with PGP 9.5, CGRP, SP, and NF200 showed that no nerve fibres were present within the fibrocartilaginous regions or the retrocalcaneal bursa of the Achilles tendon insertion at any age studied (Fig. 3.3.5-8.A-C). All 3 fibrocartilages associated with the insertion of the Achilles tendon into the calcaneus, consistently showed negative labelling at all ages studied. The acellular layer lining the insertional angle was also devoid of nerve fibres.

Retromalleolar Fat Pad

PGP 9.5

In contrast to the fibrocartilage of the enthesis organ, the retromalleolar fat pad contained an abundance of nerve fibres (Fig. 3.3.5.D-F.) the population of which varied with the age of the rat. A qualitative assessment of these fibres suggested that the number increases from birth until sexual maturity, but decreases with old age. In the neonate, very few nerve fibres were present. A nerve branch was clearly visible in the centre of the fat pad and a few fibres were seen in the tip of the pad in some animals. In 1 month rats, there was a larger population of both small and intermediate sized fibres that predominated in the central and proximal regions of the pad. The largest population of nerve fibres was evident in 4 month rats. A large nerve branch close to the midsubstance of the Achilles tendon was present along with another large nerve branch in the anterior part of the fat pad (Fig 3.3.5.D and F.). The identification of these nerve fibres acts as an internal positive control, indicating that the negative results obtained from the insertional region fibrocartilage were not a result of inappropriate technique. An abundance of small nerve fibres was also present throughout the fat pad - the fibres were either "free" or blood vessel associated. Smaller fibres were present throughout the pad although generally fewer nerve fibres were present in its fibrous tip (Fig. 3.3.5.E.). Many nerve fibres were seen in the sub-synovial layer and beneath the fibrous membrane described previously. Some nerve fibres were even present in the synovial membrane itself and within the tunica adventitia of blood vessels (Fig. 3.3.5.D.).

CGRP

Very few CGRP positive fibres were seen in the neonatal fat pad. Only a few fibres, large nerve branches and single nerve trunks were seen within the central part of the

retromalleolar fat pad, many of which were associated with blood vessels. The majority of these fibres were in the sub-synovium and in the fibrous membrane.

At 1 month, more fibres appeared to be present in comparison to neonates. Delicate “free” and blood vessel associated fibres were situated within the proximal region of the fat pad. Nerve fibres were occasionally identifiable within the tongue-like protrusion of the fat pad. Large nerve branches also showed positive labelling for CGRP, although only a small proportion of the fibres were positively labelled with the characteristic speckled foci of CGRP (Fig. 3.3.6.F.). Therefore not all fibres within the nerve branch contained CGRP. Tissue from 4 month rats showed a similar pattern. The majority of fibres were present within the proximal part of the fat pad. The smaller fibres again, predominated just deep to the synovial and fibrous membranes, and large nerve branches were identified running through the fat pad. There appeared to be a small increase in the number of nerve fibres present. At 24 months, the fibres in the fat pad were both blood vessel associated and “free”. Both types of fibres predominated in the main and proximal region of the fat pad rather than in the tip (Fig. 3.3.6.D-E.). It was not possible to determine if there was a change in the population of nerve fibres in older animals.

Substance P

SP positive nerve fibres were present within the retromalleolar fat pad - some of these fibres ran in close association with blood vessels while others were independent of blood vessels. (Fig. 3.3.7.E-G.). They displayed the characteristic fine, focal label that gives a streaky appearance of small nerve fibres found in the fat pad and the larger nerve branches. As with CGRP labelling of large nerve branches, not all the fibres in the nerve were labelled - indicating that the cells contain a mixed population of nerve fibres (Fig. 3.3.7.D.). SP fibres were also located on the superior part of the calcaneus in the periosteum; at a distance from the enthesis. Age related changes in the number of SP immunoreactive nerve fibres within the fat pad followed the same pattern as CGRP. The population of fibres increased during growth, but once again it was not possible to determine if the number of SP immunoreactive fibres changed with old age.

Neurofilament 200

The NF200 antibody allowed the identification of small “free” nerve trunks, small blood vessel associated nerve fibres, intermediate nerve fibres and large nerve bundles (Fig. 3.3.8.D-F). In all animals, a greater number of these larger fibres carrying

mechanoreceptive information were present within the fat pad in comparison to both CGRP and SP. The pattern of expression with age, as described previously with PGP 9.5, increased during growth but decreased in old age. Overall there appeared to be a larger population of nerve fibres labelling positively for NF200 than CGRP and SP.

Achilles Tendon, Plantaris Tendon and the Myotendinous Junction of the Achilles Tendon

No positive PGP 9.5 nerve fibres were seen within the tendon proper (collagen fibres or fibroblast network), however, fibres were identified between the tendon fascicles, within the endotenon and in the supportive surrounding paratenon of the Achilles tendon midsubstance. Using more specific antibodies, it was possible to identify that the endotenon and paratenon contained CGRP and SP positive nerve fibres as well as nerve fibres positive for the NF200 (Fig 3.3.7.E, Fig. 3.3.8.E.). Many of these fibres were blood vessel associated while others were “free” nerve trunks. In addition, there appeared to be no obvious correlation between the number of nerve fibres present within this tissue across the ages studied. Nerve fibres immunoreactive to all antibodies were also found in the epitenon of the plantaris tendon, although none were seen on its inner surface where this tendon and that of the Achilles were opposed.

The myotendinous junction of the Achilles tendon contained numerous fibres, mainly located in the endomysium of the muscle. Although some of these fibres were immunoreactive to SP and CGRP, the majority were NF200 immunoreactive fibres.

Age	PGP 9.5		NF200	
	EF/SF/PF/RB	FP	EF/SF/PF/RB	FP
1 day	-	+++	-	++
1 month	-	++++	-	+++
4 month	-	+++++	-	++++
24 month	-	++++	-	+++

Age	SP		CGRP	
	EF/SF/PF/RB	FP	EF/SF/PF/RB	FP
1 day	-	+	-	+
1 month	-	++	-	++
4 month	-	+++	-	+++
24 month	-	+++	-	+++

Table 3.3.1: Summary of results obtained from fluorescence labelling for nerve fibres in the rat Achilles enthesis organ. - = no nerve fibres presenting the tissue at this stage, + = denoted the presents of nerve fibres (Scale 1-5 +’s, 5 = most).

RAT ACHILLES TENDON ENTHESIS ORGAN – ROUTINE HISTOLOGY

Figure A: The components of the Achilles tendon enthesis organ. These include enthesis fibrocartilage (EF), the sesamoid fibrocartilage (SF), periosteal fibrocartilage (PF), retrocalcaneal bursa (RB), and synovial covered (arrow) fat pad (FP). C - calcaneus, T - tendon. 24m rat, H & E. Scale bar = 300µm.

Figure B: Rows of elongated tendon fibroblasts (arrows) between longitudinally running collagen fibres in the Achilles tendon of a 24m rat, H & E. Scale bar = 100µm

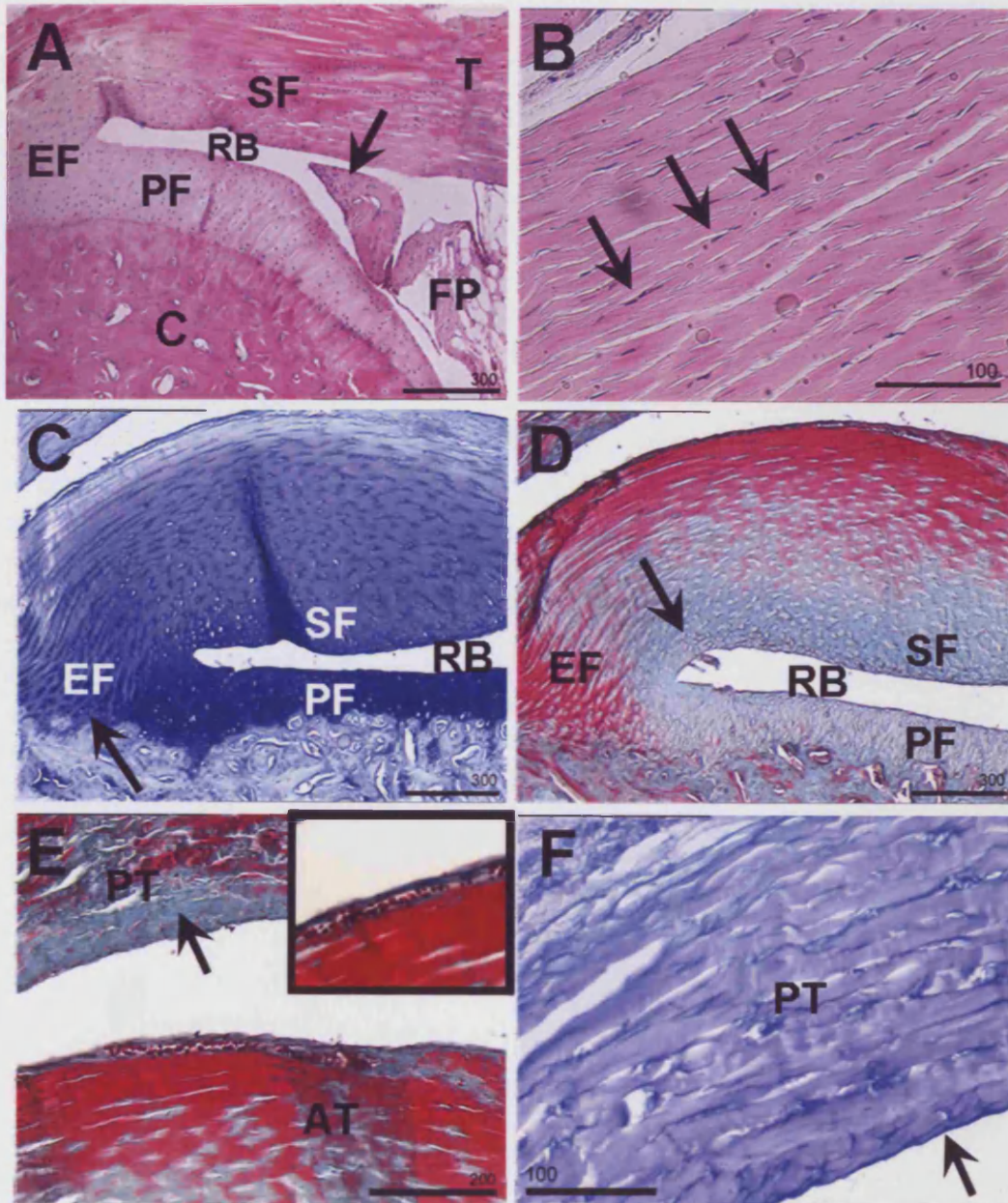
Figure C: The 3 fibrocartilaginous regions of the Achilles tendon enthesis organ in a toluidine-blue stained section. The strength of the staining increases towards the deep surface of the Achilles tendon (SF). The arrow indicates the strong staining of the pericellular matrix surrounding fibrocartilage cells in the enthesis fibrocartilage (EF). The very strong staining of the periosteal fibrocartilage can also be seen (PF). RB - retrocalcaneal bursa. 12 week rat. Scale bar = 300µm.

Figure D: The 3 fibrocartilaginous regions of the Achilles tendon enthesis organ in a Masson's stained section. Note the distinction between the periosteal (PF), sesamoid (SF), and enthesis fibrocartilages (EF). The arrow indicates the predominating fibrocartilage at the insertional angle where the collagen fibres change direction to the greatest extent. RB-retrocalcaneal bursa. 12 week rat. Scale bar = 300µm.

Figure E: The opposing surfaces of the plantaris and Achilles tendons in a Masson's stained section. The arrow indicates the presence of sesamoid fibrocartilage in the deep surface of the plantaris tendon (PT). A blood vessel runs on the surface of the Achilles tendon, within the paratenon (inset). 12 week rat. Scale bar = 200µm

Figure F: The opposing surfaces of the plantaris and Achilles tendons in a toluidine blue stained section. The arrow indicates the region of increased staining towards the deep surface of the plantaris tendon (PT). AT - Achilles tendon. 12 week rat. Scale bar = 200µm.

Figure 3.3.1



RAT ACHILLES TENDON ENTHESIS ORGAN – ROUTINE HISTOLOGY

Figure A: The Achilles tendon midsubstance in a Masson's stained section. Note the presence of a fibrocartilaginous formation in the midsubstance of the Achilles tendon. The arrow indicates fibrocartilage cells with rounded nuclei. 12 week rat. Scale bar = 100µm.

Figure B: The Achilles enthesis fibrocartilage in a Masson's stained section demonstrating the different tissues found in the region. UCFC - uncalcified fibrocartilage, TM - tidemark, CFC - calcified fibrocartilage. 12 week rat. Scale bar = 100µm.

Figure C: The Achilles enthesis fibrocartilage in a toluidine blue stained section. The uncalcified fibrocartilage (UCFC) contains large rounded nuclei of fibrocartilage cells. The calcified fibrocartilage (CFC) cells are fewer in number with slightly shrunken nuclei in comparison to those of the uncalcified fibrocartilage (arrow). The region of calcified fibrocartilage is more darkly stained than the uncalcified region. The tidemark (TM) is not obvious across the entire enthesis fibrocartilage due to the angle at which the Achilles tendon inserts into the bone. C - Calcaneus. Scale bar = 50 µm.

Figure D: The periosteal fibrocartilage in Masson's stained section. The periosteal fibrocartilage contains fibrocartilage cells that contain large rounded nuclei (white arrow). The underlying subchondral bone of the calcaneus (C) can also be clearly identified, although staining does not clearly demonstrate the zone of calcified fibrocartilage, the region can be identified by the smaller cell population which have irregular, shrunken shaped nuclei (black arrow). RB - retrocalcaneal bursa, SF - sesamoid fibrocartilage, PF - periosteal fibrocartilage. 12 week rat. Scale bar = 100µm.

Figure E: The periosteal fibrocartilage in a toluidine blue stained section. Note the stronger staining of the periosteal fibrocartilage (PF) in comparison to the sesamoid fibrocartilage (SF). The arrow indicates the darkly stained nature of the pericellular matrix in the PF. The highly irregular interface between the calcified fibrocartilage and the subchondral bone (C) can also be seen. RB - retrocalcaneal bursa. 12 week rat. Scale bar = 100µm.

Figure F: The sesamoid fibrocartilage in a Masson's stained section. The arrows indicate the large rounded character of the fibrocartilage cells populating the sesamoid fibrocartilage (SF). 12 week rat. Scale bar = 100µm

Figure 3.3.2

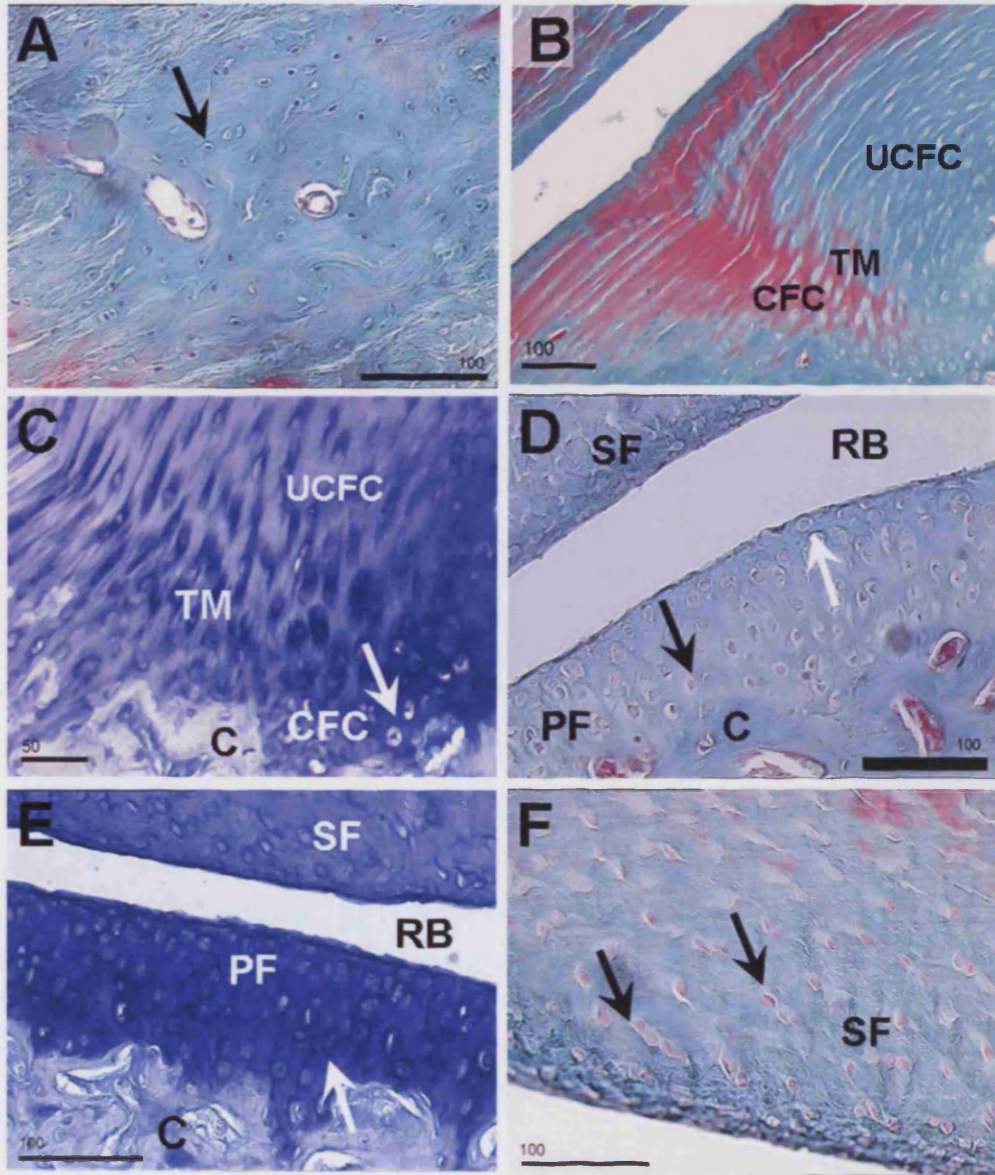
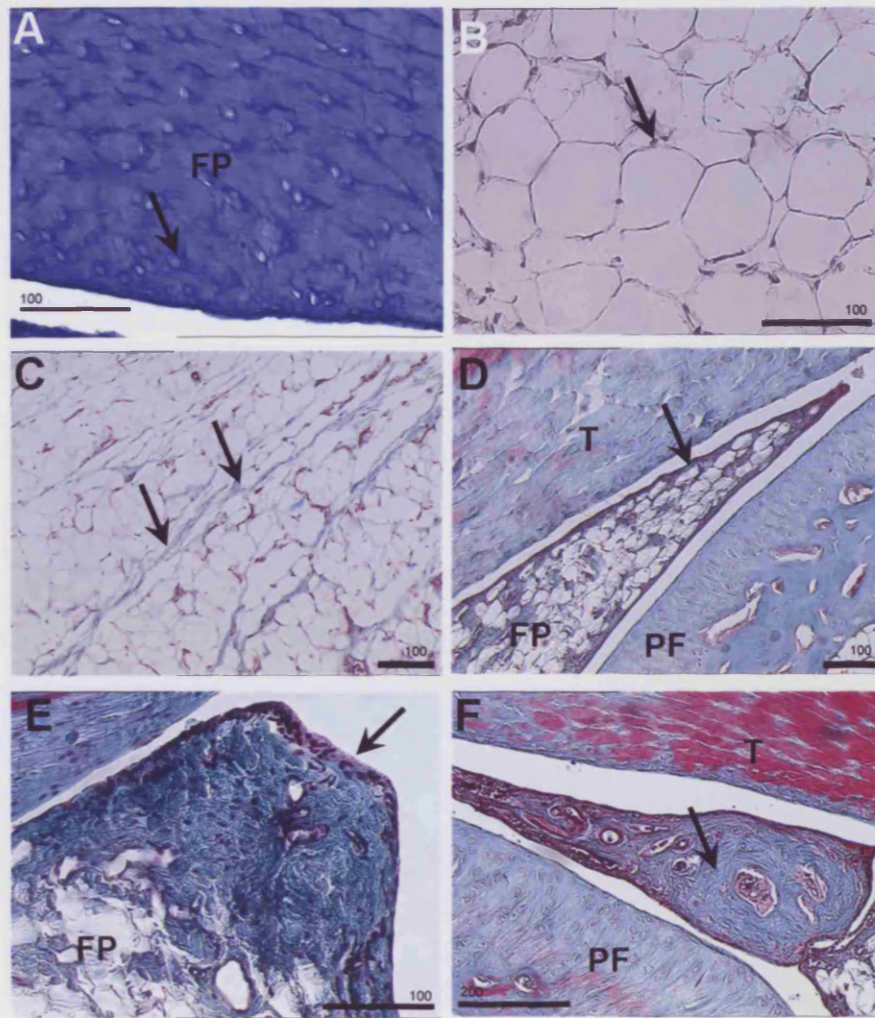


Figure 3.3.3



RAT ACHILLES TENDON ENTHESIS ORGAN – ROUTINE HISTOLOGY

Figure A: The sesamoid fibrocartilage in a toluidine blue stained section. The sesamoid fibrocartilage is darkly stained and contains fibrocartilage cells with rounded nuclei as indicated (arrow). 12 week rat. Scale bar = 100µm.

Figure B: The retromalleolar fat pad in a Masson's stained section. Note the honeycomb (hexagonal) nature of the fat cells along with their small peripheral nuclei (arrow). 12 week rat. Scale bar = 100µm.

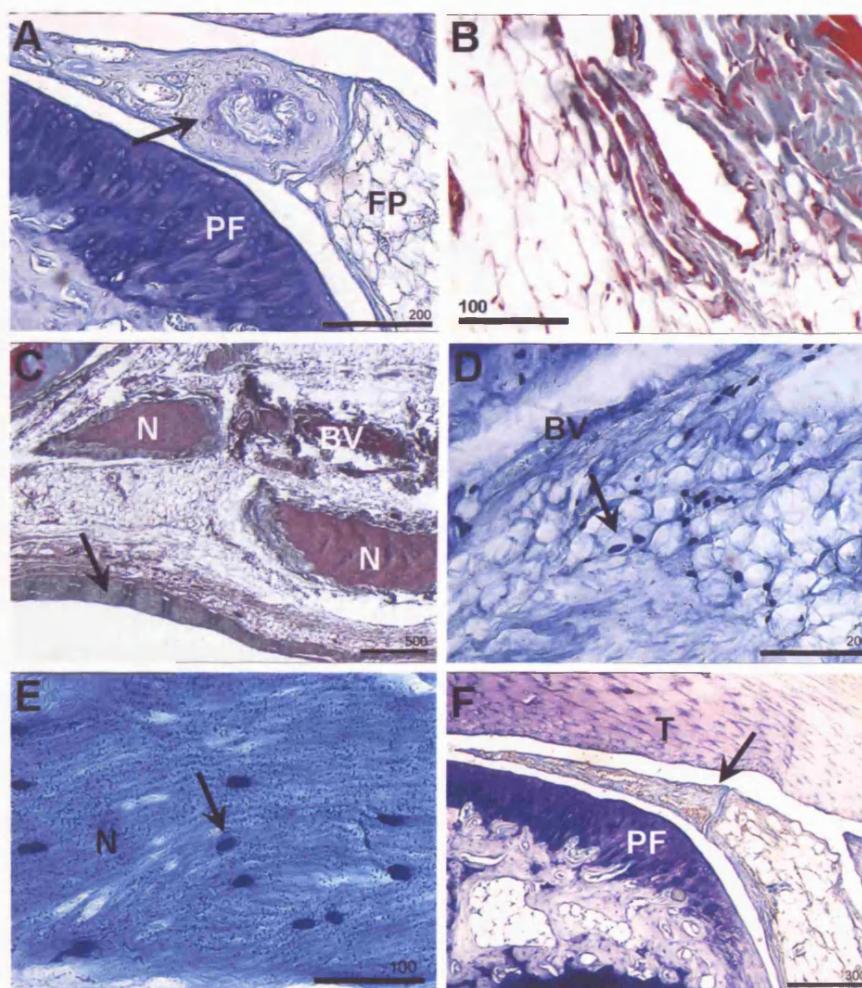
Figure C: The retromalleolar fat pad in a Masson's stained section. The arrows indicate the fibrous strands running through the fat pad. 12 week rat. Scale bar = 100µm.

Figure D: The tip of 12 week rat retromalleolar fat pad (FP) in a Masson's stained section. The figure illustrates the tip of the pad which protrudes into the retrocalcaneal bursa. The fat is covered with a synovial membrane (arrow). PF- periosteal fibrocartilage, T-tendon. Scale bar = 100µm.

Figure E: The tip of 24 month retromalleolar fat pad (FP) in a Masson's stained section. Note the highly fibrous nature of the tip of the fat pad in comparison to the pad at 12 weeks (Figure 2.3.1.P). The arrow indicates the synovial membrane. Scale bar = 100µm.

Figure F: The tip of the retromalleolar fat pad in a Masson's trichrome stained section. Note the presence of a fibrocartilaginous structure with a central bone like structure. Arrow Indicates the rounded character of the cells in at the periphery of the fibrocartilaginous cluster. T - Tendon, PF - Periosteal Fibrocartilage. 12 week rat. Scale bar = 200µm.

Figure 3.3.4



RAT ACHILLES TENDON ENTHESIS ORGAN – ROUTINE HISTOLOGY

Figure A: The fibrocartilaginous tip of the retromalleolar fat pad (FP) in a Toluidine blue stained section. The arrow indicates the dark blue staining towards the centre of the fibrocartilaginous structure in the tip of the fat pad. PF - periosteal fibrocartilage. 12 week rat. Scale bar = 200µm.

Figure B: The synovial fold in a Masson's stained section. The arrow indicates the limit of the synovial membrane following a large fold in the synovium. The structure surrounding the fat pad becomes fibrous where the synovial membrane ends. 12 week rat. Scale bar = 100µm

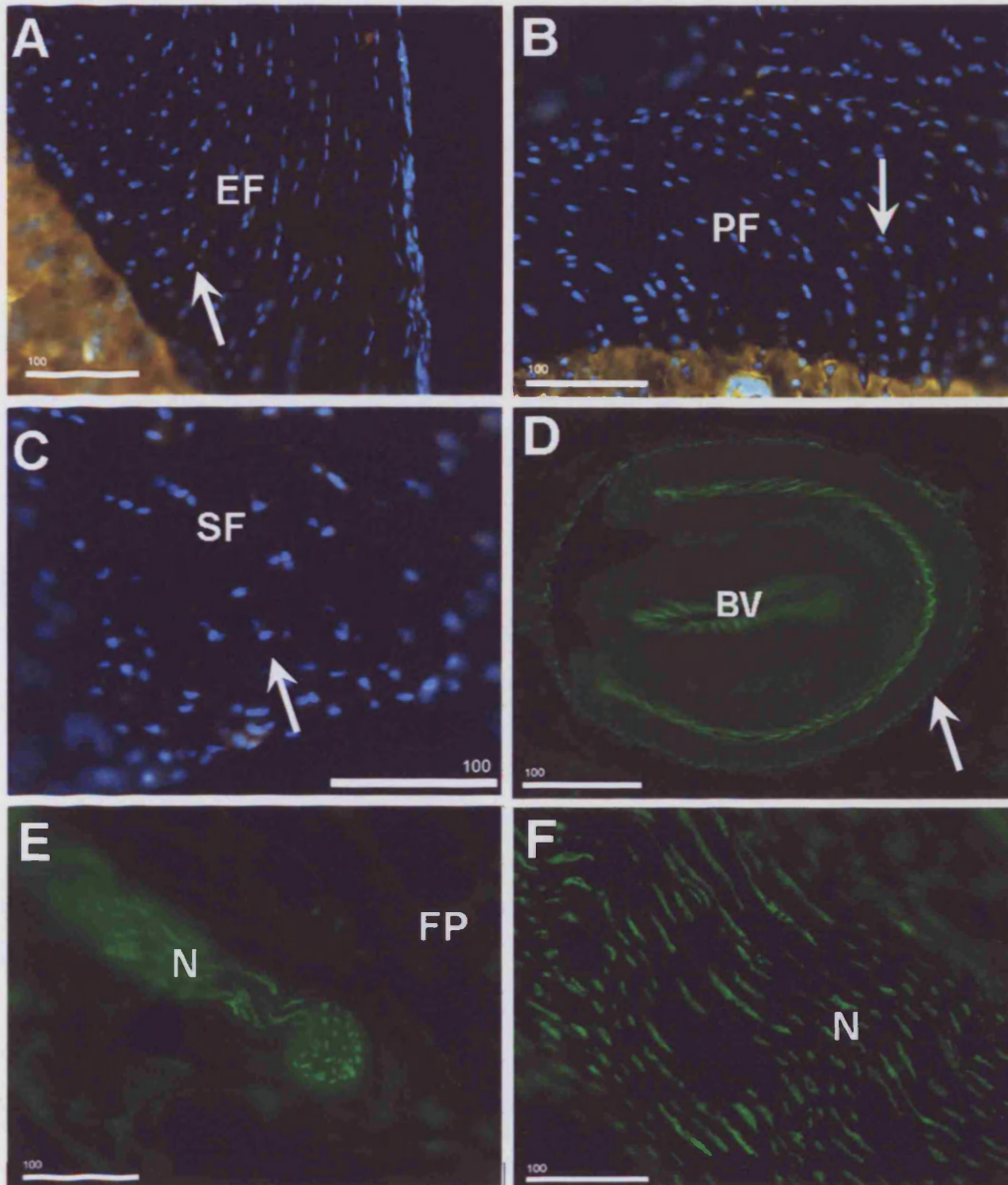
Figure C: A large neurovascular bundle containing a large peripheral nerve (N) and blood vessel (BV) in a Masson's stained section. The arrow indicates the highly fibrous nature of the proximal fat pad. 12 week rat. Scale bar = 500µm

Figure D: Numerous mast cells were present in the retromalleolar fat pad in Toluidine blue stained section (arrow). The cells are in close association with blood vessels (BV). Toluidine Blue. 12 week rat. Scale bar = 200µm

Figure E: Large peripheral nerve (N) in a Toluidine blue stained section. These nerves contained numerous mast cells (arrows). 12 week rat. Scale bar = 100µm

Figure F: The tip of the retrocalcaneal bursa in a toluidine blue stained section. Note the absence of mast cells from the tip (arrow) of the fat pad. T - tendon, PF - periosteal fibrocartilage. 12 week rat. Scale bar = 300µm.

Figure 3.3.5



**RAT ACHILLES TENDON ENTHESIS ORGAN LABELLED WITH PGP 9.5
12 week rat (Counterstained with DAPI to illustrate cell nuclei)**

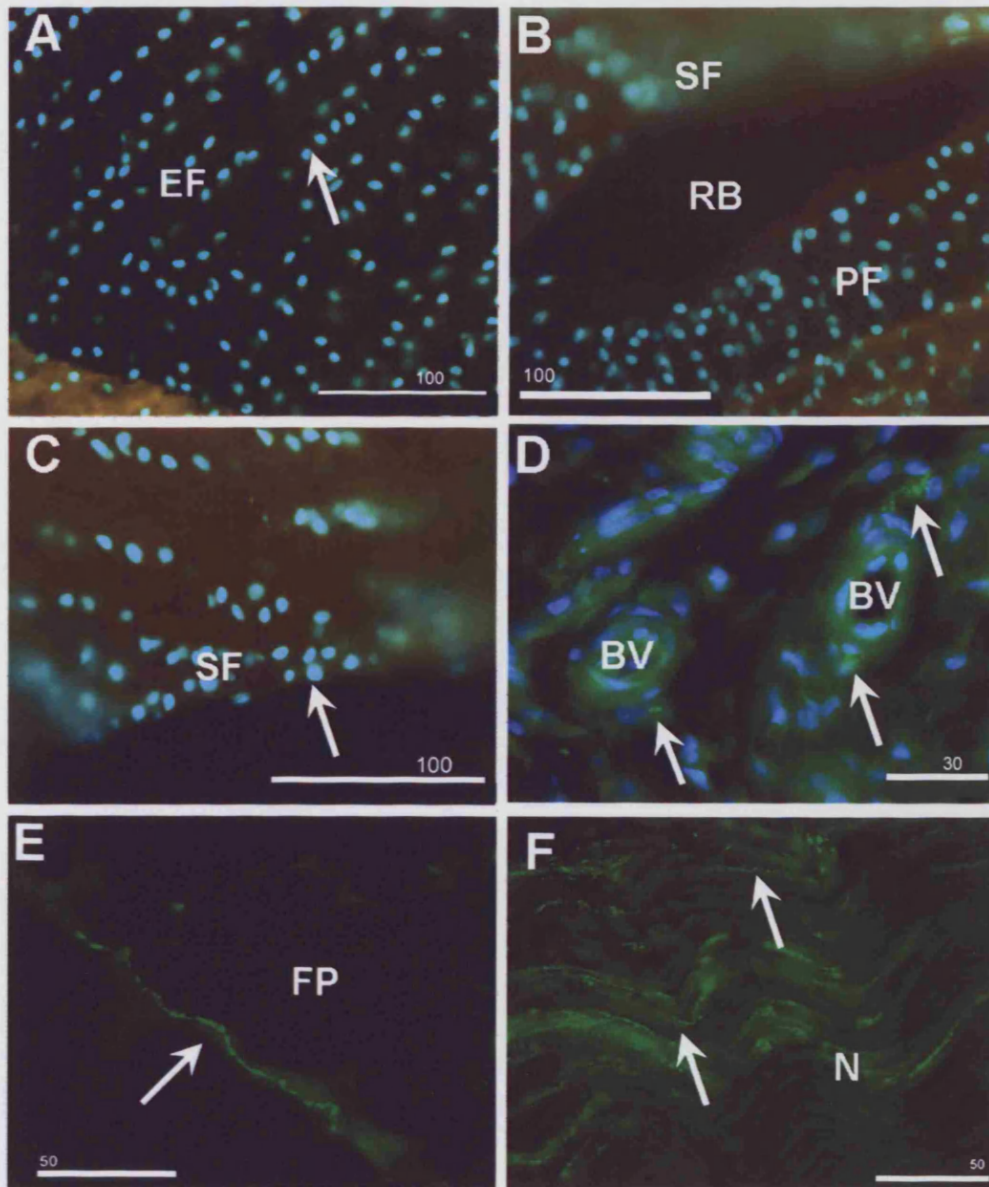
Figure A-C: Immunolabelling of the enthesis fibrocartilage (EF in A), periosteal fibrocartilage (PF in B) and sesamoid fibrocartilage (SF in C) to show the absence of nerve fibres. The arrows indicate the rounded appearance of fibrocartilage cells. Scale bar = 100µm

Figure D: A large peripheral blood vessel within the retromalleolar fat pad. Note the nerve fibres in the outer wall of the blood vessel (arrow) and also the non-specific labelling of the internal elastic lamina. Scale bar = 100µm

Figure E: An intermediate size nerve fibre (N) un-associated with blood vessels within the retromalleolar fat pad. Scale bar = 100µm

Figure F: A large peripheral nerve (N) within the retromalleolar fat pad. Scale bar = 100µm

Figure 3.3.6



**RAT ACHILLES TENDON ENTHESIS ORGAN LABELLED WITH CGRP
12 week rat (Counterstained with DAPI to illustrate cell nuclei)**

Figure A-C: The enthesis fibrocartilage (EF in A), periosteal fibrocartilage (PF in B) and sesamoid fibrocartilage (SF in C) are all devoid of nerve fibres. The arrows indicate the rounded appearance of fibrocartilage cell nuclei. B -bone. RB – retrocalcaneal bursa. Scale bar = 100µm

Figure D: CGRP positive fibres (arrows) lying in close association with small blood vessels (BV) within the retromalleolar fat pad. Scale bar = 100µm

Figure E: A small “free” CGRP immunoreactive nerve fibre within the retromalleolar fat pad (PF). Scale bar = 50µm

Figure F: A large peripheral nerve (N) in the retromalleolar fat pad demonstrating the population of CGRP containing fibres within it. Scale bar = 50µm

RAT ACHILLES TENDON ENTESIS ORGAN LABELLED WITH SUBSTANCE P
12 week rat (Counterstained with DAPI to illustrate cell nuclei)

Figure A-C: The enthesis fibrocartilage (EF in A), periosteal fibrocartilage (PF in B) and sesamoid fibrocartilage (SF in C) are all devoid of nerve fibres. The arrows indicate the rounded appearance of fibrocartilage cells. Scale bar = 50µm. RB – Retrocalcaneal bursa.

Figure D: A large peripheral nerve (N) within the retromalleolar fat pad demonstrating the population of substance P containing nerve fibres (arrows). Scale bar = 50µm

Figure E: A small, substance P containing nerve fibre within the proximal part of the Achilles paratenon (PT). T- Tendon. Scale bar = 50µm.

Figure F: A small “free” substance P containing fibre within the proximal region of the retromalleolar fat pad. Scale bar = 50µm

Figure G: A small blood vessel associated nerve fibre, immunoreactive to substance P (arrow). Note the non-specific labelling of the internal elastic lamina (IEL). Scale bar = 50µm

Figure 3.3.7

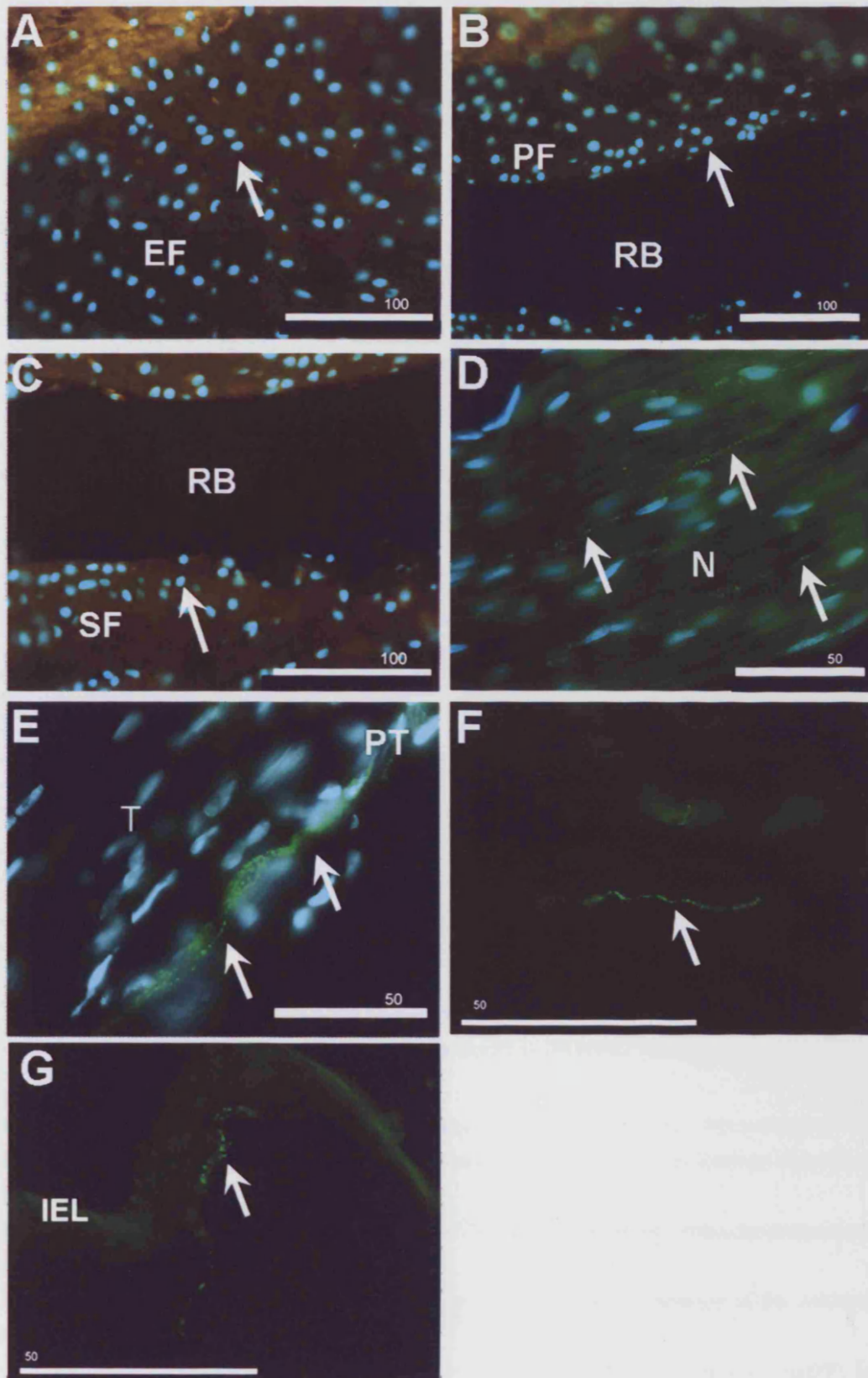
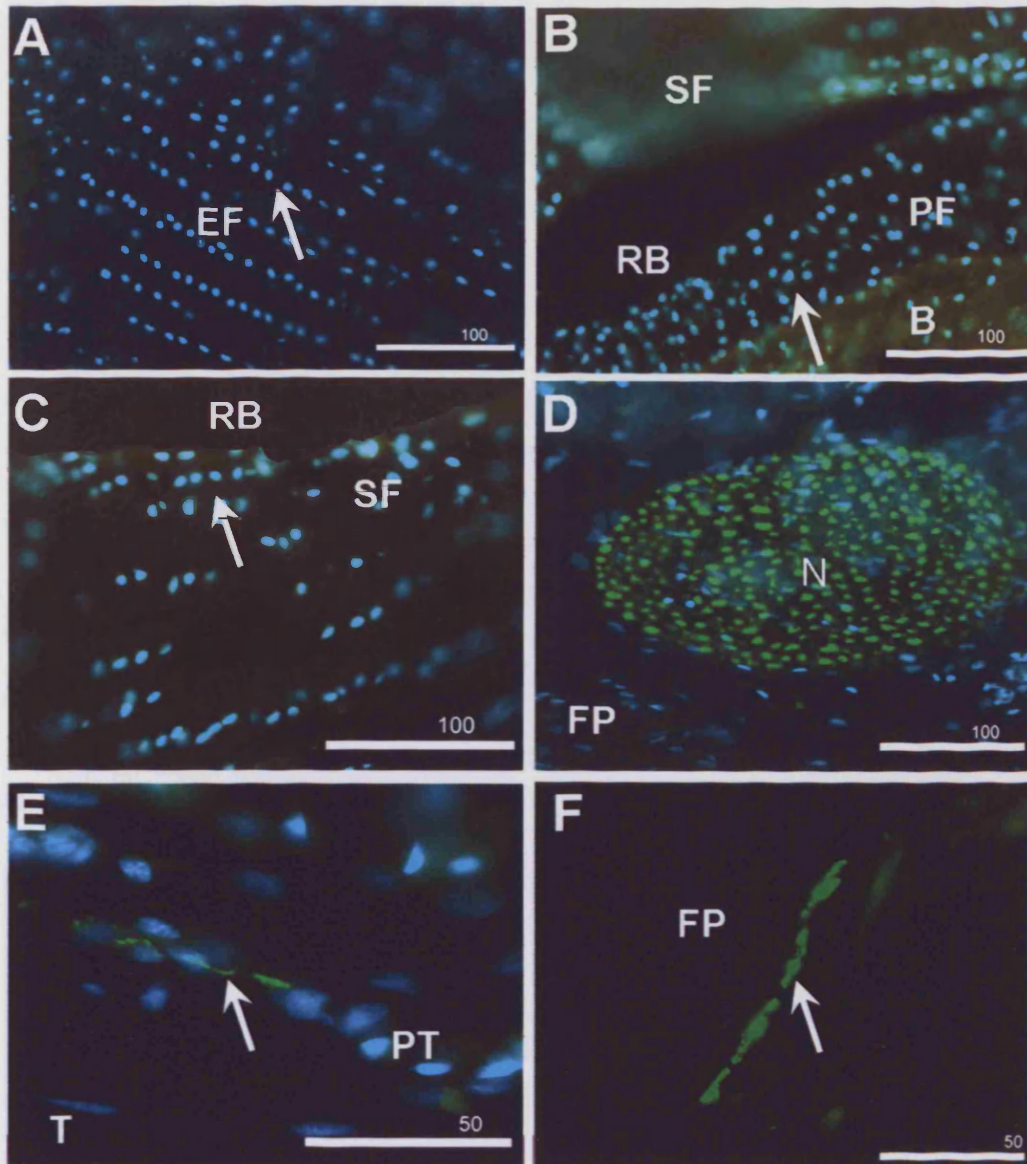


Figure 3.3.8



**RAT ACHILLES TENDON ENTHESIS ORGAN LABELLED WITH NEUROFILAMENT 200
12 week rat (Counterstained with DAPI to illustrate cell nuclei)**

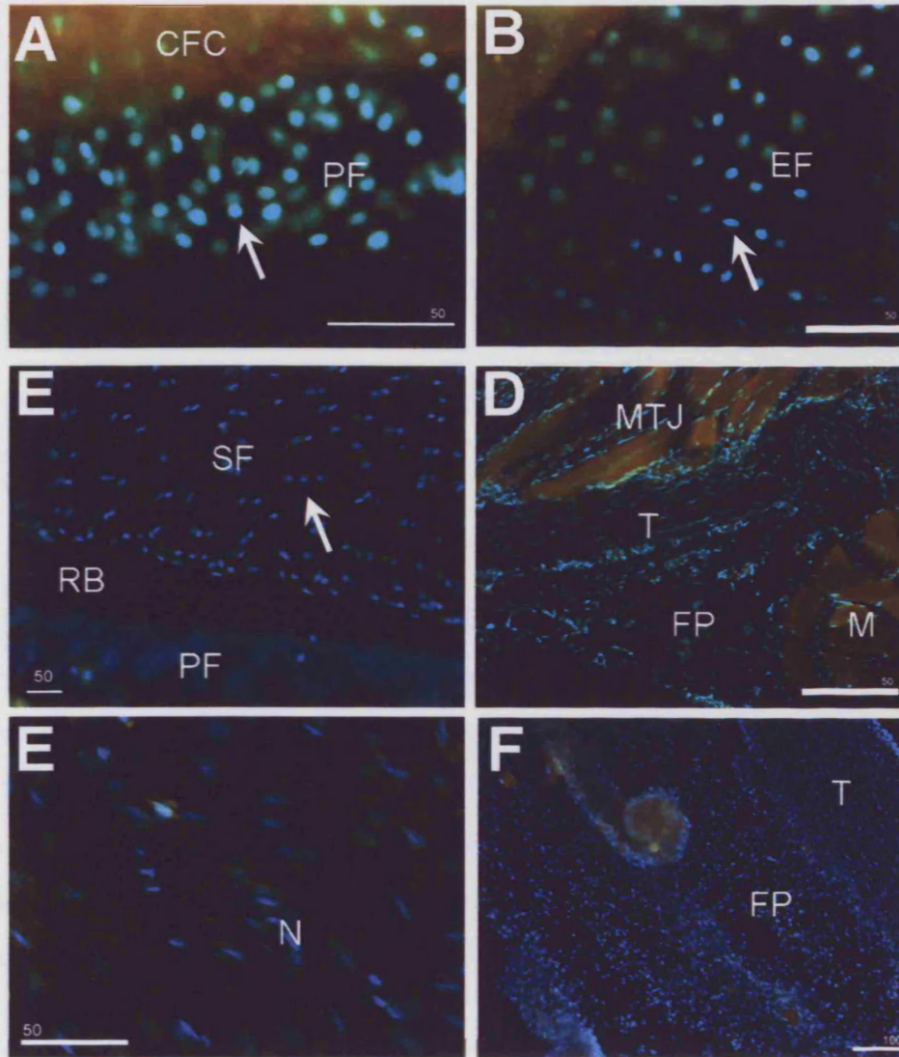
Figure A-C: The absence of nerve fibres in the enthesis fibrocartilage (EF in A), periosteal fibrocartilage (PF in B) and sesamoid fibrocartilage (SF in C). The arrows indicate the rounded appearance of the fibrocartilage cells. B-bone. RB-retrocalcaneal bursa. Scale bar = 100µm

Figure D: A large peripheral nerve (N) immunoreactive to NF200, cut in cross-section, within the proximal part of the retromalleolar fat pad (FP). Scale bar = 100µm

Figure E: A small nerve fibre (arrow) immunoreactive to NF200 within the paratenon of the Achilles tendon midsubstance. Scale bar = 50µm

Figure F: A small "free" nerve fibre (arrow) immunoreactive to NF200 within the retromalleolar fat pad (FP). Scale bar = 50µm

Figure 3.3.9



RAT ACHILLES TENDON ENTHESIS ORGAN –NEGATIVE CONTROLS

Phosphate buffer (PB) or rabbit immunoglobulins were applied to the section in place of the primary antibody. (Counterstained with DAPI to illustrate cell nuclei).

Figure A-C: The periosteal fibrocartilage (PF in A), enthesis fibrocartilage (EF in B) and sesamoid fibrocartilage (SF in C) are all devoid of non-specific labelling. The arrows indicate the rounded appearance of fibrocartilage cells. Scale bar = 50μm. RB – Retrocalcaneal bursa, CFC-calcified fibrocartilage. 12 week rat.

Figure D: The myotendinous junction (MTJ) and proximal part of the Achilles tendon (T) a region rich in nerve fibres. Note the absence of labelling. Scale bar = 50μm. FP-retromalleolar fat pad, M-muscle. 12 week rat

Figure E: A large peripheral nerve (N) within the retromalleolar fat pad. No non-specific labelling is present. Scale bar = 50μm. 12 week rat

Figure F: A low power view of the retromalleolar fat pad (FP) with rabbit immunoglobulins applied to the section in place of the primary antibody. No non-specific labelling was present. Scale bar = 100μm. T-tendon. Neonatal rat.

3.4. DISCUSSION

The results show, at all ages studied, the fibrocartilaginous regions associated with the Achilles tendon enthesis are devoid of nerve fibres. However, the retromalleolar fat pad (an integral part of the enthesis organ) contains an abundance of nerve fibres, the number of which varied according to the age of the animal. These fibres are believed to be sensory and carry both mechanoreceptive (associated with the presence of NF200 containing fibres) and nociceptive (associated with the presence of SP and CGRP containing fibres) information to the CNS. The fat pad also contained histiocytes, although the number varied between the specimens.

Innervation of the Entthesis

This study has demonstrated for the first time that contrary to many textbook/review statements (Benjamin and McGonagle, 2001; Benjamin and Ralphs, 1997; Braun et al., 2000; Khan et al., 2000; Klippel and Diepp, 1998; Niepel et al., 1966; Palesy, 1997; Resnick and Niwayama, 1983), that the rat Achilles tendon enthesis is not innervated. This absence of nerve fibres within the fibrocartilages of the enthesis organ is paralleled by their avascular nature. This is comparable to the aneural and avascular structure of articular cartilage (Kuettner and Pauli, 1983; Toynbee, 1841). In contrast to the present findings, some fibrocartilaginous structures have been shown to contain both nociceptors and mechanoreceptors. Cavalcante et al., (2004) demonstrated the presence of such receptors in the triangular fibrocartilage of the human wrist, although the nerves occurred in the more fibrous, peripheral parts of the fibrocartilage and the central cartilaginous region lacked blood vessels and nerves. This pattern is also observed in the the intervertebral disc, where the outer third of the annulus fibrosis is innervated, while the inner region and the nucleus pulposus is aneural and avascular (McCarthy et al., 1991). However, in degenerative discs, nerve fibres from the outer annulus grow into the central part of the disc. This process is driven by nerve growth factor (NGF; secreted by newly formed blood vessels) binding to the high affinity tyrosine kinase receptor (trk) – A, which is expressed on the growing nerves (Freemont et al., 2002b). It is therefore possible that a similar nerve in-growth occurs in degenerative conditions affecting the Achilles tendon enthesis. Perhaps the nerves supplying the Achilles tendon, present in the peritendinous tissue of healthy tendons, can grow into the enthesis fibrocartilage along with newly-formed blood vessels expressing NGF?

Why do the fibrocartilaginous regions associated with the Achilles tendon insertion not contain nerve fibres? It is probably associated with the mechanical load to which the enthesis is subject. The function of the enthesis fibrocartilage at the attachment site is to provide a gradual change in the mechanical properties between soft tendon and hard bone. The uncalcified fibrocartilage disperses the forces generated by tendon bending away from the bone-tendon interface to the adjacent soft tissues. This is promoted by the ECM molecule aggrecan which attracts water into the tissue - thereby making it incompressible and facilitating gradual collagen fibre bending (Benjamin et al., 1986; Kiani et al., 2002). It is therefore understandable that this region, which is subject to considerable mechanical load, is devoid of nerve fibres. This also explains why the other fibrocartilaginous regions of the enthesis organ are also aneural. These fibrocartilaginous regions reduce wear and tear which occurs on the periosteum of the superior tuberosity and the opposing tendon. However, they do also help to dissipate stress away from the insertion site itself (Benjamin et al., 2004a). As a result, these areas are subject to compression, and therefore the presence of nerve fibres in this region would probably lead to damage of delicate nerve fibres during normal movement. However, it is also possible that the compressive resistant properties of the tissue may prevent adequate compression to stimulate nerve endings therefore negating their requirement under normal conditions. The innervation of the enthesis organ can therefore be suitably compared to a synovial joint, the 3 fibrocartilaginous regions of the enthesis organ and the articular cartilage in the synovial joint function in the same way to prevent wear and tear and accordingly, both are avascular and aneural.

But what prevents these nerve fibres from growing into the fibrocartilage? It is important to recognise that all 3 fibrocartilages (enthesis, sesamoid and periosteal) contain the GAG, chondroitin sulphate (CS) in their ECM as part of the aggrecan molecule. Aggrecan first appears during growth, at load bearing age (approximately 2 weeks after birth) in the enthesis, periosteal and sesamoid fibrocartilage (Rufai et al., 1992). Recent studies have demonstrated that CS acts as an axonal growth inhibitor in the CNS (Snow and Letourneau, 1992) and also in the peripheral nervous system in the region of the intervertebral disc (Johnson et al., 2002). A number of mechanisms for this inhibition have been described including receptor mediation and masking of laminin – a growth promoting factor (Snow and Letourneau, 1992). However, most studies have concentrated on the fact that high concentrations of CS restrict nerve in-growth (Johnson et al., 2002; Snow and Letourneau,

1992) and also endothelial cell adhesion and migration (Johnson et al., 2005). The high concentrations of CS in the fibrocartilage of the enthesis organ may therefore restrict nerve growth.

During (fibro)cartilage degeneration, there is a loss of aggrecan and therefore a reduction in the concentration of CS within the tissue. This allows blood vessel and nerve in-growth into the tissue and results in pain (Johnson et al., 2002; Johnson et al., 2005). A similar mechanism may occur at the enthesis in degenerative conditions causing the pain associated with these conditions. However, nerve fibres are also absent at birth, when fibrocartilage and therefore aggrecan is not present. It could therefore be suggested that the precursor region of the enthesis may contain another form of developmental nerve growth inhibitor - such as a member of the semaphorin family (Wright et al., 1995). This may indicate that the absence of nerves is not a consequence of fibrocartilage formation, but a specified adaptation which would parallel the anti-angiogenic activity of endostatin in fibrocartilage (Pufe et al., 2004) or ChM-I in cartilage (Shukunami et al., 2005). Indeed, it may in fact be the anti-angiogenic nature of the tissue that prevents the growth of nerves into the tissue prior to cartilage formation.

Tendon Fibrocartilage

A small amount of fibrocartilage was observed on the superficial surface of the Achilles tendon and the opposing deep surface of the tendon of plantaris (i.e. where this tendon crosses posterior to the Achilles tendon). This is in line with observations made by Rufai et al., (1992). During dorsiflexion, the two tendons become opposed and, like the sesamoid fibrocartilage of the Achilles tendon itself, the tendon cells undergo metaplasia (due to the tensional and compressive forces) so that a fibrocartilaginous region develops (Benjamin and Hillen, 2003; Rufai et al., 1992; Vogel and Koob, 1989). This may indicate why nerve fibres are also absent from the Achilles paratenon in the region where the tendon of plantaris overlies the Achilles tendon.

In aged rats, a further region of fibrocartilaginous developed within the central part of the Achilles tendon – perhaps reflecting the accumulative effect of a lifetime of compressional forces imposed on the tendon. According to Vogel and Koob (1989) such a differentiation reflects metaplasia of the tendon fibroblasts into fibrocartilaginous cells, and thus the secretion of a more cartilage-like matrix which is rich in aggrecan. This matrix has a

greater ability to resist compressive forces. However, fibrocartilaginous formation has also been identified in the tendons following healing (Murrell et al., 1994) and thus an alternative interpretation of this central fibrocartilage is that it represents a pathological response to tendon damage during life.

The thin acellular layer which lines the insertional angle was also devoid of nerve fibres. By virtue of its location, it is possible that this region plays a role in relaying information about changes which occur in the insertional angle between tendon and bone with foot movements. However, it seems more likely that the fat pad is of key importance in this regard. It sits in the insertional angle between the calcaneus and the Achilles tendon, and is richly innervated nerve fibres. However, physiological evidence in support of this role is absent.

The Retromalleolar Fat Pad

The retromalleolar fat pad acts as a variable space filler, moving in and out of the retrocalcaneal bursa during plantar- and dorsiflexion (Canoso et al., 1988; Theobald et al., 2006). The pad itself is formed by a large population of adipocytes which are large globules of lipid surrounded by a thin cytoplasmic envelope (Stevens and Lowe, 2001). As these cells develop, small lipid droplets accumulate and eventually form a large lipid globule, which pushes the nucleus to one side of the cell. In the retromalleolar fat pad, as at most other locations, the adipocytes have a regular, hexagonal shape that reflects the mutual pressure exerted by neighbouring cells on each other (Thompson, 1961). The principle function of the tip of the fat pad, like the other components of the enthesis organ is to dissipate stress away from the tendon-bone interface and as a result reduce wear and tear (Benjamin et al., 2004a; Benjamin et al., 2004b; Theobald et al., 2006). However, Benjamin et al.,(2004b) demonstrated the presence of lamellated corpuscles (encapsulated, receptor nerve endings) in fat associated with other entheses, indicating that the fat pad may also have a proprioceptive function. It could collect information on ankle position which is subsequently relayed to the CNS (Benjamin et al., 2004b). The present immunohistochemical study has confirmed the presence of nerve fibres within the rat retromalleolar fat pad – suggesting that in this animal too, the fat pad may play a similar role.

Two large nerve bundles were identified in the proximal part of the fat pad. On the lateral side of the joint these are most likely sections through the sural nerve, and on the medial side sections through the medial and lateral plantar nerves - branches of the tibial nerve (Greene, 1935). The large nerve bundle in the central part of the fat pad is most likely the peroneal anastomotic branch of the sural nerve (Peyronnard and Charron, 1982). The nerve fibres in the fat pad were either "free" or blood-vessel associated. Some fibres were also present in the tunica media of larger blood vessels. The arborisation and small diameter of the nerve fibres within the fat pad indicates that these nerve fibres terminate within the pad rather than supplying other structures (although this cannot be ruled out). The presence of PGP 9.5 immunoreactive nerve fibres indicates the presence of mechanoreceptive, nociceptive, and autonomic fibres (Doran et al., 1983) in the fat pad. The large number of fibres identified within the fat pad can be compared to those fibres found within Hoffa's fat pad of the knee (Wojtys et al., 1990). This structure has been associated with the painful overuse injury commonly called 'jumper's knee', which mainly affects young active people (Sanchis-Alfonso and Alcacer-Garcia, 2001) and 'anterior knee pain syndrome', a condition in which the number of SP immunoreactive nerve fibres is significantly increased (Witonski and Wagrowska-Danielewicz, 1999). A comparable fat pad has also been identified in the equine distal phalanx. The digital cushion also contains sensory nerve fibres and an extensive capillary network (Bowker et al., 1998). In support of the observations made here, Freeman and Wyke (1967c) described the innervation of the ankle joint in the cat with silver staining. They reported that not only was the joint capsule innervated, but that the fat pad posterior to the joint (the retromalleolar fat pad) also contained many nerve fibres and in particular contained type II encapsulated nerve endings. They believed that these may play an important role in proprioception of the ankle joint (Freeman and Wyke, 1967c).

In an attempt to classify the nerve fibres found in the retromalleolar fat pad, more specific antibodies were used. Polyclonal antibodies against the sensory neuropeptides CGRP and SP demonstrate the presence of thin unmyelinated fibres which convey nociceptive information to the CNS. However, the fibres that are associated with blood vessels are primarily vasoactive and participate in pro-inflammatory mechanisms through direct binding to receptors in the endothelium (Brain, 1997; Brain and Cambridge, 1996; Jorizzo et al., 1983). Although there was no correlation between the number of CGRP and SP fibres, results previously reported with the use of radioimmunoassay suggest that the

concentration of CGRP is greater than SP in the Achilles tendon (Ackermann, 2001). CGRP facilitates the vasodilatory effect of SP in the surrounding nerve fibres (Brain, 1997; Brain and Cambridge, 1996). The population of fibres in the fat pad appeared to increase during growth of the animal up to 4 months (i.e. young sexually mature animals). However, it was not possible to determine if the number of peptidergic nerve fibres decreased in the aged rat. Studies into the somatic innervation of the mystacial fat pad of the skin (Bergman et al., 1999; Fundin et al., 1997) and the distribution of SP and CGRP in the rat urinary bladder (Mohammed and Santer, 2002) suggest that there is a decrease in the population of these fibres with old age. The same developmental observations were made for the polyclonal antibody neurofilament 200. These fibres showed the most obvious decrease in nerve fibre population with old age. These findings are in line with Bergman et al.,(1999) in which mechanoreceptive fibres are preferentially affected by age in comparison to nociceptive/peptidergic fibres. It is suggested that the decrease in the population of sensory fibres is due to age related lesions of these fibres (Bergman et al., 1999).

The neonatal fat pad demonstrated that there were a number of nerve fibres at the tip of the neonatal fat pad. In older animals, fewer fibres were present in the tip and may be due to the compression of the fat pad between the walls of the retrocalcaneal bursa during weight bearing movements in the adult. It has previously been reported that chronic low-level compression of myelinated fibres within cervical nerve roots in man, leads to a decrease in the number of fibres and thinner myelin sheaths (Oishi et al., 1995). These repeated weight bearing movements may also lead to the increasingly fibrous nature of the fat pad with age, therefore demonstrating that the fat pad is susceptible to wear and tear. The fibrous nature was also noted in the human fat pad but to a lesser extent (unpublished observations – H.M. Shaw). This may be due to the more posterior insertion of the Achilles tendon in the rat compared to that in man. It is possible that the fat pad moves further into the insertional angle and experience more compression than it does in man. The fibrous character of the fat pad tip probably enables this part of the fat to act in a similar way to the sesamoid fibrocartilage – i.e. reducing wear and tear.

It is interesting to note that in one specimen (a 4 month rat), there was fibrocartilage formation with a bony core at the tip of the fat pad. This structure may be analogous to an extraskeletal chondrosarcoma as demonstrated by Ly and Bui-Mansfield (2004) in man.

In some of these chondrosarcomas, there are regions of ring or arclike calcifications, similar to those described in the present study. It may thus be considered that the retromalleolar fat pad contains multipotent cells with the ability to transform into a number of other cell types. There is evidence that the infrapatellar fat pad, subcutaneous adipose tissue, and visceral fat deposits contain multipotent stromal cells, which have the ability to differentiate into chondrocytes, osteoblasts, and adipocytes in defined culture medium under specific biophysical factors. Such cells are attracting interest for their potential use in musculoskeletal tissue engineering (Guilak et al., 2004; Tholpady et al., 2003; Wickham et al., 2003).

The presence of mast cells in the fat pad is also intriguing. Several studies have described these cells in close association with the synovial membrane, small blood vessels and peptidergic nerve fibres (Hart et al., 1995) – observations according with those reported here in the retromalleolar fat pad. It is suggested that the release of neuropeptides from primary sensory neurons not only has a vasodilatory affect, but these neuropeptides also have the ability to increase vascular permeability, leading to inflammation and oedema, a process known as neurogenic inflammation which results in peripheral sensitisation of the local nociceptive nerve fibres (Gamse et al., 1987; Lembeck and Holzer, 1979) (Fig 3.4.1.). Peripheral sensitization can also occur through mast cells. SP release can cause mast cell degranulation and therefore the release of histamine - which can also cause stimulation of nociceptive nerve fibers (Brimble and Wallis, 1973; McQueen, 1999; Ninkovic and Hunt, 1985). A more direct route is also present by which the neuropeptides themselves cause peripheral sensitisation of local nerve fibres (Nakamura-Craig and Gill, 1991). It can therefore be hypothesised that under conditions of tissue damage which lead to peripheral sensitization, the retromalleolar fat pad will reduce the range of movement at the ankle to prevent further damage to the region.

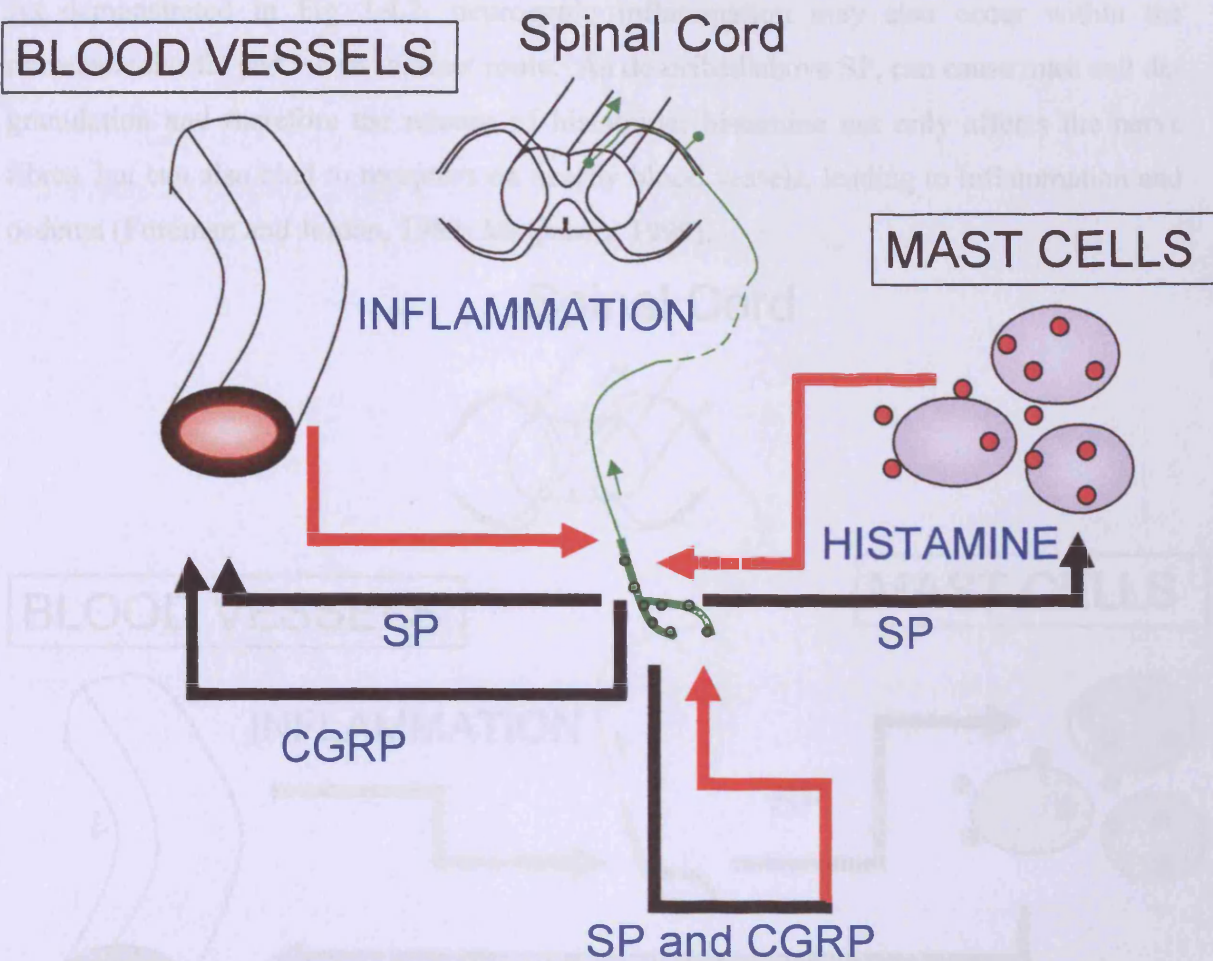


Figure 3.4.1. The peripheral release of substance P and/or calcitonin gene related peptide (black arrows) from nociceptive nerve endings under conditions of tissue damage can lead to stimulation/sensitisation (red arrows) of nociceptive nerve fibres (green fibres) via several different pathways. A) SP and CGRP can directly cause peripheral sensitization of the nerve fibres. B) SP release can cause mast cell de-granulation and therefore the release of histamine which in turn can stimulate nociceptive nerve fibres. C) Blood vessels are also affected by SP and CGRP. These neuropeptides cause vasodilation and increased vascular permeability resulting in oedema, inflammation and peripheral sensitisation of the nerve fibre.

It has even been identified that selective lesioning of unmyelinated primary sensory afferent or sympathetic postganglionic neurones can lead to a significant decrease in the number of mast cells. Therefore mast cell density may be affected by the number of active unmyelinated afferent and sympathetic postganglionic neurones (Levine et al., 1990). It has been hypothesized by Freemont et al., (2002a) that the increased number of mast cells in the diseased intervertebral disc may play a role in chronic low back pain.

As demonstrated in Fig 3.4.2. neurogenic inflammation may also occur within the retromalleolar fat pad via an indirect route. As described above SP, can cause mast cell degranulation and therefore the release of histamine; histamine not only affects the nerve fibres, but can also bind to receptors on nearby blood vessels, leading to inflammation and oedema (Foreman and Jordan, 1983; McQueen, 1999).

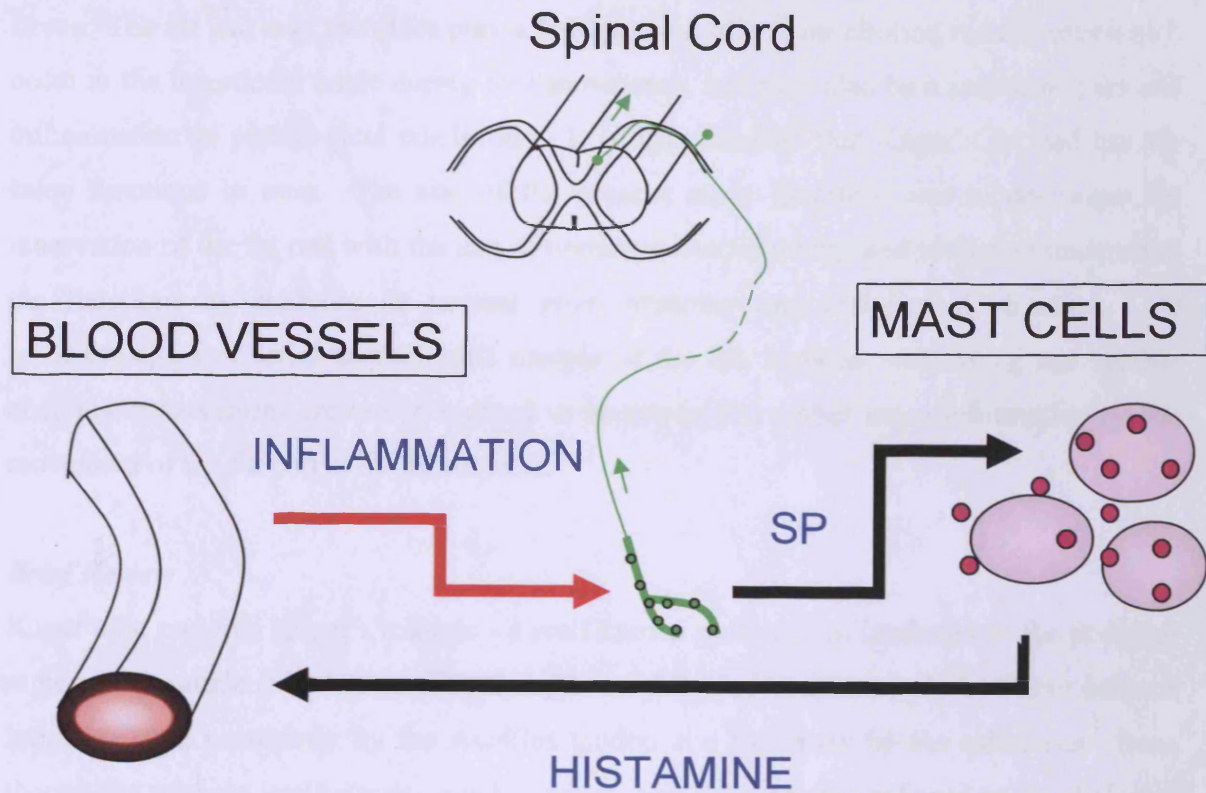


Figure 3.4.2. Neurogenic inflammation via mast cell degranulation.

Mast cells were also identified within the large peripheral nerves of the fat pad; their function in the nerve trunk is difficult to define although it should be noted that they have been identified in nerve tumors, neurofibromas and neurofibromatosis (Viskochil, 2003).

In conclusion, it is suggested that the fat pad of the rat Achilles tendon enthesis organ has unheralded proprioceptive and nociceptive roles which monitor changes in the insertional angles between tendon and bone occurring as a result of foot movements. The presence of mast cells and neuropeptide containing nerve fibres, within the retromalleolar fat pad, suggests a potential role in a neurogenic inflammatory response and peripheral sensitization – possibly restricting movement and causing pain when the region is injured.

4. ANATOMY AND INNERVATION OF KAGER'S FAT PAD

4.1. INTRODUCTION

The results presented in chapter 3 demonstrated that the retromalleolar fat pad associated with the enthesis organ of the rat Achilles tendon is highly innervated with sensory nerve fibres. The fat pad may therefore play a fundamental role in monitoring the changes which occur at the insertional angle during foot movement, and may also be a source of pain and inflammation in pathological conditions. It is hypothesised that Kager's fat pad has the same functions in man. The aim of the present study therefore was to determine the innervation of the fat pad with the use of immunohistochemistry, and to further understand the functions by studying its normal gross anatomy and histological structure. 3D reconstructions of serial sagittal MRI images of the fat, together with living and surface anatomy observations are also presented in an attempt to gather more information on the movement of the fat pad in living subjects.

Brief Review

Kager's fat pad fills Kager's triangle - a well known radiological landmark in the posterior region of the ankle (Fig 4.1.1.). The triangle itself is bordered anteriorly by flexor hallucis longus (FHL), posteriorly by the Achilles tendon and inferiorly by the calcaneus. Even though the triangle itself attracts much interest, and is commonly referred to by clinicians when evaluating problems with the ankle joint and its associated tendons (Ly and Bui-Mansfield, 2004) little attention has been paid to the fat pad itself. As a result, an extensive study was carried out on the fat pad by Theobald et al. (2006). With the use of MRI, ultrasonography, and routine histology, the pad is described as a large wedge of adipose tissue, divided into 3 regions (Figure 4.1.2). These regions are named in accordance with the structures to which they are most closely associated - a large, superficial 'Achilles-associated part', a deep 'FHL-associated part', and a 'calcaneal bursal wedge' or tongue. Theobald et al., (2006) demonstrated that the FHL-associated part of the pad was enclosed within the fascial sheath of FHL and extended beneath the Achilles-associated region to merge with the calcaneal wedge, giving it an inverted J shape. Part of the Achilles-associated region is also enclosed by the false tendon sheath - the paratenon - of the Achilles tendon (Ly and Bui-Mansfield, 2004; Theobald et al., 2006). It was suggested that the enclosure of the fat within the tendon sheath prevents excessive movement of the pad. This stabilisation is especially required in the Achilles-associated region, where numerous

blood vessels pass through it to vascularise the Achilles tendon and the pad itself. Fibrous strands are also present to further anchor the Achilles-associated region to the tendon itself (Theobald et al., 2006).

Of particular interest is the way in which the fat pad moves. Ultrasonography clearly demonstrates that during plantar flexion, the insertional angle of the Achilles tendon increases and the wedge-like tip of the fat pad moves to fill the retrocalcaneal bursa. This movement is facilitated by hyaluronic acid which is secreted by the bursal synovium (Ly and Bui-Mansfield, 2004).

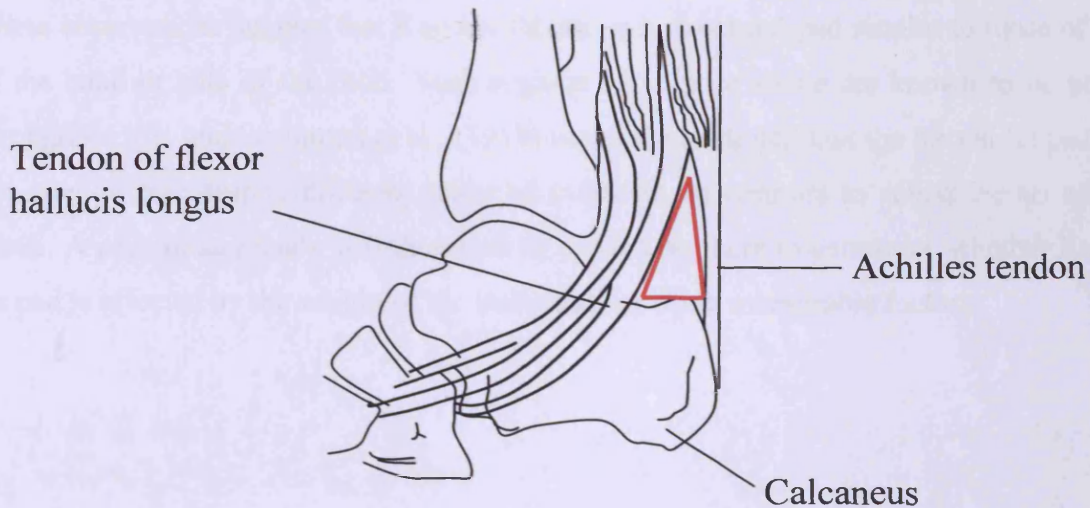


Figure 4.1.1. Kager's triangle (red) is bordered inferiorly by the calcaneus, and the Achilles tendon and the tendon of flexor hallucis longus form the sides of the triangle. Kager's fat pad is located within Kager's triangle (Ly and Bui-Mansfield, 2004)

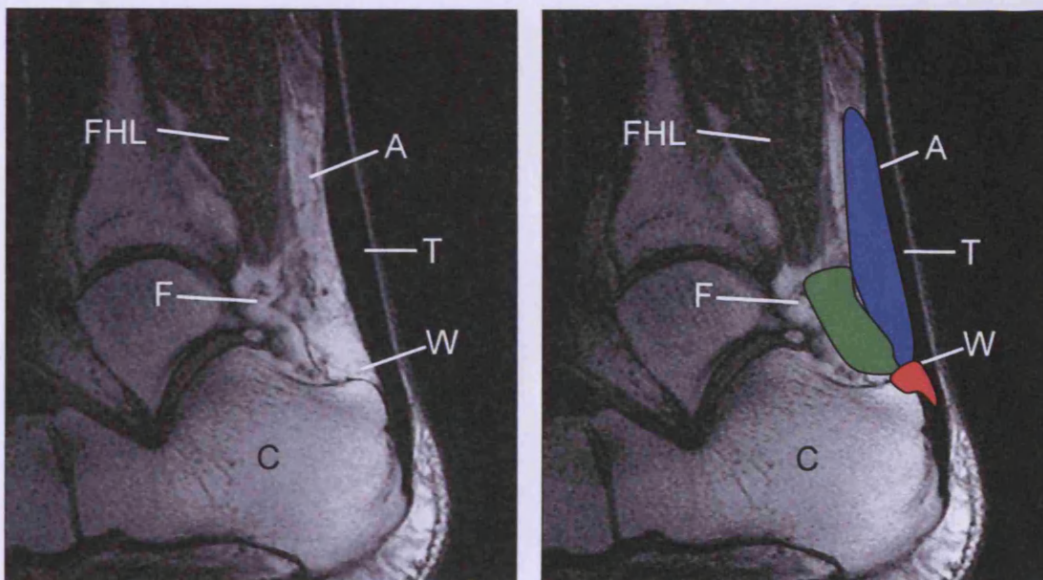


Figure 4.1.2: MRI images demonstrating Kager's pad and its identified regions. Each region is identified by the structure to which it are most closely associated. A : blue- Achilles-associated region, T -Achilles Tendon, W : red- Calcaneal bursal wedge, S – Superior tuberosity, C – Calcaneus, F : green- Flexor hallucis longus (FHL) associated region (Images provided by Prof. G. Bydder).

Theobald et al., (2006) discussed how movement of the pad may occur. Several possibilities were suggested: its movement may simply be a passive consequence of the upward movement of the calcaneus, or the pad may be sucked into the retrocalcaneal space to prevent pressure changes. It is also possible that muscular contraction may play a role in movement. One or possibly a combination of these factors may facilitate movement of the fat pad (Theobald et al., 2006). Theobald et al., (2006) highlight the importance of maintaining normal movement of the fat pad into the bursa, and therefore advise caution during surgical operations on this region to prevent adhesion formation.

These observations suggest that Kager's fat pad is a structural pad similar to those of palm of the hand or sole of the foot. Such regions of adipose tissue are known to be present throughout life, and Scammon et al., (1919) have demonstrated that the buccal fat pad does not alter in size despite different states of nutrition, in contrast to subcutaneous adipose tissue. A preliminary study will therefore be carried out here to determine whether Kager's fat pad is affected by the weight of the individual or other measurable factors.

4.2. MATERIALS AND METHODS

4.2.1. Routine Histology

To examine the general anatomy of Kager's fat pad, specimens were acquired for routine histology from dissecting room cadavers which were fixed using an ethanol/phenol/formaldehyde solution. Cadavers were donated to Cardiff University for the purposes of Anatomical investigation under the provision of the 1984 Anatomy Act and the 2004 Human Tissues Act. The central third of the Achilles tendon enthesis, along with its associated fat pad, was removed from cadavers aged 63-87 years. A number of samples had been previously prepared for histology for other purposes by Dr Koji Hayashi. Biopsy samples of Kager's fat pad were acquired from patients with symptoms of retrocalcaneal bursitis by Professor Tsukasa Kumai (Nara Medical University, Japan) during resection of the retrocalcaneal bursa and processed histologically, and digital images of these sections were used in this study. For full details of histological processing see chapter 2.

6.2.2. Macroscopic Images

The gross anatomy of the tip of Kager's fat pad was captured using a Canon IXUS55 digital camera (Canon (UK) Ltd, Surrey, UK).

6.2.3. Immunohistochemistry

Source of Material

To examine the innervation of Kager's fat pad, the pad itself in association with the Achilles tendon insertion was obtained from 10 cadavers of both sexes, at various ages, as soon as possible after death – from the Department of Forensic Medicine at the Ludwig-Maximilians-Universität, in accordance with the ethical regulations of Munich University.

Dissection Procedure

Specimens were fixed in 90% methanol (Fisher Scientific, Loughborough, UK) at 4°C for up to 7 days. The fat pad was then removed carefully with the use of scalpel and forceps from the deep surface of the Achilles tendon and the calcaneus ensuring that the tip of the fat pad remained intact (Fig 4.2.1).



Figure 4.2.1: The tip of the fat pad protruding into the retrocalcaneal bursa was removed from the specimen

Sectioning Procedure

Specimens were soaked in 10% PB sucrose solution overnight, prior to cryosectioning. Material was subsequently frozen onto a cryostat chuck and sagittal sections of the fat pad were then cryosectioned at 12 μ m using disposable blades on a Microm cryostat (HM560, Walldorf, Germany). The sections were collected on Histobond slides (RA Lamb Medical Supplies, Eastbourne, UK) and stored at -20°C for subsequent immunolabelling (see chapter 2 for further details).

Labelling

Sections were labelled with the antibodies; PGP 9.5, NF200, SP and CGRP and subsequently developed with either FITC-conjugated Fab fragments or avidin-biotin substrates. Visualisation of the primary labelling was achieved with either NovaRED or DAB (see chapter 2 for further detail).

4.2.4. Magnetic Resonance Images and 3D Reconstructions

MRI Images

Magnetic Resonance Images were obtained by Professor Graeme Bydder (University of California San Diego - Radiology). Three healthy volunteers (31-60 years) were studied on a 1.5T magnetic resonance scanner (Siemens, Erlangen, Germany). Multi-slice, T1-weighted non-fat saturated conventional spin-echo images (TR = 500 msec, TE = 16 msec, 1 mm slice thickness, 448 x 384 matrix, field of view 107 mm) were performed in the sagittal plane at varying degrees of dorsi- and plantar flexion.

3D Reconstructions

The serial MRI images were subsequently used to create three dimensional images of the hindfoot with the use of Reconstruct - a free reconstruction software download (Fiala, 2005).

4.2.5. Kager's Fat Pad Measurements

Cadavers were visually assessed by the amount of abdominal adipose tissue and classes as 'normal', 'underweight', or 'overweight'. The height and foot length of each cadaver was also recorded and Kager's fat pad was carefully dissected and weighed using electronic scales (CT200-S; OHAUS corporation, Florham park, N.J., USA). The volume of the fat pad was measured by water displacement in a Kartell[®] graduated measuring cylinder (Kartell Spa, Noviglio, Italy). The data obtained was then analysed with the used of Microsoft[®] Office Excel (2003), GraphPad Prism (version 2.01) and MINITAB (version 14).

4.3. RESULTS

Gross Anatomy and Histological Structure

The location of Kager's fat pad is shown in Figs 4.3.1.A-E. It lies in the posterior region of the ankle, filling the space between the Achilles tendon and the posterior border of FHL, to the superior surface of the calcaneus where it sends a tongue-like protrusion into the retrocalcaneal bursa. The fat itself is relatively fibrous in texture, in comparison to the greasy lobular fat found in other locations of the body – e.g. the abdominal cavity. During dissection of the fat pad, it was observed that the tip of the fat pad varied greatly between specimens (Fig 4.3.2.A-E). In some specimens the tip was relatively uniform in shape with a smooth rounded appearance (Fig 4.3.2.A). However in others, the fat pad was flattened and had a feathered appearance at its tip (Fig 4.3.2.B) or had distinct clefts which generated several discrete adipose tissue protrusions (Fig 4.3.2.C-E).

The normal histological structure of the Achilles tendon enthesis organ (Fig 4.3.3) demonstrated a structure that was composed of 3 fibrocartilages, the enthesis fibrocartilage at the attachment of the Achilles tendon to the calcaneus, a periosteal fibrocartilage covering the superior tuberosity, and a sesamoid fibrocartilage in the deep surface of the Achilles tendon. The sesamoid and periosteal fibrocartilages form the walls of the retrocalcaneal bursa, which was bordered proximally by a synovial covered protrusion of adipose tissue from Kager's fat pad. This is the focus of the current study.

During gross dissection of the fat pad, a large number of tortuous blood vessels were observed in the proximal, Achilles-associated region of the fat pad (Fig 4.3.1.B). Furthermore routine histology showed that a large anastomosing capillary network was present within the bursal-wedge (Fig 4.3.4.A). At high magnification, these capillaries could be seen to pass through small clefts between individual adipocytes (Fig 4.3.4.B). In a number of cadavers, the tip of the fat pad contained a particularly dense population of blood vessels in close association with the synovial membrane (Fig 4.3.4.C). In many individuals, the synovial membrane was infolded, forming synovial villi (Fig 4.3.4.C) - such villi were not identified in the tip of the fat pad in the rat (Fig 4.3.1.P - Chapter 3). The fat itself had a 'honeycomb' appearance, with fibrous strands, of varying thicknesses, coursing throughout the fat pad (Fig 4.3.4.D). These fibrous strands occasionally contained

elastic fibres (Fig 4.3.4.E and F). Such fibres were also identified in the walls of large arteries within the fat pad (Fig 4.3.4.G.).

A number of large nerve bundles were also seen within Kager's fat pad in routine histological sections (Fig 4.3.4.H). A Pacinian corpuscle (Fig 4.3.5.B), which was readily recognisable by its distinctive, onion-like appearance was seen in the loose connective tissue (paratenon) superficial to the Achilles tendon enthesis in one cadaver. In this particular specimen, a prominent bony spur was also present within the tendon (Fig 4.3.5.A).

Histopathology

Histological analysis of cadaveric specimens highlighted the presence of a number of pathologies and anatomical variations associated with Kager's fat pad. A number of specimens contained cartilage-like regions in the wedge-like tip of the fat pad, often on its synovial surface (Fig 4.3.5.C). The cells within these cartilaginous structures were rounded and demonstrated a strongly-staining pericellular matrix (Fig 4.3.5.C and D). Fibrous adhesions were also seen in a number of specimens. Fig 4.3.5.E. illustrates such an adhesion between the periosteal fibrocartilage and the Achilles tendon – with the adhesion crossing the retrocalcaneal bursa. These adhesions may simply bridge the gap between the two structures (Fig 4.3.5.E) as seen here or completely obliterate the bursa (not shown). The adhesions appeared to be principally fibrous in structure, and contained several blood vessels - some of which were present at the attachment of the adhesion to the Achilles tendon (Fig 4.3.5.F and G). At this attachment, fibrous strands of the adhesion can be seen to penetrate into the tendon itself (Fig 4.3.5.F). A cartilaginous-like region was also present within the central part of the adhesion (Fig 4.3.5.G and H) - this region contained rounded cells and the collagen fibre organisation was less conspicuous (Fig 4.3.5.H.). One of the most unusual variations seen in these specimens was the presence of an accessory tendon, which originated from the Achilles tendon and passed through Kager's fat pad to insert into the periosteal fibrocartilage on the superior tuberosity of the calcaneus (Fig 4.3.6.A and B).

A frequent observation was the invasion of part of Kager's fat pad into the deep surface of the Achilles tendon (Fig 4.3.6.C-E). Blood vessels were usually present within this invading tissue (Fig 4.3.6.C and E). In every specimen, the region of invagination was

consistent - proximal to the deep part of the insertion of the tendon where the synovial membrane reflects back on itself. In a number of these specimens, the blood vessels could be followed from these vascular invasions into the enthesis fibrocartilage (Fig 4.3.7.A.). In other specimens, where the blood vessels could not be seen to invade into the Achilles tendon from the fat pad, blood vessels could still occasionally be found in the enthesis fibrocartilage (not shown). Furthermore, toluidine blue staining was considerably weaker around invading blood vessels compared to the rest of the fibrocartilage (Fig 4.3.7.A).

In addition to the anatomical variations and histopathologies observed in association with the fat pad, histopathological features of the enthesis fibrocartilage were also observed. Fibrocartilage cells in the periosteal and enthesis fibrocartilage (Fig 4.3.7.B) were often hypertrophied or grouped into clusters. Such changes were also observed in the insertional angle of the enthesis (Fig 4.3.7.C). A local absence of the periosteal fibrocartilage was also noted in one cadaver – the tissue being replaced by a collection of adipocytes (Fig 4.3.7.D). Local inflammatory reactions appeared to be rare in the specimens examined. Only one specimen demonstrated the presence of mast cells within the loose connective tissue surrounding the paratenon (Fig 4.3.7.E).

Biopsy Samples from Patients with Retrocalcaneal Bursitis

Biopsy samples taken from patients with Haglund's deformity and symptoms of retrocalcaneal bursitis, demonstrated the presence of a large number of lymphocyte infiltrates within the fat pad and in several cases these cells formed dense nodules (Figs 4.3.8.A-C). Lymphocytes were also particularly prominent in the synovial and sub-synovial layers of the fat pad (Figs 4.3.8.B and D).

MRI Images and 3D Reconstructions of the Hindfoot

MRI images and 3D reconstructions of the hindfoot showed that the fat pad was compressed during foot movements. During plantarflexion, the calcaneal bursal-wedge was compressed by the superior tuberosity of the calcaneus. At the same time, the insertional angle of the tendon increases, allowing the tip of the fat pad to fill the retrocalcaneal space. Additionally, the proximal region of the 'FHL-associated part' of the fat pad is compressed by FHL during plantarflexion (Fig 4.3.9.A and C). During dorsiflexion, the 'bursal wedge' is pushed back out of the retrocalcaneal bursa as the calcaneus returned to a more horizontal position and the 'FHL associated region' was also

released from compression. However, in both positions of the foot, the 'Achilles-associated part' of the pad appeared to retain its position relatively unchanged, although it was slightly compressed by FHL (Fig 4.3.9.A).

The 3D reconstructions also highlighted the fact that during plantarflexion, the Achilles tendon itself flexed and the mid-substance of the tendon become concave (Fig 4.3.9.A and D and Fig 4.3.10). Twisting of the Achilles tendon was also seen in the reconstructions (Fig 4.3.9.D) and it was further evident that the tip of the fat pad varied in shape between individuals. Some fat pad tips had obvious lateral protrusions (Fig 4.3.9.B - bottom), while others had a more uniform shape across the width of the fat pad (Fig 4.3.9.B - top).

As illustrated in Fig 4.3.10, the Achilles tendon also undergoes marked changes in form during foot movement. The negative MRI images illustrate that from 2° (top) to 52° (bottom) of plantarflexion the Achilles tendon becomes concave, while the angle of insertion of the Achilles tendon remained the same.

Surface Anatomy of the Hindfoot

From a medial viewpoint it was clear that the Achilles tendon flexes, to become concave during plantarflexion (Fig 4.3.11.A), while from a posterior aspect, it was evident that the fat pad bulges laterally (Fig 4.3.11.E and F). During dorsiflexion from a posterior view, the flaring of the Achilles tendon at its attachment was particularly apparent (Fig 4.3.11.E and F).

Anthropometric Analysis

Comparisons between males and females in the 'normal group' demonstrated a large degree of variation between the size of the fat pad in different subjects (See Table 4.3.1). The size of the female fat pad varied to the greatest degree (between 5.94g and 16.75g). The size of the male fat pad also varied – but to a lesser extent (between 12.59g and 17.58g). There was no significant difference ($p=0.588$) in the weight of the fat pad between the sexes in the 'normal' weight group (Fig 4.3.12.A). Furthermore, there was no significant difference ($p=0.747$) in the weight of the fat pad between the three different weight groups (Fig 4.3.12.B).

Normal				
Sex	Weight of fat pad - g	Volume -ml	height -cm	foot length - cm
Male	12.59	15	184	27
Male	17.58	20	180	26
Male	13.5	10	178	25
Male	15.3	15	184	26
Female	13.42	20	170	23
Female	16.75	19	161	23
Female	5.94	4	163	23
Female	17.6	20	175	23

Overweight				
Sex	Weight of fat pad - g	Volume - ml	height - cm	foot length - cm
Male	37.42	40	171	26
Male	15.99	10	181	25.5
Female	7.06	5	166	26

Underweight				
Sex	Weight of fat pad - g	volume -ml	height - cm	foot length - cm
Male	22.02	25	176	27
Female	4.29	4	150	21
Female	9.91	10	155	24

Table 4.3.1: Measurements taken from dissecting room cadavers for anthropometric evaluation of Kager's fat pad

However there were correlations between several of the measurements made, irrespective of the sex or weight group. There was a strong positive correlation between the height and foot length of subjects used in this study (Fig 4.3.13.A). Weak positive correlations were also observed between: (a) individual height and weight of the fat pad (Fig 4.3.13.B), (b) individual height and volume of the fat pad (Fig 4.3.13.C), (c) foot length and weight of the fat pad (Fig 4.3.13.D), (d) foot length and volume of the fat pad (Fig 4.3.13.E). Furthermore there was a strongly positive correlation between the weight and volume of the fat pad in the subjects studied (Fig 4.3.13.F).

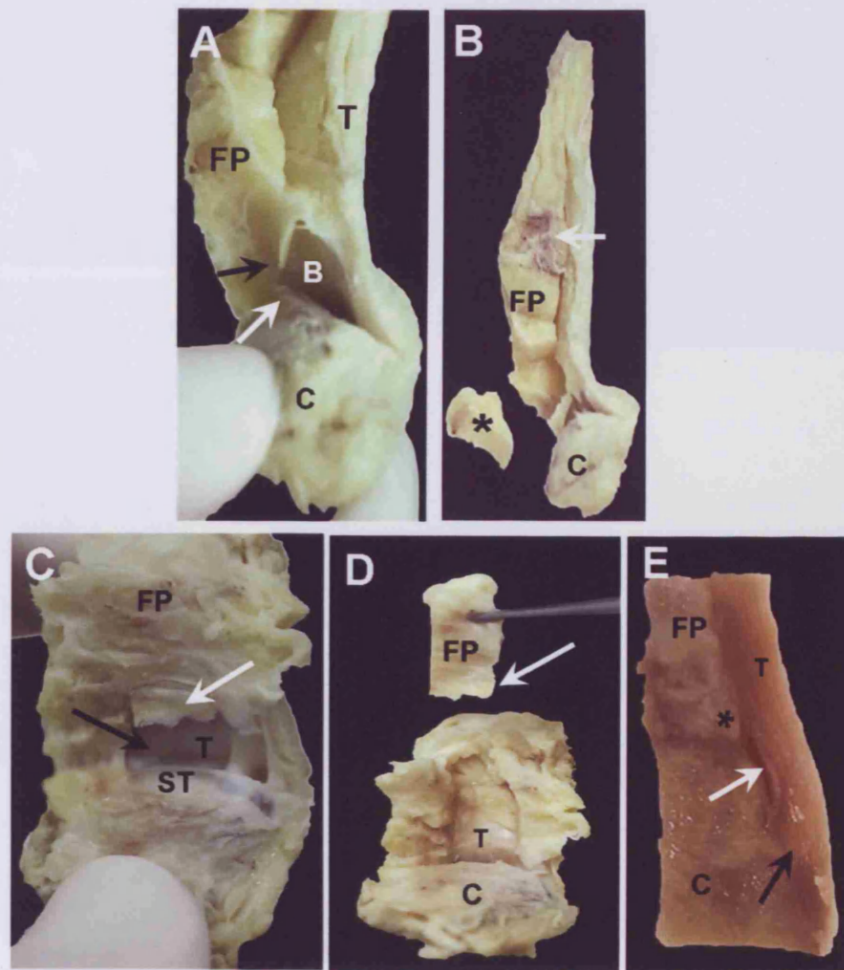
Immunohistochemistry

Nerve fibres and bundles were present within the wedge-like tip of Kager's fat pad in all 10 cadavers examined. In many of the larger nerve bundles, it was possible to see individual fibres running within them (Fig 4.3.14.A and B). Some of these nerves formed neurovascular bundles within the fat pad (Fig 4.3.14.A). Individual nerve branches were also identified. These fibres were either 'free' (Fig 4.3.14.C) or associated with blood

vessels (Fig 4.3.14.D). The 'free' nerve fibres passed through the fat pad by running within the clefts between adjacent adipocytes, while other nerve fibres were present in close association with the connective tissue strands. Nerve fibres were also identified within the walls of larger blood vessels. Structures resembling encapsulated nerve endings were also present within the 'bursal-wedge' of the fat pad (Fig 4.3.14.E). A central nerve fibre, immunoreactive to PGP 9.5, was surrounded by several layers of connective tissue (Fig 4.3.14.E).

NF200 immunoreactive nerve fibres were distributed throughout the wedge-like tip of Kager's fat pad. Large nerve bundles were present (Fig 4.3.15.A) within the fat pad, as were small branches which weaved through the clefts between adjacent adipocytes (Fig 4.3.15.B and C). Many of these nerve branches were associated with blood vessels (Fig 4.3.15.D and E). Some of these nerves lay adjacent to small capillaries which interweaved between neighbouring adipocytes (Fig 4.3.15.D). Nerve branches were also identified in close association with fibrous strands which ran throughout the bursal-wedge of the fat pad (Fig 4.3.15.F). Both immunofluorescence and immunoperoxidase labelling demonstrated the presence of SP containing nerve fibres within the bursal-wedge of Kager's fat pad. Labelling demonstrated that larger nerves contained only a small population of nerve fibres immunoreactive to SP, while a large population did not (Fig 4.3.16.A). This reflects the small number of SP containing nerve fibres found within the pad itself in comparison to PGP 9.5 labelled fibres. Nerve fibres were also a feature of the tunica adventitia of large blood vessels (not shown). A small number of nerve branches weaved between the cell membranes of adjacent adipocytes (Fig 4.3.16.B). The distribution of nerve fibres labelled positively for CGRP was very similar to that of SP labelled nerve fibres. CGRP positive fibres were either blood vessel associated (Fig 4.3.16.C) or 'free' (Fig 4.3.16.D). Negative controls incubated without the primary antibodies indicate that there was no non-specific binding of the secondary antibody to the tissue (Fig 4.3.16.E and F). Rabbit IgGs applied to the sections in place of the primary antibody, indicates that there was no non-specific labelling of the primary antibody (Fig 4.3.16.C).

Figure 4.3.1.



ACHILLES TENDON ENTHESIS ORGAN IN MAN - GROSS ANATOMY

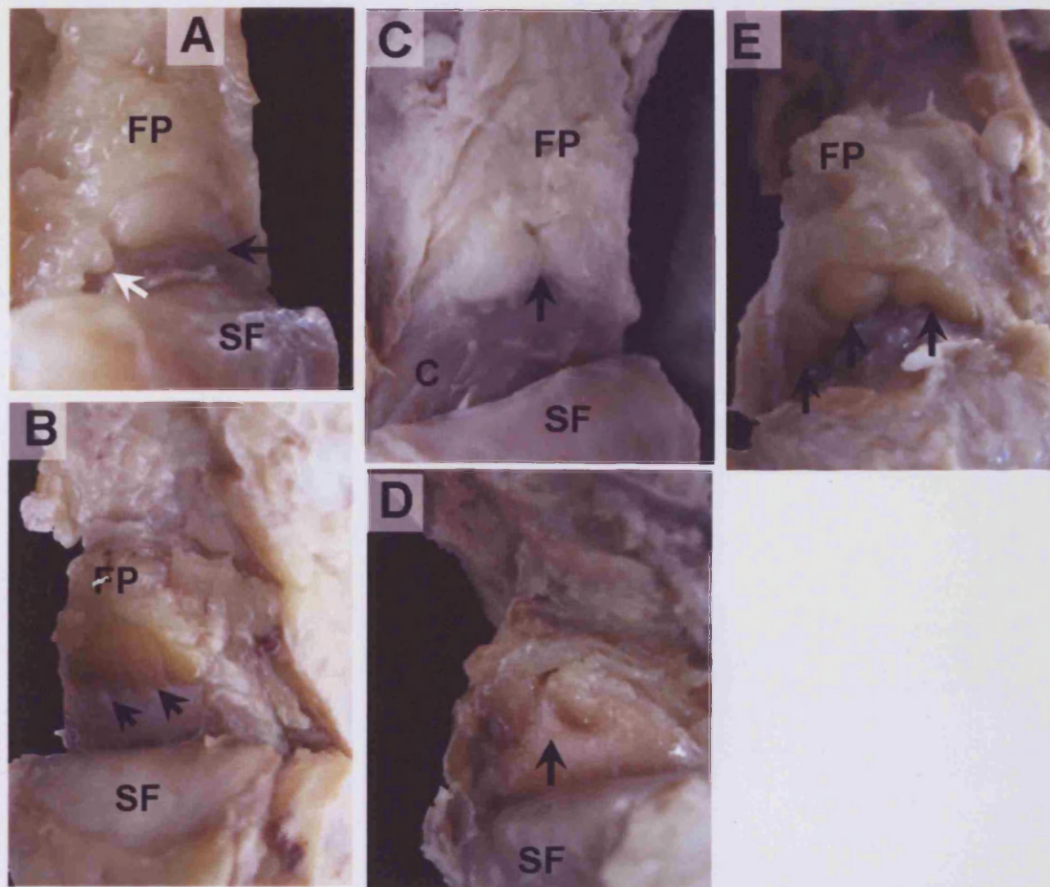
Figure A: Ventral-lateral view of the Achilles tendon (T) insertion. Note the pronounced superior tuberosity (white arrow) of the calcaneus (C) and the protruding tip (black arrow) of the fat pad (FP) which moves in and out of the retrocalcaneal bursa (B).

Figure B: Lateral view of the Achilles tendon insertion. White arrow indicates a number of tortuous blood vessels present in the Achilles associated part of the fat pad (FP). The bursal-wedge of the fat pad (*) was removed for immunohistochemistry. C—calcaneus.

Figure C and D: Ventral view of the Achilles tendon insertion. (C) Black arrow indicates the retrocalcaneal bursa between the Achilles tendon (T) posteriorly and the superior tuberosity (ST) of the calcaneus (C). White arrow indicates the tip of the fat pad (FP). (D) The bursal-wedge of the fat pad used for immunohistochemistry. Note the irregular shape of the tip of the fat pad (white arrow).

Figure E: Sagittal section through the attachment (black arrow) of the Achilles tendon (T) to the calcaneus (C). The tip (*) of the fat pad (FP) moves into the retrocalcaneal bursa (white arrow) during plantarflexion.

Figure 4.3.2.



GROSS ANATOMICAL VARIATIONS OF THE TIP OF KAGER'S FAT PAD PROTRUDING INTO THE RETROCALCANEAL BURSA IN MAN

(Dissecting room cadavers)

Figure A: The tip of Kager's fat pad (FP) in this subject is formed by a large, rounded protrusion (yellow arrow). A small protrusion (white arrow) was also present on the lateral side of the pad. SF-sesamoid fibrocartilage.

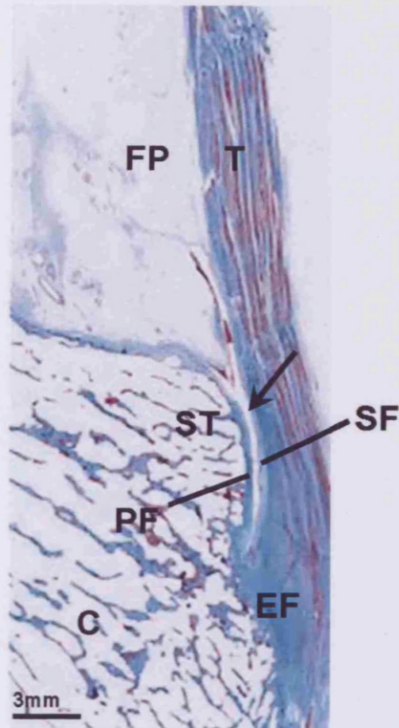
Figure B: The tip of Kager's fat pad. In this subject the tip of Kager's fat pad was formed by a single more flattened protrusion with several feathery slips extending from it into the bursa (yellow arrows). The smooth surface of the sesamoid fibrocartilage (SF) was noticeable during dissection.

Figure C: The tip of Kager's fat pad protruding into the retrocalcaneal bursa. Note that the tip of the fat pad was divided into two large rounded prongs by a large centrally located cleft (arrow). C-calcaneus.

Figure D: The tip of Kager's fat pad in this subject was divided into two uneven-protrusions by a wide cleft (arrow). Note the flattened nature and dark yellow colour of the tip.

Figure E: The tip of Kager's fat pad was formed in this subject by 3 distinct, rounded projections (arrows). The synovium covering the tip of the fat pad was particularly obvious.

Figure 4.3.3.



A sagittal-section through the attachment of the Achilles tendon enthesis organ in Man. The Achilles tendon (T) attaches to the distal part of the calcaneus (C) via the enthesis fibrocartilage (EF). The prominent superior tuberosity (ST) of the calcaneus is covered by a periosteal fibrocartilage (PF), which is opposed by a sesamoid fibrocartilage (SF) in the deep surface of the Achilles tendon. The two fibrocartilages are separated by the retrocalcaneal bursa (arrow), into which protrudes the tip of Kager's fat pad (FP) which is covered by a synovial lining. Masson's Trichrome. Scale bar = 3mm.

KAGER'S FAT PAD IN MAN – SAGITTAL ROUTINE HISTOLOGICAL SECTIONS

Figure A: A low power view of the bursal-wedge of the fat pad (FP). A large network of small capillaries (black arrows) and arteries (blue arrow) were located throughout the fat pad. Masson's trichrome. Scale bar = 500µm.

Figure B: A thin walled capillary (arrows) containing red blood cells in the bursal-wedge of Kager's pad. Note the way the capillary passes between adjacent adipocytes (A) and branches around them. Masson's trichrome. Scale bar = 200µm.

Figure C: The synovial lined tip of the fat pad. The synovial membrane of the fat pad was highly convoluted forming prominent synovial villi (arrows). Note the large population of blood vessels (*) within the villi, beneath the synovial membrane. Masson's trichrome. Scale bar = 200µm.

Figure D: Kager's fat pad contained groups of adipocytes (A) separated by fibrous strands. The size of these strands varies from small thin slips (red arrow) to thick collagenous bundles (black arrow). Masson's trichrome. Scale bar = 200µm.

Figure E and F: Kager's fat pad stained with Van Gieson's elastic stain. Elastic fibres (arrows) were stained black, illustrating their association with the fibrous connective tissue in the fat pad. Scale bar=100µm.

Figure G: A large blood vessel within Kager's fat pad stained with Van Gieson's elastic stain. Elastic fibres (arrows) were present in the internal elastic lamina. Scale bar = 100µm.

Figure H: An oblique section through a nerve bundle within the bursal-wedge of Kager's fat pad. The nerve was surrounded by a thick connective tissue sheath (arrow). Masson's Trichrome. Scale bar = 100µm



Figure 4.3.4.

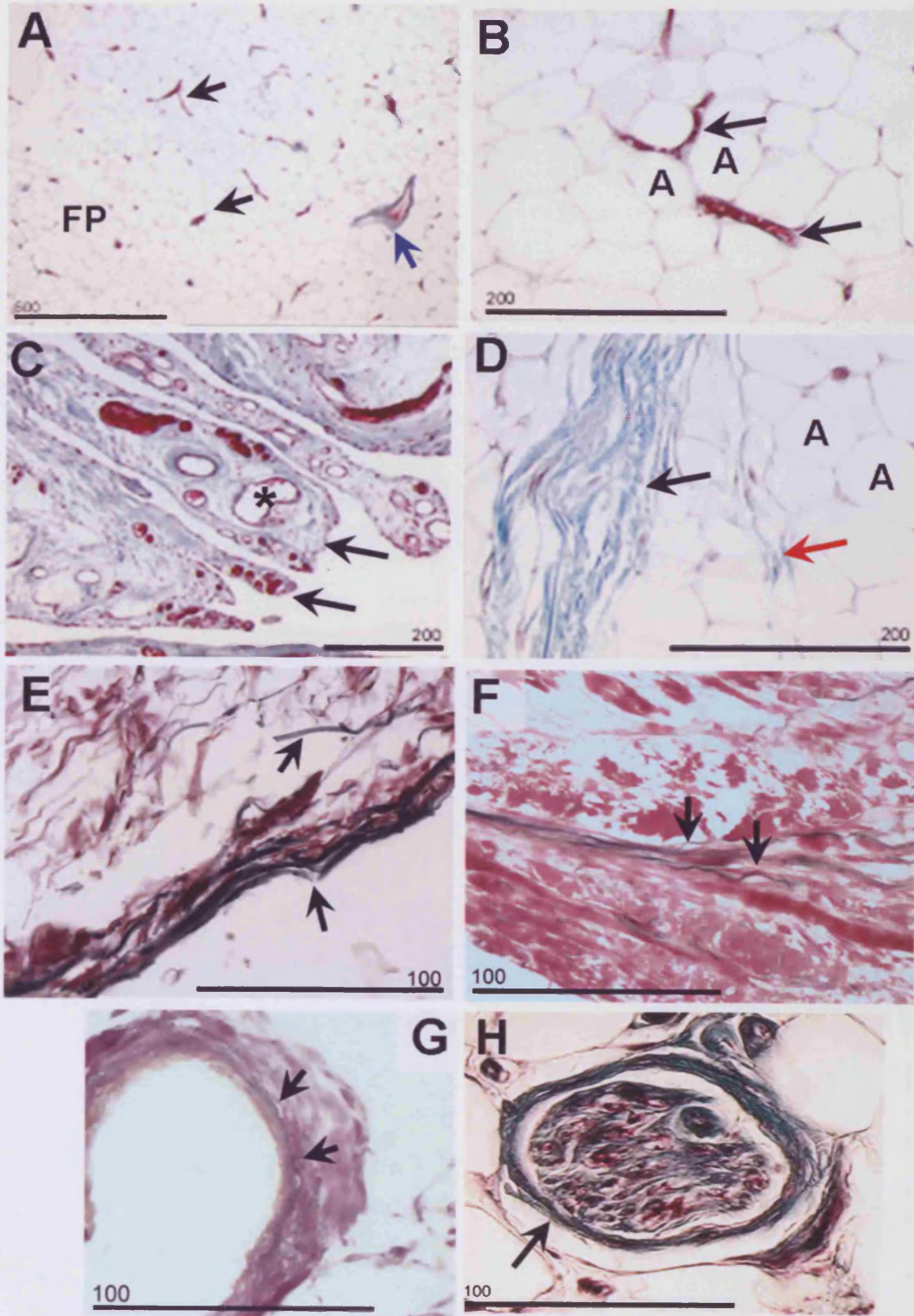


Figure A: A low-power view of the Achilles tendon insertion. Arrow indicates a large bony spur within the enthesis fibrocartilage. The black box highlights the location of the Pacinian corpuscle imaged in Fig 6.4.5.B. Masson's Trichrome.

Figure B: A Pacinian corpuscle located in the connective tissue on the posterior surface of the Achilles tendon. Note the large number of concentric fibrous lamellae which form this distinctive encapsulated nerve ending. Masson's trichrome. Scale bar = 400µm.

Figure C: A cartilage-like structure in the tip of Kager's fat pad adjacent to the Achilles tendon. Note the rounded nature of the cells within this structure (arrows). Masson's trichrome. Scale bar = 200µm.

Figure D: A toluidine blue-stained section of the cartilage-like structure in (C). Note the dark pericellular staining of its cartilage-like cells. Scale bar = 200µm.

Figures E-H: Sagittal histological sections through an adhesion between the Achilles tendon and periosteal fibrocartilage (alcian blue)

Figure E: A low-power view of the adhesion between the Achilles tendon (T) and the periosteal fibrocartilage (PF). The adhesion passes through the retrocalcaneal bursa (RB). The fat pad (FP) lies proximal to the adhesion. Scale bar=1000µm.

Figure F: The attachment of the adhesion (A) to the Achilles tendon (T). At the attachment, the adhesion fans out to increase the area of the attachment to the tendon, which is facilitated by a number of fibrous strands (*). Note the presence of blood vessels close to the attachment site. Scale bar = 300µm.

Figure G: The central part of the adhesion (A) crossing the retrocalcaneal bursa. A number of venules (arrows) were located within the adhesion, in addition to a small fibrocartilaginous structure (*). Scale bar = 200µm.

Figure H: High power view of the fibrocartilaginous region highlighted (*) in Figure 6.4.5.G. Arrows indicate rounded cells located within this structure. Note the reduced fibrillar nature. Scale bar = 200µm.

Figure 4.3.5.

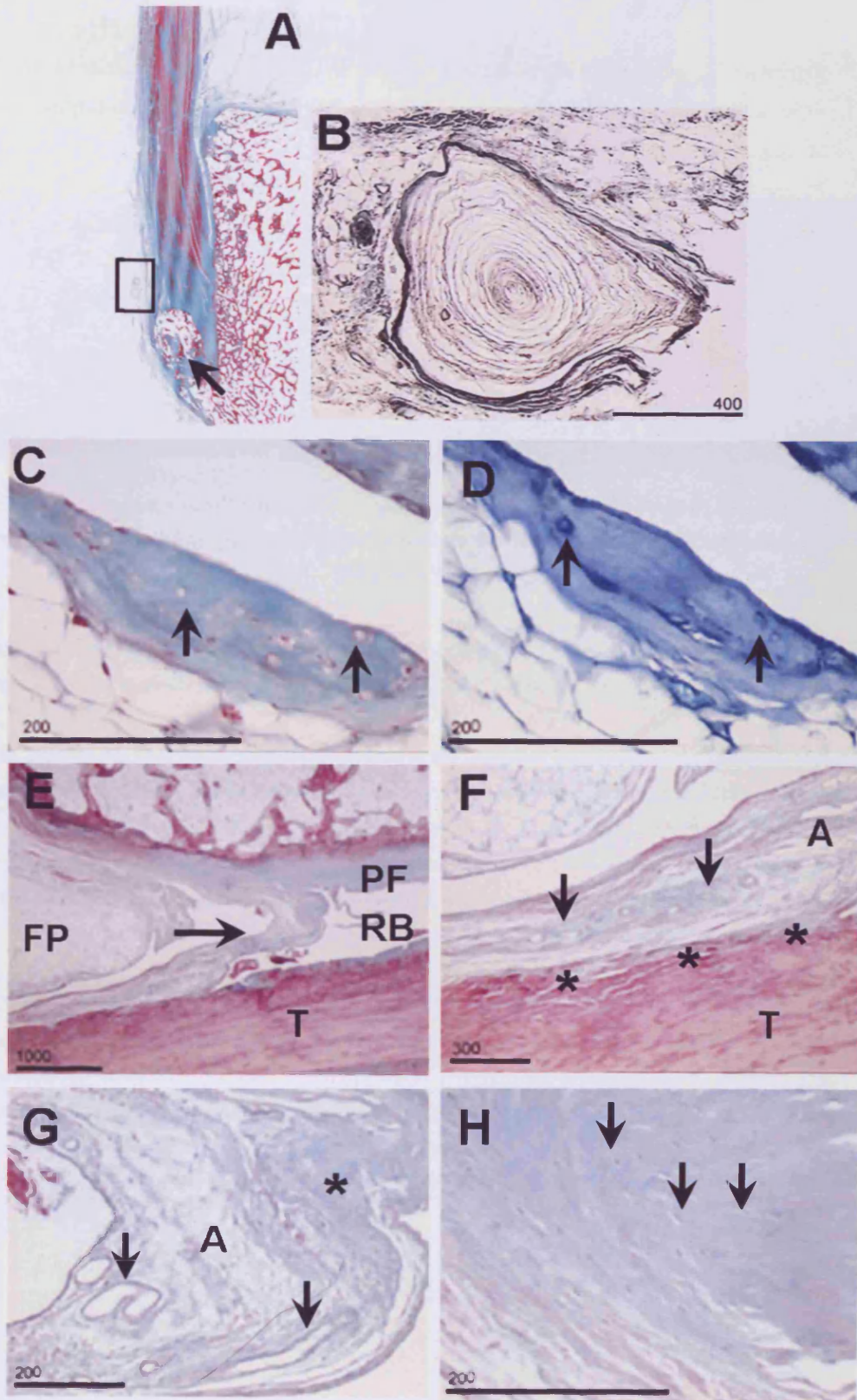
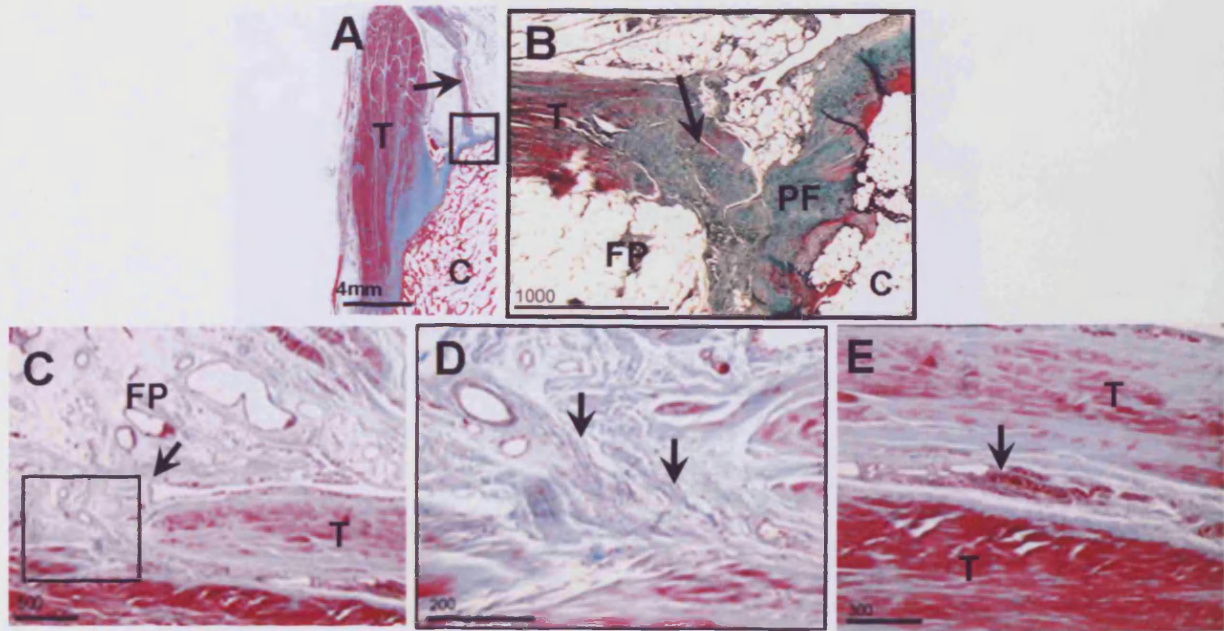


Figure 4.3.6.



Figures A and B: Sagittal histological sections through an accessory tendon passing through Kager's fat pad. (Masson's Trichrome)

Figure A: Low power view of an accessory tendon (arrow) originating from the Achilles tendon (T) passing through the tip of Kager's fat pad to attach to the periosteal fibrocartilage of the calcaneus (C). Masson's Trichrome. Scale bar = 4mm.

Figure B: High power view of the attachment (arrow) of the accessory tendon (T) to the periosteal fibrocartilage (PF) (highlighted in A). Note either side of the accessory tendon is a region of adipose tissue from the bursal-wedge of the fat pad (FP). C-calcaneus. Masson's Trichrome. Scale bar = 1mm.

Figures C – E: Sagittal histological sections illustrating the invasion of adipose tissue from the bursal-wedge of the fat pad into the deep surface of the Achilles tendon. (Masson's Trichrome)

Figure C: Vascular invasion of the Achilles tendon (T) from the bursal-wedge of the fat pad (FP). Proximal to the reflection of the synovial membrane (arrow), blood vessels and loose connective tissue invade into the deep surface of the Achilles tendon (T). Scale bar = 500 μ m

Figure D: High power view of the region highlighted in C. Note the presence of irregularly arranged fibrous strands (arrows) at the point where the fat pad invades into the tendon. Scale bar = 200 μ m.

Figure E: Blood vessels (arrow) present in the tissue invading into the deep surface of the Achilles tendon (T). Scale bar = 300 μ m.

Figure 4.3.7.

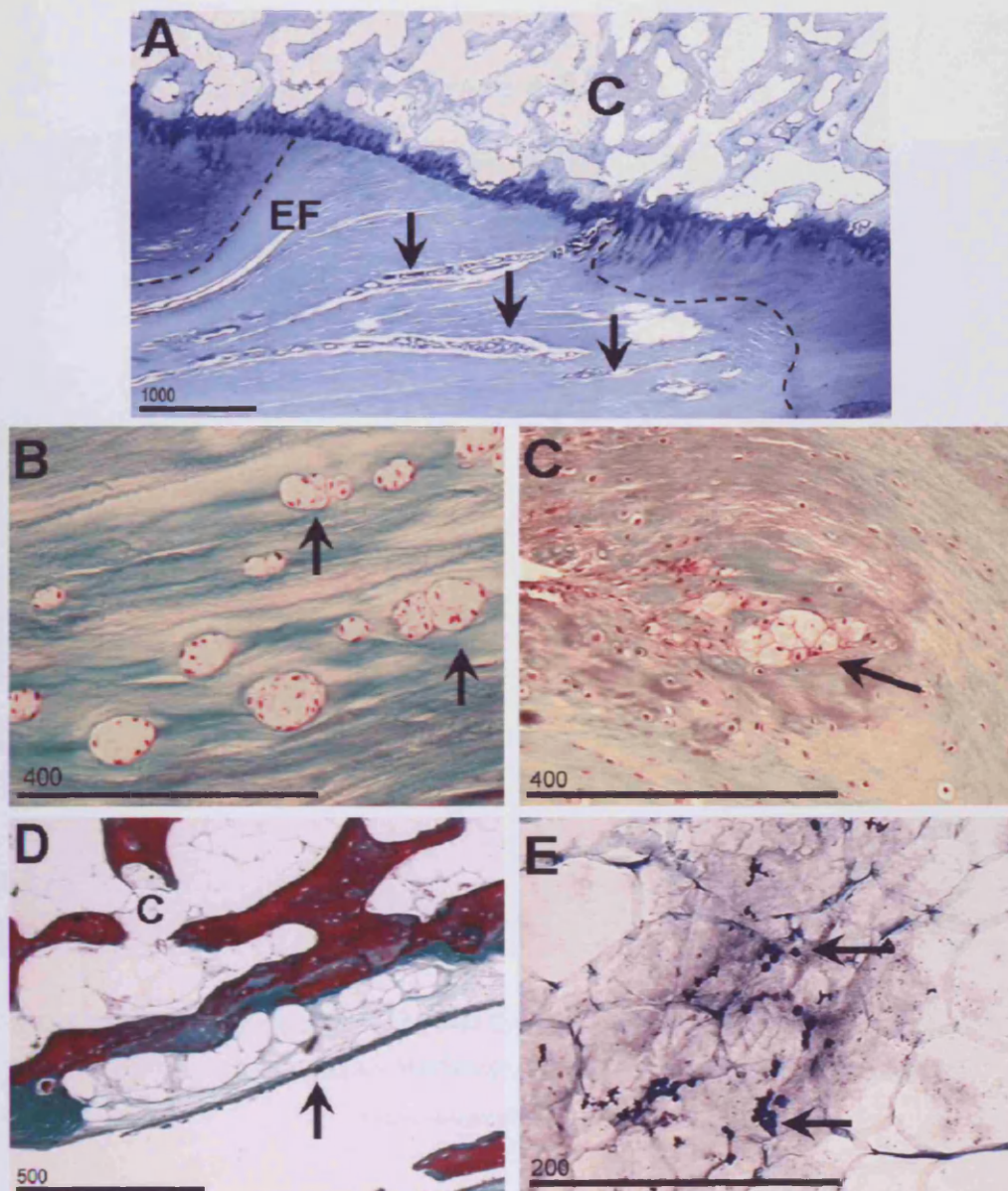


Figure A: Low power view of the Achilles tendon enthesis fibrocartilage (EF) in a toluidine blue stained section. Arrows indicate a number of blood vessels present within the fibrocartilage. Note the lighter blue stained fibrocartilage (dashed line) in the region where the blood vessels are present, while the surrounding fibrocartilage is considerably darker. C—calcaneus. Toluidine blue. Scale bar = 1000µm.

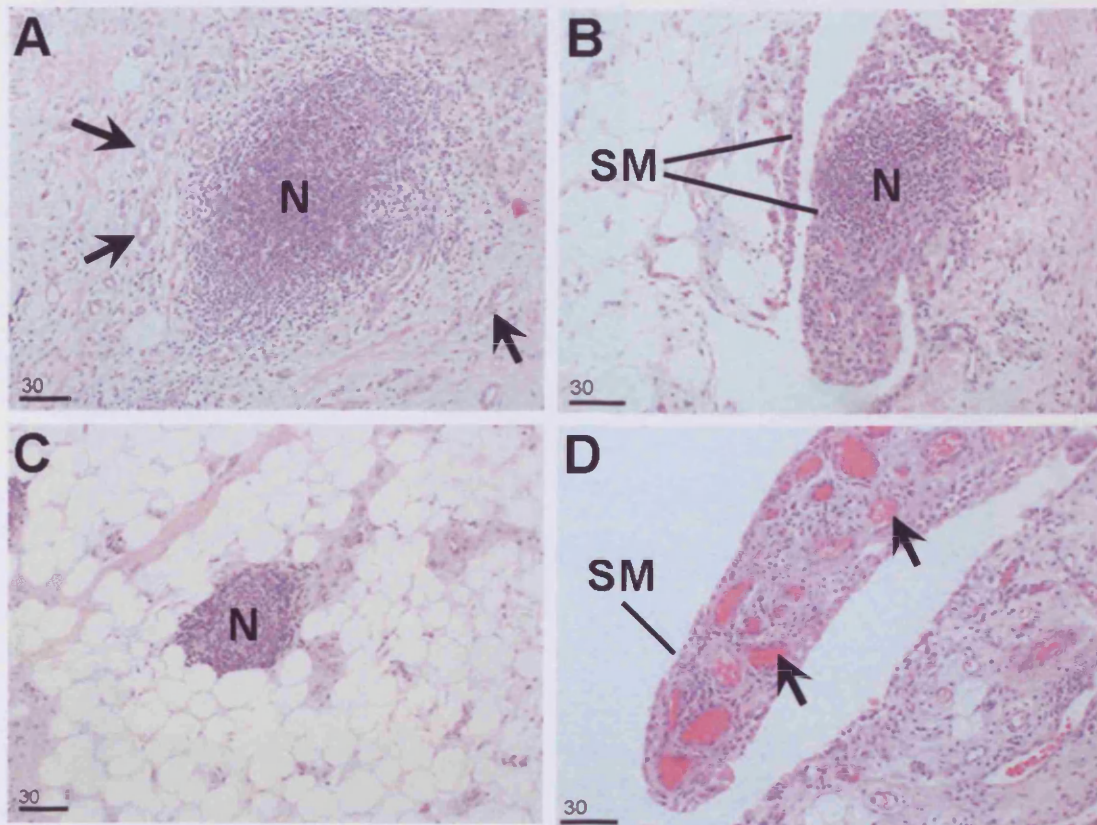
Figure B: The enthesis fibrocartilage of the Achilles tendon insertion. Arrows indicate clusters of fibrocartilage cells within the fibrocartilage. Masson's Trichrome. Scale bar = 400µm.

Figure C: The insertional angle of the Achilles tendon enthesis organ. Note the presence of a large cluster of fibrocartilage cells (arrow) and poor staining of the surrounding matrix. Masson's Trichrome. Scale bar = 400µm.

Figure D: The superior tuberosity of the calcaneus (C). A local absence of periosteal fibrocartilage was observed in this specimen; in its place were a number of adipocytes and a small quantity of fibrous tissue (arrow). Masson's trichrome. Scale bar = 500µm.

Figure E: Loose connective tissue surrounding the Achilles tendon containing a cluster of mast cells (arrows). Dark staining and surrounding granular tissue suggests that these cells were degranulating. Toluidine blue. Scale bar = 200µm.

Figure 4.3.8.



BIOPSY SAMPLES OF KAGER'S FAT PAD TAKEN FROM PATIENTS WITH HAGLUND'S DEFORMITY WHO HAD SYMPTOMS OF RETROCALCANEAL BURSTITIS.

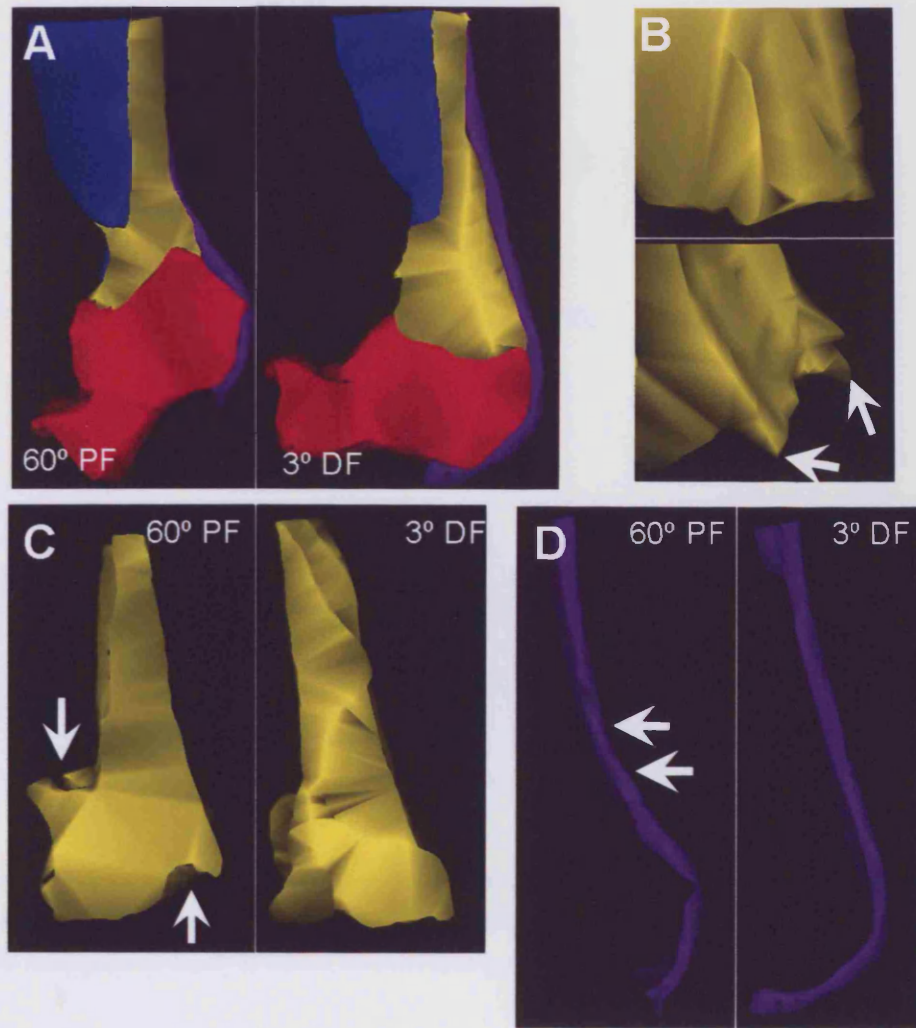
(Haematoxylin & Eosin)

Figure A: A lymph nodule (LN) within a biopsy taken from Kager's fat pad. Arrows indicate a closely associated capillary network. Scale bar =30µm.

Figure B: A lymph nodule (LN) in close association with the synovial membrane (SM) lining Kager's fat pad. Scale bar = 30µm.

Figure C: A synovial covered (SM) protrusion of Kager's fat pad containing a large number of lymphocyte. Note the presence of numerous venules (arrows) within the protrusion of the fat pad. Scale bar = 30µm.

Figure 4.3.9.



3D RECONSTRUCTIONS COMPOSED FROM SERIAL MRI IMAGES OF THE ADULT HINDFOOT IN PLANTAR (PF) AND DORSIFLEXION (DF)

(Pink = calcaneus, yellow = Kager's fat pad, purple = Achilles tendon, blue = flexor hallucis longus)

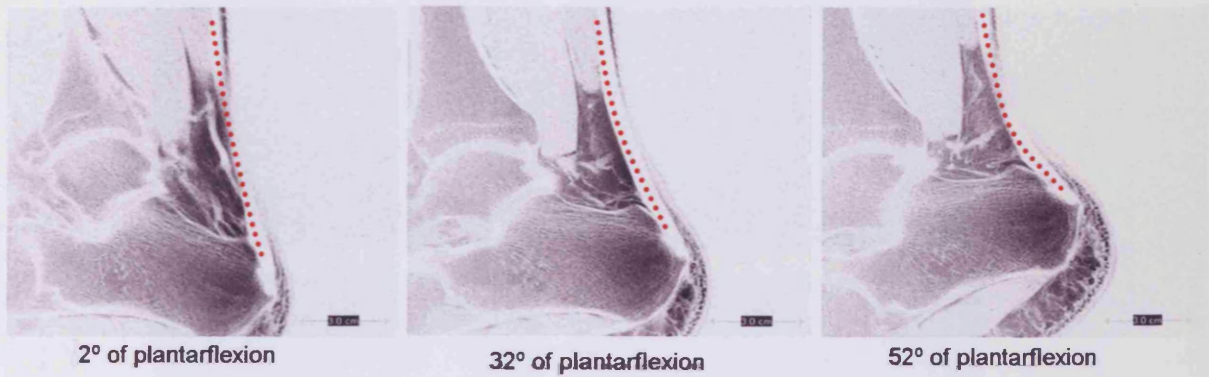
Figure A: 3D view of the hindfoot in full (60°) plantarflexion (left) and 3° dorsiflexion (right). Note the way in which Kager's pad is compressed by flexor hallucis longus and how the bursal-wedge was compressed and protuded into the retrocalcaneal bursa in full plantar flexion.

Figure B: 3D image illustrating variations in shape of the tip of the bursal wedge. One specimen (top) had a relatively uniform shape, while another (bottom) had a more irregular shape with lateral protrusions (arrows).

Figure C: 3D image of Kager's pad in isolation. Note the regions compressed by flexor hallucis longus (downward arrow) and the superior tuberosity of the calcaneus (upward arrow) during plantarflexion (left), but not in dorsiflexion (right).

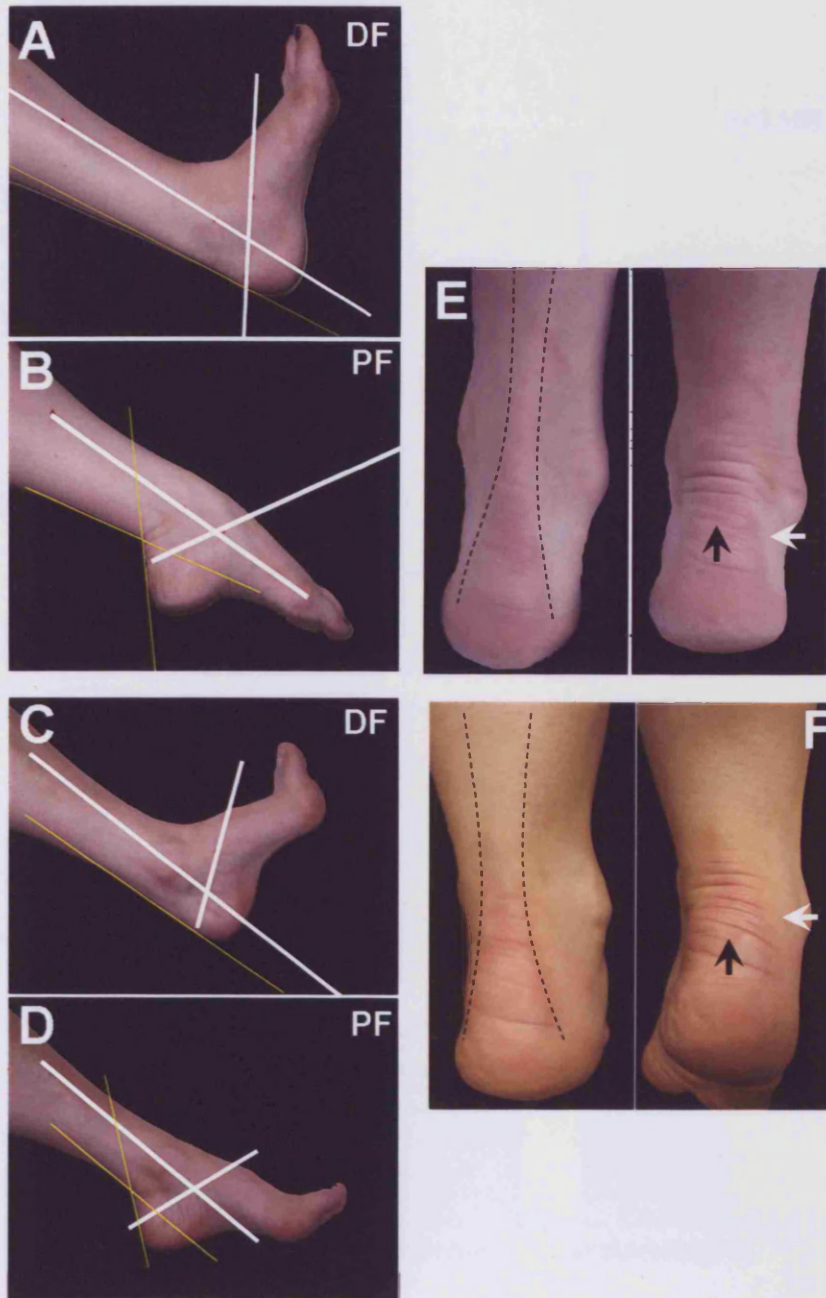
Figure D: 3D image of the Achilles tendon in plantar and dorsiflexion. Note the flexion of the tendon (arrows) which occurs during plantarflexion. Twisting of the tendon is also obvious.

Figure 4.3.10.



MRI images (negatives) illustrating the change in shape (highlighted by red dotted lines) of the Achilles tendon through 50° of plantarflexion. Note how concave the Achilles tendon becomes in plantar flexion (top). This concavity is subsequently reduced as the degree of flexion becomes smaller (middle and bottom). Scale bar = 3cm.

Figure 4.3.11.



SURFACE ANATOMY OF THE HINDFOOT IN MAN

Figures A and B: Subject 1. With the foot in full plantarflexion (B), the Achilles tendon becomes flexed.

Figures C and D: Subject 2. With the foot in full plantarflexion (D), the Achilles tendon becomes flexed.

Figure E and F: During dorsiflexion (DF), the shape of the Achilles tendon was clearly visible (dashed lines), the tendon flares out dramatically at its insertion. During plantarflexion (PF) the Achilles tendon is less visible and the skin wrinkles where the tendon flexes (black arrow). White arrow indicates the fat pad which can be seen to bulge medially and laterally during plantarflexion.

Figure 4.3.12.

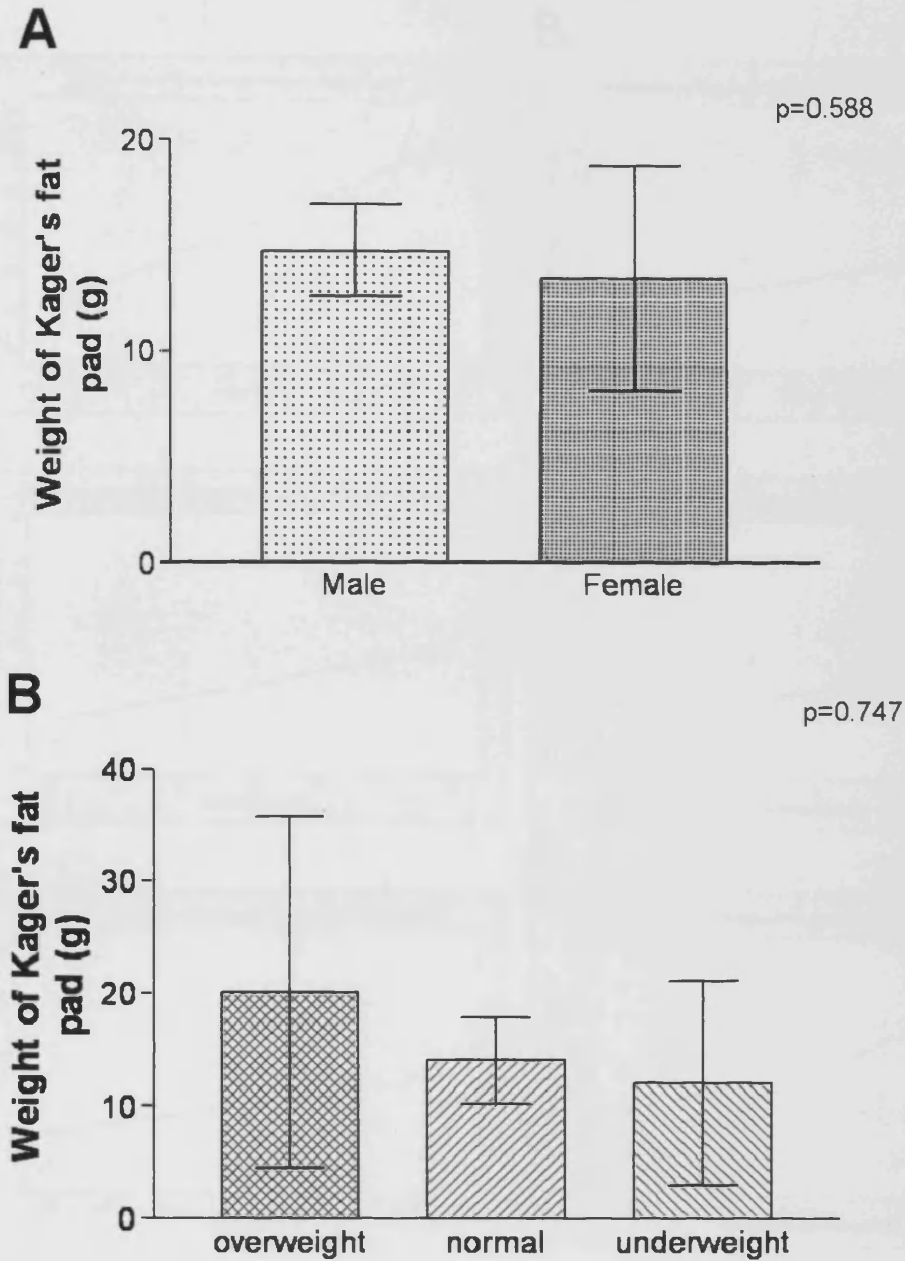


Figure A: Histogram comparing the weight of Kager's fat pad between male and female dissecting room cadavers of 'normal' weight. Means \pm Standard Deviation. No significant difference was observed ($p>0.05$). male - $n=4$; female - $n=4$

Figure B: Histogram comparing the weight of Kager's fat pad between three different weight categories: 'underweight', 'normal', and 'overweight' of dissecting room cadavers. Groups included both male and female subjects. Means \pm Standard Deviation. No significant difference was observed ($p>0.05$). normal - $n=8$, overweight - $n=3$, underweight - $n=3$.

Figure 4.3.13.

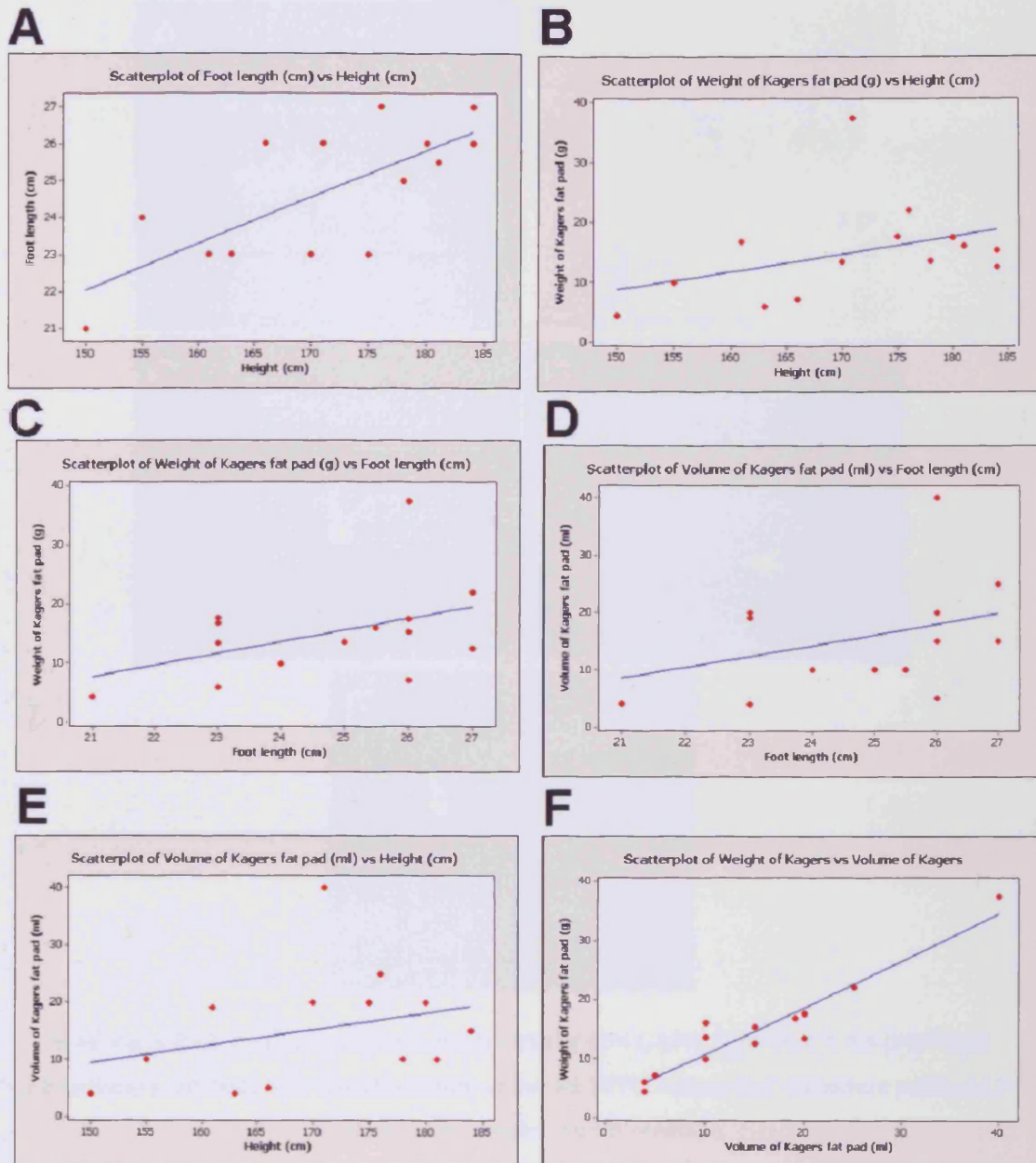


Figure A: Scattergram demonstrating a positive correlation between height and foot length in 14 dissecting room cadavers of both sexes.

Figure B: Scattergram demonstrating a weak positive correlation between the height and weight of Kager's fat pad in 14 dissecting room cadavers of both sexes.

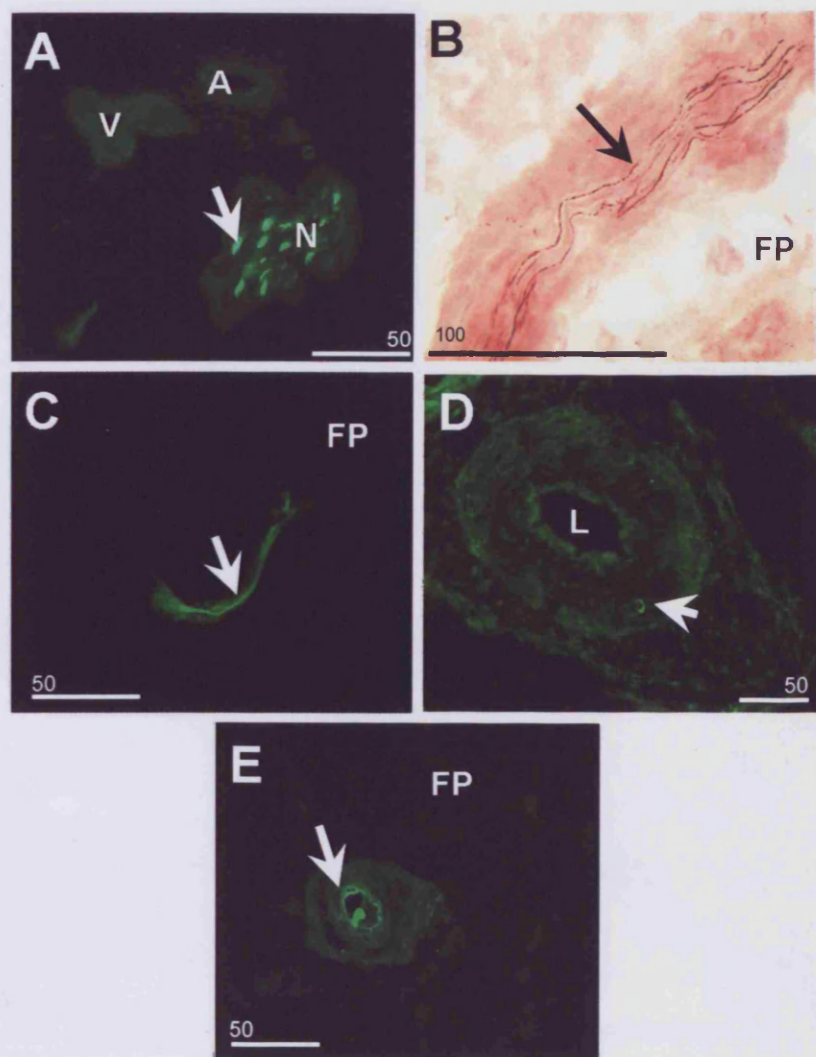
Figure C: Scattergram demonstrating a weak positive correlation between foot length and weight of Kager's fat pad in 14 dissecting room cadavers of both sexes.

Figure D: Scattergram demonstrating a weak positive correlation between foot length and volume of Kager's fat pad in 14 dissecting room cadavers.

Figure E: Scattergram demonstrating a weak positive correlation between height and volume of Kager's fat pad in 14 dissecting room cadavers.

Figure F: Scattergram demonstrating a strong positive correlation between weight and volume of Kager's fat pad in 14 dissecting room cadavers.

Figure 4.3.14.



KAGER'S FAT PAD LABELLED WITH PROTEIN GENE PRODUCT 9.5 (PGP 9.5)

The primary antibody was visualised with either an FITC conjugated secondary antibody or avidin/biotin complex and NovaRED.

Figure A: An obliquely-sectioned nerve bundle (N) in the bursal-wedge of Kager's fat pad. Such nerve bundles contained numerous axons (arrow) which labelled positively for PGP9.5. The nerve bundle was associated with two blood vessels, a venule (V) and arteriole (A) in a neurovascular bundle. FITC. Scale bar = 50µm.

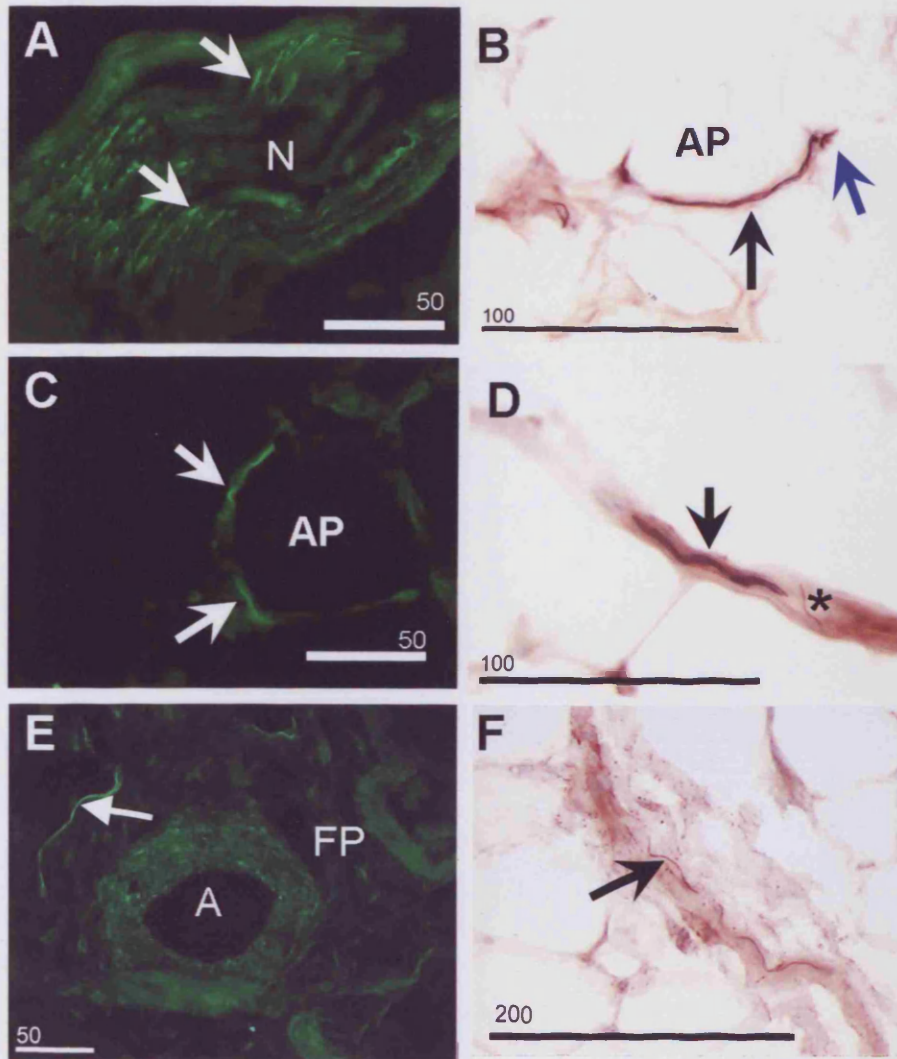
Figure B: A nerve bundle, cut longitudinally within the bursal wedge of Kager's fat pad (FP). Individual axons (arrow) can clearly be seen within the nerve. Note the wavy appearance of these axons. NovaRED. Scale bar = 100µm.

Figure C: An individual nerve fibre (arrow) within bursal wedge of Kager's fat pad (FP). The nerve fibre passes between the walls of adjacent adipocytes. FITC. Scale bar = 50µm.

Figure D: An arteriole cut in cross section, in the bursal wedge of Kager's fat pad. The arrow indicates a small nerve fibre immunoreactive to PGP 9.5 within the tunica media of the vessel wall. Note the autofluorescence of the blood vessel wall. L – Lumen. FITC. Scale bar = 50µm.

Figure E: A putative encapsulated nerve ending. A nerve fibre, immunoreactive to PGP 9.5, surrounded by several layers of connective tissue within the bursal wedge of Kager's fat pad (FP). FITC. Scale bar = 50µm.

Figure 4.3.15.



KAGER'S FAT PAD LABELLED WITH ANTI-NEUROFILAMENT 200 (NF200)

Visualised with either, an FITC conjugated secondary antibody (A,C, and E), or avidin/biotin complex and NovaRED (Figures B,D, and F).

Figure A: A large nerve bundle (N) cut obliquely in the bursal-wedge of the fat pad. Individual axons can be clearly identified (arrow) within the bundle labelled positively for NF200. FITC. Scale bar = 50 μ m.

Figure B: A nerve fibre (arrow) immunoreactive to NF200 passing between the walls of adjacent adipocytes (AP) in the bursal-wedge of Kager's fat pad. Note that one end (blue arrow) the nerve appears to branch. NovaRED. Scale bar = 100 μ m.

Figure C: A fine nerve fibre (arrows), immunoreactive to NF200, weaving between the cell membranes of neighbouring adipocytes (AP) within the bursal wedge of Kager's pad. Note the fibre dips in and out of the plane of the section. FITC. Scale bar = 50 μ m.

Figure D: A small bundle of nerves fibres (arrow) immunoreactive to NF200 running with a capillary (*) between adipocytes in the bursal wedge of Kager's fat pad. NovaRED. Scale bar = 100 μ m.

Figure E: A nerve fibre (arrow) in close association with an arteriole (A) in the bursal wedge of Kager's fat pad (FP). FITC. Scale bar = 50 μ m.

Figure F: A single nerve fibre (arrow) immunoreactive to NF200 running in association with fibrous strands within the bursal wedge of Kager's fat pad. Nova RED. Scale bar = 200 μ m.

KAGER'S FAT PAD LABELLED WITH ANTI-SUBSTANCE P

Visualised with either, and FITC conjugated secondary antibody (Fig A), or avidin/biotin complex and DAB (Fig B).

Figure A: Cross section through a nerve bundle in Kager's fat pad. Note that only a few of the fibres within the bundle contain substance P (arrows). FITC. Scale bar = 50µm.

Figure B: A fine nerve fibre immunoreactive to substance P (arrow) weaving between the walls of adipocytes (AP) in the bursal-wedge of Kager's fat pad. DAB. Scale bar = 100µm.

KAGER'S FAT PAD LABELLED WITH ANTI-CGRP

Visualised with an FITC conjugated secondary antibody (Fig C), or avidin/biotin complex and DAB (Fig D).

Figure C: A small nerve fibre immunoreactive to CGRP in the tunica adventitia of an arteriole (A) within the bursal-wedge of Kager's fat pad (FP). Note the autofluorescence of the blood vessel wall. FITC. Scale bar = 50µm.

Figure D: A small nerve fibre (arrow) immunoreactive to CGRP, weaving between neighbouring adipocytes in the bursal-wedge of Kager's fat pad. DAB. Scale bar = 100µm.

KAGER'S FAT PAD - NEGATIVE CONTROL SECTIONS

Phosphate buffer or rabbit immunoglobulins were applied to the section in place of the primary antibody.

Figure E: The bursal-wedge of Kager's fat pad. Phosphate buffer was applied to the section in place of the primary antibody and an FITC conjugated secondary antibody was applied subsequently. No non-specific labelling of the secondary antibody occurred. FP - fat pad. FITC. Scale bar = 50µm.

Figure F: A small blood vessel in the bursal wedge of Kager's fat pad, indicating that there was no non-specific binding of the secondary antibody to the specimen when phosphate buffer were applied in place of the primary antibody. Arrow indicates nuclei of endothelial cells in the small capillary. FP - fat pad. NovaRED. Scale bar = 100µm

Figure G: A blood vessel in the bursal wedge of Kager's fat pad, indicating that there was no non-specific binding of the primary antibody to the specimen when rabbit immunoglobulins were applied in place of the primary antibody. FP - fat pad. NovaRED. Scale bar = 100µm.

Figure 4.3.16.

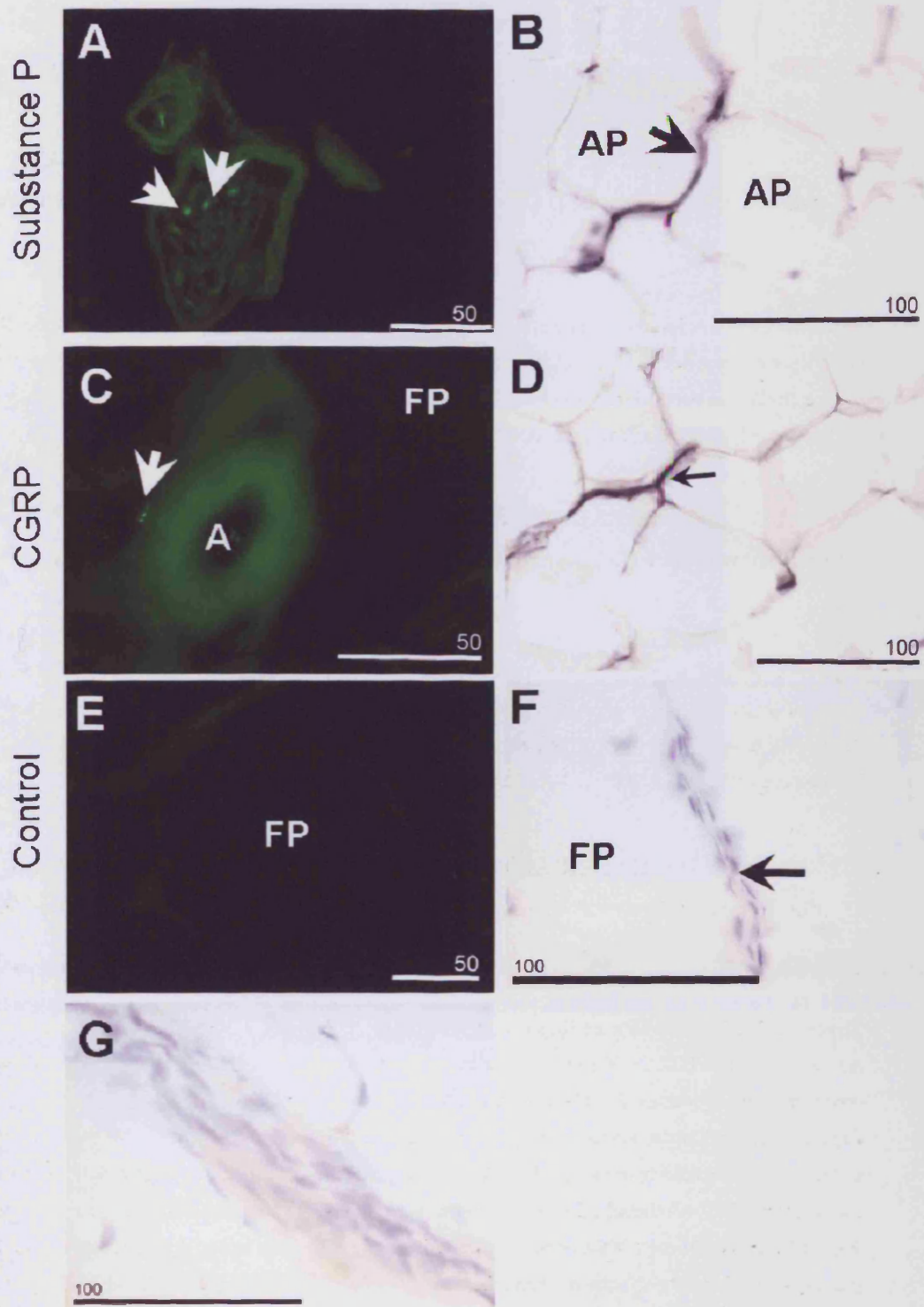
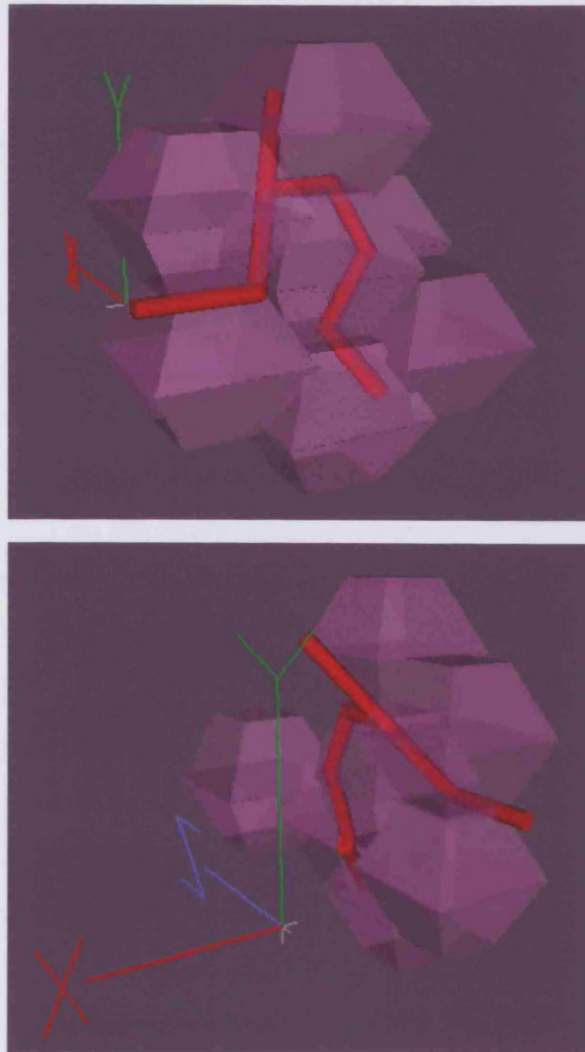


Figure 4.3.17.



Stills taken from a schematic 3D movie created by Dr. Ieuan Nicholas (Welsh e-Science Centre, Cardiff University) from serial histological sections provided by Hannah Shaw. Note the way in which the nerve fibres (red), interweave between neighbouring adipocytes (purple) in all directions (XYZ).

4.4. DISCUSSION

The results show that a number of anatomical variations and histopathological features associated with Kager's fat pad were present in elderly cadaveric specimens. The preliminary anthropometric studies suggested that the weight of a subject did not have a significant effect on the size of Kager's fat pad. However, the height and foot length of an individual do appear to be correlated with the size and volume of the fat pad. Immunohistochemical studies showed that the bursal-wedge of Kager's fat pad contains nerve fibres carrying both mechanoreceptive and nociceptive information to the CNS. Biopsy samples from the fat pad of patients with Haglund's deformity and symptoms of retrocalcaneal bursitis illustrated the presence of lymphocyte infiltrations into the synovial membrane and the formation of lymph nodules within the fat itself.

There was a marked variation in the shape of the fat pad tip between cadavers. The feathered appearance that was evident in a number of cases may indicate the presence of synovial villi. These are considered a normal characteristic of the reflected synovium (Canoso, 1981). The villi serve to increase the surface area of the membrane and therefore augment the amount of hyaluronan secreted into the bursal cavity to facilitate movement (Myers and Christine, 1983). A high density of large synovial villi is frequently associated with pathology in older individuals (Castelli et al., 1985; Pasquali-Ronchetti et al., 1992). In other cadavers, the tip of the fat pad was divided into distinct protrusions by clefts. This arrangement may enhance motility of the tip of the fat pad during foot movements (Gallagher et al., 2005). It is possible that cleft formation may reflect the influence of external factors such as footwear, lifestyle, amount or type of exercise undertaken during the lifetime of the individual etc. Unfortunately, such information was unavailable and as a result these parameters cannot be assessed and therefore no conclusions can be drawn.

MRI images and 3D reconstructions support the observations made by Theobald et al., (2006) and Canoso et al., (1988) that the fat pad moves in and out of the retrocalcaneal bursa during plantar- and dorsiflexion. Canoso et al., (1988) described the fat pad as acting as a variable plunger – and Theobald et al., (2006) suggested that the contraction of FHL leads to compression of the associated region of fat, and in turn the movement of the bursal wedge into the retrocalcaneal bursa. Movement of the fat pad may minimise pressure changes in the bursa which would otherwise occur in response to a change in the insertional

angle during foot movement. The observations in the present study suggest an additional function for the fat pad. The current MRI and surface anatomy images clearly show that the Achilles tendon maintains a smooth convexity during plantarflexion which is facilitated by a strong supporting deep fascia, located superficial to the tendon sheath. The fascia is particularly thick over the posterior part of the ankle and fuses with the fascial sheath close to the calcaneus. Thus, the fascia effectively acts as a retinaculum for the tendon (Benjamin et al., 2007a) and therefore reduces the change in the insertional angle. The retinaculum therefore provides another protective measure against wear and tear at the insertion site, and should thus also be considered to be part of the Achilles tendon enthesis organ. The fat pad anterior to the tendon adjacent to the 'fascial retinaculum' prevents the Achilles tendon from kinking when the foot is plantarflexed by filling the space anterior to the tendon with a deformable substance – i.e. adipose tissue. It is also of interest that the point at which the tendon bends is the narrowest part of the tendon and the region where most tendon failures occur (Campbell and Lawton, 1993; Reinherz et al., 1991). Therefore, repetitive flexion of the tendon at this site may lead to microdamage of the collagen fibres - resulting in tendon failure. However, a number of other factors also need to be considered as possible contributory factors to tendon failure at this point, including tendon vascularisation or lack of it (as reviewed by - Theobald et al., 2005).

The histological structure of Kager's fat pad is similar to that of the rat (as described in chapter 3). The adipocytes have a distinctive honeycomb appearance with a number of fibrous strands passing through it. These fibres are principally collagenous and most likely provide stability to the pad during its movement (Theobald et al., 2006) as it is hypothesised to do so in the calcaneal fat pad (Jahss et al., 1992; Ker, 1999; Kimani, 1984). However, elastic fibres were also observed within the fat pad associated with these fibrous strands. These may modulate the ability of the tissue to be deformed when it is subjected to compressive stresses and allowing it to return to its normal resting state (Kimani, 1984). In this way, the fat pad acts as a shock absorber (Jahss et al., 1992), dissipating stress away from the tendon-bone interface (Benjamin and Ralphs, 1998; Benjamin et al., 2004b), and protecting the highly vascularised structure during foot movement (Theobald et al., 2006). However, it also prevents the tissue from being trapped between the articulating surfaces (Davies and White, 1961).

In a number of elderly cadaveric specimens, the tip of the fat pad which protrudes into the retrocalcaneal bursa, is markedly fibrous. This may be a consequence of repeated cyclic loading and shear forces experienced by the pad during foot movement (Egerbacher et al., 2005), correlating with the role of stress dissipation of the fat pad (Benjamin et al., 2004b). There was a large capillary bed throughout the tip of the fat pad; this is a normal characteristic of adipose tissue. A principle function of adipose tissue is the storage and mobilisation of the substrates required for energy production. Fat is therefore highly vascularised in order to provide and remove substrates from the region (Gersh and Still, 1945; Stevens and Lowe, 2001). However, capillary presence at the tip of the fat pad may be considered unusual because the cyclic compression of this region could occlude the capillaries. Furthermore, it seems unlikely that Kager's fat pad has a significant metabolic function, like other structural fat pads. However, Rupnick et al., (2002) suggest that vascularisation may regulate the mass of adipose tissue by means of various anti- or angiogenic factors. Therefore it would be particularly damaging if the fat pad was deprived of blood which may lead to an alteration in the amount of adipose tissue present in Kager's triangle. This in turn could increase wear and tear to the enthesis, as has been illustrated in the knee (Stack and Chasten, 1949).

The anthropometric study indicates that Kager's fat pad is a structural pad which is not significantly affected by the weight of the individual. These results are paralleled by those of Davies and White (1961) who demonstrated that there is no correlation between the amount of subcutaneous adipose tissue and the weight of the infrapatellar (Hoffa's) fat pad. The correlation between the weight/volume of Kager's fat and the height/foot length of the individual suggests that the size of Kager's fat pad is influenced by skeletal size rather than body weight (Davies and White, 1961). However, in cases of extreme emaciation following depletion of all other adipose tissue deposits, it has been shown that both Kager's and Hoffa's fat pad can undergo significant changes in size and structure (Davies and White, 1961). No such observations were made here because of the absence of extremely emaciated individuals in the current study. Because the cadavers used were primarily for medical and dental student dissections, there were several limitations to this study which must be acknowledged. The study could only be carried out *following* dissection by the students, and therefore only estimations of the amount of abdominal adipose tissue could be made, and the number of cadavers available in this study was also reduced as the fat pad was often damaged or even missing. This also prevented comparison between the left and

right fat pads. Furthermore, it was not possible to weigh the cadavers prior to or following embalming.

In addition to the highly vascularised nature of the fat pad, immunohistochemistry illustrated that the fat pad is innervated by sensory nerve fibres carrying mechanoreceptive and nociceptive information to the CNS. Interestingly, the fibres present within the fat pad formed a network of neural elements which interweaved between individual fat cells. Nerve fibres were also seen to accompany the capillary network which also weaved between the adipocytes. This interweaving of blood vessels and nerve fibres within the clefts between adipocytes has also been visualised with the use of SEM in other mammalian adipose tissues (Motta, 1975). Some of these fibres were immunoreactive to NF200 which is known to be present in mechanoreceptive nerve fibres (Perry et al., 1991). It is therefore suggested that Kager's fat pad may play a role in collating proprioceptive information when the fat pad is compressed during ankle movement. The close association between nerve fibres and adipocytes noted here suggests that when the pad is compressed, this may deform nerve fibre between the adipocytes. The fat pad itself may therefore act as a giant mechanoreceptor. It was also demonstrated that a small number of nerve fibres within the fat pad contained the neuropeptides SP and CGRP. These are sensory neuropeptides known to be present in a population of nerve fibres conveying nociceptive information to the CNS (Hanesch et al., 1991). It is therefore possible that Kager's fat pad may be a source of pain in Achilles associated tendinopathies and enthesopathies. Of particular interest is retrocalcaneal swelling which leads to well known rheumatological sign - known as Bywaters' sign - in which the bursal wedge of the fat pad does not protrude into the bursa during plantarflexion and the bursa therefore does not become radiolucent as it would if it were filled with adipose tissue. The fat pad therefore undergoes a greater degree of compression compared to normal conditions (Canoso, 1998). This may therefore lead to the stimulation of these nociceptive nerve fibres in the bursal wedge of the fat pad, causing pain. This is one of the most likely explanations of where pain comes from in bursal swelling considering the bursal sac itself is not known to be innervated (Canoso, 1998). Kager's fat pad may therefore be comparable to the infrapatellar (Hoffa's) fat pad. Several studies have looked at the innervation of Hoffa's pad and it has been suggested that the pain associated with jumper's knee is caused by stimulation of nociceptors within the fat pad (Sanchis-Alfonso and Alcacer-Garcia, 2001). Furthermore, biopsies from the fat pad of patients with Haglund's deformity and symptoms of retrocalcaneal bursitis

contained a large number of lymphocytes. This indicates that the fat pad can become inflamed without the occurrence of spondyloarthropathies, and may be the source of pain in mechanically-associated retrocalcaneal bursitis.

A number of histopathological changes associated with Kager's fat pad were identified in the cadaveric specimens examined. In several specimens, it appears that movement of the fat pad may have been prevented by adhesions crossing the retrocalcaneal bursa, and a small accessory tendon passing through the fat pad may also have had a significant effect on movement of the fat pad. Unfortunately however, the medical histories of cadavers were unavailable and it is therefore not possible to establish whether or not the histopathologies were symptomatic.

Of particular interest was the invasion of tissue containing blood vessels from Kager's fat pad into the deep surface of the Achilles tendon. In a number of cadavers, these blood vessels could be seen to pass into the enthesis fibrocartilage at the tendon attachment. In this region a decrease in the strength of toluidine blue staining was observed around the invading vessels, indicating a lower content of sulphated glycosaminoglycans. As described in chapter 3, it is believed that the high level of CS within the fibrocartilage prevents in-growth of endothelial cells and nerve fibres (Johnson et al., 2002; Johnson et al., 2005; Snow and Letourneau, 1992). However, as seen in the intervertebral disc, degeneration of the fibrocartilage lowers the concentration of CS and may therefore allow the in-growth of blood vessels and nerve fibres causing pain (Johnson et al., 2002; Johnson et al., 2005). In the light of these observations, it is interesting to note that colour Doppler ultrasonography, has recently demonstrated a similar neovascular invasion into the deep surface of the painful Achilles tendon. It is suggested here that vascular invasion followed by the in-growth of nerve fibres may cause the pain associated with tendon pathology and no invasion was identified in the normal tendon (Alfredson et al., 2003). It may therefore be possible that vasculo-neural in-growth into the enthesis fibrocartilage may cause the pain that in some patients is associated with enthesopathies. More interestingly, are the recent studies which have demonstrated that the injection of sclerosing agents, into the "soft tissue"- now known to be Kager's or Hoffa's fat pad - on the ventral side of the tendon which target neovascular formation. This treatment has been used effectively to reduce pain associated with patellar and Achilles tendinopathies (Alfredson and Ohberg, 2005; Ohberg and Alfredson, 2002), and may therefore prove effective in treating

enthesopathies (Zeisig et al., 2006a; b). However, more studies are required especially to identify any detrimental effects this may have on the functional properties of the fat pad itself. More recently an even more radical approach has been used in a pilot study to treat jumper's knee by arthroscopically shaving away the soft tissues on the dorsal surface of the tendon (Willberg et al., 2007).

It can therefore be concluded that the function of Kager's fat pad is primarily structural, and that the size of the fat pad is determined mainly by skeletal size rather than weight of the individual. The striking innervation of Kager's fat pad in man, suggests that this structure may also have a proprioceptive role, in monitoring movement of the tendon relative to the bone during locomotion. Furthermore, the presence of nociceptive fibres suggests that it may also be a source of pain in hindfoot pathology. Inflammation of the fat pad in patients with retrocalcaneal bursitis supports this hypothesis.

5. ULTRASTRUCTURE OF THE RETROMALLEOLAR FAT PAD IN THE RAT

5.1. INTRODUCTION

A complex relationship between adipocytes and nerve fibres has been demonstrated within the retromalleolar fat pad in the rat and the equivalent fat pad (Kager's) in Man (See chapters 3 and 4). However, the extent of this relationship can only be superficially demonstrated by immunohistochemistry (Fig 5.1.1.). It is the aim of this study to describe the ultrastructure of the retromalleolar fat pad and the relationship between adipocytes and nerve fibres within the pad and use immunogold labelling to identify fibres which contain the neuropeptide CGRP. One of the nerves supplying the retromalleolar fat pad (the peroneal anastomotic branch of the sural nerve) was also studied by transmission electron microscopy (TEM), in order to determine whether there were any age-related changes in its structure.

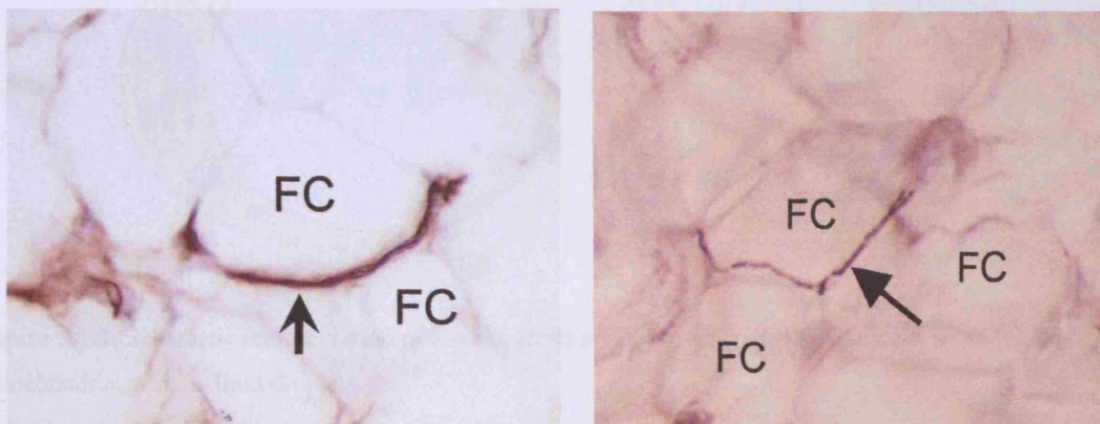


Figure 5.1.1: Left - A nerve fibre immunoreactive to neurofilament 200 (arrow) within Kager's fat pad in man. Right - A nerve fibre immunoreactive to calcitonin gene related peptide (arrow) within the retromalleolar fat pad in the rat. Note the way in which the nerve branches between adjacent fat cells (FC).

Brief Review

Adipose Tissue

Adipocytes are present in the majority of normal, healthy connective tissues, but in some regions the cells are numerous enough to form defined adipose tissue deposits such as those located at entheses. These fatty tissue accumulations are often considered to be a sign of degeneration (Jozsa and Kannus, 1997), but as demonstrated in chapters 3 and 6 that adipose tissue at entheses may also have important sensory and immunological functions under 'normal' conditions.

Classically, there are considered to be two forms of adipose tissue, white (WAT) and brown (BAT). However, it has recently been suggested that adipose tissues in the rat is not necessarily formed solely by brown or white adipocytes, and that the population of brown adipocytes within a given tissue can increase in response to different stimuli (Cousin et al., 1992). This indicates that there is a continuum between WAT and BAT. Brown fat cells are characterised histologically by their polygonal shape, abundance of large mitochondria and by the presence of lipid that is stored in multiple vacuoles (multilocular) within their relatively abundant granular cytoplasm (Napolitano and Fawcett, 1958) (Fig 5.1.2). Brown adipocytes are physiologically distinct from white adipocytes, in that they have the ability to generate heat from lipids without producing adenosine triphosphate (ATP) (Argyropoulos and Harper, 2002) for a review). This ability is created by a protein encoded by one of the genes distinct to brown adipocytes, called uncoupling protein 1 (Matthias et al., 2000).

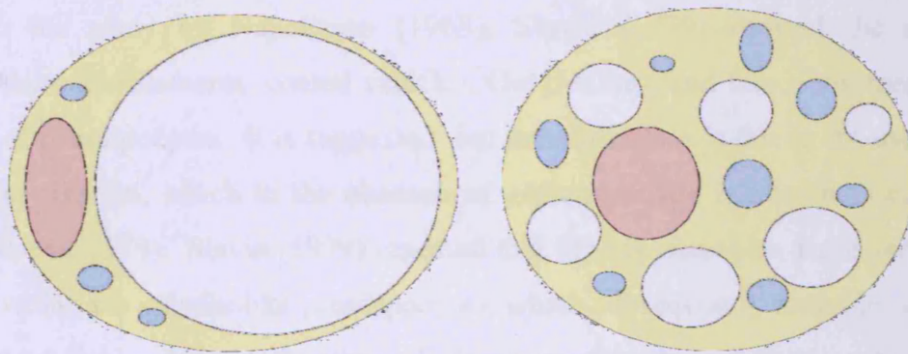


Figure 5.1.2: Schematic representation of a white (left) and a brown (right) adipocyte. Pink – nucleus, blue – mitochondria, white – lipid droplets

Histologically, the white fat cell is generally more easily recognised by its large, more spherical shape. It contains a single globule of lipid (i.e. it is unilocular) within a thin envelope of cytoplasm and the fat displaces the nucleus to one side of the cell. White adipocytes are therefore often referred to having a signet-ring shaped morphology (Fig 5.1.2.). The principle function of WAT is to store fatty acids in the form of triacylglycerols for utilisation in time of restricted food intake, although it is also known to have endocrine functions and to have the ability to metabolise glucose (Trayhurn and Beattie, 2001). However, different cell populations can have different physiological characteristics. One of the greatest differences is between visceral adipose tissue and structural fat deposits. Structural fat deposits do not undergo lipolysis as easily as visceral deposits, which can be

stimulated to release lipid by a number of hormones (Arner, 1998; Ramsey, 1959). Little is known about the mechanisms that control adipocyte differentiation in these different deposits as the majority of studies have been carried out on fibroblasts or pre-adipocytes *in vitro* (as reviewed by Smas and Sul, (1995).

Napolitano (1963) published the first ultrastructural study of adipocyte differentiation in the rat and demonstrated the similarities between presumptive adipocytes and fibroblasts, along with the process of accumulation of lipid within the cell. Further studies by (Slavin, 1979), who used primary aldehyde fixation (3% glutaraldehyde and 1% paraformaldehyde) confirmed this similarity. He also reported that the subcutaneous and inguinal fat pads developed at approximately 17 days prenatally, while the other fat pads studied, including the epididymal, mesometrial and mesenteric fat pads, did not begin to differentiate until birth. This is reminiscent of the retromalleolar fat pad in the rat, which does not undergo differentiation until after birth as documented elsewhere in this thesis (see Chapter 3). In contrast to the study by Napolitano (1963), Slavin (1979) showed the presence of microtubules, microfilaments, coated vesicles, Golgi zones, and free ribosomes within the cytoplasm of preadipocytes. It is suggested that this difference is due to the use of osmium tetroxide for fixation, which in the absence of glutaraldehyde is known to cause protein removal (Slavin, 1979). Slavin (1979) reported that lipid begins to be deposited at one pole of the cell within the spindle-like preadipocytes, which subsequently round up and continue to accumulate lipid. Eventually, the cell takes on the characteristic mature adipocyte morphology, as described above. It is now understood that adipocytes derive from multipotent mesenchymal stem cells in a two-phase process. The first stage, known as determination, takes place when pluripotent stem cells commit to an adipocyte lineage and become preadipocytes. Preadipocytes are morphologically identical to their precursors, which have the ability to differentiate into other cell types (fibroblasts, osteoblasts etc.), while preadipocytes do not. Following determination, terminal differentiation takes place in which preadipocytes mature and attain the cytoplasmic machinery required for lipid synthesis and transport, and acquire the characteristics typical of a mature adipocyte (Gregoire et al., 1998 - for a review). It has also been observed that multipotent mesenchymal stem cells remain within adult fat pads and have attracted interest as a source of multipotent cells for therapeutic use (Tholpady et al., 2003). It is also interesting to note that preadipocytes have demonstrated the ability to differentiate into macrophage-like cells both *in vitro*, when adipocyte precursor cells are grown in contact with peritoneal

macrophages; and *in vivo*, when a preadipocyte cell line is injected into the peritoneal cavity of nude mice (Charriere et al., 2003). Despite this generally accepted view, more recent studies have identified the plasticity of mature rat and human adipocytes under various conditions to acquire characteristics of the opposite form of adipocyte (Loncar, 1991).

Innervation of Adipose Tissue

Although it has long been understood that WAT is innervated by sympathetic nerves, and that these are believed to play an important role in inhibiting growth of fat pads through stimulation of lipolysis, the sensory innervation of adipose tissue deposits has raised less interest and its functional significance is unclear. The presence of sensory nerves in WAT was first identified by Fredholm in 1985 but was dismissed as originating from the nerves of adjacent muscles (Fishman and Dark, 1987). Fishman and Dark (1987) were the first to definitively demonstrate the presence of sensory nerve fibres in adipose tissue with the use of “true blue”. This is a sensitive fluorescent neuroanatomical tracer which, in its crystalline form, was implanted into the inguinal and dorsal subcutaneous fat pads. The dorsal root ganglia (DRG) from relevant levels were removed, and fluorescence microscopy demonstrated labelled cell bodies within them. This indicated that sensory neural processes are present in the fat pads tested (Fishman and Dark, 1987). The function of these nerves has been debated in visceral fat pads of the rat (Bartness and Bamshad, 1998; Bartness et al., 2005). Studies of the consequence of injecting the hormone leptin (involved in the regulation of metabolic rates) into the epididymal fat pad showed increased firing rates of sensory nerves from the pad with a simultaneous increase in the activity of sympathetic nerves. These observations suggest that the sensory nerves in the pad possess leptin receptors which, when activated, may send afferent signals to the CNS and in turn stimulate sympathetic outflow to the fat pad, thus increasing lipolysis (Nijima, 1998). The sensory nerves innervating WAT deposits may therefore convey information on adiposity levels to the brain (Bartness and Bamshad, 1998; Shi and Bartness, 2005; Shi et al., 2005) and may control lipolysis, via a feedback loop (Bartness et al., 2005). However, as described above, the physiology of visceral and structural adipose tissue deposits differ (Arner, 1998) and the majority of studies have been carried out on visceral adipose tissue deposits in the rat (Bartness and Bamshad, 1998; Bartness et al., 2005). The most frequently studied structural fat pad is that of the heel pad in man, which has attracted interest due to the occurrence of ulceration in patients with diabetes (Kao et al., 1999).

These studies suggest a link between peripheral neuropathy (primarily of autonomic but also sensory nerves) and fat pad atrophy leading to ulceration, indicating that the nervous system may also play a role in controlling lipolysis in structural fat pads. The mechanosensory role of these fibres in WAT has not yet been fully described, although neuropathy of the heel pad is associated with loss of sensory perception (Birke et al., 2000; Unger, 2004), indicating that these fibres may also play mechanosensory role.

Effect of Ageing on Peripheral Nerves

Ageing is known to affect both the structure and function of the central and peripheral nervous systems, resulting in a various neurologic diseases. In the CNS, ageing can lead to a decrease in central processing time and a decline in the effectiveness of the auditory and visual systems. In the PNS, disorders of movement are particularly common causing gait and postural abnormalities, as well as rigidity and a general state of flexion (as reviewed by - Verdu et al., 2000). It is reported that structural and biomechanical changes occur in the peripheral nerves of aged specimens and are believed to be the cause of impaired nerve function (Verdu et al., 2000). In the mouse, studies demonstrate marked fibre loss involving a decrease in the density of unmyelinated fibres to a greater degree than myelinated fibres. Where myelinated fibres are lost with ageing, there is a preferential loss of the large myelinated fibres over the smaller fibres. The morphology of myelinated fibres are also affected by age; myelinated fibres decrease in size and circularity, and a marked decrease in the thickness, while an increase in the frequency of abnormalities of the myelin sheath are observed. Other non-neuronal cells frequently identified in large peripheral nerves also undergo changes with age, including an increase in the number of mast cells and macrophages in the endoneurium (Ceballos et al., 1999).

5.2. MATERIALS AND METHODS

5.2.1. Dissection Procedure

White male Wistar rats aged 4 and 24 months (3 rats at each age) were obtained from accredited commercial suppliers and maintained up to 24 months of age Cardiff University, then killed with an overdose of CO₂. An incision was made along the medial surface of the foot and ankle to expose the fat pad which was gently reflected out of Kager's triangle to expose the nerve entering the fat on the lateral side of the foot (see figure 5.2.1.1). The fat pad and the nerve were then separated, cut into 5mm² blocks and pinned onto Sylgard with fly-pins to ensure maximum penetration of the fixative and prevent tissue deformation during fixation, respectively.

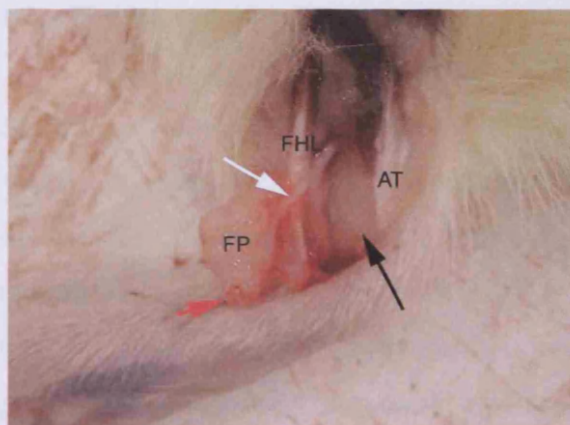


Figure 5.2.1.1: The retromalleolar fat pad (FP) reflected out of Kager's triangle (black arrow) to illustrate the nerve branch (white arrow – peroneal anastomotic branch of the sural nerve) which passes through the pad supplying it. Note the tip of the fat pad (red arrow) contains a large number of blood vessels which are visible. 24 month rat.

5.2.2. Fixation and Embedding

Following dissection, tissue was fixed in 1% paraformaldehyde 2% glutaraldehyde in 0.1 M PB, pH 7.4 (see appendix I) for a maximum of 2 hours. After washing in 0.1M PB, then distilled (d) H₂O (3 times for 5 minutes), the tissue was transferred to 1% aqueous osmium tetroxide (OsO₄; Agar Scientific, Stansted, UK) for 20 minutes. The tissue was washed again in dH₂O (3 times for 5 minutes) to remove any traces of OsO₄ and bulk stained in 2% uranyl acetate for 30 minutes. Following further washing steps the tissue was dehydrated in graded alcohols (50%, 70%, 90%) for 15 minutes each, and two changes of 100% for 30 minutes each (due to the high level of lipid present in the tissues being processed, these steps were lengthened from normal procedure times). The samples were washed again and

transferred to propylene oxide (Fisher Scientific, Loughborough, UK), two changes for 5 minutes each, and subsequently placed in a 2:1 (propylene oxide : Durcupan®; Sigma-Aldrich [Fluka-Chemika], Gillingham, UK) mixture (see appendix) for 1 hour, then a 1:1 mixture for 1 hour, and subsequently a 1:2 mixture for 1 hour. Finally the tissue was placed in Durcupan® alone for 2 hours at 37°C and then embedded in fresh Durcupan® and cured at 60°C for 20 hours.

Spinal cord sections (prepared by Dr Alan Watson), used as positive controls, were fixed as above, then cut to a thickness of 60-100µm on a vibratome and washed in 0.1M PB. Sections were prepared as above, although prior to curing sections were transferred to fresh resin for 90 minutes and flat-embedded between two sheets of acetate, and cured as above. To allow sectioning, the flat embedded sections were mounted on a blank resin stub using cyanoacrylate adhesive (super-glue).

5.2.3. Sectioning and Staining

Thick sections (1µm) were subsequently cut on a Reichert Ultracut E ultramicrotome (Reichert-Jung) using a glass knife, floated on a water bath and collected using a copper loop. The sections were then placed onto Histobond slides (RA Lamb Medical Supplies; Eastbourne, UK) and dried on a hot plate. Slides were then submerged in a solution of sodium ethoxide (see appendix I) to remove Durcupan® embedding resin. Sections were subsequently stained with toluidine blue containing 1% borax until they dried again on a hot plate, washed and mounted under DPX (RA Lamb Medical Supplies; Eastbourne, UK).

Silver or gold ultrathin (60-90nm) sections were cut on a Reichert Ultracut E ultramicrotome (Reichert-Jung) using a sapphire or diamond knife and floated on a water bath. Sections were collected on hexagonal, Pioloform-coated (see appendix I) nickel grids (Agar Scientific, Stansted, UK) and stored for subsequent immuolabelling and/or etching. Nerve sections obtained for counting purposes were collected onto 2mm slotted Pioloform-coated nickel grids (Agar Scientific, Stanstead, UK), to allow visualisation of the whole nerve.

Sections used to for axon counting and structural observations were stained using 2% aqueous uranyl acetate and Reynolds lead citrate (see appendix I). Following washing in

dH₂O the grids were dried overnight and examined with a Phillips 208 transmission electron microscope.

5.2.4. Morphometric Analysis of Electron Micrographs

The nerve supplying the fat pad was obtained from one 4 month and one 24 month animal, fixed, sectioned and stained as described above. Only one animal per age was used in this study due to the degree of variation between the nerve branches supplying the retromalleolar fat pad, and the difficulty in dissecting the nerve from the aged rat owing to the increased fibrous nature of the region. It was not possible to ensure that the sections obtained were from exactly the same level in the nerve, therefore only descriptive statistics could be carried out on the data obtained. Furthermore, nerves do not branch identically in all animals and therefore, the anatomical variation between specimens makes it impossible to be sure of equivalence between animals. The limitations of these findings will be fully detailed in the discussion.

Five sections from each nerve were examined and 3 electron micrographs taken randomly from each section (see Fig 5.2.4.1) at a magnification of x2000. Following processing the number of myelinated and unmyelinated nerve fibres were counted in each plate. In all plates, the fibres or axons overlying the bottom and left hand margins of the plate were included, while those of the top and right hand margins of the plate were excluded.

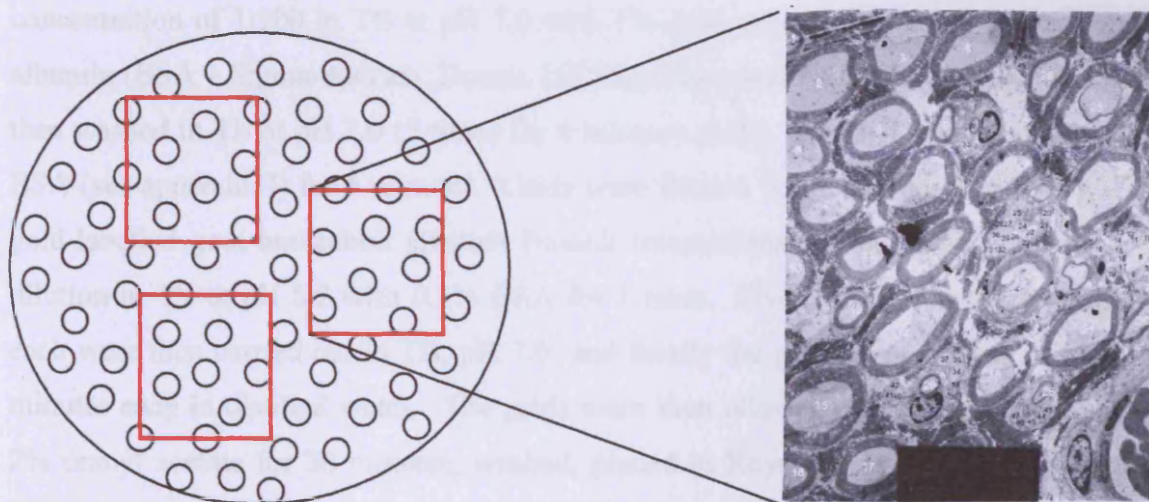


Figure 5.2.4.1: Schematic representation of a nerve used for nerve fibre counting. Image plates (red rectangles) of the nerve were taken randomly. The number of myelinated and unmyelinated nerve fibres were then counted on each plate.

The number of axons from the three plates were added together and expressed in axons per mm². The area of the entire nerve was also calculated and the total number of nerves in the axon estimated. This gave information of the density of nerve fibres which could then be compared between the two ages. From each plate, the area of 10 randomly selected myelinated axons and fibres (axon and myelin sheath) were calculated using Image J 1.37v (Rasband, 2006). The area of the myelin sheath could then be calculated and compared between the ages. A total of 150 myelinated axons were measured in the young and aged nerve. Values were compared with a Student's T-test (un-paired) using Graphpad Prism 2.

5.2.5. Standard Immunogold Labelling

Sections from the nerve and fat pad were immunogold labelled for CGRP using a postembedding, immunogold method. Sections from the dorsal root of the spinal cord were used as a positive control. All processing stages were carried out on sheets of dental wax, to ensure defined liquid droplets. Grids were etched by being floated on droplets of 2% periodic acid (Sigma-Aldrich, Gillingham, UK) for 3 minutes, and then washed in distilled water 5 times for 1 minute each. Subsequently, grids were floated on droplets of saturated sodium metaperiodate (BDH; Poole, UK - 250mg/ml at 50°C) for 3 minutes and washed again as above. Blocking non-specific binding of the secondary antibody was carried out in droplets of 5% normal goat serum (Dako UK; Ely, Cambridgeshire, UK) in Tris buffer at pH 7.0 (TB - see appendix I) for 30 minutes, the grids were subsequently placed onto droplets of the primary rabbit anti-CGRP antibody (Biomol International, Exeter, UK) at a concentration of 1:100 in TB at pH 7.0 with 1% goat serum and 3.3mg/ml bovine serum albumin (BSA – Sigma-Aldrich, Dorset, UK) for 2 hours at room temperature. Grids were then washed in TB at pH 7.0 (5 times for 4 minutes each), then in TB at pH 8.2 with 0.1% BSA (see appendix I) for 5 minutes. Grids were floated in the secondary antibody - 10nm gold-labelled goat anti-rabbit (British Biocell International, Cardiff, UK) used at a 1:30 dilution in TB at pH 8.2 with 0.1% BSA for 1 hour. Five to eight washes for 4 minutes each were then carried out in TB, pH 7.0, and finally the grids were washed 3 times for 4 minutes each in distilled water. The grids were then allowed to dry overnight, stained in 2% uranyl acetate for 20 minutes, washed, placed in Reynolds lead citrate for 5 minutes and finally washed again. Grids were again dried overnight and observed under a Phillips 208 electron microscope.

5.2.6. Detergent Method of Immunogold labelling

This method is based on the Maxwell et al., (1995) method which in turn is modified from that of de Zeeuw et al., (1988). The technique uses detergents instead of chemical etching to allow the antibody to penetrate the resin, as chemical etching may affect the antigen sites. As above, all stages were carried out on dental wax sheets. Grids were rinsed in TB, pH 7.0 (containing 0.9% NaCl; and 0.1% Triton X-100; Sigma-Aldrich, Gillingham, UK) 3 times for 5 minutes each, and then floated in the above solution also containing 5% normal goat serum (Dako UK, Ely, Cambridgeshire, UK) for 30 minutes. The grids were then incubated overnight in the primary antibody, rabbit anti-CGRP diluted to 1:75 in TB at pH 7.0, also containing 0.3mg/ml BSA, in a humidified chamber. Following a series of washes in TB at pH 7.6, the grids were incubated in TB at pH 8.2 (containing 0.9%NaCl and 0.1% Triton X-100) for 30 minutes. Grids were floated in the secondary antibody - 10 nm or 5 nm gold-labelled goat anti-rabbit (British Biocell Internatioal, Cardiff, UK) at 1:30 dilution in TB at pH 8.2 for 2 hours. Grids were again washed 3 times for 5 minutes each in TB at pH 8.2 and finally in dH₂O (5 times for 5 minutes each). They were then allowed to dry overnight, stained, and observed as above.

5.2.7. Controls

PB controls were carried out for both methods, where the primary antibody was omitted (as described previously). This ensured that non-specific binding did not occur on the tissue.

5.3. RESULTS

Semi-thin Sections

The Retromalleolar Fat Pad

The retromalleolar fat pad was made up of unilocular adipocytes (Fig 5.3.1.A) together with a small quantity of fibrous tissue (Fig 5.3.1.B and C). Each adipocyte contained a characteristic single lipid droplet which pushes the organelles and rest of the cytoplasm to the periphery of the cell, creating a very thin cytoplasmic envelope. The nucleus was also restricted to the edge of the cell and contained a darkly stained nucleolus (Fig 5.3.1.B). The cell membranes of neighbouring adipocytes appeared closely associated with each other, except when separated by fibrous strands (Fig 5.3.1.B). The size of these fibrous strands varied from thin slips which weaved between adjacent adipocytes to large bundles of collagenous matrix containing a number of fibroblasts (Fig 5.3.1.C and D). These fibroblasts stained darkly (Fig 5.3.1.D) with toluidine blue, were occasionally highly vacuolated and sent out elongated spine-like projections, which enveloped small regions of the ECM (Fig 5.3.1.C). A vast capillary network, passing between the closely associated adipocytes within the retromalleolar fat pad, was also observed. In addition to fibroblasts and adipocytes, other cell types were identified within the fat pad in toluidine blue-stained semi-thin sections. A number of these cells had large nuclei with dense chromatin concentrated around the periphery of the nucleus, and a pale staining cytoplasm containing a number of light blue stained granules/vesicles within the cytoplasm (Fig 5.3.1.E and F). In addition, mast cells containing obvious metachromatic granules were also present within the fat pad (Fig 5.3.1.F). Another unidentified cell type was also seen (infrequently) within the fat pad. These cells were large (25µm in diameter), with large spherical nuclei containing a darkly stained nucleolus (Fig 5.3.1.F) and an agranular cytoplasm. No major differences were observed between the adipocytes or fibroblasts in the 4 or 24 month rat (not shown). However, differences were observed between the synovial membranes of the young and old rats (Fig 5.3.1.G and H). The synovial membrane lining the tip of the fat pad in the 4 month rat consists predominately of pale staining cells with large translucent vacuoles in their cytoplasm. The majority of the cells in the synovium appeared to have characteristics of both type A and B synoviocytes, it was not possible to definitively identify either type of cell (Fig 5.3.1.H). Deep to the cellular layer, was a thin fibrous sub-lining layer, containing small capillaries (Fig 5.3.1.G). A small number of mast cells were also present in close association with sub-lining layer of the synovial membrane (Fig

5.3.1.G). The most marked difference observed between the 4 and 24 month rats, was an increase in the thickness of the fibrous sub-lining layer of the synovial membrane (Fig 5.3.1.G and H). In addition there appeared to be an increase in the number of fibroblast like cells in the synovium and its sub-lining layer (Fig 5.3.1.H). Mast cells were also present in the sub-lining layer in the aged rats (Fig 5.3.1.H).

The Nerve Branch Supplying the Retromalleolar Fat Pad

Semi-thin, toluidine-blue stained sections of the nerve branch supplying the retromalleolar fat pad in 4 and 24 month old rats. The myelinated axons in the aged rat were larger and accompanied by an increase in the amount of fibrous connective tissue of the endoneurium (Fig 5.3.2.A and B). There were also differences in the structure of the fibres themselves. In the nerves from young rats, axons were uniformly surrounded by thick, darkly-stained myelin sheaths (Fig 5.3.2.A). In contrast, the myelin sheaths in aged rat were often indented/infolded, irregular in shape and contained spherical myeloid bodies (Fig 5.3.2.B).

Transmission Electron Microscopy

The Retromalleolar Fat Pad

As described above, adipocytes within the retromalleolar fat pad contained a single lipid droplet within the centre of the cell; while the adipocyte nuclei and organelles were pushed to the periphery against the cell membrane. Adjacent adipocytes were closely associated with each other, although it was clear that each cell had its own thin basement membrane. In the small intercellular space ($\approx 300\text{nm}$) between neighbouring adipocytes, were irregularly-arranged, collagen fibres (Fig 5.3.3.A and B).

Bundles of collagen fibres were also observed within the main body of the fat pad. Some of these fibres were cut in cross section while others were cut longitudinally in the same TEM section, indicating that the fibres run in a number of directions (Fig 5.4.3.C and D). At high magnification, the collagen fibres within the fibrous region appeared to vary in diameter (Fig 5.4.3.E). Fibroblasts within the fibrous region, as demonstrated in thick sections, sent out cytoplasmic projections which enveloped small bundles of collagen fibres (Fig 5.3.3.F). A number of mast cells were also present within the fat pad; they contained a large number of large electron-dense vesicles distributed throughout the cell cytoplasm (Fig 5.4.3.C and D). Putative monocytes were also identified. These cells had a characteristic, irregular multi-lobular nucleus and relatively condensed chromatin (Fig 5.4.4.A).

A number of different cell types were identified within the synovial membrane lining the tip of the fat pad. A large number of such cells contained large electrolucent vacuoles, spanning up to 4µm in width (Fig 5.3.4.B). Others were smaller and contained both electrolucent and electron dense vesicles, or elongated irregular vacuoles. There was also small amount of extracellular matrix present between cells of the synovial membrane (Fig 5.3.4.B).

As described previously a large number of blood vessels and capillaries were present within the fat pad. This was also demonstrated with the use of TEM. Fig 5.3.4.C demonstrates a grazing section through a large, bifurcating blood-vessel within the fat pad. Although nerve fibres were difficult to find by TEM, nevertheless, they were occasionally identified within fat pad. The majority ran in small groups and were either thinly or non-myelinated (Fig 5.3.4.D). As demonstrated previously with the use of light microscopy immunohistochemistry, these fibres weaved between the cell membranes of closely-associated adipocytes (Figs 5.3.4.D-E). One of the most interesting observations was the finding of a single, thinly myelinated nerve fibre in the space between 3 neighbouring adipocytes (Fig 5.3.4.D). An array of collagen fibres surrounded this nerve. Some fibres were arranged concentrically, spiralling around the nerve, while others ran parallel to its longitudinal axis (Fig 5.3.4.F.).

The Nerve Supplying the Retromalleolar Fat Pad

The nerve branch supplying the retromalleolar fat pad (Fig 5.2.1) was also studied by TEM. The observations made ultrastructurally, confirmed those made with the use of semi-thin sections. The nerve contained both myelinated (Fig 5.3.5.A) and unmyelinated fibres (Fig 5.3.5.B). The former predominated, while unmyelinated nerve fibres (organised in groups) were distributed throughout the nerve (Fig 5.3.5.B). Schwann cells were seen in association with both myelinated and unmyelinated axons; although only one form of Schwann cell contributes to myelination of the nerve fibre. In myelinated nerve fibres, the Schwann cell was closely associated with a single axon and the cytoplasm wrapped concentrically around it, though there were some small indentations in the myelin sheath (Fig 5.3.5.A). By contrast, a number of unmyelinated axons were associated with a single Schwann cell; the axons were embedded irregularly within the Schwann cell cytoplasm which enveloped them completely (Fig 5.3.5.B).

The fibres in the nerve from the aged (24 month) rat differed morphologically from those in the 4 month animal. The myelin sheaths in particular were different - they were relatively uniform in the younger animals, whereas those from aged rats demonstrated infolding – i.e. where the sheath invaginated the axon, distorting its profile (Fig 5.3.5.C). In addition, oval structures composed of myelin were present within the nerve axon; which appeared to have budded off an indented part of the sheath (Fig 5.3.5.D). Double myelination of axons was also occasionally observed. Two or 3 concentric myelin sheaths, separated by unidentifiable material and degenerated myelin were occasionally noted (Fig 5.3.5.E). The axons of myelinated fibres also demonstrated age related changes. Axon shrinkage was particularly common - i.e. the axon becomes separated from the inner layer of the myelin sheath allowing the mesaxon to be seen (Fig 5.3.5.E). The axoplasm of these fibres also contained varying numbers of electron-lucent vacuoles, a sign of axon degeneration (Fig 5.3.5.E). Axons also contained small pieces of unidentified ‘debris’ and dense bodies of irregular size (Fig 5.3.5.D and E). Similar changes were occasionally observed in the 4 month rat (not shown).

In contrast to the vast number of abnormalities identified in myelinated fibres, no pathological characteristics of unmyelinated fibres could be identified within the sections examined.

CGRP-immunogold Labelling of the Nerve Branch Supplying the Retromalleolar Fat Pad

Sections from the nerve branch were also studied for the presence of CGRP with the use of immunogold labelling. Because CGRP is only located within large granular vesicles which are sparsely located in unmyelinated axons, it proved particularly difficult to find CGRP positive vesicles. Furthermore, substance P was often present or co-localised within these granules; therefore several immunogold methods were used in an attempt to amplify labelling of CGRP positive vesicles.

Standard Immunogold Labelling Procedure

None of the sections labelled demonstrated the presence of gold particles located on granular vesicles within unmyelinated nerve fibres. This was also true for PBS negative control sections. Positive control sections, stained in parallel, did however demonstrate

gold particles on granular vesicles within the superficial layers of the dorsal horn in the spinal cord.

Detergent Method

Some sections labelled for CGRP using the detergent method demonstrated a number of 10nm gold particles on dark electron-dense granular vesicles within unmyelinated nerve fibres in the peroneal anastomotic branch of the sural nerve in both old and young specimens (Figs 5.3.6.A-D). These results were supported by positive controls from the dorsal horn of the spinal cord, illustrating CGRP labelling in vesicles in synaptic and axonal profiles of the superficial layers in the dorsal horn (Fig 5.3.6.E and F).

4.3.4. Morphometric Analysis of the Nerve Supplying the Retromalleolar Fat Pad

Profiles of myelinated and unmyelinated nerve fibres could easily be identified in both young and aged animals. Representative sections are shown in Fig 5.3.7.A and B. A quantitative analysis of the results demonstrated a significant decrease in the number of both myelinated ($p < 0.001$) and unmyelinated ($p < 0.05$) nerve fibres in the aged (24 month) rat (Fig 5.3.8.A and B). There was also a significant ($p < 0.0001$) increase in the thickness of the myelin sheath in the aged (24 month) rats when compared with young (4 month) rats (Fig 5.3.8.C). Fig 5.3.9.D illustrates the changes in the area of the myelinated fibres (axon and myelin sheaths) with the age of the animal. The number of fibres with an area $< 30\mu\text{m}^2$ increased with the age of the animal; fibres between 30 and $70\mu\text{m}^2$ decreased with age, while those over $70\mu\text{m}^2$ increased with age.

THE RETROMALLEOLAR FAT PAD – TOLUIDINE BLUE STAINED, SEMI-THIN SECTIONS

Figure A: The structure of the retromalleolar fat pad in the 4 month rat. Note the close association between the cytoplasmic membranes of adjacent adipocytes (arrowheads). Lipid droplets (LD) occupy the majority of the adipocyte. Arrows indicate the presence of capillaries and venules within the fat pad. Scale bar = 100µm

Figure B: The peripherally placed, discoid nucleus of an adipocyte in the fat pad. Note the presence of a nucleolus (arrow) within the nucleus. LD – Lipid droplet. 4 month rat. Scale bar = 30µm

Figure C: A cell with fibroblastic characteristics in a fibrous region of the fat pad. Note the elongated, spindle-like processes (arrowheads) extending from the cell body (arrow) surrounding bundles of collagen fibres. 4 month rat. Scale bar = 30µm.

Figure D: Arrows indicate 3 closely associated fibroblast like cells in the fibrous region of the fat pad. They possess spindle like processes (arrowheads), but also contain unstained vacuoles within their cytoplasm. 4 month rat. Scale bar = 30µm

Figure E: A large unidentifiable cell (arrow) within the fat pad. The nucleus is located centrally with a darkly stained nucleolus and pale staining cytoplasm. LD- lipid droplet. 4 month rat. Scale bar = 30µm

Figure F: Two cells within the fat pad which contain dark blue stained granules within their cytoplasm (arrows). The cells are in close association with capillaries or venules (*). These granules differed to those metachromatic granules present in mast cells (arrowhead). LD – lipid droplet. 4 month rat. Scale bar = 30µm

Figure G and H: The synovial membrane in a 4 month (G) and 24 month (H) rat. Note the increased thickness of the sublining layer (SLL) of the synovial membrane in the aged rat. Mast cells (arrows) are present in close association with the sub-lining layer of the synovium at both ages. Arrowheads indicate synovial cells with vacuoles in the cytoplasm. Scale bar = 30µm.

Figure 5.3.1

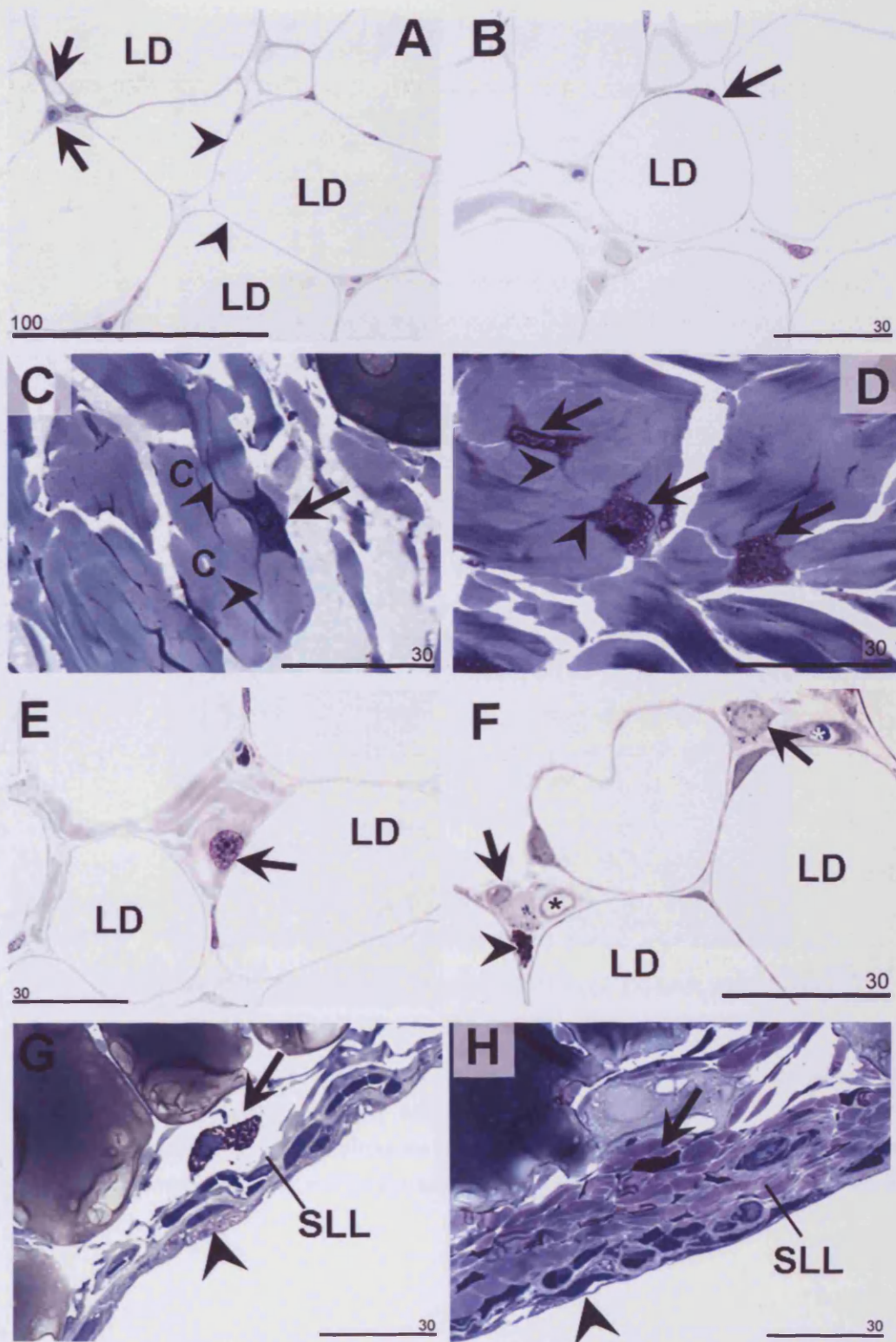
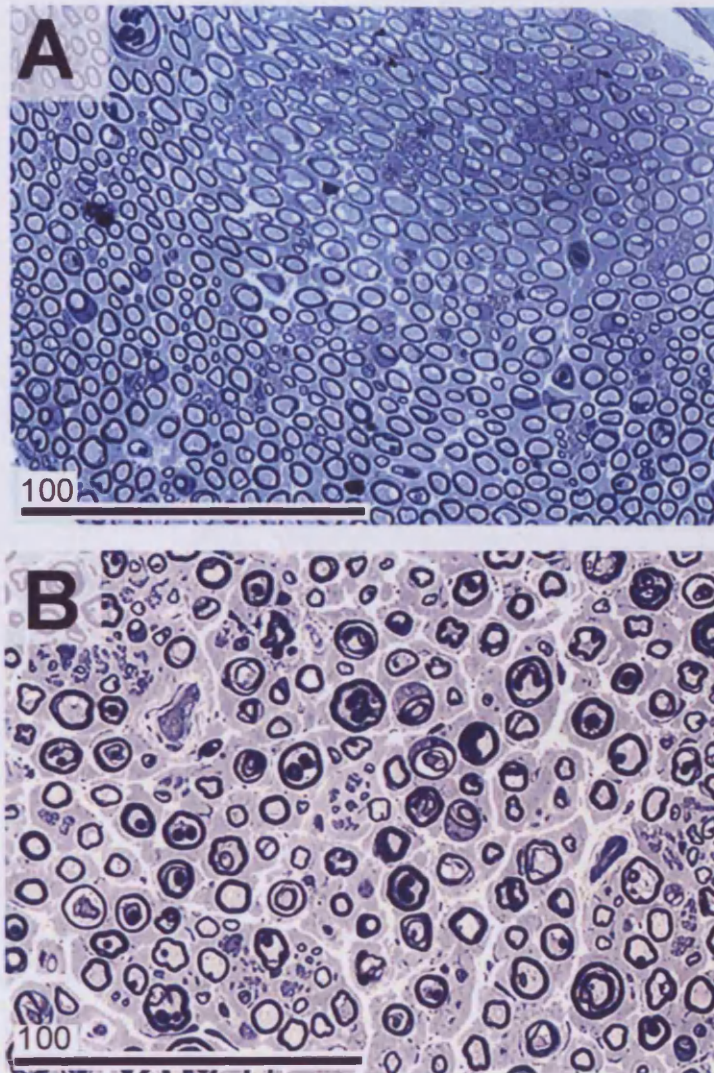


Figure 5.3.2.

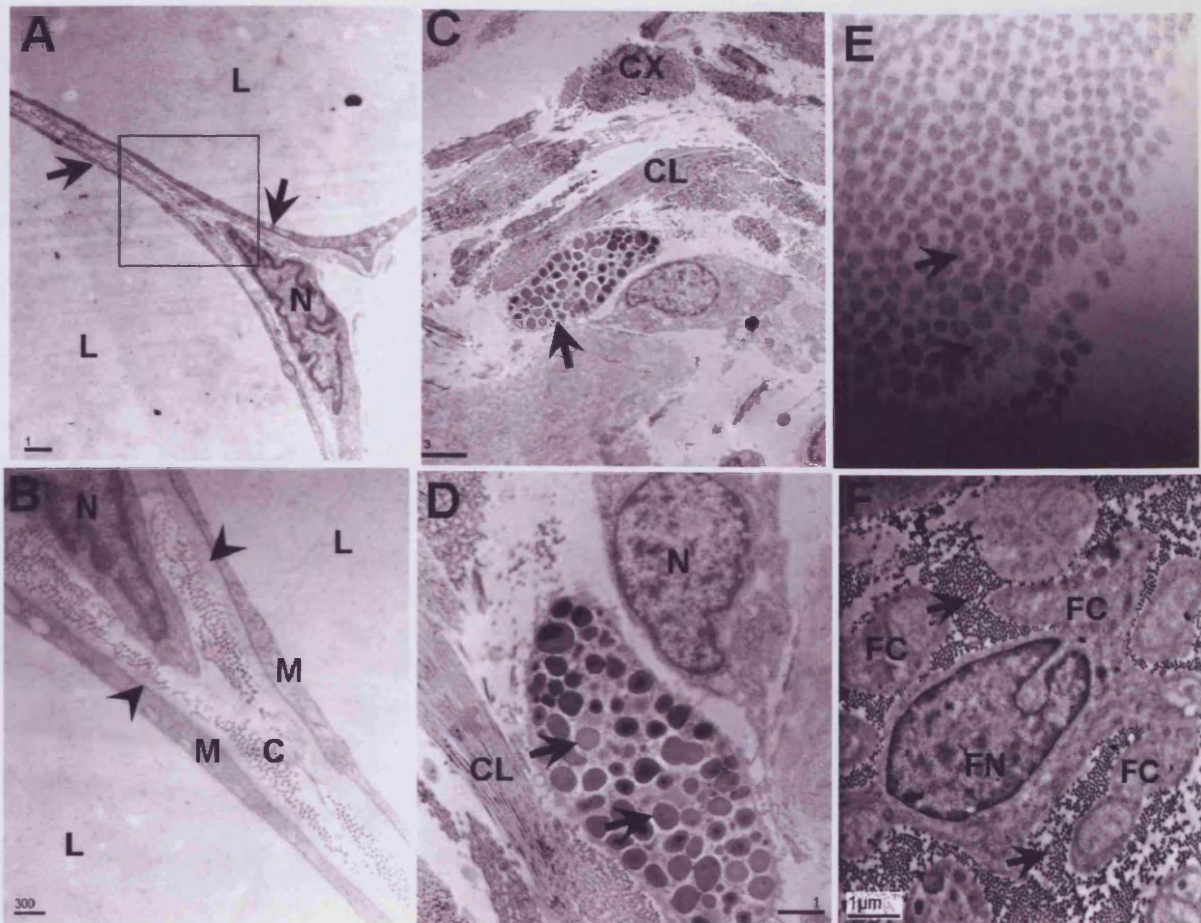


**THE NERVE SUPPLYING THE RETROMALLEOLAR FAT PAD –
TOLUIDINE BLUE STAINED, SEMI-THIN SECTIONS**

Figure A: Low power view of the nerve supplying the retromalleolar fat pad in the 4 month rat. Note the uniform size and shape of the individual fibres within the nerve. Scale bar =100 μ m.

Figure B: Low power view of the nerve supplying the retromalleolar fat pad in the 24 month rat. Note the irregular size and shape of the fibres within the nerve; and the increased amount of connective tissue present between the fibres. Scale bar = 100 μ m

Figure 5.3.3.



THE RETROMALLEOLAR FAT PAD – ULTRATHIN SECTIONS

Figure A: The cell membranes (arrows) of 2 adjacent adipocytes are closely associated. The nucleus (N) of a cell is squashed in the cleft between the two adipocytes. Large lipid droplets (LD) fill the adipocyte pushing the cytoplasm to the periphery of the cell. 24 month rat. Scale bar = 1µm.

Figure B: Higher power image of the two adjacent adipocytes in Fig A. Note the presence of collagen fibrils (C) running in different directions between the membranes (M) of the adjacent adipocytes. Arrowheads indicate amorphous material covering the adipocytes. N – nucleus, L – lipid droplet. 24 month rat. Scale bar = 300nm

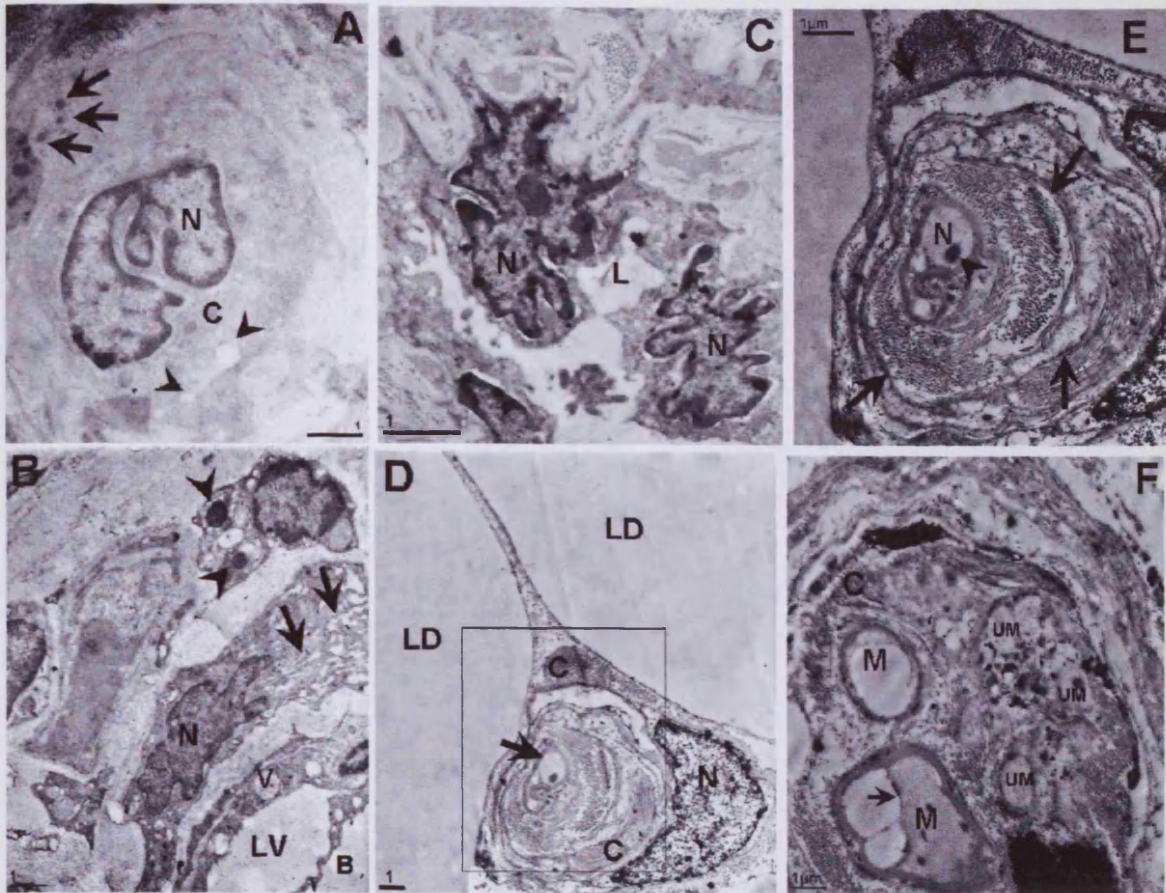
Figure C: A mast cell (arrow) in the fibrous region of the retromalleolar fat pad. Note the collagen bundles are cut both longitudinally (CL) and in cross section (CX) demonstrating that they run in a multitude of directions. 24 month rat. Scale bar = 3µm.

Figure D: High power view of the mast cell in Fig C. Note the presence of large darkly stained granules within the cell (arrows). The mast cell nucleus is not seen in this section. Note the longitudinally arranged collagen bundles adjacent to the cell (CL). N-Nucleus. 24 month rat. Scale bar = 1µm

Figure E: A bundle of collagen fibrils (arrows) within in the retromalleolar fat pad. Note how the fibrils vary in size. 4 month rat. Scale bar = 100nm.

Figure F: A fibroblast in the fibrous region of the retromalleolar fat pad. Note the way in which the fibroblast cytoplasm (FC) envelops bundles of collagen fibrils (arrow). FN- Fibroblast nucleus. 4 month rat. Scale bar = 1µm

Figure 5.3.4.



THE RETROMALLEOLAR FAT PAD – ULTRATHIN SECTIONS

Figure A: A putative monocyte within the retromalleolar fat pad. The cell has a bilobed nucleus (N) with euchromatin concentrated around the periphery of the nucleus and no nucleolus. The cytoplasm (C) contains a number of granules including electron dense (arrow) and electron leucant granules (arrowheads). 24 month rat. Scale bar = 1µm

Figure B: The synovial membrane lining the retromalleolar fat pad. Note the lining cells contain large (LV) and small vacuoles (V). Arrows indicate elongated electron-lucent regions in one synovial cell. Electron dense granules (arrowheads) were also present in some cells. N - nucleus. 4 month rat. Scale bar = 1µm

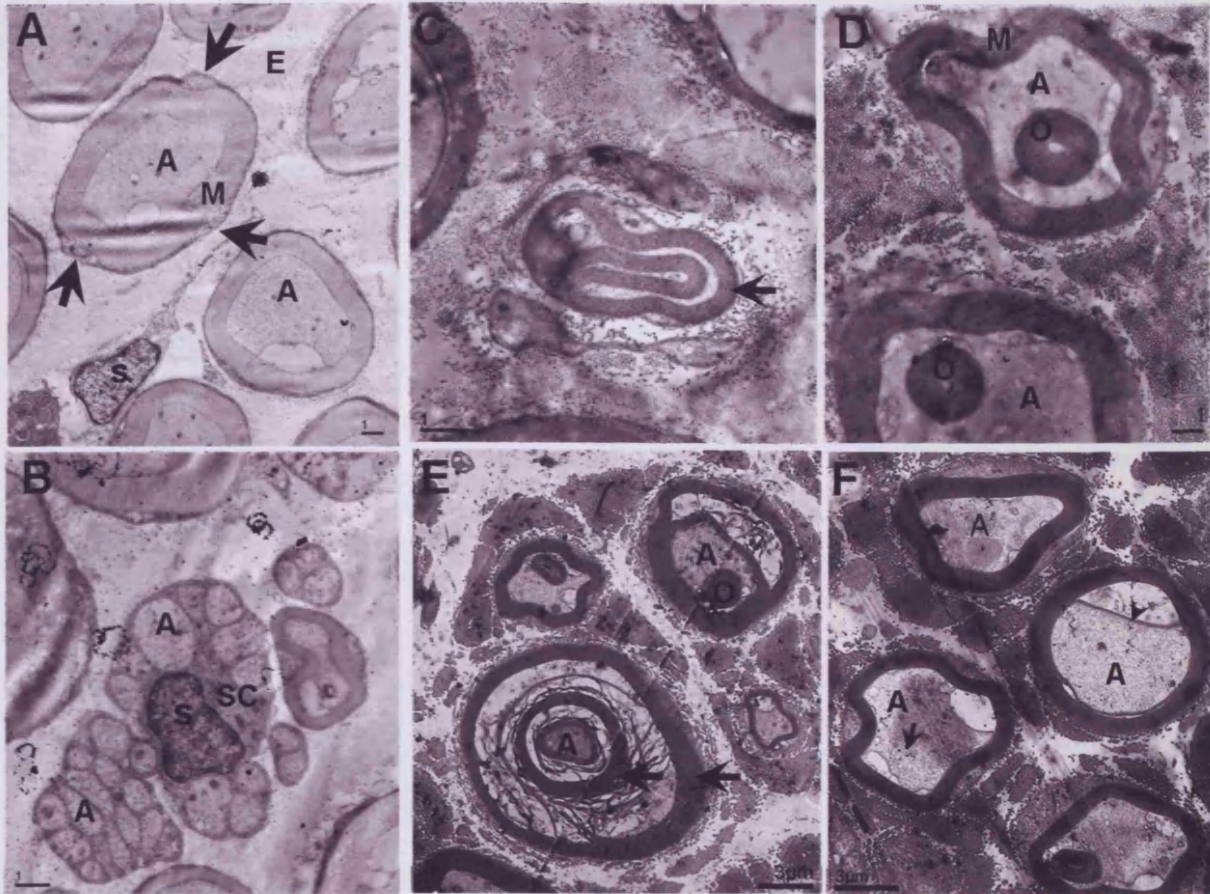
Figure C: A branching blood vessel in the retromalleolar fat pad. Note the irregular shape of the cell nuclei (N) of its lining cells. L – lumen of the blood vessel. Scale bar = 1µm.

Figure D: A thinly myelinated nerve fibre (arrow) in the cleft between adjacent adipocytes. The nerve fibre is surrounded by several whorls of collagen fibres (C). A cell nucleus (N) is present in close association with the collagen whorls. LD – lipid droplet. Scale bar = 1µm.

Figure E: A high power view of the nerve in Fig D. Arrows indicate whorls of collagen fibres which run in different directions around the thinly myelinated nerve fibre (N). Note the irregular shape of the nerve fibre which also contains an electron-dense mitochondrion (arrowhead). 24 month rat. Scale bar = 1µm.

Figure F: A collection of myelinated (M) and unmyelinated (UM) nerve fibres surrounded by collagen fibres (C) in a cleft between adjacent adipocytes. Arrow indicates where the axolemma has pulled away from the myelin sheath. 24 month rat. Scale bar = 1µm.

Figure 5.3.5.



THE NERVE SUPPLYING THE RETROMALLEOLAR FAT PAD – ULTRATHIN SECTIONS

Figure A: Axons (A) wrapped in myelin (M) surrounded by endoneurium (E) within the nerve supplying the retromalleolar fat pad. Note the presence of a Schwann cell nucleus adjacent to a myelinated axon. Arrows indicate Cajal bands of the nerve fibre. 4 month rat. Scale bar = 1 μ m.

Figure B: A collection of unmyelinated axons (A) present within the nerve supplying the retromalleolar fat pad. Note the single Schwann cell nucleus (S) which supports the group of unmyelinated axons in its cytoplasm (SC). 4 month rat. Scale bar = 1 μ m

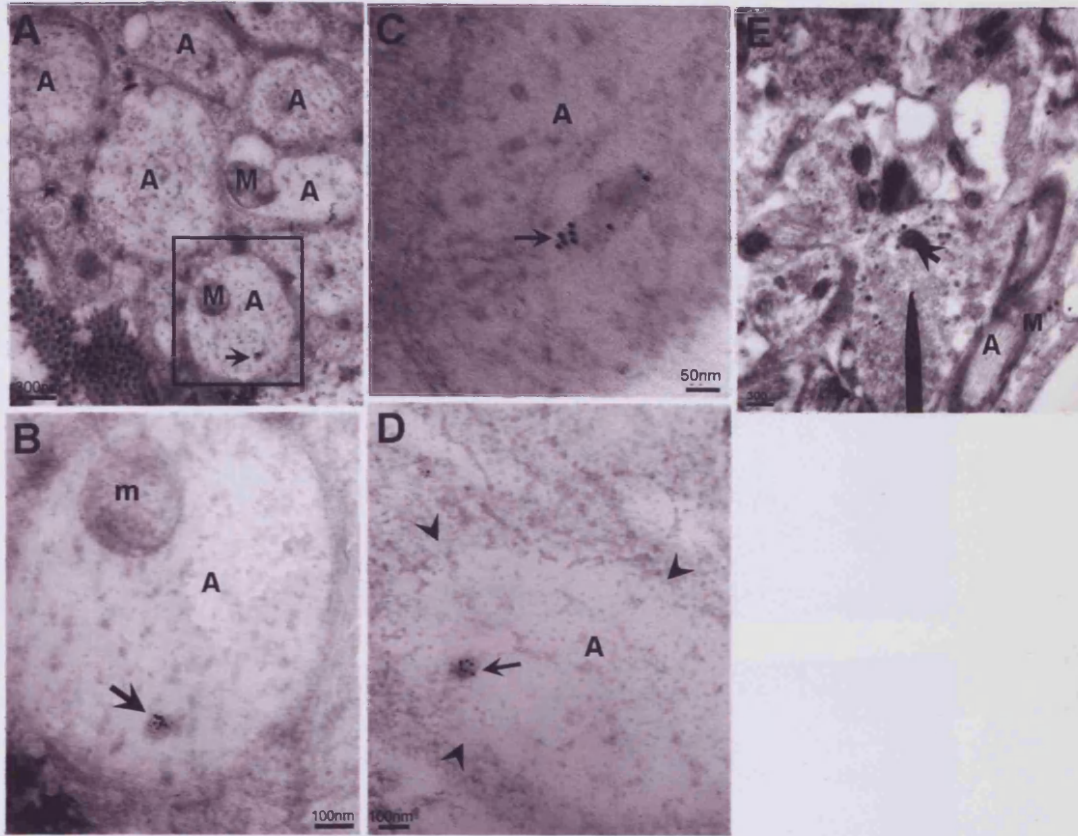
Figure C: A myelinated nerve fibre (arrow) in the nerve supplying the retromalleolar fat pad in the 24 month rat. Note the infolding of the myelin sheath into the axon. Scale bar = 1 μ m.

Figure D: Two myelinated nerve fibres in the nerve supplying the retromalleolar fat pad in the 24 month rat. Note the ovoids (O) of myelin within the axonal region (A) of the fibre. M – myelin. Scale bar = 1 μ m.

Figure E: Nerve fibres in the nerve supplying the retromalleolar fat pad in the 24 month rat. Note the presence of ovoids (O) and double myelin sheaths (arrows). Degenerating myelin and debris is located between the double myelin sheaths. Scale bar = 3 μ m.

Figure F: Nerve fibres in the nerve supplying the retromalleolar fat pad in the 24 month rat. The arrow indicates unidentified 'debris' within the fibres axon (A). The arrowhead points to the axolemma of the shrunken axon which has pulled it away from the surrounding myelin sheath. Scale bar = 3 μ m.

Figure 5.3.6.



Figures A-D: ULTRATHIN SECTIONS OF THE NERVE SUPPLYING THE RETROMALLEOLAR FAT PAD IMMUNOGOLD LABELLED FOR CALCITONIN GENE RELATED PEPTIDE (CGRP) - DETERGENT METHOD.

Figure A: A group of unmyelinated nerves (A) in the nerve supplying the retromalleolar fat pad in the 24 month rat. Several 10nm gold particles (arrow) were present on a granular vesicle within one axon. M – mitochondria. Scale bar = 300nm.

Figure B: High power image of the axon highlighted in Fig A. Arrow indicates the 10nm gold particles bound to a CGRP containing granular vesicle within the axon (A). M– mitochondria. Scale bar = 100nm.

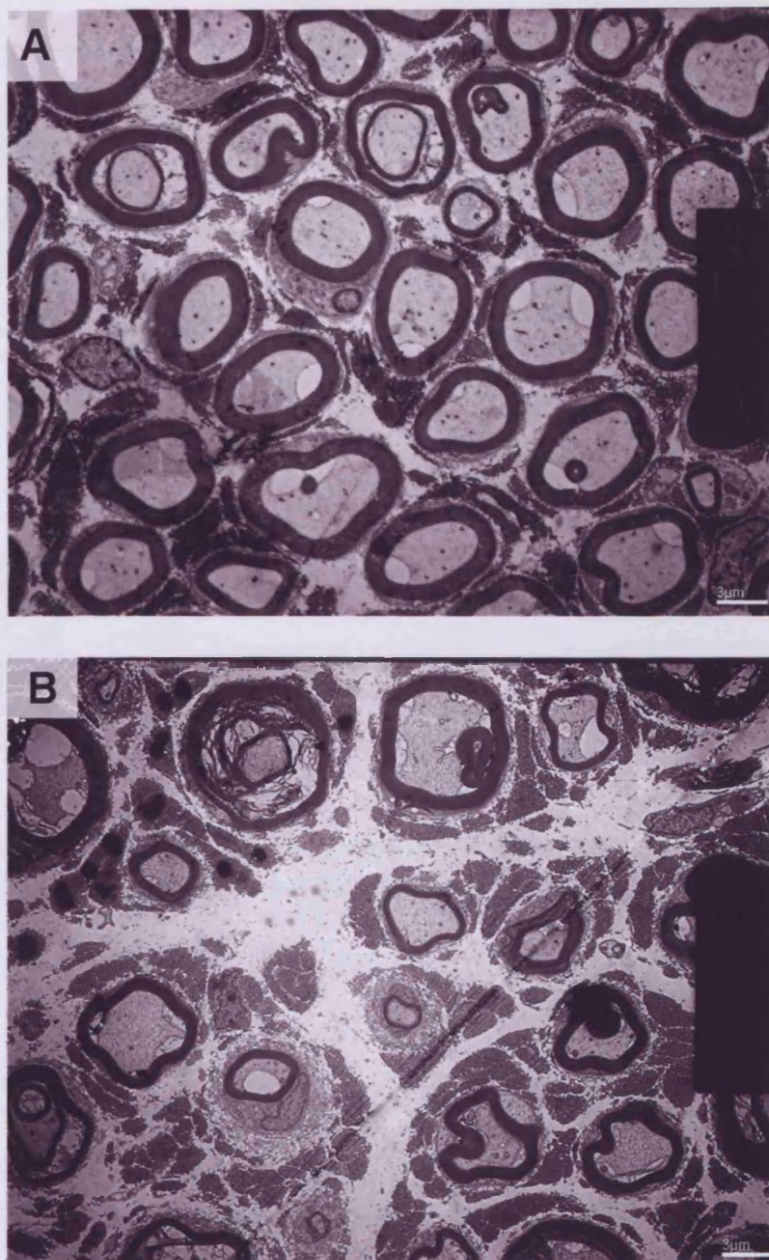
Figure C: High power image of an unmyelinated axon in the nerve supplying the retromalleolar fat pad in a 24 month rat. Arrow indicates 10nm gold particles bound to a CGRP-containing, granular vesicle within the axon (A). Scale bar = 50nm

Figure D: An unmyelinated axon in the nerve supplying the retromalleolar fat pad in a 4 month rat. The boundaries of the axon are indicated by arrowheads. Arrow indicates 10nm gold particles bound to a CGRP containing granular vesicle within the axon (a). Scale bar = 100nm.

Figures E: ULTRATHIN SECTION OF THE DORSAL HORN FROM THE SPINAL CORD IMMUNOGOLD LABELLED FOR CALCITONIN GENE RELATED PEPTIDE (CGRP) - DETERGENT METHOD.

Figure E: Arrow indicates CGRP containing granular vesicle with bound 10nm gold particles in an unmyelinated fibre in the dorsal horn of the spinal cord. A – axon, M – myelin sheath. Scale bar = 300nm.

Figure 5.3.7.



REPRESENTATIVE ULTRATHIN SECTIONS THROUGH THE NERVE SUPPLYING THE RETROMALLEOLAR FAT PAD IN THE RAT USED FOR MORPHOMETRIC ANALYSIS.

Figure A: A section through the nerve supplying the retromalleolar fat pad in the 4 month rat. Note the regular shape and size of the fibres within the nerve and their even distribution. Scale bar = 3µm.

Figure B: A section through the nerve supplying the retromalleolar fat pad in the 24 month rat. Note the irregular size and shape of the fibres within the nerve and their uneven distribution and the large amount of connective tissue between the nerve fibres. Scale bar = 3µm.

Figure 5.3.8.

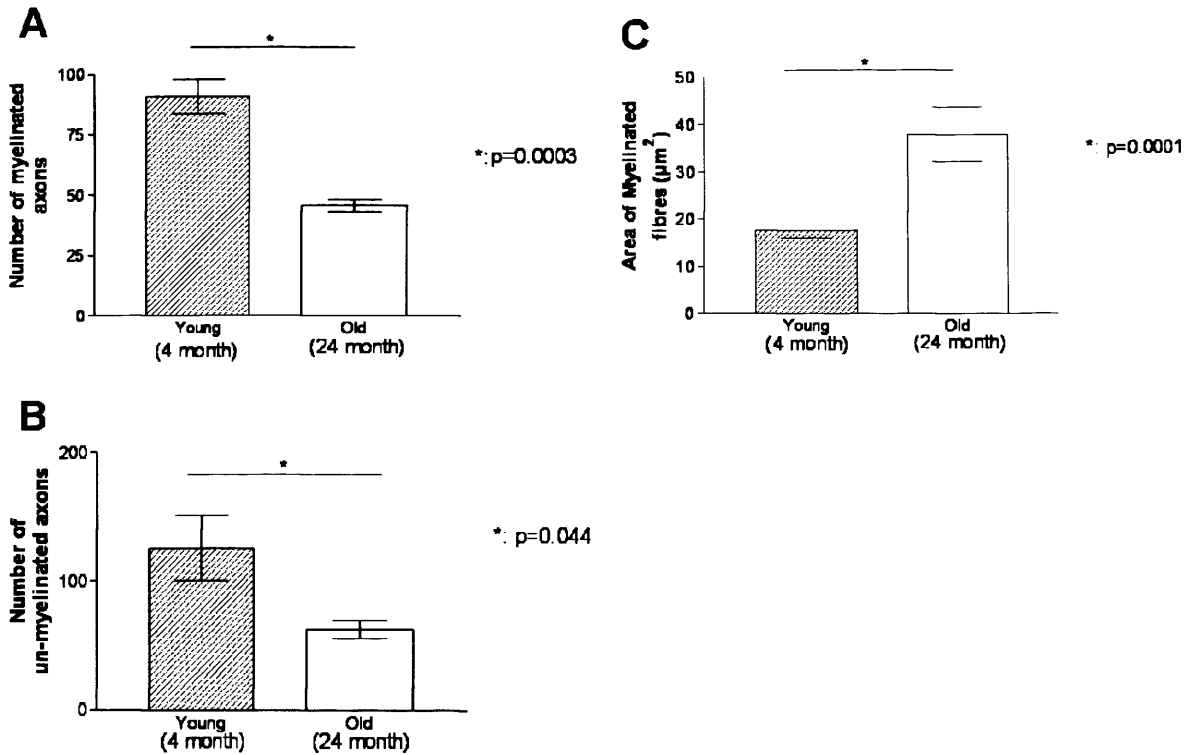


Figure A: Histograms representing the number of myelinated axons in $1,552 \mu\text{m}^2$ of the nerve supplying the retromalleolar fat pad in the 4 and 24 month rat. Means \pm Standard Errors. * = significant difference ($p < 0.05$).

AGE	N	MEAN	STANDARD ERROR
4 Month	5	30.26	0.854
24 Month	5	15.2	2.388

Figure B: Histogram representing the number of unmyelinated axons in $1,552 \mu\text{m}^2$ of the nerve supplying the retromalleolar fat pad in the 4 and 24 month rat. Mean \pm Standard Error. * = significant difference ($p < 0.05$).

AGE	N	MEAN	STANDARD ERROR
4 Month	5	41.9	8.455
24 Month	5	21	2.387

Figure C: Graph representing the thickness of the myelin sheath in $1,552 \mu\text{m}^2$ of the nerve supplying the retromalleolar fat pad in the 4 month and 24 month rat. Mean \pm Standard Deviation. * = significant difference ($p < 0.05$).

AGE	N	MEAN	STANDARD DEVIATION
4 Month	5	17.53	2.44
24 Month	5	37.92	5.79

Figure 5.3.9.

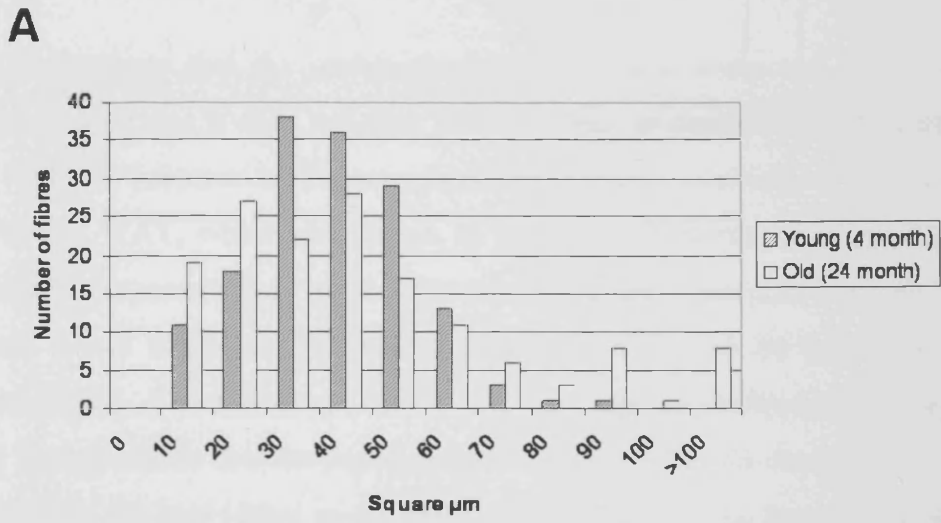


Figure A: Histogram illustrating the distribution of myelinated nerve fibre area (μm^2) in the 4 and 24 month rat.

Fibre area (μm^2)	Young (4 month)	Old (24 month)
0	0	0
10	11	19
20	18	27
30	38	22
40	36	28
50	29	17
60	13	11
70	3	6
80	1	3
90	1	8
100	0	1
>100	0	8

5.4. DISCUSSION

The results demonstrate that the retromalleolar fat pad was composed solely of white adipocytes suggesting that it does not play a role in heat production (which is associated specifically with the presence of brown adipocytes). This contrasts with a number of depots of visceral WAT, which are known to contain both forms of adipocytes (Cinti, 2005). However, the presence of “masked brown adipocytes” – i.e. cells with the ability to transform into brown adipocytes (Cousin et al., 1992) could not be ruled out with the techniques employed. These findings, along with the presence of fibrous septa within the pad, support the hypothesis that the pad is a structural adipose tissue deposit similar to that which is present in the heel (Jahss et al., 1992). It may play a role in reducing shear and dissipating stress at the Achilles tendon enthesis (Canoso et al., 1988; Theobald et al., 2006) rather than acting purely as a storage depot for triacylglycerol.

The multi-directional orientation of collagen bundles within the fat pad is of particular interest. According to Davis’ law - a corollary to the better known Wolff’s law which states that bone will remodel to adapt to the loads it experiences, soft tissue can also remodel according to the forces placed upon it (Tippett and Voight, 1995). Thus, a fat pad which experiences forces from multiple directions may form multi-directional collagen bundles within it. These are probably secreted by the resident fibroblasts noted in this study. The fibroblasts have similar characteristics to those in tendon – i.e. they have elongated, spine-like processes which envelope the surrounding collagen bundles (McNeilly et al., 1996). This characteristic fibroblast shape has been described previously with the use of TEM, by Birk and Zycband (1994), in the context of tendon development. The fibroblasts secrete the collagen extracellularly into a series of compartments. This accounts for the characteristically-complex shape of the cell, and gives the cells a greater degree of control over the secretion and organisation of their surrounding ECM (Birk and Zycband, 1994). In addition to these observations, the presence of connexin 32 in the fibrous regions of the fat pad (see chapter 6) suggests that fat pad fibroblasts have the ability to communicate with each other via gap junctions and co-ordinate the secretion of collagen in response to the mechanical loading. As in tendons, such loading might be sensed by focal contacts and adherens junctions (Ralphs et al., 2002; Waggett et al., 2006). This cell-ECM organisation, supports the concept that collagen is actively synthesised in the fat pad in response to mechanical loading.

At high magnification, collagen fibres seen in the same section, appeared to be of different diameters – possibly because collagen fibrils are known to taper towards their ends (Banfield, 1952). Those fibrils which were of small diameter may therefore be cross-sections through the tapering end of a fibril rather than representing genuinely different-sized fibrils. Small numbers of collagen fibres were also present in the small intercellular spaces between closely-adjacent neighbouring adipocytes. Such fibres have also been identified with the use of SEM (Kubo et al., 2000), but few authors have commented on their significance in fat. Kubo et al., (2000) suggest that the basement membrane of each adipocyte is interconnected to the type I collagen matrix via collagen types III, V, and VI. It is further suggested that these fibres may play an important role in the organisation of adipocytes within the fat pad (Kubo et al., 2000). The importance of the ECM in adipose tissue is highlighted by the number of studies attempting to recreate adipocyte differentiation *in vitro* with a 3D system which replicates conditions *in vivo* (Daya et al., 2007; Kang et al., 2007; Kubo et al., 2000). Adipocytes in 2D culture do not usually have the same extracellular characteristics and tissue organisation (Daya et al., 2007). It is currently thought that interstitial collagens are secreted by pre-adipocytes during differentiation and that membrane bound matrix metalloproteinases (MT-MMP) might play an important role in their breakdown (remodelling) during differentiation (Chun et al., 2006). The biomechanical role of the collagen fibres within most fatty tissues has not been clarified. In the retromalleolar fat pad, it is possible that they may play a significant role in stabilising the fat cells within the pad, providing tensile strength during loading, as Ker et al., (1999) have suggested for the heel pad in the foot.

Mast cells (as previously demonstrated in chapter 3) were present not only within the fat pad itself, but also in close association with the sub-lining layer of the synovium. These cells are known to play a role in detecting pathogens and mounting an immune response; therefore their presence in the synovium suggests that these cells may be capable of monitoring the enthesis organ for infection, and initiating an inflammatory response (Nigrovic and Lee, 2005). This is in line with the idea that the fat pad may have a significant role as an immune organ. Mast cells may thus be significant players in the autoimmune response associated with SpA (Buckley et al., 1997). In addition, it is possible that the presence of mast cells may be a factor in overuse injuries (enthesopathies) and play a similar role to that documented in osteoarthritis, where an increased number of degranulating and intact mast cells were seen when compared to normal individuals (Dean

et al., 1993). The soluble products released by the mast cell during activation can have two effects by passing into the synovial fluid and coming into direct contact with the fibro/chondrocytes. This can increase the expression of proteolytic enzymes by fibroblasts, synovial cells, and chondrocytes within the joint (Lees et al., 1994; Yoffe et al., 1984). The prolonged release of mast cell products through excessive mechanical/repetitive loading may lead to the degeneration of the fibrocartilage at the enthesis, as has been speculated in osteoarthritis (Dean et al., 1993) and rheumatoid arthritis (Bromley and Woolley, 1984a; b).

In addition to its degenerative effect, mast cell histamine is capable of stimulating fibroblast proliferation (Berton et al., 2000) and mast cell tryptase can promote collagen synthesis (Abe et al., 1998). This is particularly interesting in the light of the current observation that the sub-lining layer of the synovium showed a marked increase in fibrous tissue and mild fibroblast hyperplasia with increasing age. It may be speculated from previous data (as described above) that mechanical loading of the fat pad can lead to activation of the mast cells, and in turn stimulating fibroblast proliferation and collagen secretion over a long period of time (throughout the life of the animal). This may account for the increased thickness/fibrous nature of the synovium. Similar observations, demonstrating an increase in fibrous nature of the synovial membrane have been noted in man (Pasquali-Ronchetti et al., 1992).

The highly vascularised nature of adipose tissue is well known (Gersh and Still, 1945), and may be important in maintaining/controlling the size of the retromalleolar fat pad (Rupnick et al., 2002). It would be interesting to determine whether the size of the retromalleolar fat pad can be affected by various endocrine hormones involved in adipogenesis in the same manner as has been demonstrated for visceral WAT.

With the use of TEM, it was possible to demonstrate the presence of nerve fibres in the space between adjacent adipocytes. Although, these fibres were only occasionally observed, this may be explained by the small amount of tissue that had to be used for each block of tissue to ensure penetration of the osmium. Even though the samples were small, the osmium did not fully penetrate the tissue due to its high lipid content. This may also account for the poor contrast of the images presented here. Where fibres were observed, they were fine, thinly-myelinated or unmyelinated axons - indicating a sensory function

(Bear et al., 2006). No nerve fibres were found to contain CGRP-containing granular vesicles with any of the techniques used. CGRP-containing vesicles were however identified in unmyelinated axons within the nerve supplying the fat pad and in the dorsal horn of the spinal cord. This indicated that labelling was effective - although only using the detergent method. The absence of labelling may be attributed to the paucity of nerves in the small volume of tissue examined. The nerves themselves were surrounded by concentric rings of ECM. The role of these fibres is unknown; however, their appearance suggests that they may have a sensory role, rather than a role in regulating the size of the fat pad (Bartness and Bamshad, 1998), although this cannot be ruled out. The collagen surrounding the nerve may play a role in protecting the nerve from mechanical stress and/or shear exerted on the fat pad.

In contrast to the structure of the fat pad, there were significant differences between the young and aged animals with regard to the nerve supplying it. Age-related changes to peripheral nerves are well documented (Verdu et al., 2000), and morphological observations correlate with those changes demonstrated here. The increasingly irregular shape of the fibres within the aged nerve is believed to be a consequence of the myelin abnormalities described. These are associated with a decrease in the expression of myelin protein with age (Verdu et al., 2000) and changes in the shape and structure of the myelin sheath are suggestive of axonal degeneration (Krinke et al., 1988). In the aged rat, an increase in the amount of collagen was observed between the nerve fibres, in line with previous studies (Ceballos et al., 1999). It is believed that the denervated Schwann cells influence adjacent fibroblasts to synthesize collagen in order to fill the space left by degenerated nerve fibres (Ceballos et al., 1999; Eather et al., 1986).

Significant decreases in the number of myelinated fibres and unmyelinated axons with old age together with a general decrease in the average size of the axons remaining have previously been demonstrated in a variety of species and nerves (Verdu et al., 2000). The changes in number and morphology of the myelinated fibres of the nerve examined here may result in a decrease in conduction velocity associated with old age (Verdu et al., 2000). The histological and cellular changes described here are believed have a marked impact on the function of the nerve (Verdu et al., 2000) and may manifest themselves as an age-related alteration in the sensory function proposed for the retromalleolar fat pad. However, in contrast to these studies, the loss of myelinated axons was more marked than of

unmyelinated fibres, and particularly affected fibres that had a diameter between 30-40 μm^2 rather than large myelinated fibres. In addition, there was a significant increase in the thickness of the myelin sheath with age. It is difficult to explain these observations, but it may be associated with the use of a single animal at each age in the present study, or due to the levels at which the sections were obtained from each nerve. It should also be noted that the rat sural nerve, unlike its equivalent in man contains motoneurones axons (Peyronnard and Charron, 1982) and that these constitute “no more than one fourth” of the fibres within the nerve studied here (the peroneal anastomatic branch of the sural nerve). These axons are believed to innervate the plantar muscles of the foot and may explain some of the differences observed. In future studies, it would be important to confirm these observations with the use of more animals. However, as discussed above (see section 5.2.5), the interpretation of the results would still be limited by the likelihood of inter-individual variation.

In summary, the present results suggest that the retromalleolar fat pad is a structural fat pad, which contains a number of cell types other than adipocytes. These include mast cells which may play an important role in pathology of the enthesis organ. The nerves within the fat pad pass via clefts between adjacent adipocytes and are surrounded by concentric layers of collagenous ECM. This is reminiscent of the arrangement for nerve fibres within Pacinian corpuscles – i.e. the nerves are not in direct contact with the adipocytes. Collectively, the results suggest a mechanosensory role for the fat pad, rather than one concerned with regulating its adipogenicity. The nerve supplying the fat pad undergoes a number of morphometric and ultrastructural changes with age, which would be consistent with decline in the proposed mechanosensory function of the fat pad. This in turn may result in gait abnormalities.

6. CELL INTERACTIONS AND CELL COMPOSITION OF THE RETROMALLEOLAR FAT PAD IN THE RAT

6.1. INTRODUCTION

The presence of adipose tissue at entheses has recently attracted renewed interest, for it occurs not only within the enthesis itself, but also in the angle which the tendon/ligament makes with the bone (Benjamin et al., 2004b). Elsewhere in tendons and ligaments, it is often dismissed as a sign of degeneration; however Benjamin et al., (2004b) have proposed a number of functions for adipose tissue at entheses. These include facilitating movement between tendon fascicles, and between the tendon or ligament and bone, and dissipating stress concentration at attachment sites. It has been demonstrated above (see chapter 3/5) that the retromalleolar fat pad is composed of adipocytes and a fibrous ECM. This organisation is likely to play an important role in the structure-function relationships of the fat pad. It is therefore the purpose of this study to provide information on cell-cell and cell-matrix interactions of adipocytes and fibroblasts within retromalleolar fat pad which would support the suggestion that the fat pad may modulate its fibrous nature according to the mechanical loading it experiences.

Adipose tissue, in other locations is recognized to have important immunological functions (Fantuzzi, 2005) for a review). The presence of mast cells in the retromalleolar fat pad, as described above (see chapter 3), suggests that this fat pad may also have immunological properties. Thus, a further aim of the present chapter is to identify by immunohistochemistry, the presence of a phagocyte and inflammatory cell population in the rat Achilles tendon enthesis organ and record changes in their expression with the age of the animal. The cells identified may have an immunoprotective role for the Achilles tendon enthesis organ, and may also play a role in SpA (McGonagle et al., 2002).

Brief Review

Cell-Matrix Interactions

Actin, a major component of the cell cytoskeleton, is present in two forms, at equal ratios. Individual subunits of actin - known as globular-actin (G-actin) - can polymerise into double stranded flexible helical filaments known as filamentous actin (F-actin). These microfilaments are found throughout the cytoplasm but are principally concentrated beneath the plasma membrane, in the cell cortex (Alberts et al., 1994). Here F-actin

operates as networks or bundles, with actin associated proteins allowing the cell to alter the profile of the overlying plasma membrane (Amato et al., 1983), or transport vesicles within the cell (Goldberg et al., 1980). In response to tension, temporary bundles of contractile stress fibres are formed by the interaction of actin filaments and the actin associated protein tropomyosin. Tropomyosin binds along the length of the actin filaments to stabilise the structure, and promote binding of myosin II – a muscle associated protein - which leads to the generation of contractile forces. These stress fibres insert into the plasma membrane via a series of proteins that form specialised sites of adhesion which anchor the fibres to the underlying ECM or a neighbouring cell (Alberts et al., 1994; Burridge et al., 1987). Focal contacts (also known as focal adhesions) anchor actin filaments to the ECM via a cytoskeletal complex composed of many proteins, including α -actinin, vinculin, talin, focal adhesion kinase, tensin and paxillin, which in turn anchor with a member of the transmembrane family of integrins. The integrins subsequently bind to an RGD (Arg-Gly-Asp) sequence of an ECM molecule such as collagen, laminin, fibronectin. Integrins are able to transduce the force applied to the cell and stimulate re-organisation of the cytoskeleton in response to the force applied. Reciprocally the intracellular actin filaments can influence the orientation of secreted fibronectin mediated by integrins (Alberts et al., 1994; Burridge et al., 1987). Focal contacts in tendon and the annulus fibrosus of the intervertebral disc are known to have a role in organising the orientation of fibroblasts and the direction of ECM deposition during development (Hayes et al., 1999; Ralphs et al., 2002).

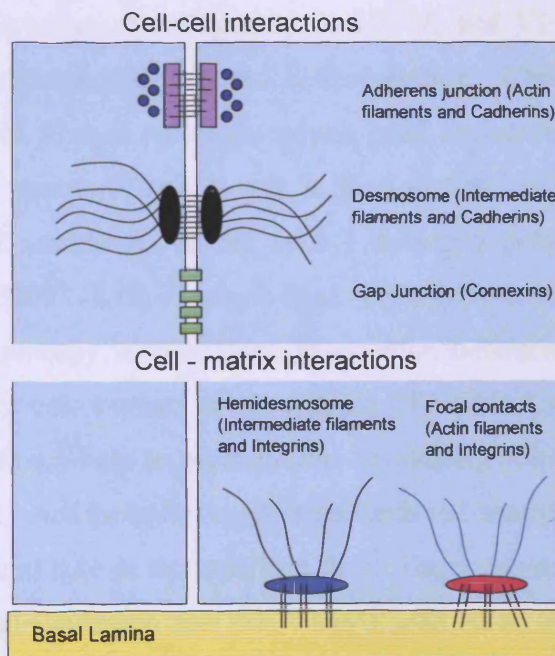


Figure 6.1.1: Cell-cell and cell-matrix interactions (Alberts et al., 1994)

Focal contacts are also known to be important in the early stages of adipocyte differentiation. This is a complex process involving multiple stages. During adipocyte differentiation, the cell dramatically alters its morphology from a stellate-shaped cell (resembling a fibroblast) to a spherical one. Several authors have demonstrated, *in vitro*, a decrease in the mRNA levels of actin and other components of cell-matrix interactions (Rodriguez Fernandez and Ben-Ze'ev, 1989; Spiegelman and Farmer, 1982). This suggests that such a downregulation is a key event in generating the differentiated phenotype of the cell (Rodriguez Fernandez and Ben-Ze'ev, 1989). Even though these studies are carried out on established cell lines known to develop into fat pads when injected into animals (Green and Kehinde, 1979), it has not been established whether adipocytes in mature adipose tissue re-express cell-matrix interactions *in vivo* or in 3D cultures.

A recent study of the 3D culture of adipocytes (Kubo et al., 2000) has demonstrated an important role in the ECM during differentiation, which is secreted and degraded throughout differentiation. Fibronectin secretion by preadipocytes provides an ECM which promotes adipocyte differentiation and the organisation of interstitial collagen during the initial stages of adipogenesis. However, at later stages, fibronectin inhibits differentiation and must be proteolytically degraded. Following fibronectin degradation, expression and secretion of laminin and type IV collagen is observed. Once again these ECM components are broken down, but later re-expressed in the form of cell-surface associated proteins forming the basement membrane which is characteristic of the mature adipocyte. During the mid-stages of differentiation collagen types III, V, and VI are secreted, followed by type I collagen expression during terminal differentiation. These fibres form an intricate extracellular network of fibrous collagens which bind unilocular adipocytes together into clusters resembling the structure *in vivo*. It is thought that collagen types III, V and VI connect the basement membrane to the type I collagen network to anchor the tissue together (Kubo et al., 2000). Kuri-Harcuch et al., (1984) have demonstrated with the use of scanning electron microscopy, a very close association between the fibrillar ECM and the differentiated adipocyte cell surface *in vitro* using 3T3-F442A cells. It is suggested here that the collagen fibres may help to organise the developing adipocytes into lobules as seen *in vivo* (Motta, 1975). Additionally, membrane tethered matrix metalloproteinases (MT-MMP) play an important role in remodelling the collagenous matrix during development. Chun et al., (2006) demonstrated that MT1-MMP null mice are lipodystrophic, because development of WAT is aborted due to a build up of collagen in the ECM. It would

therefore appear unusual for such a highly organised ECM to develop during adipogenesis without the occurrence of cell-matrix interactions.

Hemidesmosomes (half desmosomes) are generally associated with polarised cells, attaching the basal surface of the cell to the underlying basement membrane. They are composed of intermediate filaments, which anchor to a cluster of integrins via a cytoplasmic plaque. The integrins are in turn anchored to a part of the underlying membrane. Intermediate filaments are polymers of fibrous proteins – variations of these proteins result in different types of filaments including: keratin, vimentin, desmin. These filaments are often found in tissues subject to large amounts of mechanical stress, such as epithelia (Alberts et al., 1994). The expression of hemidesmosomes has not been fully addressed in mature adipocytes. Nonetheless, once again, vimentin levels have been measured during adipogenesis. In contrast to other cytoskeletal proteins, vimentin levels are increased during the differentiation of preadipocytes isolated from rat and human adipose tissues (Teichert-Kuliszewska et al., 1996). It is suggested that vimentin plays a role in lipid storage, metabolism and adipocyte differentiation (Franke et al., 1987; Teichert-Kuliszewska et al., 1996).

Cell-Cell Interactions

Cells have the ability to interact with each other in a number of ways: for anchorage, communication or occlusion of the intercellular space (Alberts et al., 1994). Adherens junctions - one form of anchoring junction - connect the actin cytoskeleton of adjacent cells via cadherin junctional proteins. Cadherins are single transmembrane glycoproteins which interact homophilically with cadherins on the adjacent cell – mediated by calcium (Takeichi, 1988). The cytoplasmic domain of cadherin glycoprotein is anchored to the actin cytoskeleton via a multimolecular protein consisting of catenins α , β , and γ , vinculin, α -actinin and plakoglobin. Cadherins are highly involved in cell adhesion during development and have been identified throughout the developing embryo - providing the ability to link dividing cells and co-ordinating their orientation. This regulates the shape and structure of the tissue (Alberts et al., 1994; Geiger et al., 1987). In the adult, cadherins connect cells together to maintain tissue integrity. In tendon, the expression of adherens junctions is upregulated *in vitro* under cyclic tensile load (Ralphs et al., 2002). A number of *in vitro* studies have demonstrated a decrease in the expression of all cadherins during adipocyte differentiation (Shin et al., 2000). However, another homophilic cell adhesion

molecule – adipocyte adhesion molecule (ACAM) - has recently been identified by Eguchi et al., (2005) on the surface of mature adipocytes, *in vivo*. Its expression is upregulated during differentiation and in obesity and is therefore believed to have a role in these processes; however, its role in mature adipocytes is not yet understood (Eguchi et al., 2005).

Gap junctions are communicating junctions that allow co-ordination of the cell population. They are found in many tissue types and are composed of two hemichannels that coalesce from adjacent cells to form an open channel, which has the ability to mediate the exchange of small metabolites and ions between the connected cytoplasm thereby generating an integrated cell population. Each hemichannel, called a connexon, is assembled from six transmembrane connexins (cxn) bound together to form a hexamer (Alberts et al., 1994; Goodenough, 1976). Tendon fibroblasts and periodontal ligament cells express both cxn 32 and 43. It has been hypothesized that stimulation of fibroblasts under mechanical loading causes cellular deformation. As a consequence there is an increase in intracellular calcium concentration that leads to the transposition of inositol phosphate (IP₃) through open gap junctions, and an increase in the intracellular calcium concentration in the connected cell. This allows the cell population to mount a co-ordinated response to mechanical loading (Banes et al., 1999). Waggett et al., (2006) further demonstrated that *in vitro*, tendon fibroblast signalled via cxn 32 to increase collagen synthesis and secretion while signalling via cxn 43 inhibits collagen synthesis.

Gap junctions (cxn43 but not cxn32) have been identified in differentiating bone marrow stromal cells, and are known to play an important role in the mitogenic clonal expansion during adipogenesis (Umezawa and Hata, 1992; Yanagiya et al., 2007). During differentiation, Ras independent (Brownell et al., 1996), closure of gap junctions induces adipocyte differentiation in a similar manner to the decrease in cell-matrix interaction components. Interestingly, if gap junctions are inhibited during osteoblast differentiation, *in vitro*, these cells accumulate triacylglycerol lipid droplets and express several adipocytic markers indicating that signals downstream of gap junction communication have the ability to control cell phenotype (Schiller et al., 2001). *In vivo*, gap junctions are not believed to be present in the plasma membrane of mature adipocytes due to the occurrence of a basement membrane surrounding them. Therefore, in this study, only the fibrous regions of the retromalleolar fat pad will be examined.

Macrophages in Adipose Tissue

Approximately 10% of the cells from the stromo-vascular fraction of WAT are resident tissue macrophages (Curat et al., 2004). Furthermore, several studies have demonstrated that the number of macrophages is directly linked to the number and size of adipocytes in the deposit, with no significant differences between subcutaneous and visceral deposits (Curat et al., 2004; Weisberg et al., 2003). Although macrophages and preadipocytes show some structural similarities, the cell types are distinct and with the use of mouse bone marrow chimeras it has been demonstrated that macrophages in WAT are not differentiated from preadipocytes - but from monocytes derived from bone marrow, that circulated in the bloodstream and infiltrate into WAT (Weisberg et al., 2003). Recruitment of macrophages into WAT may be stimulated by a number of factors: High doses of leptin induce the adhesion and transmigration of monocytes in blood vessels (Curat et al., 2004) and chemokines such as monocyte chemoattractant protein 1 (MCP1) are released by adipocytes at levels which correlate with adiposity (Christiansen et al., 2005; Takahashi et al., 2003). These observations correlate with a number of studies that demonstrate obese individuals/animals have larger populations of macrophages within WAT deposits. Furthermore, Lumeng et al., (2007) have demonstrated a novel population of macrophages in WAT of obese mice which may contribute to a proinflammatory state and insulin resistance.

McGonagle et al., (2002) has demonstrated that macrophages are the primary cell infiltrate in lesions of plantar enthesal fibrocartilage in patients with SpA. This explains the beneficial effect of anti-tumor necrosis factor alpha (TNF- α) on patients with SpA. TNF- α is secreted by activated macrophages and stimulates the endothelium to recruit other inflammatory cells and induces the release of other inflammatory cytokines. It is suggested that anti-TNF α reduces migration of inflammatory cells through deactivation of adhesion molecules in the endothelium (Paleolog et al., 1996). The presence of macrophages in the rat Achilles tendon enthesis organ (a site commonly affected by enthesopathies in patients with SpA) will be studied with the use of the pan-macrophage marker CD68. The effect of age on the phagocyte cell population will also be observed. Myeloid-related protein (MRP14) - a marker for inflammatory macrophages/neutrophils will also be used in this study. MRP14 is a calcium-binding protein belonging to the S100 protein family (also known as S-100A9). Under inflammatory, conditions MRP14 is expressed by monocytes and granulocytes during early stages of differentiation (Odink et al., 1987). Furthermore,

MRP14 is secreted, as a heterodimer with MRP8 (S-100A8), during the interaction of monocytes with TNF-stimulated endothelial cells (Frosch et al., 2000). In several inflammatory conditions - such as rheumatoid arthritis (RA) and SpA - levels of MRP14/MRP8 are increased in synovial tissue, synovial fluid, and blood serum (De Rycke et al., 2005; Youssef et al., 1999).

6.2. MATERIALS AND METHODS

6.2.1. Source of Material

White male Wistar rats aged 1 day, 1 month, 4 months, and 24 months (3 from each age group) were used in this study. 4 month rats and pregnant female rats were obtained from accredited commercial suppliers. Following parturition the offspring were maintained at Cardiff University until the appropriate age.

6.2.2. Dissection Procedure

Adult rats were killed with an overdose of carbon dioxide followed by cervical dislocation. Neonates were stunned and then killed by cervical dislocation. The hind-limbs from adult rats were skinned and amputated. The ankle region was removed from the limb by cutting through the tibia and fibula midway down the hind-limb. The forefoot removed from the ankle by cutting through the proximal part of the metatarsus leaving the Achilles tendon intact and attached to the calcaneus. The whole hind-limbs were removed and used from neonatal rats. Tissues were kept moist at all stages during dissection with 0.1M PB.

6.2.3. Immunohistochemistry

Immunofluorescence and immunoperoxidase labelling was carried out as described in chapter 2 using the antibodies against actin, vinculin, N-cadherin, connexin 32, CD68 (ED1), and MRP14 (see Table 2.1).

6.3. RESULTS

6.3.1. Immunohistochemistry

Cellular Composition of the Retromalleolar Fat Pad

Connexin 32, Actin, Vinculin, and N-cadherin

Within the fat pad, the connective tissue between fascicles of large nerve bundles labelled positively for cxn32 (Fig 6.3.1.A). Where fibroblasts were present within the fibrous connective tissue of the fat pad, positive cxn32 labelling was present between cytoplasmic extensions (Fig 6.3.1.A). Labelling for Alexa 488 conjugated Phalloidin demonstrated the presence of filamentous actin within the cytoplasm of adipocytes in the fat pad (Fig 6.3.1.B) labelling was particularly prominent in the blood vessels within the fat pad (not shown). Vinculin labelling was also present within the adipocyte cytoplasm (Fig 6.3.1.C). In contrast; N-cadherin labelling was not widely distributed. It was not a feature of the adipocyte cytoplasm; however, clusters of un-identified cells within the fat pad were positive for N-cadherin (Fig 6.3.1.D). Negative controls did not demonstrate any non specific labelling (Fig 6.3.2.A-E).

Histiocytes of the Achilles enthesis organ

The results are summarised in Table 6.3.1.

CD68 - Neonate

In the neonatal rat, no CD68 positive cells were identified within the any of the fibrocartilaginous regions of the enthesis organ (Fig 6.3 3.A). A large number of CD68 positive cells were however present within the presumptive fat pad (Fig 6.3.3.B) of the Achilles enthesis organ. In comparison to the size of the presumptive fat pad, CD68 cells were particularly numerous, although the number of positive cells did vary between animals of the same age. The shape of CD68 positive cells within the presumptive fat pad varied from rounded cells (Fig 6.3.3.C), which were often in close association with blood vessels, to more spindle-like cells with several cytoplasmic projections (Fig 6.3.3.D). The synovial membrane lining the tip of the presumptive fat pad did not contain any CD68 positive cells (Fig 6.3.3.E).

CD68 - 1 month

At 1 month of age there were few differences to the observations made from the neonatal rat. As above, the fibrocartilaginous regions of the enthesis organ were negative (Figs 6.3.3.F and 6.3.4.A) and a number of CD68 positive cells were present in the fat pad, which is now enlarged and adipocyte differentiation has occurred. The number of CD68 positive cells in the fat pad did however appear to be reduced and the positive cells more widely distributed throughout the wedge of adipose tissue than in the neonatal rat. CD68 positive cells were often in association with blood vessels (Fig 6.3.4.B) and the synovial membrane was negative for CD68 (not shown).

CD68 – 4 month

At 4 months, the enthesis fibrocartilage did not contain CD68 positive cells (Fig 6.3.4.C); however, several CD68 positive cells were present on the bursal surface of the periosteal, and more frequently of the sesamoid fibrocartilage (Fig 6.3.4.D). Interestingly, a number of positive CD68 cells were also identified in one specimen, within the fibrocartilage at the point where the fat pad reflects back and attaches to the periosteum (Fig 6.3.4.F). The fat pad, as above, contained CD68 positive cells (Fig 6.3.4.E), and there appeared to be a slight increase in the number of CD68 positive cells compared to the 1 month rat, although this difference did vary between specimens. In addition, a large number of cells in the synovial membrane were positively labelled for CD68 (Fig 6.3.5.A), although regional variations were evident.

CD68 – 24 month

By 24 months, there was once again an increase in the number of cells labelled for CD68 in the fat pad (Fig 6.3.5.B), and most of the synovial membrane contained CD68 positive cells (Fig 6.3.5.C). There was also a large nerve bundle within the fat pad which had large oval cells expressing CD68 (Fig 6.3.5.D). CD68 positive cells were also identified on the surface of both the sesamoid (Fig 6.3.5.E) and periosteal fibrocartilages; however, several rounded cells within the fibrocartilage also strongly expressed CD68 (Fig 6.3.5.F). In addition to this, several elongated CD68 positive cells were seen just in the tendon just proximal to the enthesis fibrocartilage (not shown).

Inflammatory Cell Populations in the Achilles Tendon Enthesis Organ

The results are summarised in Table 6.3.1.

MRP 14 - neonate

The fibrocartilage associated with the neonatal entheses organ was negative (Fig 6.3.6.A), as was the retrocalcaneal bursa and the synovial membrane (Fig 6.3.6.B) when labelled with anti-MRP14. A small number of cells within the presumptive fat pad were however, positively labelled. These cells, had large rounded nuclei, surrounded by a MRP14 positive cytoplasm which was distinct from the adipocyte precursors as they do not send out elongated cytoplasmic projections (Fig 6.3.6.C and D).

MRP 14 - 1 month

At 1 month labelling with MRP 14 demonstrated the presence of a marked number of positive cells in the retromalleolar fat pad. These cells were rounded and usually present within or in close association with capillaries or larger blood vessels (Fig 6.3.6.E). Clusters of adipocytes also labelled positively for MRP14, these cells were smaller than the majority of the other adipocytes, which remained unlabelled (Fig 6.3.6.F). The synovial membrane was negative in all specimens examined (not shown). In two out of the three specimens examined, the entheses, sesamoid and periosteal fibrocartilages were all negative. However, one specimen demonstrated the presence of what appeared to be a small tear/rupture in the entheses fibrocartilage, which contained a number of positively labelled cells. These cells were irregular in shape, one of which was sending out strongly labelled cytoplasmic projections, extending over the surface of the tear in the fibrocartilage (Figs 6.3.7.A and B).

MRP 14 - 4 month

The entheses (Fig 6.3.7.C), sesamoid and periosteal fibrocartilages were negative for MRP 14 in all specimens examined at 4 months of age. However, the fat pad – as above – contained a number of rounded positively labelled cells within and in association with blood vessels (Fig 6.3.7.D). As above, a small number of adipocytes also labelled positively for MRP 14.

MRP 14 - 24 month

In the 24 month rat, the fibrocartilages associated with the entheses were negative, while positive cells were present in the retromalleolar fat pad. The number of positive cells appeared to be higher than at 4 months of age. In contrast to the observations from previous ages, there was a large amount of labelling associated with endothelial lining of

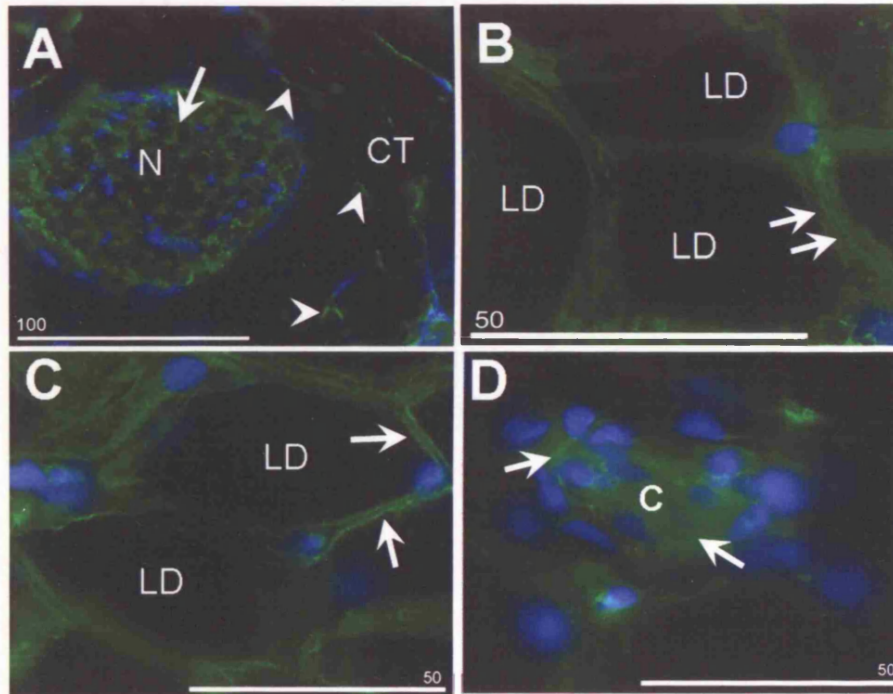
blood vessels (Fig 6.3.7.E). Negative control sections did not demonstrate non-specific labelling (Fig 6.3.8.A-C).

CD68					
Age	FP	EF	SF	PF	RB
1 day	++++	-	-	-	-
1 month	+	-	-	-	-
4 month	++	-	+	+	+
24 month	+++	+/-	++	++	++

MRP14					
Age	FP	EF	SF	PF	RB
1 day	+	-	-	-	-
1 month	++	-	-	-	-
4 month	+++	+/-	-	-	-
24 month	++++	-	-	-	-

Table 6.3.1. Summary of results obtained by peroxidise labelling for immunocompetent cells in the rat Achilles enthesis organ. - = no labelling was present in the tissue at this stage, + = labelling present within the tissue on a scale of 1-4, +/- = labelling in some but not all specimens. FP – Retromalleolar fat pad, EF – enthesis fibrocartilage, SF – sesamoid fibrocartilage, PF – periosteal fibrocartilage, RB – retrocalcaneal bursa.

Figure 6.3.1



THE RETROMALLEOLAR FAT PAD LABELLED WITH CONNEXIN 32, ACTIN, VINCULIN, OR N-CADHERIN. 12 week rat (Counterstained with DAPI to highlight cell nuclei)

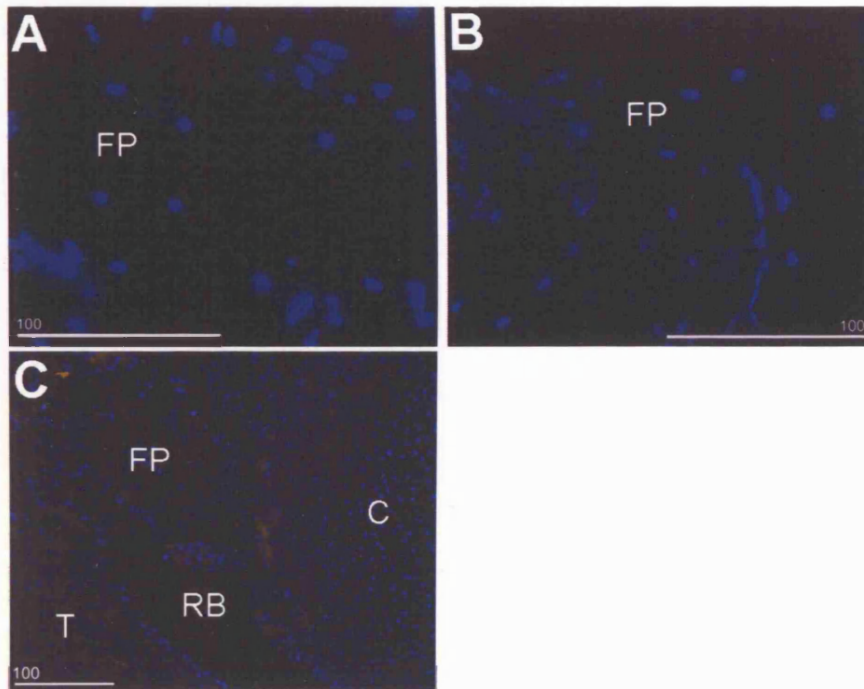
Figure A: A section through a large nerve bundle (N) and fibrous connective tissue (CT) in the retromalleolar fat pad labelled with connexin 32. Labelling was present in the connective tissue (arrow) of a large nerve bundle. Connexin 32 labelling was also present between fibroblasts in the fibrous region of the fat pad (arrowheads). Scale bar = 100μm.

Figure B: A grazing section through adipocytes in the retromalleolar fat pad labelled with Alexa488 - conjugated Phalloidin. Note the presence of actin filaments (arrows) within the adipocyte cytoplasm. LD - Lipid droplet. Scale bar = 50μm.

Figure C: Adipocytes in the retromalleolar fat pad labelled for vinculin. Speckled labelling was present in the adipocyte cytoplasm (arrows). LD – lipid droplet. Scale bar = 50μm.

Figure D: A cluster (C) of unidentified cells within the retromalleolar fat pad labelled for N-cadherin. Note the cytoplasmic labelling (arrows) of cells within the cluster. Scale bar = 50μm.

Figure 6.3.2



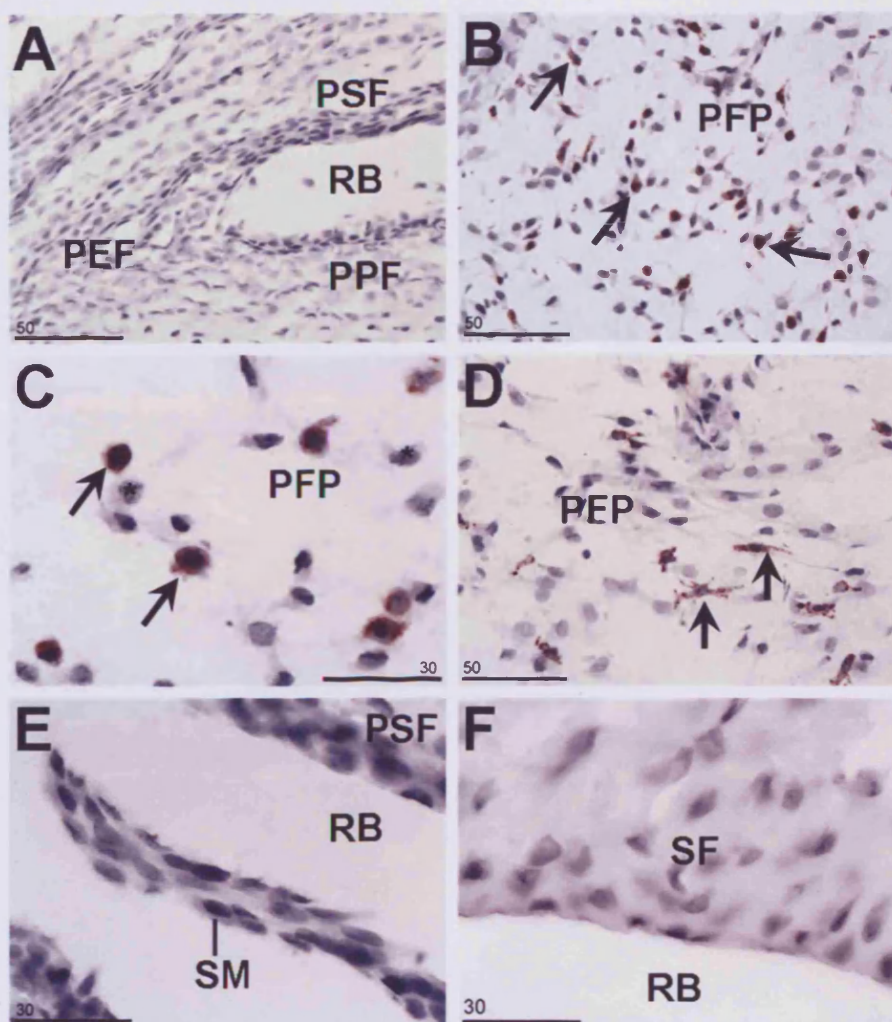
**THE RAT ACHILLES TENDON ENTHESIS ORGAN - NEGATIVE CONTROL SECTIONS
(Counterstained with DAPI to illustrate cell nuclei)**

Figure A: The retromalleolar fat pad (FP) demonstrated no non-specific labelling in a section where PBS was applied in place of the primary antibody. Secondary antibody - goat anti-mouse FITC. 12 week rat. Scale bar = 100µm.

Figure B: The retromalleolar fat pad (FP) demonstrated no non-specific labelling in a section with mouse IgG 1 fragments applied in place of the primary antibody. Secondary antibody - goat anti-mouse FITC. 12 week rat. Scale bar = 100µm.

Figure C: The rat Achilles tendon enthesis organ demonstrated no non-specific labelling in a section with mouse IgG 2a fragments applied in place of the primary antibody. Secondary antibody - goat anti- mouse FITC, FP- fat pad, RB – Retrocalcaneal bursa, T – Tendon, C – Calcaneus. Neonatal rat. Scale bar = 100µm.

Figure 6.3.3



THE RAT ACHILLES TENDON ENTHESIS ORGAN AT VARIOUS AGES, LABELLED WITH CD68

(Visualized with NovaRED and counterstained with Mayer's Haematoxylin to highlight cell nuclei)

Figure A: The rat Achilles tendon enthesis in the neonate. No positive labelling was present in the presumptive enthesis (PEF), sesamoid (PSF), or periosteal fibrocartilage (PPF). RB – retrocalcaneal bursa. Scale bar = 50µm.

Figure B: The presumptive fat pad (PFP) of the rat Achilles tendon enthesis organ. A large number of CD68 positive cells (arrows) were present in the fat pad. Neonatal rat. Scale bar = 50µm.

Figure C: High power view of the CD68 positive cells (arrows) in the presumptive fat pad (PFP). Note the rounded nature of these cells and their nuclei. Neonatal rat. Scale bar = 30µm

Figure D: CD68 positive cells (arrows) in the presumptive fat pad (PFP) of the rat Achilles tendon enthesis organ. Note the spindle-like shape of these cells. Neonatal rat. Scale bar = 50µm

Figure E: The tip of the retromalleolar fat pad in the neonatal rat. No positively labelled cells were present in the synovial membrane (SM) lining the tip of the fat pad or in the retrocalcaneal bursa (RB). PSF – presumptive sesamoid fibrocartilage. Scale bar = 30µm.

Figure F: The sesamoid fibrocartilage (SF) of the rat Achilles tendon enthesis organ. Note the absence of CD68 positive cells. 1 month rat. RB – retrocalcaneal bursa. Scale bar = 30µm.

Figure 6.3.4

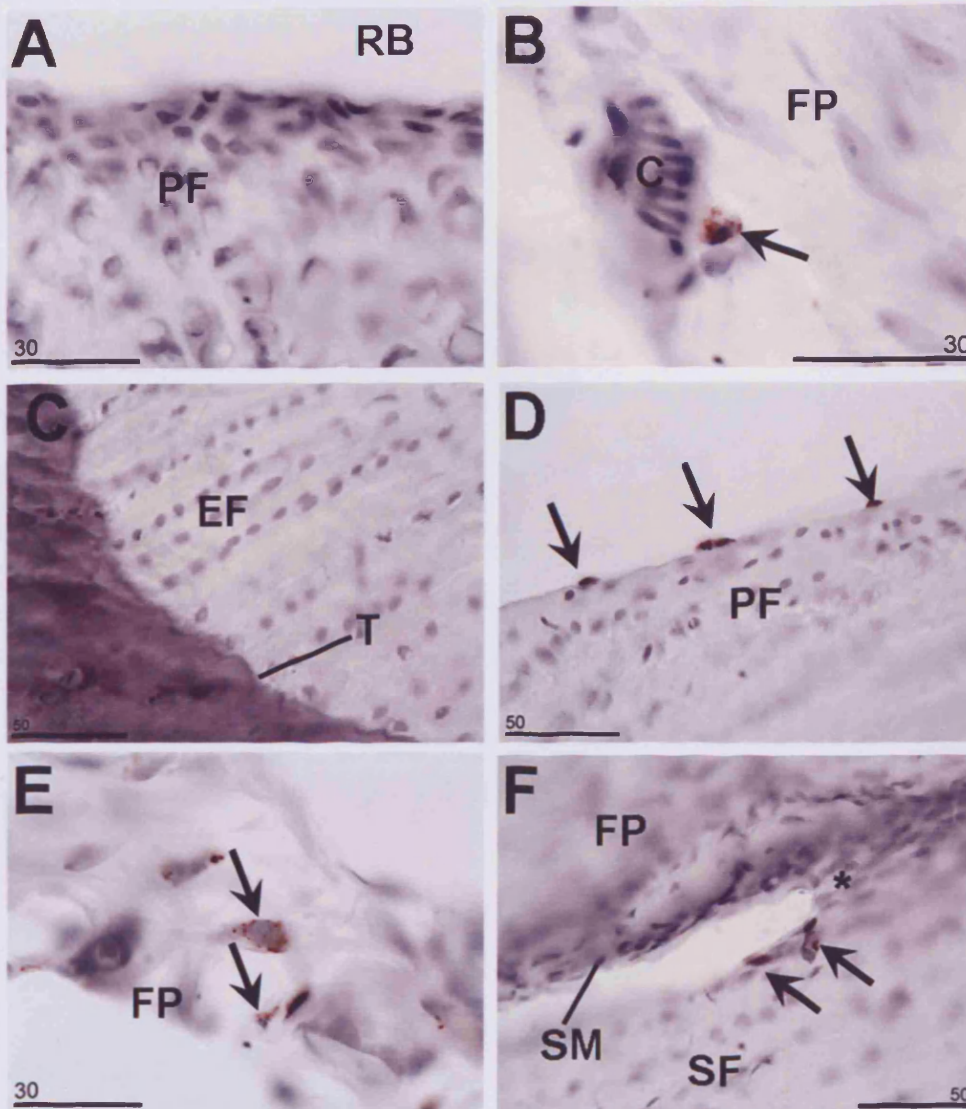


Figure A: The periosteal fibrocartilage (PF) of the rat Achilles tendon enthesis organ. Note the absence of CD68 positive cells. 1 month rat. RB – retrocalcaneal bursa. Scale bar = 30µm.

Figure B: A CD68 positive cell (arrow) in close association with a capillary (C) in the retromalleolar fat pad (FP). 1 month rat. Scale bar = 30µm.

Figure C: The entheses fibrocartilage (EF) of a 4 month rat. No positively labelled cells were present. T – tidemark. Scale bar = 50µm.

Figure D: The periosteal fibrocartilage (PF) of a 4 month rat. Arrows indicate CD68 positive cells on the surface of the periosteal fibrocartilage. Scale bar = 50µm.

Figure E: CD68 positive cells (arrows) in the retromalleolar fat pad (FP). Note the speckled labelling within the cell cytoplasm. 4 month rat. Scale bar = 30µm.

Figure F: CD68 positive cells (arrows) in the sesamoid fibrocartilage (SF) close to the attachment (*) of the reflected synovial membrane (SM) lining the tip fat pad (FP). 4 month rat. Scale bar = 50µm.

Figure 6.3.5

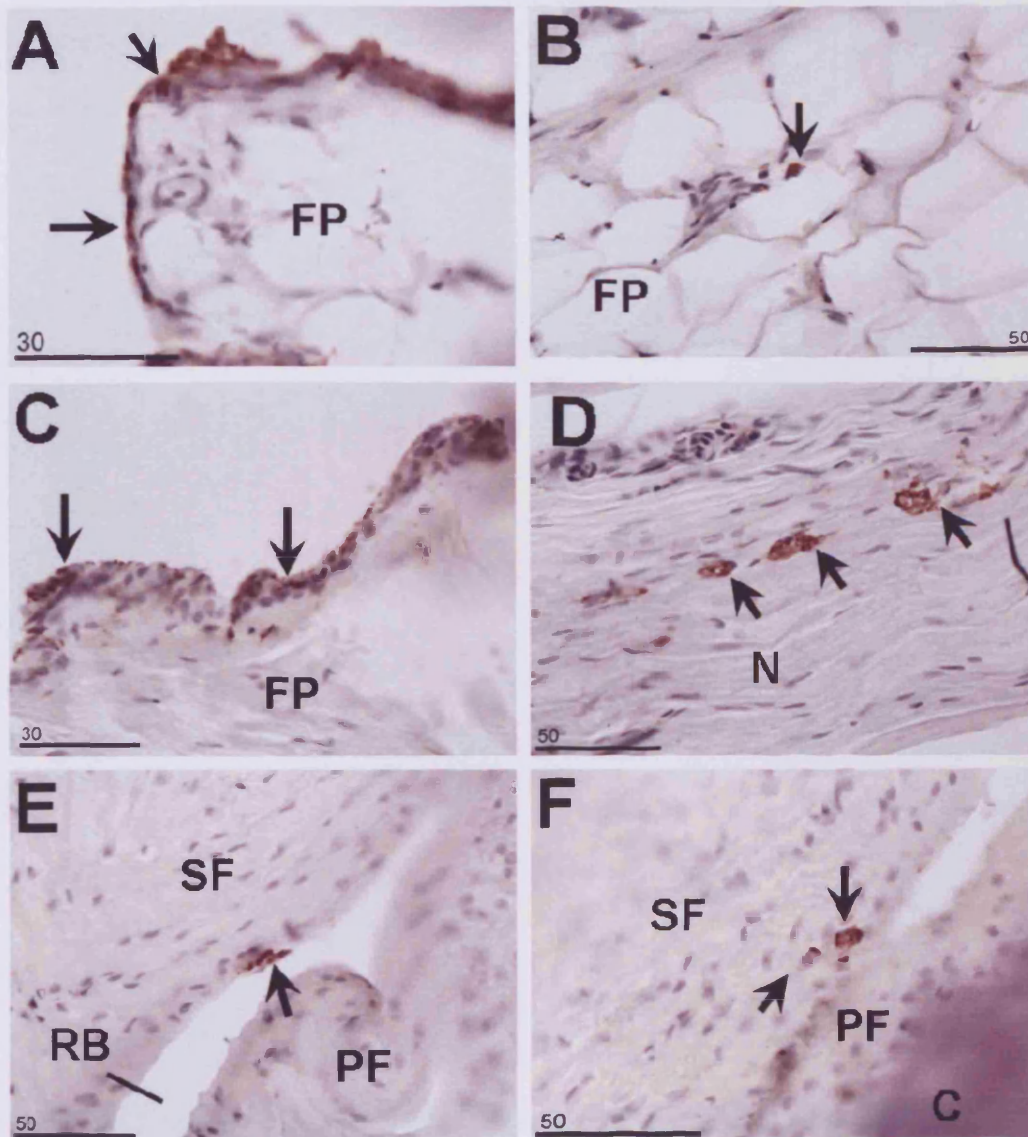


Figure A: The synovial membrane (arrows) lining the retromalleolar fat pad (FP) positively labelled for CD68 in a 4 month rat. Scale bar = 30µm

Figure B: CD68 positive cell (arrow) in the retromalleolar fat pad (FP). 24 month rat. Scale bar = 50µm.

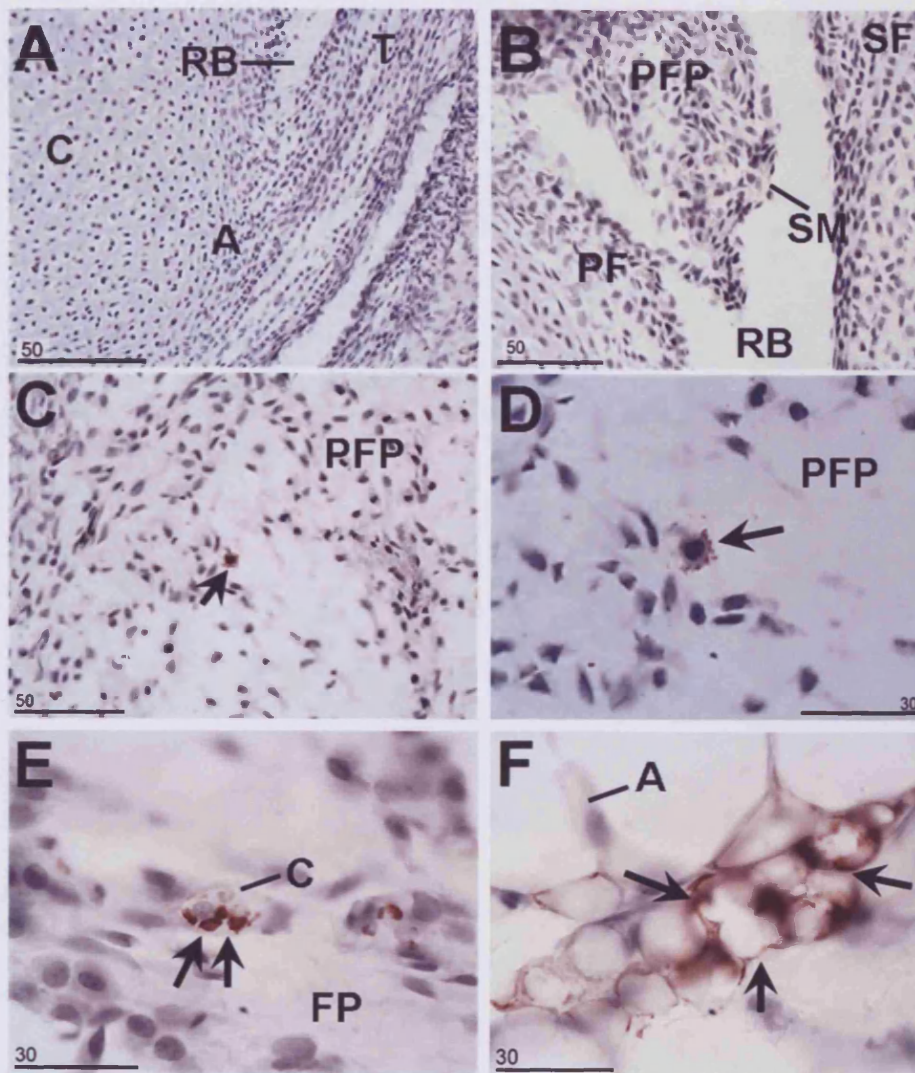
Figure C: CD68 positive cells in the synovial membrane (arrows) of a 24 month rat. FP - Fat pad. Scale bar = 30µm

Figure D: A large nerve bundle (N) in the proximal part of the retromalleolar fat pad. Arrows indicate CD68 positive cells in the connective tissue of the nerve bundle. 24 month rat. Scale bar = 50µm.

Figure E: The sesamoid (SF) and periosteal fibrocartilages (PF) of the rat Achilles tendon enthesis organ. Arrow indicates a pair of CD68 positive cells on the surface of the sesamoid fibrocartilage. RB - Retrocalcaneal bursa. 24 month rat. Scale bar = 50µm

Figure F: The sesamoid (SF) and periosteal fibrocartilages (PF) of the rat Achilles tendon enthesis organ. Arrows indicate rounded CD68 positive cell within the sesamoid fibrocartilage. C - Calcaneus. 24 month rat. Scale bar = 50µm

Figure 6.3.6



THE RAT ACHILLES TENDON ENTHESIS ORGAN LABELLED WITH MRP 14

(Visualized with NovaRED and counterstained with Mayer's Haematoxylin to highlight the cell nuclei)

Figure A: The attachment (A) of the Achilles tendon (T) to the cartilaginous anlagen of the calcaneus (C) of a neonatal rat. Note the absence of MRP14 labelling in all regions. RB - Retrocalcaneal bursa. Scale bar = 50µm.

Figure B: The tip of the presumptive retromalleolar fat pad (PFP) protruding into the retrocalcaneal bursa (RB). No labelling was present in the tip of the fat pad, synovial membrane (SM), sesamoid (SF), or periosteal fibrocartilage (PF). Neonatal rat. Scale bar = 50µm.

Figure C: The presumptive fat pad (PFP) associated with the rat Achilles tendon enthesis organ. Arrow indicates a single cell positively labelled for MRP 14 in the fat pad. Neonatal rat. Scale bar = 50µm.

Figure D: High power view of the MRP14 positive cell (arrow) in C. Note the rounded nucleus and lamellopodia/filopodia of the the cell. PFP - presumptive fat pad. Neonatal rat. Scale bar = 30µm

Figure E: A cross section through a small capillary (C), within the fat pad (FP). A number of MRP14 positive cells were present within the capillary. 1month rat. Scale bar =30µm.

Figure F: A cluster of small MRP 14 positively labelled adipocytes (arrows) in the retromalleolar fat pad. Larger adipocytes in the fat pad were unlabelled (A). 1month rat. Scale bar = 30µm

Figure 6.3.7

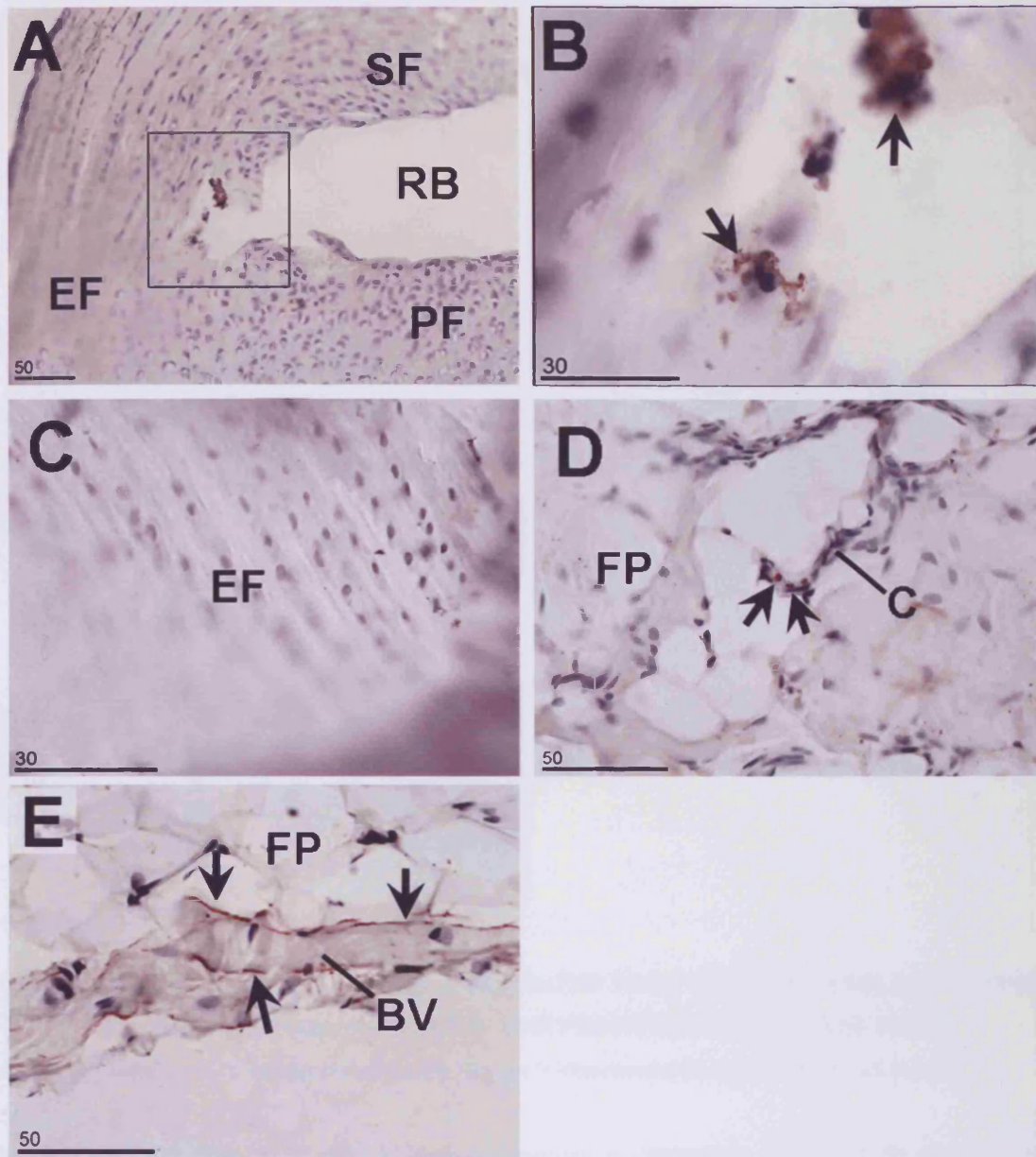


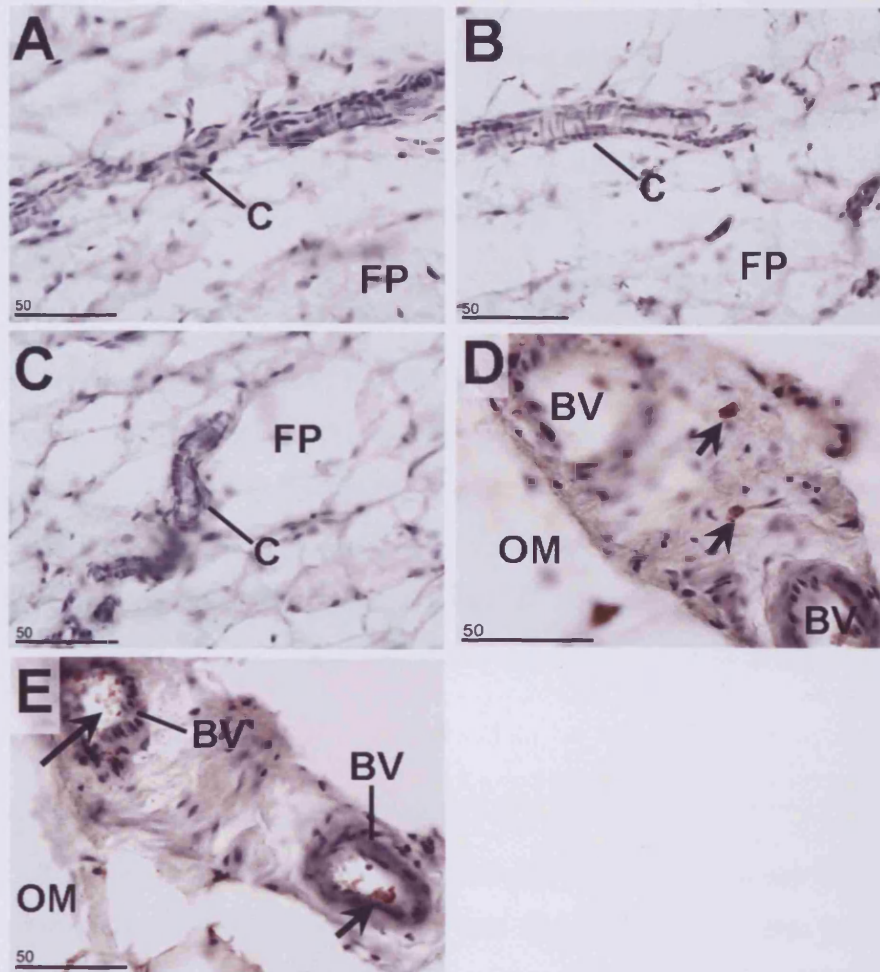
Figure A and B: A small tear/rupture at the insertional angle (square in A, highlighted in B) in the enthesis fibrocartilage (EF) of the rat Achilles tendon enthesis organ. A small number of MRP 14 positive cells (arrows) were present within the tear. Note the irregular shape, and extending cytoplasmic membrane of one of these positive cells. RB – retrocalcaneal bursa, SF – sesamoid fibrocartilage, PF – periosteal fibrocartilage. 1 month rat. Scale bar = 30 μ m.

Figure C: The enthesis fibrocartilage (EF) of the rat Achilles tendon enthesis organ. Note the absence of positively labelled cells. 4 month rat. Scale bar = 30 μ m.

Figure D: The retromalleolar fat pad (FP) associated with the rat Achilles tendon enthesis organ. A capillary (C) within the fat pad containing 3 MRP 14 positively labelled cells (arrows). 4 month rat. Scale bar = 50 μ m.

Figure E: Blood vessels in the retromalleolar fat pad (FP) associated with the rat Achilles tendon enthesis organ. Strong MRP14 labelling (arrows) was associated with the blood vessel (BV) endothelium. 24 month rat. Scale bar = 50 μ m.

Figure 6.3.8.



**THE RETROMALLEOLAR FAT PAD-ASSOCIATED WITH THE RAT ACHILLES TENDON
ENTHESIS ORGAN – NEGATIVE AND POSITIVE CONTROL SECTIONS
4 month rat (Counterstained with Mayer's Haematoxylin to illustrate cell nuclei)**

Figure A: The rat Achilles tendon enthesis organ demonstrated no non-specific labelling of the primary antibody. Mouse IgG 2a fragments were applied to the section in place of the primary antibody. Secondary antibody - biotinylated horse anti- mouse. C - Capillary. Scale bar = 50µm.

Figure B: The rat Achilles tendon enthesis organ demonstrated no non-specific labelling of the primary antibody. Mouse IgG 1 fragments were applied to the section in place of the primary antibody. Secondary antibody - biotinylated horse anti- mouse. C - Capillary. Scale bar = 50µm.

Figure C: The rat Achilles tendon enthesis organ demonstrated no non-specific labelling of the secondary antibody. Phosphate buffer was applied to the section in place of the primary antibody. Secondary antibody - biotinylated horse anti-mouse secondary antibody. C - Capillary. Scale bar = 50µm

Figure D: The rat omentum (OM) labelled with CD68. Positive cells (arrows) were present throughout the tissue. BV - Blood vessel. Scale bar = 50µm.

Figure E: The rat omentum (OM) labelled with MRP 14. Positive cells (arrows) were present in close association with the blood vessel (BV) endothelium. Scale bar = 50µm.

6.4. DISCUSSION

The results show that adipocytes and fibroblasts within the retromalleolar fat pad contain filamentous actin and vinculin. N-cadherin labelling was present in clusters of unidentified cells in the retromalleolar fat pad, but not the mature adipocytes of the fat pad. Cxn 32 was observed between fibroblasts in the fibrous region of the fat pad and in nerve bundles within the fat pad.

Macrophages were present throughout the fat pad in animals of all ages. In older rats macrophages were also present on the bursal surfaces and within the sesamoid and periosteal fibrocartilages (4 and 24 month rat only). The number of MRP14 positive cells, which were usually blood vessel associated, increased with the age of the rat and pervascular labelling was particularly prominent in aged rats. In one animal, in a tear/rupture of the enthesis fibrocartilage was observed which contained MRP14 positively labelled cells.

Cell Interactions in the Retromalleolar Fat Pad

Although most studies have demonstrated that actin and vinculin levels are reduced during adipocyte differentiation (Rodriguez Fernandez and Ben-Ze'ev, 1989) this has only been confirmed in 2D cell culture systems which do not accurately reflect the 3D nature of adipose tissue *in vivo*. The 3D structure of adipose tissue displays complex interstitial collagen arrangements that are laid down and remodelled during adipocyte differentiation (Chun et al., 2006; Kubo et al., 2000; Kuri-Harcuch et al., 1984). This collagen network is now believed to play an important role in the structure and organisation of adipose tissue during development (Chun et al., 2006; Kubo et al., 2000; Kuri-Harcuch et al., 1984; Nakajima et al., 2002; Nakajima et al., 1998). Despite these observations no studies have looked into the expression of cell-matrix interactions in terminally differentiated adipose tissue *in vivo*. The present study demonstrated the presence of actin filaments and vinculin within the adipocyte cytoplasm in the retromalleolar fat pad. Due to the absence of N-cadherin, it may be suggested that these components belong to cell-matrix interactions, such as focal contacts, which may play an important role in sensing mechanical load experienced by the fat pad during foot movement, although further confirmation of this is required. Loading may initiate a cellular response to remodel the ECM via collagen synthesis (Ooshima, 1977) or degeneration (Chun et al., 2006).

The actin filaments observed here in the adipocyte cytoplasm may also play a role in the transportation of glucose vesicles from the plasma membrane during glucose uptake (Kanzaki and Pessin, 2001). Additionally, it must be considered that actin filaments – in conjunction with vinculin and vimentin may form cell-matrix interactions, called podosomes. Podosomes are present in cells of mesenchymal origin, but have also been identified in epithelial, smooth muscle cells and src-transformed fibroblasts (Linder and Aepfelbacher, 2003) for a review). Interestingly, the matrix degrading MT1-MMP - associated with ECM turnover in adipose tissue (Chun et al., 2006) - is also localised at podosome sites in osteoclasts (Sato et al., 1997). Podosomes are also associated with tissue invasion through cell migration and ECM degeneration - in addition to cell adhesion (Linder and Aepfelbacher, 2003). It is obvious from these initial observations that further investigation is required in this aspect of adipocyte biology.

N-cadherin was not present in the cytoplasm of mature adipocytes within the fat pad indicating that adherens junctions were not present. This is supported by previous *in vitro* observations (Shin et al., 2000). N-cadherin was however, observed in clusters of unidentified cells. These may be clusters of preadipocytes or mesenchymal stem cells. N-cadherin may be preventing differentiation of these cells down a specific pathway (Shin et al., 2000). It may be differentiation of these cells that results in the formation of bone/fibrocartilaginous structures in retromalleolar fat pad (as observed in chapter 3 and 4).

Gap junctions were seen between fibroblasts in the fibrous region of the retromalleolar fat pad. Communication via cxn32 may stimulate collagen synthesis in response to mechanical loading sensed through integrin signalling, in a similar way to fibroblasts in the tendon (Waggett et al., 2006). This may explain the increasingly fibrous nature of the retromalleolar fat pad in aged rats (see chapter 3) and elderly cadavers (see chapter 4) which have been subject to mechanical loading during foot movement, thereby stimulating collagen synthesis over a prolonged period. Similarly, the presence of cxn32 in the connective tissue of the large nerve bundle may explain the increased amount of collagen demonstrated in the nerve supplying the retromalleolar fat pad in the aged rat (see chapter 5). These junctions may co-ordinate the fibroblast cell population to increase collagen secretion in response to axonal degeneration (Ceballos et al., 1999; Eather et al., 1986) or mechanical loading (Waggett et al., 2006).

Inflammatory Cell Populations in the Rat Achilles Tendon Entesis Organ

Adipose tissues are well known to have immunological functions (as reviewed by - Fantuzzi, 2005) and the retromalleolar fat pad is no exception. A large population of histiocytes were demonstrated within the fat pad, for many cells within the tissue expressed CD68 – a member of the lysosomal/endosomal-associated membrane glycoprotein family, highly characteristic of monocytes and macrophages (Damoiseaux et al., 1994). Two morphologically different populations of macrophages were identified in the fat pad; one round, the other dendritic. This parallels the two populations of macrophages reported in the greater omentum (Fischer et al., 1970). The latter structure provides a route for macrophages to enter the peritoneal cavity (Krist et al., 1995). If the macrophages present in the fat pad pass into the bursa in an analogous fashion, they may help to combat infection and remove cellular debris generated by wear and tear of the periosteal and sesamoid fibrocartilages during foot movement (Rufai et al., 1995). The demonstration that these cells were present on the fibrocartilages in older animals supports this idea, as there would be a build up of debris with wear and tear with age (Milz et al., 2004). This finding is however surprising, as these cells would be compressed during dorsiflexion between the sesamoid and periosteal fibrocartilages; however, this may be explained by looking at similar tissues; such as the intervertebral disc and periodontal ligament in which macrophages have also been identified (Carreon et al., 1996; Kawahara et al., 1992). These tissues are also under large levels of compression suggesting that such cells are resilient to compressive stresses. Interestingly, a small number of cells within the sesamoid fibrocartilage were also shown to express CD68. It may be that these cells are not invading macrophages at all, but resident fibrocartilage cells with the ability to phagocytose the surrounding extracellular matrix. Similar findings have been identified by Nerlich et al., (2002) in the intervertebral disc. These phagocytic fibrocartilage cells may play a role in degeneration and/or remodelling (Nerlich et al., 2002) of the sesamoid/periosteal fibrocartilages of the Achilles tendon entesis organ.

The large population of histiocytes in the presumptive fat pad suggests that monocytes migrate to the fat pad, possibly attracted through the expression of MCP-1 expressed by preadipocytes (Gerhardt et al., 2001). This would ensure that macrophages are present within the fat pad at birth to migrate into the synovium and also retain a population within the fat pad throughout life. The apparent decrease in number of CD68 positive cells in the fat pad is most likely due to differentiation of preadipocytes into mature adipocytes which

express MCP-1 at lower levels (Gerhardt et al., 2001). Therefore, the reduced recruitment of monocytes, accompanied with the increasing size of the fat pad and differentiation of preadipocytes into large lipid filled adipocytes, may give the illusion that the number of histiocytes in the fat pad decreases. A qualitative assessment demonstrated a small increase in the number of histiocytes in the fat pad from the age of 1 month. This may also be related to the increasing amounts of cellular debris generating by wear and tear at the enthesis with increasing age (Milz et al., 2004). Furthermore, this may account for the increasing number of macrophages in the synovial membrane with age. Adipose tissue at entheses could also be a source of the macrophages present in patients with SpA (McGonagle et al., 2002). It is interesting to note that along with the Achilles tendon, other entheses commonly affected in SpA are also associated with significant quantities of fat at their entheses – e.g. the proximal and distal attachments of the patellar tendon and the calcaneal enthesis of the plantar aponeurosis (Benjamin et al., 2004a).

MRP14 labelling demonstrated a small population of infiltrating inflammatory cells (Odink et al., 1987) within the retromalleolar fat pad, which were usually associated with capillaries. These cells may have been attracted to the retromalleolar fat pad through secretion of TNF- α by macrophages or mast cells as they have been demonstrated to do so in inflammation of the peritoneum (Zhang et al., 1992). The number of positive cells increased with the age of the animal indicating that the region becomes more susceptible to damage – resulting in inflammation with increasing age. Labelling of the endothelium was particularly prominent in the 24 month rat. Such labelling indicates that a large number of activated monocytes have migrated through the TNF- α activated endothelium suggesting chronic or acute inflammation of the tissue (Frosch et al., 2000). The co-expression of inflammatory cytokines and peptidergic fibres (see chapter 3) in aged specimens supports the idea that the fat pad may be a site of inflammation and pain in enthesopathies and old age. Cytokines (SP, CGRP and mast cell products) expressed by the immune cells described here are able to induce sensitisation of nociceptors indirectly through increasing production of nerve growth factor (NGF – a neurotrophic factor), which in turn results in an increase in the synthesis of SP and CGRP leading to hyperalgesia of nerve fibres (Donnerer et al., 1992; Leon et al., 1994; Lewin et al., 1993).

Cell-cell and cell-matrix interactions may play an important role in sensing mechanical loading in the fat pad. This may result in the increasingly fibrous nature of the fat pad with

Cell Interactions and Cell Composition of the Retromalleolar Fat Pad in the Rat

age in an attempt to reduce mechanical stress experienced. Additionally, adipose tissue may also be an important immune organ at healthy attachment sites. Macrophages within the fat pad may function by removing cellular debris and possibly protecting the enthesis organ from infection. They may also be implicated in autoimmune or autoinflammatory conditions such as SpA or RA.

7. DEVELOPMENT OF KAGER'S FAT PAD IN MAN

7.1. INTRODUCTION

In earlier chapters, a number functions have been considered for Kager's fat pad, including stress dissipation, proprioception and providing a source of macrophages to protect the enthesis and remove debris from the retrocalcaneal bursa. Although, it is known that the retromalleolar fat pad of the rat develops within the first two postnatal weeks (H. Shaw, Unpublished observations), little is known of the development of Kager's fat pad in man. Thus the aim of the present study is to describe the development of this fat pad in relation to that of the rest of the Achilles tendon enthesis organ and the neighbouring fat pad in the heel. It may be hypothesized that due to the similarities between an enthesis organ and a typical synovial joint, the sequence of development may be similar – i.e. beginning with joint cavitation and followed by the formation of the articular cartilages (equivalent of the sesamoid and periosteal fibrocartilages).

Brief Review

Despite the lack of information available on the development of the human Achilles tendon enthesis organ, the development of the enthesis organ in the rat has been well studied (Rufai et al., 1992). This is most likely due to the availability of material and ethical considerations. At birth the highly cellular Achilles tendon attaches to the cartilage anlagen of the calcaneus, and with continuing development, the cartilage rudiment is eroded through endochondral ossification, leaving only a small region of fibrocartilage at the attachment site derived from the cartilage rudiment. However, at the same time, fibrocartilage begins to develop and spread into the tendon itself to form the tendon attachment (Rufai et al., 1992). It is believed that fibrocartilage within the tendon develops in response to mechanical loading at the time when muscle activity and strength increases. This induces metaplasia of the tendon fibroblasts into fibrocartilage cells (Vogel and Koob, 1989) - thus explaining the arrangement of the cells within longitudinal rows in the tendon (Rufai et al., 1992). This hypothesis has recently been confirmed by Thomopolous et al., (2007) in the shoulder of mice. The authors paralysed the supraspinatus muscle using botulism toxin A at birth and at several postnatal time points, the development of the fibrocartilaginous enthesis of supraspinatus was studied. The results demonstrated that paralysis of the muscle had little effect on the early development of the enthesis, indicating that at this stage, development is driven purely by genetic programming. However, 21 days

postpartum, the development of the enthesis was dramatically affected – delaying fibrocartilage development within the tendon and reducing bone mineralization. This substantiates the view that mechanical factors are essential for maturation of the enthesis fibrocartilage (Thomopoulos et al., 2007). In the neonatal rat, the sesamoid fibrocartilage in the deep surface of the Achilles tendon is absent, only developing at around 2 weeks after birth. With increasing age, the fibrocartilage becomes more metachromatic, but type II collagen is not present until at least 2 years of age suggesting that the sesamoid fibrocartilage also develops through metaplasia of tendon fibroblasts (Rufai et al., 1992). Again, the periosteal fibrocartilage also develops around 2 weeks postnatally, deriving primarily from the perichondrium of the calcaneus adjacent to the Achilles tendon. However, a small contribution may also be made from the synovial membrane which lines the retrocalcaneal bursa at birth (Rufai et al., 1992). Rufai et al., (1992) suggest that the stimulus for the development of the sesamoid and periosteal fibrocartilages is likely to be the onset of locomotion which leads to an increase in muscle power and thereby compression of the two regions is increased during movement. The retromalleolar fat pad was not considered in this study.

The development of Kager's fat pad has however been briefly described by Fritsch, (1996) in man. At birth, Kager's pad is not fully developed and in contrast to the adult, it is located at the medial border of the Achilles tendon. As a result, the Achilles tendon is pushed against the fascial covering of flexor hallucis longus and its associated tendon. Why the pad is located medially in the newborn is unknown, although it is likely that the short body of the calcaneus and the way in which the Achilles tendon curves medially and coils up under the calcaneus in the newborn may be responsible. During postnatal growth several changes occur; a gradual increase in size of the posterior segment of the calcaneus and an increase in the strength of the contractions of triceps surae, causing the Achilles tendon to be pulled into a more ventral and upright position, and pulling with it the growing Kager's pad into its adult position, ventral to the Achilles tendon and posterior to the tendon of FHL (Fritsch, 1996).

7.2. MATERIALS AND METHODS

7.2.1. Source of Material

The sections of embryonic material were part of the developmental biology collection in the department of Human Anatomy and Embryology at the Universidad Complutense, Madrid. Miscarried embryos were donated to the university with parents consent in accordance with Spanish law. All foetuses were staged by the curators of the collections, according to their cranial-rump length in mm (Patten, 1968).

7.2.2. Routine Histology

Routine histology was carried out as described in chapter 2. Additional stains used included Hansen's Haematoxylin, VOF stain (VOF: light green – orange G – acid fuchsin), Azan technique, and Bielchowsky (silver) technique.

7.3. RESULTS

The development of Kager's fat pad was considered in relation to the development of the other components of the enthesis organ and also the neighbouring heel pad. The results are presented according to the CRL of the foetus and summarised in Table 7.3.1.

45mm Foetus - The highly cellular Achilles tendon showed little evidence of collagen fibrillogenesis and was attached to the perichondrium of the cartilage anlagen of the calcaneus (Fig 7.3.1 A and B). The continuation of the Achilles tendon insertion with the plantar fascia could clearly be seen (Fig 7.3.1.C). Anterior to the Achilles tendon, was a large mesenchymal condensation containing characteristic spindle shaped cells (Fig 7.3.1.B and D). This condensation was located in the presumptive Kager's triangle, between the Achilles tendon, calcaneus and FHL. It was therefore considered to be the prospective Kager's fat pad. A number of small blood vessels were present within the mesenchymal condensation (Fig 7.3.1.D). Furthermore, at this stage the presumptive heel pad was also mesenchymal in nature – with no evidence of fat cell differentiation (Fig 7.3.1.E). The retrocalcaneal bursa of the enthesis organ was first observed at this stage and appeared as a small cavitation, lined with synovial cells, in the angle proximal to where the Achilles tendon attaches to the calcaneus (Fig 7.3.1.A and B). No other components of the enthesis organ were observed at this stage.

53mm Foetus – Transverse sections of the Achilles tendon insertion at this stage indicated that the tendon appeared to attach primarily to the medial side of the calcaneus and the fat pad mesenchyme was located between the Achilles tendon and the bone (Figs 7.3.2.A and B).

57mm Foetus – Sagittal sections confirmed the presence of the fat pad mesenchyme within Kager's triangle at this stage. As at previous stages, the only evidence of enthesis organ differentiation was cavitation of the retrocalcaneal bursa (Fig 7.3.3.A).

110mm Foetus - The synovial bursa at this stage had increased in size and invaginating into the bursa, was the tip of the mesenchymal condensation which was destined to become the tip of Kager's fat pad (Fig 7.3.4.A and B). However, adipocyte differentiation had yet to occur. The tip of the condensation was lined with synovium which reflected back on itself

to line the proximal region of the retrocalcaneal bursa (Fig 7.3.4.B). Furthermore, large blood vessels could also be seen in the presumptive fat pad. However, in silver stained sections, no nerve fibres were evident (Fig 7.3.4.C), though they were present near the dorsal surface of the foot (Fig 7.3.4.D). At the same time, the periosteum on the posterior surface of the calcaneus had thickened (but without fibrocartilage differentiation) suggesting an early stage in the formation of the periosteal fibrocartilage (Fig 7.3.4.B).

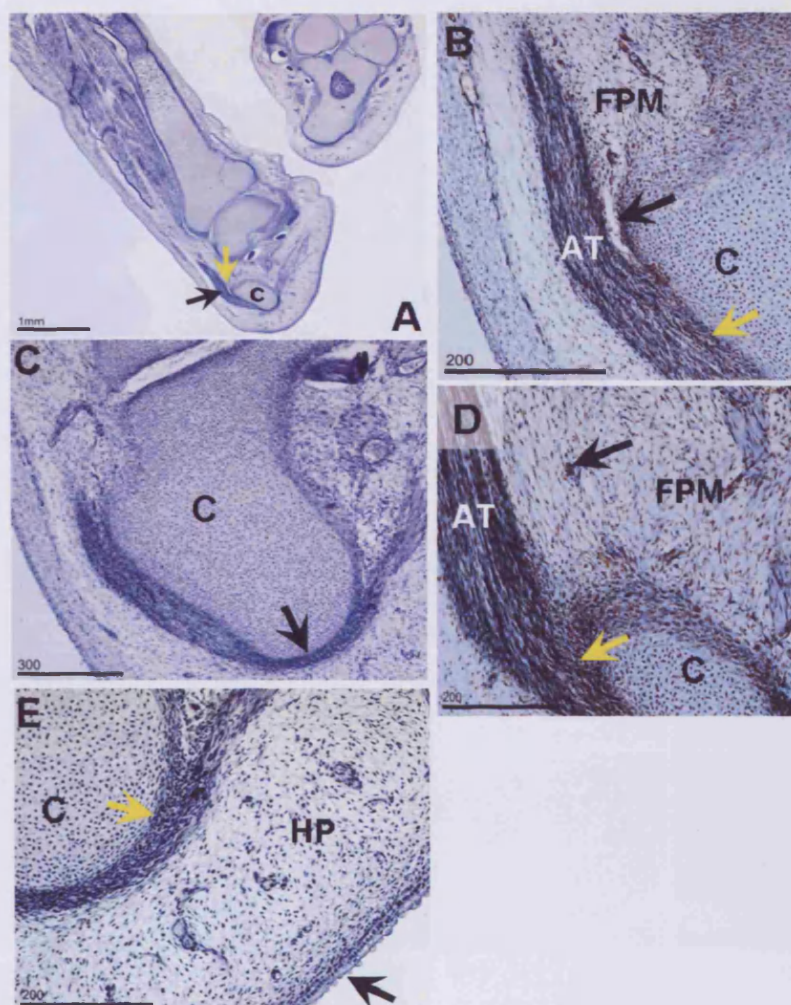
177mm Foetus – This was the first stage at which adipogenesis was evident within Kager's fat pad (Fig 7.3.5.A, and B). However, in the fat pad of the heel, adipocyte differentiation had still not commenced, although thick fibrous septa were evident between collections of mesenchymal condensations (Fig 7.3.5.E) and Pacinian corpuscles were found in the region (Fig 7.3.5.F). With reference to the rest of the entheses organ at this stage, the retrocalcaneal bursa was considerably larger and more defined; furthermore the superior tuberosity of the calcaneus had differentiated (Fig 7.3.5.C). On the posterior surface of the tuberosity, the perichondrium was still thickened – but had not differentiated into a distinct fibrocartilage (Fig 7.3.5.D). Furthermore, at this stage, although fibrocartilage cells could not be identified at the Achilles tendon insertion, it was clear that the tendon was bending to allow the collagen fibres to insert at right angles to the calcaneus (Figs 7.3.5.C inset). This suggested that the matrix was somehow stiffened in this region.

332mm Foetus - At this stage, Kager's fat pad contained a large number of adipocytes (although not fully enlarged) separated by a number of large fibrous septa. The pad also contained a number of nerve branches and blood vessels (Fig 7.3.6.A and B). Furthermore, the tip of the fat pad protruding into the retrocalcaneal bursa was slightly fibrous in nature (Fig 7.3.6.C) and adipogenesis had now also begun in the neighbouring heel pad (Fig 7.3.6.D). It was also evident at this stage that rounded fibrocartilage cells were present on the surface of the developing sesamoid and periosteal fibrocartilages (Fig 7.3.6.E).

Crown-rump length	Weeks of gestation	Bursa	Kager's fat pad adipogenesis	Hoffa's fat pad adipogenesis	Heel pad adipogenesis	Sesamoid fibrocartilage	Periosteal fibrocartilage
45mm	9.5	+	-	-	-	-	-
53mm	10.5	+	-	-	-	-	-
57mm	10.5	+	-	-	-	-	-
110mm	14.5	+	-	-	-	-	-
177mm	19.5	+	+	+	-	-	-
332mm	32.5	+	+	+	+	+	+

Table 7.3.1: Summary of the development of the Kager's fat pad in the context of the development of the rest of the Achilles tendon enthesis organ. + or - indicates whether a particular feature was present or absent.

Figure 7.3.1.



45mm FOETUS.

Figure A: A low power view of the Achilles tendon (black arrow) inserting into the calcaneus (C). The yellow arrow indicates the region highlighted in Fig B where a small cavitation was present between the superior surface of the calcaneus and the deep surface of the Achilles tendon. Hansen Haematoxylin. Scale bar = 1mm

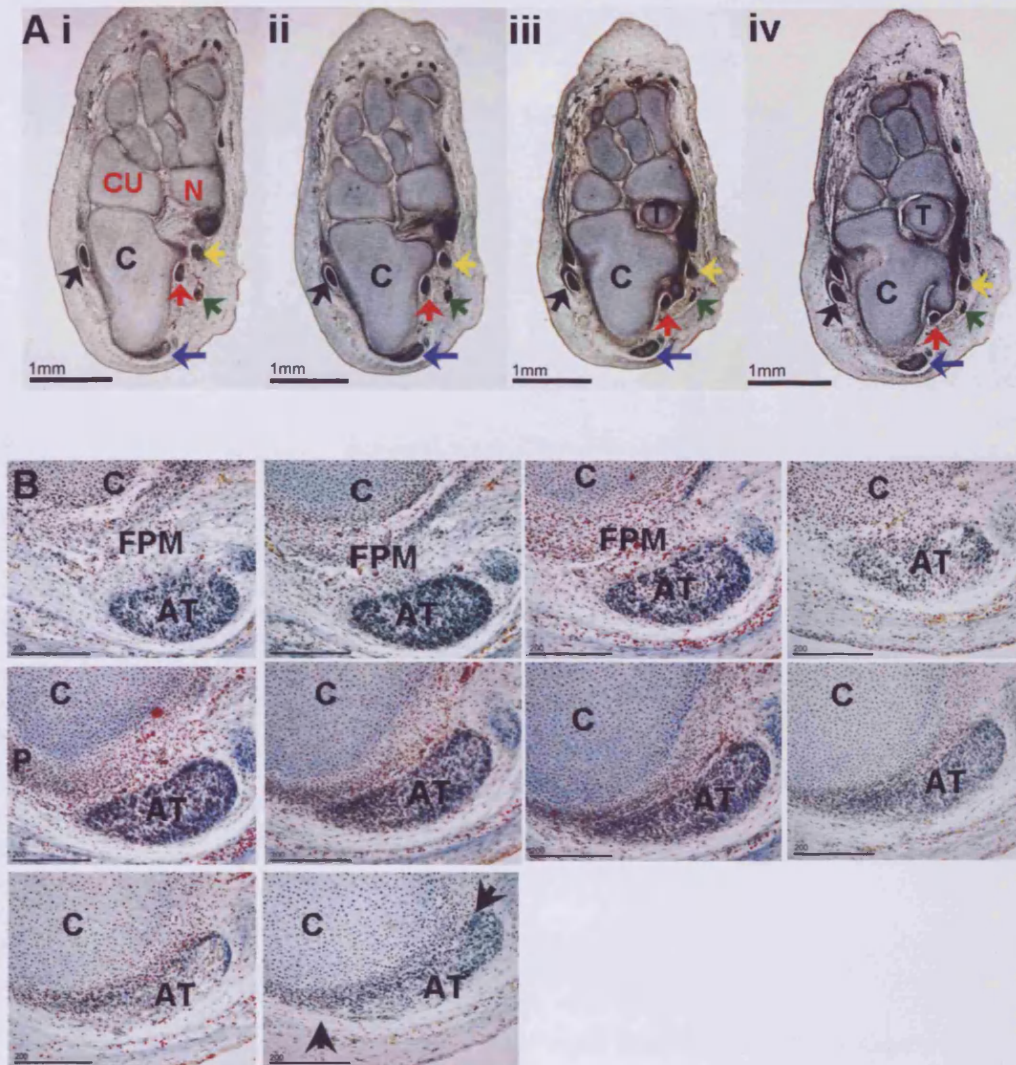
Figure B: High power view of the retrocalcaneal bursa (black arrow). The yellow arrow indicates the point at which the highly cellular Achilles tendon (AT) attaches to the calcaneal (C) perichondrium. Superior to the retrocalcaneal bursa is a mesenchymal structure, believed to develop into Kager's fat pad (FPM – Fat pad mesenchyme). VOF technique (light green, orange G and acid fuschin). Scale bar = 200 μ m

Figure C: High-power view of the continuation between the Achilles tendon and the plantar fascia via the perichondrium. Scale bar = 300 μ m

Figure D: High-power view of the prospective fat pad (which is mesenchymal at this stage - FPM), proximal to the insertion (yellow arrow) of the Achilles tendon (AT) to the calcaneus (C). The black arrow indicates a small capillary present in the presumptive fat pad. This figure also shows that the retrocalcaneal bursa does not extend across the width of the entire tendon. VOF technique. Scale bar = 200 μ m

Figure E: The attachment of the plantar fascia (yellow arrow) to the calcaneal (C) perichondrium. Not that at this stage, the presumptive heel pad (HP) is also mesenchymal in nature. The black arrow indicates the plantar surface of the foot. Scale bar = 200 μ m

Figure 7.3.2.

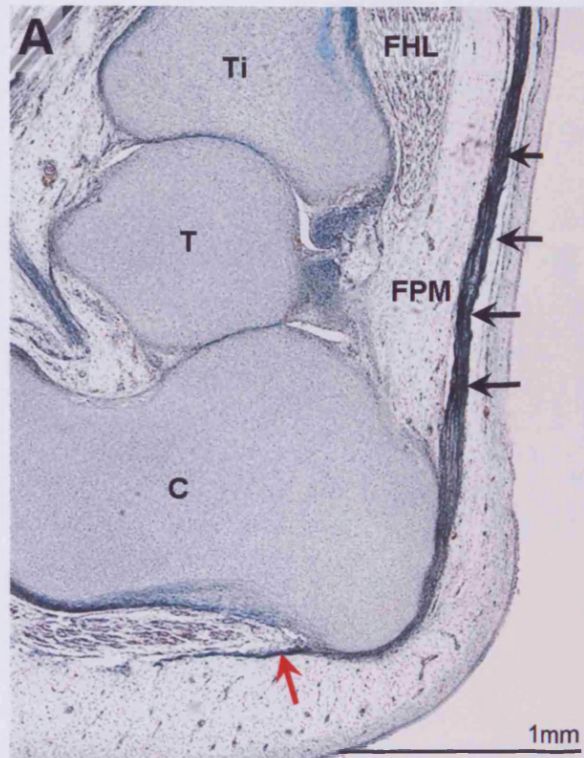


53mm FOETUS

Figure A i-iv: Transverse sections through the right foot. Note the attachment of the Achilles tendon (blue arrow) predominates on the medial side of the calcaneus (C) while the lateral aspect appears to remain free and rounded in appearance. Black arrow – peroneus longus tendon, Red arrow – flexor hallucis longus tendon, Yellow arrow – flexor digitorum longus tendon, Green arrow – posterior tibial artery, T – talus., N – Navicular, Cu – Cuneiform. Figures A i and iii - VOF technique, Figure A iv - azan technique. Scale bar = 1mm.

Figure B: High power view of transverse sections through the attachment of the Achilles tendon (AT) to the calcaneus (C) from proximal to distal, emphasizing its bilateral attachment (arrows). P - Perichondrium, FPM – fat pad mesenchyme. Scale bar = 200µm.

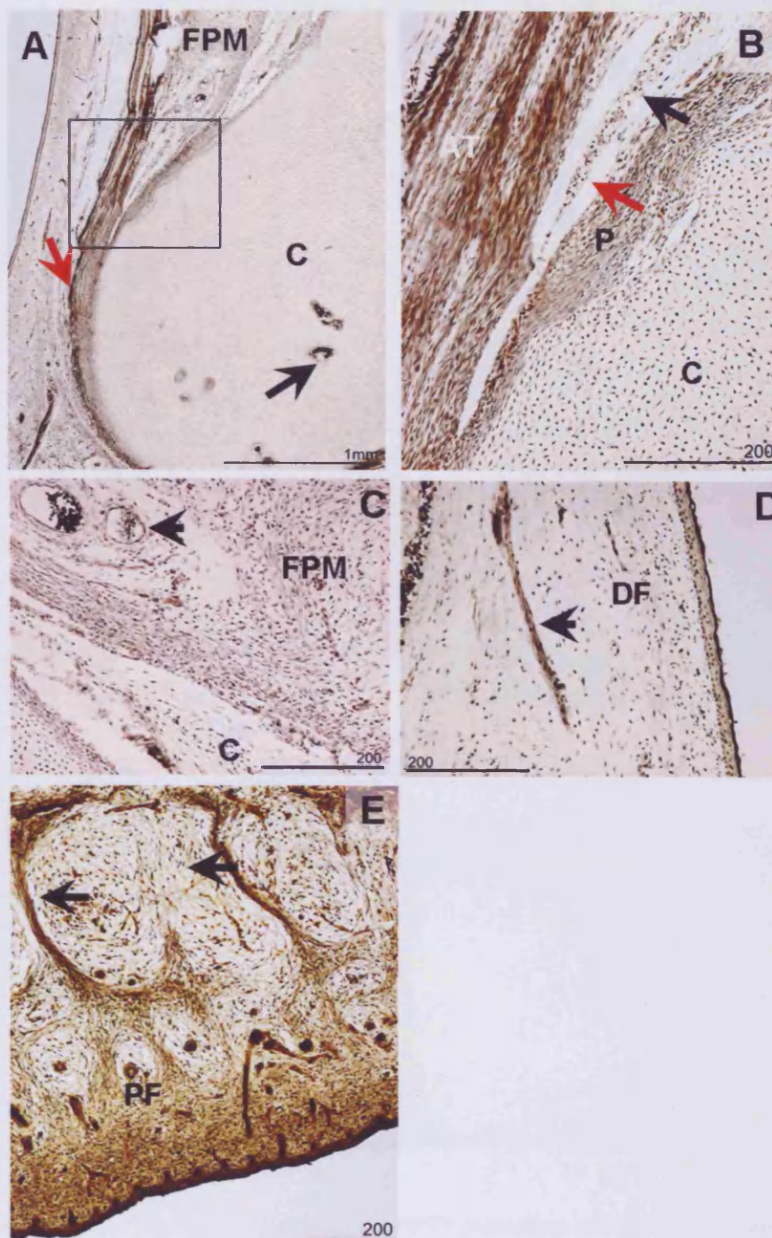
Figure 7.3.3.



57mm FOETUS

Figure A: A sagittal section showing the location of Kager's pad mesenchyme (FPM) in Kager's triangle which is bordered by the Achilles tendon posteriorly (black arrows), the calcaneus (c) inferiorly and flexor hallucis longus (FHL) anteriorly. Ti – Tibia, T-Talus, red arrow – plantar fascia. VOF technique. Scale bar = 1mm.

Figure 7.3.4.



110mm FOETUS (Bielchowsky technique)

Figure A: Low power view of the Achilles tendon enthesis (red arrow). Note the presence of cartilage canals (black arrow) in the calcaneus (C). Highlighted area is enlarged in Fig B. . Scale bar = 1mm.

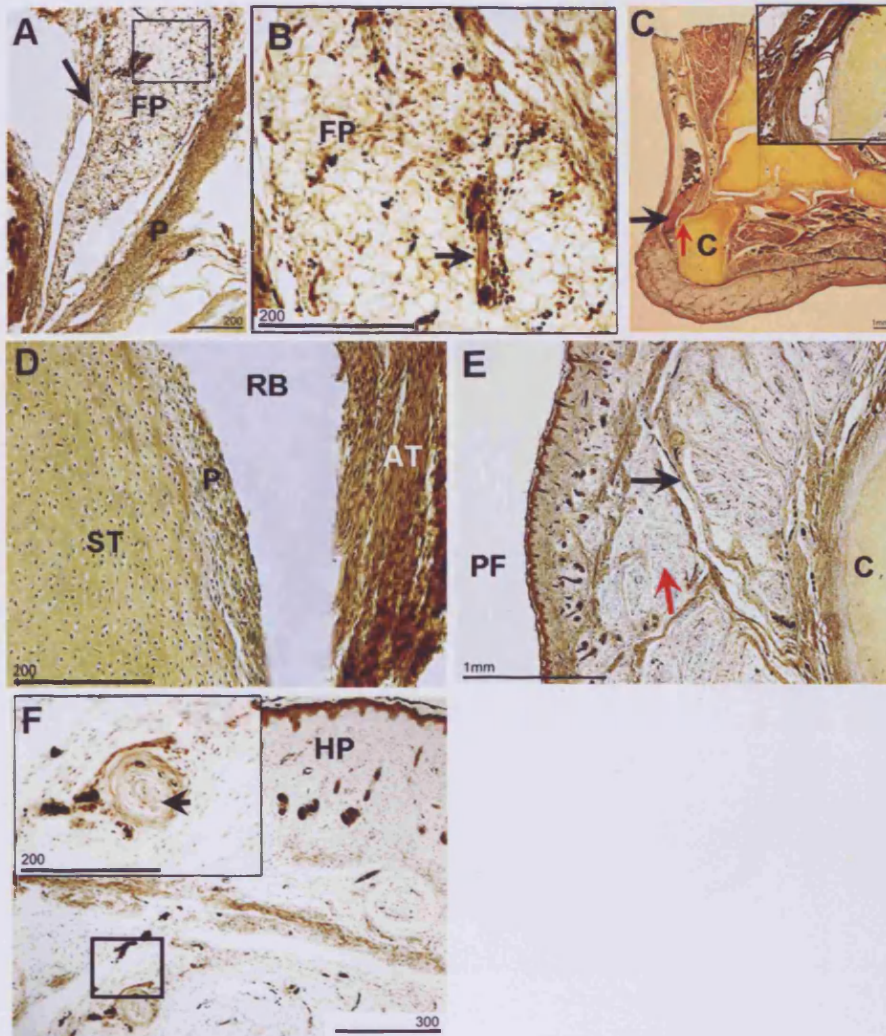
Figure B: High power view of the tip of the fat pad mesenchyme (black arrow) protruding into the retrocalcaneal bursa (red arrow). Note the thickened periosteum (P) on the posterior surface of the calcaneus. Scale bar = 200µm

Figure C: The fat pad mesenchyme (FPM) in a silver stained section. Note the absence of visible nerve fibres. Arrow indicates a venule in the fat pad mesenchyme. Scale bar = 200µm.

Figure D: A positively-stained nerve fibre – believed to be a digital nerve – (arrow) was present in the mesenchyme near the dorsal surface of the foot (DF). Scale bar = 200µm.

Figure E: The plantar surface of the foot demonstrating the mesenchymal heel pad containing a large number of thick fibrous septa (black arrows). PF - plantar surface of the foot. Scale bar = 200µm.

Figure 7.3.5.



177mm FOETUS (Bielchowsky technique).

Figure A: Low power view of the tip of Kager's fat pad (FP) protruding into the retrocalcaneal bursa (red arrow) C-calcaneus. Note the reflections of the synovial membrane (black arrow) lining the tip of the fat pad and the proximal part of the retrocalcaneal bursa. P – periosteum. Scale bar = 200µm.

Figure B: High power view of the region highlighted in fig A. Note the differentiated adipocytes and the small capillary (arrow) within the fat pad (FP). Scale bar = 200µm.

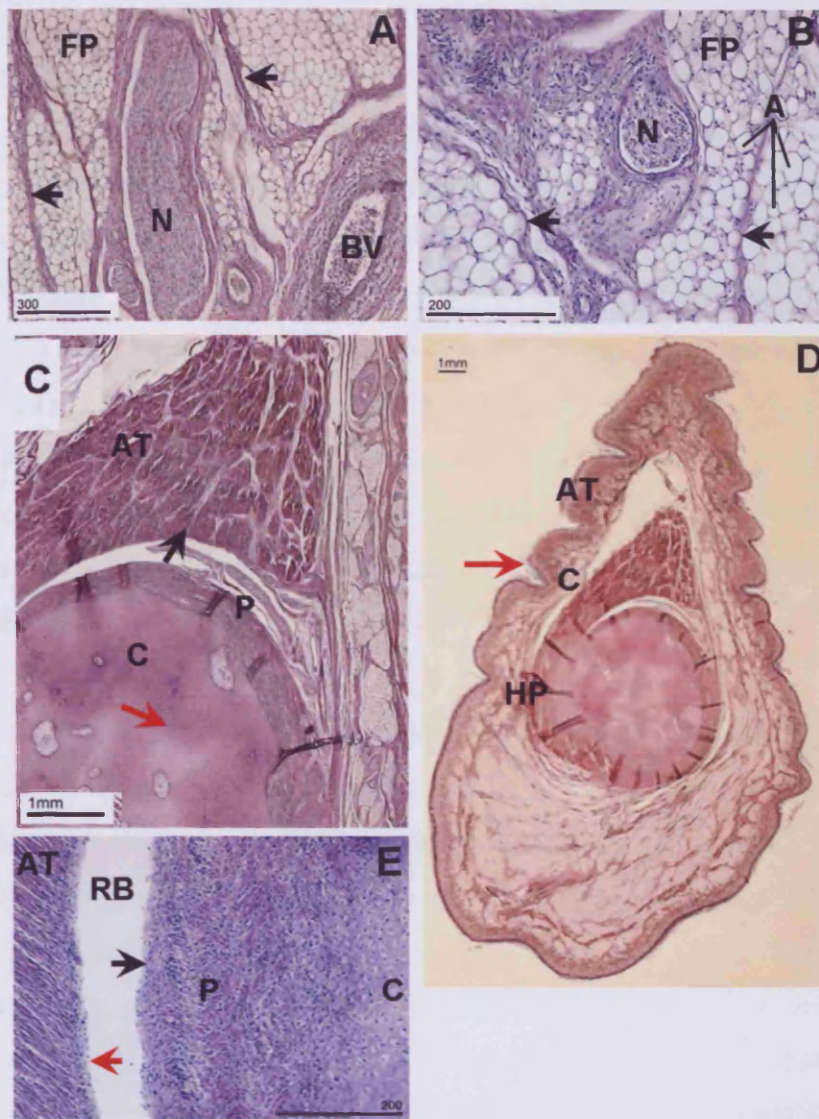
Figure C: Low power view of the posterior region of the foot. Note the prominent superior tuberosity (red arrow) of the calcaneus (C) and bending of the collagen fibres in the Achilles tendon close to the insertion (black arrow and inset). T-tibia. Scale bar = 1mm.

Figure D: The retrocalcaneal bursa (RB) – note the thickened perichondrium (P) on the superior tuberosity (ST) of the calcaneus adjacent to the Achilles tendon (AT). Scale bar = 200µm.

Figure E: The plantar surface of the foot (PF) illustrating the absence of any adipocyte differentiation (red arrow) in the heel pad of the foot. Note the thick fibrous septa (black arrow) separating collections of mesenchymal cells. C-calcaneus. Scale bar = 1mm.

Figure F: Low power view of the heel pad (HP) containing a Pacinian corpuscle. Sale bar = 300µm. **Inset:** High power view of the highlighted Pacinian corpuscle. Scale bar = 300µm.

Figure 7.3.6.



332mm FOETUS (Hansen Hematoxylin)

Figures A and B: A high power view of Kager's fat pad (FP). Note the single lipid droplets present within the adipocytes (A) and thick fibrous septa (arrows) separating groups of fat cells. Large nerve bundle (N) and blood vessels (BV) were also present within the fat pad. Scale bars = 300 μ m (A) and 200 μ m (B).

Figure C: Higher power view of the fat pad (black arrow) – fibrous in nature and protruding into the retrocalcaneal bursa. Note the thick perichondrium (P) covering the cartilaginous calcaneus (C) and the presence of cartilage canals (red arrow) in the calcaneus. AT- Achilles tendon. Scale bar = 1mm.

Figure D: Low power view of the Achilles tendon (AT) attaching to the calcaneus (C). Note the medial attachment of the tendon to the calcaneus (red arrow). The heel pad (HP) contains a large number of terminally differentiated adipocytes containing lipid droplets. Scale bar = 1mm. Coronal section.

Figure E: High power view of the retrocalcaneal bursa (RB) Note the formation of the sesamoid (red arrow) in the deep surface of the Achilles tendon (AT), and the developing fibrocartilaginous nature (black arrow) of the perichondrium (P) on the posterior surface of the calcaneus (C). Scale bar = 200 μ m.

7.4. DISCUSSION

The formation of the retrocalcaneal bursa (lined with synovial cells) was the first evidence of the differentiation of the Achilles tendon enthesis organ during development. Subsequently, the bursa became larger and more defined, and the tip of the mesenchymal condensation, destined to become the bursal wedge of Kager's fat pad, protruded into it. At the same stage, the perichondrium lining the posterior surface of the calcaneus thickened. At a later stage, the posterior tuberosity of the calcaneus became prominent, bending of collagen fibres was observed in the tendon at its attachment, and adipogenesis of Kager's fat pad commenced. Intriguingly, mature adipocytes were evident in Kager's fat pad before they appeared in the neighbouring heel pad. Differentiation of the periosteal and sesamoid fibrocartilages was the final stage in the appearance of an enthesis organ that was typical of an adult foot.

Initially, the developing Achilles tendon attached to the perichondrium of the calcaneus, as did the plantar fascia. However, previous studies have debated the continuity of these entheses in the adult (Milz et al., 2002; Snow et al., 1995). The current work shows that the continuity between the Achilles tendon and plantar fascia entheses reflects their development. As discussed previously, the linking of these two structures may be a functional adaptation to aid stress dissipation at the tendon insertion over a larger area (Benjamin et al., 2006). Therefore this connection during development may be particularly important as recent studies have demonstrated that the immature enthesis is 35% weaker than the mature, fully developed attachment site (Furikado et al., 2002).

Another observation highlighted by the current developmental study, was the apparent medial attachment of the Achilles tendon to the calcaneus. Similar observations have previously been reported by Fritsch (1996) who attributed this to the torsion of the calcaneus (Straus Jr, 1927) and therefore when sectioned this may give the illusion that the Achilles tendon does not attach across the width of the calcaneus - whereas in reality it does. This needs to be confirmed by further studies in which the whole area is reconstructed in 3D. However, in contrast to the view of Fritsch (1996), it is here suggested that the presumptive fat pad was located within Kager's triangle, between the Achilles tendon and flexor hallucis longus, rather than laterally. Once again 3D reconstructions are necessary to resolve the issue more satisfactorily.

The first component of the enthesis organ to differentiate was the retrocalcaneal bursa and this appeared at 9.5 weeks of gestation. At this stage, the bursa, unlike that of the adult, was lined by synovial cells. It is likely that synoviocytes differentiated from the mesenchyme (continuous with the mesenchymal presumptive fat pad) which filled the space between the presumptive periosteal and sesamoid fibrocartilages i.e the interzone. Such a mechanism has previously been observed during the formation of synovial membrane in joints (Andersen, 1963; Andersen and Bro-rasmussen, 1961). This is the most logical part of the enthesis organ to develop first, as the hyaluronan-rich synovial fluid secreted by the synovium would facilitate movement of the Achilles tendon relative to the calcaneus during foot movements. With continued development, the bursa gradually increased in size and the tip of the presumptive fat pad protruded into the bursa. This is in line with the proposal of Theobald et al., (2006) that a protruding fat pad tip is required to prevent pressure changes occurring in the bursa during foot movements. During later development, the synovium lining the walls of the bursa disappeared, but remained as a covering for the tip of the presumptive fat pad protruding into the bursa. This is in line with earlier findings in the rat (Rufai et al., 1992). The retention of synovium over the tip of the presumptive fat pad is likely to facilitate the movement of the fat pad in and out of the bursa (Canoso et al., 1988). Loss of the synovial membrane on the surfaces of the Achilles tendon and perichondrium during development may be the result of compression of these two surfaces together during foot movement. However, it has also been suggested by Rufai et al., (1992) in the rat that the synovial membrane may contribute to the formation of the sesamoid and periosteal fibrocartilages. Clearly, the same may be true for man.

Although this study does not allow us to understand *exactly* at which stage of development, the 3 individual fibrocartilages of the enthesis organ differentiate, it was possible to conclude that they do not develop until adipogenesis has begun within Kager's fat pad (around 19.5 weeks of gestation). The purpose of ensuring that adipocyte maturation in the fat pad occurred prior to fibrocartilage differentiation is unknown, although it may be an adaptation to ensure that the enthesis is protected from wear and tear during development, at a stage when fibrocartilage has yet to appear. Several changes were however observed in the presumptive fibrocartilaginous regions at this point. It was clear that the collagen fibres of the Achilles tendon began to bend to a greater degree proximal to its insertion and this may be facilitated by an increase in PG-rich matrix that was not evident in routine

histology sections. Furthermore, the perichondium opposing the tendon became thicker and the superior tuberosity of the calcaneus was pronounced; while the deep surface of the Achilles tendon remained purely tendinous. These observations suggest that the presumptive enthesis and periosteal fibrocartilages begin to develop prior to the presumptive sesamoid fibrocartilage. This sequence of fibrocartilage formation was also observed in the rat by Rufai et al. (1992).

As described above, the presumptive Kager's fat pad appeared at 9.5 weeks of gestation as a loose mesenchymal mass located in Kager's triangle. However, due to the similar appearance of mesenchymal cells and pre-adipocytes it was impossible to differentiate between the two cell types in routine sections. Therefore, immunolabelling for pre-adipocytes (possibly with the use of Pref-1 (Smas and Sul, 1993) may prove useful for further studies to identify when the cells in this region become specified into pre-adipocytes. Mature fat cells were not present within Kager's fat pad until 19.5 weeks of gestation, at which stage they were also be seen in Hoffa's fat pad (H. Shaw, Unpublished observations). However, mature adipocytes were still not present in the heel fat pad at this stage. This may reflect the structural function of these pads in dissipating stress during movement. The observations suggest that adipocytes have differentiated in the knee and ankle to protect their associated structures – i.e. entheses, while adipocytes within the heel pad have not differentiated as cushioning in this region in not yet required. However, it was clear that the heel pad was beginning to develop with the formation of fibrous septa, separating groups of mesenchymal cells/pre-adipocytes which will eventually develop into mature adipocytes. The fibrous compartments within the heel pad have previously been observed by Jahss et al., (1992) who suggested that this may contribute to the effective cushioning function of the fat pad. The formation of fibrous septa prior to adipogenesis contrasts with the observations in Kager's fat pad, where thick fibrous septa are only observed later in development (32.5 weeks of gestation). In addition, nerve bundles could clearly be seen at 32.5 weeks of gestation within Kager's fat pad, suggesting that the pad may contribute at this early stage to ankle joint proprioception. However, in further studies it would be necessary to identify the developmental stage at which nerve fibres can be found in the fat pad.

Although further studies are clearly required to obtain more information on the development of the enthesis organ, this study has demonstrated that the retrocalcaneal

bursa was the first component of the enthesis organ to differentiate, in order to facilitate movement between the tendon and bone. Furthermore, it has also been established that adipocytes within Kager's fat pad mature prior to the differentiation of the fibrocartilages of the enthesis. However, due to the rare nature of the material used in this study, only 1 foetus at each stage could be examined which is a limitation that should be addressed in further work.

8. THE STRUCTURE AND INNERVATION OF OTHER ENTHESES

8.1. INTRODUCTION

As described previously, there are two distinct types of tendon and ligament entheses namely; fibrocartilaginous and fibrous entheses. However, some muscles attach to bone without a tendon and these attachments are known as 'fleshy' or 'muscular' entheses. Chapter 3 discusses the structure and innervation of the classical fibrocartilaginous entheses of the Achilles tendon in the rat. The purpose of the present chapter is to explore the structure and innervation of other entheses by routine histology and immunohistochemistry: The chosen entheses include (a) a muscular entheses (the origin of tibialis anterior in the rat) (b) a classical fibrous entheses – the tibial insertion of the rat MCL and (c) the attachment of the suspensory ligament to the plantar surface of the third metatarsal bone in the horse. The suspensory ligament is a common sight of pathology leading to lameness in thoroughbred race horses.

Brief Review

8.1.1. Fibrous Entesis of the Medial Collateral Ligament

A large number of studies use the rat or rabbit MCL as a model for ligament research, and as a result its development and growth has been studied in detail (Dorfl, 1980a; b; Gao et al., 1996; Hurov, 1986; Muhl and Gedak, 1986; Wei and Messner, 1996). The innervation of the mid portion of the MCL has also been considered (Ackermann et al., 1999; Delgado-Baeza et al., 1999; McDougall et al., 1997), however, the innervation of its fibrous entesis has not been fully described.

Gross Anatomy

The MCL is located on the medial side of the knee, originating from the femoral diaphysis and inserting onto the tibial metaphysis. Its principle function is to stabilise and prevent lateral movement of the knee. In man, the tendons of sartorius, gracilis and semitendinosus cross the ligament to insert into the tibia, forming a multi-layered structure known as pes anserinus. This helps to strengthen and stabilise the medial aspect of the joint (Mochizuki et al., 2004), however, this structure is not seen in the rat. The proximal insertion of the MCL onto the medial epicondyle of the femur is fibrocartilaginous; this permits bending of the ligament during flexion and extension of the knee without causing damage and fraying

of the ligament (Benjamin et al., 1986; Matyas et al., 1995). In contrast, the distal insertion of the MCL is fibrous and inserts onto the shaft of the tibia. (Fig 8.1.1.1.)

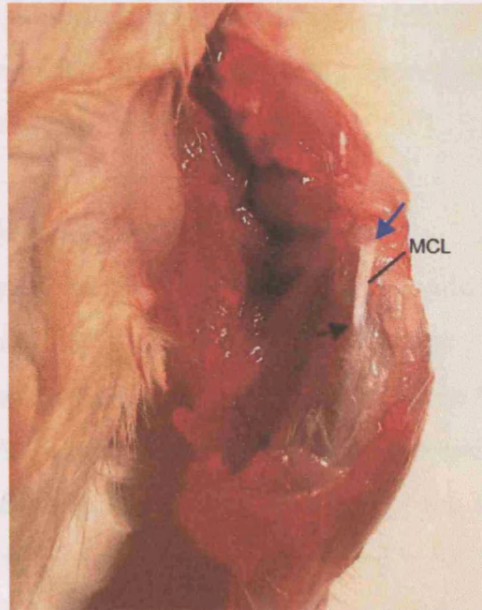


Figure 8.1.1.1: The location of the medial collateral ligament (MCL) in the rat knee. Blue arrow indicates the proximal fibrocartilaginous enthesis attaching to the medial condyle of the femur. Black arrow indicates the distal fibrous enthesis attaching to the shaft of the tibia.

Histological and Biochemical Structure of the MCL

Due to the distinct similarity between the histological and biochemical structure of tendons and ligaments, this topic will only be briefly discussed here (for more information see chapter 1). However, it must be remembered that the proportion and arrangement of the molecular components varies within and between ligaments and tendons, primarily because of differences in loading patterns exerted (Rumian et al., 2007). Ligaments, like tendons, are dense fibrous connective tissues, composed primarily of bundles of type I collagen which are produced by the resident fibroblasts lying between these bundles. Chi et al., (2005) show that fibroblasts which reside in the MCL have a more complex structure than initially believed. With the use of SEM and TEM they showed that the cells, like those of the tendon, send out cytoplasmic projections from the cell body to envelop adjacent collagen bundles. However, these cells are not uniformly distributed along the row in which they lie and in contrast to tendons, a single row of cells cannot be followed along the length of the ligament. Instead, the cells weave - in a twisted fashion - through the ECM of the ligament (Chi et al., 2005). They also demonstrated by TEM, that an extensive pericellular matrix surrounds the fibroblasts, and that these cells interact with this matrix

via short membrane extensions to increase the surface area. This arrangement may facilitate the exchange of information and material between the cell and the surrounding ECM (Chi et al., 2005). Furthermore, the shape of the fibroblasts residing within the ligament is altered in response to mechanical loading (Matyas et al., 1994). This, in turn may alter the metabolism of the fibroblast allowing appropriate modification of the ECM (Banes et al., 1999; Matyas et al., 1994).

Innervation and Blood Supply of the MCL

The innervation of the knee joint has been widely studied with various techniques including silver-staining, gold chloride and immunohistochemistry. Such techniques have demonstrated that both myelinated and un-myelinated nerve fibres occur most frequently within the epiligament. McDougall et al., (1997) have reported that these fibres run parallel to the collagen strands of the epiligamentous tissue, and the fibres subsequently enter the main substance of the MCL via accompanying blood vessels or as free nerve endings. These fibres then branch into the deeper layers of the tissue. The myelinated nerve fibres within the tissue usually end as simple (type IV - un-encapsulated) nerve endings (74%), however, some terminate in specialised Golgi (type III endings - 4%), Ruffini (type I endings - 9%), or Panican (type II endings - 11%) endings conveying mechanoreceptive information to the CNS (Delgado-Baeza et al., 1999). The presence of such endings confirms the complex role that the MCL plays in knee joint proprioception (McDougall et al., 1997). Ackermann et al., (1999) have also demonstrated the presence of nociceptive nerve fibres containing SP and CGRP in the epiligamentous tissue of the MCL. These fibres are believed to play an important role in vasoregulation, pro-inflammatory processes, and possibly healing of the tissues in which they are contained (Ackermann et al., 1999; McDougall et al., 1997). In addition, sensory modulating fibres containing galanin and somatostatin have also been identified in the ligament and its surrounding tissue. These fibres inhibit inflammation and nociception. With the use of radioimmunoassay, it was established that ligaments and capsules contain a greater number of sensory modulating fibres than sensory peptidergic fibres when compared with tendons. It is suggested that this may reflect the greater vulnerability to pain and inflammation in tendons, as well as the difference in function of these two connective tissues (Ackermann et al., 1999)

The sympathetic nervous system may also play an important role in the structure of the MCL. Dwyer et al., (2004) blocked the sympathetic nervous system in the rat MCL with

quanethidine - used to treat pain in orthopaedic diseases. They demonstrated that this treatment lead to alterations in the levels of degenerative enzymes within the tissue, which may at a later stage lead to pathology (Dwyer et al., 2004). Furthermore, innervation of the rabbit MCL is believed to be essential for early healing responses. Neuropeptides released from nerves at damaged sites may function to improve angiogenesis through increasing vascularity or may directly help to repair the damaged tissue (Ivie et al., 2002).

The vasculature of the MCL may also have an important role in healing. The normal ligament is relatively hypovascular, with the majority of the blood vessels contained within the loose connective tissue of the epiligament. These vessels are randomly dispersed, which contrasts with the intra-ligamentous vessels that run, in an organised fashion, parallel to the collagen fibres bundles of the ECM. Despite the gross visible presence of blood vessels in the ligament, only approximately 1.5% of the total available ligament matrix is occupied by vasculature. The number of blood vessels in the ligament increases dramatically during healing, these vessels are organised randomly, in contrast to the normal structure (Eng et al., 1992). With continued healing this vasculature regresses, and is replaced with a more organised arrangement in the scar tissue (Bray et al., 1996).

Structure of the Fibrous Enthesis of the MCL

As described previously, fibrous entheses can be categorised into two groups: (a) periosteal - where the tendon attaches to the periosteum, which in turn attaches to the underlying cortical bone and (b) bony - where the periosteum is absent and the tendon inserts directly into the bone. In most animals a periosteal entheses can become a bony one following closure of the growth plate. As described in detail in chapter 1, the insertion of the MCL onto the tibia is a complex multi-layered structure that alters during development and growth. In the adult, the attachment is composed of four layers. Layer I is a delicate, connective-tissue continuous with the superficial layer of the periosteum distally. Layer II, formed from densely packed collagen fibres of the ligament pass through the periosteum. Some of these fibres insert into the underlying cortical bone – these are believed to be the perforating fibres of Sharpey. Layer IV (layer III is lost during development) is a thin layer of mineralised ligament which thickens progressively with age. Collagen fibres of this layer are continuous with layer II, however the layers are distinguished by a mineralization front which is basophilic in haematoxylin and eosin stained sections. The lamellar bone of the tibial cortex forms the final layer (layer V) (Matyas et al., 1990).

Development and Postnatal Growth of the fibrous enthesis of MCL

Wei and Messner (1996) studied in detail, the postnatal growth of the MCL in the rat knee, by routine histology. At birth, the fibres of the MCL attach obliquely to the periosteum forming three layers; the ligament, periosteum, and metaphysial bone. With growth, the cellular nature of the ligament is reduced and the collagen fibres become more longitudinally arranged. From day 8, osteoclastic activity on the periosteal side of the bone, increasingly erodes the bone to form a metaphysial depression which is deepest at its proximal part. As a result, osteoclasts are present primarily in this region up to day 55. Following this stage, their numbers reduce and the periosteum thins out. At the distal part of the depression, the fibres of the ligament and periosteum weave together and attach obliquely into the underlying trabecular bone, where some of these fibres become cemented into the bone. At day 90, the ligament is still attached to bone via the periosteum, however, by this time the periosteum is much thinner. The cells within it are elongated and flattened, and only a very small number of osteoclasts are present. It is only at day 120 that development of the insertion is complete, the ligament inserts directly into the bone to form a bony enthesis and all osteoblast or osteoclast activity has ended (Wei and Messner, 1996). The use of metallic markers has shown that the insertion migrates at the same speed, and in the same direction as the neighbouring periosteum. Therefore the indirect attachment of the ligament to bone during early stages of development allows the ligament to migrate towards the epiphysis, ensuring that it maintains its position with respect to the joint cavity (Dorfl, 1980a; b; Muhl and Gedak, 1986).

8.1.2. 'Muscular' Enthesis of Tibialis Anterior

The principle function of a tendon is to transfer the force generated by muscle to bone in order to produce locomotion. However, some muscles do not possess tendons because the angle at which the muscle acts is insignificant (Benjamin and Ralphs, 1997). The attachment of such muscles is described as forming 'fleshy' or 'muscular' entheses. However, such entheses are little studied and textbook descriptions simply suggest that the mechanism of attachment is via the connective tissue (epimysium) which surrounds the attaching muscle. The connective tissue then attaches to the periosteum and the periosteum in turn attaches to the underlying cortical bone (Benjamin et al., 2002).

It is surprising that this form of attachment site has not previously been studied because it is suggested that repeated microtrauma to the fleshy origin of *tibialis anterior* or *tibialis posterior* may cause the pain associated with shin splints. However, 'shin splints', is used as an umbrella term to describe chronic pains in the area between the knee and ankle. Pain in this region can be the result of a number of different problems including - tibial periostitis, exertional compartment syndrome, and also stress fractures of the tibia. These pathologies are usually a consequence of extended periods of excessive strain (Pecina and Bojanic, 1993). As a result there has been much debate as to the cause of pain in this region. Therefore, describing the innervation of the muscular attachment of *tibialis anterior* may shed some light on this discussion.

Only a small number of articles have referred to the presence of muscular/fleshy attachments, and no detailed study focussing on this form of attachments has been made (Benjamin et al., 2002). Suzuki et al., (2002) provides one of the most comprehensive descriptions from the limb muscles of the lizard. They reported that these fibres approach the bone at varying angles, some of these muscle fibres appeared to be in direct contact with the periosteum without the presence of loose connective tissue from the epimysium. The significance of this is not been discussed. Hurov et al., (1986) described the fleshy attachment of popliteus. The author has shown that the epimysial connective tissue inserts into the periosteum and that some of these fibres pass through the periosteum and terminate on the surface of the lamellar bone. He also demonstrated the presence of periosteal elastic fibres arranged in layers at the attachment site (Hurov, 1986).

Recently, (Chen et al., 2006) used a lacZ reporter construct, under control of endogenous PTHrP in an attempt to illustrate the widespread expression of PTHrP. The authors demonstrate that lacZ positive cells are present at muscular attachment sites. It appears as though these cells are present within the connecting epimysium of the muscle attachment, however, the function of PTHrP at these sites is not understood (Chen et al., 2006). PTHrP may have a role in regulating local growth of the periosteum in response to mechanical stimulation/periosteal tension from the attached muscle (Hurov, 1986).

Gross Anatomy of Tibialis Anterior

The principle function of tibialis anterior is dorsiflexion and inversion of the foot. The muscle originates from the margin of the lateral condyle, the tuberosity, and the ventral

crest of the tibia, passing superficially over the antero-lateral surface of the leg (Fig 8.1.2.1 and 2). Its tendon passes under the annular ligament, crosses to the medial surface of the foot and inserts into the first cuneiform bone and the proximal end of the first metatarsal. Tibialis anterior is vascularised by the anterior tibial recurrent and muscular branch of anterior tibial arteries and receives its innervation from the deep peroneal nerve (Greene, 1935).

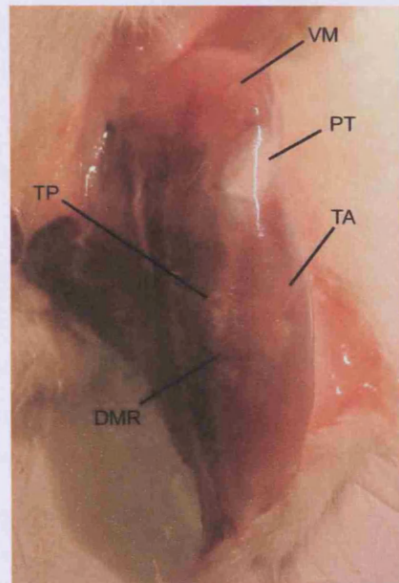


Figure 8.1.2.1. The location of tibialis anterior (TA) in the shank of the rat. PT – patellar tendon, TP – Tibialis posterior, DMR – dorso-medial ridge of the tibia.



Figure 8.1.2.2: The anatomy of the rat tibia and fibula indicating the lateral condyle, tuberosity and the ventral crest of the tibia where tibialis anterior originates (Greene, 1935).

The Myotendinous Junction

The myotendinous junction (MTJ) shows both molecular and morphological specialisations for the transmission of force from cytoskeletal proteins in a contractile muscle cell to extracellular structural proteins of the tendon. The interface membrane between muscle and tendon is highly convoluted and the tendinous collagen fibrils insert into deep recesses which are formed by the finger-like processes of the muscle cells. These invaginations increase the surface area, leading to a reduction in the force-per-unit area applied and plays an important role in reducing stress and dissipating shear caused by high levels of muscular contraction (Tidball, 1991). A similar structure is seen at the myofascial junction in the rat calf muscles (Jarvinen et al., 1992). Force, generated by the muscle, is transmitted through a chain of proteins namely, vinculin, talin, integrin, fibronectin and collagen, which form strong focal contacts. However, other structural proteins such as myonexin and dystrophin, which are specifically found at MTJs may also play a role in force transmission (Tidball, 1991). Jarvinen et al., (1991) describe the presence of heparin sulphate, chondroitin

sulphate and or dermatan sulphate specifically in the sarcolemma and ECM of terminal muscle cells. The presence of these various polysaccharides may increase the adhesive force between the muscle cell membrane and the collagen fibres of the tendon (Jarvinen et al., 1991). Tenascin-C, an ECM glycoprotein, is also present at the myotendinous junction, and other locations which transmit high mechanical forces from one tissue to another (Jarvinen et al., 1999; Jarvinen et al., 2000; Kannus et al., 1998). At the myotendinous junction, tenascin-c expression is regulated by mechanical loading (Jarvinen et al., 2003). Despite its highly specialized adaptations, the myotendinous junction is described as the weakest point in the muscle-tendon unit (Jarvinen et al., 1991). Therefore, this study will examine the expression of actin and vinculin at the muscular entesis to establish if there are any similarities to the myotendinous junction even though there is effectively no tendon present.

The main collagenous component of the myotendinous junction is type I collagen. However, type III is also present at the tissue interface - on the surface of the muscle cells (Jarvinen et al., 1991). In addition, a novel collagen type (collagen XXII) has been identified which is present only at tissue interfaces, such as the myotendinous junction in skeletal muscle. Collagen XXII, a member of the fibril-associated collagens with interrupted triple helices (FACIT), is synthesized by muscle cells close to the MTJ and deposited into the basement membrane between the finger-like processes of the muscle cells. It is hypothesized that collagen XXII at the MTJ may play a role in binding the ECM components of the basement membrane (Koch et al., 2004). Furthermore, Astrow et al., (1992) have generated a monoclonal antibody named 3G2 against a 41 kDa protein. This protein is present at the myotendinous junction but is also identified within the subsarcolemma where it outlines the synaptic gutters of the neuromuscular junction. It is believed that this protein may also have a function in stabilizing the connection between the extracellular matrices, thereby maintaining structural integrity during muscular contraction at both myotendinous and neuromuscular junctions (Astrow et al., 1992).

Experiments into the effect of immobilization on the MTJ have demonstrated that degenerative changes occur, causing a decrease in the tensile strength and may predispose the region to rupture. The main changes identified with immobilisation include a reduction in the contact area between the muscle cells and collagen fibres, a shallowing or atrophy of the muscle finger-like processes and a significant decrease in the quantity of sulphated

GAGs. In addition, the amount of collagen type III was seen to increase, although the quantity of collagen type I was unaffected (Kannus et al., 1992). Similar degenerative changes are also observed when soleus is tenotomised at the muscle-tendon junction. These changes were almost completely restored 5-6 weeks following tenotomy (Abou Salem et al., 1993a; Abou Salem et al., 1993b).

During development, the formation of the MTJ begins with an accumulation of ECM in the presumptive junctional region at the end of the myotube. Subsequently, the basement membrane appears; initially in the form of membrane-associated ECM accumulations on the lateral surfaces of the cells. Both fibroblasts and myogenic cells contribute to the deposition of this ECM material. Laminin is the first major basement protein to be identified in the developing MTJ. Myofibrils then associate with the developing junctional membrane where subsarcolemmal densities of mitochondria are present corresponding with increasing levels of talin (involved in membrane fold formation and mediate myofibril - cell membrane associations). Following the appearance of talin, membrane folding occurs and the muscle cells form digit like extensions into the surrounding connective tissues. Once the initial structure is formed, the only changes which occur are increases in the number of subsarcolemmal densities, myofibril-membrane associations, and increased junctional membrane folding (Tidball and Lin, 1989).

Innervation of the Myotendinous Junction

As described previously, the MTJ is under a large degree of mechanical stress at the tissue interface. Consequently, there is a need for movements occurring in this region to be monitored. For this reason, the myotendinous junction has a large population of various mechanoreceptors along with free nerve endings which conduct sensory information to the CNS. Ruffini corpuscles are present in both the muscular and tendinous regions, while Pacinian corpuscles predominate on the tendon side. In contrast, Golgi-tendon organs are present primarily on the muscular side within the anchoring connective tissue (Jozsa et al., 1993). During development, a temporary neuromuscular contact is present in the MTJ. Up to the 5th postnatal day, sensory axon terminals form neuromuscular contacts in the muscle fibre fascicles connected with differentiated Golgi tendon organs. However, following the 5th day postpartum, the terminals become detached from the muscle fibres leaving only

those present within the collagen bundles of the tendon organ. The function and significance of these temporary neuromuscular contacts is unknown (Zelena, 1976).

8.1.3. The Origin of the Suspensory Ligaments in the Horse

Gross Anatomy

The suspensory ligament attaches proximally to the plantar surface of the third metatarsal bone at the hock joint; but also arises in part from the plantar tarsal fascia (Fig 8.1.3.1). The ligament extends down to posterior surface of the metatarsal, flanked by the 2nd and 4th metatarsal bones, deep to the deep flexor tendon. There is a considerable amount of muscle contained within the ligament - forming the third interosseous muscle. This muscle is believed to play an important role in storing elastic energy during locomotion, and dampening low frequency vibrations (Soffler and Hermanson, 2006). At the distal part of the metatarsus the ligament bifurcates and each branch attaches to a sesamoid bone at the back of the fetlock. From here, the ligament has several attachments: (a) two paired extensor processes pass medially and laterally around the digit and inset onto the tendon of the common digital extensor muscle, (b) a straight sesamoidian ligament, continues caudally inserting onto the 2nd phalanx, (c) the straight ligament is flanked by two oblique sesamoidean ligaments attach to the 1st phalanx. The primary function of the ligament is to support the fetlock joint (metatarso-phalangeal joint) and protect it from hyperextension during exercise (Soffler and Hermanson, 2006).

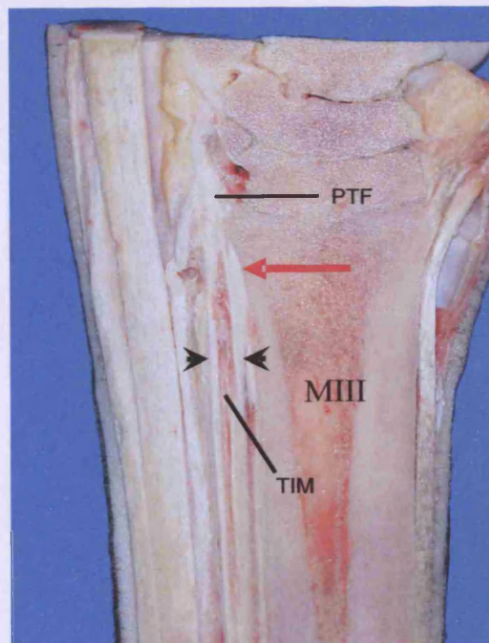


Figure 8.1.3.1: Sagittal section through the proximal attachment (red arrow) of the suspensory ligament (arrows) to the third metatarsal bone (MIII). Part of the ligament also arises from the plantar tarsal fascia

Pathology of the Origin of the Suspensory Ligament

The proximal attachment of the suspensory ligament is prone to pathology causing lameness in thoroughbred race horses. Pathologies associated with the entesis of the ligament are generally either associated with the bone, leading to enthesophytes, sclerosing and re-orientation of the trabeculae, and avulsion fractures; or soft tissue lesions at the entesis (Dyson, 1988). The majority of studies on the suspensory ligament use ultrasonography and radiology to assess pathological changes (Dyson, 1991), while few histological assessments have been made of normal or pathological enteses. Consequently, very little is known about the cause of pain and pathology in these regions. Current strategies for treatment of these pathologies are minimal but include, extracorporeal shock wave therapy (Crowe et al., 2002; McClure et al., 2004), and neuroectomy associated with fasciotomy (Bathe, 2001). Both treatments have been shown to have beneficial results.

8.2. MATERIALS AND METHODS

8.2.1. Source of Material

Five white male Wistar rats aged 4 months were obtained from accredited commercial suppliers for this study on the MCL and tibialis anterior. Equine material (1 normal foal, 1 normal adult, 1 pathological adult limb) was obtained by Andrew P. Bathe from Rosssdales Equine Hospital, Newmarket, UK.

8.2.2. Rat Dissection Procedure

Rats were killed with an overdose of carbon dioxide followed by cervical dislocation. The hind-limbs were skinned and amputated. The knee was disarticulated by cutting through the cruciate and collateral ligaments. The tibia and fibula were cut midway down the shank with bone cutters and the tibia bisected sagittally, leaving the origin of tibialis anterior attached to the lateral side of the head of the tibia. Finally, the distal attachment of the MCL was dissected – ensuring that the ligament remained attached to the medial side of the tibia. Tissues were kept moist at all stages during dissection with 0.1M PB.

8.2.3. Routine Histology

Routine histology was carried out as described in chapter 2.

8.2.4. Immunohistochemistry

Immunofluorescence and immunoperoxidase labelling was carried out as described in chapter 2 using the antibodies against, PGP 9.5, NF200, CGRP, SP, actin and vinculin (see Table 2.1).

8.3. RESULTS

8.3.1. Routine Histology

The Fibrous Insertion of the Medial Collateral Ligament

The MCL approached the bone at an acute angle and its attachment was spread over a wide area. The MCL was composed of regularly arranged collagen bundles interspersed with elongated cell nuclei (Fig 8.3.1.A). At the insertion, the 4 layers of the attachment can be seen (Fig 8.3.1.A). The most superficial layer (layer i) merged with the superficial fibrous layer of the periosteum at the distal end of the attachment. Deep to this, layer ii contained tightly packed parallel bundles of collagen fibres; the cells which reside in this layer resembled those of the ligament itself – containing flat elongated nuclei. It was possible to see the fibres from this layer insert into the underlying bone (Fig 8.3.1.B). The deepest layer (layer iii) of the attachment, lay just above the cortical bone and was composed of relatively loose, disorganised fibrous connective tissue containing rounded nuclei. This layer is continuous with the osteogenic layer of the periosteum proximal to the attachment and is thickest at the proximal part of the attachment site where the metaphyseal depression is located (Fig 8.3.1.A). Layers ii and iii are both highly cellular (Fig 8.3.1.A-C). The tibial bone forms the final layer of the attachment.

However, this 4 layered structure is difficult to identify, especially in fluorescence images. Therefore a simplified description will be used in this study. The ligament attachment will be described with 3 layers which can be easily distinguished from each other – (1) the ligament itself (identified by the elongate nuclei arranged in rows) (2) the attachment of the ligament to the periosteum (which can be distinguished by its highly cellular appearance) (3) the underlying cortical bone (Fig 8.3.1.C).

The ‘Muscular’ Attachment of Tibialis Anterior

The muscle fibres of tibialis anterior (TA) are anchored to the fibrous layer of the periosteum by loose connective tissue (Fig 8.3.2.A and B). The fibrous layer of the periosteum in turn attaches to the highly cellular, osteogenic layer, which subsequently attaches to the underlying cortical bone (Fig 8.3.2.A-D). The junction between the fibrous and osteogenic periosteum is relatively smooth while the border between the cortical bone and osteogenic periosteum is irregular. This irregular border is present throughout the periosteum (Fig 8.3.2.A-D). Blood vessels were present at the muscle attachment site,

either running at right angles to the bone or running along the surface of the periosteum (not shown).

Muscle fibres at the attachment arise from the bone at varying angles depending largely on their location. Where the muscle fibres arise from the shaft of the bone, the fibres leave at an acute angle (Fig 8.3.2.C), while those attached to the underside of the condyle arise at right angles (Fig 8.3.2.B). It was also noted that where the muscle fibres attach at right angles to the periosteum, the fibrous layer of the periosteum was thicker and a large amount of connective tissue anchoring the muscle to the periosteum appears to be present, in contrast to where the muscle fibres arise at a more acute angle (Fig 8.3.2.A-B). In addition, mast cells were present at the junction between the muscle and the periosteum (Fig 8.3.2.D). It is also clear from Fig 8.3.2.A. that the fibres of the fibrous and osteogenic periosteum appear to run in opposite directions. The fibres of the fibrous periosteum are coarser and run downwards at an oblique angle, whereas the fibres of the osteogenic periosteum are finer and pass obliquely upwards.

The Origin of the Suspensory Ligament of the Horse

Normal ligament: In the foal, the origin of the suspensory ligament was mixed with both fibrous and fibrocartilagenous attachments (Fig 8.3.3.A). The most proximal part of the attachment merged with the articular cartilage of the metatarsal bone (Fig 8.3.3.B). The distal part of the attachment is purely fibrous, attaching first to the thick periosteum (Fig 8.3.3.C). A small amount of fat was present in the insertional angle between the ligament and the bone (Fig 8.3.3.C) and muscle fibres were obviously present within the ligament at a distance from the enthesis (Fig 8.3.3.D).

In the adult, the enthesis of the ligament was primarily fibrocartilagenous. Its proximal attachment showed an obvious tidemark, and a layer of CFC. The amount of uncalcified fibrocartilage, was however minimal with only a small number of rounded chondrocytes on the ligament side of the tidemark (Fig 8.3.4.A). The attachment of the ligament was frequently invaded by blood vessels and adipocytes originating from the ligament proper (Fig 8.3.4.B). Small bony spur formations were also observed (Fig 8.3.4.C). The quantity of insertional angle fat was much larger than in the foal. Several slips from the distal part of the ligament were observed to pass through this fat, to attach onto the shaft of the bone. The attachment of these slips appeared to be bony rather than fibrocartilagenous (Fig

8.3.4.D). The wedge of adipose tissue at the insertional angle contained a large number of blood vessels and some nerve branches (Fig 8.3.4.E) along with a number of type II nerve endings (Pacinian corpuscles - between 400 and 800µm in size) within the adipose tissue. These encapsulated nerve endings were of characteristic appearance; an ovoid structure composed of a central nerve surrounded by a large number of connective tissue layers (Fig 8.3.4.F). In some sections, Pacinian corpuscles were observed at the insertional angle – i.e. between the ligament and the periosteum (Fig 8.3.4.G). Muscle fibres, as in the foal were present, within the ligament (Fig 8.3.4.H).

Pathological Ligament: There was a large amount of adipose tissue (Fig 8.3.5.A) within the ligament, just posterior to the enthesis. This adipose tissue contained a large number of blood vessels and nerve bundles (Fig 8.3.5.B). The pathological tissue appeared to originate from the posterior surface of the ligament, by following blood vessels. Small groups of inflammatory cells were also observed within the pathological adipose tissue located within the ligament (Fig 8.3.5.C). Due to difficulties with sectioning this material it was difficult to determine differences between the normal and pathological entheses, however a number of blood vessels invaded into the enthesis itself from the adipose tissue within the ligament (Fig 8.3.5.D).

8.3.2. Immunohistochemistry

Innervation of the Fibrous Insertion of the Medial Collateral Ligament

Immunohistochemical labelling with PGP 9.5, CGRP, SP, and NF200 illustrate that no nerve fibres were present within any layer of the fibrous attachment of the medial collateral ligament (Fig 8.3.6-8.A-D). In contrast to the aneural nature of the attachment of the MCL, nerve fibres immunoreactive to PGP 9.5 were identified in the loose connective tissue surrounding the ligament (epiligament). These nerve fibres were either 'free' or associated with small blood vessels. Proximal to the ligament attachment, nerve fibres were present in the connective tissue between the deep surface of the MCL and the underlying periosteum – i.e. in the insertional angle (Fig 8.3.6.F). Nerve fibres were also present in the periosteum adjacent to the attachment site (Fig 8.3.6.E). Nerve fibres immunoreactive to NF200 were present primarily in the connective tissue, on both surfaces of the ligament (Fig 8.3.7.E). The periosteum adjacent to the attachment was also innervated with NF200 immunoreactive nerve fibres (not shown).

Substance P and CGRP labelling demonstrated a similar pattern of nerve fibre distribution. Blood vessel associated fibres immunoreactive to SP and CGRP were present in the connective tissue between the MCL and the periosteum (Fig 8.3.8.E-G). In addition, nerve fibres were present in the periosteum adjacent to the ligament (not shown). Although the pattern of SP and CGRP nerve fibres were similar, there appeared to be a predominance of CGRP fibres in comparison to SP fibres.

Structure and Innervation of the ‘Muscular’ Attachment of Tibialis Anterior

Many nerve fibres immunoreactive to PGP 9.5 were present within the muscle body of tibialis anterior and the periosteum (Fig 8.3.10.A and B). Some of these nerve fibres were associated with blood vessels (Fig 8.3.10.A). A number had a characteristic coiling pattern (Fig 8.3.10.C) and others resembled motor-end plates (Fig 8.3.10.D). Of particular interest was the occurrence of nerve fibres at the musculature entesis – they were frequently present within the connective tissue which attaches the muscle fibres to the periosteum (Fig 8.3.10.E-F). In the majority of specimens, spindle-like structures were present close to the point where the muscle attaches to the periosteum (Fig 8.3.10.G-H).

Neurofilament 200 immunoreactive nerve fibres were also distributed at and around the muscular entesis. As seen in PGP labelling, bundles of nerve fibres ran along the surface of the periosteum and between the fascicles in the muscle body. A large number of these were blood vessel associated (not shown). Once again, spindle like structures were present close to and at the muscle attachment site (Fig 8.3.11.A-E). In addition, there were many NF200-immunoreactive nerve fibres in both layers of the periosteum (Fig 8.3.11.F).

Substance P and CGRP immunoreactive nerve fibres were a feature of both the fibrous and osteogenic layers of the periosteum of the muscular entesis (Fig 8.3.12.A, B and E). However, neither fibre was observed on the muscle side of the attachment unless they were in association with blood vessels (Fig 8.3.12.C, D and F). Furthermore, where tibialis anterior attaches to its overlying fascia, blood-vessel associated and free CGRP and SP immunoreactive nerve fibres were present (not shown). No coiled nerve fibres were seen in sections labelled with CGRP or SP.

At the muscular entesis, vinculin was observed in the muscle at its most distal point (Fig 8.3.13.A). The labelling pattern showed that the distal part of the muscle fibre was highly

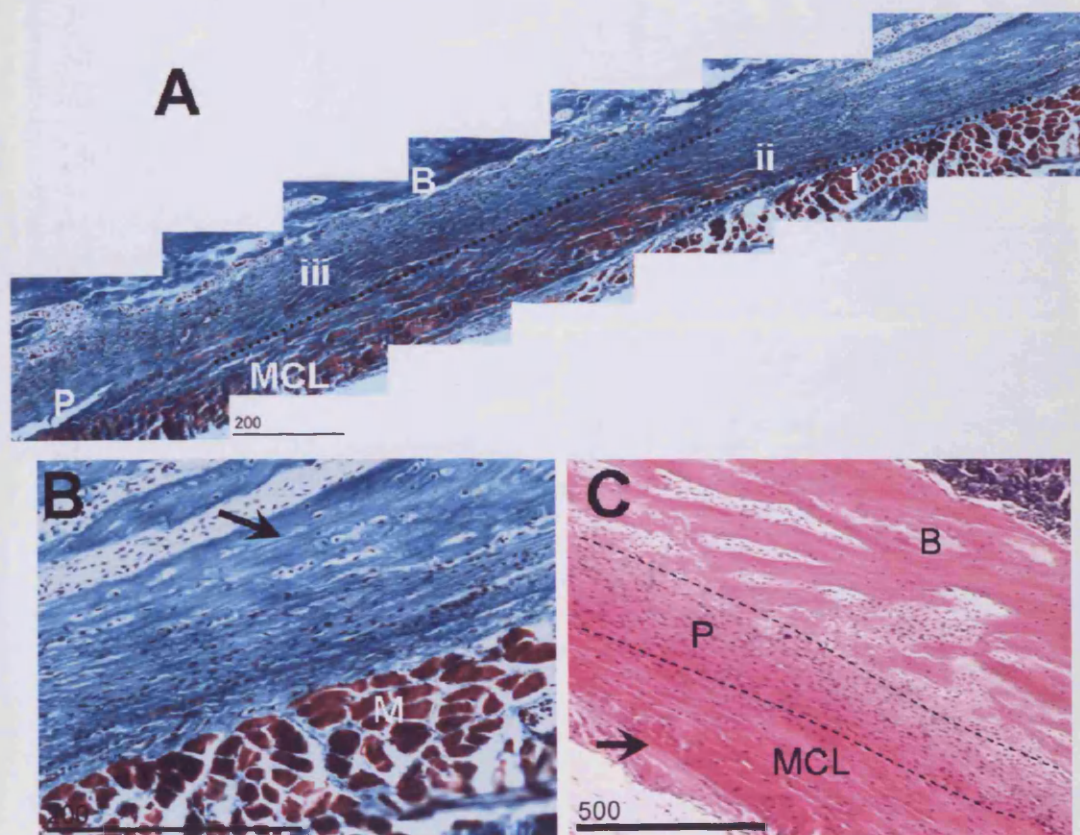
invaginated and these invaginations labelled strongly for vinculin (Fig 8.3.13.B). Actin labelling was present throughout the muscle fibres (Fig 8.3.13.C). At the distal part of the muscle fibre, the invaginations could be seen again as terminations of the actin filaments (Fig 8.3.13.D). Figures 8.3.13 E, F and G (PB, rabbit IgGs and mouse IgGs respectively) illustrated that labelling could not be dismissed as non-specific.

Innervation of the Origin of the Suspensory Ligament in the Horse

Normal ligament: There were no PGP 9.5 immunoreactive nerve fibres present within the cartilaginous attachment of the ligament in the foal (Fig 8.3.14.A). Neither were any fibres present at the fibrous attachment of the ligament to the thick outer layer of the periosteum (Fig 8.3.14.B). However, a number of nerve fibres were observed between the inner and outer layers of the periosteum (Fig 8.3.14.B) and isolated nerve bundles and blood-vessel associated nerve fibres were present in the endoligament. Nerve fibres were also seen in the insertional angle fat (i.e. the fat located between the ligament entheses and bone). These fibres were either 'free' or blood-vessel associated (Fig 8.3.14.C and D). Within the insertional angle fat, specialised nerve endings, resembling Meissner's corpuscles, were identified (Fig 8.3.14.E). The labelling pattern was similar in the adult. The insertional angle fat – was highly innervated with a large number of nerve bundles and blood-vessel associated nerve fibres (Fig 8.3.15.A and B). Some of these nerve bundles were located very close to the insertional angle (Fig 8.3.15.A). The fibrocartilaginous entheses of the ligament was largely aneural, although small nerve fibres were present within regions where blood vessels and adipocytes invaded into the entheses fibrocartilage (Fig 8.3.15.C and D). In addition, a large number of nerve fibres were identified in the inner layer of the periosteum covering the metatarsus (Fig 8.3.15.E).

Pathological Ligament: A large number of nerve bundles and endings (Fig 8.3.17.A and B) were observed within the 'pathological' adipose tissue present within the suspensory ligament, a large number of which were associated with blood vessels. Negative control sections (PB and rabbit IgGs) illustrate that labelling was not non-specific (Figs 8.3.18.A-C).

Figure 8.3.1



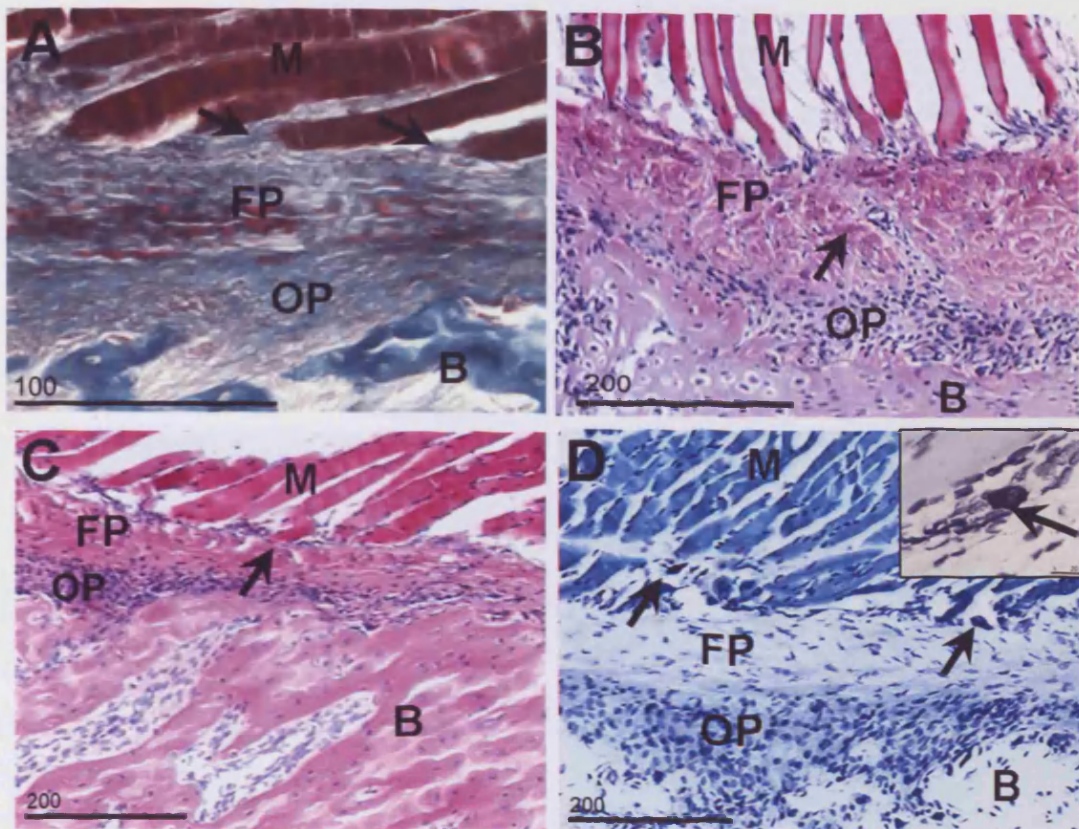
THE FIBROUS ENTESIS OF THE MEDIAL COLLATERAL LIGAMENT ONTO THE SHAFT OF THE TIBIA - ROUTINE HISTOLOGICAL SECTIONS. 12 week rat.

Figure A: A composite image of the fibrous enthesis of the medial collateral ligament (MCL) onto the shaft of the tibia. The three layers of the insertion can be seen (separated by dotted lines). The superficial layer (i) merges with the fibrous layer of the periosteum distal to the attachment site. Layer ii is a dense fibrous layer where the fibres of the ligament insert into the underlying periosteum (P) and bone (B) and the deepest layer (iii) is composed of poorly organised loose fibrous tissue which is continuous with the osteogenic layer of the periosteum. Masson's Trichrome. Scale bar = 200µm.

Figure B: High power image of the medial collateral ligament inserting into the tibia. Arrow indicates the presence of Sharpey's fibres penetrating into the underlying bone. Masson's trichrome. M – muscle. Scale bar = 200µm.

Figure C: The fibrous enthesis of the MCL to the tibia. The 3 simplified layers of the enthesis can clearly be seen. The MCL approaches the bone at an acute angle, inserting into the highly cellular periosteum (P) and the underlying bone (B). These 3 simplified layers will be used to describe the MCL attachment in the forthcoming fluorescence images. Haematoxylin & Eosin. Scale bar = 500µm.

Figure 8.3.2



THE MUSCULAR ENTESIS OF TIBIALIS ANTERIOR ONTO THE TIBIA - ROUTINE HISTOLOGICAL SECTIONS. 12 week rat

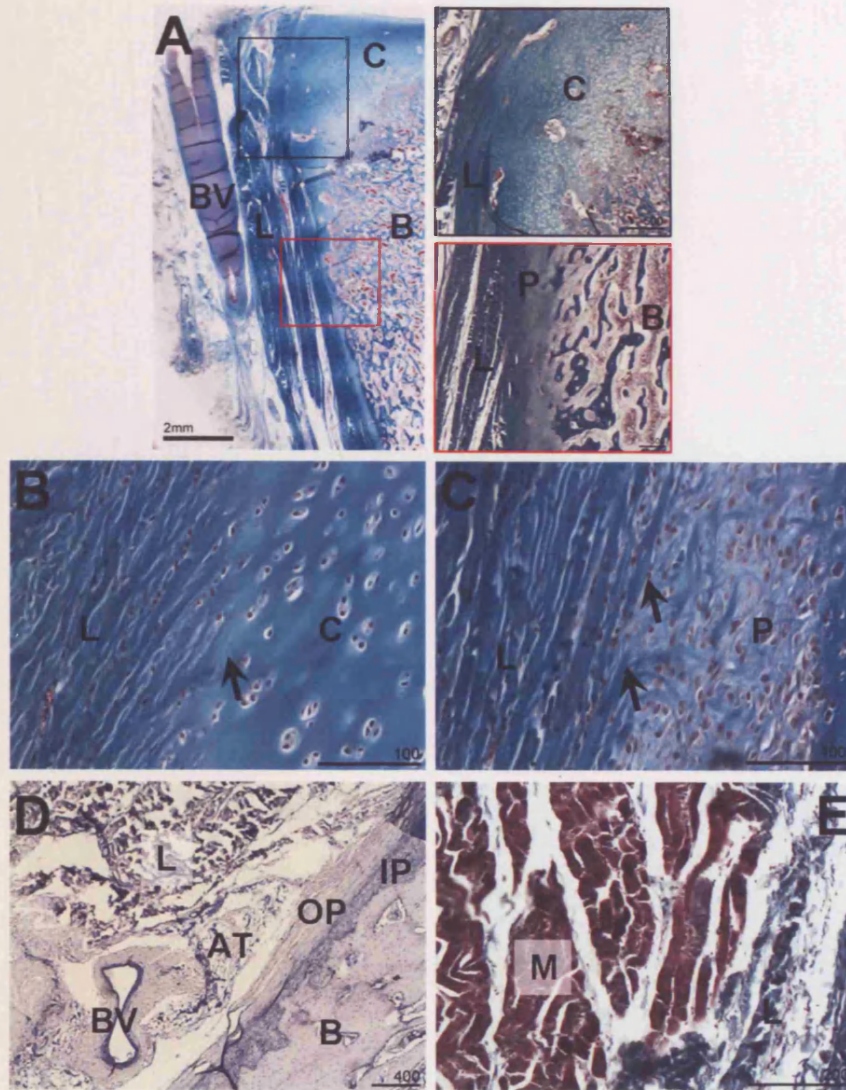
Figure A: The muscular entesis of tibialis anterior (M) in a Masson's trichrome stained section. Arrows indicate the connective tissue attaching the muscle fibres to the fibrous layer of the periosteum (FP). The fibrous layer of the periosteum is in turn attached to the osteogenic periosteum (OP) which subsequently attaches to the underlying bone (B). Scale bar = 100µm.

Figure B: The muscular attachment of tibialis anterior to the underside of the lateral condyle of the tibia. The muscle fibres (M) arise at right angles from the bone, and attach by a large amount of connective tissue. Note the thickness of the fibrous periosteum (FP) in this region. OP-osteogenic periosteum. B-Bone. Haematoxylin & Eosin. Scale bar = 200µm.

Figure C: The muscular attachment of tibialis anterior to the shaft of the tibia. The muscle fibres (M) arise at an acute angle from the bone. There appears to be a minimal amount of connective tissue attaching the muscle to the tibia (arrow). Note that the fibrous periosteum (FP) is substantially thinner than in figure B. OP-osteogenic periosteum. B-Bone. Haematoxylin & Eosin. Scale bar = 200µm

Figure D: The muscular attachment of tibialis anterior in a toluidine blue stained section. Note the presence of mast cells close to the attachment of the muscle to the periosteum (arrows). B-bone, M-muscle, FP-fibrous periosteum. OP-osteogenic periosteum. Scale Bar = 200µm. **Inset:** A high power view of a mast cell at the muscle-entesis junction. Toluidine blue. Scale bar =20µm.

Figure 8.3.3



ORIGIN OF THE SUSPENSORY LIGAMENT FROM THE 3RD METATARSAL BONE - ROUTINE HISTOLOGICAL SECTIONS. Foal.

Figure A: Low power view of the attachment of the suspensory ligament (L) to the 3rd metatarsal. The black highlighted region illustrates the attachment of the ligament to cartilage (C) of the metatarsus. Red highlighted region illustrates the attachment of the ligament to the periosteum (P). B-bone, BV-blood vessel. Scale bar = 2mm

Figure B: High power view of the attachment of the ligament (L) to cartilage (C) of the metatarsus. Note that the fibres of the ligament merge imperceptibly into the cartilage (arrow). Masson's Trichrome. Scale bar = 100µm.

Figure C: High power view of the attachment of the ligament (L) to the outer layer of the periosteum (P). Arrows indicate relatively thick fibres from the ligament penetrating into the periosteum. Masson's Trichrome. Scale bar = 100µm

Figure D: Adipose tissue (AT) in the insertional angle between the ligament (L) and bone (B). OP-outer periosteum, IP-inner periosteum, BV-blood vessel. Toluidine blue. Scale bar =400µm.

Figure E: The 3rd interosseus muscle (M) located within the suspensory ligament (L). Masson's Trichrome. Scale bar = 200µm.

**THE ORIGIN OF THE SUSPENSORY LIGAMENT FROM THE 3RD METATARSAL BONE -
ROUTINE HISTOLOGICAL SECTIONS. Adult Horse.**

Figure A: The proximal, fibrocartilagenous attachment of the ligament (L) to bone (B) of the metatarsus. Note that the region of uncalcified fibrocartilage (UCFC) is small (dashed line) but the calcified fibrocartilage (CFC) is prominent. Tidemark. Toluidine blue. Scale bar = 300µm.

Figure B: The fibrocartilagenous attachment of the ligament (L) to bone (B) of the metatarsus. Arrow indicates a blood vessel accompanied by a number of adipocytes invading from the ligament proper into the fibrocartilage of the ligament attachment. Toluidine blue. Scale bar = 500µm.

Figure C: A region of the fibrocartilagenous attachment of the suspensory ligament (L). Arrow indicates bony spur formation at the entesis. B-bone. Toluidine blue. Scale bar = 200µm.

Figure D: A small slip of ligament (L) attaching directly (arrow) to the shaft of the metatarsal bone (B) without the presence of fibrocartilage (inset – dashed line). Masson's trichrome. Scale bar = 300µm. Inset – Toluidine blue. Scale bar = 200µm.

Figure E: Insertional angle fat (IAF) at the attachment of the suspensory ligament (L). The adipose tissue at the insertional angle contained large nerve bundles (arrow). LS-ligament slip. Masson's trichrome. Scale bar = 300µm

Figure F: A Pacinian corpuscle (arrow) in the insertional angle fat (IAF) at the attachment of the suspensory ligament. Note the concentric arrangement of the collagen around the central nerve fibre (N) within the corpuscle. Masson's trichrome. Scale bar = 200µm.

Figure G: A collection of Pacinian corpuscles (arrows) in the fat at the insertional angle (IAF) close to the attachment of the ligament (L). P-periosteum. Masson's trichrome. Scale bar = 300µm.

Figure H: Muscle fibres (M) of the 3rd interosseous muscle within the suspensory ligament. Masson's trichrome. Scale bar = 200µm.

Figure 8.3.4

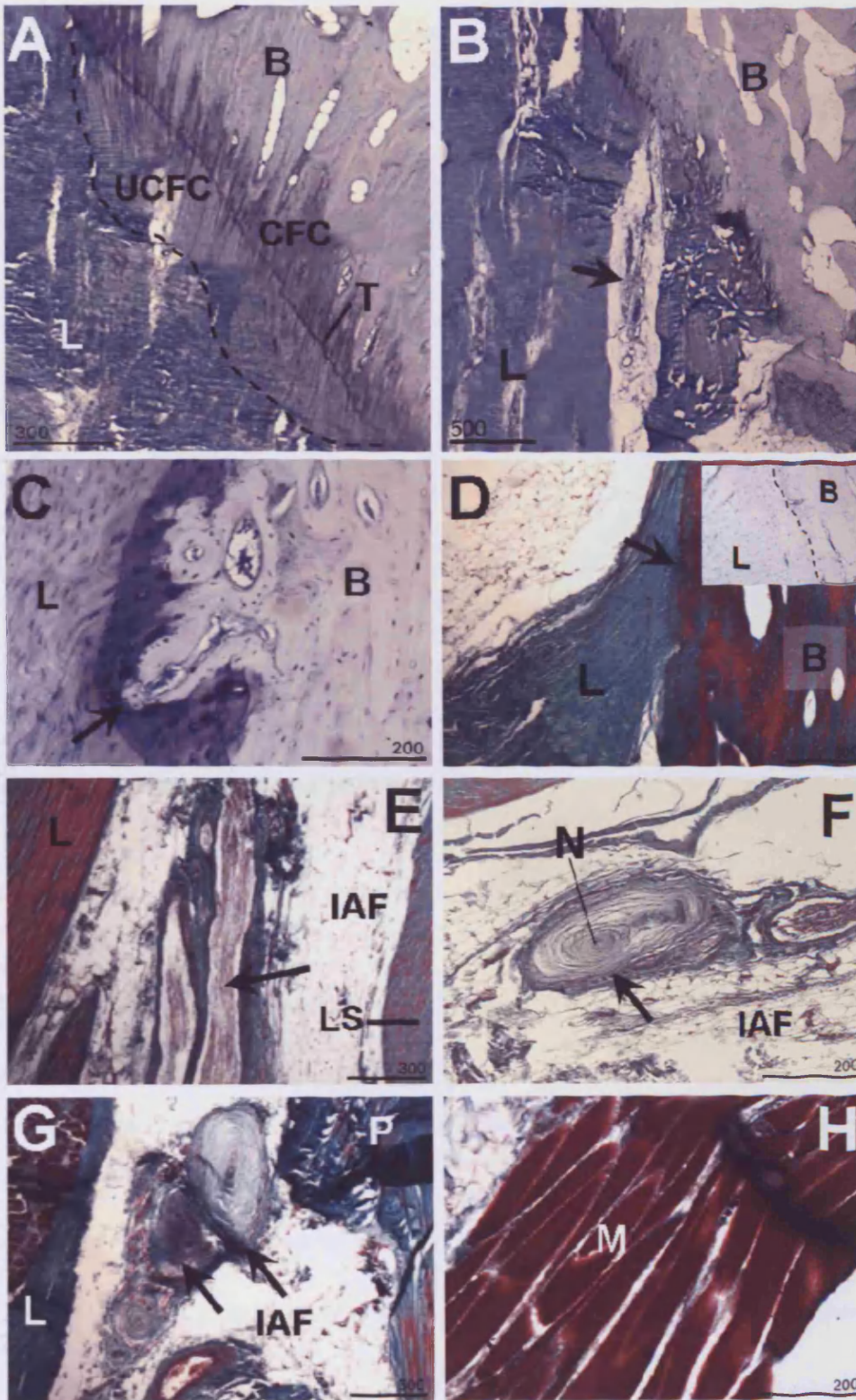
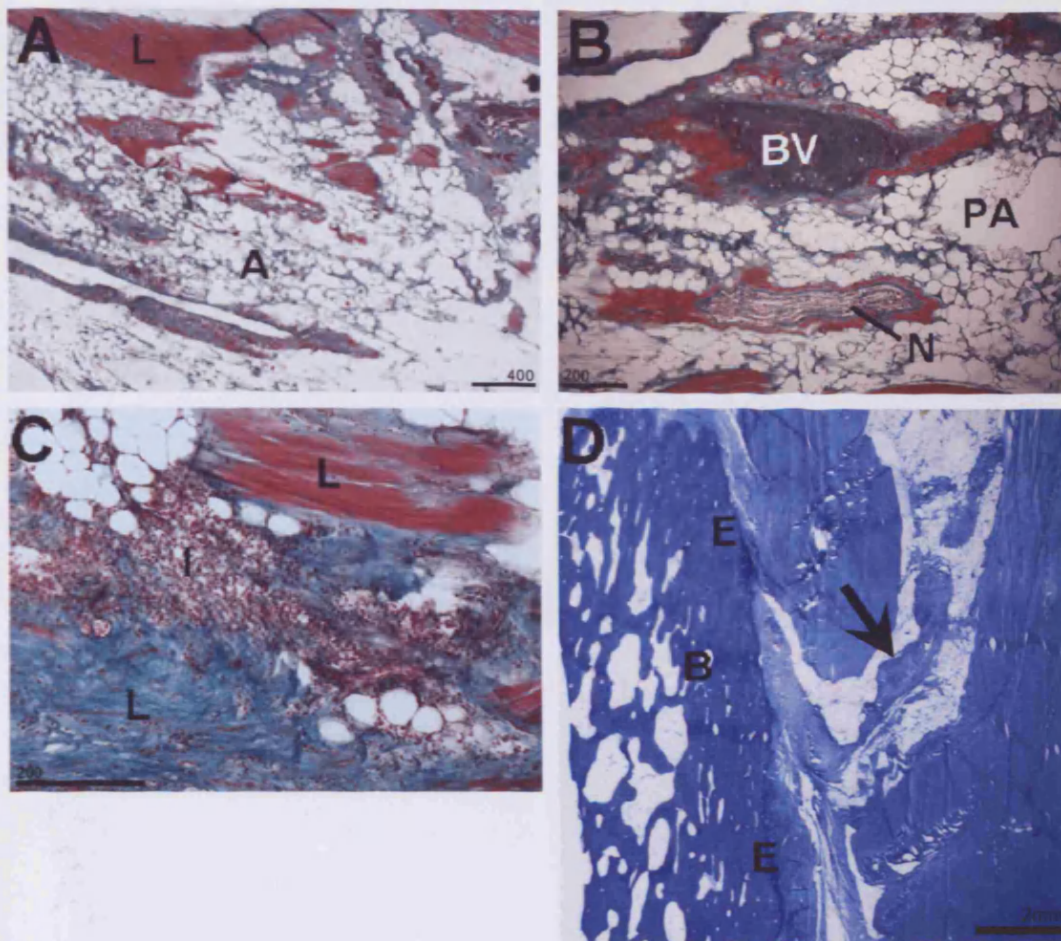


Figure 8.3.5



THE ORIGIN OF THE SUSPENSORY LIGAMENT FROM THE 3RD METATARSAL BONE -
ROUTINE HISTOLOGICAL SECTIONS. Pathological Specimens.

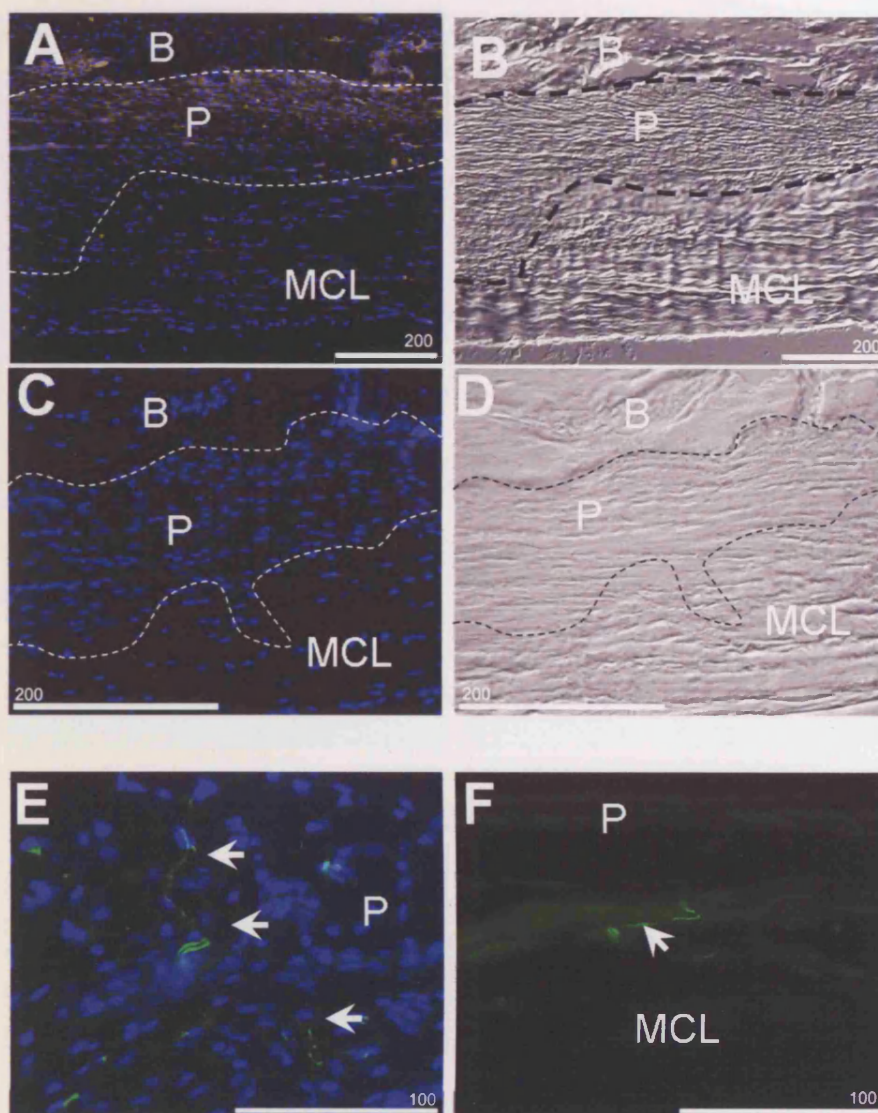
Figure A: A large wedge of adipose tissue (A) located within the suspensory ligament (L) of the pathological specimen with suspected enthesopathy. Scale bar = 400µm.

Figure B: A large blood vessel (BV) and accompanying nerve (N) bundle within the pathological adipose tissue within the suspensory ligament of a pathological equine specimen with suspected enthesopathy. Masson's Trichrome. Scale bar = 200µm.

Figure C: An inflammatory cell population (I) located within the suspensory ligament (L) of an equine specimen with suspected enthesopathy. Masson's Trichrome. Scale bar = 200µm.

Figure D: A region of fibrous and adipose tissue (arrow) invading into the enthesis (E) of the origin of the suspensory ligament in an equine specimen with suspected enthesopathy. Toluidine blue. Scale bar = 2mm.

Figure 8.3.6



**FIBROUS INSERTION OF THE MEDIAL COLLATERAL LIGAMENT (MCL) INTO THE TIBIA
LABELLED WITH PRTIEN GENE PRODUCT 9.5 (PGP 9.5)**

(counterstained with DAPI to illustrate cell nuclei)

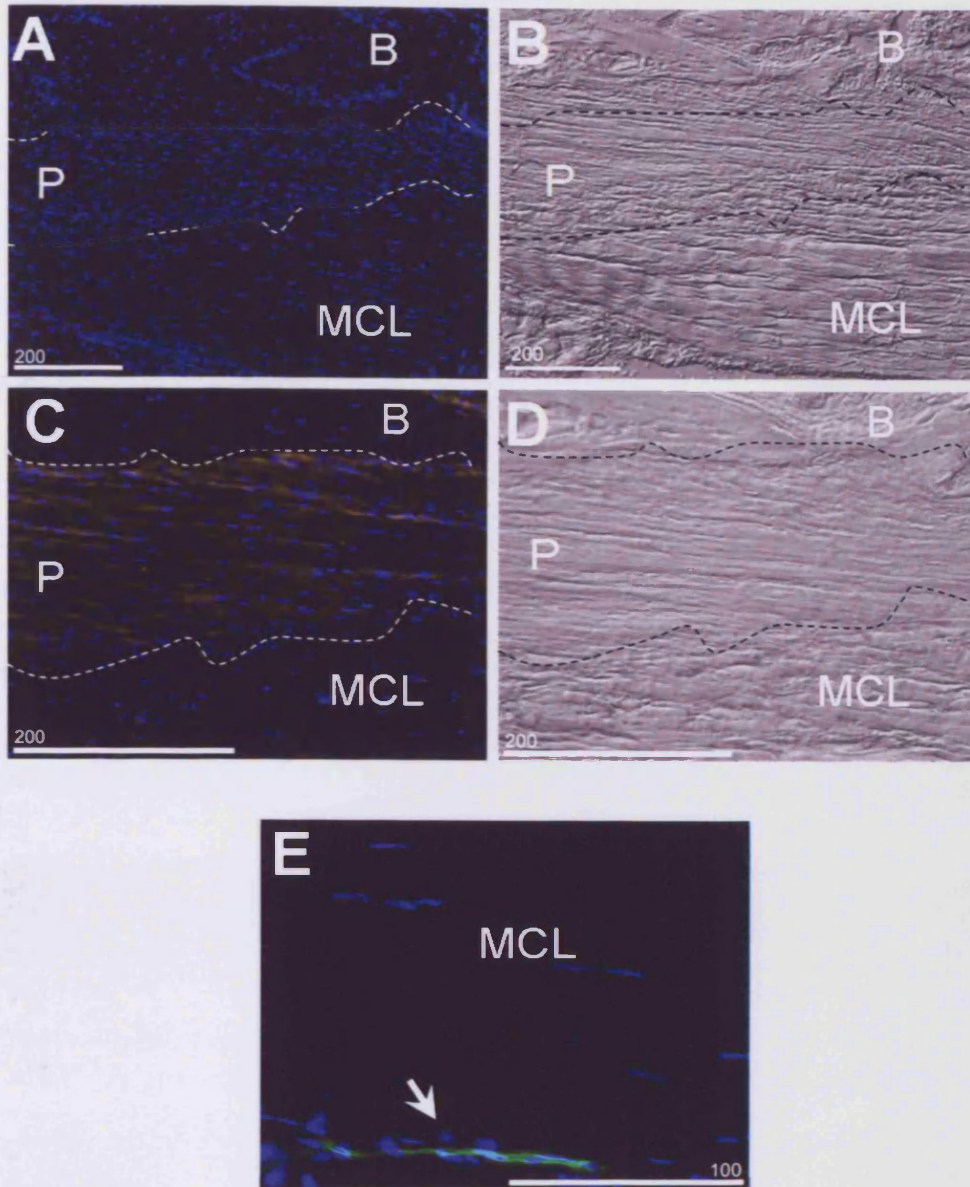
Dashed lines demonstrate the boundaries of the fibrous insertion. B–bone, P–periosteum. 12 week rat.

Figure A and B: Low power fluorescence image (A) and corresponding differential interference contrast image (B) demonstrates that all layers of the fibrous insertion are devoid of nerve fibres. Scale bar = 200μm.

Figure C and D: High power fluorescence image (C) and corresponding differential interference contrast image (D) demonstrating that no nerve fibres are present at the fibrous insertion of the MCL. Scale bar = 200μm.

Figure E and F: Nerve fibres immunoreactive to PGP 9.5 were however present within the periosteum (P) (E) and between the periosteum and the deep surface of the medial collateral ligament (MCL) (F); proximal to the fibrous insertion. Scale bar = 100μm.

Figure 8.3.7



FIBROUS INSERTION OF THE MEDIAL COLLATERAL LIGAMENT (MCL) INTO THE TIBIA LABELLED WITH NEUROFILAMENT 200 (NF200) (Counterstained with DAPI to illustrate cell nuclei)

Dashed lines demonstrate the boundaries of the fibrous insertion. B–bone, P–periosteum. 12 week rat.

Figure A and B: Low power fluorescence image (A) and corresponding differential interference contrast image (B) demonstrates that all regions of the fibrous insertion are devoid of nerve fibres. Scale bar = 200µm.

Figure C and D: High power fluorescence image (C) and corresponding differential interference contrast image (D) demonstrating that no nerve fibres are present at the fibrous insertion of the MCL. Scale bar = 200µm.

Figure E: Nerve fibre immunoreactive to NF200 were however present in the connective tissue (epi-ligament of the medial collateral ligament (MCL)). Scale bar = 100µm

FIBROUS INSERTION OF THE MEDIAL COLLATERAL LIGAMENT (MCL) INTO THE TIBIA LABELLED WITH ANTIBODIES AGAINST EITHER CALCITONIN GENE RELATED PEPTIDE (CGRP) OR SUBSTANCE P (SP)

(Counterstained with DAPI to illustrate cell nuclei)

Dashed lines demonstrate the boundaries of the fibrous insertion. B–bone, P–periosteum. 12 week rat.

Figure A and B: Low power fluorescence image (A) and corresponding differential interference contrast image (B) demonstrating that all regions of the fibrous insertion are devoid of CGRP immunoreactive nerve fibres. Scale bar = 200µm.

Figure C and D: High power fluorescence image (C) and corresponding differential interference contrast image (D) demonstrating that no nerve fibres immunoreactive to CGRP are present at the fibrous insertion of the MCL. Scale bar = 200µm.

Figure E: A free nerve fibre immunoreactive to CGRP (arrow) in the epiligament between the medial collateral ligament (MCL) and the periosteum (P) proximal to the fibrous insertion. Note the elongate nuclei of the MCL. Scale bar = 100µm.

Figure F: Differential interference contrast image of Figure E. Arrow indicates the location of the nerve fibre in E in the epiligament. Note the wavy nature of the fibres in the medial collateral ligament (MCL) and the cellular nature of the periosteum (P). Scale bar = 100µm.

Figure G: A blood vessel associated nerve fibre immunoreactive to substance P (SP) (arrow) in the epiligament surrounding the medial collateral ligament. Scale bar = 100µm

Figure 8.3.8

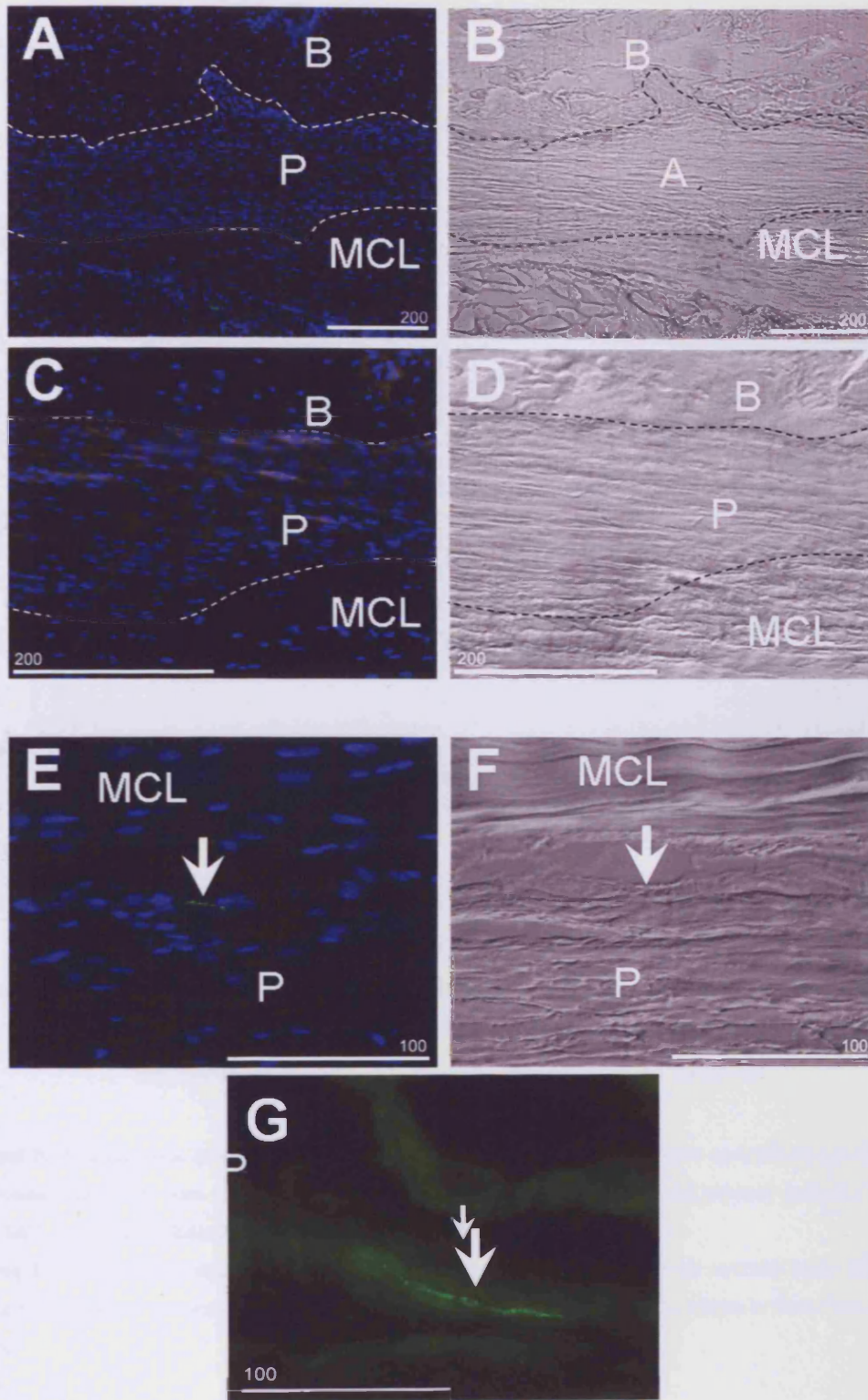
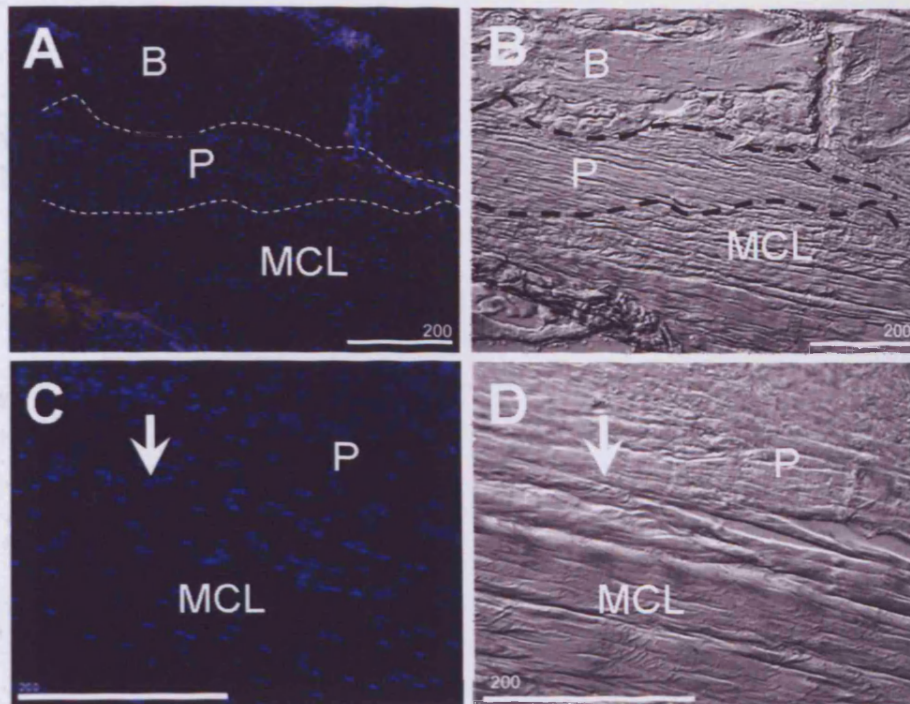


Figure 8.3.9



**FIBROUS INSERTION OF THE MEDIAL COLLATERAL LIGAMENT (MCL) INTO THE TIBIA –
NEGATIVE CONTROL SECTIONS.**

Phosphate buffer (PB) or rabbit immunoglobulins were applied to the sections instead of the primary antibody. (Counterstained with DAPI to illustrate cell nuclei). Dashed lines indicate the boundaries of the fibrous insertion. B- bone, P- periosteum. 12 week rat.

Figure A and B: Fluorescence image (A) and corresponding differential interference contrast image (B) demonstrates that the secondary antibody does not bind to the tissue without the presence of the primary antibody. B – bone, P – periosteum, MCL – medial collateral ligament. Scale bar = 200µm.

Figure C and D: Fluorescence image (C) and corresponding differential interference contrast image (D) demonstrates that non-specific binding is not occurring. Arrow indicates the point where the MCL comes to insert into the bone. Scale bar = 200µm.

THE MUSCULAR ORIGIN OF TIBIALIS ANTERIOR FROM THE TIBIA.

**Immunofluorescence or immunoperoxidase sections labelled with Protein Gene Product 9.5 (PGP 9.5).
12 week rat.**

Figure A: Blood vessel and associated nerve fibres (arrows) passing through the muscle (M) and along the surface of the periosteum (P). Blue-cell nuclei. Scale bar = 300µm.

Figure B: PGP 9.5 immunoreactive nerve fibres (arrows) within the periosteum (P) where the muscle (M) is anchored. Blue-cell nuclei. Scale bar = 200µm.

Figure C: A spindle-like structure (arrow) within the muscle (M) body of tibialis anterior. Blue-cell nuclei. Scale bar = 100µm.

Figure D: A motor endplate (arrows) present in the muscle (M) body of tibialis anterior. Scale bar = 100µm.

Figure E and F: Fluorescence image (E) and corresponding differential interference contrast image (F) demonstrates a small nerve fibre in the connective tissue attaching the muscle (M) to the periosteum (P). Blue-cell nuclei. Scale bar = 100µm.

Figure G and H: Low power view (G) of the muscular enthesis and high power view (H) of the highlighted area. A spindle-like structure was present at the muscle (M) - periosteum (P) interface. Scale bar = 100µm.

Figure 8.3.10

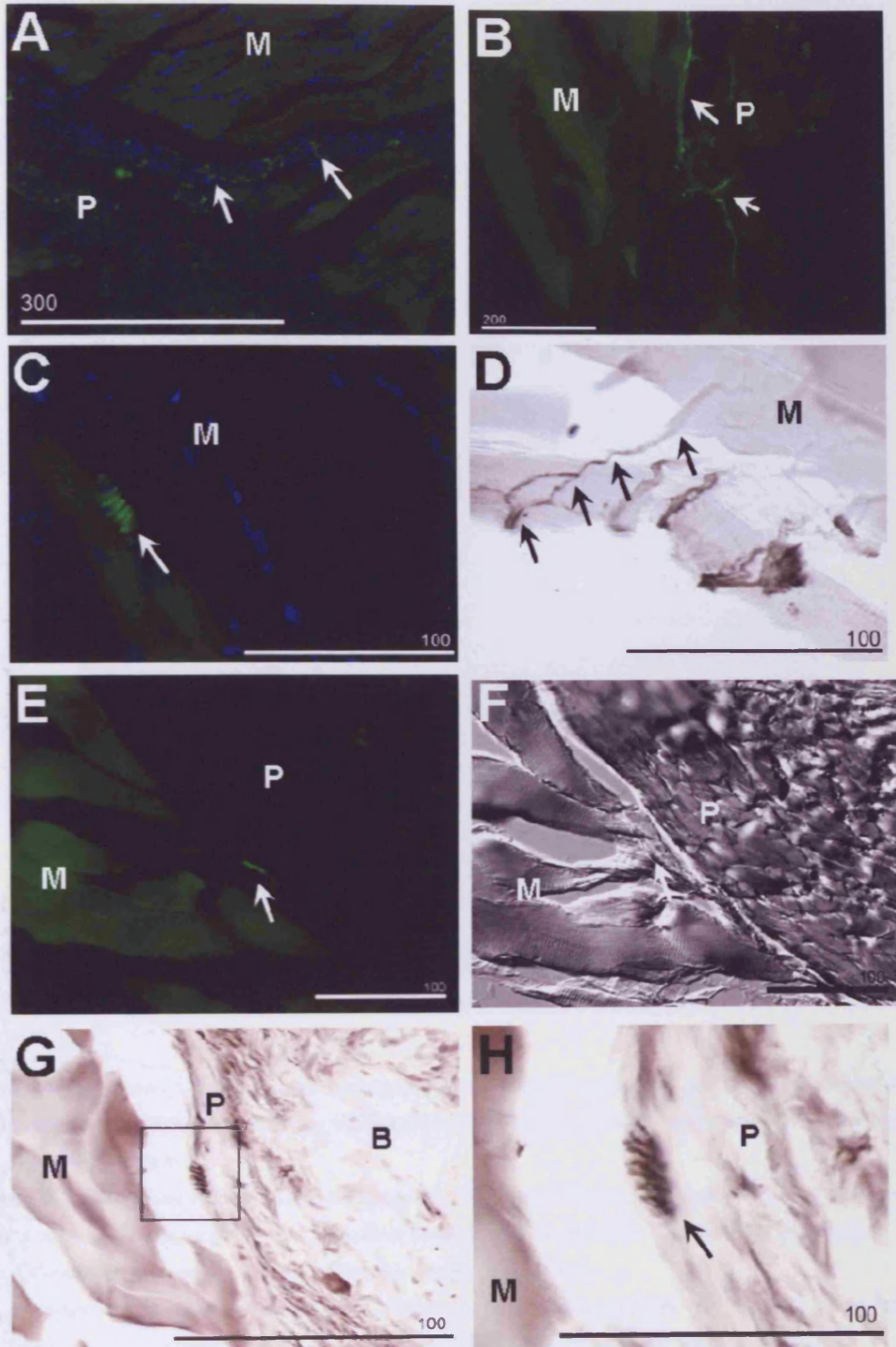
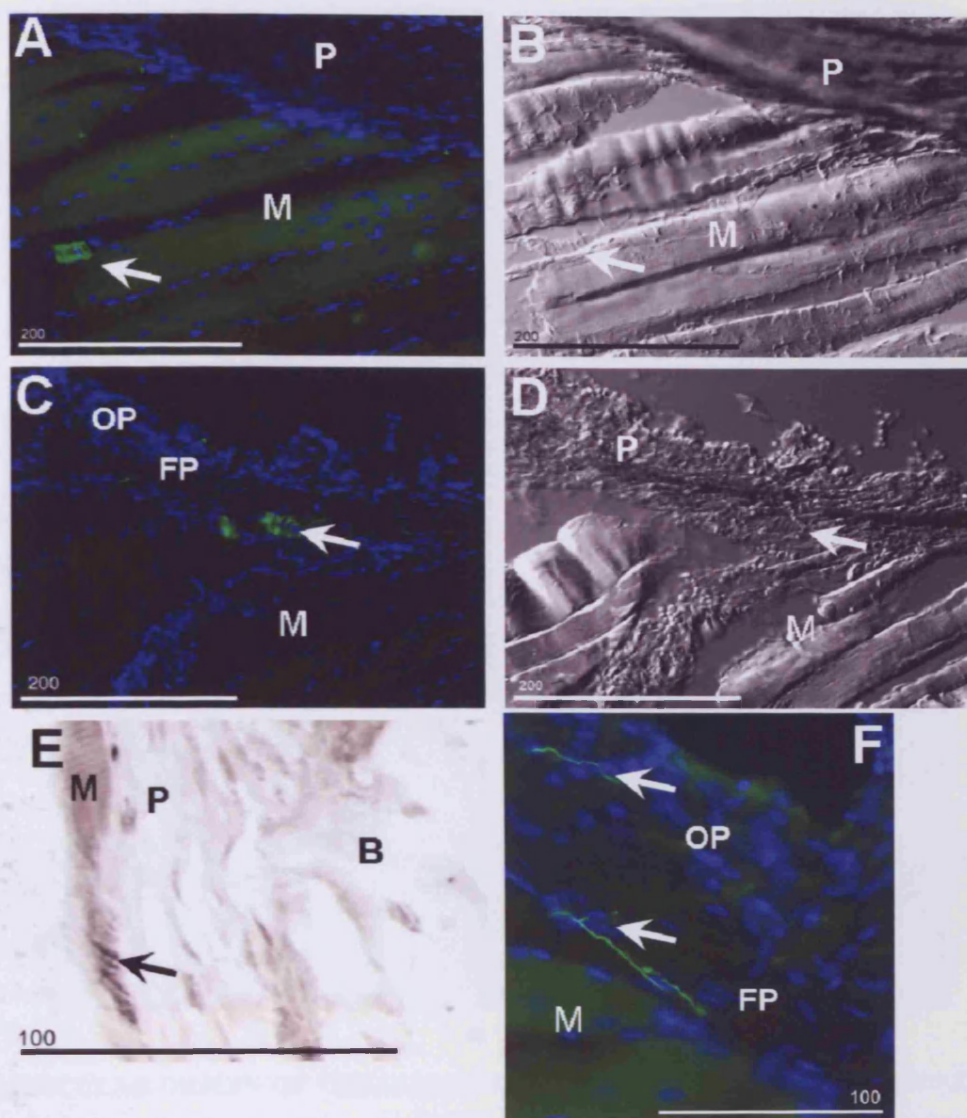


Figure 8.3.11



THE MUSCULAR ORIGIN OF TIBIALIS ANTERIOR FROM THE TIBIA - LABELLED WITH NEUROFILAMENT 200 (NF200). 12 week rat.

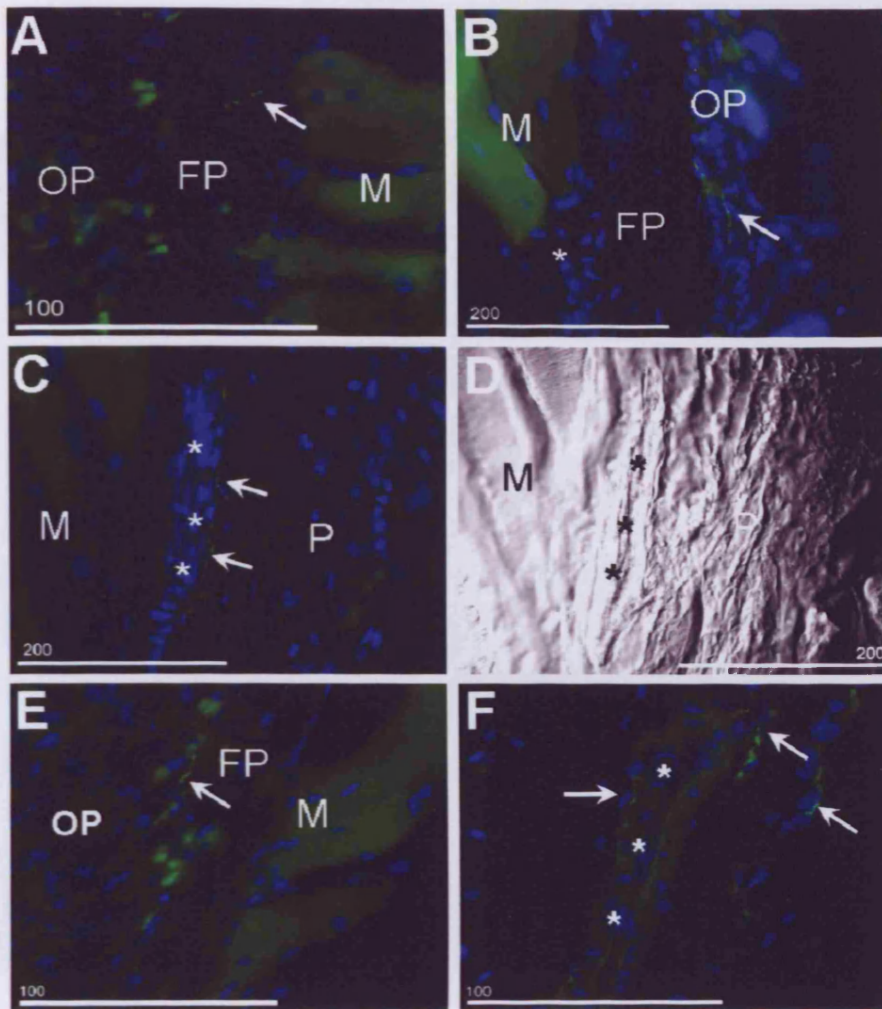
Figure A and B: Fluorescence image (A) and corresponding differential interference contrast image (B) demonstrates the presence of a spindle-like structure (arrow) in tibialis anterior close to its attachment. M-muscle, P-periosteum. Blue - cell nuclei. Scale bar = 200µm.

Figure C and D: Fluorescence image (C) and corresponding differential interference contrast image (D) demonstrates the presence of a spindle-like structure in the connective tissue at the muscle (M) - periosteum (P) interface. FP-fibrous periosteum, OP-osteogenic periosteum. Blue-cell nuclei. Scale bar = 200µm.

Figure E: Spindle-like structure (arrow) in an immunoperoxidase labelled section. Note the spindle is located in the connective tissue attaching the muscle (M) to the underlying periosteum (P). B-bone. Scale bar = 100µm.

Figure F: Nerve fibres (arrows) immunoreactive to neurofilament 200 in the fibrous (FP) and the osteogenic (OP) of the periosteum where tibialis anterior attaches. Scale bar = 100µm.

Figure 8.3.12



THE MUSCULAR ORIGIN OF TIBIALIS ANTERIOR FROM THE TIBIA LABELLED WITH SUBSTANCE P (SP) OR CALCITONIN GENE RELATED PEPTIDE (CGRP) (Counterstained with DAPI to illustrate cell nuclei). 12 week rat.

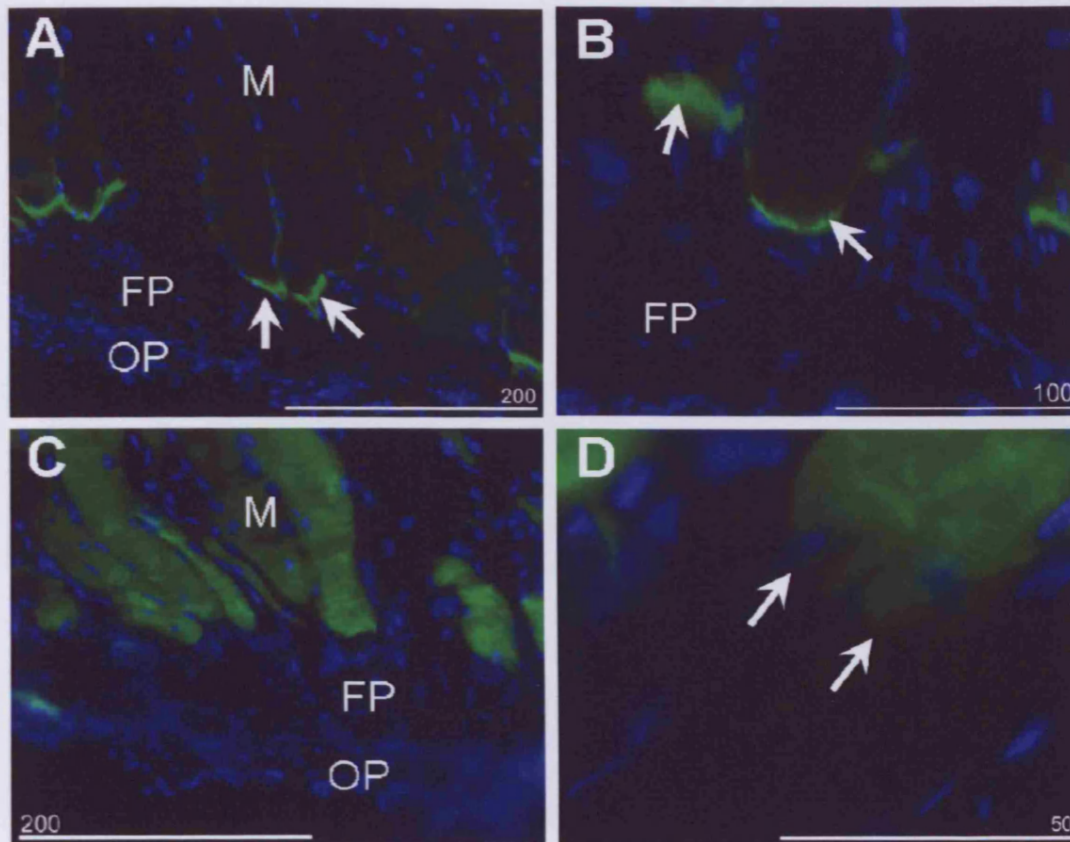
Figure A and B: Small nerve fibres (arrows) immunoreactive to substance P in the fibrous (FP-A) and osteogenic layer of the periosteum (OP-B) where tibialis anterior attaches. M-muscle.

Figure C and D: Fluorescence image (C) and corresponding differential interference contrast image (D) of a small blood vessel (***) associated nerve fibre, immunoreactive to substance P, in the connective tissue attaching the muscle (M) to the periosteum (P). Scale bar = 200µm.

Figure E: A small nerve fibre (arrow) immunoreactive to CGRP between the fibrous (FP) and osteogenic layer of the periosteum (OP) where tibialis anterior (M) attaches. Scale bar = 100µm.

Figure F: A number of blood vessel (***) associated nerve fibres (arrows), immunoreactive to CGRP, at the attachment of tibialis anterior to the periosteum. Scale bar = 100µm.

Figure 8.3.13



THE MUSCULAR ORIGIN OF TIBIALIS ANTERIOR FROM THE TIBIA. SECTIONS WERE LABELLED WITH VINCULIN OR ACTIN (Counterstained with DAPI to illustrate cell nuclei). 12 week rat.

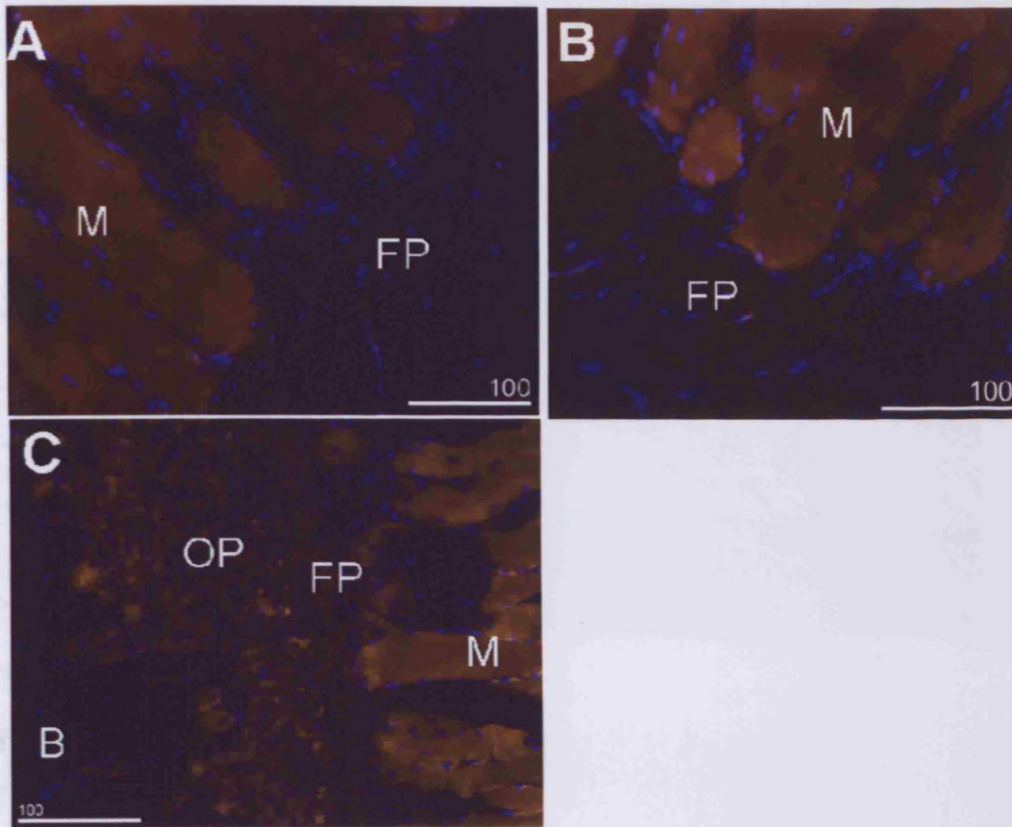
Figure A: Low power view of the muscular enthesis of tibialis anterior labelled with vinculin. Note the localisation of vinculin (arrows) in the tip of the muscle (M) fibres closest to the attachment to the fibrous periosteum (FP). OP-osetogenic periosteum. Scale bar = 200µm.

Figure B: High power view of the muscular enthesis of tibialis anterior labelled with vinculin. Arrows indicate the invaginations in the tip of the muscle fibres labelled positively for vinculin. FP-fibrous periosteum. Scale bar = 100µm.

Figure C: Low power view of the muscular enthesis of tibialis anterior labelled with actin. The muscle (M) fibres labelled positively for actin. FP-Fibrous periosteum. OP-osetogenic periosteum. Scale bar = 200µm.

Figure D: High power view of the muscular enthesis of tibialis anterior labelled with actin. Arrows indicate the termination of actin filaments as finger-like processes in the tip of the muscle fibre. Scale bar = 100µm.

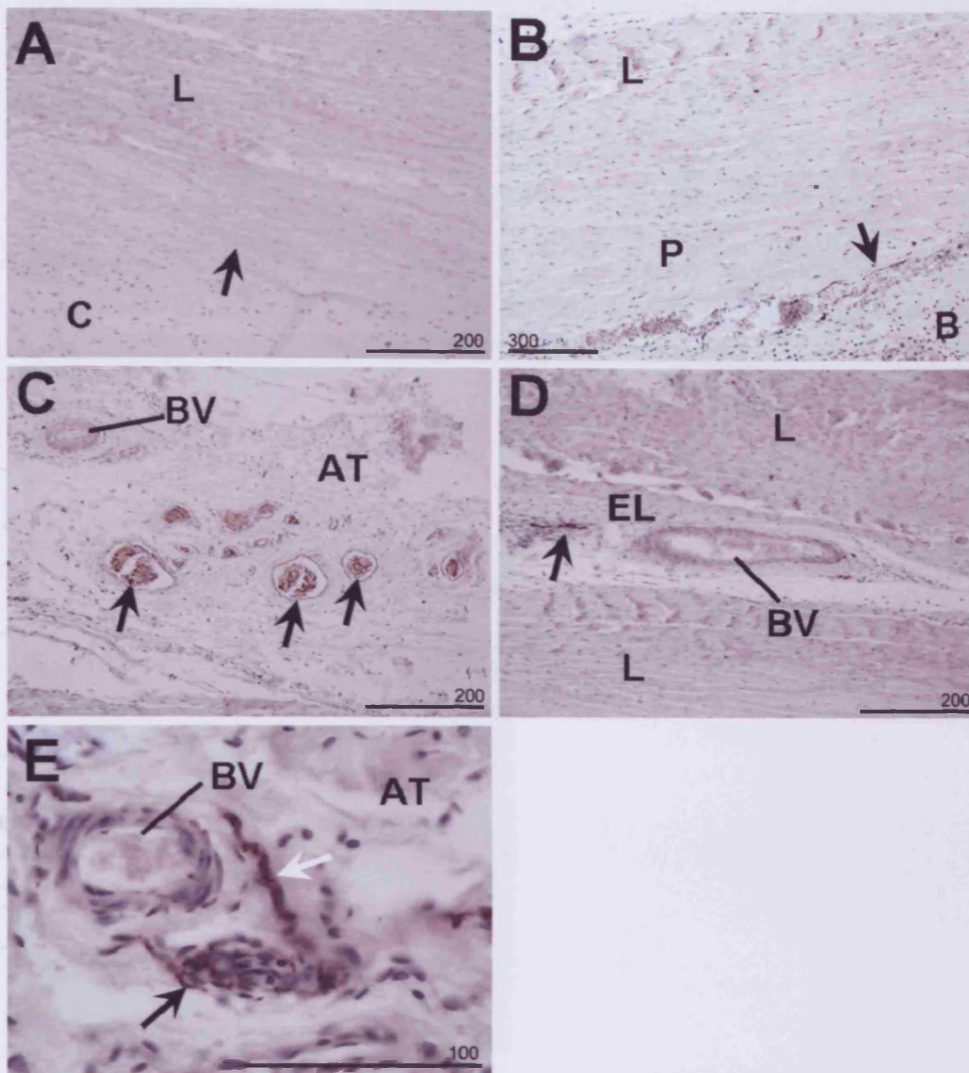
Figure 8.3.14



THE MUSCULAR ORIGIN OF TIBIALIS ANTERIOR FROM THE TIBIA - NEGATIVE CONTROL SECTIONS (Counterstained with DAPI to illustrate cell nuclei). 12 week rat.

Figure A, B and C: Negative control sections of the muscular enthesis of tibialis anterior illustrating that no non-specific labelling was present. Phosphate buffer (A), mouse immunoglobulins (B) or rabbit immunoglobulins (C) were applied to the sections in place of the primary antibody. Note the autofluorescence of the muscle fibres. B-bone, FP-fibrous periosteum, OP-osteogenic periosteum, M-muscle. Scale bar = 100µm.

Figure 8.3.15



ORIGIN OF THE SUSPENSORY LIGAMENT ONTO THE 3RD METATARSAL LABELLED WITH PROTEIN GENE PRODUCT 9.5 (PGP 9.5)

(Visualised with NovaRED and counterstained with Mayer's Haematoxylin). Foal.

Figure A: The insertion of the ligament (L) into the cartilage (C) of the 3rd metatarsal. Note that no nerve fibres were present within the insertion. Arrow indicates the fibres of the ligament inserting into the cartilage. Scale bar = 200µm.

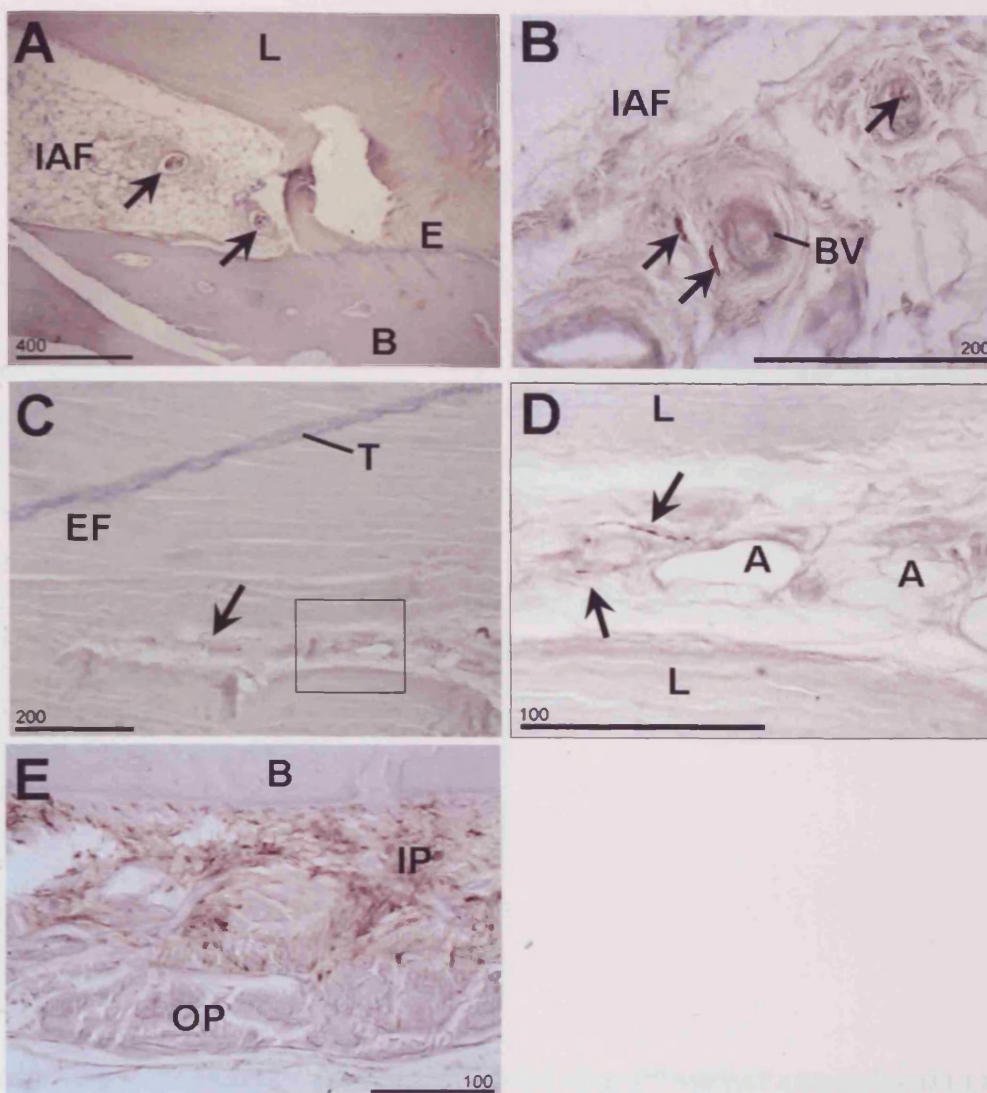
Figure B: The insertion of the ligament (L) into the periosteum (P) of the 3rd metatarsal. No nerve fibres were present at the insertion of the ligament to the periosteum. Arrow indicates nerve fibres in the deep layer of the periosteum adjacent to the bone (B) beneath the insertion of the ligament. Scale bar = 200µm.

Figure C: Nerve bundles (arrows) immunoreactive to PGP 9.5 in the adipose tissue (AT) at the entesis of the suspensory ligament. BV-blood vessel. Scale bar = 200µm.

Figure D: The suspensory ligament (L) immunolabelled with PGP 9.5. Arrow indicates a nerve fibre in the endoligament (EL) associated with an large blood vessel (BV). Scale bar = 200µm.

Figure E: Adipose tissue (AT) at the insertional angle of the suspensory ligament immunolabelled with PGP 9.5. White arrow indicates a blood vessel associated nerve fibre within the adipose tissue. Black arrow indicates a specialised nerve ending, resembling a Ruffini ending, within the adipose tissue. Scale bar = 100µm.

Figure 8.3.16



ORIGIN OF THE SUSPENSORY LIGAMENT ONTO THE 3RD METATARSAL LABELLED WITH PROTEIN GENE PRODUCT 9.5 (PGP 9.5)

(Visualised with NovaRED and counterstained with Mayer's Haematoxylin). Adult horse.

Figure A: The enthesis (E) of the suspensory ligament (L) immunolabelled with PGP 9.5. The insertional angle fat (IAF) contained numerous positively labelled nerve bundles (arrows). B-bone. Scale bar = 400µm.

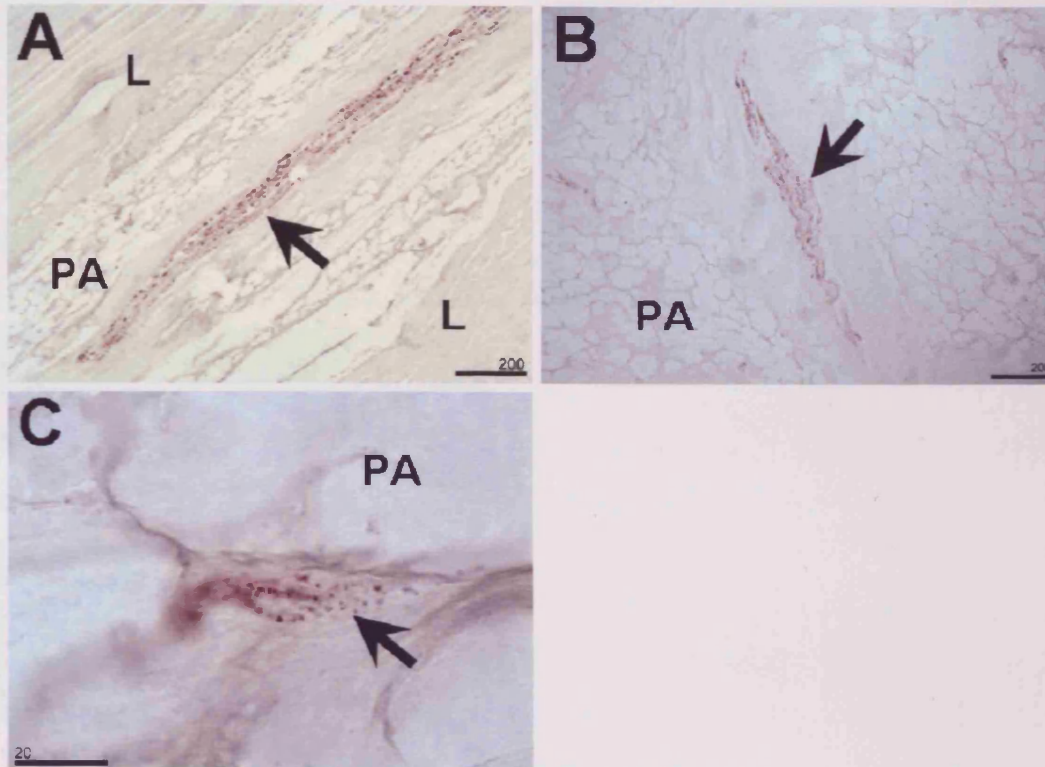
Figure B: The insertional angle fat (IAF) of the ligament insertion immunolabelled with PGP 9.5. Nerve fibres (arrows) within the adipose tissue were either blood vessel (BV) associated or 'free'. Scale bar = 200µm.

Figure C: The enthesal fibrocartilage (EF) of the ligament insertion immunolabelled with PGP 9.5. No nerve fibres were present within the fibrocartilage. Nerve fibres were however present in regions of blood-vessel invasion (arrow). T-tidemark. Scale bar = 200µm

Figure D: High power view of the region highlighted in (C). Arrows indicate the PGP 9.5 immunoreactive nerve fibres invading the enthesal fibrocartilage. L-ligament, A-adipocyte. Scale bar = 100µm.

Figure E: The periosteum of the 3rd metatarsal bone immunolabelled with PGP 9.5. Note the inner layer of the periosteum (IP) contains a large number of nerve fibres. OP-outer periosteum, B-bone. Scale bar = 100.

Figure 8.3.17

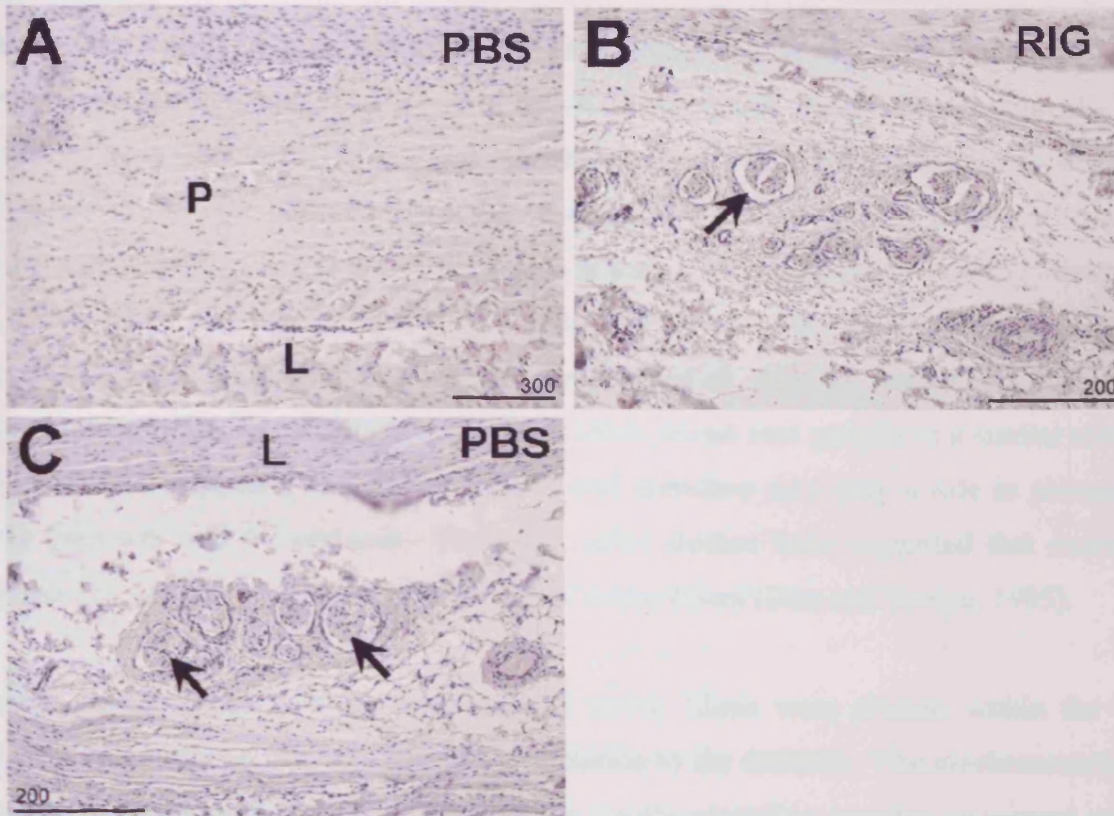


ORIGIN OF THE SUSPENSORY LIGAMENT ONTO THE 3RD METATARSAL LABELLED WITH PROTEIN GENE PRODUCT 9.5 (PGP 9.5) (Visualised with NovaRED). Pathological specimen.

Figures A and B: The enthesis (E) of the suspensory ligament (L) with suspected enthesopathy, immunolabelled with PGP 9.5. The pathological adipose tissue (PA) within the ligament contained numerous positively labelled nerve bundles (arrow). Scale bar = 200µm.

Figure C: The enthesis (E) of the suspensory ligament (L) with suspected enthesopathy, immunolabelled with PGP 9.5. An arborising nerve ending in the pathological adipose tissue (PA) located in the suspensory ligament. Scale bar = 20µm.

Figure 8.3.18



THE ORIGIN OF THE SUSPENSORY LIGAMENT - NEGATIVE CONTROL SECTIONS

(Sections were counter stained with Mayer's Haematoxylin). Adult horse.

Figure A: The fibrous insertion of the suspensory ligament onto the 3rd metatarsal bone. PBS was applied to the section in place of the primary antibody. No non-specific labelling was observed. L-ligament, P-periosteum. Scale bar = 300µm.

Figure B: A collection of nerve bundles in the insertional angle fat. Rabbit immunoglobulins were applied to the section in place of the primary antibody. Note that the nerves were devoid of labelling (arrow). Scale bar = 200µm.

Figure C: A collection of nerve bundles in the insertional angle fat. Phosphate buffer was applied to the section in place of the primary antibody. Note that the nerves were devoid of labelling (arrows). L-ligament. Scale bar = 200µm.

8.4. DISCUSSION

8.4.1. Fibrous Entesis of the Medial Collateral Ligament

Innervation

Like the fibrocartilaginous entesis of the rat Achilles tendon, the fibrous entesis of the medial collateral ligament was devoid of nerve fibres. It also appeared to be avascular and this may be a functional adaptation which increases the strength of the attachment. However, unlike the fibrocartilaginous entesis, the fibrous one does not contain chondroitin sulphate (Gao et al., 1996) which is known to inhibit nerve growth (Johnson et al., 2002; Snow and Letourneau, 1992). The MCL and its fibrous entesis do however contain dermatan sulphate rich proteoglycans (Gao et al., 1996). Dermatan sulphate has been shown to inhibit axonal outgrowth from chick dorsal root ganglia in a similar manner to chondroitin sulphate (Verna et al., 1989) and therefore may play a role in preventing nerve ingrowth into the entesis. However, other studies have suggested that dermatan sulphate has little or no effect on the growth of nerve fibres (Dou and Levine, 1995).

Putative mechanoreceptive and nociceptive nerve fibres were present within the epiligament and in the periosteum, in close association to the entesis. The mechanoreceptive fibres in the deep surface of the ligament are ideally placed to monitor movement of the ligament and may play a role in proprioception of the joint when stimulated. The peptidergic fibres in the ligament may be stimulated under conditions of joint stress or high levels of mechanical loading which may prevent damaging movement of the joint (Hanesch et al., 1991). In addition, the peptidergic fibres in the epiligament close to the entesis may play a role in ligament healing (Ivie et al., 2002; Salo et al., 2007). The periosteum surrounding the entesis was also innervated with nociceptive and mechanoreceptive nerve fibres. Such observations, in other regions of periosteum, have previously been reported by other authors (Bjurholm et al., 1988; Gajda et al., 2004; Hill and Elde, 1991). It is suggested that the fibres within the periosteum may be associated with pain in various pathologies of the skeletal system (Mach et al., 2002). In addition to their role in conveying nociceptive information to the CNS, peptidergic fibres containing CGRP may also influence bone remodelling at the insertion during growth or healing (Hukkanen et al., 1993). SP has also demonstrated similar osteogenic promoting properties *in vitro* (Shih and Bernard, 1997). CGRP may influence remodelling either directly, by acting on the cells

within the periosteum itself or through indirect action, by affecting the vascular flow in the periosteum (Irie et al., 2002).

8.4.2. Muscular Entesis of Tibialis Anterior

Adaptations of Muscular Enteses

Muscular enteses are not as common as tendinous ones and this is reflected in the lack of information available on such enteses; the majority of studies have focused on the muscular attachments of the facial muscles (Chong and Evans, 1982). The muscular attachment of tibialis anterior in the rat originates from the periosteum of the lateral condyle and the ventral crest of the tibia. The attachment of the muscle to the periosteum is facilitated by a small amount of connective tissue. Furthermore, the fibrous attachment of the muscle to the periosteum shows considerable similarities to the attachment of muscle fibres to tendon (Chong and Evans, 1982). At the muscle-bone interface of the masticatory muscles, this fibrous tissue has been shown to contain collagen types I, III and V, tenascin, laminin and fibronectin (Kawagoe et al., 1997), all of which are present in the connective tissue at the MTJ. At the MTJ Goss (1944) described the tissue as - “reticular (argyrophil) connective tissue fibrillae” or “argentofibrillae”. Chong and Evans, (1982) however, termed this connective tissue perimysium or terminal endomysium. Either of these terms could therefore also be applied to the fibrous tissue at muscular enteses on long bones – although the latter may be the most appropriate.

The similarities between the MTJ and the muscular entesis do not end here. The tip of the muscle fibre at entesis was highly invaginated (Schippel and Reissig, 1968). The invaginations in the muscle membrane may be considered a mechanical adaptation to dissipate the contractile stress generated by the cell over a larger area, thereby reducing stress at the tissue interface. In addition to reducing stress, a highly infolded membrane ensures that the tissue interaction primarily experiences shear loading. This increases the strength of the adhesion compared to a tissue interface which is loaded under tensile stress where membrane invaginations are not present. The similarities to the MTJ continue with the presence of vinculin (Shear and Bloch, 1985) in the tip of the muscle fibre at the entesis. At these sites, vinculin may form part of the cell-substrate interaction, anchoring actin filaments of the muscle to the collagenous extracellular matrix, thereby facilitating the transmission of force across the muscle membrane. It may therefore be speculated that the other proteins located at myotendinous junctions, such as talin (Tidball et al., 1986),

paxillin (Turner et al., 1991), and the transmembrane linkers – integrins (Bozyczko et al., 1989; Swasdison and Mayne, 1989) may also be present at the muscular enthesis. At the periosteal side of the enthesis the mode of attachment is less clear. It appears that the attachment of the terminal endomysium is facilitated by inserting into the fibrous layer of the periosteum. The fibrous layer in turn attaches to the osteogenic layer of the periosteum and subsequently the underlying bone. This is similar to the periosteal mode of attachment described by Chong and Evans, (1982). As the fibres of the endomysium do not appear to penetrate very deeply into the periosteum, unlike fibrous entheses of tendons and ligaments, this may be the potential site pathology or rupture.

Gross anatomical adaptations are present at muscular enthesis in addition to the microscopic adaptations described above. The area of the attachment of tibialis anterior is certainly larger than its tendinous attachment in the foot. This – in a similar fashion to the membrane invaginations of the muscle membrane – reduces the stress at the enthesis by distributing it over a wide area (Benjamin et al., 2006). It was also observed that the muscle fibres arise from the periosteum at various angles depending on their location. Those fibres attaching to the underside of the tibial condyle arise at right angles; while the muscle fibres arising from the shaft of the tibia do so at a more acute angle. This most likely reflects the unipennate shape of the muscle, where the muscle fibres converge onto a single tendon. This fibre arrangement also ensures a large surface area at the attachment. It was observed that where the muscle fibres arise from the periosteum; those arising at right angles were attached to the periosteum by a larger amount of connective tissue in comparison to fibres arising at more acute angles. This difference may reflect the higher load experienced by the attachment of perpendicular muscle fibres, because the load is not distributed in as many directions as it is where the fibres attach at an angle (Figure 8.4.2.1). Therefore, a larger amount of terminal epimysium may be present to provide a stronger attachment. This is supported by the observations made by Kawagoe et al., (1997), that the molecular components of the muscle-bone junction differ in each masticatory muscle according to the amount of stretch or tension experienced by that particular attachment. However, care must be taken when assessing the amount of connective tissue, as even slight alterations in the angle of the section can affect the results observed, due to the small size of this structure (Goss, 1944).

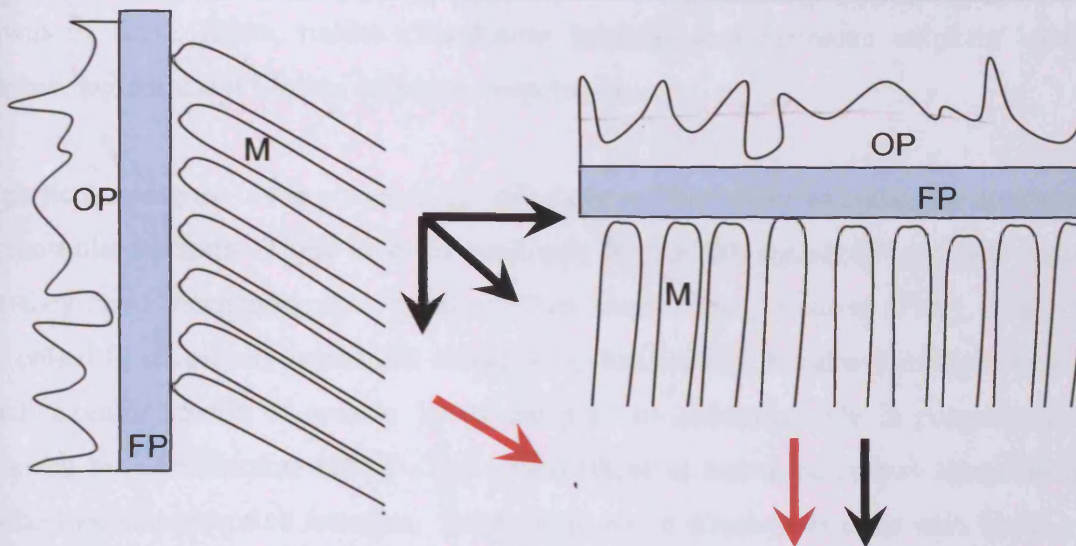


Figure 8.4.2.1: Schematic diagram of the muscular entesis of tibialis anterior. Muscle fibres arising at an angle from the periosteum (left) dissipate the tensile load experienced (red arrow) in a number of directions (black arrows) while, the stress is unable to be dissipated where the muscles arise perpendicular to the periosteum; resulting in a higher level of tensile load exerted on the entesis.

Developmentally, the indirect attachment of the muscle to the periosteum is advantageous as this allows movement and growth of the muscle in a similar manner to fibrous enteses of tendons and ligaments, ensuring that the muscle position is maintained relative to bone growth (Dorfl, 1980a; b).

Blood Supply and Innervation of the Muscular Enteses

In contrast to fibrous and fibrocartilaginous enteses - which are characteristically avascular - muscular enteses appear to be relatively well vascularised. Blood vessels were frequently observed passing between the muscle fibres and occasionally come directly into contact with the underlying periosteum at the entesis. It is possible that the difference in vascularisation is due to the large area of the attachment site which reduces stress concentration. This may be explained by the simple engineering formula, $\text{stress} = \text{force} / \text{contact area}$, which is used to calculate stress at an interface (Benham et al., 1996).

It is interesting to note the relatively high level of innervation at the muscular entesis. This in complete contrast to the results obtained from both fibrous and fibrocartilaginous enteses - which were aneural (see chapter 3 and chapter 8). Once again, the large surface area of the attachment site and therefore reduced stress concentration at the entesis may allow the presence of nerve fibres at the entesis. Furthermore, the molecular composition of the terminal endomysium, as described by Kawagoe et al., (1997), does not inhibit

growth of nerve fibres, unlike chondroitin sulphate and dermatan sulphate located at fibrocartilaginous and fibrous enteses, respectively.

Of particular interest is the presence of coiled nerve fibres close to and at the attachment of the muscular entesis. These labelled positively for NF200, but not SP or CGRP indicating that they have mechanoreceptive, rather than nociceptive functions (Perry et al., 1991). The coiled fibres closely resembled muscle-spindles usually found within the muscle body, which monitor stretch of muscle fibres and play an important role in proprioception (as reviewed by - Prochazka, 1981). The coiled fibres at the entesis may therefore have a similar mechanoreceptive function. Peptidergic nerve fibres associated with blood-vessels were also present at the entesis and these fibres are likely to be stimulated under conditions of tissue damage or extremes of movement causing pain when the entesis is damaged. As described previously (chapter 3), the neuropeptides - substance P and CGRP can cause vasodilation and increased vascular permeability by binding to receptors in the endothelium when released from the peripheral terminals of the nerve fibre (Holzer, 1988; Kenins, 1981; Kenins et al., 1984). These vasoactive properties may result in inflammation at the muscle attachment site. Furthermore, mast cells were located at the entesis. The release of SP from nerve fibres at the entesis in response to tissue damage may cause mast cell de-granulation which may produce inflammation or directly result in stimulation of local nerve fibres (Brimble and Wallis, 1973; Foreman and Jordan, 1983; Foreman, 1987; Ninkovic and Hunt, 1985). The aforementioned nociceptive pathways may therefore cause pain at the entesis when tissue damage has occurred as a result of overuse and might be causing the pain associated with shin splints. Nociceptive and mechanoreceptive nerve fibres were also present in the periosteum, suggesting that the periosteum itself be a source of pain in overuse injuries.

8.4.3. Origin of the Suspensory Ligament in the Horse

The suspensory ligament in the horse originates from the proximal part of the 3rd metatarsal bone and partly from the plantar tarsal fascia. In the foal, the proximal fibres of the suspensory ligament insert into the cartilaginous epiphysis of the metatarsal bone, and during development the cartilage is eroded and replaced by bone. In the adult, the superficial fibres of the ligament attach to the metatarsal bone via a small region of fibrocartilage, which generates the four layers characteristic of a fibrocartilaginous entesis similar to those seen in man (Benjamin et al., 1986). The region of uncalcified

fibrocartilage at the insertion of the suspensory ligament entheses is considerably smaller than the uncalcified fibrocartilage located at the insertion of the rat Achilles tendon and this may be attributed to the small range of motion that the ligament experiences at its origin. This is supported by observations made by Frowen and Benjamin (1995) in man. In contrast, the more distal fibres of the ligament origin attach to the metatarsus via a periosteal fibrous entheses in the foal and in the adult the small slips of ligament that remain more distally, insert directly into the cortical bone forming a bony entheses. Enteses with mixed modes of attachment are not unusual. Benjamin et al., (1986) point out that the most distal region of the Achilles tendon entheses in man is fibrous while the main part of the attachment is fibrocartilaginous. Furthermore, Hems and Tillman (2000) emphasised the mixed nature of the attachments of the human masticatory muscles.

The origin of the suspensory ligament however, does not have a distinctive “entheses organ” (Benjamin et al., 2004a). Neither the periosteum on the posterior surface of the metatarsus or the opposing deep surface of the ligament is fibrocartilaginous, indicating that these regions do not experience high levels of compression (Rufai et al., 1996; Vogel and Koob, 1989). Fibrocartilage is therefore not required to prevent wear and tear (Rufai et al., 1995, 1996). However, in both the foal and the adult horse, a region of adipose tissue is located in the insertional angle between the ligament and bone. Interestingly, this region of adipose tissue contained a large number of blood vessels and also Pacinian corpuscles. These specialised nerve endings may contribute to proprioceptive input (Willis and Coggeshall, 1991) from the hock joint and entheses during movement. Immunohistochemical labelling of the entheses confirmed the presence of nerve fibres within the adipose tissue. The nerve fibres within the wedge of adipose tissue and within the endoligament, may gather nociceptive information associated with pathology of the suspensory ligament. This supports the findings made by Bathe, (2001) who found that neurectomy of the plantar metatarsal nerves, which innervate the area, significantly improves cases of persistent lameness linked to enthesopathy.

It was further established that at both ages the entheses (fibrocartilaginous and fibrous regions) was aneural, correlating with the observations made previously (see chapters 3 and 8). However, in the adult specimen, a small number of blood vessels and nerve fibres associated with adipose tissue were observed to invade into the entheses fibrocartilage from the endoligament. This was seen to a much larger degree within the pathological sample.

As described previously (chapters 3 and 6) this may be the result of a decrease in the concentration of aggrecan, allowing the ingrowth of the blood vessels and nerve fibres (Freemont et al., 2002b; Johnson et al., 2002; Snow and Letourneau, 1992). It may be further postulated that the small amount of uncalcified fibrocartilage located at the enthesis may predispose the attachment to neurovascular invasion and may explain the frequency of the enthesopathy.

9. THE EFFECT OF GHRELIN ON THE RAT ACHILLES TENDON ENTHESES ORGAN

9.1. INTRODUCTION

This chapter aims to describe the effect of ghrelin, its naturally occurring isoform Des-Octanoyl Ghrelin, and the growth hormone secretagogue receptor 1a (GHS-R1a) antagonist - L163,255, on the retromalleolar fat pad and the rest of the rat Achilles tendon enthesis organ. Ghrelin is a peptide which has recently been demonstrated to affect adipogenesis directly (Choi et al., 2003; Tschop et al., 2000). However, the function of the retromalleolar fat pad is believed to be primarily structural, and previous studies in man have suggested that the weight of an individual does not affect to the size of Kager's fat pad in man (see chapter 6). Therefore it may be hypothesised that ghrelin, des-octanoyl ghrelin, and the GHS-R1a antagonist will not affect the size of the retromalleolar fat pad; thereby confirming its primary structural role. Because ghrelin is also believed to induce chondrocyte hypertrophy and bone formation (Caminos et al., 2005) signs of ossification will also be evaluated in the fibrocartilages of the enthesis organ. Finally, the effect of these peptides on the innervation of the Achilles tendon enthesis organ will be assessed as recent reports have suggested that ghrelin can also induce neurogenesis (Sato et al., 2006). It is possible that ghrelin or its isoform may induce nerve in-growth in what has been shown previously (see chapter 3) to be a largely aneural enthesis organ.

Brief Review

The peptide Ghrelin, an endogenous ligand for the GHS-R1a, was first identified by Kojima et al., (1999) in the rat stomach. Various tissue extracts were used to stimulate a cell line expressing GHS-R and the changes were monitored by recording intracellular Ca^{2+} levels. Surprisingly, the stomach demonstrated the greatest activity and the peptide was named ghrelin – 'ghre' meaning 'grow'. The name refers to the ability of ghrelin to stimulate growth hormone secretion (Kojima et al., 1999). Two major forms of the peptide have been identified; ghrelin, and des-octanoyl ghrelin (also known as non-actylated). Ghrelin itself is formed from a 28 amino acid peptide, in which the third serine has an n-octanoic acid attached via an ester bond. This octanoylated modification is essential to allow ghrelin to activate its receptor GHS-R1a. Des-octanoyl ghrelin is also a major circulating form of ghrelin in the rat and does not contain the octanoic acid attached to the 3rd serine residue (Ser3) (Hosoda et al., 2000).

Ghrelin is currently known to have a number of functions including stimulating the release of growth hormone (GH) from the pituitary and stimulating appetite when it is secreted by the stomach under fasting conditions. However, with increasing research into the function of this peptide, a wide expression pattern has been demonstrated in a variety of different tissues. Of particular interest is the finding that ghrelin affects adipogenesis (Choi et al., 2003). It has been demonstrated that *in vitro* ghrelin stimulates preadipocyte differentiation and prevents lipolysis in adipocytes isolated from epididymal and parametrial adipose tissue (Choi et al., 2003). *In vivo* studies support these observations; Tschöp et al., (2000) demonstrated that following 2 weeks of subcutaneous and intracerebroventricular administration of ghrelin, rats and mice demonstrated significant increases in fat mass, as assessed by dual energy X-ray absorptiometry. It is therefore suggested that adipocytes are directly affected by ghrelin. However, Patel et al., (2006) have shown that the receptor for ghrelin - GHS-R1a is not present in some adipose tissue deposits, such as peri-renal fat. The authors demonstrated that des-octanoyl/ghrelin does not affect insulin-stimulated glucose uptake in adipocytes isolated from peri-renal deposits, unlike the effects of GHS-R1a on epididymal adipose tissue deposits (Patel et al., 2006). In contrast, Thompson et al., (2004) have shown that tibial bone marrow adipocytes (even though they do not express GHS-R1a) are directly affected by both ghrelin and des-octanol ghrelin resulting in adipogenesis. This suggests that des-octaoyl/ghrelin binds to an as-yet-unidentified receptor.

Caminos et al., (2005) have shown that chondrocytes located in the proliferative and maturation zones of the growth plate expressed ghrelin but not the GHS-R1a. The authors suggest a number of functions for the expression of ghrelin by these chondrocytes. Principally, it increases the production of cyclic adenosine monophosphate (cAMP) in a dose-dependent manner. Such an increase is believed to be related to an alteration in the extent of PG and hyaluronan synthesis and also to an induction of apoptosis. It is therefore suggested that ghrelin may participate in chondrocyte metabolism by promoting chondrocyte hypertrophy and bone formation (Caminos et al., 2005). In support of this hypothesis, it should be pointed out that ghrelin has also been shown to promote proliferation and differentiation of osteoblasts (Fukushima et al., 2005; Maccarinelli et al., 2005). Therefore, this study will also describe whether the fibrocartilage of the Achilles tendon enthesis organ is affected by ghrelin. It is further suggested that ghrelin, through increasing fatty acid uptake and the downregulation of enzymes involved in the formation

of reactive oxygen species, may reduce the synthesis of inflammatory mediators in cartilage. Ghrelin may therefore have potential use as a therapeutic pharmaceutical agent for articular inflammatory conditions – e.g. rheumatoid arthritis (Caminos et al., 2005). Furthermore, ghrelin and des-octanoyl ghrelin also have the ability to stimulate neurogenesis in the spinal cord during development - both dependently and independently of the GHS-R1a (Sato et al., 2006). It may therefore be interesting to assess whether the innervation of the Achilles enthesis organ is altered by ghrelin administration.

9.2. MATERIALS AND METHODS

9.2.1. Ghrelin Infusion Programme (carried out by Dr. T Wells and Dr. J. Davies)

Sprague-Dawley rats, obtained from accredited commercial suppliers were housed individually in metabolic cages for the purposes of recording their food and water consumption. All rats were allowed food (Harlan Powdered Food, Cat ~2014, 14% protein) and water *ad libitum*. All were fitted with a jugular vein cannula connected to an osmotic mini-pump (Alzet, Cat# 2001) containing an appropriate infusate (Vehicle, Ghrelin, Des-Octanoyl Ghrelin and L163,255 – 3 rats in each group), and were infused at 1µl/hour for 7 days.

Infusates: **Vehicle** – Sterile saline (NaCl) solution containing 0.1% BSA and 10U/ml Heparin. **Ghrelin** – 3.3µg/µl of ghrelin in sterile saline (NaCl) solution containing 0.1% BSA and 10U/ml Heparin (80µg of ghrelin every 24 hours). **Des-Octanoyl Ghrelin** – 3.3µg/µl of Des-Octanoyl ghrelin in sterile saline (NaCl) solution containing 0.1% BSA and 10U/ml Heparin (80µg of des- octanoyl ghrelin every 24 hours). **L163,255** - 6.6µg/µl of L163,255 in sterile saline (NaCl) solution containing 0.1% BSA and 10U/ml Heparin (160µg of L163,255 every 24 hours).

All rats were given an intraperitoneal injection of Bromodeoxyuridine (BrdU) (50mg/kg – see appendix I), 1 hour before the animals were killed by Halothane anaesthesia and subsequent decapitation.

9.2.2. Dissection and Fixation

Following decapitation, both ankles of the rat were removed, ensuring the fat pad was not disturbed. The left ankle was subsequently used for immunohistochemistry, while the right ankle was used for routine histology.

9.2.3. Routine Histology

Specimens were fixed in 4% paraformaldehyde in 0.1M phosphate buffer (PB) (see appendix I) for 1 week and decalcified in 5% nitric acid (see appendix I). Samples were subsequently washed in 0.1M PB (see appendix I) and dehydrated in graded alcohols (70%, 95%, and 100% with two changes of 20 minutes each), cleared in xylene (two changes of 20 minutes) and embedded in 58°C paraffin wax. Routine histology was carried out as described in chapter 2.

9.2.4. Immunohistochemistry

Indirect immunofluorescence was carried out using the antibodies PGP 9.5, Neurofilament 200, anti-substance P and anti-CGRP as described in chapter 2.

Anti-Bromodeoxyuridine (BrdU) labelling

Indirect immunofluorescence was carried out in a light-proof, humidified chamber. Slides were removed from the freezer and allowed to adjust to ambient room temperature. A ring was drawn around the specimens with a waterproof pen (Zymed® Laboratories, San Francisco, US) to retain solutions on the slide. The samples were re-hydrated in 0.1M PB containing 0.1% Triton X (Sigma-Aldrich Company Ltd, Gillingham, UK; see appendix I) and 2N HCl in dH₂O was applied to the slides for 30 minutes at 37°C in a humidified incubator to permeabilize the nucleus. The sections were washed well using 0.1M PB containing 0.1% triton X and then nuclear proteins were denatured using 0.25% trypsin (Gibco) for 20 minutes at 37°C to allow visualization of the incorporated BrdU. Following another series of washing steps, 20% normal goat serum (Dako UK, Ely, Cambridgeshire, UK) was applied to the sections for 1 hour. The blocking serum was gently poured off the slide and the primary antibody anti-BrdU (Sigma-Aldrich, Gillingham, UK) applied (see Table 2.1) directly without washing. The antibody-treated sections were incubated for 2 hours at 37°C. Following incubation, the slides were washed 3 times for 5min in 0.1M PB. The sections were incubated for 1 hour with the secondary antibody goat anti-mouse FITC (Dako UK, Ely, Cambridgeshire, UK) following pre-incubation with 1% normal rat serum (Invitrogen, Paisley, UK) for 1h at 4°C. After several washes, the slides were mounted under 22mm x 50mm coverslips (RA Lamb Medical Supplies, Eastbourne, UK) using Vectorshield containing DAPI (Vector Labs, Peterborough, UK).

Controls

Negative control sections were incubated with 0.1M PB and mouse immunoglobulins (IgG1; Dako, Cambridgeshire, UK) in place of the primary antibody.

Microscopy

Sections were examined by epifluorescence microscopy using an Olympus BX-61 (Olympus UK Ltd, London, UK) and captured using AnalySIS software using a Leitz DMRB (Leica Microsystems Ltd; Milton Keynes, UK), and processed using Adobe Photoshop (Version 6).

9.3. RESULTS

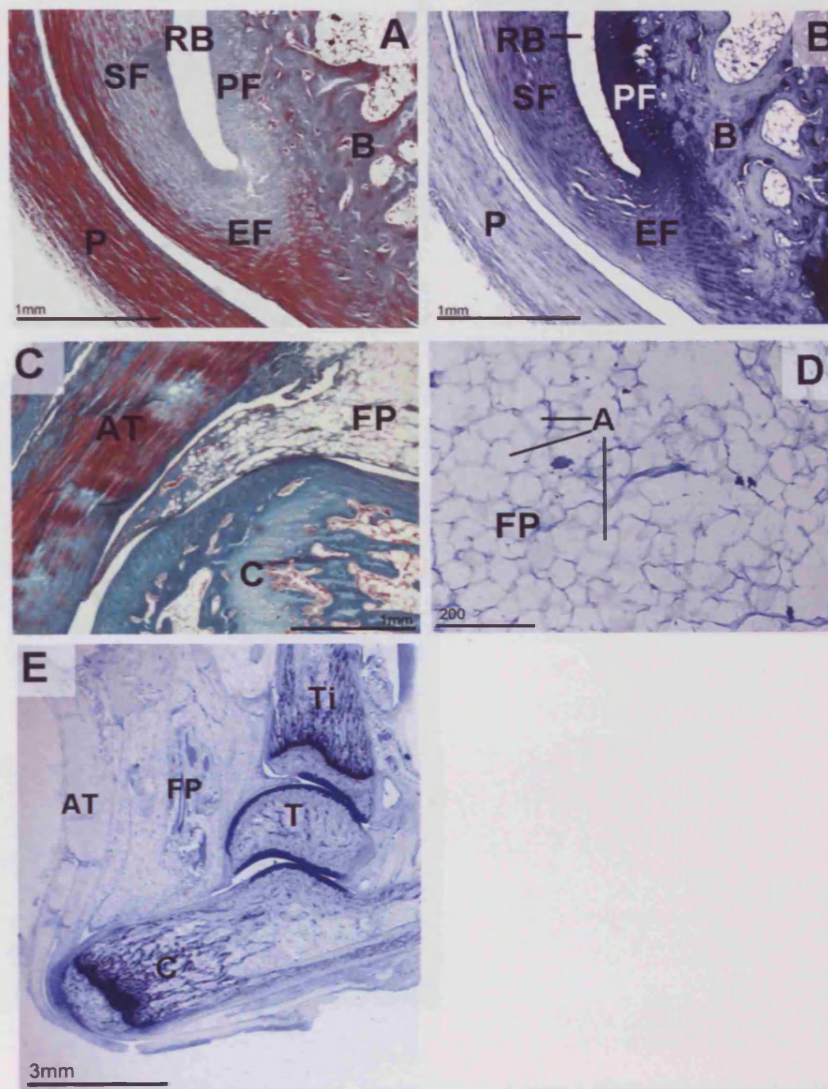
Routine Histology

The structure of the Achilles tendon enthesis organ was comparable in all rats from the 4 different groups treated with ghrelin, des-octanoyl ghrelin, L163,255, and vehicle (representative images - Figs 9.3.1.A-B) and was no different from the Achilles tendon enthesis organ described in chapter 3. Specifically, no ectopic bone formation or chondrocyte hypertrophy was observed in the enthesis fibrocartilage in any of the 4 test groups. Furthermore, in all animals the retromalleolar fat pad was present, contained unilocular adipocytes and sent a tongue-like protrusion into the retrocalcaneal bursa. There was no obvious difference in the size of the fat pad between the 4 groups. In all animals, the retromalleolar fat pad filled a space in the region of the ankle, posterior to the Achilles tendon, anterior to the tendon of flexor hallucis longus, and superior to the calcaneus (representative images - Figs 9.3.1.C-E).

Immunohistochemistry

The innervation of the Achilles tendon enthesis organ was equivalent in all rats from the 4 different treatment groups and comparable to the innervation of the Achilles tendon enthesis organ as described in chapter 3. The enthesis, sesamoid and periosteal fibrocartilages of the enthesis organ were aneural in all groups, as was the retrocalcaneal bursa (Figs 9.3.2.A-C). In addition, the retromalleolar fat pad contained nerve fibres immunoreactive to PGP 9.5, NF200, SP and CGRP. No marked differences were observed between any of the treatment groups (Figs 9.3.2.D-E). Labelling for BrdU demonstrated that only a small number of adipocytes within the retromalleolar fat pad were proliferating, and there were no obvious differences between the 4 treatment groups (Fig 9.3.3.A-F). The majority of positively labelled cells in the fat pad were either fibroblasts or endothelial cells.

Figure 9.3.1.



GHRELIN TREATED RATS - ROUTINE HISTOLOGY

Images presented are representative of all 4 treatment groups.

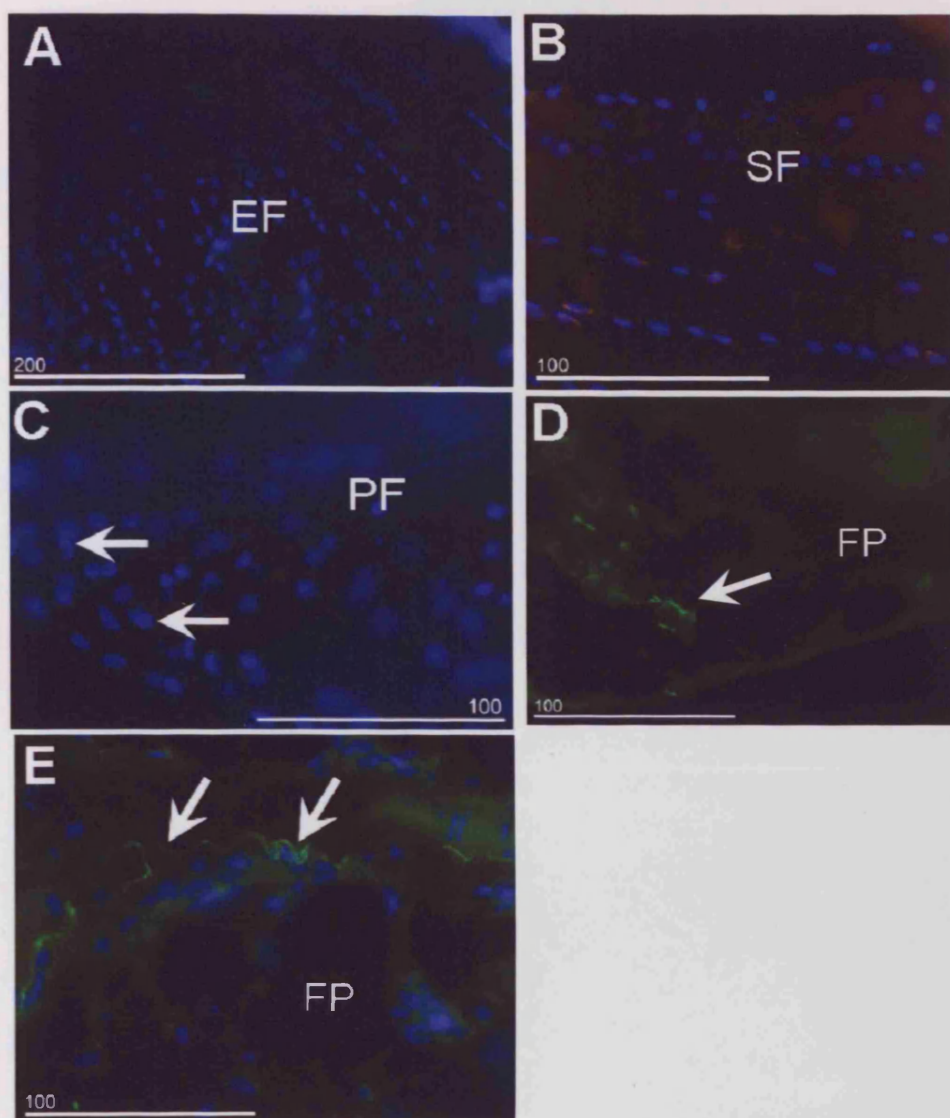
Figure A and B: The enthesis (EF), sesamoid (SF) and periosteal fibrocartilages (PF) of the rat Achilles tendon enthesis organ in a Masson's trichrome (A) and toluidine blue (B) stained section. Note the normal appearance of these structures. B-bone, P-plantaris tendon. RB-retrocalcaneal bursa. Scale bar = 1mm.

Figure C: The tip of the retromalleolar fat pad (FP) protruding into the retrocalcaneal bursa. C-calcaneus, AT-Achilles tendon. Masson's trichrome. Scale bar = 1mm.

Figure D: A high power view of the retromalleolar fat pad (FP). Note the unilocular appearance of the adipocytes (A). Toluidine blue. Scale bar = 200µm.

Figure E: Low power view of the posterior region of the ankle. Note that the fat pad (FP) fills the region equivalent to Kager's triangle. AT-Achilles tendon, C-calcaneus, T-talus, Ti-Tibia. Toluidine blue. Scale bar = 3mm.

Figure 9.3.2.



GHRELIN TREATED RATS – IMMUNOLABELLING OF NERVE FIBRES

Images presented are representative of all 4 treatment groups (All sections are counterstained with DAPI to illustrate cell nuclei).

Figure A: The enthesion fibrocartilage (EF) of the Achilles tendon insertion in a section labelled with PGP 9.5. Note the absence of nerve fibres located in the fibrocartilage. RB-retrocalcaneal bursa. Scale bar = 200µm.

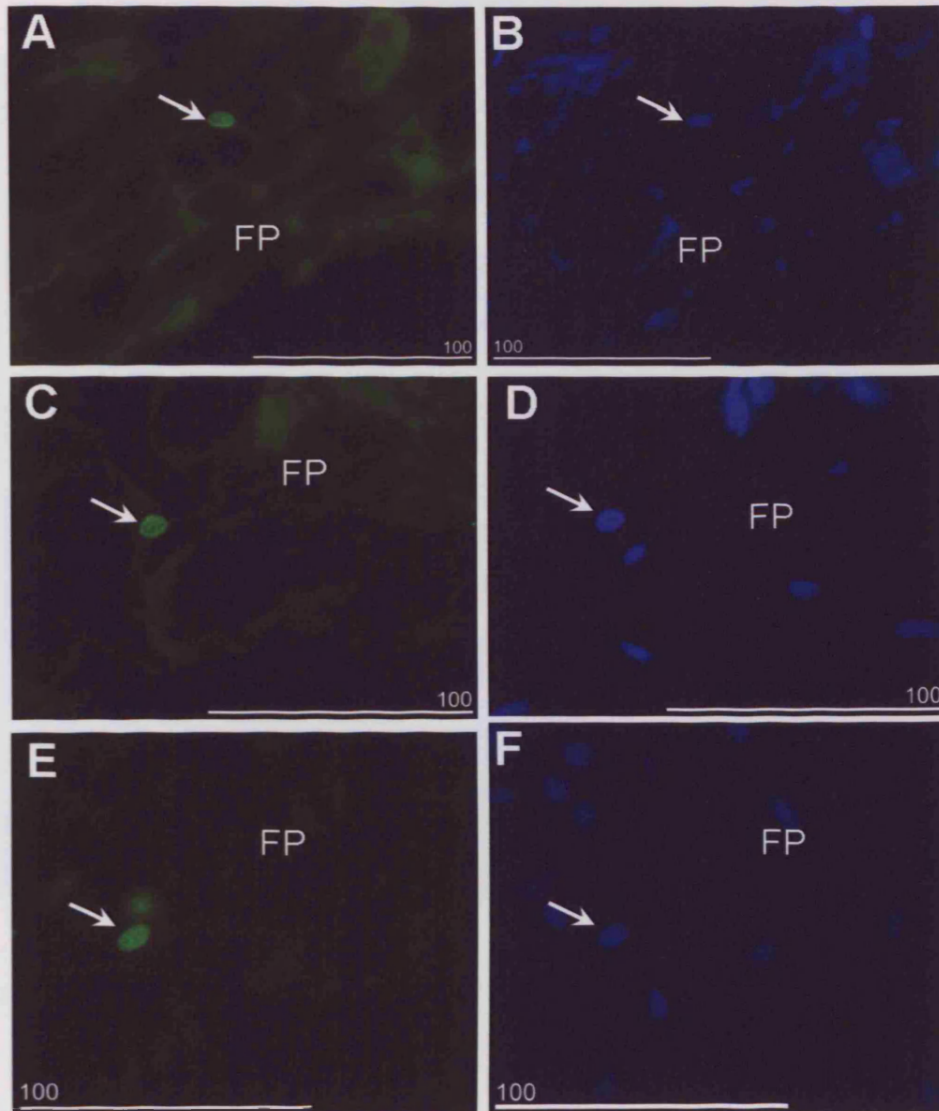
Figure B: The sesamoid fibrocartilage (SF) in a section labelled with PGP 9.5. No nerve fibres were present. Scale bar = 100µm.

Figure C: The periosteal fibrocartilage (PF) in a section labelled with PGP 9.5. No nerve fibres were present. Note the rounded appearance of the fibrocartilage cell nuclei (arrows). Scale bar = 100µm.

Figure D: The retromalleolar fat pad (FP) in a PGP 9.5 labelled section. Arrow indicates a nerve fibre within the fat pad. Scale bar = 100µm.

Figure E: The retromalleolar fat pad (FP) in a CGRP labelled section. Arrows indicate a nerve fibre containing CGRP within the fat pad. Scale bar = 100µm.

Figure 9.3.3.



THE RETROMALLEOLAR FAT PAD OF THE ACHILLES TENDON ENTESIS ORGAN LABELLED FOR BROMODEOXYURIDINE (BrdU) WHICH INDICATES PROLIFERATING CELLS.

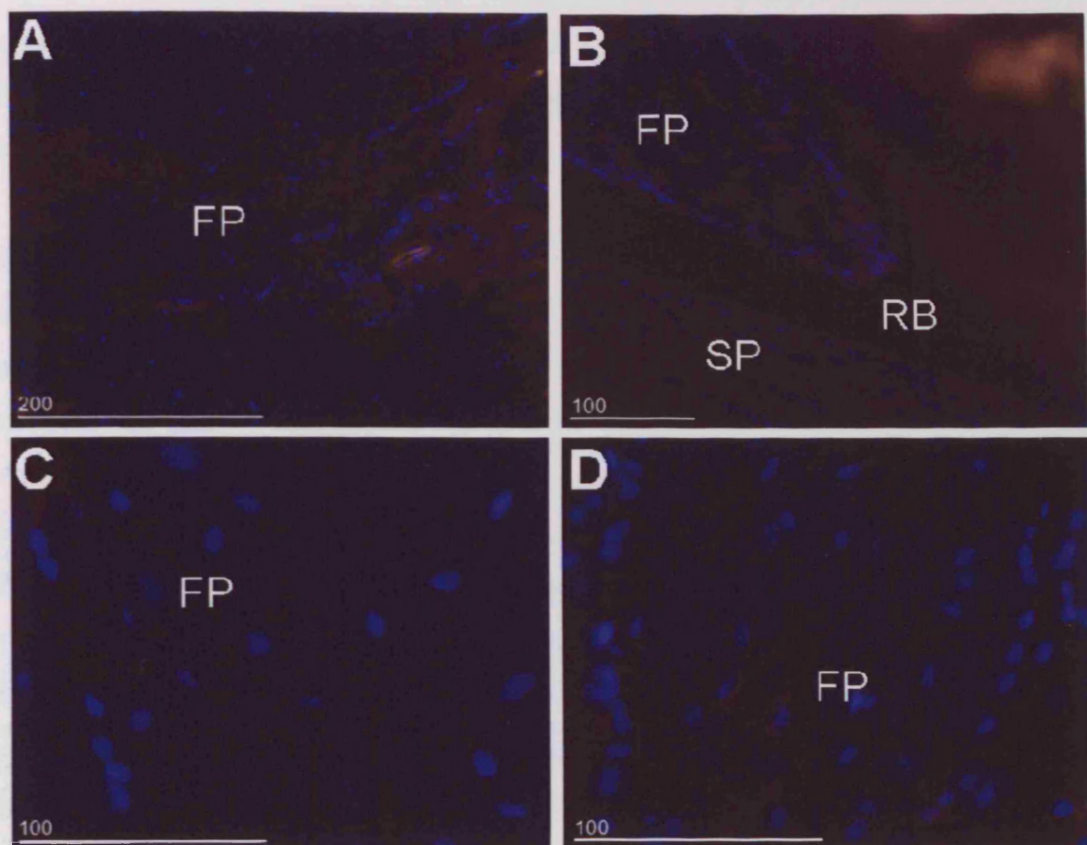
(All sections are counterstained with DAPI to illustrate cell nuclei).

Figure A and B: The retromalleolar fat pad (FP) in a Des-Octanoyl Ghrelin treated rat. Arrow indicates the presence of a BrdU positively labelled cell nucleus (A) and corresponding DAPI positive nucleus (B). Scale bar = 100µm.

Figure C and D: The retromalleolar fat pad (FP) in a vehicle treated rat. Arrow indicates the presence of a BrdU positively labelled cell nucleus (C) and corresponding DAPI positive nucleus (D). Scale bar = 100µm

Figure E and F: The retromalleolar fat pad (FP) in a L163,255 treated rat. Arrow indicates the presence of a BrdU positively labelled cell nucleus (E) and corresponding DAPI positive nucleus (F). Scale bar = 100µm.

Figure 9.3.4



**NEGATIVE CONTROL SECTIONS OF THE ACHILLES TENDON ENTESIS ORGAN.
(All sections are counterstained with DAPI to illustrate cell nuclei).**

Figure A: The retromalleolar fat pad (FP) of a Ghrelin treated rat. Phosphate buffer was applied to the section in place of a neuronal related primary antibody. Non-specific binding of the secondary antibody was not observed. Scale bar = 200µm.

Figure B: The retromalleolar fat pad (FP) protruding into the retrocalcaneal bursa (RB) of a Ghrelin treated rat. Rabbit immunoglobulins were applied to the section in place of a neuronal related primary antibody. Non-specific binding of the primary antibody was not observed. Scale bar = 100µm.

Figure C: The retromalleolar fat pad (FP) of a Ghrelin treated rat. Phosphate buffer was applied to the section in place of the anti-BrdU primary antibody. Non-specific binding of the secondary antibody was not observed. Scale bar = 100µm.

Figure D: The retromalleolar fat pad (FP) of a Ghrelin treated rat. Mouse immunoglobulins were applied to the section in place of the anti-BrdU primary antibody. Non-specific binding of the primary antibody was not observed. Scale bar = 100µm.

9.4. DISCUSSION

The results demonstrated that treatments with ghrelin, des-octanoyl ghrelin and L163,255 had no effect on the size or innervation of the retromalleolar fat pad associated with the rat Achilles tendon enthesis organ. Neither did they affect the structure or innervation of the enthesis, sesamoid, or periosteal fibrocartilages of the enthesis organ.

Ghrelin and des-octanoyl ghrelin are currently understood to play a role in directly inducing adipogenesis dependently and independently of GHS-R1a. However, the results presented here suggest that neither peptide markedly increased the size of the retromalleolar fat pad. Furthermore the GHS-R antagonist L163,255 did not reduce the size of the fat pad, or induce lipolysis. This is in line with the results presented in chapter 6 showing that the weight and volume of Kager's fat pad are not affected by the weight of the individual (Davies and White, 1961). Thus, the current results provide further support for the hypothesis that the fat pad associated with the Achilles tendon enthesis organ is a structural fat pad rather than one which is altered according to the metabolic needs of the individual (Davies and White, 1961). Furthermore, there appeared to be no difference in the structure of the fibrocartilages of the enthesis organ. This too is in line with the finding that the size of the fat pad was not altered; as such an alteration could have resulted in an increased wear and tear to the fibrocartilages - as the fat pad plays a role in dissipating stress at the tendon attachment (Benjamin et al., 2004b).

Finally, as mentioned earlier, ghrelin is synthesised and expressed by chondrocytes in the growth plate. The molecule is believed to play a role in promoting bone formation (Camino et al., 2005). As entheses are often described as miniature growth plates, it is possible that ghrelin administration might have induced fibrocartilage cell hypertrophy and apoptosis. However, such changes were not observed. This may be related to the avascular nature of the fibrocartilage - an intravenous (iv) injection of ghrelin may not affect the cells within it.

10. *IN VITRO* STUDY OF TARGET DERIVED NERVE GROWTH

10.1. INTRODUCTION

It has been demonstrated above that only the retromalleolar fat pad of the rat Achilles tendon enthesis organ is innervated, while the enthesis, sesamoid and periosteal fibrocartilages are aneural (see chapter 3). It is interesting to note that even though fibrocartilage has yet to differentiate in the neonatal rat, the precursors of the fibrocartilages are still aneural, whereas the fat pad contains nerve fibres at birth and throughout postnatal development into old age (see chapter 3). It may therefore be suggested that during development, nerve fibres are guided by factors released from the developing adipose tissue in the retromalleolar fat pad to innervate this structure, while inhibitory signals may be released from the developing fibrocartilage to prevent neural invasion. It was therefore the aim of the present study to determine *in vitro* whether axons are attracted from DRG to the retromalleolar fat pad, presumably through the release of chemical signals, and whether the developing and mature enthesis fibrocartilage inhibits axonal nerve growth.

Brief Review

It is currently believed that axons are guided to their targets during development by a combination of diffusible, membrane bound, and extracellular matrix cues/signals (as reviewed by - Mueller, 1999; Tessier-Lavigne and Goodman, 1996). These signals can have attractive or repulsive effects on the specialised receptive ending – known as a growth cone – at the peripheral terminal of the developing axon. Molecular cues bind to surface receptors located on the growth cone which transduce the signal by triggering intracellular pathways. Activation of these pathways regulates motility of the growth cone through polymerisation and depolymerisation of actin filaments in the filopodia, located in the distal region of the growth cone. Growing axons may respond to cues in a temporal sequence in addition to being influenced by signals secreted by the target organ (i.e. long distance cues) and signals from the underlying substrata (i.e. short distance cues). In most cases a combination of signals facilitate fine control over axon guidance and as a result it is clearly a very complex process (Mueller, 1999; Tessier-Lavigne and Goodman, 1996).

Target tissues secrete molecular cues such as neurotrophins - which guide axons towards them and regulate survival of these axons (Cohen, 1960; Gundersen and Barrett, 1979; Lumsden and Davies, 1983). Neurotrophins also have a role in nerve repair following

injury (as reviewed by - Ebadi et al., 1997). Sensory axons from DRG are guided by one of the most well known, classical neurotrophins – NGF which is expressed by targets of sensory axons and also by intermediate tissues to guide them along their pathway (Wyatt et al., 1990). Since the identification of NGF, a number of other structurally related neurotrophins have been identified with the use of blocking antibodies and gene targeting systems, including: brain derived neurotrophic factor (BDNF), neurotrophin-3 (NT3), and neurotrophin 4/5. It is understood that one or a combination of these factors may promote survival of a specific collection of embryonic sensory neurons (Paves and Saarna, 1997).

Signalling via these neurotrophins is mediated by various neurotrophin receptors, of which there are 2 distinct forms. High affinity binding of the ligands occurs at the tyrosine kinase receptor family (Trk), of which there are 3 types - A, B, and C. NGF is the preferred ligand for trkA, while both BDNF and NT4/5 bind to trkB, and NT3 primarily interacts with trkC although it is able to bind to all 3 trk receptors (Barbacid, 1995).

Knockout mice, lacking either a specific receptor or ligand have shown that distinct classes of peripheral sensory neurons depend on specific neurotrophic factors. Ruit et al., (1992) demonstrated through *in vivo* administration of antibodies against NGF, that axons responding to NGF are small diameter sensory neurones which project to laminae I and II of the spinal cord, indicating that they have nociceptive/thermoreceptive roles. However, larger axons which project to the more ventral regions of the spinal laminae and therefore have proprioceptive functions, do not require NGF for survival. These axons depend instead on NT-3, which was identified with the use of knockout mice (Ernfors et al., 1994; Zhou and Rush, 1995). Thereby, trkA is expressed on the growth cones of NGF-dependent nociceptive nerve fibres (Averill et al., 1995; McMahon et al., 1994), while trkB and C are expressed on NT-3-dependent proprioceptive axons (Genc et al., 2004; Klein et al., 1994). Furthermore, trkB expressing nerve fibres dependant on BDNF indicates a subpopulation of intermediate-size mechanoreceptive neurons (McMahon et al., 1994). Downstream events following ligand binding lead to the internalisation of the receptor/ligand complex which has a local, stimulatory, effect on the actin filaments of the growth cone leading to extension of the filpodia and lamellopodia in the direction of the signalling molecule, but is also transported via microtubules to the cell body where it promotes cell survival (as reviewed by - Letourneau, 1996).

However, different neurotrophins act on developing sensory neurones at different time points determining not only their survival, but also their phenotype. A particularly striking example is the switch in nociceptive nerve fibres which do not contain neuropeptides (isolectin B4 (IB4) positive fibres). During embryonic development IB4 positive neurons are dependent on NGF and express *trkA*, however following 2 days of postnatal development, *trkA* expression is down-regulated and the growing axons are no longer dependent on NGF, but instead become dependent on another family of neurotrophins - the glial cell line-derived neurotrophic factor (GDNF) family - and express the corresponding receptor, GDNF family receptor (GFR) $\alpha 1$. In contrast, nerve fibres that continue to depend on NGF and express *trkA* following 2 postnatal days of development become peptidergic (SP) fibres with a nociceptive function (Molliver et al., 1997).

Inhibitory molecular signals also play an important role in guiding sensory neurons to their targets. The semaphorin family are among the best characterised repellent factors and *Sema3A* (also known as collapsin -1) is a potent factor which repels and leads to the collapse of growth cones on sensory axons (Luo et al., 1993; Messersmith et al., 1995) through binding with its receptor complex containing the glycoprotein - neurophilin-1 (He and Tessier-Lavigne, 1997). Wright et al., (1995) demonstrated that during development of the rat embryo *Sema3A* mRNA is spatially and temporally expressed in the peripheral mesoderm to guide sensory DRG axons to their targets. *Sema3A* functions through binding with its receptor, thereby initiating downstream signals which rapidly induce depolymerisation of the actin cytoskeleton within the leading edge of the growth cone. As a result of this cytoskeletal reorganisation, the growth cones exhibit a thin, needle-like shape and cease to draw the axon with them due to lack of traction (Fan et al., 1993).

In a similar manner to neurotrophins, temporal expression *Sema3A*, and the neurophilin-1 subunit of the *Sema3A* receptor expressed by neurons plays an important part in controlling patterning of sensory neurons. The sensitivity of the growth cones to *Sema3A* is increased by up-regulation of neurophilin-1, or decreased through loss of neurophilin-1. This controls the timing and final location at which sub-populations (NGF and NT dependent neurons, respectively) of sensory axons invade and terminate in spinal cord. It is further proposed that a similar mechanism may function in the periphery (Pond et al., 2002).

It has been indicated that adipose tissue releases several neurotrophic factors including NGF (Peeraully et al., 2004) and adipocyte derived angiopoietin – 1 (Kosacka et al., 2006) which have chemoattractive effects on axons thus supporting the hypothesis that nerves may be attracted to innervate the adipose tissue located at entheses. In contrast however, Sema3A may play a role in inhibiting innervation of the Achilles enthesis during development.

Nonetheless, it must be remembered that the ECM also has a significant effect on axonal outgrowth. A permissive substrate must be present for growth cone filopodia to attach to and this occurs through the presence of cell-surface molecules such as integrins and cadherins expressed on the membrane of the growth cone. These cell-surface molecules anchor to the polymerising actin cytoskeleton at the leading edge of the growth cone, therefore holding it in place, and exerting traction on the developing axon, which subsequently increases in length. Studies have identified the ECM molecule laminin to be a highly permissive substrate to which growth cones bind (Dodd and Jessell, 1988; Gundersen, 1987). Of particular interest are the ECM molecules - proteoglycans which are able to act as both permissive and inhibitory substrata in the CNS and PNS during development (Bovolenta and Feraud-Espinosa, 2000) for a review). If such an inhibitory substratum is present, then anchorage of the filopodia does not occur and the filopodia will retract, causing the growth cone to turn and grow in a more permissive direction. Aggrecan is one such proteoglycan which has an inhibitory effect on nerve growth from DRG (Johnson et al., 2002; Snow and Letourneau, 1992)}. These authors demonstrated that aggrecan isolated from the intervertebral disc inhibits nerve growth *in vitro* in a dose dependent manner. This resulted in the suggestion that loss of aggrecan in the degenerating central cartilaginous region of the IVD results in the invasion of nerve fibres which are believed to cause pain in some chronic back conditions (Freemont et al., 2002a; Freemont et al., 2002b; Johnson et al., 2002) and the hypothesis that aggrecan in the fibrocartilage of the Achilles tendon enthesis may inhibit nerve growth in a similar manner.

10.2. MATERIALS AND METHODS

10.2.1. Source of Material

Pregnant female white Wistar rats were obtained from accredited commercial suppliers at 16 days after fertilisation and maintained at Cardiff University until parturition. Neonatal rats were killed by cervical dislocation 7 days postpartum. Three 12-17 week Wistar rats were obtained as described previously (see chapter 3.2).

10.2.2. Dissection Procedure

Adult rats were killed with an overdose of carbon dioxide while neonates were stunned and then killed by cervical dislocation. Under sterile conditions, using a dissecting microscope (Olympus SZ40, Southall, UK) both DRG at L4 and L5 were removed following exposure by removing the dorsal part of the spinal cord. Dissected ganglia were subsequently immersed in L15 dissecting media (see appendix I) and the connective tissue capsule was removed from the DRG with the use of fine tungsten needles and the ganglia were subsequently placed in Ham's F12 washing media (see appendix I).

A single incision was then made along the medial side of the ankle. The fat pad was then removed from the ankle of the rats and placed in L15 dissecting media. The tendon, presumptive Achilles enthesis fibrocartilage and the enthesis fibrocartilage from adult rats were then obtained and placed in L15 dissecting media.



Figure 10.2.2.1: Sterile setup for removal of DRG and the fat pad and fibrocartilage of the Achilles tendon enthesis organ.

10.2.3. Culture Procedure

Growth factor reduced - phenol red free, Matrigel[®] (BD Biosciences Discovery Labware; Fred Baker, Runcorn, UK) was thawed overnight, at 4°C, to a viscous liquid, then kept on ice throughout the procedure. 100µl of Matrigel[®] was pipetted (using cooled pipettes) into the centre of a well in a cooled 12 well plate (Corning; Fisher Scientific, Loughborough, UK – Fig 10.2.A). A DRG was then placed into the centre of the Matrigel[®] droplet and on either side of the DRG, the retromalleolar fat pad, tendon or the enthesis (see Table 10.2.1) were placed within the Matrigel[®] (Fig 10.2.B). Control cultures contained DRG only (Fig 10.2.C). The plates were then placed in an incubator (Forma Scientific, Marietta, OH, USA) for 10 minutes to ensure the Matrigel[®] solidified into a gel. 1ml of F14 growth medium (see appendix) was then added gently into the well, taking care not to disturb the culture. The plates were then incubated at 37°C in a CO₂ regulated humidified incubator (Forma Scientific, Marietta, OH, USA). Phase contrast images of the cultures were captured using a digital CCD camera mounted on an inverted microscope (Olympus IX-81F, Olympus UK Ltd, London) for the next 13 days. The protocol was modified from Lumsden and Davies (1983).

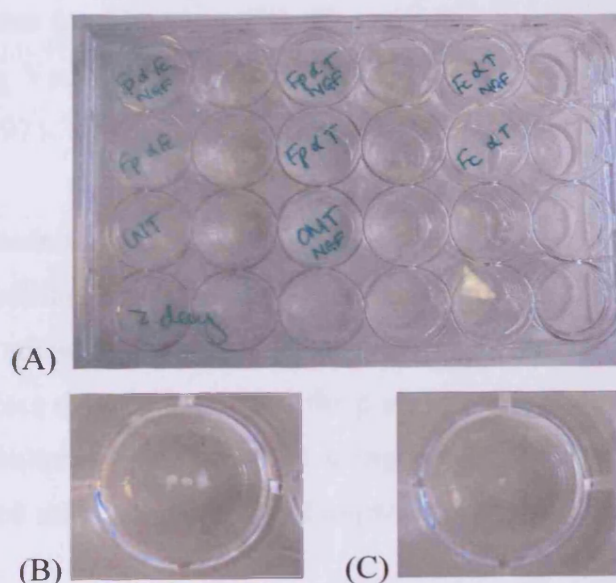


Figure 10.2.3.1: (A) 12 well plate containing DRG co-cultures, (B) DRG co-culture from the 7 day rat containing fat pad and fibrocartilage. (C) Control culture containing a DRG only.

	FP against FC	FP against T	FC against T	Control
Neonate	n = 11	n = 3	n = 3	n = 6
Adult	n = 6	n = 0	n = 0	-

Table 10.2.3.1: The number and character of co-cultures used during this experiment. FP – Fat pad, FC – Fibrocartilage, T – Tendon.

10.2.4. Immunohistochemistry

Cultures were fixed in 4% paraformaldehyde for 1.5 hours at 37°C and subsequently washed with 0.1M PB. The cultures were then blocked in 3% (w/v) BSA containing 0.1% triton-x for 1 hour at 4°C. The primary antibody – NF200 (Sigma-Aldrich, Gillingham, UK) - diluted to a concentration of 1:1000 in 3% BSA was incubated on the cultures overnight at 4°C. The following day the cultures were washed 5 times in 0.1M PB on an orbital shaker (SO1, Stuart Scientific, Redhill, Surrey, UK). During this process the plates were wrapped in silver foil to protect from the light. The secondary antibody (swine anti-rabbit FITC, Dako UK, Ely, Cambridgeshire, UK) diluted to 1:100 in 3% BSA was incubated on the cultures for 2 hours at 4°C. The cultures were washed again overnight and finally mounted using Vectorshield (Vector Labs, Peterborough, UK). Protocol modified from Tonge et al., (1997).

10.2.5. Oil Red - O Staining

Following immunolabelling, plates were washed three times with dH₂O and 1ml of Oil Red - O dye solution was added to each well. The dye was incubated on the cultures for 1.5h, following this the excess dye removed, and the plate was washed 3 times in dH₂O. Bright field images of the cultures were captured using a digital Nikon coolpix 4500 camera mounted on an inverted microscope (Nikon Eclipse TS100; Jencons – PLS, East Grinstead, UK).

10.3. RESULTS

Neonatal Targets

Day 2

Axonal outgrowth was observed on the 2nd day of culture, where a small number of axons could be seen to branch out from the DRG. The axons projecting from the ganglion could clearly be seen to have elaborate arborisations at the peripheral terminal of the axon (Fig 10.3.1.A). Axonal outgrowth was first seen in cultures where the target tissues were situated closest to ganglia, and in the majority of cases axonal growth was directed towards both of the target tissues (Fig 10.3.1.B). It was noted that at this point the tendon attachment did not inhibit neurite outgrowth from the ganglia (Fig 10.3.1.B). A small number of DRG within the co-cultures failed to show any axon outgrowth. This was seen more frequently in the cultures containing the fat pad and the tendon attachment site, while it was less frequently observed in those cultures which contained tendon and either the fat pad or the tendon attachment.

Day 3

On the 3rd day in culture, the number of axons projecting from the ganglia increased and the axons themselves were considerably longer and their growth was still directed towards the targets. By viewing the cultures by phase contrast microscopy, qualitative assessment indicated that the axons had no particular preference towards the fat pad and in many cases the axons grew preferentially towards the tendon attachment (Fig 10.3.1.C and D). Similar observations were also observed in cultures where fat pad and the tendon were placed in culture together – i.e the axons grew preferentially towards the tendon over the fat pad (Figs 10.3.1.E and F).

Day 6

On the 6th day in culture, the axons were considerably greater in number. This highlighted the observations made previously that axons from the ganglia grew preferentially towards the tendon (Fig 10.3.1.G) and the tendon attachment (not shown). In contrast however, although the number of axons growing towards the fat pad increased, these axons had not increased in length and the terminal projections of the axons rounded up. Therefore no contact could be seen between the fat pad and the axons growing from the ganglion (Fig 10.3.1.G).

Day 10-13

During the final stages of culture, no significant differences were observed from the previous stage apart from a continued increase in the number of axons projecting from the ganglia. The inhibition of axon elongation towards the fat pad was particularly prominent at this stage, while axons continued to elongate towards the tendon and the tendon attachment (Fig 10.3.2.A). As described previously, the peripheral terminals of the axons which grew out towards the fat pad rounded up. At high power, it was seen that the peripheral parts of the axon had undergone considerable arborisation, and that the terminals of these branches were round (Fig 10.3.2.B).

A number, but not all, of the axons within the culture were positively immunolabelled for NF200 (Figs 10.3.2.C and D). These axons grew towards the tendon attachment (Figs 10.3.2.C and D) but did not appear to pass into the tissue itself, but around and under it (Figs 10.3.2.E and F). A number of the axons growing towards the fat pad were also positive for NF200 (Figs 10.3.3.A and B). This confirmed that the axons grew towards the fat pad but stopped elongating a short distance away from the tissue (Figs 10.3.3.A - C). In some cultures, the axons grouped together into bundles to grow towards their targets (Fig 10.3.3.D). Where axonal growth occurred in the opposite direction to the targets, the axons did not grow in a uniform direction but grew randomly and changed direction a number of times (Fig 10.3.3.E). At high power, the NF200 axons within the culture were seen to branch several times (Fig 10.3.3.F) and in a single case case, one branch went toward the tendon attachment target while another was directed towards the fat pad (not shown).

However, by 13 days in culture a number of cells had migrated out of the tissue explants into the Matrigel[®]. These cells could be seen around the tendon, tendon attachment and the fat pad explants (Fig 10.3.4.A and B). The cells had a varied morphology, some where fibroblast-like with multiple spindle-like extensions, while others contained lucent droplets which stained positive for lipid in oil red O staining (Fig 10.3.4.C and D). The size and number of which varied between cells (Fig 10.3.4.B and D). It was also observed in the majority of cultures that a large number of cells within both the tendon (Fig 10.3.4 E and F) and the tendon attachment (Fig 10.3.4.G and H) contained large numbers of lipid droplets within the tissue itself. Lipid containing cells were present in the tendon or tendon attachments irrespective of whether a fat pad explant was present in the culture, although the numbers of lipid containing cells were considerably fewer where the fat pad was absent.

Adult Targets

Day 2-3

As above, no axonal outgrowth was observed on the 1st day in culture (not shown), however by day 2 outgrowth was seen predominately towards the fibrocartilage of the Achilles tendon enthesis in 3 out of the 6 cultures (Fig 10.3.5.A and B). In the other 3 cultures no outgrowth was observed. On the 3rd day in culture, where outgrowth was seen, axon growth continued preferentially towards the fibrocartilage in 1 co-culture (Fig 10.3.5.C). At this stage the other cultures illustrated no preferential axon outgrowth.

Day 6 - 10

With increasing time in culture the number and length of axons projecting from the DRG increased. On the 6th day in culture the axons which grew towards the fibrocartilage could be seen to grow around the explant (Fig 10.3.5.D). The axons growing towards the fat pad did not elongate as close towards the explant (Fig 10.3.5.E). On the 10th day in culture this pattern was seen clearly in all cultures where axon growth occurred. The axons growing towards the fat pad stopped elongating and avoided the tissue, while the axons growing towards the fibrocartilage were not inhibited but grew around the explant (Fig 10.3.5.F).

Day 13

This pattern of axon outgrowth was confirmed on the 13th day in culture with the use of immunolabelling for neurofilament 200 (Fig 10.3.6.A-D).

Although a small number of migrating cells containing lipid droplets were seen within the cultures with adult targets (not shown), the fibrocartilage explants themselves were not invaded with lipid-containing cells (Fig 10.3.6.E and F).

Controls

Five out of the 6 control cultures in which the DRG cultured alone (no target tissues) did not show any axonal outgrowth (Fig 10.3.7.A). The one DRG which did show axonal outgrowth, sent out projections of uniform size in all directions. Negative controls for a culture stained with oil red – O confirmed that no non-specific labelling occurred in the culture (Fig 10.3.7.B). PB (10.3.7.C and D) and rabbit IgGs (10.3.7.E and F) were applied to cultures to indicate that no non-specific labelling occurred in the cultures, although autofluorescence was particularly strong in the tissue explants.

TARGET DERIVED NERVE GROWTH – NEONATAL TARGETS

Phase contrast images of the first 6 days of competitive nerve growth *in vitro*.

Figure A: An axon protruding from a dorsal root ganglion (DRG) on the 2nd day in culture towards a fat pad (FP). Note the numerous arborisations at the peripheral terminal of the axon (arrow). Day 2. Scale bar = 100µm.

Figure B: Numerous axons protruding from the dorsal root ganglion (DRG) towards both the tendon attachment (TA) and the fat pad (FP). Note that the TA did not inhibit neurite outgrowth. Day 2. Scale bar = 100µm.

Figure C and D: Axons (arrows) growing from the dorsal root ganglion (DRG) towards the fat pad (FP in C) and the tendon attachment (TA in D). There was no obvious preference for axons to grow towards the FP, while axons grew in large numbers towards the tendon attachment. Day 3. Scale bar = 100µm.

Figure E: Axons growing preferentially (arrow) from the dorsal root ganglion (DRG) towards the tendon (T) over the fat pad (FP). Day 3. Scale bar = 200µm.

Figure F: Axons growing preferentially (arrow) from the dorsal root ganglion (DRG) towards the tendon (T) over the fat pad (FP). Day 3. Scale bar = 200µm.

Figure G: Axons growing from the dorsal root ganglion (DRG) towards the fat pad (FP) increased in number but did not increase in length (black arrow), while axons growing towards the tendon (T) continued to grow in length and in number (white arrow) from the previous stage. Day 6. Scale bar = 200µm.

Figure 10.3.1.

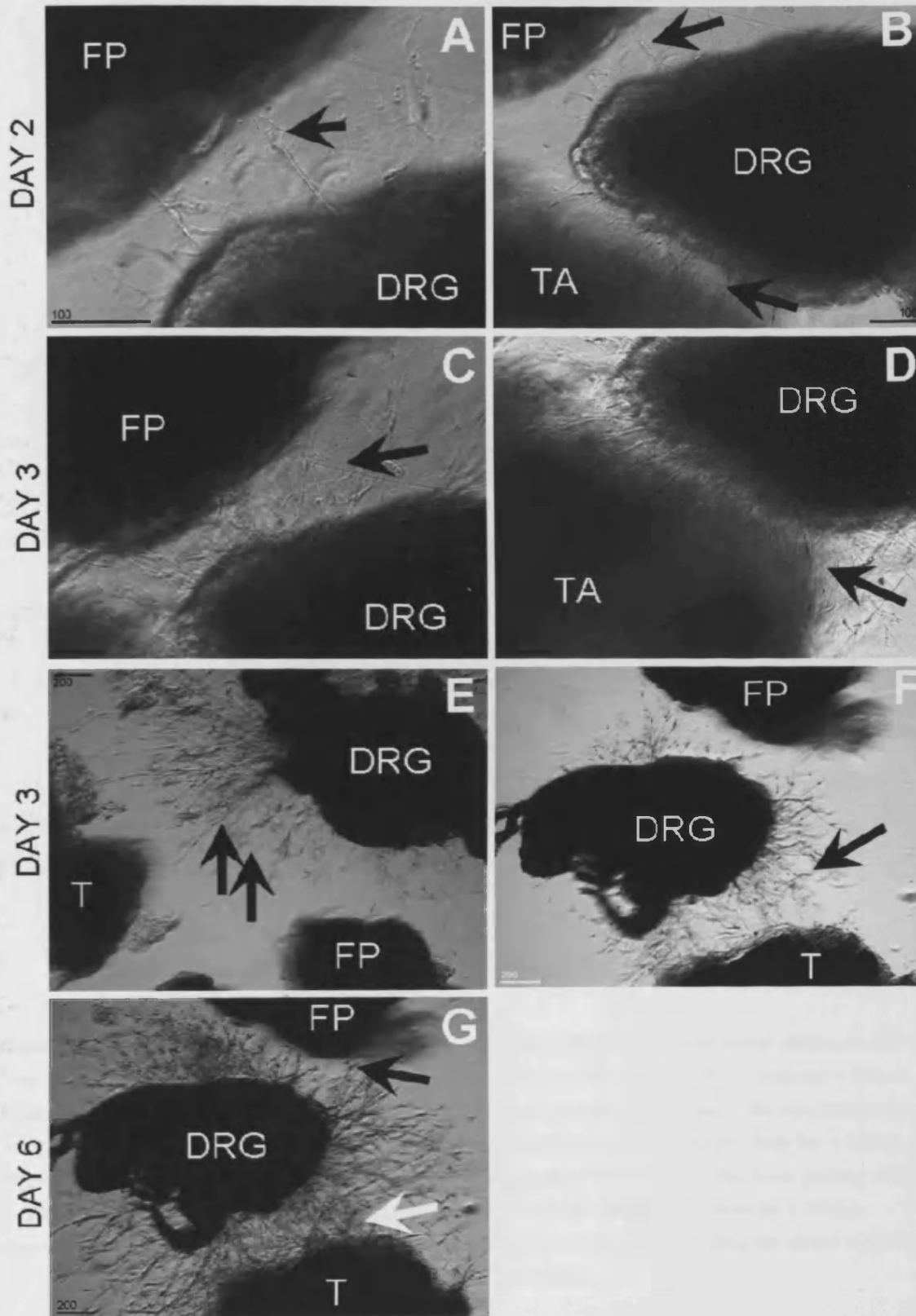
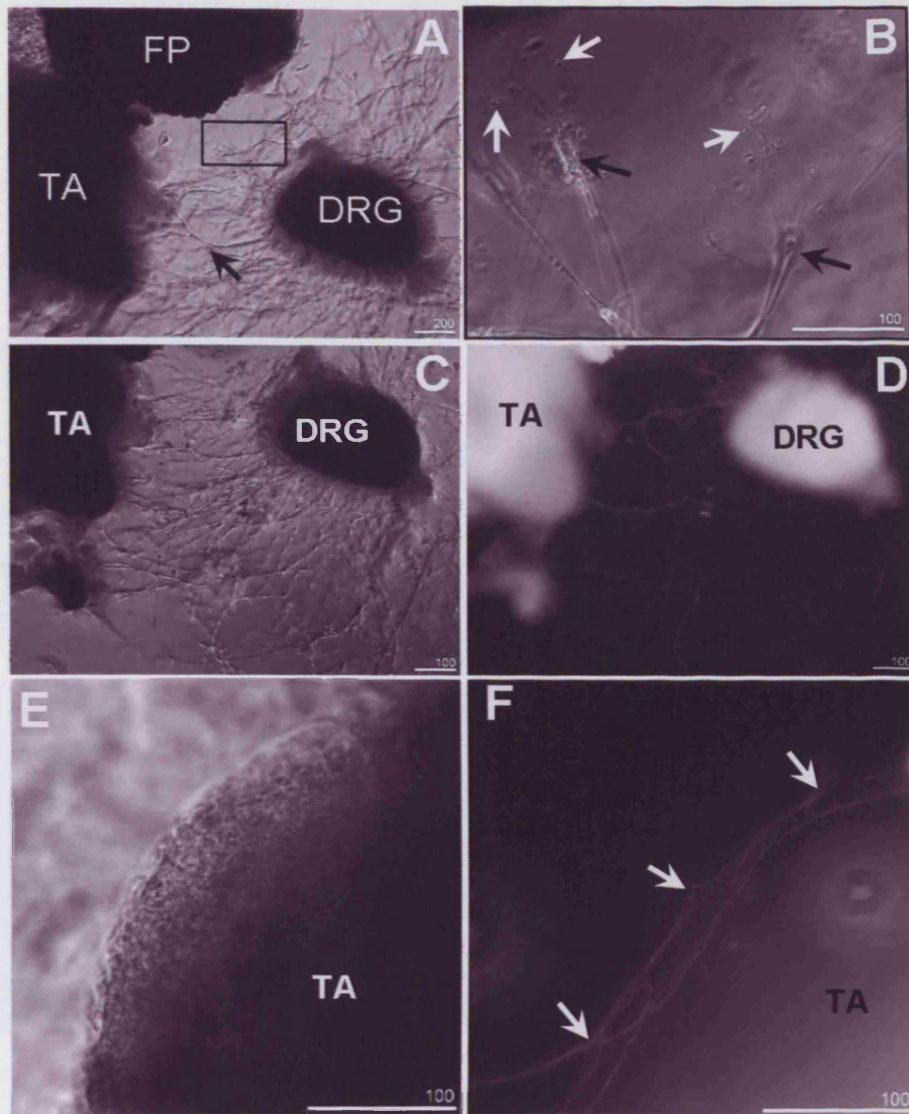


Figure 10.3.2.



TARGET DERIVED NERVE GROWTH – NEONATAL TARGETS

Phase contrast and fluorescence images of day 13 of competitive nerve growth *in vitro*.

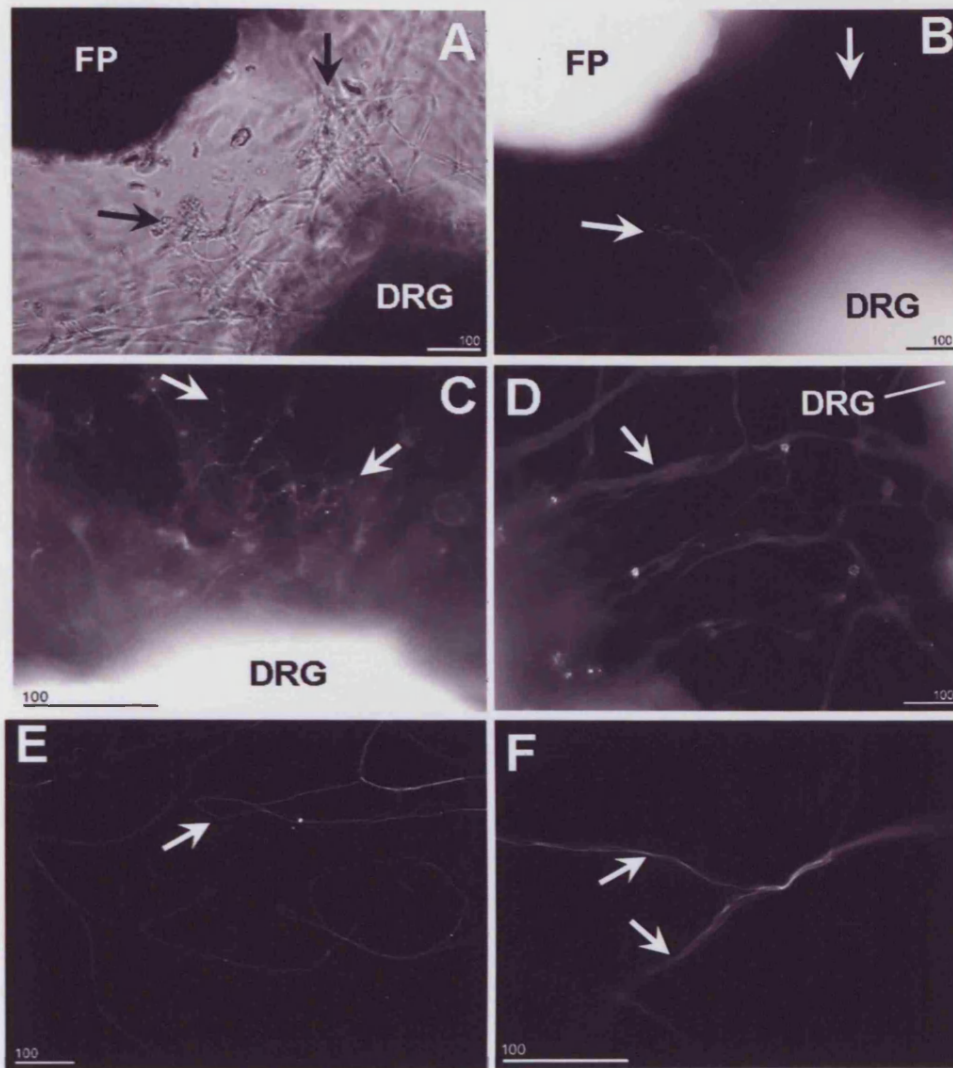
Figure A: Axons from the dorsal root ganglion (DRG) grew preferentially towards the tendon attachment (TA - arrow). Note that the axons growing towards the fat pad stopped elongating towards the target (box). Scale bar = 200µm.

Figure B: High power view of the region highlighted in A. Note the peripheral terminal of the axon (black arrows) gives rise to a large number of fine arborisations (white arrows) which end in a rounded structure. Scale bar = 100µm.

Figure C and D: Phase contrast (C) and corresponding fluorescence (D) image of the axons growing preferentially towards the tendon attachment (TA). Neurofilament 200. DRG – dorsal root ganglion. Scale bar = 100µm.

Figure E and F: Phase contrast (A) and corresponding fluorescence image (B) illustrating the growth of axon over the surface of the tendon attachment. Neurofilament 200. Scale bar = 100µm.

Figure 10.3.3.



TARGET DERIVED NERVE GROWTH – NEONATAL TARGETS

Phase contrast and fluorescence images of day 13 of competitive nerve growth *in vitro*.

Figure A and B: Phase contrast (E) and corresponding fluorescence (F) image of the axons (arrows) which stopped growing towards the fat pad (FP). Neurofilament 200. DRG – dorsal root ganglion. Scale bar = 100µm.

Figure C: Neurite terminals growing towards the fat pad from the dorsal root ganglion (DRG). Note the irregular appearance of the axons towards their peripheral terminals (arrows). Neurofilament 200. Scale bar = 100µm.

Figure D: Co-culture immunolabelled for neurofilament 200 to illustrate positively labelled axons growing from the dorsal root ganglion (DRG) towards the tendon (T). Note that the axons follow 3 main pathways (arrows) towards the tendon. Scale bar = 100µm.

Figure E: Co-culture immunolabelled for neurofilament 200 to illustrate positively labelled axons (arrows) growing in a random, disorganised fashion in the opposite direction from the targets. Scale bar = 100µm.

Figure F: High power view of a neurofilament 200 positive axon branching (arrows) towards a target. Scale bar = 100µm.

TARGET DERIVED NERVE GROWTH – NEONATAL TARGETS

Phase contrast and oil red O stained bright field images of day 13 of competitive nerve growth *in vitro*.

Figure A: Phase contrast image of cells containing several lucent droplets (arrows) surrounding the adjacent regions of the tendon attachment (TA) and the fat pad (FP). Scale bar = 200 μ m.

Figure B: Oil red – O stained culture to illustrate the presence of lipid droplets within the cells located between and around the tissue explants. Scale bar = 500 μ m.

Figure C: Phase contrast image of numerous cells migrated from the tissue explants into the surrounding Matrigel[®]. These cells had various morphologies from fibroblastic spindle-like cells (white arrow) to more rounded cells containing several lucent droplets of various sizes (black arrow). Scale bar = 200 μ m.

Figure D: Oil red – O stained culture to illustrate the presence of lipid droplets within the rounded cells (black arrow) migrated from the tissue explants. Scale bar = 200 μ m.

Figure E: Phase contrast image of a tendon (T) explant in a co-culture containing a large number of cells with lucent droplets (arrow). Scale bar = 100 μ m.

Figure F: Oil red – O stained culture to illustrate the presence of lipid droplets within and surrounding the tendon explant. Scale bar = 500 μ m.

Figure G: Phase contrast image of a tendon attachment in a co-culture. Several cells within the tendon attachment contained cells with numerous lipid droplets (arrows). Scale bar = 100 μ m.

Figure H: Oil red – O stained culture to illustrate the presence of lipid droplets (arrow) within cells in the tendon attachment explant. Scale bar = 200 μ m.

Figure 10.3.4.

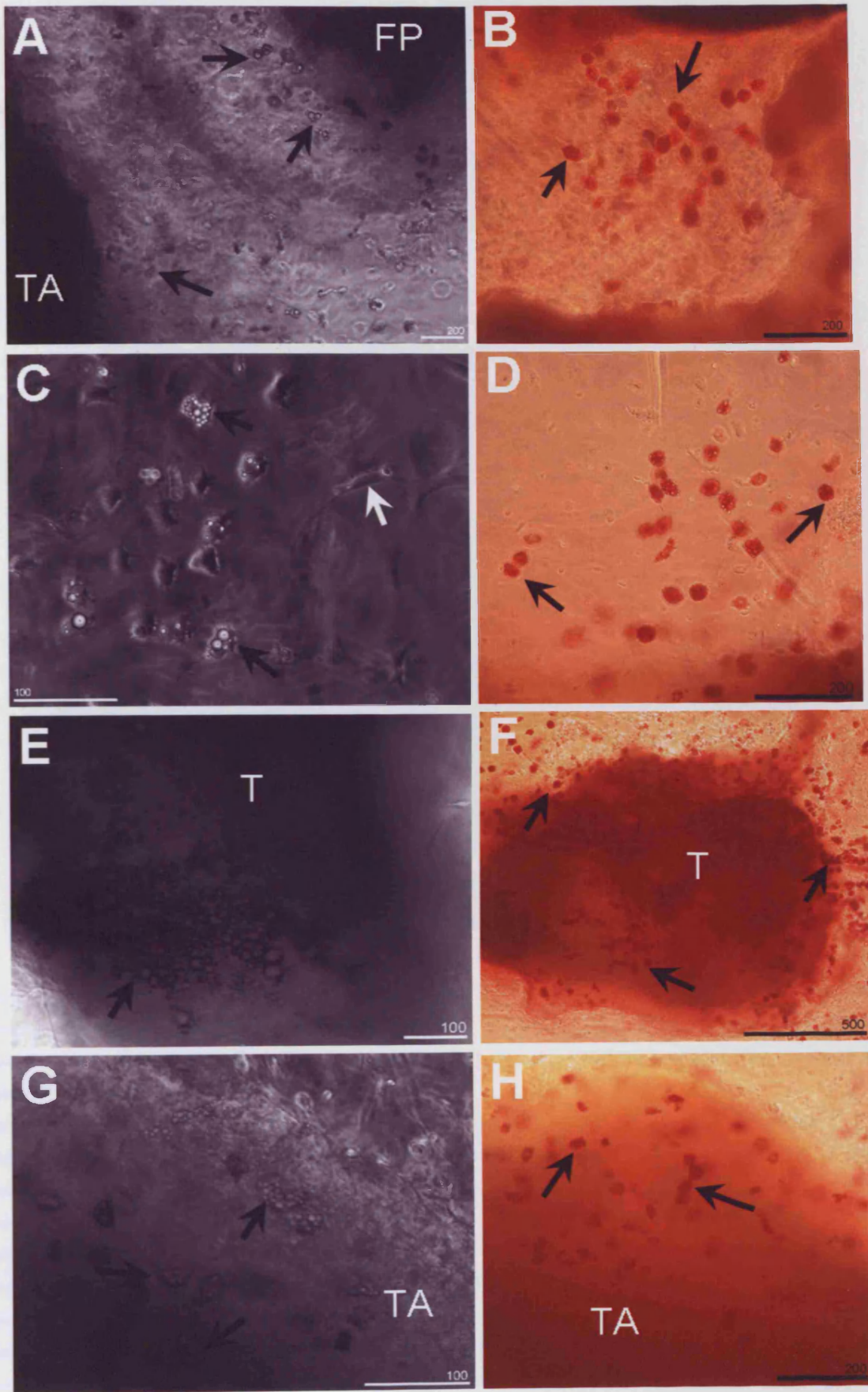
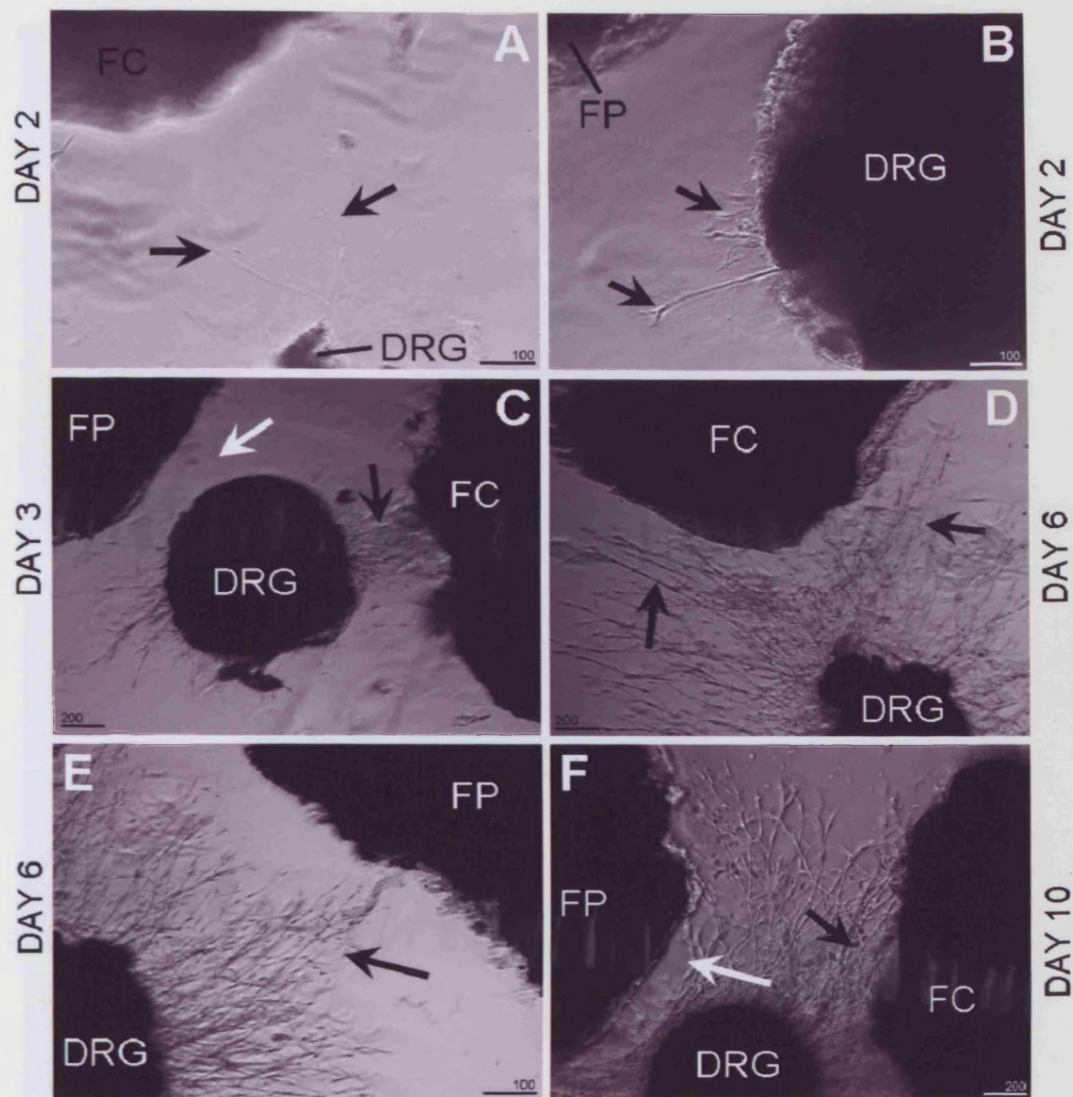


Figure 10.3.5.



TARGET DERIVED NERVE GROWTH – ADULT TARGETS

Phase contrast images of first 6 days of competitive nerve growth *in vitro*.

Figure A: Axons (arrows) growing from the dorsal root ganglion (DRG) towards a fibrocartilage (FC) explant from the Achilles tendon enthesis organ. Day 2. Scale bar = 100µm.

Figure B: Axons (arrows) from the dorsal root ganglion (DRG) growing away from an explant from the retromalleolar fat pad (FP). Day 2. Scale bar = 100µm.

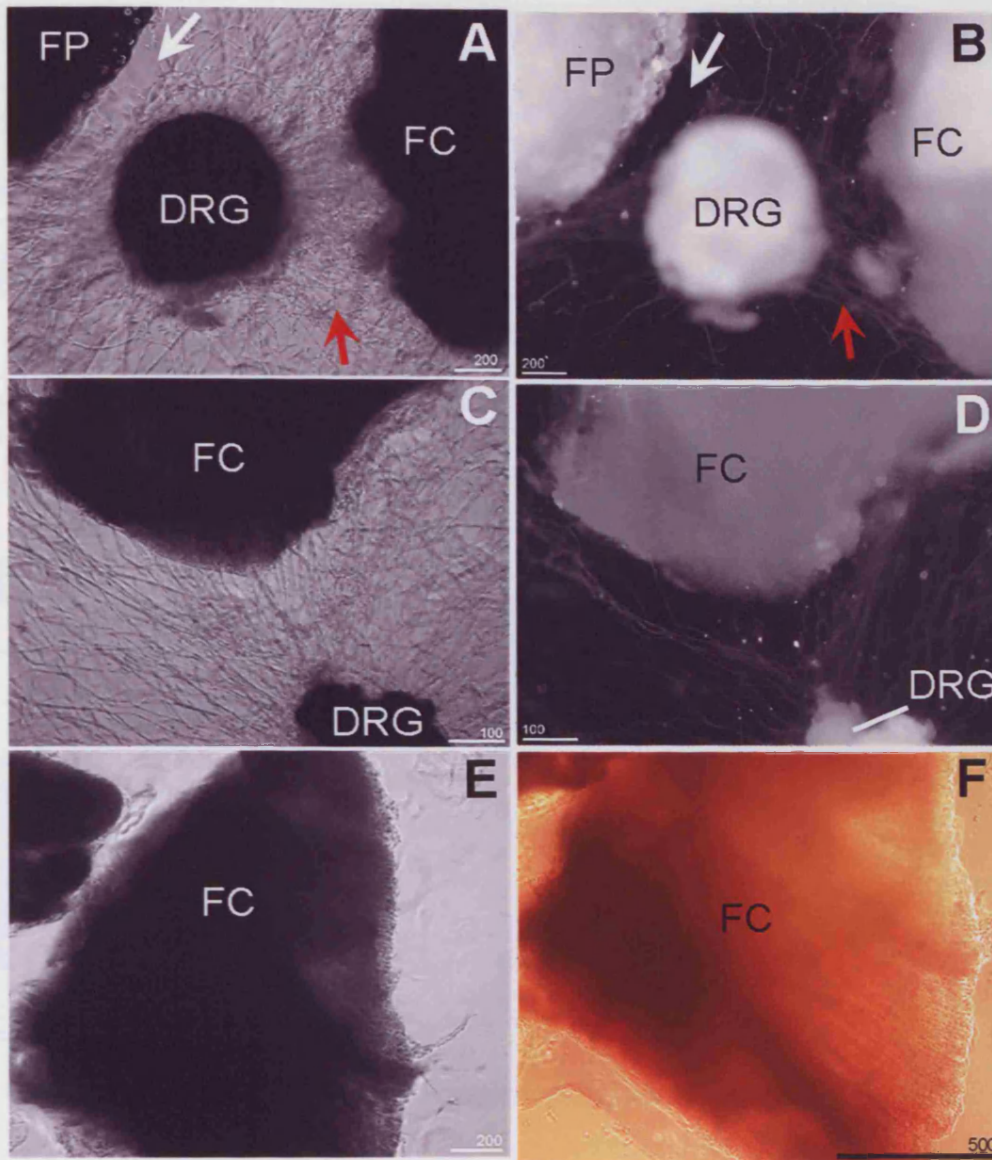
Figure C: Axons from the dorsal root ganglion (DRG) growing preferentially towards the fibrocartilage (FC) of the tendon attachment (black arrow) over an explant from the retromalleolar fat pad (FP – white arrow). Day 3. Scale bar = 200µm.

Figure D: Axons (black arrows) growing from the dorsal root ganglion (DRG) around the fibrocartilage (FC) of the Achilles tendon enthesis. Day 6. Scale bar = 200µm.

Figure E: Axons (arrow) growing from the dorsal root ganglion (DRG) towards the fat pad (FP). Note the axons unlike those in figure E do not extend to the fat pad. Day 6. Scale bar = 100µm.

Figure F: Axons growing from the dorsal root ganglion (DRG) following 10 days of culture. White arrow indicates that axons are no growing towards the fat pad while they do grow towards the fibrocartilage (FC). Scale bar = 200µm.

Figure 10.3.6.



TARGET DERIVED NERVE GROWTH – ADULT TARGETS

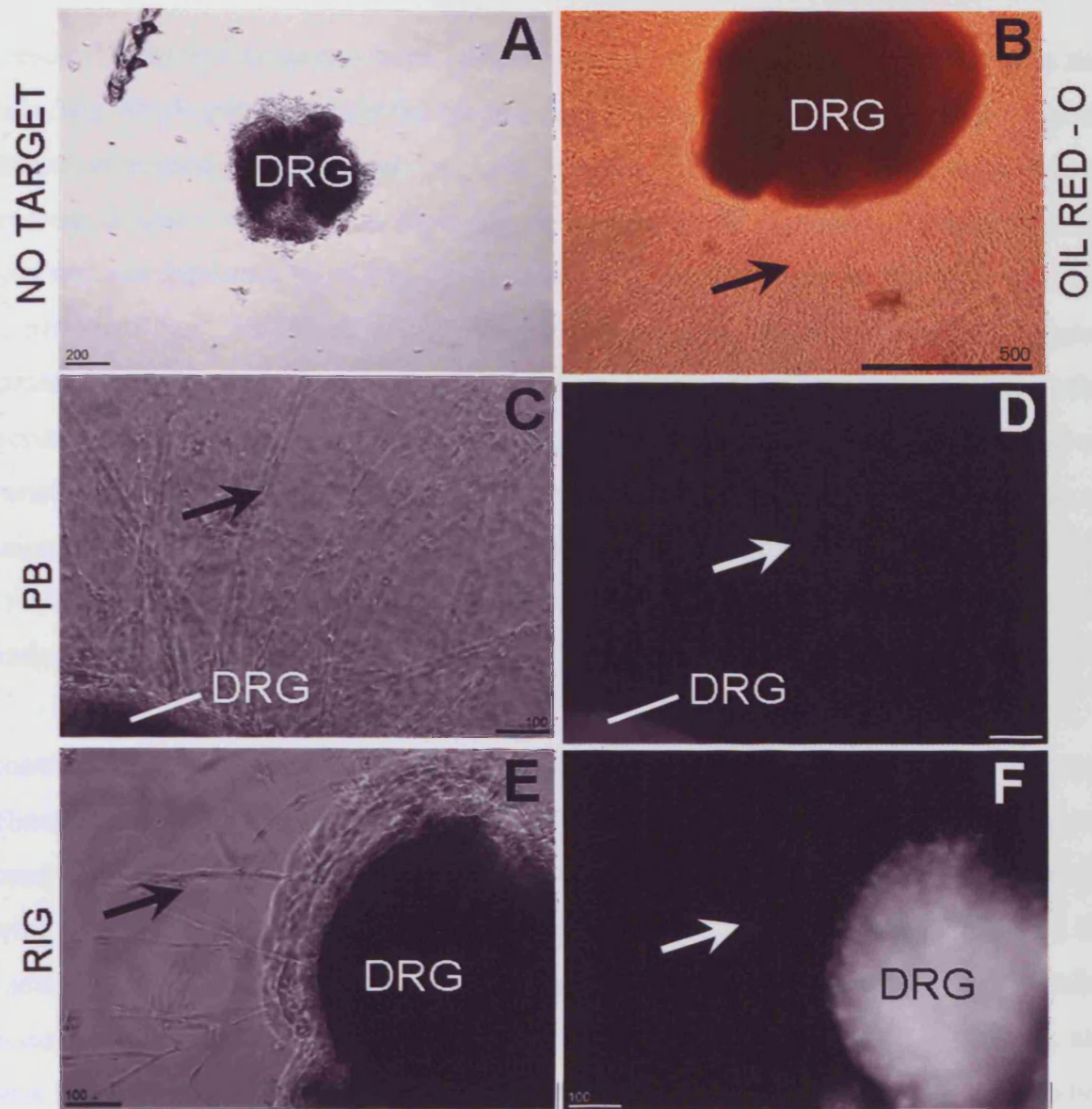
Phase contrast, fluorescence and bright field images from 13 days of competitive nerve growth *in vitro*.

Figure A and B: Phase contrast (A) and corresponding fluorescence (B) image to illustrate axons growing towards and around (red arrow) the fibrocartilage (FC) explant and avoiding (white arrow) the fat pad (FP) explant. DRG - dorsal root ganglion. Scale bar = 200μm.

Figure C and D: Phase contrast (C) and corresponding fluorescence (D) image to illustrate axons growing towards but around a fibrocartilage (FC) explant. DRG - dorsal root ganglion. Scale bar = 100μm.

Figure E and F: Phase contrast (E) and corresponding brightfield images of an oil red – O stained culture (F) to illustrate the absence of cells containing lipid within and surrounding a fibrocartilage (FC) explant from the Achilles tendon enthesis. Scale bar = (E) 200μm and (F) 500μm.

Figure 10.3.7.



TARGET DERIVED NERVE GROWTH – CONTROLS

Phase contrast, fluorescence and bright field images from 13 days of competitive nerve growth *in vitro*.

Figure A: Dorsal root ganglion (DRG) without any targets. Note the absence of axon outgrowth from the ganglion. Day 13. Scale bar = 200µm.

Figure B: Oil red - O stained culture containing only a dorsal root ganglion (DRG). Note the absence of lipid containing cells in this explant. However, in this culture axons grew out uniformly from the entire ganglion. Day 13. Scale bar = 500µm.

Figure C and D: Phase contrast (C) and corresponding fluorescent (D) images of cultures where phosphate buffer (PB) was applied to the section in place of the primary antibody to illustrate there was non non-specific labelling present. Note the autofluorescence of the dorsal root ganglion (DRG) explant. Scale bar = 100µm

Figure E and F: Phase contrast (E) and corresponding fluorescent (F) images of cultures where rabbit immunoglobulins (RIG) were applied to the culture in place of the primary antibody to illustrate non non-specific labelling of the primary antibody was occurring. Note the autofluorescence of the dorsal root ganglion (DRG) explant. Scale bar = 100µm.

10.4 DISCUSSION

The results illustrate that axons from DRG are not preferentially attracted to adipose tissue and neurites which grew towards the fat pad stopped elongating a short distance away from the tissue, at around 6 days in culture. These observations were made for tissue explants taken from animals at 7 days postpartum and adult tissue explants. Furthermore, axon growth was not inhibited by either the neonatal tendon attachment or the fully developed adult fibrocartilage. However, the axons growing towards the enthesis did not appear to penetrate the tissue but grew around it. These results therefore reject the hypothesis suggested denoted at the beginning of this chapter. In addition, it was observed that non-neuronal cells migrated out of the target tissue explants, and the majority of these cells contained lipid droplets. Lipid containing cells were identified within the neonatal tendon and tendon attachment explants but not in the adult fibrocartilage explants, in fact fewer migrating cells were seen in cultures containing adult explants.

In contrast to the original expectation, axons grew preferentially towards the tendon attachment, or fibrocartilage of the Achilles tendon enthesis. These observations are in contrast to the suggestion made by Johnson et al., (2002) in which axons are inhibited from growing over the ECM molecule - aggrecan isolated from the intervertebral disc, and those by Lidslot et al., (2000) who illustrated that explants from the nucleus pulposus inhibited axon outgrowth. However, it has been shown that with increasing time in culture, axons are able to adapt to an inhibitory substratum such as aggrecan by increasing the number of integrin receptors expressed on the growth cone (Condic et al., 1999). This adaptation may be occurring in this co-culture system, allowing axon growth over the fibrocartilage explant. More recently however, Johnson et al., (2006) indicated that aggrecan, co-cultured with cells from the IVD, did not inhibit axon outgrowth as drastically but permitted axons to grow over the matrix. The authors suggest that this may be due to neurotrophins such as NGF released by chondrocytes, as identified by Gigante et al, (2003) in various cartilages including the intervertebral disc. Therefore, a combination of cell-secreted factors and inhibitory matrix may carefully control through - as yet unknown - complex mechanisms, axon guidance around but not necessarily into the tissue (Johnson et al., 2006). This may explain the observations made here in which the explants contain both cells and extracellular matrix, and therefore the axons are not inhibited from growing towards or over the fibrocartilage explant but their growth is controlled around it. Furthermore, it has

been demonstrated that significantly more chondrocytes in osteoarthritic cartilage from knee joints express NGF (Iannone et al., 2002). Although the authors suggest this is likely to play a role in cell metabolism and has no bearing on the innervation of the articular cartilage (Iannone et al., 2002), if the same increase in cells expressing NGF holds true for the enthesis, these cells may play a role in neo-innervation of the tissue under pathological conditions, as has been suggested in the IVD (Abe et al., 2007).

However, this does not explain the observations made concerning the tendon attachment prior to fibrocartilage differentiation. In contrast to the hypothesis, axons were attracted to the tendon attachment and grew around the explant, suggesting that this region does not express inhibitory factors such as Sema3A to inhibit nerve growth during development. It may be that the expression of inhibitory factors was down-regulated before the age at which this study was carried out, and therefore it may be interesting to identify in further research (possibly with the use of *in situ* hybridisation) the presence or absence of attractive or inhibitory neuronal factors during pre-natal development of the rat Achilles tendon enthesis organ.

It is well known that tendons are innervated (Ackermann, 2001; Ackermann et al., 1999), however, little is known about the developmental control of this innervation. The present study suggests that neurotrophins may be expressed by the tendon to attract nerve fibres towards it. Further studies are required to confirm this and identify which neurotrophins are involved although the presence of peptidergic and mechanoreceptive fibres (as identified previously – see chapter 3 and by Ackermann et al., (1999) suggests that NGF and BDNF may be implicated.

Although, as described above, several studies have demonstrated that adipose tissue expresses neurotrophins which attract axon outgrowth including NGF (Peeraully et al., 2004), it was demonstrated here that axons growing from lumbar DRG were inhibited by adipose tissue explants from the retromalleolar fat pad and the growth cones at the peripheral terminal of these axons appeared to round up following arborisation. This indicates that an inhibitory signal, such as Sema3A, was present within the adipose tissue that prevented further outgrowth of the axons. This correlates with the observations made by Giordano et al., (2003) who identified the expression of Sema3A from white adipocytes in rodent white adipose tissue, correlating with other studies which have demonstrated that

adipose tissue inhibits nerve growth during peripheral nerve regeneration (Weis and Schroder, 1989a; b). However, previous studies have demonstrated (see chapter 3) that the pre-adipocyte containing fat pad in the neonatal rat is highly innervated, therefore the fat pad may be specified to become innervated prior to differentiation of the adipocytes (although the exact time point is unknown), possibly through the higher expression of NGF from the pre-adipocytes (Peeraully et al., 2004). Following differentiation, NGF and Sema3A may carefully control the innervation and plasticity of nerve fibres within the fat pad preventing over-innervation (Giordano et al., 2003), which may also have a profound effect on the adipocytes themselves (Nijima, 1998). This may therefore explain the inhibition of nerve fibres growing towards the fat pad in this experiment as it was already innervated at birth - a mechanism which may be controlled through up-regulation of neurophilin-1 on the growth cones during this period of development (Pond et al., 2002); resulting in increased sensitivity to Sema3A released by differentiated adipocytes (Giordano et al., 2003). However this needs to be determined in further studies. It would also be interesting to understand the expression of the relative neurotrophins, semaophorins, and their receptors in adipose tissue in pathology of tendons and entheses, where adipose tissue accumulation is observed.

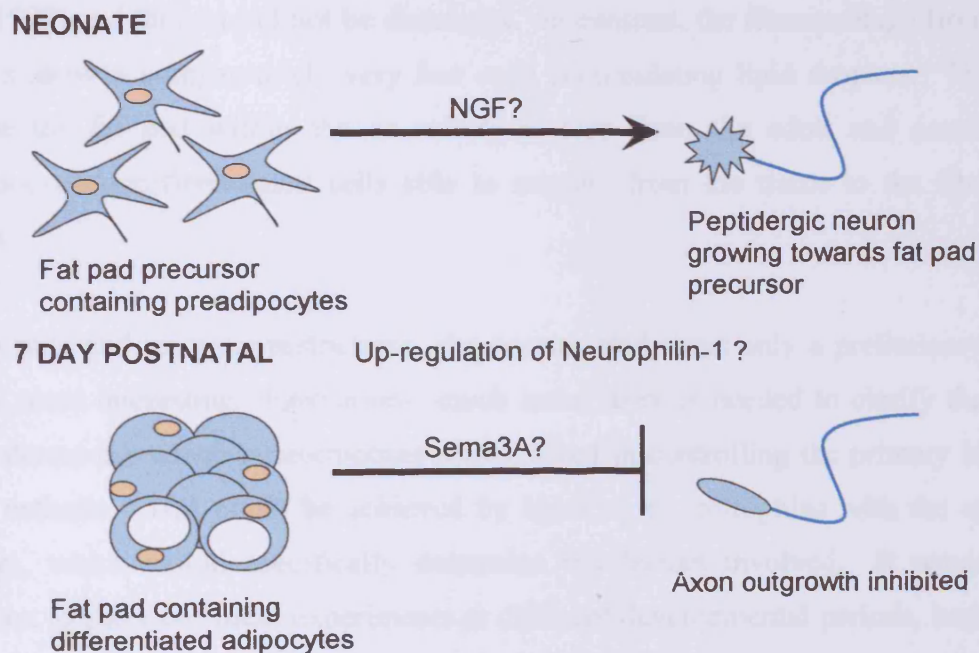


Figure 10.4.1: Proposed mechanism for the temporal regulation of the innervation of the retromalleolar fat pad.

It was also observed during this experiment that a number of cells migrated from the tissue explants into the surrounding Matrigel[®]. A large population of these cells contained large

and numerous lipid droplets suggesting they were differentiating adipocytes (Slavin, 1979). It is likely that these cells had migrated out of the fat pad explant. These migrating cells were more frequently observed in tissue cultures obtained from 7 day animals than adult explants; this may reflect that a larger number of pre-adipocytes are present within the developing fat pad than the mature fat pad. However, developing adipocytes were also observed within and around tendon and tendon attachment tissue explants. It is possible that pre/adipocytes attached to the explants were not removed during dissection and differentiated. This may not however, explain the large number of developing adipocytes within the tissue itself. It has recently been demonstrated that a large population of tendon fibroblasts isolated from human adolescent tendons have the ability to transdifferentiate into adipocytes in the presence of adipogenic media (de Mos et al., 2007). Furthermore, it is also understood that adipocytes are able to secrete large numbers of cytokines including adipogenic factors such as adiponectin (Fu et al., 2005); therefore the adipocytes from the fat pad within the co-culture may have stimulated the transdifferentiation of fibroblasts within the tendon and tendon attachment site. This may therefore have implications in understanding the pathogenesis of enthesopathies and tendonoses where lipid accumulation is frequently observed (de Mos et al., 2007; Jarvinen et al., 1997; Jozsa and Kannus, 1997). However, it is understood that connective tissue cells can accumulate lipid *in vitro* (Gordon et al., 1977) and this should not be dismissed. In contrast, the fibrocartilage from the adult enthesis showed comparatively very few cells accumulating lipid droplets. This may be because the fat pad within the co-culture is also from the adult and contains fewer preadipocytes/undifferentiated cells able to migrate from the tissue to the fibrocartilage explant.

Due to time and resource restrictions, the current study was only a preliminary one, and despite some interesting observations, much more work is needed to clarify the situation e.g. to determine which neurotrophins are involved in controlling the primary innervation of the enthesis. This could be achieved by blocking neurotrophins with the appropriate anti-sera, which would specifically determine the factors involved. It would also be important to carry out these experiments at different developmental periods, both pre- and postnatally, in order to find an explanation for some of the observations made here. In addition, quantification of the number and length of axon outgrowth would allow statistically based comparison between experiments.

In summary, this preliminary study has illustrated that there is a complex control mechanism over the innervation of the rat Achilles tendon enthesis organ. It appears that the precursor of the enthesis fibrocartilage, and the fibrocartilage of the enthesis itself do not release inhibitory signals to prevent innervation. It is likely that the innervation of the enthesis fibrocartilage is regulated by both the extracellular matrix and the cells within the tissue. Furthermore, the retromalleolar fat pad becomes innervated prior to adipocyte differentiation, and following this differentiation the fat pad releases inhibitory signals to growing sensory axons, possibly to prevent over-innervation of the fat pad.

11. GENERAL DISCUSSION

It is the purpose of this chapter is to bring together the different aspects of this thesis that for organisational reasons have been presented as separate chapters, discuss some of the clinical implications of the work and outline possible directions for further research. An attempt has been made to summarise the findings that have been presented in earlier chapters in such a way as to highlight the rationale underpinning the overall study design and the evolution of ideas.

Summary of findings – the progression of ideas and their clinical importance

As enthesopathies are known to be painful conditions, the study began with an extensive investigation into the innervation of the rat Achilles tendon enthesis organ. Somewhat surprisingly, this showed that the enthesis fibrocartilage and its associated sesamoid and periosteal fibrocartilages were aneural at all ages studied. In the ‘normal’ animal, it was thus clear that the avascular and aneural nature of the fibrocartilages paralleled that of articular cartilage (Kuettner and Pauli, 1983; Toynbee, 1841)} and other cartilaginous tissues – e.g. the nucleus pulposus of the intervertebral disc (McCarthy et al., 1991).

The only part of the rat Achilles tendon enthesis organ that was innervated was the retromalleolar fat pad. Previous studies had shown that the fat pad moves in and out of the retrocalcaneal bursa during foot movements (Canoso et al., 1988; Theobald et al., 2006) and the 3D reconstructions of the hindfoot presented in chapter 6 suggest that it but is compressed as these movements occur. Movement of the fat pad may stimulate nerve fibres within it and allow the fat to have a proprioceptive role in monitoring insertional angle change between tendon and bone. This proposition was supported by the observations presented in chapters 4 and 5, which highlight the intimate relationship between the nerve fibres and adipocytes within the fat pad. A schematic 3D representation of this association was created it illustrate this point. In the light of these findings, the question was subsequently posed: what is the ultrastructural relationship between the adipocytes and the nerve fibres? Transmission electron microscopy of the retromalleolar fat pad in the rat showed that nerve fibres weaved between the very small spaces that existed between adjacent adipocytes, but were surrounded by varying amounts of fibrous connective tissue. Consequently, nerves did not come into direct contact with adipocytes. This may be an adaptation to protect the nerve from damage during compression of the fat

pad during foot movement. The contribution of the intra- and extra-articular fat pads to ankle and knee joint proprioception has previously been suggested by Freeman and Wyke, (1965, 1967a, 1967b, 1967c) in the cat, who demonstrated their innervation with free and encapsulated nerve endings.

The retromalleolar fat pad may also be a source of pain in pathology associated with the enthesis and/or the Achilles tendon itself, in a similar manner to Hoffa's fat pad in the knee which has been implicated in anterior knee pain (Bennell et al., 2004). The peptidergic nerve fibres within the retromalleolar fat pad may be stimulated if the fat becomes impinged between the tendon and superior calcaneal tuberosity, or in patients with retrocalcaneal bursitis where the fat pad is prevented from moving in and out of the bursa (Canoso, 1998). This study also suggests that neo-vascular invasion of entheses could be a source of pain in enthesopathies. The blood vessels penetrating into the enthesis were frequently seen to originate from the region of Kager's fat pad that was associated with the Achilles tendon. In line with this hypothesis, Alfredson and colleagues have demonstrated with colour Doppler ultrasound that neo-vascular invasion is present in patients with painful tennis elbow (Zeisig et al., 2006a; b), and patients with painful Achilles and patellar tendinosis (Alfredson and Ohberg, 2005; Alfredson et al., 2003), while neo-vascular invasion was not present in patients without symptoms. The latter studies also illustrate (but do not discuss) that neo-vascular invasion is most prominent in the deep part of the tendon adjacent to Hoffa's or Kager's fat pads. It may therefore be suggested that structural deposits of adipose tissue located at entheses (Benjamin et al., 2004b) could be a source of neo-vascular invasion of attachment sites, and thus be a source of pain. Adipose tissue should therefore be considered as a possible target for treatments in enthesopathies. However, the mechanical role of these fat pads must be remembered before taking drastic measures to stop or prevent pain, as any procedure that reduces the size of the fat pad (e.g. surgery) may well adversely affect the ability of the fat pad to dissipate stress and monitor movement at these locations (Benjamin et al., 2004b).

In view of the aneural nature of all the fibrocartilages associated with the attachment of the Achilles tendon, a question that now needed to be addressed was 'what inhibits the in-growth of nerve fibres into the fibrocartilage?' It has previously been demonstrated that high levels of aggrecan inhibit axonal outgrowth from DRG (Johnson et al., 2002), and it was therefore anticipated that the presence of aggrecan in the fibrocartilage of the rat

Achilles tendon enthesis organ could inhibit its innervation, as suggested in the IVD (Johnson et al., 2002). However, aggrecan is not present at the attachment site until 2 weeks postpartum (Rufai et al., 1992). Therefore, it is possible that inhibitory nerve growth factors may control axon growth during development of the enthesis to prevent its innervation. This hypothesis was tested using *in vitro* target derived nerve growth which demonstrated that axons from lumbar DRG are not inhibited from growing towards the attachment of the Achilles tendon in the 7 day-old rat; the nerve fibres however did not grow into the tissue itself. Further investigation is therefore necessary to identify how nerve growth is controlled during development of the enthesis organ and the stages at which this occurs. In addition, this study established that explants from the fully differentiated fibrocartilage in the adult rat Achilles tendon enthesis did not inhibit axon growth either. This may be explained by the presence of fibrocartilage cells within the explant which may promote axonal growth over an aggrecan rich tissue (Johnson et al., 2006). These observations suggest that there is a complex mechanism controlling the innervation of fibrocartilaginous structures such as entheses, which is balanced by an inhibitory extracellular matrix (Johnson et al., 2002) and the growth-promoting resident cells (Johnson et al., 2006). Loss of this equilibrium in the enthesis fibrocartilage under pathological conditions is therefore likely result in neurovascular invasion of the tissue – as suggested in the IVD (Abe et al., 2007; Freemont et al., 2002b; Johnson et al., 2006).

The interesting observation that the retromalleolar fat pad is highly innervated and is able to move in and out of the retrocalcaneal bursa to prevent pressure changes indicates that the fat pad is not merely a passive space-filler in the posterior region of the ankle. Other possible functions of the fat thus needed to be considered in this thesis. In view of the immunological functions of adipose tissue in other locations of the body such as the peritoneal cavity (Krist et al., 1995), it is possible that the retromalleolar fat pad has similar functions. Thus, the presence of inflammatory macrophages and neutrophils in the fat was explored and it was demonstrated that the retromalleolar fat pad may be a source and possible conduit for macrophages and other inflammatory cells to pass into the retrocalcaneal bursa. Under normal conditions these cells may phagocytose cellular debris generated by wear and tear at the entheses. However in susceptible individuals, the fat pad could also act as a source of inflammatory cells in autoinflammatory conditions. The fat pad, here and at other locations such as the knee joint, should therefore also be considered as a site for treatment in such conditions, and the functional importance of these regions

should be remembered during surgical procedures. The inflammatory cells located within the fat pad may also play a role in hyperalgesia through the release inflammatory cytokines, such as tumour necrosis factors, interleukins and histamine under conditions of tissue damage (Cunha et al., 1992; Foreman, 1987; Jancso et al., 1968). Furthermore, it is the current popular view that pathological conditions affecting tendons and entheses are primarily degenerative in nature and rarely inflammatory (Khan et al., 1999a); however, authors rarely look at structures located in the close vicinity of tendons (such as the fat pad), where inflammation may be present. Furthermore, Benjamin and McGonagle (2007) have recently demonstrated the presence of inflammatory cells at numerous entheses in dissecting room cadavers, and suggest that these cells may be involved in early mechanisms of pathology associated with attachment sites.

Given that the retromalleolar fat pad may function as an important proprioceptive, immunological and stress dissipating organ, the next question addressed was 'does the fat pad vary in size according to the weight of the individual?'. It was demonstrated that unlike other adipose tissue deposits, Kager's fat pad does not vary with the weight of the individual. Instead, the size of the fat pad correlates better with the skeletal size of the individuals. This supports the idea of Benjamin et al., (2004b) and Theobald et al.,(2006) that the fat pad plays an essential role in dissipating stress away from the tendon-bone interface. The dietary independence of the fat pad was confirmed with the use of rats injected with the appetite-inducing hormone Ghrelin. The lack of influence of Ghrelin on the size of the fat pad is in line with the observations of Davies and White (1961) who demonstrated that only in extremely emaciated individuals, does Kager's or Hoffa's fat pad undergo lypolysis. This might be of particular interest to athletes with very low body fat content – e.g. distance runners. Loss of adipose tissue in joints and at entheses may have severe implications on the amount of stress experienced at these sites.

Since it was understood that the retromalleolar fat pad is a structural adipose tissue deposit, it was now considered of interest to determine the time point at which the fat pad develops in relation to the rest of the Achilles tendon enthesis organ. The results of the developmental study presented in chapter 7 showed that adipogenesis occurred in Kager's fat pad *prior* to differentiation of the sesamoid and periosteal fibrocartilages, but *after* the formation of the retrocalcaneal bursa. The early differentiation of adipose tissue in Kager's fat pad reflects its proposed importance in proprioception, stress dissipation and

immunological protection. In the light of the developmental study, it would be interesting to know the effect of developmental abnormalities (e.g. clubfoot), on the structure, function and development of Kager's fat pad and the effect this may have on its now known functions. Ethical considerations however make it unlikely that such a question could be easily addressed.

Much of this thesis focussed on the fibrocartilaginous enthesis of the Achilles tendon, but the question was also posed as to whether other types of entheses are also aneural. Furthermore, are entheses in other animals, other than the rat, also aneural? To answer such questions, the innervation of the fibrous enthesis of the MCL, and the muscular enthesis of tibialis anterior in the rat were described along, with the innervation of the proximal enthesis of the equine suspensory ligament. The fibrous enthesis of the MCL proved also to be aneural, however, the muscular entheses of tibialis anterior had a large sensory nerve supply, and spindle-like nerve endings were located in the connective tissue which anchored the muscle to the underlying periosteum. The nerve fibres at muscular entheses are likely to play a significant role in proprioception by monitoring stretch of the collagen fibres at the attachment, in a similar manner to Golgi-tendon organs (Houk and Simon, 1967). Nociceptive nerve fibres were also present at the muscular enthesis, indicating that this region is also a potential source of pain in injuries and may be involved in conditions such as shin splints. The most obvious difference between fibrous/fibrocartilaginous entheses and muscular entheses is the surface area of the attachment. Tendinous attachments are considerably more discrete than muscular attachments which may reduce the stress concentration significantly enough to allow their innervation. The proximal enthesis of the equine suspensory ligament was described histologically as a mixed enthesis with both fibrous and fibrocartilaginous regions, both of which were aneural in the asymptomatic animal. Interestingly, this enthesis was also associated with a region of adipose tissue, located between the ligament and the bone which contained a large number of encapsulated nerve endings and free nerve fibres. It is therefore proposed that in the majority of mammals, adipose tissue at entheses has proprioceptive functions, but may also be involved in entheses pathology and pain at these sites. The substantial importance of adipose tissue at entheses and in other musculoskeletal regions should therefore be recognised by practising clinicians.

Future Research

This study identified numerous novel functions of the retromalleolar fat pad of the Achilles tendon enthesis organ. Suggested below are points for future research associated with this structure and the innervation of entheses in general which may shed more light on proprioception within the musculoskeletal system and the genesis of pain at attachment sites.

- ❖ The role of the retromalleolar fat pad in the seronegative spondyloarthropathies requires further investigation. This may be done with the use of the IILA-B27 transgenic mouse model, ANKENT, which develops mild inflammation, progressive stiffening, cartilage proliferation at entheses and finally ossification of the ankle and tarsal joints in the hindlimb (Eulderink et al., 1998; Weinreich et al., 1995). It would be interesting to assess the contribution of inflammatory cells from the fat pad during the development of the disease; in addition to the effect of TNF- α blockers and non-steroidal anti-inflammatory drugs (NSAID) on this animal model when applied to the fat pad. Furthermore, it is essential to assess the effect of these treatments on the fat pad throughout the lifetime of the animal and their influence on lipolysis.
- ❖ The importance of adipose tissue at entheses may be confirmed with the use of a different animal model. The A-ZIP/-1 transgenic mouse strain lacks white adipose tissue throughout their lifetime (Moitra, 1998). The ability to evaluate any structural differences between control and transgenic mice in the nature of the Achilles tendon enthesis organ in the absence of the retromalleolar fat pad would be invaluable – if indeed this animal model does not possess a fat pad at all.
- ❖ It has been suggested in this thesis that the retromalleolar fat pad contains pluripotent mesenchymal stem cells (MSCs) as numerous fibrocartilaginous/bony condensations were observed within it the fat pad in both man and rat. Confirming the presence of MSCs within the retromalleolar fat pad, possibly with the use of flow-cytometry, may shed some light on the ability of entheses to repair themselves (Newsham-West et al., 2007; Silva et al., 2002). At present the occurrence of stem cells at entheses/enthesis organs has yet to be determined and is clearly an avenue worth exploring, considering the frequency at which the surgical reattachment of tendons and ligaments is performed (Wagner et al., 2006), and the current interest in stem cells in tissue engineering.

- ❖ The biochemical composition of the fat pad has not been addressed in this thesis, but is necessary to understand fully the biology and function of the fat pad. The fatty acid composition, protein content, rate of fatty acid synthesis and incorporation, rate of insulin induced lipogenesis, and glucose utilisation should be compared with other adipose tissue deposits such as the subcutaneous, peritoneal, cardiac, and calcaneal fat pads.
- ❖ A recent study by Langberg et al., (1999) demonstrated that levels of inflammatory cytokines (prostaglandin E2), carbohydrate and lipid metabolism increased in the Achilles associated region of Kager's fat pad (tested as what the authors described as "peritendinous tissue") with dynamic loading. This was assessed with the use of microdialysis in healthy human volunteers. In the light of these observations, it would be interesting to assess the alteration in levels of the same factors in the tip of Kager's fat pad with active loading of the Achilles tendon and flexor hallucis longus. This could be addressed using the same microdialysis approach.
- ❖ Current investigations on musculoskeletal innervation usually focus primarily on just one part of the musculoskeletal unit. Indeed, this has been the approach in the current thesis. However, to understand the system as a whole, it would be beneficial to examine an entire muscle-tendon-bone unit and quantitatively assess the density of innervation by injecting each region with neuronal tracers, and counting the number and type of cell bodies highlighted within the corresponding DRG. This would pinpoint regions of the musculoskeletal system which are particularly important in proprioception or nociception. The innervation of specialised regions within the muscle-tendon-bone unit such as 'functional entheses' is also of interest. It may be hypothesized that they are also likely to be aneural because they are commonly fibrocartilaginous.
- ❖ Although the topic was only briefly addressed in this thesis, further research is required to determine the mechanisms which control the development and innervation of entheses. The *in vitro* investigation described in chapter 10 needs to be repeated at different developmental time points. Furthermore, the application of antibodies to block the receptors for NGF/BDNF and semaphorins would indicate which signalling mechanisms which control enthesal innervation. This might also highlight possible treatments that could be used to prevent or slow neo-vascular invasion in enthesopathies/tendinopathies.

LIST OF REFERENCES

- Abe, M., Kurosawa, M., Ishikawa, O., Miyachi, Y. & Kido, H. (1998) Mast cell tryptase stimulates both human dermal fibroblast proliferation and type I collagen production. *Clin Exp Allergy*, 28, 1509-1517.
- Abe, Y., Akeda, K., An, H. S., Aoki, Y., Pichika, R., Muehleman, C., Kimura, T. & Masuda, K. (2007) Proinflammatory cytokines stimulate the expression of nerve growth factor by human intervertebral disc cells. *Spine*, 32, 635-642.
- Abou Salem, E. A., Fujimaki, N. & Ishikawa, H. (1993a) Ultrastructural changes of myotendinous junctions in tenotomized soleus muscles of the rat. *J Submicrosc Cytol Pathol*, 25, 181-191.
- Abou Salem, E. A., Saito, K. & Ishikawa, H. (1993b) Scanning electron microscopy of tenotomized soleus muscles of the rat. *Arch Histol Cytol*, 56, 49-63.
- Ackermann, P. (2001) Peptidergic innervation of periarticular tissue. Karolinka Institutet.
- Ackermann, P. W., Finn, A. & Ahmed, M. (1999) Sensory neuropeptidergic pattern in tendon, ligament and joint capsule. A study in the rat. *Neuroreport*, 10, 2055-2060.
- Ackermann, P. W., Li, J., Lundberg, T. & Kreicbergs, A. (2003) Neuronal plasticity in relation to nociception and healing of rat achilles tendon. *J Orthop Res*, 21, 432-441.
- Ahmed, I. M., Lagopoulos, M., Mcconnell, P., Soames, R. W. & Sefton, G. K. (1998) Blood supply of the Achilles tendon. *J Orthop Res*, 16, 591-596.
- Alberts, B., Bray, D., Lewis, J., Raff, M., Roberts, K. & Watson, J. D. (1994) *Molecular Biology of the Cell*, New York. 3rd Edition ed, Garland Publishing Inc.
- Alfredson, H. & Ohberg, L. (2005) Neovascularisation in chronic painful patellar tendinosis--promising results after sclerosing neovessels outside the tendon challenge the need for surgery. *Knee Surg Sports Traumatol Arthrosc*, 13, 74-80.
- Alfredson, H., Ohberg, L. & Forsgren, S. (2003) Is vasculo-neural ingrowth the cause of pain in chronic Achilles tendinosis? An investigation using ultrasonography and colour Doppler, immunohistochemistry, and diagnostic injections. *Knee Surg Sports Traumatol Arthrosc*, 11, 334-338.
- Amato, P. A., Unanue, E. R. & Taylor, D. L. (1983) Distribution of actin in spreading macrophages: a comparative study on living and fixed cells. *J Cell Biol*, 96, 750-761.
- Andersen, H. (1963) Histochemistry and Development of the Human Shoulder and Acromioclavicular Joints with Particular Reference to the Early Development of the Clavicle. *Acta Anat (Basel)*, 55, 124-165.
- Andersen, H. & Bro-Rasmussen, F. (1961) Histochemical Studies on the Histogenesis of the Joints in Human Fetuses with Special Reference to the Development of the Joint Cavities in the Hand and Foot. *American Journal of Anatomy*, 108 111-122.
- Argyropoulos, G. & Harper, M. E. (2002) Uncoupling proteins and thermoregulation. *J Appl Physiol*, 92, 2187-2198.
- Arner, P. (1998) Not all fat is alike. *Lancet*, 351, 1301-1302.
- Astrom, M. & Rausing, A. (1995) Chronic Achilles tendinopathy. A survey of surgical and histopathologic findings. *Clin Orthop*, 151-164.
- Astrow, S. H., Sutton, L. A. & Thompson, W. J. (1992) Developmental and neural regulation of a subsarcolemmal component of the rat neuromuscular junction. *J Neurosci*, 12, 1602-1615.
- Averill, S., McMahon, S. B., Clary, D. O., Reichardt, L. F. & Priestley, J. V. (1995) Immunocytochemical localization of trkA receptors in chemically identified subgroups of adult rat sensory neurons. *Eur J Neurosci*, 7, 1484-1494.

- Banes, A. J., Weinhold, P., Yang, X., Tsuzaki, M., Bynum, D., Bottlang, M. & Brown, T. (1999) Gap junctions regulate responses of tendon cells ex vivo to mechanical loading. *Clin Orthop Relat Res*, S356-370.
- Banfield, W. G. (1952) Occurrence of tapered collagen fibrils from human sources with observations on mesenchymal neoplasms. *Proc Soc Exp Biol Med*, 81, 658-660.
- Banks, A. S., Downey, R., Martin, D. E. & Miller, J. S. (2001) *McGlamry's comprehensive textbook of foot and ankle surgery*, 3rd ed, Lippincott Williams and Wilkins.
- Barbacid, M. (1995) Structural and functional properties of the TRK family of neurotrophin receptors. *Ann NY Acad Sci*, 766, 442-458.
- Barfred, T. (1973) Achilles tendon rupture. Aetiology and pathogenesis of subcutaneous rupture assessed on the basis of the literature and rupture experiments on rats. *Acta Orthop Scand Suppl*, 3-126.
- Bartness, T. J. & Bamshad, M. (1998) Innervation of mammalian white adipose tissue: implications for the regulation of total body fat. *Am J Physiol*, 275, R1399-1411.
- Bartness, T. J., Kay Song, C., Shi, H., Bowers, R. R. & Foster, M. T. (2005) Brain-adipose tissue cross talk. *Proc Nutr Soc*, 64, 53-64.
- Bathe, A. (2001) Neurectomy and fasciotomy for the surgical treatment of hindlimb proximal suspensory desmitis. *40th Congress of the British Equine Veterinary Association*.
- Bear, M. F., Connors, A. & Paradiso, M. (2006) *Neuroscience: Exploring the brain*, 3rd Edition ed, Lippincott, Williams and Wilkins.
- Bell J, B. S., Holmes Mh. (1994) The structure and function of Pacinian corpuscles: a review. *Prog Neurobiol*, 42, 79-128.
- Benham, P. P., Crawford, R. J. & Armstrong, C. G. (1996) *Mechanics of Engineering Materials*, London. Prentice Hill.
- Benjamin, M., Evans, E. J. & Copp, L. (1986) The histology of tendon attachments to bone in man. *J Anat*, 149, 89-100.
- Benjamin, M. & Hillen, B. (2003) Mechanical influences on cells, tissues and organs - 'Mechanical Morphogenesis'. *Eur J Morphol*, 41, 3-7.
- Benjamin, M., Kumai, T., Milz, S., Boszczyk, B. M., Boszczyk, A. A. & Ralphs, J. R. (2002) The skeletal attachment of tendons-tendon 'entheses'. *Comp Biochem Physiol A Mol Integr Physiol*, 133, 931-945.
- Benjamin, M. & McGonagle, D. (2001) The anatomical basis for disease localisation in seronegative spondyloarthropathy at entheses and related sites. *J Anat*, 199, 503-526.
- Benjamin, M., Moriggl, B., Brenner, E., Emery, P., McGonagle, D. & Redman, S. (2004a) The "entheses organ" concept: Why enthesopathies may not present as focal insertional disorders. *Arthritis Rheum*, 50, 3306-3313.
- Benjamin, M., Qin, S. & Ralphs, J. R. (1995) Fibrocartilage associated with human tendons and their pulleys. *J Anat*, 187 (Pt 3), 625-633.
- Benjamin, M. & Ralphs, J. R. (1997) Tendons and ligaments--an overview. *Histol Histopathol*, 12, 1135-1144.
- Benjamin, M. & Ralphs, J. R. (1998) Fibrocartilage in tendons and ligaments--an adaptation to compressive load. *J Anat*, 193 (Pt 4), 481-494.
- Benjamin, M. & Ralphs, J. R. (2004) Biology of fibrocartilage cells. *Int Rev Cytol*, 233, 1-45.
- Benjamin, M., Redman, S., Milz, S., Buttner, A., Amin, A., Moriggl, B., Brenner, E., Emery, P., McGonagle, D. & Bydder, G. (2004b) Adipose tissue at entheses: the rheumatological implications of its distribution. A potential site of pain and stress dissipation? *Ann Rheum Dis*, 63, 1549-1555.

- Benjamin, M., Theobald, P., Suzuki, D. & Toumi, H. (2007a) The Anatomy of the Achilles Tendon. In Maffulli, N. & Almekinders, L.C., (Eds.) *The Achilles Tendon*. London, Springer-Verlang.
- Benjamin, M., Toumi, H., Ralphs, J. R., Bydder, G., Best, T. M. & Milz, S. (2006) Where tendons and ligaments meet bone: attachment sites ('entheses') in relation to exercise and/or mechanical load. *J Anat*, 208, 471-490.
- Benjamin, M., Toumi, H., Suzuki, D., Redman, S., Emery, P. & Mcgonagle, D. (2007b) Microdamage and altered vascularity at the enthesis-bone interface provides an anatomic explanation for bone involvement in the HLA-B27-associated spondylarthritides and allied disorders. *Arthritis Rheum*, 56, 224-233.
- Bennell, K., Hodges, P., Mellor, R., Bexander, C. & Souvlis, T. (2004) The nature of anterior knee pain following injection of hypertonic saline into the infrapatellar fat pad. *J Orthop Res*, 22, 116-121.
- Bergman, E., Fundin, B. T. & Ulfhake, B. (1999) Effects of aging and axotomy on the expression of neurotrophin receptors in primary sensory neurons. *J Comp Neurol*, 410, 368-386.
- Berton, A., Levi-Schaffer, F., Emonard, H., Garbuzenko, E., Gillery, P. & Maquart, F. X. (2000) Activation of fibroblasts in collagen lattices by mast cell extract: a model of fibrosis. *Clin Exp Allergy*, 30, 485-492.
- Biermann, H. (1957) [Ossification in the region of periosteal-diaphysial tendon- and ligament insertion.]. *Z Zellforsch Mikrosk Anat*, 46, 635-671.
- Biewenga, J., Van Der Ende, M. B., Krist, L. F., Borst, A., Ghufon, M. & Van Rooijen, N. (1995) Macrophage depletion in the rat after intraperitoneal administration of liposome-encapsulated clodronate: depletion kinetics and accelerated repopulation of peritoneal and omental macrophages by administration of Freund's adjuvant. *Cell Tissue Res*, 280, 189-196.
- Birk, D. E., Fitch, J. M., Babiarz, J. P., Doane, K. J. & Linsenmayer, T. F. (1990) Collagen fibrillogenesis in vitro: interaction of types I and V collagen regulates fibril diameter. *J Cell Sci*, 95 (Pt 4), 649-657.
- Birk, D. E. & Mayne, R. (1997) Localization of collagen types I, III and V during tendon development. Changes in collagen types I and III are correlated with changes in fibril diameter. *Eur J Cell Biol*, 72, 352-361.
- Birk, D. E. & Zycband, E. (1994) Assembly of the tendon extracellular matrix during development. *J Anat*, 184 (Pt 3), 457-463.
- Birke, J. A., Patout, C. A., Jr. & Foto, J. G. (2000) Factors associated with ulceration and amputation in the neuropathic foot. *J Orthop Sports Phys Ther*, 30, 91-97.
- Bjur, D., Alfredson, H. & Forsgren, S. (2005) The innervation pattern of the human Achilles tendon: studies of the normal and tendinosis tendon with markers for general and sensory innervation. *Cell Tissue Res*, 320, 201-206.
- Bjurholm, A., Kreicbergs, A., Brodin, E. & Schultzberg, M. (1988) Substance P- and CGRP-immunoreactive nerves in bone. *Peptides*, 9, 165-171.
- Bonaldo, P., Russo, V., Bucciotti, F., Doliana, R. & Colombatti, A. (1990) Structural and functional features of the alpha 3 chain indicate a bridging role for chicken collagen VI in connective tissues. *Biochemistry*, 29, 1245-1254.
- Borman, P., Koparal, S., Babaoglu, S. & Bodur, H. (2006) Ultrasound detection of enthesal insertions in the foot of patients with spondyloarthritis. *Clin Rheumatol*, 25, 373-377.
- Bovolenta, P. & Feraud-Espinosa, I. (2000) Nervous system proteoglycans as modulators of neurite outgrowth. *Prog Neurobiol*, 61, 113-132.
- Bowker, R. M., Van Wulfen, K. K., Springer, S. E. & Linder, K. E. (1998) Functional anatomy of the cartilage of the distal phalanx and digital cushion in the equine foot

- and a hemodynamic flow hypothesis of energy dissipation. *Am J Vet Res*, 59, 961-968.
- Bozyczko, D., Decker, C., Muschler, J. & Horwitz, A. F. (1989) Integrin on developing and adult skeletal muscle. *Exp Cell Res*, 183, 72-91.
- Brain, S. D. (1997) Sensory neuropeptides: their role in inflammation and wound healing. *Immunopharmacology*, 37, 133-152.
- Brain, S. D. & Cambridge, H. (1996) Calcitonin gene-related peptide: vasoactive effects and potential therapeutic role. *Gen Pharmacol*, 27, 607-611.
- Braun, J., Khan, M. A. & Sieper, J. (2000) Enthesitis and ankylosis in spondyloarthritis: what is the target of the immune response? *Ann Rheum Dis*, 59, 985-994.
- Bray, R. C., Rangayyan, R. M. & Frank, C. B. (1996) Normal and healing ligament vascularity: a quantitative histological assessment in the adult rabbit medial collateral ligament. *J Anat*, 188 (Pt 1), 87-95.
- Brimble, M. J. & Wallis, D. I. (1973) Histamine H1 and H2-receptors at a ganglionic synapse. *Nature*, 246, 156-158.
- Bromley, M. & Woolley, D. E. (1984a) Chondroclasts and osteoclasts at subchondral sites of erosion in the rheumatoid joint. *Arthritis Rheum*, 27, 968-975.
- Bromley, M. & Woolley, D. E. (1984b) Histopathology of the rheumatoid lesion. Identification of cell types at sites of cartilage erosion. *Arthritis Rheum*, 27, 857-863.
- Brownell, H. L., Narsimhan, R. P., Corbley, M. J., Mann, V. M., Whitfield, J. F. & Raptis, L. (1996) Ras is involved in gap junction closure in proliferating fibroblasts or preadipocytes but not in differentiated adipocytes. *DNA Cell Biol*, 15, 443-451.
- Buckley, M. G., Walters, C., Wong, W. M., Cawley, M. I., Ren, S., Schwartz, L. B. & Walls, A. F. (1997) Mast cell activation in arthritis: detection of alpha- and beta-tryptase, histamine and eosinophil cationic protein in synovial fluid. *Clin Sci (Lond)*, 93, 363-370.
- Buckwalter, J. A. & Mankin, H. J. (1998) Articular cartilage: tissue design and chondrocyte-matrix interactions. *Instr Course Lect*, 47, 477-486.
- Burridge, K., Molony, L. & Kelly, T. (1987) Adhesion plaques: sites of transmembrane interaction between the extracellular matrix and the actin cytoskeleton. *J Cell Sci Suppl*, 8, 211-229.
- Byers, M. R. (1985) Sensory innervation of periodontal ligament of rat molars consists of unencapsulated Ruffini-like mechanoreceptors and free nerve endings. *J Comp Neurol*, 231, 500-518.
- Caminos, J. E., Gualillo, O., Lago, F., Otero, M., Blanco, M., Gallego, R., Garcia-Caballero, T., Goldring, M. B., Casanueva, F. F., Gomez-Reino, J. J. & Dieguez, C. (2005) The endogenous growth hormone secretagogue (ghrelin) is synthesized and secreted by chondrocytes. *Endocrinology*, 146, 1285-1292.
- Campbell, P. & Lawton, J. O. (1993) Spontaneous rupture of the Achilles tendon: pathology and management. *Br J Hosp Med*, 50, 321-325.
- Canoso, J. (1981) Bursae, tendons and ligaments. *Clin. Rheum. Dis.*, 7, 189-221.
- Canoso, J. J. (1998) The premiere enthesis. *J Rheumatol*, 25, 1254-1256.
- Canoso, J. J., Liu, N., Traill, M. R. & Runge, V. M. (1988) Physiology of the retrocalcaneal bursa. *Ann Rheum Dis*, 47, 910-912.
- Carreon, L. Y., Ito, T., Yamada, M., Uchiyama, S., Takahashi, H. & Ikuta, F. (1996) Histologic changes in the disc after cervical spine trauma: evidence of disc absorption. *J Spinal Disord*, 9, 313-316.
- Carvalho, H. F., Felisbino, S. L., Keene, D. R. & Vogel, K. G. (2006) Identification, content, and distribution of type VI collagen in bovine tendons. *Cell Tissue Res*, 325, 315-324.

- Castelli, W. A., Nasjleti, C. E., Diaz-Perez, R. & Caffesse, R. G. (1985) Histopathologic findings in temporomandibular joints of aged individuals. *J Prosthet Dent*, 53, 415-419.
- Cavalcante, M. L., Rodrigues, C. J. & Mattar, R., Jr. (2004) Mechanoreceptors and nerve endings of the triangular fibrocartilage in the human wrist. *J Hand Surg [Am]*, 29, 432-435; discussion 436-438.
- Ceballos, D., Cuadras, J., Verdu, E. & Navarro, X. (1999) Morphometric and ultrastructural changes with ageing in mouse peripheral nerve. *J Anat*, 195 (Pt 4), 563-576.
- Charriere, G., Cousin, B., Arnaud, E., Andre, M., Bacou, F., Penicaud, L. & Casteilla, L. (2003) Preadipocyte conversion to macrophage. Evidence of plasticity. *J Biol Chem*, 278, 9850-9855.
- Chen, X., Macica, C. M., Dreyer, B. E., Hammond, V. E., Hens, J. R., Philbrick, W. M. & Broadus, A. E. (2006) Initial characterization of PTH-related protein gene-driven lacZ expression in the mouse. *J Bone Miner Res*, 21, 113-123.
- Chi, S. S., Rattner, J. B., Sciore, P., Boorman, R. & Lo, I. K. (2005) Gap junctions of the medial collateral ligament: structure, distribution, associations and function. *J Anat*, 207, 145-154.
- Chihlas, C. N., Lodocsi, L. T., Sholley, M. M., Loughran, T. P. & Krieg, R. J. (1993) Position of the fabella relative to the path of the common peroneal nerve across the lateral head of the gastrocnemius muscle. *Clinical Anatomy*, 6, 163-166.
- Childs, S. G. (2004) Diffuse idiopathic skeletal hyperostosis: Forestier's disease. *Orthop Nurs*, 23, 375-382; quiz 383-374.
- Choi, K., Roh, S. G., Hong, Y. H., Shrestha, Y. B., Hishikawa, D., Chen, C., Kojima, M., Kangawa, K. & Sasaki, S. (2003) The role of ghrelin and growth hormone secretagogues receptor on rat adipogenesis. *Endocrinology*, 144, 754-759.
- Chong, D. A. & Evans, C. A. (1982) Histologic study of the attachment of muscles to the rat mandible. *Arch Oral Biol*, 27, 519-527.
- Christiansen, T., Richelsen, B. & Bruun, J. M. (2005) Monocyte chemoattractant protein-1 is produced in isolated adipocytes, associated with adiposity and reduced after weight loss in morbid obese subjects. *Int J Obes (Lond)*, 29, 146-150.
- Chun, T. H., Hotary, K. B., Sabeh, F., Saltiel, A. R., Allen, E. D. & Weiss, S. J. (2006) A pericellular collagenase directs the 3-dimensional development of white adipose tissue. *Cell*, 125, 577-591.
- Cinti, S. (2005) The adipose organ. *Prostaglandins Leukot Essent Fatty Acids*, 73, 9-15.
- Clark, J. & Stechschulte, D. J., Jr. (1998) The interface between bone and tendon at an insertion site: a study of the quadriceps tendon insertion. *J Anat*, 192 (Pt 4), 605-616.
- Cohen, S. (1960) Purification of a Nerve-Growth Promoting Protein from the Mouse Salivary Gland and Its Neuro-Cytotoxic Antiserum. *Proc Natl Acad Sci U S A*, 46, 302-311.
- Condic, M. L., Snow, D. M. & Letourneau, P. C. (1999) Embryonic neurons adapt to the inhibitory proteoglycan aggrecan by increasing integrin expression. *J Neurosci*, 19, 10036-10043.
- Cooper, R. R. & Misol, S. (1970) Tendon and ligament insertion. A light and electron microscopic study. *J Bone Joint Surg Am*, 52, 1-20.
- Corps, A. N., Robinson, A. H., Movin, T., Costa, M. L., Hazleman, B. L. & Riley, G. P. (2006) Increased expression of aggrecan and biglycan mRNA in Achilles tendinopathy. *Rheumatology (Oxford)*, 45, 291-294.

- Corps, A. N., Robinson, A. H., Movin, T., Costa, M. L., Ireland, D. C., Hazleman, B. L. & Riley, G. P. (2004) Versican splice variant messenger RNA expression in normal human Achilles tendon and tendinopathies. *Rheumatology (Oxford)*, 43, 969-972.
- Cousin, B., Cinti, S., Morroni, M., Raimbault, S., Ricquier, D., Penicaud, L. & Casteilla, L. (1992) Occurrence of brown adipocytes in rat white adipose tissue: molecular and morphological characterization. *J Cell Sci*, 103 (Pt 4), 931-942.
- Crowe, O., Wright, I. M., Schramme, M. C. & Smith, R. K. W. (2002) Treatment of 45 cases of chronic hindlimb proximal suspensory desmitis by radial extracorporeal shockwave therapy. *American Association of Equine Practitioners (AAEP)*.
- Cunha, F. Q., Poole, S., Lorenzetti, B. B. & Ferreira, S. H. (1992) The pivotal role of tumour necrosis factor alpha in the development of inflammatory hyperalgesia. *Br J Pharmacol*, 107, 660-664.
- Curat, C. A., Miranville, A., Sengenès, C., Diehl, M., Tonus, C., Busse, R. & Bouloumie, A. (2004) From blood monocytes to adipose tissue-resident macrophages: induction of diapedesis by human mature adipocytes. *Diabetes*, 53, 1285-1292.
- Currey, J. D. (1984) Effects of differences in mineralization on the mechanical properties of bone. *Philos Trans R Soc Lond B Biol Sci*, 304, 509-518.
- D'agostino, M. A. & Olivieri, I. (2006) Enthesitis. *Best Pract Res Clin Rheumatol*, 20, 473-486.
- Damoiseaux, J. G., Dopp, E. A., Calame, W., Chao, D., Macpherson, G. G. & Dijkstra, C. D. (1994) Rat macrophage lysosomal membrane antigen recognized by monoclonal antibody ED1. *Immunology*, 83, 140-147.
- Davies, D. V. & White, J. E. (1961) The structure and weight of synovial fat pads. *J Anat*, 95, 30-37.
- Daya, S., Loughlin, A. J. & Macqueen, H. A. (2007) Culture and differentiation of preadipocytes in two-dimensional and three-dimensional in vitro systems. *Differentiation*, 75, 360-370.
- De Mos, M., Koevoet, W. J., Jahr, H., Verstegen, M. M., Heijboer, M. P., Kops, N., Van Leeuwen, J. P., Weinans, H., Verhaar, J. A. & Van Osch, G. J. (2007) Intrinsic differentiation potential of adolescent human tendon tissue: an in-vitro cell differentiation study. *BMC Musculoskelet Disord*, 8, 16.
- De Rycke, L., Baeten, D., Foell, D., Kruihof, E., Veys, E. M., Roth, J. & De Keyser, F. (2005) Differential expression and response to anti-TNFalpha treatment of infiltrating versus resident tissue macrophage subsets in autoimmune arthritis. *J Pathol*, 206, 17-27.
- De Zeeuw, C. I., Holstege, J. C., Calkoen, F., T.J.H., R. & Voogd, J. (1988) A new combination of WGA-HRP anterograde tracing and GABA immunocytochemistry applied to afferents of the cat inferior olive at the ultrastructural level. *Brain Res*, 447, 369-375.
- Dean, G., Hoyland, J. A., Denton, J., Donn, R. P. & Freemont, A. J. (1993) Mast cells in the synovium and synovial fluid in osteoarthritis. *Br J Rheumatol*, 32, 671-675.
- Delgado-Baeza, E., Utrilla-Mainz, V., Contreras-Porta, J., Santos-Alvarez, I. & Martos-Rodriguez, A. (1999) Mechanoreceptors in collateral knee ligaments: an animal experiment. *Int Orthop*, 23, 168-171.
- Dodd, J. & Jessell, T. M. (1988) Axon guidance and the patterning of neuronal projections in vertebrates. *Science*, 242, 692-699.
- Dolgo-Saburoff, B. (1929) Über ursprung und Inserttion der Skelettmuskeln. *Anat Anz.*, 68, 8-87.
- Donahue, S. P. & English, A. W. (1989) Selective elimination of cross-compartmental innervation in rat lateral gastrocnemius muscle. *J Neurosci*, 9, 1621-1627.

- Donnerer, J., Schuligoi, R. & Stein, C. (1992) Increased content and transport of substance P and calcitonin gene-related peptide in sensory nerves innervating inflamed tissue: evidence for a regulatory function of nerve growth factor in vivo. *Neuroscience*, 49, 693-698.
- Doran, J. F., Jackson, P., Kynoch, P. A. & Thompson, R. J. (1983) Isolation of PGP 9.5, a new human neurone-specific protein detected by high-resolution two-dimensional electrophoresis. *J Neurochem*, 40, 1542-1547.
- Dorfl, J. (1980a) Migration of tendinous insertions. I. Cause and mechanism. *J Anat*, 131, 179-195.
- Dorfl, J. (1980b) Migration of tendinous insertions. II. Experimental modifications. *J Anat*.
- Dou, C. L. & Levine, J. M. (1995) Differential effects of glycosaminoglycans on neurite growth on laminin and L1 substrates. *J Neurosci*, 15, 8053-8066.
- Dwyer, K. W., Provenzano, P. P., Muir, P., Valhmu, W. B. & Vanderby, R., Jr. (2004) Blockade of the sympathetic nervous system degrades ligament in a rat MCL model. *J Appl Physiol*, 96, 711-718.
- Dyson, S. (1988) Some observations on lameness associated with pain in the proximal metacarpal region. *Equine Vet J Suppl*, 43-52.
- Dyson, S. (1991) Proximal suspensory desmitis: clinical, ultrasonographic and radiographic features. *Equine Vet J*, 23, 25-31.
- Eather, T., Pollock, M. & Myer, D. (1986) Proximal and distal changes in collagen content of peripheral nerve that follow transection and crush lesions. *Experimental Neurology*, 92, 299-310.
- Ebadi, M., Bashir, R. M., Heidrick, M. L., Hamada, F. M., Refaey, H. E., Hamed, A., Helal, G., Baxi, M. D., Cerutis, D. R. & Lassi, N. K. (1997) Neurotrophins and their receptors in nerve injury and repair. *Neurochem Int*, 30, 347-374.
- Edwards, D. A. (1946) The blood supply and lymphatic drainage of tendons. *J Anat*, 80, 147-152 142.
- Egerbacher, M., Helmreich, M., Probst, A., Konig, H. & Bock, P. (2005) Digital cushions in horses comprise coarse connective tissue, myxoid tissue, and cartilage but only little unilocular fat tissue. *Anat Histol Embryol*, 34, 112-116.
- Eguchi, J., Wada, J., Hida, K., Zhang, H., Matsuoka, T., Baba, M., Hashimoto, I., Shikata, K., Ogawa, N. & Makino, H. (2005) Identification of adipocyte adhesion molecule (ACAM), a novel CTX gene family, implicated in adipocyte maturation and development of obesity. *Biochem J*, 387, 343-353.
- Eng, K., Rangayyan, R. M., Bray, R. C., Frank, C. B., Anscornb, L. & Veale, P. (1992) Quantitative analysis of the fine vascular anatomy of articular ligaments. *IEEE Trans Biomed Eng*, 39, 296-306.
- Ernfors, P., Lee, K. F., Kucera, J. & Jaenisch, R. (1994) Lack of neurotrophin-3 leads to deficiencies in the peripheral nervous system and loss of limb proprioceptive afferents. *Cell*, 77, 503-512.
- Eulderink, F., Ivanyi, P. & Weinreich, S. (1998) Histopathology of murine ankylosing enthesopathy. *Pathol Res Pract*, 194, 797-803.
- Ezura, Y., Chakravarti, S., Oldberg, A., Chervoneva, I. & Birk, D. E. (2000) Differential expression of lumican and fibromodulin regulate collagen fibrillogenesis in developing mouse tendons. *J Cell Biol*, 151, 779-788.
- Fairclough, J., Hayashi, K., Toumi, H., Lyons, K., Bydder, G., Phillips, N., Best, T. M. & Benjamin, M. (2006) The functional anatomy of the iliotibial band during flexion and extension of the knee: implications for understanding iliotibial band syndrome. *J Anat*, 208, 309-316.

- Fairclough, J., Hayashi, K., Toumi, H., Lyons, K., Bydder, G., Phillips, N., Best, T. M. & Benjamin, M. (2007) Is iliotibial band syndrome really a friction syndrome? *J Sci Med Sport*, 10, 74-76; discussion 77-78.
- Fan, J., Mansfield, S. G., Redmond, T., Gordon-Weeks, P. R. & Raper, J. A. (1993) The organization of F-actin and microtubules in growth cones exposed to a brain-derived collapsing factor. *J Cell Biol*, 121, 867-878.
- Fantuzzi, G. (2005) Adipose tissue, adipokines, and inflammation. *J Allergy Clin Immunol*, 115, 911-919; quiz 920.
- Fenwick, S. A., Hazleman, B. L. & Riley, G. P. (2002) The vasculature and its role in the damaged and healing tendon. *Arthritis Res*, 4, 252-260.
- Fiala, J. C. (2005) Reconstruct: a free editor for serial section microscopy. *J Microsc*, 218, 52-61.
- Fietzek, P. P. & Kuhn, K. (1976) The primary structure of collagen. *Int Rev Connect Tissue Res*, 7, 1-60.
- Fischer, H., Ax, W., Freund-Molbert, E., Holub, M., Krusmann, W. & Matthes, M. (1970) Studies on phagocytic cells of the Omentum. In Van Furth R (Ed.) *Mononuclear Phagocytes*. Oxford, Blackwell Scientific Publications.
- Fish, R. (2006) Cell-cell and cell-matrix interactions in tendon development. *Cardiff School of Biosciences*. Cardiff, University of Wales, Cardiff.
- Fishman, R. B. & Dark, J. (1987) Sensory innervation of white adipose tissue. *Am J Physiol*, 253, R942-944.
- Foreman, J. & Jordan, C. (1983) Histamine release and vascular changes induced by neuropeptides. *Agents Actions*, 13, 105-116.
- Foreman, J. C. (1987) Substance P and calcitonin gene-related peptide: effects on mast cells and in human skin. *Int Arch Allergy Appl Immunol*, 82, 366-371.
- Francois, R. J., Braun, J. & Khan, M. A. (2001) Entheses and enthesitis: a histopathologic review and relevance to spondyloarthritides. *Curr Opin Rheumatol*, 13, 255-264.
- Franke, W. W., Hergt, M. & Grund, C. (1987) Rearrangement of the vimentin cytoskeleton during adipose conversion: formation of an intermediate filament cage around lipid globules. *Cell*, 49, 131-141.
- Freeman, M. A. & Wyke, B. (1965) Reflex innervation of the ankle joint. *Nature*, 207, 196.
- Freeman, M. A. & Wyke, B. (1967a) Articular reflexes at the ankle joint: an electromyographic study of normal and abnormal influences of ankle-joint mechanoreceptors upon reflex activity in the leg muscles. *Br J Surg*, 54, 990-1001.
- Freeman, M. A. & Wyke, B. (1967b) The innervation of the ankle joint. An anatomical and histological study in the cat. *Acta Anat (Basel)*, 68, 321-333.
- Freeman, M. A. & Wyke, B. (1967c) The innervation of the knee joint. An anatomical and histological study in the cat. *J Anat*, 101, 505-532.
- Freemont, A. J., Jeziorska, M., Hoyland, J. A., Rooney, P. & Kumar, S. (2002a) Mast cells in the pathogenesis of chronic back pain: a hypothesis. *J Pathol*, 197, 281-285.
- Freemont, A. J., Watkins, A., Le Maitre, C., Baird, P., Jeziorska, M., Knight, M. T., Ross, E. R., O'Brien, J. P. & Hoyland, J. A. (2002b) Nerve growth factor expression and innervation of the painful intervertebral disc. *J Pathol*, 197, 286-292.
- Fritsch, H. (1996) Sectional anatomy of connective tissue structures in the hindfoot of the newborn child and the adult. *Anat Rec*, 246, 147-154.
- Frosch, M., Strey, A., Vogl, T., Wulffraat, N. M., Kuis, W., Sunderkotter, C., Harms, E., Sorg, C. & Roth, J. (2000) Myeloid-related proteins 8 and 14 are specifically secreted during interaction of phagocytes and activated endothelium and are useful markers for monitoring disease activity in pauciarticular-onset juvenile rheumatoid arthritis. *Arthritis Rheum*, 43, 628-637.

- Frowen, P. & Benjamin, M. (1995) Variations in the quality of uncalcified fibrocartilage at the insertions of the extrinsic calf muscles in the foot. *J Anat*, 186 (Pt 2), 417-421.
- Fu, Y., Luo, N., Klein, R. L. & Garvey, W. T. (2005) Adiponectin promotes adipocyte differentiation, insulin sensitivity, and lipid accumulation. *J Lipid Res*, 46, 1369-1379.
- Fujioka, H., Wang, G. J., Mizuno, K., Balian, G. & Hurwitz, S. R. (1997) Changes in the expression of type-X collagen in the fibrocartilage of rat Achilles tendon attachment during development. *J Orthop Res*, 15, 675-681.
- Fukushima, N., Hanada, R., Teranishi, H., Fukue, Y., Tachibana, T., Ishikawa, H., Takeda, S., Takeuchi, Y., Fukumoto, S., Kangawa, K., Nagata, K. & Kojima, M. (2005) Ghrelin directly regulates bone formation. *J Bone Miner Res*, 20, 790-798.
- Fundin, B. T., Bergman, E. & Ulfhake, B. (1997) Alterations in mystacial pad innervation in the aged rat. *Exp Brain Res*, 117, 324-340.
- Furikado, K., Fujioka, H., Kurosaka, M., Yoshiya, S., Makino, T. & Fujita, K. (2002) Comparison of mechanical and histological properties between the immature and mature tendon attachment. *Int Orthop*, 26, 318-321.
- Gajda, M., Litwin, J. A., Adriaensen, D., Timmermans, J. P. & Cichocki, T. (2004) Segmental distribution and morphometric features of primary sensory neurons projecting to the tibial periosteum in the rat. *Folia Histochem Cytobiol*, 42, 95-99.
- Galera, V. & Garralda, M. D. (1993) Enthesopathies in a spanish medieval population: anthropological, epidemiological and ethnohistorical aspects. *International Journal of Anthropology*, 8, 247-258.
- Gallagher, J., Tierney, P., Murray, P. & O'brien, M. (2005) The infrapatellar fat pad: anatomy and clinical correlations. *Knee Surg Sports Traumatol Arthrosc*, 13, 268-272.
- Galtes, I., Rodriguez-Baeza, A. & Malgosa, A. (2006) Mechanical morphogenesis: a concept applied to the surface of the radius. *Anat Rec A Discov Mol Cell Evol Biol*, 288, 794-805.
- Gamse, R., Posch, M., Saria, A. & Jancso, G. (1987) Several mediators appear to interact in neurogenic inflammation. *Acta Physiol Hung*, 69, 343-354.
- Gao, J., Messner, K., Ralphs, J. R. & Benjamin, M. (1996) An immunohistochemical study of entheses development in the medial collateral ligament of the rat knee joint. *Anat Embryol (Berl)*, 194, 399-406.
- Gatehouse, P. D. & Bydder, G. M. (2003) Magnetic resonance imaging of short T2 components in tissue. *Clin Radiol*, 58, 1-19.
- Geiger, B., Volk, T., Volberg, T. & Bendori, R. (1987) Molecular interactions in adherens-type contacts. *J Cell Sci Suppl*, 8, 251-272.
- Genc, B., Ozdinler, P. H., Mendoza, A. E. & Erzurumlu, R. S. (2004) A chemoattractant role for NT-3 in proprioceptive axon guidance. *PLoS Biol*, 2, e403.
- Gerhardt, C. C., Romero, I. A., Canello, R., Camoin, L. & Strosberg, A. D. (2001) Chemokines control fat accumulation and leptin secretion by cultured human adipocytes. *Mol Cell Endocrinol*, 175, 81-92.
- Gersh, I. & Still, M. A. (1945) Blood vessels in fat tissues. *J Exper. Med*, 219, 219-232.
- Gigante, A., Bevilacqua, C., Pagnotta, A., Manzotti, S., Toesca, A. & Greco, F. (2003) Expression of NGF, Trka and p75 in human cartilage. *Eur J Histochem*, 47, 339-344.
- Giordano, A., Cesari, P., Capparuccia, L., Castellucci, M. & Cinti, S. (2003) Sema3A and neuropilin-1 expression and distribution in rat white adipose tissue. *J Neurocytol*, 32, 345-352.
- Goldberg, D. J., Harris, D. A., Lubit, B. W. & Schwartz, J. H. (1980) Analysis of the mechanism of fast axonal transport by intracellular injection of potentially

- inhibitory macromolecules: evidence for a possible role of actin filaments. *Proc Natl Acad Sci U S A*, 77, 7448-7452.
- Goncharova, E. J., Kam, Z. & Geiger, B. (1992) The involvement of adherens junction components in myofibrillogenesis in cultured cardiac myocytes. *Development*, 114, 173-183.
- Goodenough, D. A. (1976) The structure and permeability of isolated hepatocyte gap junctions. *Cold Spring Harb Symp Quant Biol*, 40, 37-43.
- Goodenough, D. A., Paul, D. L. & Jesaitis, L. (1988) Topological distribution of two connexin32 antigenic sites in intact and split rodent hepatocyte gap junctions. *J Cell Biol*, 107, 1817-1824.
- Gordon, G. B., Barcza, M. A. & Bush, M. E. (1977) Lipid accumulation of hypoxic tissue culture cells. *Am J Pathol*, 88, 663-678.
- Goss, C. M. (1944) The attachment of skeletal muscle fibers. *Am. J. Anat*, 259-289.
- Gratzner, H. G. (1982) Monoclonal antibody to 5-bromo- and 5-iododeoxyuridine: A new reagent for detection of DNA replication. *Science*, 218, 474-475.
- Green, H. & Kehinde, O. (1979) Formation of normally differentiated subcutaneous fat pads by an established preadipose cell line. *J Cell Physiol*, 101, 169-171.
- Greene (1935) *Anatomy of the rat*, Philadelphia. Hafner.
- Gregoire, F. M., Smas, C. M. & Sul, H. S. (1998) Understanding adipocyte differentiation. *Physiol Rev*, 78, 783-809.
- Guilak, F., Awad, H. A., Fermor, B., Leddy, H. A. & Gimple, J. M. (2004) Adipose-derived adult stem cells for cartilage tissue engineering. *Biorheology*, 41, 389-399.
- Gundersen, R. W. (1987) Response of sensory neurites and growth cones to patterned substrata of laminin and fibronectin in vitro. *Dev Biol*, 121, 423-431.
- Gundersen, R. W. & Barrett, J. N. (1979) Neuronal chemotaxis: chick dorsal-root axons turn toward high concentrations of nerve growth factor. *Science*, 206, 1079-1080.
- Haines, R. W. & Mohuiddin, A. (1968) Metaplastic bone. *J Anat*, 103, 527-538.
- Hanesch, U., Heppelmann, B. & Schmidt, R. F. (1991) Substance P- and calcitonin gene-related peptide immunoreactivity in primary afferent neurons of the cat's knee joint. *Neuroscience*, 45, 185-193.
- Hart, D., Frank, C. B. & Bray, R. C. (1995) Inflammatory Processes in Repetitive Motion and Overuse Syndromes: Potential Role of Neurogenic mechanisms in tendons and ligaments. In Gordon, S. L., Blair, S. J. & Fine, L. J. (Eds.) *Repetitive Motion Disorders of the Upper Extremity*. Rosemont, American Academy of Orthopaedic surgeons.
- Havelka, S. & Horn, V. (1999) Observations on the Tidemark and Calcified Layer of Articular Cartilage. In Archer, C. W., Caterson, B., Benjamin, M. & Ralphs, J. R. (Eds.) *Biology of the Synovial joint*. Amsterdam, Harwood Academic Publishers.
- Hayami, T., Pickarski, M., Wesolowski, G. A., Mclane, J., Bone, A., Destefano, J., Rodan, G. A. & Duong Le, T. (2004) The role of subchondral bone remodeling in osteoarthritis: reduction of cartilage degeneration and prevention of osteophyte formation by alendronate in the rat anterior cruciate ligament transection model. *Arthritis Rheum*, 50, 1193-1206.
- Hayes, A. J., Benjamin, M. & Ralphs, J. R. (1999) Role of actin stress fibres in the development of the intervertebral disc: cytoskeletal control of extracellular matrix assembly. *Dev Dyn*, 215, 179-189.
- He, Z. & Tessier-Lavigne, M. (1997) Neuropilin is a receptor for the axonal chemorepellent Semaphorin III. *Cell*, 90, 739-751.
- Hebel, R. & Stromberg, M. W. (1986) *Anatomy an Embryology of the Laboratory Rat*, Germany. BioMed Verlag.

- Hems, T. & Tillmann, B. (2000) Tendon entheses of the human masticatory muscles. *Anat Embryol (Berl)*, 202, 201-208.
- Heppelmann, B. (1997) Anatomy and histology of joint innervation. *J Peripher Nerv Syst*, 2, 5-16.
- Heppelmann, B., Messlinger, K., Neiss, W. F. & Schmidt, R. F. (1990) Ultrastructural three-dimensional reconstruction of group III and group IV sensory nerve endings ("free nerve endings") in the knee joint capsule of the cat: evidence for multiple receptive sites. *J Comp Neurol*, 292, 103-116.
- Heppelmann, B., Messlinger, K. & Schmidt, R. F. (1989) Serial sectioning, electron microscopy, and three-dimensional reconstruction of fine nerve fibres and other extended objects. *J Microsc*, 156 (Pt 2), 163-172.
- Hill, E. L. & Elde, R. (1991) Distribution of CGRP-, VIP-, D beta H-, SP-, and NPY-immunoreactive nerves in the periosteum of the rat. *Cell Tissue Res*, 264, 469-480.
- Holzer, P. (1988) Local effector functions of capsaicin-sensitive sensory nerve endings: involvement of tachykinins, calcitonin gene-related peptide and other neuropeptides. *Neuroscience*, 24, 739-768.
- Hosoda, H., Kojima, M., Matsuo, H. & Kangawa, K. (2000) Ghrelin and des-acyl ghrelin: two major forms of rat ghrelin peptide in gastrointestinal tissue. *Biochem Biophys Res Commun*, 279, 909-913.
- Houk, J. & Simon, W. (1967) Responses of Golgi tendon organs to forces applied to muscle tendon. *J Neurophysiol*, 30, 1466-1481.
- Hoyle, C. H., Chakrabarti, G., Pendleton, N. P. & Andrews, P. L. (1998) Neuromuscular transmission and innervation in the urinary bladder of the insectivore *Suncus murinus*. *J Auton Nerv Syst*, 69, 31-38.
- Hukkanen, M., Kontinen, Y. T., Santavirta, S., Paavolainen, P., Gu, X. H., Terenghi, G. & Polak, J. M. (1993) Rapid proliferation of calcitonin gene-related peptide-immunoreactive nerves during healing of rat tibial fracture suggests neural involvement in bone growth and remodelling. *Neuroscience*, 54, 969-979.
- Hurov, J. R. (1986) Soft-tissue bone interface: how do attachments of muscles, tendons, and ligaments change during growth? A light microscopic study. *J Morphol*, 189, 313-325.
- Iannone, F., De Bari, C., Dell'accio, F., Covelli, M., Patella, V., Lo Bianco, G. & Lapadula, G. (2002) Increased expression of nerve growth factor (NGF) and high affinity NGF receptor (p140 TrkA) in human osteoarthritic chondrocytes. *Rheumatology (Oxford)*, 41, 1413-1418.
- Irie, K., Hara-Irie, F., Ozawa, H. & Yajima, T. (2002) Calcitonin gene-related peptide (CGRP)-containing nerve fibers in bone tissue and their involvement in bone remodeling. *Microsc Res Tech*, 58, 85-90.
- Ivie, T. J., Bray, R. C. & Salo, P. T. (2002) Denervation impairs healing of the rabbit medial collateral ligament. *J Orthop Res*, 20, 990-995.
- Jahss, M. H., Michelson, J. D., Desai, P., Kaye, R., Kummer, F., Buschman, W., Watkins, F. & Reich, S. (1992) Investigations into the fat pads of the sole of the foot: anatomy and histology. *Foot Ankle*, 13, 233-242.
- Jancso, N., Jancso-Gabor, A. & Szolcsanyi, J. (1968) The role of sensory nerve endings in neurogenic inflammation induced in human skin and in the eye and paw of the rat. *Br J Pharmacol Chemother*, 33, 32-41.
- Jarvinen, M., Jozsa, L., Kannus, P., Jarvinen, T. L., Kvist, M. & Leadbetter, W. (1997) Histopathological findings in chronic tendon disorders. *Scand J Med Sci Sports*, 7, 86-95.

- Jarvinen, M., Jozsa, L., Kvist, M., Lehto, M., Vieno, T., Isola, J. & Kannus, P. (1992) Ultrastructure and collagen composition of the myo-fascial junction in rat calf muscles. *Acta Anat (Basel)*, 145, 216-219.
- Jarvinen, M., Kannus, P., Kvist, M., Isola, J., Lehto, M. & Jozsa, L. (1991) Macromolecular composition of the myotendinous junction. *Exp Mol Pathol*, 55, 230-237.
- Jarvinen, T. A., Jozsa, L., Kannus, P., Jarvinen, T. L., Hurme, T., Kvist, M., Peltto-Huikko, M., Kalimo, H. & Jarvinen, M. (2003) Mechanical loading regulates the expression of tenascin-C in the myotendinous junction and tendon but does not induce de novo synthesis in the skeletal muscle. *J Cell Sci*, 116, 857-866.
- Jarvinen, T. A., Jozsa, L., Kannus, P., Jarvinen, T. L., Kvist, M., Hurme, T., Isola, J., Kalimo, H. & Jarvinen, M. (1999) Mechanical loading regulates tenascin-C expression in the osteotendinous junction. *J Cell Sci*, 112 Pt 18, 3157-3166.
- Jarvinen, T. A., Kannus, P., Jarvinen, T. L., Jozsa, L., Kalimo, H. & Jarvinen, M. (2000) Tenascin-C in the pathobiology and healing process of musculoskeletal tissue injury. *Scand J Med Sci Sports*, 10, 376-382.
- Johnson, D. L., Urban, W. P., Jr., Caborn, D. N., Vanarthos, W. J. & Carlson, C. S. (1998) Articular cartilage changes seen with magnetic resonance imaging-detected bone bruises associated with acute anterior cruciate ligament rupture. *Am J Sports Med*, 26, 409-414.
- Johnson, W. E., Caterson, B., Eisenstein, S. M., Hynds, D. L., Snow, D. M. & Roberts, S. (2002) Human intervertebral disc aggrecan inhibits nerve growth in vitro. *Arthritis Rheum*, 46, 2658-2664.
- Johnson, W. E., Caterson, B., Eisenstein, S. M. & Roberts, S. (2005) Human intervertebral disc aggrecan inhibits endothelial cell adhesion and cell migration in vitro. *Spine*, 30, 1139-1147.
- Johnson, W. E., Sivan, S., Wright, K. T., Eisenstein, S. M., Maroudas, A. & Roberts, S. (2006) Human intervertebral disc cells promote nerve growth over substrata of human intervertebral disc aggrecan. *Spine*, 31, 1187-1193.
- Jones, F. (1982) *Structure and function as seen in the foot*, London. 2nd edition ed, Bailliere, Tindall and Cox.
- Jorizzo, J. L., Coutts, A. A., Eady, R. A. & Greaves, M. W. (1983) Vascular responses of human skin to injection of substance P and mechanism of action. *Eur J Pharmacol*, 87, 67-76.
- Jozsa, L., Balint, J., Kannus, P., Jarvinen, M. & Lehto, M. (1993) Mechanoreceptors in human myotendinous junction. *Muscle Nerve*, 16, 453-457.
- Jozsa, L., Kvist, M., Kannus, P., Vieno, T., Jarvinen, M. & Lehto, M. (1991) Structure and macromolecular composition of the myotendineal junction. Histochemical, immunohistochemical and electron microscopic study of the rat calf muscles. *Acta Morphol Hung*, 39, 287-297.
- Jozsa, L. G. & Kannus, P. (1997) *Human Tendons. Anatomy, Physiology and Pathology*, Champaigne. Human Kinetics.
- Kamel, M., Eid, H. & Mansour, R. (2003) Ultrasound detection of heel enthesitis: a comparison with magnetic resonance imaging. *J Rheumatol*, 30, 774-778.
- Kang, X., Xie, Y., Powell, H. M., James Lee, L., Belury, M. A., Lannutti, J. J. & Kniss, D. A. (2007) Adipogenesis of murine embryonic stem cells in a three-dimensional culture system using electrospun polymer scaffolds. *Biomaterials*, 28, 450-458.
- Kannus, P. (2000) Structure of the tendon connective tissue. *Scand J Med Sci Sports*, 10, 312-320.

- Kannus, P., Jozsa, L., Jarvinen, T. A., Jarvinen, T. L., Kvist, M., Natri, A. & Jarvinen, M. (1998) Location and distribution of non-collagenous matrix proteins in musculoskeletal tissues of rat. *Histochem J*, 30, 799-810.
- Kannus, P., Jozsa, L., Kvist, M., Lehto, M. & Jarvinen, M. (1992) The effect of immobilization on myotendinous junction: an ultrastructural, histochemical and immunohistochemical study. *Acta Physiol Scand*, 144, 387-394.
- Kanzaki, M. & Pessin, J. E. (2001) Insulin-stimulated GLUT4 translocation in adipocytes is dependent upon cortical actin remodeling. *J Biol Chem*, 276, 42436-42444.
- Kao, P. F., Davis, B. L. & Hardy, P. A. (1999) Characterization of the calcaneal fat pad in diabetic and non-diabetic patients using magnetic resonance imaging. *Magn Reson Imaging*, 17, 851-857.
- Kawagoe, T., Sato, I. & Sato, T. (1997) Distribution of macromolecular components in the muscle-bone junction of human masticatory muscles. *Okajimas Folia Anat Jpn*, 74, 1-7.
- Kawahara, I., Takano, Y., Sato, O., Maeda, T. & Kannari, K. (1992) Histochemical and immunohistochemical demonstration of macrophages and dendritic cells in the lingual periodontal ligament of rat incisors. *Arch Histol Cytol*, 55, 211-217.
- Kellgren, J. H. & Samuel, E. P. (1950) The sensitivity and innervation of the articular capsule. *J. Bone Joint Surg. Br.*, 32, 84-92.
- Kenins, P. (1981) Identification of the unmyelinated sensory nerves which evoke plasma extravasation in response to antidromic stimulation. *Neurosci Lett*, 25, 137-141.
- Kenins, P., Hurley, J. V. & Bell, C. (1984) The role of substance P in the axon reflex in the rat. *Br J Dermatol*, 111, 551-559.
- Ker, R. F. (1999) The design of soft collagenous load-bearing tissues. *J Exp Biol*, 202, 3315-3324.
- Khan, K., Cook, J., Maffulli, N. & Kannus, P. (2000) Where is the pain coming from in tendinopathy? It may be biochemical, not only structural, in origin. *Br J Sports Med*, 34, 81-83.
- Khan, K. M., Bonar, F., Desmond, P. M., Cook, J. L., Young, D. A., Visentini, P. J., Fehrmann, M. W., Kiss, Z. S., O'Brien, P. A., Harcourt, P. R., Dowling, R. J., O'Sullivan, R. M., Crichton, K. J., Tress, B. M. & Wark, J. D. (1996) Patellar tendinosis (jumper's knee): findings at histopathologic examination, US, and MR imaging. Victorian Institute of Sport Tendon Study Group. *Radiology*, 200, 821-827.
- Khan, K. M., Cook, J. L., Bonar, F., Harcourt, P. & Astrom, M. (1999a) Histopathology of common tendinopathies. Update and implications for clinical management. *Sports Med*, 27, 393-408.
- Khan, M. (2002a) *The 2nd international enthesitis meeting*. Leeds General infirmary.
- Khan, M. A. (2002b) Update on spondyloarthropathies. *Ann Intern Med*, 136, 896-907.
- Khan, M. A., Dashwood, M. R., Thompson, C. S., Mumtaz, F. H., Morgan, R. J. & Mikhailidis, D. P. (1999b) Time-dependent up-regulation of neuronal 5-hydroxytryptamine binding sites in the detrusor of a rabbit model of partial bladder outlet obstruction. *World J Urol*, 17, 255-260.
- Kiani, C., Chen, L., Wu, Y. J., Yee, A. J. & Yang, B. B. (2002) Structure and function of aggrecan. *Cell Res*, 12, 19-32.
- Kido, M. A., Kiyoshima, T., Kondo, T., Ayasaka, N., Moroi, R., Terada, Y. & Tanaka, T. (1993) Distribution of substance P and calcitonin gene-related peptide-like immunoreactive nerve fibers in the rat temporomandibular joint. *J Dent Res*, 72, 592-598.

- Kimani, J. K. (1984) The structural and functional organization of the connective tissue in the human foot with reference to the histomorphology of the elastic fibre system. *Acta Morphol Neerl Scand*, 22, 313-323.
- Klein, R., Silos-Santiago, I., Smeyne, R. J., Lira, S. A., Brambilla, R., Bryant, S., Zhang, L., Snider, W. D. & Barbacid, M. (1994) Disruption of the neurotrophin-3 receptor gene *trkC* eliminates Ia muscle afferents and results in abnormal movements. *Nature*, 368, 249-251.
- Klippel, J. & Diepp, P. (1998) *Rheumatology*, London. Mosby.
- Knese, K. H. (1957) [Diaphysial chondral osteogenesis before birth.]. *Z Zellforsch Mikrosk Anat*, 47, 80-113.
- Knese, K. H. & Biermann, H. (1958) [Osteogenesis in tendon and ligament insertions in the area of the original chondral apophyses.]. *Z Zellforsch Mikrosk Anat*, 49, 142-187.
- Koch, M., Schulze, J., Hansen, U., Ashwodt, T., Keene, D. R., Brunken, W. J., Burgeson, R. E., Bruckner, P. & Bruckner-Tuderman, L. (2004) A novel marker of tissue junctions, collagen XXII. *J Biol Chem*, 279, 22514-22521.
- Kojima, M., Hosoda, H., Date, Y., Nakazato, M., Matsuo, H. & Kangawa, K. (1999) Ghrelin is a growth-hormone-releasing acylated peptide from stomach. *Nature*, 402, 656-660.
- Kosacka, J., Nowicki, M., Kacza, J., Borlak, J., Engele, J. & Spanel-Borowski, K. (2006) Adipocyte-derived angiopoietin-1 supports neurite outgrowth and synaptogenesis of sensory neurons. *J Neurosci Res*, 83, 1160-1169.
- Kraus, B. L., Kirker-Head, C. A., Kraus, K. H., Jakowski, R. M. & Steckel, R. R. (1995) Vascular supply of the tendon of the equine deep digital flexor muscle within the digital sheath. *Vet Surg*, 24, 102-111.
- Krinke, G., Froehlich, E., Herrmann, M., Schnider, K., Da Silva, F., Suter, J. & Traber, K. (1988) Adjustment of the myelin sheath to axonal atrophy in the rat spinal root by the formation of infolded myelin loops. *Acta Anat (Basel)*, 131, 182-187.
- Krist, L. F., Eestermans, I. L., Steenbergen, J. J., Hoefsmit, E. C., Cuesta, M. A., Meyer, S. & Beelen, R. H. (1995) Cellular composition of milky spots in the human greater omentum: an immunochemical and ultrastructural study. *Anat Rec*, 241, 163-174.
- Kruzynska-Frejtag, A., Wang, J., Maeda, M., Rogers, R., Krug, E., Hoffman, S., Markwald, R. R. & Conway, S. J. (2004) Periostin is expressed within the developing teeth at the sites of epithelial-mesenchymal interaction. *Dev Dyn*, 229, 857-868.
- Kubo, Y., Kaidzu, S., Nakajima, I., Takenouchi, K. & Nakamura, F. (2000) Organization of extracellular matrix components during differentiation of adipocytes in long-term culture. *In Vitro Cell Dev Biol Anim*, 36, 38-44.
- Kuettner, K. E. & Pauli, B. U. (1983) Inhibition of neovascularization by a cartilage factor. *Ciba Found Symp*, 100, 163-173.
- Kuri-Harcuch, W., Arguello, C. & Marsch-Moreno, M. (1984) Extracellular matrix production by mouse 3T3-F442A cells during adipose differentiation in culture. *Differentiation*, 28, 173-178.
- Lagasse, E. & Weissman, I. L. (1992) Mouse MRP8 and MRP14, two intracellular calcium-binding proteins associated with the development of the myeloid lineage. *Blood*, 79, 1907-1915.
- Lahm, A., Erggelet, C., Steinwachs, M. & Reichelt, A. (1998) Articular and osseous lesions in recent ligament tears: arthroscopic changes compared with magnetic resonance imaging findings. *Arthroscopy*, 14, 597-604.
- Lahm, A., Uhl, M., Erggelet, C., Haberstroh, J. & Mrosek, E. (2004) Articular cartilage degeneration after acute subchondral bone damage: an experimental study in dogs with histopathological grading. *Acta Orthop Scand*, 75, 762-767.

- Langberg, H., Skovgaard, D., Karamouzis, M., Bulow, J. & Kjaer, M. (1999) Metabolism and inflammatory mediators in the peritendinous space measured by microdialysis during intermittent isometric exercise in humans. *J Physiol*, 515 (Pt 3), 919-927.
- Lawlor, P., Marcotti, W., Rivolta, M. N., Kros, C. J. & Holley, M. C. (1999) Differentiation of mammalian vestibular hair cells from conditionally immortal, postnatal supporting cells. *J Neurosci*, 19, 9445-9458.
- Lees, M., Taylor, D. J. & Woolley, D. E. (1994) Mast cell proteinases activate precursor forms of collagenase and stromelysin, but not of gelatinases A and B. *Eur J Biochem*, 223, 171-177.
- Lembeck, F. & Holzer, P. (1979) Substance P as neurogenic mediator of antidromic vasodilation and neurogenic plasma extravasation. *Naunyn Schmiedebergs Arch Pharmacol*, 310, 175-183.
- Lemont, H., Ammirati, K. M. & Usen, N. (2003) Plantar fasciitis: a degenerative process (fasciosis) without inflammation. *J Am Podiatr Med Assoc*, 93, 234-237.
- Leon, A., Buriani, A., Dal Toso, R., Fabris, M., Romanello, S., Aloe, L. & Levi-Montalcini, R. (1994) Mast cells synthesize, store, and release nerve growth factor. *Proc Natl Acad Sci U S A*, 91, 3739-3743.
- Letourneau, P. C. (1996) The cytoskeleton in nerve growth cone motility and axonal pathfinding. *Perspect Dev Neurobiol*, 4, 111-123.
- Levine, J. D., Coderre, T. J., Covinsky, K. & Basbaum, A. I. (1990) Neural influences on synovial mast cell density in rat. *J Neurosci Res*, 26, 301-307.
- Lewin, G. R., Ritter, A. M. & Mendell, L. M. (1993) Nerve growth factor-induced hyperalgesia in the neonatal and adult rat. *J Neurosci*, 13, 2136-2148.
- Lidslot, L., Olmarker, K., Kayama, S., Larsson, K. & Rydevik, B. (2000) Nucleus pulposus inhibits the axonal outgrowth of cultured dorsal root ganglion cells. *Eur Spine J*, 9, 8-13.
- Linder, S. & Aepfelbacher, M. (2003) Podosomes: adhesion hot-spots of invasive cells. *Trends Cell Biol*, 13, 376-385.
- Lloyd, D. P. C. (1943) Neuron patterns controlling transmission of ipsilateral hind limb reflexes in cat. *J Neurophysiol*, 6, 293-315.
- Loncar, D. (1991) Convertible adipose tissue in mice. *Cell Tissue Res*, 266, 149-161.
- Lories, R. J., Daans, M., Derese, I., Matthys, P., Kasran, A., Tylzanowski, P., Ceuppens, J. L. & Luyten, F. P. (2006) Noggin haploinsufficiency differentially affects tissue responses in destructive and remodeling arthritis. *Arthritis Rheum*, 54, 1736-1746.
- Lovell, A. G. & Tanner, H. H. (1908) Synovial Membranes, with Special Reference to those related to the Tendons of the Foot and Ankle. *J Anat Physiol*, 42, 415-432.
- Lumeng, C. N., Bodzin, J. L. & Saltiel, A. R. (2007) Obesity induces a phenotypic switch in adipose tissue macrophage polarization. *J Clin Invest*, 117, 175-184.
- Lumsden, A. G. & Davies, A. M. (1983) Earliest sensory nerve fibres are guided to peripheral targets by attractants other than nerve growth factor. *Nature*, 306, 786-788.
- Luo, Y., Raible, D. & Raper, J. A. (1993) Collapsin: a protein in brain that induces the collapse and paralysis of neuronal growth cones. *Cell*, 75, 217-227.
- Ly, J. Q. & Bui-Mansfield, L. T. (2004) Anatomy of and abnormalities associated with Kager's fat Pad. *AJR Am J Roentgenol*, 182, 147-154.
- Lyons, T. J., McClure, S. F., Stoddart, R. W. & McClure, J. (2006) The normal human chondro-osseous junctional region: evidence for contact of uncalcified cartilage with subchondral bone and marrow spaces. *BMC Musculoskelet Disord*, 7, 52.
- Lyons, T. J., Stoddart, R. W., McClure, S. F. & McClure, J. (2005) The tidemark of the chondro-osseous junction of the normal human knee joint. *J Mol Histol*, 36, 207-215.

- Maccarinelli, G., Sabilia, V., Torsello, A., Raimondo, F., Pitto, M., Giustina, A., Netti, C. & Cocchi, D. (2005) Ghrelin regulates proliferation and differentiation of osteoblastic cells. *J Endocrinol*, 184, 249-256.
- Mach, D. B., Rogers, S. D., Sabino, M. C., Luger, N. M., Schwei, M. J., Pomonis, J. D., Keyser, C. P., Clohisy, D. R., Adams, D. J., O'leary, P. & Mantyh, P. W. (2002) Origins of skeletal pain: sensory and sympathetic innervation of the mouse femur. *Neuroscience*, 113, 155-166.
- Maffulli, N., Reaper, J., Ewen, S. W., Waterston, S. W. & Barrass, V. (2006) Chondral metaplasia in calcific insertional tendinopathy of the Achilles tendon. *Clin J Sport Med*, 16, 329-334.
- Maffulli, N., Testa, V., Capasso, G. & Sullo, A. (2004) Calcific insertional Achilles tendinopathy: reattachment with bone anchors. *Am J Sports Med*, 32, 174-182.
- Maganaris, C. N., Narici, M. V., Almekinders, L. C. & Maffulli, N. (2004) Biomechanics and pathophysiology of overuse tendon injuries : ideas on insertional tendinopathy. *Sports Med*, 34, 1005-1017.
- Marshall, K. W., Theriault, E. & Homonko, D. A. (1994) Distribution of substance P and calcitonin gene related peptide immunoreactivity in the normal feline knee. *J Rheumatol*, 21, 883-889.
- Mason, R. M., Levick, J. R., Coleman, P. J. & Scott, D. (1999) Biochemistry of the Synovium and Synovial Fluid. In Archer, C. W., Caterson, B., Benjamin, M. & Ralphs, J. R. (Eds.) *Biology of the Synovial Joint*. Amsterdam, Harwood Academic Publishers.
- Matthias, A., Ohlson, K. B., Fredriksson, J. M., Jacobsson, A., Nedergaard, J. & Cannon, B. (2000) Thermogenic responses in brown fat cells are fully UCP1-dependent. UCP2 or UCP3 do not substitute for UCP1 in adrenergically or fatty acid-induced thermogenesis. *J Biol Chem*, 275, 25073-25081.
- Matyas, J., Edwards, P., Miniaci, A., Shrive, N., Wilson, J., Bray, R. & Frank, C. (1994) Ligament tension affects nuclear shape in situ: an in vitro study. *Connect Tissue Res*, 31, 45-53.
- Matyas, J. R., Anton, M. G., Shrive, N. G. & Frank, C. B. (1995) Stress governs tissue phenotype at the femoral insertion of the rabbit MCL. *J Biomech*, 28, 147-157.
- Matyas, J. R., Bodie, D., Andersen, M. & Frank, C. B. (1990) The developmental morphology of a "periosteal" ligament insertion: growth and maturation of the tibial insertion of the rabbit medial collateral ligament. *J Orthop Res*, 8, 412-424.
- Maxwell, D. J., Ottersen, O. P. & Storm-Mathisen, J. (1995) Synaptic organization of excitatory and inhibitory boutons associated with spinal neurons which project through the dorsal columns of the cat. *Brain Res*, 676, 103-112.
- Mayne, R. (1988) Preparation and applications of monoclonal antibodies to different collagen types. *Clin Biochem*, 21, 111-115.
- Mccarthy, P. W., Carruthers, B., Martin, D. & Petts, P. (1991) Immunohistochemical demonstration of sensory nerve fibers and endings in lumbar intervertebral discs of the rat. *Spine*, 16, 653-655.
- Mcclure, S. R., Vansickle, D., Evans, R., Reinertson, E. L. & Moran, L. (2004) The effects of extracorporeal shock-wave therapy on the ultrasonographic and histologic appearance of collagenase-induced equine forelimb suspensory ligament desmitis. *Ultrasound Med Biol*, 30, 461-467.
- Mcdougall, J. J., Bray, R. C. & Sharkey, K. A. (1997) Morphological and immunohistochemical examination of nerves in normal and injured collateral ligaments of rat, rabbit, and human knee joints. *Anat Rec*, 248, 29-39.
- Mcgonagle, D. & Emery, P. (2000) Enthesitis, osteitis, microbes, biomechanics, and immune reactivity in ankylosing spondylitis. *J Rheumatol*, 27, 2302-2304.

- McGonagle, D., Marzo-Ortega, H., O'connor, P., Gibbon, W., Hawkey, P., Henshaw, K. & Emery, P. (2002) Histological assessment of the early enthesitis lesion in spondyloarthritis. *Ann Rheum Dis*, 61, 534-537.
- McMahon, S. B., Armanini, M. P., Ling, L. H. & Phillips, H. S. (1994) Expression and coexpression of Trk receptors in subpopulations of adult primary sensory neurons projecting to identified peripheral targets. *Neuron*, 12, 1161-1171.
- McNeilly, C. M., Banes, A. J., Benjamin, M. & Ralphs, J. R. (1996) Tendon cells in vivo form a three dimensional network of cell processes linked by gap junctions. *J Anat*, 189 (Pt 3), 593-600.
- McQueen, D. S. (1999) *Inflammatory pain and the joint*, Basel. Birkhauser.
- Messersmith, E. K., Leonardo, E. D., Shatz, C. J., Tessier-Lavigne, M., Goodman, C. S. & Kolodkin, A. L. (1995) Semaphorin III can function as a selective chemorepellent to pattern sensory projections in the spinal cord. *Neuron*, 14, 949-959.
- Messner, K., Wei, Y., Andersson, B., Gillquist, J. & Rasanen, T. (1999) Rat model of Achilles tendon disorder. A pilot study. *Cells Tissues Organs*, 165, 30-39.
- Miller, B. F., Hansen, M., Olesen, J. L., Schwarz, P., Babraj, J. A., Smith, K., Rennie, M. J. & Kjaer, M. (2006) Tendon collagen synthesis at rest and after exercise in women. *J Appl Physiol*.
- Milz, S., Benjamin, M. & Putz, R. (2005) Molecular parameters indicating adaptation to mechanical stress in fibrous connective tissue. *Adv Anat Embryol Cell Biol*, 178, 1-71.
- Milz, S., Rufai, A., Buettner, A., Putz, R., Ralphs, J. R. & Benjamin, M. (2002) Three-dimensional reconstructions of the Achilles tendon insertion in man. *J Anat*, 200, 145-152.
- Milz, S., Tischer, T., Buettner, A., Schieker, M., Maier, M., Redman, S., Emery, P., McGonagle, D. & Benjamin, M. (2004) Molecular composition and pathology of entheses on the medial and lateral epicondyles of the humerus: a structural basis for epicondylitis. *Ann Rheum Dis*, 63, 1015-1021.
- Mine, T., Kimura, M., Sakka, A. & Kawai, S. (2000) Innervation of nociceptors in the menisci of the knee joint: an immunohistochemical study. *Arch Orthop Trauma Surg*, 120, 201-204.
- Mochizuki, T., Akita, K., Muneta, T. & Sato, T. (2004) Pes anserinus: layered supportive structure on the medial side of the knee. *Clin Anat*, 17, 50-54.
- Mohammed, H. A. & Santer, R. M. (2002) Distribution and changes with age of calcitonin gene-related peptide- and substance P-immunoreactive nerves of the rat urinary bladder and lumbosacral sensory neurons. *Eur J Morphol*, 40, 293-301.
- Moitra J, M. M., Olive M, Krylov D, Gavrilova O, Marcus-Samuels B, Feigenbaum L, Lee E, Aoyama T, Eckhaus M, Reitman Ml, Vinson C (1998) Life without white fat: a transgenic mouse. *Genes Dev*, 12, 3168-3181.
- Molliver, D. C., Wright, D. E., Leitner, M. L., Parsadanian, A. S., Doster, K., Wen, D., Yan, Q. & Snider, W. D. (1997) IB4-binding DRG neurons switch from NGF to GDNF dependence in early postnatal life. *Neuron*, 19, 849-861.
- Morel, M., Boutry, N., Demondion, X., Legroux-Gerot, I., Cotten, H. & Cotten, A. (2005) Normal anatomy of the heel entheses: anatomical and ultrasonographic study of their blood supply. *Surg Radiol Anat*.
- Motta, P. (1975) Scanning electron-microscopic observations of mammalian adipose cells. *J Microsc Biol Cell* 22.
- Mueller, B. K. (1999) Growth cone guidance: first steps towards a deeper understanding. *Annu Rev Neurosci*, 22, 351-388.
- Muhl, Z. F. & Gedak, G. K. (1986) The influence of periosteum on tendon and ligament migration. *J Anat*, 145, 161-171.

- Murrell, G. A., Lilly, E. G., 3rd, Goldner, R. D., Seaber, A. V. & Best, T. M. (1994) Effects of immobilization on Achilles tendon healing in a rat model. *J Orthop Res*, 12, 582-591.
- Myers, S. L. & Christine, T. A. (1983) Hyaluronate synthesis by synovial villi in organ culture. *Arthritis Rheum*, 26, 764-770.
- Myers, T. W. (2001) *Anatomy Train. Myofascial Meridians for Manual and Movement Therapists*, Edinburgh. Churchill Livingstone.
- Nakajima, I., Muroya, S., Tanabe, R. & Chikuni, K. (2002) Extracellular matrix development during differentiation into adipocytes with a unique increase in type V and VI collagen. *Biol Cell*, 94, 197-203.
- Nakajima, I., Yamaguchi, T., Ozutsumi, K. & Aso, H. (1998) Adipose tissue extracellular matrix: newly organized by adipocytes during differentiation. *Differentiation*, 63, 193-200.
- Nakamura-Craig, M. & Gill, B. K. (1991) Effect of neurokinin A, substance P and calcitonin gene related peptide in peripheral hyperalgesia in the rat paw. *Neurosci Lett*, 124, 49-51.
- Napolitano, L. (1963) The Differentiation of White Adipose Cells. an Electron Microscope Study. *J Cell Biol*, 18, 663-679.
- Napolitano, L. & Fawcett, D. (1958) The fine structure of brown adipose tissue in the newborn mouse and rat. *J Biophys Biochem Cytol*, 4, 685-692.
- Nerlich, A. G., Weiler, C., Zipperer, J., Narozny, M. & Boos, N. (2002) Immunolocalization of phagocytic cells in normal and degenerated intervertebral discs. *Spine*, 27, 2484-2490.
- Newsham-West, R., Nicholson, H., Walton, M. & Milburn, P. (2007) Long-term morphology of a healing bone-tendon interface: a histological observation in the sheep model. *J Anat*, 210, 318-327.
- Niepel, G. A., Kostka, D., Kopecky, S. & Manaca, S. (1966) Enthesopathy. *Acta Rehm. Balneol.*, 1, 1-64.
- Niepel, G. A. & Sit'aj, S. (1979) Enthesopathy. *Clinics in Rheumatic disease*, 5, 857-872.
- Nigrovic, P. A. & Lee, D. M. (2005) Mast cells in autoantibody responses and arthritis. *Novartis Found Symp*, 271, 200-209; discussion 210-204.
- Nijijima, A. (1998) Afferent signals from leptin sensors in the white adipose tissue of the epididymis, and their reflex effect in the rat. *J Auton Nerv Syst*, 73, 19-25.
- Ninkovic, M. & Hunt, S. P. (1985) Opiate and histamine H1 receptors are present on some substance P-containing dorsal root ganglion cells. *Neurosci Lett*, 53, 133-137.
- Nolte, J. (2002) *The Human Brain An introduction to its functional anatomy*, Missouri. Fifth ed, Mosby, inc.
- O'brien, M. (1997) Structure and metabolism of tendons. *Scand J Med Sci Sports*, 7, 55-61.
- Odink, K., Cerletti, N., Bruggen, J., Clerc, R. G., Tarcsay, L., Zwadlo, G., Gerhards, G., Schlegel, R. & Sorg, C. (1987) Two calcium-binding proteins in infiltrate macrophages of rheumatoid arthritis. *Nature*, 330, 80-82.
- Ohberg, L. & Alfredson, H. (2002) Ultrasound guided sclerosis of neovessels in painful chronic Achilles tendinosis: pilot study of a new treatment. *Br J Sports Med*, 36, 173-175; discussion 176-177.
- Oishi, Y., Ohnishi, A., Suzuki, K. & Hojo, T. (1995) Lower number and thinner myelin of large myelinated fibers in human cervical compression radiculopathy. *J Neurosurg*, 83, 342-347.
- Olivieri, I., Barozzi, L., Padula, A., De Matteis, M., Pierro, A., Cantini, F., Salvarani, C. & Pavlica, P. (1998) Retrocalcaneal bursitis in spondyloarthritis: assessment by ultrasonography and magnetic resonance imaging. *J Rheumatol*, 25, 1352-1357.

- Ooshima, A. (1977) Immunohistochemical localization of prolyl hydroxylase in rat tissues. *J Histochem Cytochem*, 25, 1297-1302.
- Paleolog, E. M., Hunt, M., Elliott, M. J., Feldmann, M., Maini, R. N. & Woody, J. N. (1996) Deactivation of vascular endothelium by monoclonal anti-tumor necrosis factor alpha antibody in rheumatoid arthritis. *Arthritis Rheum*, 39, 1082-1091.
- Palesy, P. D. (1997) Tendon and ligament insertions--a possible source of musculoskeletal pain. *Cranio*, 15, 194-202.
- Pasquali-Ronchetti, I., Frizziero, L., Guerra, D., Baccarani-Contri, M., Focherini, M. C., Georgountzos, A., Vincenzi, D., Cicchetti, F., Perbellini, A. & Govoni, E. (1992) Aging of the human synovium: an in vivo and ex vivo morphological study. *Semin Arthritis Rheum*, 21, 400-414.
- Patel, A. D., Stanley, S. A., Murphy, K. G., Frost, G. S., Gardiner, J. V., Kent, A. S., White, N. E., Ghatei, M. A. & Bloom, S. R. (2006) Ghrelin stimulates insulin-induced glucose uptake in adipocytes. *Regul Pept*, 134, 17-22.
- Patten, B. (1968) *Human Embryology*, New York. 3rd edition ed, McGraw-Hill.
- Paves, H. & Saarma, M. (1997) Neurotrophins as in vitro growth cone guidance molecules for embryonic sensory neurons. *Cell Tissue Res*, 290, 285-297.
- Peacock, E. E., Jr. (1959) A study of the circulation in normal tendons and healing grafts. *Ann Surg*, 149, 415-428.
- Pecina, M. M. & Bojanic, I. (1993) *Overuse Injuries of the Musculoskeletal System*, Boca Raton. CRC Press.
- Peeraully, M. R., Jenkins, J. R. & Trayhurn, P. (2004) NGF gene expression and secretion in white adipose tissue: regulation in 3T3-L1 adipocytes by hormones and inflammatory cytokines. *Am J Physiol Endocrinol Metab*, 287, E331-339.
- Peloso, P. M. & Braun, J. (2004) Expanding the armamentarium for the spondyloarthropathies. *Arthritis Res Ther*, 6 Suppl 2, S36-43.
- Pendegrass, C. J., Oddy, M. J., Cannon, S. R., Briggs, T., Goodship, A. E. & Blunn, G. W. (2004) A histomorphological study of tendon reconstruction to a hydroxyapatite-coated implant: regeneration of a neo-enthesis in vivo. *J Orthop Res*, 22, 1316-1324.
- Pereira Da Silva, J. A. & Carmo-Fonseca, M. (1990) Peptide containing nerves in human synovium: immunohistochemical evidence for decreased innervation in rheumatoid arthritis. *J Rheumatol*, 17, 1592-1599.
- Perry, M. J., Lawson, S. N. & Robertson, J. (1991) Neurofilament immunoreactivity in populations of rat primary afferent neurons: a quantitative study of phosphorylated and non-phosphorylated subunits. *J Neurocytol*, 20, 746-758.
- Petersen, H. (1930) Die organe des skelettsystems. IN MOLLENDORF, W. (Ed.) *Handbuch der Mikroskopischen Anatomie des Menschen*. Berlin, Springer.
- Petersen, W., Pufe, T., Kurz, B., Mentlein, R. & Tillmann, B. (2002) Angiogenesis in fetal tendon development: spatial and temporal expression of the angiogenic peptide vascular endothelial cell growth factor. *Anat Embryol (Berl)*, 205, 263-270.
- Petersen, W., Pufe, T., Zantop, T., Tillmann, B., Tsokos, M. & Mentlein, R. (2004) Expression of VEGFR-1 and VEGFR-2 in degenerative Achilles tendons. *Clin Orthop Relat Res*, 286-291.
- Peyronnard, J. M. & Charron, L. (1982) Motor and sensory neurons of the rat sural nerve: a horseradish peroxidase study. *Muscle Nerve*, 5, 654-660.
- Pfirschmann, C. W., Chung, C. B., Theumann, N. H., Trudell, D. J. & Resnick, D. (2001) Greater trochanter of the hip: attachment of the abductor mechanism and a complex of three bursae--MR imaging and MR bursography in cadavers and MR imaging in asymptomatic volunteers. *Radiology*, 221, 469-477.

- Pond, A., Roche, F. K. & Letourneau, P. C. (2002) Temporal regulation of neuropilin-1 expression and sensitivity to semaphorin 3A in NGF- and NT3-responsive chick sensory neurons. *J Neurobiol*, 51, 43-53.
- Prochazka, A. (1981) Muscle spindle function during normal movement. *Int Rev Physiol*, 25, 47-90.
- Pufe, T., Petersen, W., Kurz, B., Tsokos, M., Tillmann, B. & Mentlein, R. (2003) Mechanical factors influence the expression of endostatin--an inhibitor of angiogenesis--in tendons. *J Orthop Res*, 21, 610-616.
- Pufe, T., Petersen, W. J., Miosge, N., Goldring, M. B., Mentlein, R., Varoga, D. J. & Tillmann, B. N. (2004) Endostatin/collagen XVIII--an inhibitor of angiogenesis--is expressed in cartilage and fibrocartilage. *Matrix Biol*, 23, 267-276.
- Ralphs, J. R., Waggett, A. D. & Benjamin, M. (2002) Actin stress fibres and cell-cell adhesion molecules in tendons: organisation in vivo and response to mechanical loading of tendon cells in vitro. *Matrix Biol*, 21, 67-74.
- Ramsey, H. J. (1959) Fat in the epidural space in young and adult cats. *Am J Anat*, 104, 345-379.
- Rasband, W. (2006) Image J. Version 1.37 ed.
- Redler, I., Mow, V. C., Zimny, M. L. & Mansell, J. (1975) The ultrastructure and biomechanical significance of the tidemark of articular cartilage. *Clin Orthop*, 357-362.
- Rees, S. G., Waggett, A. D., Dent, C. M. & Caterson, B. (2007) Inhibition of aggrecan turnover in short-term explant cultures of bovine tendon. *Matrix Biol*, 26, 280-290.
- Reinherz, R. P., Granoff, S. R. & Westerfield, M. (1991) Pathologic afflictions of the Achilles tendon. *J Foot Surg*, 30, 117-121.
- Resnick, D. & Niwayama, G. (1983) Entheses and enthesopathy. Anatomical, pathological, and radiological correlation. *Radiology*, 146, 1-9.
- Rijkelijkhuizen, J. M., Baan, G. C., De Haan, A., De Ruyter, C. J. & Huijing, P. A. (2005) Extramuscular myofascial force transmission for in situ rat medial gastrocnemius and plantaris muscles in progressive stages of dissection. *J Exp Biol*, 208, 129-140.
- Robbins, J. R., Evanko, S. P. & Vogel, K. G. (1997) Mechanical loading and TGF-beta regulate proteoglycan synthesis in tendon. *Arch Biochem Biophys*, 342, 203-211.
- Robertson, A., Jones, S. C., Paes, R. & Chakrabarty, G. (2004) The fabella: a forgotten source of knee pain? *Knee*, 11, 243-245.
- Robson, M. D., Benjamin, M., Gishen, P. & Bydder, G. M. (2004) Magnetic resonance imaging of the Achilles tendon using ultrashort TE (UTE) pulse sequences. *Clin Radiol*, 59, 727-735.
- Rodriguez Fernandez, J. L. & Ben-Ze'ev, A. (1989) Regulation of fibronectin, integrin and cytoskeleton expression in differentiating adipocytes: inhibition by extracellular matrix and polylysine. *Differentiation*, 42, 65-74.
- Rooney, P., Walker, D., Grant, M. E. & McClure, J. (1993) Cartilage and bone formation in repairing Achilles tendons within diffusion chambers: evidence for tendon-cartilage and cartilage-bone conversion in vivo. *J Pathol*, 169, 375-381.
- Ros, M. A., Rivero, F. B., Hinchliffe, J. R. & Hurle, J. M. (1995) Immunohistological and ultrastructural study of the developing tendons of the avian foot. *Anat Embryol (Berl)*, 192, 483-496.
- Rowe, R. W. (1985) The structure of rat tail tendon. *Connect Tissue Res*, 14, 9-20.
- Rufai, A., Benjamin, M. & Ralphs, J. R. (1992) Development and ageing of phenotypically distinct fibrocartilages associated with the rat Achilles tendon. *Anat Embryol (Berl)*, 186, 611-618.
- Rufai, A., Ralphs, J. R. & Benjamin, M. (1995) Structure and histopathology of the insertional region of the human Achilles tendon. *J Orthop Res*, 13, 585-593.

- Rufai, A., Ralphs, J. R. & Benjamin, M. (1996) Ultrastructure of fibrocartilages at the insertion of the rat Achilles tendon. *J Anat*, 189 (Pt 1), 185-191.
- Ruit, K. G., Elliott, J. L., Osborne, P. A., Yan, Q. & Snider, W. D. (1992) Selective dependence of mammalian dorsal root ganglion neurons on nerve growth factor during embryonic development. *Neuron*, 8, 573-587.
- Rumian, A. P., Wallace, A. L. & Birch, H. L. (2007) Tendons and ligaments are anatomically distinct but overlap in molecular and morphological features--a comparative study in an ovine model. *J Orthop Res*, 25, 458-464.
- Rupnick, M. A., Panigrahy, D., Zhang, C. Y., Dallabrida, S. M., Lowell, B. B., Langer, R. & Folkman, M. J. (2002) Adipose tissue mass can be regulated through the vasculature. *Proc Natl Acad Sci U S A*, 99, 10730-10735.
- Salo, P., Bray, R., Seerattan, R., Reno, C., McDougall, J. & Hart, D. A. (2007) Neuropeptides regulate expression of matrix molecule, growth factor and inflammatory mediator mRNA in explants of normal and healing medial collateral ligament. *Regul Pept*, 142, 1-6.
- Samuel, E. P. (1952) The autonomic and somatic innervation of the articular capsule. *Anat Rec*, 113, 53-70.
- Sanchis-Alfonso, V. & Alcacer-Garcia, J. (2001) Extensive osteolytic cystlike area associated with polyethylene wear debris adjacent to an aseptic, stable, uncemented unicompartamental knee prosthesis: case report. *Knee Surg Sports Traumatol Arthrosc*, 9, 173-177.
- Sato, M., Nakahara, K., Goto, S., Kaiya, H., Miyazato, M., Date, Y., Nakazato, M., Kangawa, K. & Murakami, N. (2006) Effects of ghrelin and des-acyl ghrelin on neurogenesis of the rat fetal spinal cord. *Biochem Biophys Res Commun*, 350, 598-603.
- Sato, T., Del Carmen Ovejero, M., Hou, P., Heegaard, A. M., Kumegawa, M., Foged, N. T. & Delaisse, J. M. (1997) Identification of the membrane-type matrix metalloproteinase MT1-MMP in osteoclasts. *J Cell Sci*, 110 (Pt 5), 589-596.
- Scammon, R. (1919) On the development and finer structure of the corpus adiposum buccae. *Anat Rec*, 267.
- Schaffer, M., Beiter, T., Becker, H. D. & Hunt, T. K. (1998) Neuropeptides: mediators of inflammation and tissue repair? *Arch Surg*, 133, 1107-1116.
- Schaible, H. G. & Schmidt, R. F. (1985) Effects of an experimental arthritis on the sensory properties of fine articular afferent units. *J Neurophysiol*, 54, 1109-1122.
- Schiller, P. C., D'ippolito, G., Brambilla, R., Roos, B. A. & Howard, G. A. (2001) Inhibition of gap-junctional communication induces the trans-differentiation of osteoblasts to an adipocytic phenotype in vitro. *J Biol Chem*, 276, 14133-14138.
- Schippel, K. & Reissig, D. (1968) [On the fine structure of the musculotendinal junction]. *Z Mikrosk Anat Forsch*, 78, 235-255.
- Schmidt-Rohlfing, B., Graf, J., Schneider, U. & Niethard, F. U. (1992) The blood supply of the Achilles tendon. *Int Orthop*, 16, 29-31.
- Schneider, H. (1956) Zur Struktur der sehnenansatzzonen. *Zeitschrift fuer Anatomie und Entwicklungsgeschichte*, 119, 431-456.
- Schultz, T. W. & Swett, J. E. (1974) Ultrastructural organization of the sensory fibers innervating the Golgi tendon organ. *Anat Rec*, 179, 147-162.
- Schubert, T. E., Weidler, C., Lerch, K., Hofstadter, F. & Straub, R. H. (2005) Achilles tendinosis is associated with sprouting of substance P positive nerve fibres. *Ann Rheum Dis*, 64, 1083-1086.
- Scott, J. E. (1996) Proteodermatan and proteokeratan sulfate (decorin, lumican/fibromodulin) proteins are horseshoe shaped. Implications for their interactions with collagen. *Biochemistry*, 35, 8795-8799.

- Shaffer, S. W. & Harrison, A. L. (2007) Aging of the somatosensory system: a translational perspective. *Phys Ther*, 87, 193-207.
- Shear, C. R. & Bloch, R. J. (1985) Vinculin in subsarcolemmal densities in chicken skeletal muscle: localization and relationship to intracellular and extracellular structures. *J Cell Biol*, 101, 240-256.
- Shi, H. & Bartness, T. J. (2005) White adipose tissue sensory nerve denervation mimics lipectomy-induced compensatory increases in adiposity. *Am J Physiol Regul Integr Comp Physiol*, 289, R514-R520.
- Shi, H., Song, C. K., Giordano, A., Cinti, S. & Bartness, T. J. (2005) Sensory or sympathetic white adipose tissue denervation differentially affects depot growth and cellularity. *Am J Physiol Regul Integr Comp Physiol*, 288, R1028-1037.
- Shibakawa, A., Yudoh, K., Masuko-Hongo, K., Kato, T., Nishioka, K. & Nakamura, H. (2005) The role of subchondral bone resorption pits in osteoarthritis: MMP production by cells derived from bone marrow. *Osteoarthritis Cartilage*, 13, 679-687.
- Shih, C. & Bernard, G. W. (1997) Neurogenic substance P stimulates osteogenesis in vitro. *Peptides*, 18, 323-326.
- Shin, C. S., Lecanda, F., Sheikh, S., Weitzmann, L., Cheng, S. L. & Civitelli, R. (2000) Relative abundance of different cadherins defines differentiation of mesenchymal precursors into osteogenic, myogenic, or adipogenic pathways. *J Cell Biochem*, 78, 566-577.
- Shukunami, C., Oshima, Y. & Hiraki, Y. (2005) Chondromodulin-I and tenomodulin: A new class of tissue-specific angiogenesis inhibitors found in hypovascular connective tissues. *Biochem Biophys Res Commun*, 333, 299-307.
- Silva, M. J., Boyer, M. I., Ditsios, K., Burns, M. E., Harwood, F. L., Amiel, D. & Gelberman, R. H. (2002) The insertion site of the canine flexor digitorum profundus tendon heals slowly following injury and suture repair. *J Orthop Res*, 20, 447-453.
- Slavin, B. G. (1979) Fine structural studies on white adipocyte differentiation. *Anat Rec*, 195, 63-72.
- Smas, C. M. & Sul, H. S. (1993) Pref-1, a protein containing EGF-like repeats, inhibits adipocyte differentiation. *Cell*, 73, 725-734.
- Smas, C. M. & Sul, H. S. (1995) Control of adipocyte differentiation. *Biochem J*, 309 (Pt 3), 697-710.
- Snow, D. M. & Letourneau, P. C. (1992) Neurite outgrowth on a step gradient of chondroitin sulfate proteoglycan (CS-PG). *J Neurobiol*, 23, 322-336.
- Snow, S. W., Bohne, W. H., Dicarlo, E. & Chang, V. K. (1995) Anatomy of the Achilles tendon and plantar fascia in relation to the calcaneus in various age groups. *Foot Ankle Int*, 16, 418-421.
- Soffler, C. & Hermanson, J. W. (2006) Muscular design in the equine interosseus muscle. *J Morphol*, 267, 696-704.
- Spalazzi, J. P., Gallina, J., Fung-Kee-Fung, S. D., Konofagou, E. E. & Lu, H. H. (2006) Elastographic imaging of strain distribution in the anterior cruciate ligament and at the ligament-bone insertions. *J Orthop Res*, 24, 2001-2010.
- Spiegelman, B. M. & Farmer, S. R. (1982) Decreases in tubulin and actin gene expression prior to morphological differentiation of 3T3 adipocytes. *Cell*, 29, 53-60.
- Stack, J. K. & Chasten, S. (1949) Intra-articular lesions caused by fat pad hypertrophy. *Am J Surg*, 78, 570-573; Disc, 580.
- Standring, S. (2004) *Gray's Anatomy: The anatomical basis of clinical practice*, 39th edition ed, Churchill Livingstone.
- Steinbach, L. S., Palmer, W. E. & Schweitzer, M. E. (2002) Special focus session. MR arthrography. *Radiographics*, 22, 1223-1246.

- Stevens, A. & Lowe, J. (2001) *Human Histology*, Barcelona. second ed, Mosby.
- Stilwell, D. L., Jr. (1957) The innervation of tendons and aponeuroses. *Am J Anat*, 100, 289-317.
- Stovitz, S. D. & Johnson, R. J. (2006) "Underuse" as a cause for musculoskeletal injuries: is it time that we started reframing our message? *Br J Sports Med*, 40, 738-739.
- Straus Jr, W. (1927) Growth of the Human Foot and its Evolutionary Significance. *Contributions to embryology*, 19, 93-134.
- Suzuki, D., Murakami, G. & Minoura, N. (2002) Histology of the bone-tendon interfaces of limb muscles in lizards. *Ann Anat*, 184, 363-377.
- Svensson, L., Aszodi, A., Reinholt, F. P., Fassler, R., Heinegard, D. & Oldberg, A. (1999) Fibromodulin-null mice have abnormal collagen fibrils, tissue organization, and altered lumican deposition in tendon. *J Biol Chem*, 274, 9636-9647.
- Swadison, S. & Mayne, R. (1989) Location of the integrin complex and extracellular matrix molecules at the chicken myotendinous junction. *Cell Tissue Res*, 257, 537-543.
- Takahashi, K., Mizuarai, S., Araki, H., Mashiko, S., Ishihara, A., Kanatani, A., Itadani, H. & Kotani, H. (2003) Adiposity elevates plasma MCP-1 levels leading to the increased CD11b-positive monocytes in mice. *J Biol Chem*, 278, 46654-46660.
- Takeichi, M. (1988) Cadherins: key molecules for selective cell-cell adhesion. *IARC Sci Publ*, 76-79.
- Teichert-Kuliszewska, K., Hamilton, B. S., Roncari, D. A., Kirkland, J. L., Gillon, W. S., Deitel, M. & Hollenberg, C. H. (1996) Increasing vimentin expression associated with differentiation of human and rat preadipocytes. *Int J Obes Relat Metab Disord*, 20 Suppl 3, S108-113.
- Tessier-Lavigne, M. & Goodman, C. S. (1996) The molecular biology of axon guidance. *Science*, 274, 1123-1133.
- Theobald, P., Benjamin, M., Nokes, L. & Pugh, N. (2005) Review of the vascularisation of the human Achilles tendon. *Injury*, 36, 1267-1272.
- Theobald, P., Bydder, G., Dent, C., Nokes, L., Pugh, N. & Benjamin, M. (2006) The functional anatomy of Kager's fat pad in relation to retrocalcaneal problems and other hindfoot disorders. *J Anat*, 208, 91-97.
- Tholpady, S. S., Katz, A. J. & Ogle, R. C. (2003) Mesenchymal stem cells from rat visceral fat exhibit multipotential differentiation in vitro. *Anat Rec A Discov Mol Cell Evol Biol*, 272, 398-402.
- Thomopoulos, S., Kim, H. M., Rothermich, S. Y., Biederstadt, C., Das, R. & Galatz, L. M. (2007) Decreased muscle loading delays maturation of the tendon enthesis during postnatal development. *J Orthop Res*.
- Thomopoulos, S., Marquez, J. P., Weinberger, B., Birman, V. & Genin, G. M. (2006) Collagen fiber orientation at the tendon to bone insertion and its influence on stress concentrations. *J Biomech*, 39, 1842-1851.
- Thomopoulos, S., Williams, G. R., Gimbel, J. A., Favata, M. & Soslowsky, L. J. (2003) Variation of biomechanical, structural, and compositional properties along the tendon to bone insertion site. *J Orthop Res*, 21, 413-419.
- Thompson, D. A. W. (1961) *On Growth and Form*, London. Cambridge University Press.
- Thompson, N. M., Gill, D. A., Davies, R., Loveridge, N., Houston, P. A., Robinson, I. C. & Wells, T. (2004) Ghrelin and des-octanoyl ghrelin promote adipogenesis directly in vivo by a mechanism independent of the type 1a growth hormone secretagogue receptor. *Endocrinology*, 145, 234-242.
- Tidball, J. G. (1991) Force transmission across muscle cell membranes. *J Biomech*, 24 Suppl 1, 43-52.

- Tidball, J. G. & Lin, C. (1989) Structural changes at the myogenic cell surface during the formation of myotendinous junctions. *Cell Tissue Res*, 257, 77-84.
- Tidball, J. G., O'halloran, T. & Burridge, K. (1986) Talin at myotendinous junctions. *J Cell Biol*, 103, 1465-1472.
- Tillmann, B. & Koch, S. (1995) [Functional adaptation processes of gliding tendons]. *Sportverletz Sportschaden*, 9, 44-50.
- Tippett, S. R. & Voight, M. L. (1995) *Functional Progressions for Sport Rehabilitation*, Champlain. Human Kinetics.
- Tonge, D. A., Golding, J. P., Edbladh, M., Kroon, M., Ekstrom, P. E. & Edstrom, A. (1997) Effects of extracellular matrix components on axonal outgrowth from peripheral nerves of adult animals in vitro. *Exp Neurol*, 146, 81-90.
- Tortora, G. J. & Grabowski, S. R. (1996) *Principles of Anatomy and Physiology*, New York. Eighth Edition ed, HarperCollins.
- Toumi, H., Higashiyama, I., Suzuki, D., Kumai, T., Bydder, G., Mcgonagle, D., Emery, P., Fairclough, J. & Benjamin, M. (2006) Regional variations in human patellar trabecular architecture and the structure of the proximal patellar tendon enthesis. *J Anat*, 208, 47-57.
- Toynbee, J. (1841) Researches, tending to prove the non-vascularity and the peculiar uniform mode of organization and nutrition of certain animal tissues, viz. articular cartilage and the cartilage of the different classes of fibro-cartilage. *Philos Trans R Soc Lond*, 159-192.
- Trayhurn, P. & Beattie, J. H. (2001) Physiological role of adipose tissue: white adipose tissue as an endocrine and secretory organ. *Proc Nutr Soc*, 60, 329-339.
- Tschop, M., Smiley, D. L. & Heiman, M. L. (2000) Ghrelin induces adiposity in rodents. *Nature*, 407, 908-913.
- Turner, C. E., Kramarcy, N., Sealock, R. & Burridge, K. (1991) Localization of paxillin, a focal adhesion protein, to smooth muscle dense plaques, and the myotendinous and neuromuscular junctions of skeletal muscle. *Exp Cell Res*, 192, 651-655.
- Uthoff, H. K., Sarkar, K. & Maynard, J. A. (1976) Calcifying tendinitis: a new concept of its pathogenesis. *Clin Orthop*, 164-168.
- Umezawa, A. & Hata, J. (1992) Expression of gap-junctional protein (connexin 43 or alpha 1 gap junction) is down-regulated at the transcriptional level during adipocyte differentiation of H-1/A marrow stromal cells. *Cell Struct Funct*, 17, 177-184.
- Unger, J. (2004) Diabetic Neuropathy: Early clues, effective management *Consultant*, 44 1549-1556
- Verdu, E., Ceballos, D., Vilches, J. J. & Navarro, X. (2000) Influence of aging on peripheral nerve function and regeneration. *J Peripher Nerv Syst*, 5, 191-208.
- Verna, J. M., Fichard, A. & Saxod, R. (1989) Influence of glycosaminoglycans on neurite morphology and outgrowth patterns in vitro. *Int J Dev Neurosci*, 7, 389-399.
- Viskochil, D. H. (2003) It takes two to tango: mast cell and Schwann cell interactions in neurofibromas. *J Clin Invest*, 112, 1791-1793.
- Vogel, K. G. (2004) What happens when tendons bend and twist? Proteoglycans. *J Musculoskelet Neuronal Interact*, 4, 202-203.
- Vogel, K. G., Keller, E. J., Lenhoff, R. J., Campbell, K. & Koob, T. J. (1986) Proteoglycan synthesis by fibroblast cultures initiated from regions of adult bovine tendon subjected to different mechanical forces. *Eur J Cell Biol*, 41, 102-112.
- Vogel, K. G. & Koob, T. J. (1989) Structural specialization in tendons under compression. *Int Rev Cytol*, 115, 267-293.
- Vogel, K. G. & Meyers, A. B. (1999) Proteins in the tensile region of adult bovine deep flexor tendon. *Clin Orthop Relat Res*, S344-355.

- Volk, T. & Geiger, B. (1984) A 135-kd membrane protein of intercellular adherens junctions. *Embo J*, 3, 2249-2260.
- Von Schroeder, H. P. & Botte, M. J. (1993) The functional significance of the long extensors and juncturae tendinum in finger extension. *J Hand Surg [Am]*, 18, 641-647.
- Von Schroeder, H. P., Botte, M. J. & Gellman, H. (1990) Anatomy of the juncturae tendinum of the hand. *J Hand Surg [Am]*, 15, 595-602.
- Waggett, A. D., Benjamin, M. & Ralphs, J. R. (2006) Connexin 32 and 43 gap junctions differentially modulate tenocyte response to cyclic mechanical load. *Eur J Cell Biol*, 85, 1145-1154.
- Waggett, A. D., Ralphs, J. R., Kwan, A. P., Woodnutt, D. & Benjamin, M. (1998) Characterization of collagens and proteoglycans at the insertion of the human Achilles tendon. *Matrix Biol*, 16, 457-470.
- Wagner, E., Gould, J. S., Kneidel, M., Fleisig, G. S. & Fowler, R. (2006) Technique and results of Achilles tendon detachment and reconstruction for insertional Achilles tendinosis. *Foot Ankle Int*, 27, 677-684.
- Waite, J. H., Lichtenegger, H. C., Stucky, G. D. & Hansma, P. (2004) Exploring molecular and mechanical gradients in structural bioscaffolds. *Biochemistry*, 43, 7653-7662.
- Wakabayashi, Y., Maeda, T., Tomoyoshi, T. & Kwok, Y. N. (1998) Increase of growth-associated protein-43 immunoreactivity following cyclophosphamide-induced cystitis in rats. *Neurosci Lett*, 240, 89-92.
- Wei, X. & Messner, K. (1996) The postnatal development of the insertions of the medial collateral ligament in the rat knee. *Anat Embryol (Berl)*, 193, 53-59.
- Weihe, E., Nohr, D., Millan, M. J., Stein, C., Muller, S., Gramsch, C. & Herz, A. (1988) Peptide neuroanatomy of adjuvant-induced arthritic inflammation in rat. *Agents Actions*, 25, 255-259.
- Weinreich, S., Eulderink, F., Capkova, J., Pla, M., Gaede, K., Heesemann, J., Van Alphen, L., Zurcher, C., Hoebe-Hewryk, B., Kievits, F. & Et Al. (1995) HLA-B27 as a relative risk factor in ankylosing enthesopathy in transgenic mice. *Hum Immunol*, 42, 103-115.
- Weis, J. & Schroder, J. M. (1989a) Differential effects of nerve, muscle, and fat tissue on regenerating nerve fibers in vivo. *Muscle Nerve*, 12, 723-734.
- Weis, J. & Schroder, J. M. (1989b) The influence of fat tissue on neuroma formation. *J Neurosurg*, 71, 588-593.
- Weisberg, S. P., Mccann, D., Desai, M., Rosenbaum, M., Leibel, R. L. & Ferrante, A. W., Jr. (2003) Obesity is associated with macrophage accumulation in adipose tissue. *J Clin Invest*, 112, 1796-1808.
- Wickham, M. Q., Erickson, G. R., Gimble, J. M., Vail, T. P. & Guilak, F. (2003) Multipotent stromal cells derived from the infrapatellar fat pad of the knee. *Clin Orthop*, 196-212.
- Willberg, L., Sunding, K., Ohberg, L., Forssblad, M. & Alfredson, H. (2007) Treatment of Jumper's knee: promising short-term results in a pilot study using a new arthroscopic approach based on imaging findings. *Knee Surg Sports Traumatol Arthrosc*, 15, 676-681.
- Williams, P. L. (1987) The painful heel. *Br J Hosp Med*, 38, 562-563.
- Willis, W. D. & Coggeshall, R. (1991) Peripheral Nerves and Sensory Receptors. *Sensory Mechanisms of the Spinal Cord*. 2nd Edition ed. New York, Plenum Press.
- Witonski, D. & Wagrowska-Danielewicz, M. (1999) Distribution of substance-P nerve fibers in the knee joint in patients with anterior knee pain syndrome. A preliminary report. *Knee Surg Sports Traumatol Arthrosc*, 7, 177-183.

- Wojtys, E. M., Beaman, D. N., Glover, R. A. & Janda, D. (1990) Innervation of the human knee joint by substance-P fibers. *Arthroscopy*, 6, 254-263.
- Woo, S. L. & Buckwalter, J. A. (1988) AAOS/NIH/ORS workshop. Injury and repair of the musculoskeletal soft tissues. Savannah, Georgia, June 18-20, 1987. *J Orthop Res*, 6, 907-931.
- Wright, D. E., White, F. A., Gerfen, R. W., Silos-Santiago, I. & Snider, W. D. (1995) The guidance molecule semaphorin III is expressed in regions of spinal cord and periphery avoided by growing sensory axons. *J Comp Neurol*, 361, 321-333.
- Wyatt, S., Shooter, E. M. & Davies, A. M. (1990) Expression of the NGF receptor gene in sensory neurons and their cutaneous targets prior to and during innervation. *Neuron*, 4, 421-427.
- Yaksh, T. L. (1988) Substance P release from knee joint afferent terminals: modulation by opioids. *Brain Res*, 458, 319-324.
- Yanagiya, T., Tanabe, A. & Hotta, K. (2007) Gap-junctional communication is required for mitotic clonal expansion during adipogenesis. *Obesity (Silver Spring)*, 15, 572-582.
- Yoffe, J. R., Taylor, D. J. & Wooley, D. E. (1984) Mast cell products stimulate collagenase and prostaglandin E production by cultures of adherent rheumatoid synovial cells. *Biochem Biophys Res Commun*, 122, 270-276.
- Yokokawa, K., Sakanaka, M., Shiosaka, S., Tohyama, M., Shiotani, Y. & Sonoda, T. (1985) Three-dimensional distribution of substance P-like immunoreactivity in the urinary bladder of rat. *J Neural Transm*, 63, 209-222.
- Yokokawa, K., Tohyama, M., Shiosaka, S., Shiotani, Y., Sonoda, T., Emson, P. C., Hillyard, C. V., Girgis, S. & Macintyre, I. (1986) Distribution of calcitonin gene-related peptide-containing fibers in the urinary bladder of the rat and their origin. *Cell Tissue Res*, 244, 271-278.
- Youssef, P., Roth, J., Frosch, M., Costello, P., Fitzgerald, O., Sorg, C. & Bresnihan, B. (1999) Expression of myeloid related proteins (MRP) 8 and 14 and the MRP8/14 heterodimer in rheumatoid arthritis synovial membrane. *J Rheumatol*, 26, 2523-2528.
- Zantop, T., Tillmann, B. & Petersen, W. (2003) Quantitative assessment of blood vessels of the human Achilles tendon: an immunohistochemical cadaver study. *Arch Orthop Trauma Surg*, 123, 501-504.
- Zeisig, E., Ohberg, L. & Alfredson, H. (2006a) Extensor origin vascularity related to pain in patients with Tennis elbow. *Knee Surg Sports Traumatol Arthrosc*, 14, 659-663.
- Zeisig, E., Ohberg, L. & Alfredson, H. (2006b) Sclerosing polidocanol injections in chronic painful tennis elbow-promising results in a pilot study. *Knee Surg Sports Traumatol Arthrosc*, 14, 1218-1224.
- Zelena, J. (1976) Sensory terminals on extrafusal muscle fibres in myotendinous regions of developing rat muscles. *J Neurocytol*, 5, 447-463.
- Zhang, Y., Ramos, B. F. & Jakschik, B. A. (1992) Neutrophil recruitment by tumor necrosis factor from mast cells in immune complex peritonitis. *Science*, 258, 1957-1959.
- Zhang, Y., Shi, S., Ciurli, C. & Poole, A. R. (2002) Animal models of ankylosing spondylitis. *Curr Rheumatol Rep*, 4, 507-512.
- Zhou, X. F. & Rush, R. A. (1995) Peripheral projections of rat primary sensory neurons immunoreactive for neurotrophin 3. *J Comp Neurol*, 363, 69-77.
- Zimny, M. L. (1988) Mechanoreceptors in articular tissues. *Am J Anat*, 182, 16-32.
- Zumwalt, A. (2005) A new method for quantifying the complexity of muscle attachment sites. *Anat Rec B New Anat*, 286, 21-28.

Solutions

100mM Phosphate Buffer (PB)

100mls 200mM sodium dihydrogen orthophosphate ($\text{NaH}_2\text{PO}_4 \cdot 2\text{H}_2\text{O}$ – 31.2g/litre) (Fisher Scientific, Loughborough, UK)

400mls 200mM di-sodium hydrogen orthophosphate anhydrous (Na_2HPO_4 – 28.4g/litre) (Fisher Scientific, Loughborough, UK)

500mls distilled H_2O

100mM Phosphate Buffer (PB) 0.01% triton X

100mls 200mM sodium dihydrogen orthophosphate ($\text{NaH}_2\text{PO}_4 \cdot 2\text{H}_2\text{O}$ – 31.2g/litre)

400mls 200mM di-sodium hydrogen orthophosphate anhydrous (Na_2HPO_4 – 28.4g/litre)

500mls distilled H_2O

1ml Triton X (Sigma-Aldrich, Gillingham, UK)

4% Paraformaldehyde (PFA) in 100mM PB

200mls distilled H_2O

16g PFA powder (Fisher Scientific, Loughborough, UK)

4 drops NaOH (1M - Fisher Scientific, Loughborough, UK)

4 drops HCl (1M - Fisher Scientific, Loughborough, UK)

40mls 200mM sodium dihydrogen orthophosphate ($\text{NaH}_2\text{PO}_4 \cdot 2\text{H}_2\text{O}$ – 31.2g/litre)

160mls 200mM di-sodium hydrogen orthophosphate anhydrous (Na_2HPO_4 – 28.4g/litre)

4% Paraformaldehyde (PFA) and 2% Gluteraldehyde in 100mM PB

200mls distilled H_2O

16g PFA powder (Fisher Scientific, Loughborough, UK)

4 drops NaOH (1M - Fisher Scientific, Loughborough, UK)

4 drops HCl (1M - Fisher Scientific, Loughborough, UK)

40mls 200mM sodium dihydrogen orthophosphate ($\text{NaH}_2\text{PO}_4 \cdot 2\text{H}_2\text{O}$ – 31.2g/litre)

160mls 200mM di-sodium hydrogen orthophosphate anhydrous (Na_2HPO_4 – 28.4g/litre)

10mls 25% Gluteraldehyde (Agar Scientific, Stansted, UK)

10% ethylenediaminetetraacetic acid (EDTA) disodium salt solution

100mls 100mM PB

12.5g NaOH pellets (Fisher Scientific, Loughborough, UK)

10g ethylenediaminetetraacetic acid (EDTA) disodium salt (Fisher Scientific, Loughborough, UK)

5% Sucrose solution

100mls 100mM PB

10g Sucrose (Fisher Scientific, Loughborough, UK)

Tris Buffer (TB) pH 7.0

5mls 200mM Tris stock solution (4.8g Tris Base (Fisher Scientific, Loughborough, UK) in 100mls dH₂O)

1.7mls 1N HCl (Sigma-Aldrich, Gillingham, UK)

3.3mls H₂O

TB pH 8.2

5mls 200mM Tris stock solution

1.2mls 1N HCl (Sigma-Aldrich, Gillingham, UK)

4.3mls H₂O

TB, 0.1% Bovine serum albumin (BSA)

10mls TB pH 7.0 or 8.2 solution

3.3mg BSA (Sigma-Aldrich, Gillingham, UK)

Reynold's Lead citrate solution

1.33g Lead Nitrate (Fisher Scientific, Loughborough, UK)

1.76g Sodium Citrate (Fisher Scientific, Loughborough, UK)

30mls H₂O

0.7% Pioloform solution

50mls 1,2 Dichloroethane

0.35g Pioloform Powder (Agar Scientific, Stansted, UK)

Sodium Ethoxide

100mls 100% Ethanol (Fisher Scientific, Loughborough, UK)

5.5g Sodium Hydroxide (Fisher Scientific, Loughborough, UK)

Bromodeoxyuridine solution

10mls Tris pH7.6

250mg BrdU

500µl = 12.5mg given to a 250g rat (50mg/kg)

L15 dissecting media (Gift from Prof. A. Davies)

1 pot of L15 powder (Gibco-Invitrogen, Paisley, UK)

1L dH₂O and mix thoroughly

60mg Penicillin (Sigma-Aldrich, Gillingham, UK)

100mg Streptomycin (Sigma-Aldrich, Gillingham, UK)

Mix and make to pH 7.2-7.4

Filter using sterile pump filter (Millipore, Watford, UK)

Ham's F15 culture media (Gift from Prof. A. Davies)

1 pot of F12 powder (Gibco-Invitrogen, Paisley, UK)

1L dH₂O and mix thoroughly

60mg Penicillin (Sigma-Aldrich, Gillingham, UK)

100mg Streptomycin (Sigma-Aldrich, Gillingham, UK)

Remove 100ml of the solution then add 100ml horse serum (Sigma-Aldrich, Gillingham, UK)

Filter using sterile pump filter (Millipore, Watford, UK)

F14 final growth medium (Gift from Prof A. Davies)

500mg sodium hydrogen carbonate (BDH Laboratory Supplies, Poole, UK)

250ml distilled water and mix

Remove 25ml and discard

25mls F14 stock solution

10mls L-Glutamine

5.5ml Albumax I (20g/100ml - Gibco-Invitrogen, Paisley, UK) containing -

160mg Putrescine

1ml Progesterone (0.625mg/ml in ethanol)

10ml L-thyroxine (0.4mg/ml in ethanol)

10ml Sodium selenite (0.4mg/ml in PBS)

10ml Tri-Iodothyroxine (0.34mg/ml in ethanol)

Filter using sterile pump filter (Millipore, Watford, UK)

Durcopan[®]

10mls A/M resin

10mls solution B

0.35mls solution C

0.15mls solution D

Procedures

Haematoxylin & Eosin stain

De-wax in xylene and rehydrate in alcohol

Wash in running tap water (5 min)

Stain in Mayer's Haematoxylin (10 min - RA Lamb Medical Supplies, Eastbourne, UK))

Wash in running tap water until clear

Stain in 1% Aqueous Eosin (5 min - RA Lamb Medical Supplies, Eastbourne, UK)

Wash in running tap water (30 sec)

Rehydrate in alcohol and clear in xylene

Mount in DPX and coverslip

Masson's trichrome stain

De-wax in xylene and rehydrate in alcohol
Stain in Celestine blue B (10 min)
Wash in running tap water until clear
Stain in Mayer's Haematoxylin (10 min - RA Lamb Medical Supplies, Eastbourne, UK)
Wash in running tap water until clear
Stain in Ponceau/acid fuchin (5 min)
Wash in running tap water (30 sec)
Differentiate in 1% phosphomolydic acid (5 mns)
Transfer directly to light green stain (2 min)
Wash in running tap water until clear
Wash in 1% acetic acid
Wash briefly in running tap water (30 sec)
Rehydrate in alcohol and clear in xylene
Mount in DPX and coverslip

Van Gieson stain

De-wax in xylene and rehydrate in alcohol
Stain slides in Miller's elastic stain at 60°C
Wash in 95% alcohol
Wash in running tap water until clear
Stain in Celestine blue B (10 min)
Wash in running tap water (1 min)
Stain in Mayer's Haematoxylin (10 min - RA Lamb Medical Supplies, Eastbourne, UK)
Wash in running tap water (5 min)
Stain in Van Gieson's stain (3 min)
Wash briefly in tap water (30s)
Dehydrate in alcohol and clear in xylene
Mount in DPX and coverslip

Toluidine blue

De-wax in xylene and rehydrate in alcohol
Apply toluidine blue to sections (30 sec)
Wash in running tap water until clear
Drain and blot slides dry with filter paper
Air dry for a few minutes
Clear in xylene
Mount using DPX and coverslip

APPENDIX II

TURNS 10 - 2000				TURNS 2001 - 3000				TURNS 3001 - 4000				TURNS 4001 - 5000			
Q1S1	Q1S2	Q1S3	Q1S4	Q1S1	Q1S2	Q1S3	Q1S4	Q1S1	Q1S2	Q1S3	Q1S4	Q1S1	Q1S2	Q1S3	Q1S4
1	1	1	1	1	1	1	1	1	1	1	1	1	1	1	1
2	2	2	2	2	2	2	2	2	2	2	2	2	2	2	2
3	3	3	3	3	3	3	3	3	3	3	3	3	3	3	3
4	4	4	4	4	4	4	4	4	4	4	4	4	4	4	4
5	5	5	5	5	5	5	5	5	5	5	5	5	5	5	5
6	6	6	6	6	6	6	6	6	6	6	6	6	6	6	6
7	7	7	7	7	7	7	7	7	7	7	7	7	7	7	7
8	8	8	8	8	8	8	8	8	8	8	8	8	8	8	8
9	9	9	9	9	9	9	9	9	9	9	9	9	9	9	9
10	10	10	10	10	10	10	10	10	10	10	10	10	10	10	10

Q1S1	Q1S2	Q1S3	Q1S4												
1	1	1	1	1	1	1	1	1	1	1	1	1	1	1	1
2	2	2	2	2	2	2	2	2	2	2	2	2	2	2	2
3	3	3	3	3	3	3	3	3	3	3	3	3	3	3	3
4	4	4	4	4	4	4	4	4	4	4	4	4	4	4	4
5	5	5	5	5	5	5	5	5	5	5	5	5	5	5	5
6	6	6	6	6	6	6	6	6	6	6	6	6	6	6	6
7	7	7	7	7	7	7	7	7	7	7	7	7	7	7	7
8	8	8	8	8	8	8	8	8	8	8	8	8	8	8	8
9	9	9	9	9	9	9	9	9	9	9	9	9	9	9	9
10	10	10	10	10	10	10	10	10	10	10	10	10	10	10	10

Publications Arising from this Work

FULL LENGTH PUBLICATIONS

Shaw H.M, Santer R.M, Watson A.H.D, and Benjamin M. (2007) Structure – function relationships of entheses in relation to mechanical load and exercise. *Scand. J. Med and Sci in Sports*. Aug; 17 (4): 303-15.

Shaw H.M, and Benjamin M. (2007) Adipose tissue at Entheses: The Innervation and cell composition of the retromalleolar fat pad associated with the Achilles tendon. *J.Anat*. Aug 3; Epub ahead of print.

ABSTRACTS

Shaw H.M, Santer R.M, Watson A.H.D, and Benjamin M. (2006) The innervation of the enthesis organ of the rat Achilles tendon. *J. Anat* March 208 (3) pp 204. Paper #21. (Oral presentation).

Shaw H.M, Milz S, Büettner A, Santer R.M, Watson A.H.D, and Benjamin M. (2006) The Innervation of Kager’s Fat Pad in Man. *Winter meeting of the ASGBI in Oxford* (Poster Presentation).

Shaw H.M, Milz S, Büettner A, Santer R.M, Watson A.H.D, and Benjamin M. (2006) The Innervation of the enthesis organ of the rat Achilles tendon. *Medicine and Science in Sports and Exercise*. May 38 (Supplement No.5) Paper #2426 (Poster Presentation).

Shaw H.M, Santer R.M., Watson A.H.D., and Benjamin M. (2006) The Structure and Innervation of the Muscular Origin of Tibialis Anterior in the Rat. *Joint summer meeting of the ASGBI and Spanish Anatomical Society (SPA) in Madrid* (Poster Presentation)

Summer meeting of the ASGBI in Cardiff (2005) (Oral Presentation)

Published in Journal of Anatomy (2006); March 208 (3) pp 204. Paper #21

The innervation of the enthesis organ of the rat Achilles tendon

H.M. Shaw, R.M. Santer, A.H.D. Watson, and M. Benjamin

School of Biosciences, Cardiff University, Cardiff, UK.

The enthesis (bony insertion site) is a common site of overuse injuries in sport and a region that is also commonly affected in patients with ankylosing spondylitis. Because insertional tendinopathies can be very painful, it is often assumed that entheses are richly innervated. However there is little evidence to confirm this assumption, and thus we have investigated the nerve supply to the Achilles tendon enthesis in the rat. This insertion site is one of the most complex of tendon attachments. Together with adjacent structures, it forms part of an 'enthesis organ'. The other structures include a sesamoid fibrocartilage in the tendon, a periosteal fibrocartilage on the calcaneus, and Kager's fat pad which protrudes into the retrocalcaneal bursa. Enthesis organs were removed from 3 male Wistar rats at each of the following ages - neonates, 4 week, 12 week and 24 month. The tissue was prepared for indirect immunofluorescence and cryosections cut in the sagittal plane. The presence of nerve fibres in the different parts of the enthesis organ was evaluated in serial sections immunolabelled with polyclonal antibodies against protein gene product 9.5, substance P, calcitonin gene related peptide, and neurofilament 200. At all ages, the enthesis itself and the sesamoid and periosteal fibrocartilages were not innervated, but the fat pad was supplied by nerve fibres immunoreactive to substance P, calcitonin gene related peptide, and neurofilament 200. We suggest that healthy entheses are not innervated because insertion sites experience high levels of mechanical load. However, the striking innervation of the fat pad suggests that it may have an unheralded proprioceptive role monitoring changes in insertional angle between tendon and bone that occur as a result of foot movements. Prominent mast cells seen in toluidine blue sections within the fat pad may play a role in neurogenic inflammatory responses.

American Collagen of Sports Medicine (ACSM) 53rd Annual Meeting in Denver, Colorado (2006). Published in the Abstract issue of Medicine and Science in Sports and Exercise (2006); May 38 (Supplement No.5) Paper #2426 (Poster Presentation)

The Innervation of the enthesis organ of the rat Achilles tendon

H.M. Shaw¹, S. Milz², A. Büettner³, R.M. Santer¹, A. Watson¹, and M. Benjamin¹ ¹School of Biosciences, Cardiff University, ² AO Research Institute, Davos, Switzerland and ³Institut für Rechtsmedizin, Ludwig-Maximilians-Universität, Munich, Germany

PURPOSE: The enthesis (bony insertion of a tendon or ligament) is a common site of overuse injuries in sport. Because enthesopathies can be painful, it is often assumed that the enthesis is highly innervated – but with little evidence to support the assumption. The Achilles tendon has one of the most complex of attachment sites, for together with adjacent tissues, the enthesis itself forms part of an ‘enthesis organ’ which reduces stress concentration at the bony interface. These adjacent structures include a ‘sesamoid fibrocartilage’ in the tendon, a ‘periosteal fibrocartilage’ on the superior tuberosity of the calcaneus, and a fat pad which extends into the retrocalcaneal bursa during plantarflexion. The purpose of the present study is to investigate the innervation of the whole enthesis organ complex. **METHODS:** The tendon attachment site was removed from one leg of 3 male Wistar rats at each of the following ages – neonates, 4 weeks, 12 weeks, and 24 months. The tissue was fixed in 4% paraformaldehyde, prepared for routine indirect immunohistochemistry and cryosectioned in the sagittal plane. Serial sections were immunolabelled with polyclonal antibodies to protein gene product 9.5, substance P, calcitonin gene related peptide and neurofilament 200. Histology reference sections were stained with toluidine blue. **RESULTS:** No nerve fibres were detected at the enthesis itself or in the sesamoid and periosteal fibrocartilages in rats of any age. However, the fat pad was richly supplied by nerve fibres which immunolabelled with all of the antibodies used. It also contained abundant mast cells. The innervation of the fat pad was confirmed in 10 human Achilles tendons obtained from the Department of Forensic Medicine at the Ludwig-Maximilians-Universität, in accordance with the ethical regulations of Munich University. The nerve fibres again immunolabelled with all antibodies and formed an intricate network in which the fibres lay between individual fat cells. **CONCLUSION:** We suggest that healthy entheses are not innervated because of the high levels of mechanical loading experienced at insertion sites. However, the striking innervation of the adjacent fat pad suggests that it may have an unheralded proprioceptive role monitoring changes in insertional angle between tendon and bone that occur as a result of foot movements.

The Innervation of Kager's Fat Pad in Man

H.M. Shaw¹, S. Milz², A. Büettner³, R.M. Santer¹, A.D.H. Watson¹, and M. Benjamin¹

¹School of Biosciences, Cardiff University and ²AO Research Institute, Davos, Switzerland, ³Institut für Rechtsmedizin, Ludwig-Maximilians-Universität, Munich, Germany.

The enthesis (bony attachment of a tendon or ligament) is a common site of overuse injuries and the primary 'target organ' in the spondyloarthropathies. Because enthesopathies can be painful, it is often assumed that the enthesis is highly innervated – but with little evidence to support the assumption. The Achilles tendon has one of the most complex of attachment sites, for together with adjacent tissues, the enthesis itself forms part of an 'enthesis organ' which reduces stress concentration at the bony interface. These adjacent structures include a prominent fat pad which extends into the retrocalcaneal bursa during plantarflexion. We have previously demonstrated in both young and aged rats that this is the only region of the enthesis organ which is innervated. It is heavily supplied by both nociceptive and mechanoreceptive nerve fibres. The purpose of the present study was to investigate the innervation of the comparable fat pad (Kager's fat pad) in man. The fat pad was removed from 10 human cadaveric specimens of various ages (11-84 years) obtained from the Department of Forensic Medicine at the Ludwig-Maximilians-Universität (Germany), in accordance with the ethical regulations of Munich University. The tissue was fixed in 100% ethanol and serial sections were immunolabelled with polyclonal antibodies to protein gene product 9.5, substance P, calcitonin gene related peptide and neurofilament 200. Antibody binding was detected both with a Vectastain ABC 'Elite' avidin/biotin kit and for confocal microscopy, with immunofluorescence, using a FITC-conjugated goat anti-rabbit Fab fragments as a secondary antibody. Histology reference sections were stained with toluidine blue and Masson's Trichrome. The fat pad was richly supplied by nerve fibres which immunolabelled with all the antibodies used. The delicate nerve fibres insinuated in a complex manner between adjacent adipocytes in association with a rich capillary network. The striking innervation of the fat pad suggests that it may be a source of pain in enthesopathies and have a proprioceptive role in monitoring movement of the tendon relative to the bone during locomotion.

Joint summer meeting of the ASGBI and Spanish Anatomical Society (SPA) in Madrid (2006) (Poster Presentation)

The Structure and Innervation of the Muscular Origin of Tibialis Anterior in the Rat

Shaw H.M., Santer R.M., Watson A.H.D., and Benjamin M.

School of Biosciences, Cardiff University, Cardiff, UK.

The term enthesis is usually associated with the bony attachment of a tendon or ligament; however, some muscles attach to bone via a small amount of loose connective tissue. Such “fleshy” entheses have not been widely studied. This region is of particular interest as this may be the site where pain arises in overuse injuries, such as shin splints. The purpose of this study is to investigate the structure and innervation of the fleshy attachment of tibialis anterior in the rat. The attachment site was removed from 5 male Wistar rats at 12 weeks of age, fixed in 4% paraformaldehyde, stored overnight in 10% sucrose buffer and cryosectioned. Sections were immunolabelled with antibodies to protein gene product 9.5 (PGP 9.5), substance P (SP), CGRP and neurofilament 200 (NF200). Antibody binding was detected with; Vectastain avidin/biotin kit or FITC-conjugated goat anti-rabbit Fab fragments. Reference sections were stained with toluidine blue and Masson’s Trichrome. The muscle itself is attached indirectly to the fibrous layer of the periosteum via a small amount of loose connective tissue; this in turn attaches to the osteogenic layer of the periosteum which subsequently attaches to the underlying bone. In contrast to the aneural nature of fibrocartilaginous entheses, “fleshy” entheses are innervated with a large number of both nociceptive (SP and CGRP) and mechanoreceptive (NF200) nerve fibres. Nociceptive fibres may play a significant role in pain caused by microtrauma and pathology associated with this region. In addition, muscle spindle-like structures immunoreactive to NF200 close to the enthesis were common. These structures may play role similar to Golgi tendon organs in monitoring stretch at myotendinous junctions.

Summer meeting of the ASGBI in Durham (2007) (Poster Presentation, Young Cave investigator of the year award)

Could the retromalleolar fat pad of the rat Achilles tendon enthesis organ function as an immune organ?

Shaw H.M. , Santer R.M., Watson A.H.D., and Benjamin M.

School of Biosciences, Cardiff University, Cardiff, UK.

Adipose tissue is a conspicuous, though greatly neglected component of entheses (bony attachments of tendons or ligaments) and a number of functions for this fat have been proposed, including stress dissipation and sensory perception. As adipose tissue elsewhere in the body is known to function as an immune organ, we have sought to determine whether the retromalleolar fat pad component of the Achilles tendon enthesis organ contains monocytes and/or macrophages which may play a similar role at attachment sites. The Achilles tendon enthesis organ was removed from male Wistar rats at 1 day, 1 month, 4 months, and 24 months of age (3 of each age), fixed in 4% paraformaldehyde, stored overnight in 10% sucrose buffer and cryosectioned. Sections were immunolabelled with the PAN macrophage/monocyte marker - CD68 (ED1), and inflammation marker - myeloid related protein (MRP) 14. Antibody binding was detected with a biotinylated secondary antibody using a Vector avidin/biotin kit. Labelling was developed with NovaRED and the sections were counterstained with Mayer's haematoxylin. In all animals and at all ages, CD68 positive macrophages were present within the retromalleolar fat pad. In aged (24month) rats, such macrophages were additionally present within the sesamoid and periosteal fibrocartilages and on their bursal surfaces. Blood vessel-associated MRP14 labelling was also seen in the fat pads of 24 month rats. This enthesis-associated adipose tissue may therefore play a role in protecting the attachment site from infection and/or removing cellular debris from the retrocalcaneal bursa. If similar findings can be confirmed in human entheses, this may have implications for understanding the seronegative spondyloarthropathies - debilitating, rheumatic conditions in which the enthesis is generally considered to be the primary 'target organ'.

Review

Structure–function relationships of entheses in relation to mechanical load and exercise

H. M. Shaw, M. Benjamin

Cardiff School of Biosciences, Cardiff University, Cardiff, UK

Corresponding author: M Benjamin, Cardiff School of Biosciences, Cardiff University, Cardiff, UK. Tel: +44 (0)2920875041, Fax: +44 (0)2920874116, E-mail: Benjamin@cardiff.ac.uk

Accepted for publication 7 February 2007

Entheses are regions of high-stress concentration that are commonly affected by overuse injuries in sport. This review summarizes current knowledge of their structure–function relationships – at the macroscopic, microscopic and molecular levels. Consideration is given to how stress concentration is reduced at fibrocartilaginous entheses by various adaptations which ensure that stress is dissipated away from the hard–soft tissue interface. The fundamental question of how a tendon or ligament is anchored to bone is addressed – particularly in relation to the paucity of compact bone at fibrocartilaginous entheses. The concept of an “enthesis organ” is reviewed – i.e. the idea of a collection of tissues

adjacent to the enthesis itself, which jointly serve a common function – stress dissipation. The archetypal enthesis organ is that of the Achilles tendon and the functional importance of its subtendinous bursa, with its fibrocartilaginous walls and protruding fat pad, is emphasized. The distribution of adipose tissue elsewhere at entheses is also explained and possible functions of insertion-site fat are evaluated. Finally, a brief consideration is given to enthesopathies, with attention drawn to the possibility of degenerative changes affecting other regions of an enthesis organ, besides the enthesis itself.

What are entheses and why are they important?

An enthesis is the attachment of a tendon, ligament or joint capsule to bone. It is also called an insertion site, osteotendinous or osteoligamentous junction. Benjamin and McGonagle (2001) have coined the term “enthesis organ” to emphasize the point that structures adjacent to the enthesis itself also help to reduce stress concentration at the attachment site. Stress concentration is a key issue at an enthesis, because any insertion site represents the meeting point between two materials of very different physical properties (i.e. a “soft and flexible” tendon/ligament and a hard bone). Mechanical engineers know that such a recipe makes the region vulnerable to failure. Benjamin and McGonagle (2001) have also introduced the term “functional enthesis” to describe the wrap-around regions of tendons or ligaments (TL), where there is a change in direction around a bony or fibrous pulley (Vogel & Koob, 1989). This highlights the parallels between wrap-around regions and “true” entheses. However, the current review primarily focuses on the structure and function of entheses and enthesis organs and the reader is referred elsewhere for any further consideration of functional entheses (Benjamin & Ralphs,

1998; Benjamin & McGonagle, 2001). We have given particular emphasis in the current article to mechanical issues that relate to sport and exercise.

Functionally, entheses provide strong and stable anchorage that promotes musculo-skeletal movement with the necessary, concomitant joint integrity. However, they must serve as more than simple anchors, for in linking soft to hard tissue, entheses also need to minimize the risk of damage in the face of high levels of mechanical loading. They do this by facilitating the smooth transfer of force between soft and hard tissue. This can occur in either direction, and particularly in the context of sport it is important to remember that ground reaction forces can place enormous strain on TL entheses. An enthesis is thus a key link in any muscle–tendon–bone or bone–ligament–bone unit – and one that may experience considerably more stress than the TL itself. Curiously, however, Rijkelijhuizen et al. (2005) have claimed that not all of the force generated by a muscle is transferred to bone via its connecting tendon. They argue that force transmission can continue even when a tendon is severed, provided that the connection between the epimysium and the epitendinous tissue is substantial and intact (Rijkelijhuizen et al., 2005).

Despite the stress concentration at entheses, they are less likely to fail than other parts of the musculo-skeletal chain, because of their ability to withstand high mechanical loads. Nonetheless, they are vulnerable to overuse injuries and these present as a number of poorly understood, pathological changes that are collectively referred to as enthesopathies. Any such injury can have a significant impact on the ability of athletes to pursue their sport. Pathologies such as the epicondyloses (tennis and little league elbow), proximal patellar tendinopathy (jumper's knee), a variety of Achilles insertional disorders and plantar fasciosis ("fasciitis" is probably a less appropriate synonym) are well known to sports medicine practitioners.

In the differential diagnosis of overuse injuries associated with sport and exercise, clinicians must recognize that entheses are also targeted in the seronegative spondyloarthropathies (SpA) (Benjamin and McGonagle, 2001). These are a diverse collection of chronic, autoimmune joint diseases that are among the most prevalent of rheumatic conditions. They include ankylosing spondylitis, reactive arthritis, psoriatic arthritis, and arthritis associated with inflammatory bowel disease. Similarly, Diffuse Idiopathic Skeletal Hyperostosis (DISH, formerly known as Forestier's disease Cammisa et al., (1998)) is also characterized by excessive bone deposition at entheses that leads to the formation of bony spurs.

Entheses are of particular concern to orthopedic surgeons who treat sporting injuries because of the common need to re-attach TL to bone – e.g. during the reconstruction of an anterior cruciate ligament. It is uniquely challenging to recreate the natural smooth transfer of load from TL to bone that typifies the healthy, original attachment site (Pende-grass et al., 2004). A variety of techniques have been pioneered surgically that attempt to do so, but most simply involve stapling the TL to the bone. More recently, however, various materials with viscous properties (e.g. hydroxyapatite) have been coated on the attachment site of the implanted TL (Pende-grass et al., 2004).

The reader concerned more broadly with the influence of exercise on the musculo-skeletal system should note that skeletal attachment sites have long been of interest to archaeologists in relation to physical activity. The focus of archaeologists has been exclusively on the characteristic markings left by entheses following skeletal maceration. The premise is that the appearance of dried bones conveys useful information about the lifestyle of ancient populations (Galera & Garralda, 1993). Greater physical activity (e.g. between males and females) is reflected by different entheses markings. The constant stressing of a muscle from daily repetitive tasks of various types gives the archaeologist a skeletal record

of habitual activity patterns and this has contributed to understanding a wide range of issues relating to ancient populations (social, cultural, labor, the development, and use of tools, etc. – Galera and Garralda (1993)).

Enthesis structure

Macroscopic structure

As TL approach bone, they flare out in order to increase the surface area of the attachment. A good example of this is the attachment of the Achilles tendon to the calcaneus or the combined insertion of the tendons of sartorius, gracilis, and semitendinosus onto the tibia. These three tendons constitute the *pes anserinus* (literally "duck's foot") because of their highly flared appearance. Both the Achilles tendon and the *pes anserinus* are also illustrative of the general principle that neighboring entheses often interconnect to form stronger and more stable attachments. Indeed, this may be reflected in their development – as with the Achilles tendon and the plantar fascia. In the fetus, these two structures are continuous over the posteroinferior aspect of the calcaneus, because both initially attach to the perichondrium, rather than to the cartilaginous anlagen itself (Snow et al., 1995). With growth, this continuity is certainly reduced, but may still be evident in adulthood (Milz et al., 2002) – although Snow et al. (1995) disagree. The direct continuity of one entheses with another has also been observed between the insertion of the quadriceps tendon and origin of the patellar ligament (Toumi et al., 2006). Fibers from the former pass over the anterior surface of the patella (to which they also attach) to become directly continuous with the patellar ligament at its proximal entheses. The convergence of entheses and the blending of attachment sites with adjacent fasciae is an adaptation for dissipating stress between one TL and another and thus reducing the risk of local failure. There are numerous, largely unnamed, fibrous connections between one TL and another in the immediate vicinity of their attachment sites. It may also account for why patients with enthesopathies can complain of pain and tenderness in areas adjacent to the principal entheses involved. Thus, in considering cases of lateral epicondylosis, the clinician should note that the attachment of the common extensor tendon merges imperceptibly with the entheses of the lateral collateral ligament and that this in turn fuses with the annular ligament of the superior radioulnar joint (Milz et al., 2004).

On the other hand, there is a need to ensure that certain tendons attach to bone discretely in order to promote precise and highly intricate movements. It is interesting to consider whether this relates to a

particular propensity of tendons with small areas of bony attachment (relative to the size of the whole musculo-skeletal unit) for avulsion. A whole series of imaginatively named, avulsion fractures have been described in the hand and wrist (where TL often have small entheses) – e.g. mallet finger, coach's finger, and gamekeeper's thumb. However, it should be recognized that load may be reduced at a given attachment site (thus reducing the risk of avulsion) by dissipating the action of a single muscle belly over more than one tendon – e.g. as with the digital tendons. In other regions of the body, stress dissipation can be promoted by a single tendon attaching to a number of bones. Thus, fibularis (peroneus) longus attaches to both the medial cuneiform and the first metatarsal, and tibialis posterior sends tendinous slips to every tarsal bone except the talus.

Microscopic structure

Classification of entheses

Because the pioneering, histological descriptions of entheses were largely published in German, one of the key early classifications distinguished between *die diaphysären-periostalen Ansätze* (“diaphysial–periosteal attachments”) and *die chondralen-apophysären Ansätze* (chondral–apophyseal attachments) (Biermann, 1957; Knese & Biermann, 1958). However, these terms only refer to the attachments of TL to long bones and cannot be easily applied to other parts of the skeleton. Thus, more recently, broader terminologies have been devised to encompass the entire musculo-skeletal system. Benjamin and co-workers (Benjamin & McGonagle, 2001; Benjamin et al., 2002, 2006) have regarded entheses as being either fibrous or fibrocartilaginous, depending on the character of the tissue at the TL–bone interface [Fig. 1(a)–(c)]. Fibrous entheses are usually present where TLs attach to the diaphysis or metaphysis of a long bone – e.g. the tibial attachment of the medial collateral ligament (MCL) of the knee. They equate to the diaphysial–periosteal attachments of Biermann (1957) or to the “indirect” insertions of Woo et al. (1988). The former authors have sub-classified such entheses as “areal” or “circumscribed,” with the distinction relating to the surface area (i.e. the footprint) of the attachment. Areal entheses have fibers that flare out over a larger area than circumscribed attachments. Hems and Tillmann (2000) consider that regarding entheses as either fibrous or fibrocartilaginous is an oversimplification and argue that fibrous entheses can be sub-classified into “bony” or “periosteal” attachments to indicate whether the tendon inserts directly into the bone [Fig. 1(b)] or indirectly into it via the periosteum [Fig. 1(c)]. It should be recognized, however, that as

development proceeds, periosteal entheses can become bony ones (Gao et al., 1996).

Fibrocartilaginous entheses (the “direct insertions” of Woo et al. (1988) or the chondral–apophyseal attachments of Knese and Biermann (1958) are more common than fibrous entheses and predominate at the epiphyses and apophyses of long bones and in the short bones of the carpus and tarsus (Benjamin et al., 1986). The archetypal fibrocartilaginous attachment is exemplified by that of the Achilles tendon on the calcaneus [Fig. 1(a) and (d)]. It should be noted, however, that the structure of a given enthesis can vary greatly from region to region. Hems and Tillmann (2000) emphasized this in their study of the attachments of the masticatory muscles, and both Benjamin et al. (1986) and Woo et al. (1988) have pointed out that what are termed fibrocartilaginous entheses are not cartilaginous in all regions. Thus, at the Achilles tendon insertion for example, the most superficial part of the attachment is purely fibrous (Benjamin et al., 2002). The significance of this in understanding the differential load transfer across the footprint of an enthesis has yet to be thoroughly explored, although it is recognized by Maganaris et al. (2004).

Although this review focuses on TL entheses, it is also important to remember that some muscles have fleshy attachments to bone and thus lack a tendinous link to the skeleton – although usually at one end only. Even at such attachment sites, however, muscle fibers do not anchor directly to the underlying periosteum, but attach to it via a small amount of connective tissue associated with the muscle fibers. These entheses correspond to the muscular or “fleshy” attachment sites of Biermann (1957).

Fibrocartilaginous entheses

Dolgo-Saburoff (1929) described a four-layered, bony attachment of the cat patellar ligament in which the zones defined were the ligament itself, uncalcified fibrocartilage, calcified fibrocartilage, and bone. The zonal concept, which is widely credited to have originated with this author, remains a cornerstone of descriptions today, although Benjamin et al. (2007) have pointed out that one or more of the zones may be locally absent. Cooper and Misol (1970) later showed that each of the zones has different characteristics, but emphasized how the zones can blend imperceptively with each other. Typically, the tendon or ligament region (i.e. the zone furthest away from the bone at an enthesis) is characterized by the presence of parallel bundles of collagen fibers, with rows of elongate fibroblasts lying between them. Within the zone of uncalcified fibrocartilage, these collagen fibers may become less obvious, as their staining properties are masked by

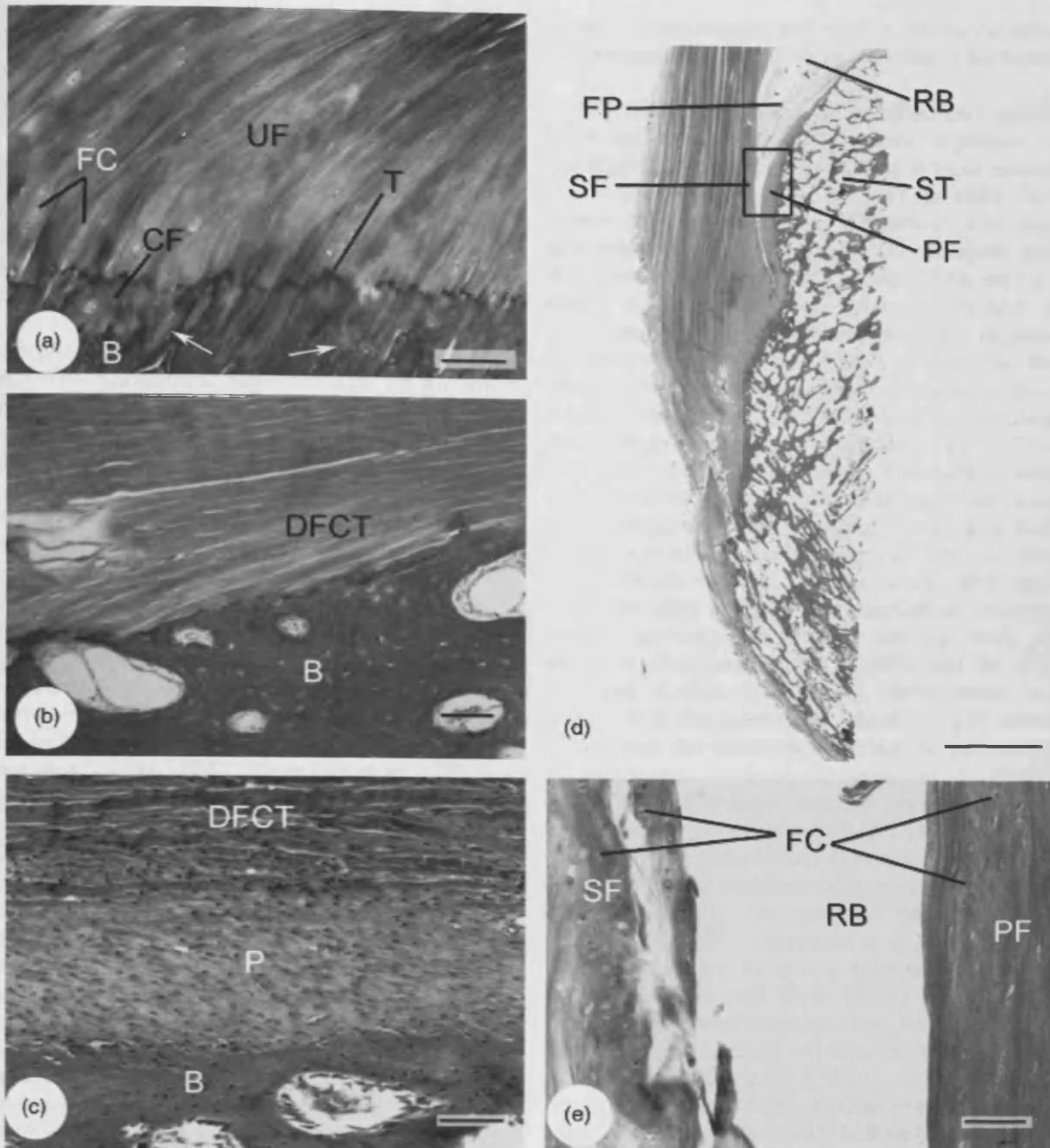


Fig. 1. Histological structure of entheses and the concept of an enthesis organ. (a) The fibrocartilaginous enthesis of the human Achilles tendon. Zones of calcified (CF) and uncalcified (UF) fibrocartilage are readily visible and large rounded fibrocartilage cells (FC) are conspicuous in the former. Note that a calcification front (the tidemark – T) separates hard from soft tissue, but that this is subtly different from the tissue boundary between tendon and bone (B). This boundary is marked by an irregular cement line (arrows). Scale bar = 100 μ m. (b) The purely fibrous enthesis of pronator teres in the adult forearm. The dense fibrous connective tissue (DFCT) of the tendon approaches the bone at a very oblique angle and attaches directly to the bone – i.e. no periosteum is present. Scale bar = 200 μ m. (c) The periosteal fibrous attachment of a horse ligament. Note that the ligament attaches indirectly to the bone via the thick periosteum. P, periosteum. Scale bar = 100 μ m. (d) Low-power view of the enthesis organ associated with the human Achilles tendon. The enthesis organ comprises the enthesis itself (E), sesamoid (SF) and periosteal (PF) fibrocartilages, the retrocalcanal bursa (RB) and the tip of Kager's fat pad (FP). Note the virtual absence of compact bone at the enthesis. ST, superior tuberosity. Scale bar = 3 mm. (e) Higher-power view of the sesamoid and periosteal fibrocartilages in a region similar to that enclosed in the rectangle in (d). Note the presence of rounded fibrocartilage cells (FC). Scale bar = 100 μ m.

those of the proteoglycan-rich, extracellular matrix (ECM), and the fibroblasts are replaced by fibrocartilage cells. These latter cells are more rounded and lie in lacunae, surrounded by a small amount of amorphous ECM. Again, they are typically arranged in longitudinal rows – reflecting their metaplastic origin from fibroblasts during development (see Benjamin & McGonagle, 2001 for further details). A basketweave arrangement of collagen fibers is sometimes evident within enthesis fibrocartilage and may spread the load of the TL over a broader area.

Functional significance of uncalcified enthesis fibrocartilage. The uncalcified fibrocartilage at an enthesis promotes a gradual change of elastic modulus that encourages the smooth transfer of load across the hard–soft tissue interface (Hems & Tillmann, 2000). It allows the gradual bending of TL collagen fibers as they approach the bone, in much the same way that a grommet on an electrical plug controls the bending of the lead that enters it (Schneider 1956). The “bending-control” function is supported by the correlation that exists between the quantity of uncalcified fibrocartilage at different entheses, and the range of insertional angle change that occurs with joint movement – the greater the angle change, the more fibrocartilage is present (Evans et al., 1990; Benjamin et al., 1991, 1992; Boszczyk et al., 2003). Fibrocartilage may also act as a “stretching brake” for tendons during muscular contraction (Knese & Biermann, 1958). In other words, it may prevent a tendon from narrowing as it elongates. Any significant narrowing too close to a bony interface may weaken the tendon attachment site. In all of these functions, fibrocartilage should primarily be viewed as a tissue geared toward resisting compression and/or shear (Benjamin & Ralphs, 1998).

Knese and Biermann (1958) highlighted the specialized nature of fibrocartilage cells and this issue has been addressed in much further detail by Benjamin and Ralphs (2004). These latter authors have commented on the transitional character of fibrocartilage and emphasized that the term fibrocartilage embraces a wide spectrum of tissues with properties intermediate between those of dense fibrous connective tissue and hyaline cartilage. However, it is the cartilage-like molecules in the ECM that are of particular importance in providing a TL with the ability to withstand compression (Milz et al., 2005). Such loading is an inevitable consequence of the changing insertional angle of a TL that accompanies joint movement. More recently, the orientation of collagen fibers at the insertion site has also attracted attention in relation to mechanisms for reducing stress concentration. Thomopoulos et al. (2006) demonstrated that a changing orientation of the collagen fibers from tendon to the bone results in changes to the predicted

stress concentrations; this may therefore influence the cell phenotype and matrix production at the insertion.

Tidemarks. The layers of calcified and uncalcified fibrocartilage at an enthesis are separated by a calcification front [Fig. 1(a)] that is most commonly called the tidemark, but which in the older German literature was called *die Grenzlinie*. Occasionally (particularly in older people), the tidemark may be duplicated (Benjamin et al., 1986). Although a tidemark separates calcified from uncalcified fibrocartilage, collagen fibers in the two regions are continuous. Few authors have studied the importance of the tidemark at entheses, but the presence of a comparable boundary within articular cartilage has attracted greater attention. Redler et al. (1975) have raised the possibility that the tidemark tethers the perpendicularly orientated, collagen fibers in articular cartilage to reduce shearing stresses and Havelka and Horn (1999) have suggested that it prevents blood vessels from penetrating uncalcified cartilage. It is certainly a region of mechanical weakness at which horizontal clefts can develop both at TL entheses (Benjamin et al., 2007) and in articular cartilage (Kumar et al., 1991). Furthermore, in both tissues, it is the interface at which the soft tissues fall away from the hard ones, during the preparation of an anatomical skeleton (Benjamin et al., 1986). It is also pertinent to note that the presence of multiple tidemarks in articular cartilage has long been associated with osteoarthritis (Lane & Bullough, 1980) and that tendon entheses too can show osteoarthritic-like degenerative changes and multiple tidemarks (Rufai et al., 1995; Benjamin et al., 2007).

The exact structure of a tidemark is difficult to define. Havelka and Horn (1999) have described a wide spectrum of appearances, from fibrillated to granular, and pointed out that the tidemark may be ill-defined (particularly if the tissue is pathological), may vary with age and may change with the degree of loading. Lyons et al. (2005) believe that the tidemark in articular cartilage is formed by two juxtaposed laminae with differing biochemical characteristics. They suggest that it inhibits hydroxyapatite crystal formation and growth after musculo-skeletal maturity. In this way, the cartilage is protected from progressive mineralization. Clearly, this could also apply to the fibrocartilage at entheses and it may help to bear this in mind when considering the significance of multiple tidemarks that can be a feature of degenerative insertional tendinopathies. Curiously, Zoeger et al. (2006) have found that tidemarks in articular cartilage have a particular propensity for accumulating lead, although the significance of this is unclear. The calcified (fibro)cartilage cells immediately deep to the tidemark have characteristics similar to those in the neighboring uncalcified region and

their viability has been confirmed by a number of authors, as reviewed in articular cartilage by Havelka and Horn (1999).

Subchondral bone plate. Although the tidemark is the mechanical boundary of an enthesis, it is subtly distinct from the tissue boundary – i.e. the interface between TL and bone (Hems & Tillmann, 2000). This is represented by a cement line [Fig. 1(a)]. In sharp contrast to the straightness of a normal tidemark, the cement line is highly convoluted, and the increased surface area it creates between TL and bone promotes firm anchorage and resistance to shear. As Hems and Tillmann (2000) have explained, the two interfaces have conflicting mechanical demands and thus need to be spatially distinct. The tidemark has to be as straight and smooth as possible at a healthy enthesis so that movement of soft tissue over hard tissue does not result in damage to the former. On the other hand, a straight boundary between hard and soft tissues does not make for the most secure mechanism of attaching a TL to a bone. Anchorage is thus better promoted by increasing the surface area of contact between the two tissues. Hence, the arrangement is that the terminal part of the TL is represented by a zone of calcified fibrocartilage that has an irregular interface (i.e. a cement line) with the underlying bone. The irregularity gives good resistance to shear – essential because TLs pull on bone from typically oblique angles. Whether or not there is significant continuity of collagen fibers across the cement line (i.e. from TL to bone) at a fibrocartilaginous enthesis is debatable. The traditional view is that TL attach to bone via “Sharpey’s fibers” and indeed, such fibers are obviously present at certain fibrous entheses (Hems & Tillmann, 2000). However, Benjamin et al. (2007) point out that compact bone may be virtually absent at even the largest of fibrocartilaginous entheses and that the cortical shell is often no more than a continuum of spongy bone trabeculae. Thus, there would seem to be insufficient cortical bone at the attachment site itself [see Fig. 1(d)], to accommodate many/any deeply penetrating collagen fibers. It is worth noting, however, that Haines and Mohuiddin (1968) suggest that the fibers that cross the tidemark between uncalcified and calcified fibrocartilage at TL entheses could be considered as equivalent to Sharpey’s fibers, because calcified fibrocartilage can be viewed as metaplastic bone. Although such considerations are valid, Milz et al. (2002) suggest that it is the highly interdigitating nature of the calcified fibrocartilage zone of the inserting TL and underlying bone that is of fundamental importance in promoting attachment.

Why is there so little compact bone at fibrocartilaginous entheses? One possibility is that this contributes to stress dissipation by allowing slight

deformation of the bone during loading of the TL (Benjamin et al., 2007). In other words, stress dissipation is not the sole prerogative of the soft tissue side of an enthesis, but continues within the bone itself via the trabecular network. In addition, the absence of compact bone may be an adaptation to promote access of the soft tissue to marrow blood vessels, for there are local areas at the enthesis where both the subchondral bone and calcified fibrocartilage are completely missing (Benjamin et al., 2007). Such “holes” may also provide access to immunocompetent cells and stem cells in the underlying bone marrow. Similar defects have been reported in the subchondral bone plate that supports articular cartilage (Shibakawa et al., 2005). It has been suggested that these holes could reflect bone resorption and remodeling, and that they may also trigger proteoglycan degradation in the adjacent articular cartilage (Shibakawa et al., 2005). This could occur via the osteoclastic expression of matrix metalloproteinases. Although such a potential for remodeling may be construed as beneficial, the formation of local defects in any subchondral plate (i.e. either that which supports articular cartilage or a TL enthesis) might equally create an imbalance in stress transduction within the overlying (fibro)cartilage. Clearly this could promote local degeneration (Shibakawa et al., 2005). In the light of the above considerations, it is interesting to note that damage to the subchondral bone (i.e. fractures) can lead to lesions in the overlying articular cartilage (Lahm et al., 2004). Intriguingly, when alendronate (an inhibitor of bone resorption) was given to rats with subchondral bone fractures, remodeling of the subchondral plate was suppressed and the formation of cartilage lesions was prevented (Hayami et al., 2004). Whether similar findings could apply to the enthesis is unknown.

Molecular composition of enthesis fibrocartilage.

The reader is referred to earlier reviews by Benjamin and McGonagle (2001) and Milz et al. (2005) for a comprehensive account of the great variety of different molecules that have been found at entheses. Clearly, the ECM molecules in enthesis fibrocartilage must play an important role in force transfer at attachment sites, and the type of molecule present is directly related to the mechanical demands at the interface. This is the basic premise developed in the extensive monograph of Milz et al. (2005). They emphasize how the expression of the glycosaminoglycans (GAGs), chondroitin – 4 and 6 – sulfate is elevated at fibrocartilaginous entheses, reflecting the compressive loading to which the attachment site is subject. These GAGs are usually associated with aggrecan – a large, aggregating proteoglycan that is a major constituent of the ECM in hyaline articular cartilage. Aggrecan is a hydrophilic molecule that

imbibes water and thus allows a TL to withstand compression (Yoon & Halper, 2005). It is probably the aggrecan content of entheses that accounts for the ability of the uncalcified fibrocartilage to dissipate collagen fiber bending and prevent TL narrowing from occurring too close to the bony interface, under load. Other small, leucine-rich, proteoglycans such as decorin, fibromodulin and lumican have also been detected immunohistochemically in enthesis fibrocartilage. They may have an important role in regulating collagen fibril formation and thus determining the tensile strength of the TL (Milz et al., 2005).

The importance of cartilage-like molecules in tendons has been highlighted by Corps et al. (2004, 2006). They demonstrate that levels of aggrecan and biglycan in painful tendinopathy are increased and may reflect the change in mechanical loading at the site of the lesion, leading to a more cartilage-like phenotype of the tissue. Such an increased expression of these proteoglycans would also be expected to occur at entheses, as changes in mechanical loading are also experienced here in injured tendons. These changes may in turn cause a further alteration in the mechanical loading and consequently trigger a vicious cycle of increased pathology (Maffulli et al., 2006).

While type I collagen generally predominates in the midsubstance of a TL, and in bone, type II collagen (the typical collagen of cartilage) is only characteristic of the fibrocartilage zones (Milz et al., 2005). Although types III and IV collagen show no significant regional variations across the TL-bone unit, the expression of the latter does vary between the midsubstance of the TL and the fibrocartilage zones. In the TL itself, type IV collagen is found throughout the ECM, while in the fibrocartilaginous regions it has a more restricted and pericellular distribution. This suggests that type IV collagen has different matrix-binding functions in these regions (Waggett et al., 1998). Type III collagen has the ability to form heterotypic fibrils with types I and V collagen and is believed to play a role in controlling fibril diameter (Birk & Mayne, 1997; Waggett et al., 1998). Type X collagen has also been identified at entheses (within the zone of calcified fibrocartilage) and is thought to be important in controlling calcification (Fujioka et al., 1997). Interestingly, Kruzynska-Frejtag et al. (2004) have recently demonstrated the presence of a cell-adhesion molecule called “periostin” at the periodontal ligament enthesis that may also be involved in controlling mineralization. They suggest that high levels of periostin present at hard–soft tissue interfaces may prevent ligament cells near the soft–hard tissue boundary from differentiating into an osteogenic phenotype. In other words, the molecule helps to maintain the ligament as a non-mineralized tissue.

It would thus be of interest to know whether periostin is expressed at other entheses and whether a reduction in its expression is associated with the spread of mineralization into soft tissues. Finally, it must be acknowledged that we know little about the turnover of any enthesis ECM molecules, but in the rest of the TL, it seems that men have elevated levels of collagen synthesis following exercise compared with women (Miller et al., 2007). This has been related to the greater incidence of exercise-related musculo-skeletal injuries in women.

Fibrous entheses

Fibrous entheses have attracted far less interest than fibrocartilaginous attachments, probably because they are less frequently involved in enthesopathies. Nevertheless, a number of large and powerful muscles (e.g. deltoid, pectoralis major and latissimus dorsi; Benjamin et al., 1986) and important ligaments (e.g. the knee joint MCL; Woo et al., 1988) have fibrous entheses. The footprint of fibrous entheses is generally broad and this helps to dissipate the stress over a wide area and minimize stretching.

As outlined earlier, there are two forms of fibrous entheses – those that attach directly to cortical bone and those that attach indirectly to it via the periosteum [Fig. 1(b) and (c)]. Following closure of the growth plate, a periosteal fibrous enthesis can become a bony one, although some TL attach to the periosteum throughout life (Hems & Tillmann, 2000). It is important to recognize that the initial periosteal attachment of a metaphyseal TL to a long bone allows the TL to migrate as the bone lengthens, so that the relative position of the ligament remains unchanged. This is because the periosteum can grow interstitially, but the bone itself cannot – it can only grow by appositional means. A periosteal, fibrous enthesis is inevitably weaker than a bony one and this is a fact that should be recognized by those concerned with coaching young children in sport, for it has a bearing on the loading of entheses during puberty in athletic children.

The enthesis organ concept and its relevance in sports medicine

Benjamin and McGonagle (2001) coined the term “enthesis organ” to denote a collection of structures adjacent to the attachment site itself that are functionally associated with the enthesis and that also play an important part in reducing stress concentration at the soft–hard tissue interface. The concept of an enthesis organ explains why patients may present with symptoms adjacent to an enthesis as well as at the enthesis itself.

The archetypal enthesis organ is that of the Achilles tendon [Fig. 1(d)], which Canoso (1998) described as the “première enthesis.” Canoso was aware of the contribution of neighboring structures to the role of the enthesis itself and had made particularly pertinent observations on the functions of Kager’s fat pad that protrudes into the retrocalcaneal bursa (Canoso et al., 1988). The triangular tip of this fat pad, the retrocalcaneal bursa itself and the fibrocartilages that form its walls collectively constitute the enthesis organ of the Achilles tendon, together with the enthesis itself [Fig. 1(d)]. The two fibrocartilages in the bursal walls comprise a variably thick, periosteal fibrocartilage on the superior tuberosity of the calcaneus, and a sesamoid fibrocartilage within the deep surface of the opposing tendon [Fig. 1(e)]. They are an adaptation to resist compression and/or shear when the foot is dorsiflexed and the tendon is brought in contact with the tuberosity. The fluid-filled bursa facilitates a change in insertional angle between the tendon and the bone during foot movements. By analogy with synovial joints, the presence of hyaluronan within the bursa might be expected to reduce the coefficient of friction substantially and thus prevent the buildup of heat. Bursal fluid may also be important as a source of nutrients and oxygen for the avascular fibrocartilages.

In understanding the general concept of an enthesis organ, the reader should note that the bone immediately adjacent to the Achilles tendon enthesis (i.e. the superior tuberosity) acts as a mini pulley for the tendon and that contact between tendon and pulley reduces stress concentration at the enthesis itself, albeit, this is at the expense of increasing wear and tear in the contact zone. The corollary is that the surgical removal of a prominent superior calcaneal tuberosity in patients with Haglund’s deformity will inevitably increase the stress concentration on the enthesis itself. When the contact zone between tendon and tuberosity is no longer present (i.e. when the tuberosity is removed by the surgeon), none of the tensile loading placed on the Achilles tendon can be dissipated as compressive loading on the bone, adjacent to the insertion site. Instead, all of the loading on the tendon is transferred directly to the enthesis itself. It is thus conceivable that if the patient is an athlete who loads their Achilles tendon heavily during the course of their sport, this might produce a new set of problems – a possibility that merits further consideration. Evidence of increased wear and tear in the tendon–bone contact zone adjacent to the Achilles tendon enthesis is common in the walls of the retrocalcaneal bursa of elderly individuals (Rufai et al., 1995).

It should be noted that as dorsiflexion begins and the Achilles tendon presses against the tuberosity, the insertional angle of the tendon is not altered with

further foot movement. Similarly, even the most cursory of observations on a living foot shows that as the foot is plantarflexed, any large change in insertional angle is greatly reduced by the controlling influence of the deep fascia in the lower part of the leg. This acts as an unheralded retinaculum to prevent bowstringing of the Achilles tendon and should probably be added to the list of structures that form part of its enthesis organ. Whether it is involved in Achilles tendon sheath problems is a question that has not been addressed. It is difficult to distinguish the two structures in a dissection of the terminal part of the Achilles tendon.

Enthesis organs are found elsewhere in the body and many sites have been listed by Benjamin et al. (2004a, b). Because of its relevance to the sports medicine practitioner, the attention of the reader is drawn to the presence of an enthesis organ at the talar end of the anterior talofibular ligament of the ankle joint – a ligament commonly damaged in ankle sprains. The contact that occurs between the ligament and the talus in a plantarflexed and inverted foot, immediately adjacent to the attachment site, is associated with the presence of a sesamoid fibrocartilage near the deep surface of the ligament (Kumai et al., 2002). This is likely to reduce the stress concentration at the enthesis itself. Kumai et al. (2002) relate the presence of this distally located enthesis organ in the ligament to the greater tendency of the *proximal* enthesis to avulse in ankle sprains. Clearly, however, differences in bone density between the talar and fibular entheses are also important.

In generalizing from the specific features of the Achilles tendon enthesis organ to concepts that apply elsewhere in the body, it is important to recognize that TLs often attach to bone near tuberosities or are sunken into pits. In either case, the TL enthesis is sited below the level of the adjacent bone. The presence of a tuberosity is exemplified by that at the insertion of biceps brachii and patellar tendons, and the presence of a pit by the attachment of the tendon of popliteus and by the collateral ligaments of the interphalangeal joints. It should be noted that wherever a TL sinks into a pit at its attachment, the adjacent bone surface can also act as a pulley, dissipating stress away from the attachment site itself.

Kager’s fat pad is an important part of the Achilles tendon enthesis organ that is often ignored. It is also known as the retromalleolar or pre-Achilles fat pad and it has a number of functions. Its tip moves in and out of the bursal cavity during plantar and dorsiflexion like a variable plunger (Canoso et al., 1988; Theobald et al., 2006). This minimizes pressure changes in the bursal cavity and ensures that the space is a potential, rather than a real one, at a healthy attachment site. The fat pad may also pre-

vent adhesions from developing between the tendon and the bone. All these observations on the function of this region of adipose tissue, together with other comments on its significance detailed below, should be of interest to surgeons who perform any operation that disturbs Kager's triangle.

According to Theobald et al. (2006), Kager's fat pad has three distinct regions: an Achilles-associated part (which is enclosed within the paratenon of the Achilles tendon), the flexor hallucis longus (FHL)-associated region (which is partly enveloped by the tendon sheath of FHL) and a distal bursal wedge or tip that protrudes into the bursal cavity. The movement of the fat pad in and out of the bursa is promoted both by pushing (contraction of FHL) and by pulling (it is sucked into the bursa to prevent the volume from increasing during the upward motion of the calcaneus during plantarflexion). In addition, the fat pad cushions the deep surface of the Achilles tendon offering protection to the blood vessels that enter it, and prevents the tendon from kinking during plantar flexion (Theobald et al., 2006). It may also have a proprioceptive role in monitoring changes in the insertional angle of the tendon during foot movement (Benjamin et al., 2004a, b; Shaw et al., 2005). The latter hypothesis is supported by the demonstration of an abundant sensory nerve supply within the fat pad (Shaw et al., 2005). Finally, as the fat pad contains peptidergic nerve fibers involved in nociception, it may be a source of pain in enthesopathies (Shaw et al., 2005). This could be mediated either through direct stimulation of nerve endings or by neurogenic inflammation. It is important to recognize that in the rat at least, the fat pad is the only part of the normal Achilles tendon enthesis organ that is innervated (Shaw et al., 2005). However, in humans, nerve fibers often accompany blood vessels in the vascular invasion of entheses that so often occurs in elderly individuals (Benjamin et al., 2007).

The presence of adipose tissue at other entheses is also common. However, its significance is often misinterpreted and many authors automatically equate it with TL degeneration. Although Benjamin et al. (2004a, b) agree that fat in TL may be pathological, they also argue for a variety of normal functions of fat at or near entheses. They have shown that adipose tissue is present not only at the insertional angle of many entheses but also in the epitendon and endotenon near the attachment site (Benjamin et al., 2004a, b). The fat is often innervated and may have a mechanosensory role. Endotenon fat is particularly characteristic of certain entheses where the TL flares out [e.g. fibularis (peroneus) longus insertion and the tibial attachment of the ACL]. It may thus contribute as a space filler and/or promote the independent movement of fascicles (Benjamin et al., 2004a, b).

Enthesopathies

Despite the adaptations that occur at entheses for preventing wear and tear, they are still prone to pathological changes. Overuse injuries in particular are common in athletes and account for a high proportion of all sports injuries. They are best termed "enthesopathies" (a term that embraces both tendons and ligaments), but have also been called "enthesiopathies," "insertional tendinopathies," or "insertional tendinoses" – although the last two can of course only be applied to tendons. The reader should also note that some authors use a more general pathological term, which applies to a whole tendon or ligament, when discussing enthesopathies. "Achillodynia" for example, covers the whole spectrum of Achilles tendon problems commonly reported in athletes and the term may disguise the fact that an author is at least partly considering enthesopathies. The term "enthesitis" may be appropriate for some enthesopathies (e.g. in patients with SpA), but carries with it the implication that an attachment site is inflamed (the suffix *.itis*). The reader should note therefore that the current consensus view is that most overuse injuries at entheses are degenerative rather than inflammatory. Where inflammation does occur, it may be a secondary change related to tissue damage and repair. This suggestion was made by Rufai et al. (1995) in relation to retrocalcaneal bursitis. They suggested that the synovial inflammation that is characteristic of the bursitis may not be a primary event, but a secondary change triggered by degeneration (fissuring, fragmentation and calcification) of the periosteal and sesamoid fibrocartilages that line the bursal walls and form part of the Achilles tendon enthesis organ – i.e. retrocalcaneal bursitis is primarily a problem related to fibrocartilage degeneration. This is also a reminder that the clinical symptoms of an enthesopathy need not necessarily affect only the enthesis.

The etiology of enthesopathies is often unclear, although as with tendinopathies in general, both intrinsic and extrinsic factors are involved. The former include anatomical variations, malalignment problems, muscle imbalance, or weakness and flexibility issues (Wilder & Sethi, 2004). The latter may relate to changes in training programs (including terrain, mileage coverage, duration, and intensity of training), inappropriate footwear, poor technique, or equipment (Wilder & Sethi, 2004). Maganaris et al. (2004) have made the interesting suggestion that some "overuse" insertional injuries would be better regarded as "underuse" injuries. They argue that parts of entheses may be stress shielded, so that when increased loading occurs, that particular region of the attachment site is unable to adapt sufficiently. They point out that the stress-shielded area is often

subject to greater compressive (rather than tensile) loading than the rest of the enthesis. Such regions are characterized by fibrocartilage (Benjamin & Ralphs, 1998) – a tissue that can show a variety of pathological changes at the certain entheses – e.g. that of the Achilles tendon (Rufai et al., 1995). Maganaris et al. (2004) suggest that tensile loading at entheses is non-uniform and it is the less heavily loaded regions that are the most vulnerable. Commonly, these are on the joint side of an attachment site – e.g. in rotator cuff problems, jumper's knee and Achilles insertional disorders. Certainly, so-called “fibrocartilaginous entheses” are of non-uniform composition and are purely fibrous in some parts of the enthesis (Benjamin et al., 1986; Woo et al., 1988). This is likely to reflect regional differences in tensile loading. It must be remembered, however, that an increase in compressive loading in what is regarded as a “stress-shielded” site of an enthesis may lead to degenerative changes that parallel those in osteoarthritic articular cartilage (Rufai et al., 1995). These may contribute to the histopathological basis of overuse injuries. It should also be noted that Toumi et al. (2006) highlight regional differences in trabecular architecture at the patellar enthesis of the patellar tendon. As Wolff's law dictates that mechanical stress governs the architecture of cancellous bone, Toumi et al. (2006) suggest that the medial part of the attachment site is subject to greater tensile loading than the lateral – it is this region of the enthesis that is most typically associated with jumper's knee.

Enthesopathies can affect a wide variety of different TLs and among the most common (and relevant to sport) are those that affect the Achilles tendon, patellar tendon, quadriceps tendon, supraspinatus and the common extensor and flexor tendons of the forearm (Khan et al., 1999). In addition, it should be noted that Fairclough et al. (2006) have suggested that iliotibial band (ITB) syndrome could be viewed as a form of enthesopathy. It is a well-recognized overuse injury that is common in runners and cyclists and is characterized by pain and tenderness over the lateral epicondyle of the femur when the knee is flexed to 30°. ITB syndrome is traditionally believed to be caused by repetitive friction between the band and the lateral epicondyle of the femur, when the ITB “rolls over” the epicondyle during knee movement. However, Fairclough et al. (2006) point out that the ITB cannot move in an anterior–posterior direction as the knee is flexed, because the band is firmly anchored to the distal part of the femur – i.e. it has an enthesis in the region of the lateral femoral epicondyle. They have suggested that the antero-posterior “movement” of the band is actually an illusion created by a sequential shifting of tensile load from anterior to posterior ITB fibers, during knee flexion. Their magnetic resonance

imaging (MRI) data suggest that the tract moves in a medial–lateral direction during knee flexion. This creates a change in the insertional angle of the femoral enthesis of the ITB. They have also demonstrated the presence of highly vascularized and innervated adipose tissue between the ITB and the lateral epicondyle that is the equivalent of the insertional angle fat at many entheses Benjamin et al. (2004a, b). Evidently, the fat must be compressed by any medial–lateral movement of the ITB. Intriguingly, there are MRI signal changes in this fat in patients with ITB syndrome, and Fairclough et al. (2006) consider this to be of key importance in understanding the pain and edema associated with ITB syndrome.

Finally, it should be noted that Knobloch et al. (2006) have demonstrated a significant increase in the microcirculatory blood flow at painful Achilles tendon entheses. This is in-line with earlier studies which have shown that angiogenesis occurs in painful mid-portion tendinopathies (Alfredson et al., 2003; Alfredson & Ohberg, 2005) and has led to the suggestion that enthesopathies or tendinopathies could be treated with agents that affect neovascular development (Ohberg & Alfredson, 2002).

Enthesophytes (bony spurs)

Particular mention is made of bony spurs (enthesophytes) as they are commonly found in athletes – especially at the attachment of the Achilles tendon, common extensor origin and plantar fascia. The molecular pathways that lead to their formation have not yet been clearly elucidated, although loss of *noggin* (an antagonist of bone morphogenetic protein expression) can induce ectopic bone formation in ankylosis (Lories et al., 2006). Some spurs may exceed 1 cm in length (Maffulli et al., 2004), but even large ones may not be symptomatic. However, spurs may be associated histologically with evidence of degenerative change elsewhere at the enthesis (Rufai et al., 1995). Enthesophytes in the Achilles tendon must be distinguished from what are simply areas of soft tissue calcification at the enthesis (Rufai et al., 1995). The term “enthesophyte” implies specifically that ossification has extended from the bone into the TL at the attachment site, whereas soft tissue calcification merely means the deposition of calcium salts. It is commonly reported in tendons as calcifying tendonitis or tendinopathy and is more typical of males than females at the attachment of the Achilles tendon (M. Benjamin, unpublished observations). It should be understood that *calcification* accompanies ossification, but can occur in its absence – this is a point of common confusion among those new to the field. The distinction between soft tissue calcification at an enthesis and bony spur formation can easily be

made in histological sections, but may also be made radiologically (Rufai et al., 1995).

Perspectives

Overuse injuries at tendon or ligament attachment sites (entheses) are common and can seriously jeopardize a subject's ability to pursue their sport. However, there is often a lack of awareness among sports medicine practitioners about many fundamental aspects of the structure–function relationships of insertion sites that are essential for understanding the basis of enthesopathies. In particular, the tendency of one enthesis to interconnect with another and the concept of an “enthesis organ” (a collection of structures adjacent to entheses, which, together with the attachment site itself, serve to reduce stress concentration at the hard–soft tissue interface) have a number of implications for understanding (a) why

symptoms associated with enthesopathies may be diffuse and (b) why the surgical removal of a structure close to an enthesis e.g. the superior tuberosity of the calcaneus may alter the mechanics of the enthesis itself. It is argued that a good understanding of the structural adaptations of entheses, and an appreciation that one attachment site may be very different from another, should be helpful to an orthopedic surgeon concerned with the reattachment of a tendon or ligament to a bone.

Key words: tendons, ligaments, osteotendinous junction, enthesopathy, fibrocartilage, overuse injuries.

Acknowledgement

We wish to thank Andrew Bathe of the Rossdale Equine Hospital, Newmarket, UK for supplying the horse tissue from which Fig 1(c) was taken.

References

Alfredson H, Ohberg L. Neovascularisation in chronic painful patellar tendinosis-promising results after sclerosing neovessels outside the tendon challenge the need for surgery. *Knee Surg Sports Traumatol Arthrosc* 2005; 3: 74–80.

Alfredson H, Ohberg L, Forsgren S. Is vasculo-neural ingrowth the cause of pain in chronic Achilles tendinosis? An investigation using ultrasonography and colour Doppler, immunohistochemistry, and diagnostic injections. *Knee Surg Sports Traumatol Arthrosc* 2003; 1: 334–338.

Benjamin M, Evans EJ, Copp L. The histology of tendon attachments to bone in man. *J Anat* 1986; 149: 89–100.

Benjamin M, Evans EJ, Rao RD, Findlay JA, Pemberton DJ. Quantitative differences in the histology of the attachment zones of the meniscal horns in the knee joint of man. *J Anat* 1991; 177: 127–134.

Benjamin M, Toumi H, Suzuki D, Redman S, Emery P, McGonagle D. Microdamage and altered vascularity at the enthesis-bone interface provides an anatomic explanation for bone involvement in the HLA-B27 associated spondyloarthritides and allied disorders. *Arthritis Rheum* 2007; 56: 224–233.

Benjamin M, Kumai T, Milz S, Boszczyk BM, Boszczyk AA, Ralphs JR. The skeletal attachment of tendons–tendon ‘entheses’. *Comp Biochem Physiol A Mol Integr Physiol* 2002; 133: 931–945.

Benjamin M, McGonagle D. The anatomical basis for disease localisation in seronegative spondyloarthropathy at entheses and related sites. *J Anat* 2001; 199: 503–526.

Benjamin M, Moriggl B, Brenner E, Emery P, McGonagle D, Redman S. The “enthesis organ” concept: why enthesopathies may not present as focal insertional disorders. *Arthritis Rheum* 2004a; 50: 3306–3313.

Benjamin M, Newell RL, Evans EJ, Ralphs JR, Pemberton DJ. The structure of the insertions of the tendons of biceps brachii, triceps and brachialis in elderly dissecting room cadavers. *J Anat* 1992; 180: 327–332.

Benjamin M, Ralphs JR. Fibrocartilage in tendons and ligaments – an adaptation to compressive load. *J Anat* 1998; 193: 481–494.

Benjamin M, Ralphs JR. Biology of fibrocartilage cells. *Int Rev Cytol* 2004; 233: 1–45.

Benjamin M, Redman S, Milz S, Buttner A, Amin A, Moriggl B, Brenner E, Emery P, McGonagle D, Bydder G. Adipose tissue at entheses: the rheumatological implications of its distribution. A potential site of pain and stress dissipation? *Ann Rheum Dis* 2004b; 63: 1549–1555.

Benjamin M, Toumi H, Ralphs JR, Bydder G, Best TM, Milz S. Where tendons and ligaments meet bone: attachment sites (‘entheses’) in relation to exercise and/or mechanical load. *J Anat* 2006; 208: 471–490.

Biermann H. Die Knochenbildung im Bereich periostaler-diaphysarer Sehnen- und Bandansätze. *Z Zellforsch* 1957; 46: 635–671.

Birk DE, Mayne R. Localization of collagen types I, III and V during tendon development. Changes in collagen types I and III are correlated with changes in fibril diameter. *Eur J Cell Biol* 1997; 72: 352–361.

Boszczyk AA, Boszczyk BM, Putz R, Benjamin M, Milz S. Expression of a wide range of fibrocartilage molecules at the entheses of the alar ligaments – possible antigenic targets for rheumatoid arthritis? *J Rheum* 2003; 30: 1420–1425.

Cammisa M, De Serio A, Guglielmi G. Diffuse idiopathic skeletal hyperostosis. *Eur J Radiol* 1998; 27(Suppl 1): S7–S11.

Canoso JJ. The premiere enthesis. *J Rheumatol* 1998; 25: 1254–1256.

Canoso JJ, Liu N, Traill MR, Runge VM. Physiology of the retrocalcaneal bursa. *Ann Rheum Dis* 1988; 47: 910–912.

Cooper RR, Misol S. Tendon and ligament insertion. A light and electron microscopic study. *J Bone Jt Surg* 1970; 52A: 1–20.

Corps AN, Robinson AH, Movin T, Costa ML, Hazleman BL, Riley GP. Increased expression of aggrecan and biglycan mRNA in Achilles tendinopathy. *Rheumatology* 2006; 45: 291–294.

Corps AN, Robinson AH, Movin T, Costa ML, Ireland DC, Hazleman BL, Riley GP. Versican splice variant messenger RNA expression in normal human Achilles tendon and tendinopathies. *Rheumatology* 2004; 43: 969–972.

- Dolgo-Saburoff B. Uber ursprung und insertion der Skelettmuskeln. *Anat Anz* 1929: 68: 8–87.
- Evans EJ, Benjamin M, Pemberton DJ. Fibrocartilage in the attachment zones of the quadriceps tendon and patellar ligament of man. *J Anat* 1990: 171: 155–162.
- Fairclough J, Hayashi K, Toumi H, Lyons K, Bydder G, Phillips N, Best TM, Benjamin M. The functional anatomy of the iliotibial band during flexion and extension of the knee: implications for understanding iliotibial band syndrome. *J Anat* 2006: 208: 309–316.
- Fujioka H, Wang GJ, Mizuno K, Balian G, Hurwitz SR. Changes in the expression of type-X collagen in the fibrocartilage of rat Achilles tendon attachment during development. *J Orthop Res* 1997: 15: 675–681.
- Galera V, Garralda MD. Enthesopathies in a spanish medieval population: anthropological, epidemiological and ethnohistorical aspects. *Int J Anthropol* 1993: 8: 247–258.
- Gao J, Messner K, Ralphs JR, Benjamin M. An immunohistochemical study of entheses development in the medial collateral ligament of the rat knee joint. *Anat Embryol (Berl)* 1996: 194: 399–406.
- Haines RW, Mohuiddin A. Metaplastic bone. *J Anat* 1968: 103: 527–538.
- Havelka S, Horn V. Observations on the tidemark and calcified layer of articular cartilage. In: Archer CW, Caterson B, Benjamin M, Ralphs JR, eds. *Biology of the synovial joint*. Amsterdam: Harwood Academic Publishers, 1999: 331–346.
- Hayami T, Pickarski M, Wesolowski GA, McLane J, Bone A, Destefano J, Rodan GA, Duong Le T. The role of subchondral bone remodeling in osteoarthritis: reduction of cartilage degeneration and prevention of osteophyte formation by alendronate in the rat anterior cruciate ligament transection model. *Arthritis Rheum* 2004: 50: 1193–1206.
- Hems T, Tillmann B. Tendon entheses of the human masticatory muscles. *Anat Embryol (Berl)* 2000: 202: 201–208.
- Khan KM, Cook JL, Bonar F, Harcourt P, Astrom M. Histopathology of common tendinopathies. Update and implications for clinical management. *Sports Med* 1999: 27: 393–408.
- Knese K-H, Biermann H. Die Knochenbildung an sehnen- und Bandsätzen im beriech ursprünglich chondraler apophysen. *Z Zellforsch* 1958: 49: 142–187.
- Knobloch K, Kraemer R, Lichtenberg A, Jagodzinski M, Gossling T, Richter M, Zeichen J, Hufner T, Krettek C. Achilles tendon and paratendon microcirculation in midportion and insertional tendinopathy in athletes. *Am J Sports Med* 2006: 34: 92–97.
- Kruzynska-Freitag A, Wang J, Maeda M, Rogers R, Krug E, Hoffman S, Markwald RR, Conway SJ. Periostin is expressed within the developing teeth at the sites of epithelial–mesenchymal interaction. *Dev Dyn* 2004: 229: 857–868.
- Kumai T, Takakura Y, Rufai A, Milz S, Benjamin M. The functional anatomy of the human anterior talofibular ligament in relation to ankle sprains. *J Anat* 2002: 200: 457–465.
- Kumar P, Oka M, Nakamura T, Yamamuro T, Delecrin J. Mechanical strength of osteochondral junction. *Nippon Seikeigeka Gakkai zasshi* 1991: 65: 1070–1077.
- Lahm A, Uhl M, Erggelet C, Haberstroh J, Mrosek E. Articular cartilage degeneration after acute subchondral bone damage: an experimental study in dogs with histopathological grading. *Acta Orthop Scand* 2004: 75: 762–767.
- Lane LB, Bullough PG. Age-related changes in the thickness of the calcified zone and the number of tidemarks in adult human articular cartilage. *J Bone Jt Surg* 1980: 62B: 372–375.
- Lories RJ, Daans M, Derese I, Matthys P, Kasran A, Tylzanowski P, Ceuppens JL, Luyten FP. Noggin haploinsufficiency differentially affects tissue responses in destructive and remodeling arthritis. *Arthritis Rheum* 2006: 54: 1736–1746.
- Lyons TJ, Stoddart RW, McClure SF, McClure J. The tidemark of the chondro-osseous junction of the normal human knee joint. *J Mol Histol* 2005: 36: 207–215.
- Maffulli N, Reaper J, Ewen SW, Waterston SW, Barrass V. Chondral metaplasia in calcific insertional tendinopathy of the Achilles tendon. *Clin J Sport Med* 2006: 16: 329–334.
- Maffulli N, Testa V, Capasso G, Sullo A. Calcific insertional Achilles tendinopathy: reattachment with bone anchors. *Am J Sports Med* 2004: 32: 174–182.
- Maganaris CN, Narici MV, Almekinders LC, Maffulli N. Biomechanics and pathophysiology of overuse tendon injuries: ideas on insertional tendinopathy. *Sports Med* 2004: 34: 1005–1017.
- Miller BF, Hansen M, Olesen JL, Schwarz P, Babraj JA, Smith K, Rennie MJ, Kjaer M. Tendon collagen synthesis at rest and after exercise in women. *J Appl Physiol* 2007: 102: 541–546.
- Milz S, Benjamin M, Putz R. Molecular parameters indicating adaptation to mechanical stress in fibrous connective tissue. *Adv Anat Embryol Cell Biol* 2005: 178: 1–71.
- Milz S, Rufai A, Buettner A, Putz R, Ralphs JR, Benjamin M. Three-dimensional reconstructions of the Achilles tendon insertion in man. *J Anat* 2002: 200: 145–152.
- Milz S, Tischer T, Buettner A, Schieker M, Maier M, Redman S, Emery P, McGonagle D, Benjamin M. Molecular composition and pathology of entheses on the medial and lateral epicondyles of the humerus: a structural basis for epicondylitis. *Ann Rheum Dis* 2004: 63: 1015–1021.
- Ohberg L, Alfredson H. Ultrasound guided sclerosis of neovessels in painful chronic Achilles tendinosis: pilot study of a new treatment. *Br J Sports Med* 2002: 36: 173–175.
- Pendegrass CJ, Oddy MJ, Cannon SR, Briggs T, Goodship AE, Blunn GW. A histomorphological study of tendon reconstruction to a hydroxyapatite-coated implant: regeneration of a neo-entheses in vivo. *J Orthop Res* 2004: 22: 1316–1324.
- Redler I, Mow VC, Zimny ML, Mansell J. The ultrastructure and biomechanical significance of the tidemark of articular cartilage. *Clin Orthop* 1975: 112: 357–362.
- Rijkelijkhuisen JM, Baan GC, de Haan A, de Ruiter CJ, Huijing PA. Extramuscular myofascial force transmission for in situ rat medial gastrocnemius and plantaris muscles in progressive stages of dissection. *J Exp Biol* 2005: 208: 129–140.
- Rufai A, Ralphs JR, Benjamin M. Structure and histopathology of the insertional region of the human Achilles tendon. *J Orthop Res* 1995: 13: 585–593.
- Schneider H. Zur Struktur der Sehnenansatzzonen. *Z Anat Entwicklung* 1956: 119: 431–456.
- Shaw HM, Santer RM, Watson AHD, Benjamin M. The innervation of the entheses organ of the rat Achilles tendon. *J Anat* 2005: 208: 402.
- Shibakawa A, Yudoh K, Masuko-Hongo K, Kato T, Nishioka K, Nakamura H. The role of subchondral bone resorption pits in osteoarthritis: MMP production by cells derived from bone marrow. *Osteoarthritis Cart* 2005: 13: 679–687.
- Snow SW, Bohne WH, DiCarlo E, Chang VK. Anatomy of the Achilles tendon and plantar fascia in relation to the calcaneus in various age groups. *Foot Ankle Int* 1995: 16: 418–421.
- Theobald P, Bydder G, Dent C, Nokes L, Pugh N, Benjamin M. The functional

- anatomy of Kager's fat pad in relation to retrocalcaneal problems and other hindfoot disorders. *J Anat* 2006; 208: 91–97.
- Thomopoulos S, Marquez JP, Weinberger B, Birman V, Genin GM. Collagen fiber orientation at the tendon to bone insertion and its influence on stress concentrations. *J Biomech* 2006; 39: 1842–1851.
- Toumi H, Higashiyama I, Suzuki D, Kumai T, Bydder G, McGonagle D, Emery P, Fairclough J, Benjamin M. Regional variations in human patellar trabecular architecture and the structure of the proximal patellar tendon enthesis. *J Anat* 2006; 208: 47–57.
- Vogel KG, Koob TJ. Structural specialization in tendons under compression. *Int Rev Cytol* 1989; 115: 267–293.
- Waggett AD, Ralphs JR, Kwan AP, Woodnutt D, Benjamin M. Characterization of collagens and proteoglycans at the insertion of the human Achilles tendon. *Matrix Biol* 1998; 16: 457–470.
- Wilder RP, Sethi S. Overuse injuries: tendinopathies, stress fractures, compartment syndrome, and shin splints. *Clin Sports Med* 2004; 23: 55–81.
- Woo S, Maynard J, Butler D, Lyon R, Torzilli P, Akeson W, Cooper R, Oakes B. Ligament, tendon, and joint capsule insertions to bone. In: Woo SL-Y, Buckwalter JA, eds. *Injury and repair of the musculoskeletal soft tissues*. Park Ridge: American Academy of Orthopaedic Surgery, 1988: 133–166.
- Yoon JH, Halper J. Tendon proteoglycans: biochemistry and function. *J Musc Neur Int* 2005; 5: 22–34.
- Zoeger N, Roschger P, Hofstaetter JG, Jokubonis C, Pepponi G, Falkenberg G, Fratzl P, Berzlanovich A, Osterode W, Strelci C, Wobraschek P. Lead accumulation in tidemark of articular cartilage. *Osteoarthritis Cart* 2006; 14: 906–913.

Adipose tissue at entheses: the innervation and cell composition of the retromalleolar fat pad associated with the rat Achilles tendon

H. M. Shaw, R. M. Santer, A. H. D. Watson and M. Benjamin

Cardiff School of Biosciences, Cardiff University, UK

Abstract

This study set out to determine whether the fat pad at the attachment of the Achilles tendon has features enabling it to function as an immune organ and a mechanosensory device, and to be a source of pain in insertional tendon injuries. Sections for histology and immunohistochemistry were cut from the Achilles tendon enthesis organ of 1 day old, 1 month, 4 month and 24 month old rats. For fluorescence and peroxidase immunohistochemistry, cryosections were labelled with primary antibodies directed against PGP9.5, substance P, neurofilament 200, calcitonin gene related peptide, CD68, CD36, myeloid related protein 14, actin and vinculin. The fat pad contained not only adipocytes, but also fibrous tissue, mast cells, macrophages, fibroblasts and occasional fibrocartilage cells. It was richly innervated with nerve fibres, some of which were likely to be nociceptive, and others mechanoreceptive (myelinated fibres, immunoreactive for neurofilament 200). The fibres lay between individual fat cells and in association with blood vessels. In marked contrast, the enthesis itself and all other components of the enthesis organ were aneural at all ages. The presence of putative mechanoreceptive and nociceptive nerve endings between individual fat cells supports the hypothesis that the fat pad has a proprioceptive role monitoring changes in the insertional angle of the Achilles tendon and that it may be a source of pain in tendon injuries. The abundance of macrophages suggests that the adipose tissue could have a role in combating infection and/or removing debris from the retrocalcaneal bursa.

Key words Achilles tendon; adipose tissue; entheses; innervation; spondyloarthropathies.

Introduction

Adipose tissue is a conspicuous, though greatly neglected, component of entheses and enthesis organs (Benjamin et al. 2004b). It occurs not only within the enthesis itself, but also in the angle which the tendon/ligament makes with the bone ('insertional angle fat'; Benjamin et al. 2004b). Elsewhere in tendons and ligaments, its presence is often dismissed as a sign of degeneration, but Benjamin et al. (2004b) have proposed a number of functions for adipose tissue at entheses. These include facilitating movement between tendon fascicles, and between the tendon or ligament and bone, dissipating stress concentration at attachment sites, and sensory perception. Kager's fat pad, which lies at the insertion of the human Achilles tendon, is one of the largest and most distinctive regions of adipose tissue associated with any enthesis. In man, it is also known

as the retromalleolar fat pad (Canoso et al. 1988) and it fills the triangular space (Kager's triangle) in the posterior region of the ankle, between the tendon of flexor hallucis longus (FHL) anteriorly, the Achilles tendon posteriorly and the superior border of the calcaneus inferiorly (Ly & Bui-Mansfield, 2004). Even though the triangle itself is a well-known radiological landmark, and radiolucency of the retrocalcaneal recess in MRI images is used to rule out retrocalcaneal bursitis (Canoso et al. 1988), the structure and functions of the fat pad have remained largely unstudied. Recently however, Theobald et al. (2006) have shown that the fat has three distinctive parts, which they named according to the structures with which each is closely associated – i.e. a large superficial Achilles-associated region, a deep FHL-associated region, and a calcaneal bursal wedge that protrudes into the retrocalcaneal bursa. These authors confirmed and extended the earlier pioneering work of Canoso et al. (1988) which showed that the bursal wedge moves into the retrocalcaneal bursa during plantar flexion and out again during dorsiflexion. Both Theobald et al. (2006) and Canoso et al. (1988) have suggested that these movements minimise pressure changes within the bursa that might otherwise occur. Canoso et al. (1988) have likened the bursal wedge of fat to a freely moveable spacer that permits

Correspondence

M. Benjamin, School of Biosciences, Cardiff University, Museum Avenue, Cardiff, CF10 3US, UK. T: +44 (0)2920875041; F: +44 (0)2920874116; E: Benjamin@cardiff.ac.uk

Accepted for publication 27 April 2007

the tendon and bone to move apart, without creating excessive surface tension, and have made the important observation that its bursal movements are compromised in patients with seronegative spondyloarthropathy (SpA). The fat pad movements are thought to be promoted by the secretion of hyaluronan-rich synovial fluid by the fibroblast-like lining cells of its covering synovial membrane (Canoso et al. 1983).

We believe that the bursal wedge of fat has other functions that have yet to be properly investigated. (1) It could monitor the changing insertional angle which the Achilles tendon makes with the calcaneus as the foot moves and be a source of pain in insertional tendinopathies. (2) As adipose tissue is known to have immunological functions (Fantuzzi, 2005), Kager's fat pad could have an immunoprotective role for the retrocalcaneal bursa – removing debris which is known to be produced by wear and tear of its lining tissues (Rufai et al. 1995). It could also represent a source of inflammatory cells seen in SpA – conditions which commonly target the Achilles tendon.

The purpose of the present study is to provide further information on the structure of the bursal wedge of fat associated with the Achilles tendon in order to improve our understanding of the significance of such insertional angle fat. There is a comparable region of adipose tissue associated with the retrocalcaneal bursa of the rat (Rufai et al. 1996) and because of the need to examine the fat at different developmental stages, we have used this species for the current work. Our findings emphasise the importance of considering fat as a significant tissue at entheses and an integral part of many 'enthesis organs' (Benjamin et al. 2004a,b).

Materials and methods

Routine histology

White male Wistar rats aged 4 months were obtained from accredited commercial suppliers; 24 month old rats were bred in house at Cardiff University. The left ankle was removed from 3 rats at each age and fixed in 4% paraformaldehyde (PFA) in 0.1 M phosphate buffer (PB) for 3–5 days, decalcified in 5% nitric acid, dehydrated in graded alcohols and embedded in paraffin wax. Serial sagittal sections were cut at 8 µm throughout each block and sections stained with Masson's trichrome, haematoxylin & eosin, van Gieson's elastic stain, or toluidine blue.

Immunohistochemistry

Rats aged 1 day, 1 month, 4 months and 24 months old were obtained as above, and the ankle region dissected and fixed in 4% PFA for up to 4 h. Three animals were used at each age – one limb per animal. Specimens were subsequently washed in 0.1 M PB and soaked in 10% sucrose in PB overnight at 4 °C. The tissue was then frozen in Serotec cryoprotectant (RA Lamb Medical Supplies; Eastbourne, UK) onto a cryostat

chuck. Sagittal sections were cut at 10 µm on a cryostat (OFT5000; Bright Instrument Co. Ltd, Huntingdon, UK) and collected on Histobond slides (RA Lamb Medical Supplies). All labeling was carried out in a humidified chamber at room temperature unless otherwise stated.

Immunofluorescence

Sections were rehydrated with 0.1 M PB and incubated with 20% swine or goat serum for 1 h, prior to incubation with the primary antibodies – see Table 1. Following several washes with PB, the sections were incubated with the secondary antibody, swine anti-rabbit FITC (Dako UK, Ely, Cambridgeshire, UK) or goat anti-mouse FITC (Dako UK) (following pre-incubation with 1% normal rat serum (Invitrogen, Paisley, UK) for 1 h at 4 °C) for 1 h, washed in PB and mounted under coverslips using Vectorshield containing DAPI to label cell nuclei (Vector Labs, Peterborough, UK). The tendon component of the enthesis organ acted as a convenient internal positive control for the actin and vinculin antibodies (Ralphs et al. 2002), and the base of the rat bladder was used as a positive control for the neuronal antibodies (Yokokawa et al. 1985; Yokokawa et al. 1986; Wakabayashi et al. 1998; Khan et al. 1999). For negative controls, representative sections were treated with 0.1 M PB, rabbit or mouse immunoglobulins (IgG; Dako UK) in place of the primary antibody.

Immunoperoxidase

Sections were rehydrated with 0.1 M PB and, where necessary, antigen retrieval procedures were performed (Table 1). Endogenous peroxidase activity was blocked with 3% hydrogen peroxide in distilled H₂O for 10 min. Following washing, 20% goat, horse or swine serum was applied to the sections for 1 h, depending on the species in which the secondary antibody was raised (Table 1). All primary antibodies (Table 1) were incubated on the sections in PB, containing 0.1% Tween 20 (Sigma-Aldrich, Gillingham, UK), overnight at 4 °C. Following washing, the appropriate biotinylated secondary antibody was applied for 1 h at room temperature (following pre-incubation with 1% normal rat serum for 1 h at 4 °C) and an avidin-biotin complex (Vector Labs) applied for 30 min, following a further wash in PB. Sections were washed yet again and developed either with NovaRED or DAB substrate kits (Vector Labs). The greater omentum of 4 month rats was used as a positive control for CD68, CD36, and myeloid related protein 14 antibodies (Lagasse & Weissman, 1992; Biewenga et al. 1995). As above, negative control sections were incubated with 0.1 M, Mouse IgG1 (Dako, Cambridgeshire, UK), Mouse IgG2a (Dako, Cambridgeshire, UK), or rabbit IgG (Dako, Cambridgeshire, UK) in place of the primary antibody.

Results

The basic structure of the enthesis organ associated with the rat Achilles tendon is similar to that previously

Table 1 List of primary antibodies used along with pretreatments, dilutions and sources. M – monoclonal antibody, P – polyclonal antibody

Antibody	M/P	Unmasking treatment	Dilution/ Concentration	Source	Reference
Rabbit anti-PGP 9.5	P	None	1:400	Ultraclone, Isle of Wight, UK	Doran et al. (1983)
Rabbit anti-substance P	P	None	1:2000	Biomol, Exeter, UK	Hoyle et al. (1998)
Rabbit anti-calcitonin gene related peptide (ARP296/1)	P	None	1:500	Biomol, Exeter, UK	Skofitsch & Jacobowitz (1985)
Rabbit anti-neurofilament 200	P	None	1:2000	Sigma-Aldrich, Poole, UK	Nakamura et al. (1987)
Mouse anti-hVin1 (binds to vinculin)	M	None	10 µg/mL	Sigma-Aldrich, Poole, UK	Goncharova et al. (1992)
Alexa 488- conjugated phalloidin (for filamentous actin)	N/A	None	1 U/mL	Molecular Probes, Chemicon Europe Ltd., Chandlers Ford, UK	
Mouse anti-COL-1 (for collagen I)	M	Hyaluronidase 30 min at 37 °C	1:2000	Sigma-Aldrich, Poole, UK	Mayne (1988)
Mouse anti-CD68 (macrophage marker for lysosome-associated antigens)	M	None	1:400	AbD Serotec, Oxford, UK	Damoiseaux et al. (1994)
Mouse anti-CD36 (UA009) (leucocyte marker)	M	None	1:10	Hycult biotechnology, Uden, NL	
Mouse anti-S100A9 (1C10) – for myeloid-related protein 14	M	None	1:200	Abnova, Stratech Scientific Ltd., Newmarket, UK	
Rabbit IgG Normal Fraction.	N/A	None	5 µg/mL	Dako, Ely Cambridgeshire, UK	
Negative control					
Mouse IgG1 Negative control	N/A	None	5 µg/mL	Dako, Ely, Cambridgeshire, UK	
Mouse IgG2a Negative control	N/A	None	5 µg/mL	Dako, Ely Cambridgeshire, UK	

described in man (Benjamin & McGonagle, 2001). Briefly, the tendon attachment is associated with 3 different fibrocartilages – an *enthesis fibrocartilage* (EF) at the tendon-bone junction, a *sesamoid fibrocartilage* within the deep surface of the tendon, and an opposing *periosteal fibrocartilage* covering the calcaneus (Fig. 1a). Further regions of fibrocartilage were also observed both near the superficial surface of the Achilles tendon and in the opposing tendon of plantaris (Fig. 1a – inset). The sesamoid and periosteal fibrocartilages form the walls of the retrocalcaneal bursa into which protrudes the tip of the synovial-covered wedge of adipose tissue (Fig. 1b) that is the focus of the current study. There were no marked differences between the fat pad of the sexually mature (4 months) and aged (24 months) rats, other than a tendency for the tip of the fat pad to become more fibrous with age (Fig. 1c).

Cellular composition

The fat pad was composed of unilocular adipocytes, separated by small bundles of elastic fibres and type I collagen fibres (Fig. 1d). The fat pad was anchored to the walls of the bursa by fibrous strands. Small nodules of fibrocartilage were occasionally seen near the tip of the fat pad and in one 4 month rat, the central core of this fibrocartilage contained bone (Fig. 1e).

Mast cells were readily identifiable in the fat pad by the metachromasia of their granules in toluidine blue stained sections, and some lay close to blood vessels, nerves or the synovial membrane (Fig. 1f). Immunolabeling for

actin with alexa488-conjugated phalloidin demonstrated the presence of filamentous actin within the cytoplasm of adipocytes and resident fibroblasts (Fig. 2a). In addition, speckled labelling for vinculin was seen both in adipocytes and in the occasional fibroblasts present between the fat cells (Fig. 2b).

In rats of all ages, CD68 positive macrophages were identifiable within the fat pad (Fig. 3a), though the number varied greatly between animals. Such cells were rarely seen within the synovial membrane of the neonatal rat, but the number increased with age (Fig. 3b). Many of the CD68 macrophages were closely associated with blood vessels and the connective tissue of large nerve bundles (Fig. 3c). Neonates had a particularly large number of positive cells in relation to the size of the developing fat pad (Fig. 3d). In 24 month old rats, positive cells were present not only in the fat pad, but also on the surface of the sesamoid and periosteal fibrocartilages in the retrocalcaneal bursa (Fig. 3e). In contrast, there were very few positive cells labeling at any age with CD36 (not shown). Myeloid related protein 14 (MRP14) expression was most commonly detected in cells adjacent to blood vessels and in their endothelium – particularly in 24 month old rats (Fig. 3f).

Innervation

Immunohistochemical labeling of rat tissue with the general nerve marker – PGP 9.5 – showed that the fat pad was the only component of the enthesis organ which

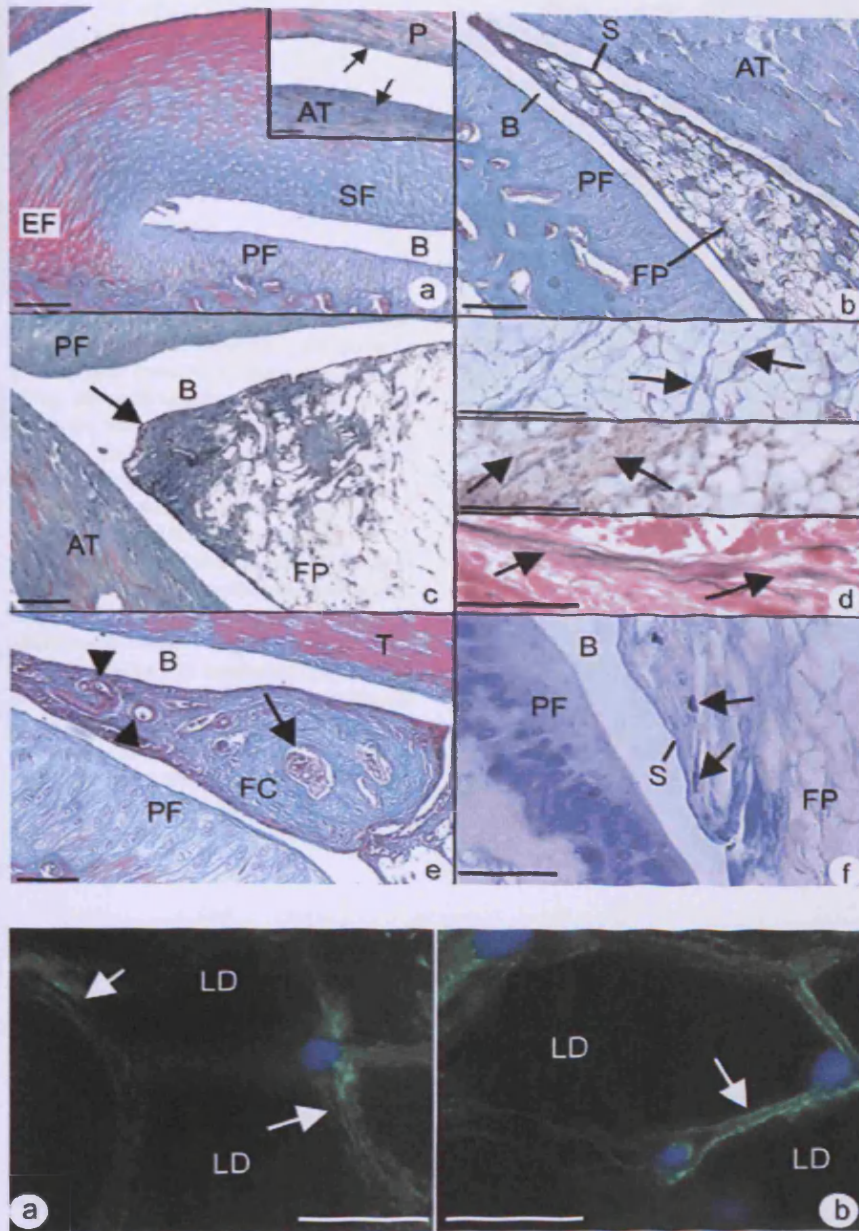


Fig. 1 (a) The Achilles enthesis organ in a 4 month old rat showing the enthesis (EF), sesamoid (SF) and periosteal fibrocartilages (PF). SF and PF form the walls of the retrocalcaneal bursa (B) into which the fat pad protrudes more proximally. Masson's trichrome. Scale bar = 200 μ m. Inset: opposing regions of the Achilles (AT) and plantaris (P) tendons. The surface of both is fibrocartilaginous (arrows). Masson's trichrome. Scale bar = 100 μ m. (b) The synovial-covered tip (S) of the fat pad (FP) protrudes into the retrocalcaneal bursa. The enthesis itself is located beyond the top left corner of the figure. 4 month rat. Masson's trichrome. Scale bar = 100 μ m. (c) The tip of the fat pad (arrow) becomes more fibrous in the 24 month old rat. Masson's trichrome. Scale bar = 100 μ m. (d - top) Fibrous strands (arrows) run between groups of adipocytes within the fat pad. 4 month old rat. Masson's trichrome. Scale = 200 μ m. (d - middle) Fibrous strands within the fat pad immunolabelled for type I collagen (arrows). 4 month old rat. Scale bar = 100 μ m. (d - bottom) Elastic fibres (arrows) in the fat pad within the fibrous strands. 4 month old rat. Van Gieson's elastic stain. Scale bar = 50 μ m. (e) A bony nodule (arrow) within the tip of the fat pad of a 4 month old rat, surrounded by a region of fibrocartilage (FC) and prominent blood vessels near the tip of the pad (arrow heads) Masson's trichrome. Scale bar = 100 μ m. (f) Mast cells (arrows) present within the fat pad in close association with the synovial lining (S). Toluidine blue. Scale bar = 10 μ m.

Fig. 2 (a) Adipocytes within the fat pad immunolabelled with alexa488-conjugated phalloidin. The array of actin filaments is associated with the peripheral cytoplasm (arrow). Note that the region containing the central lipid droplet (LD) in each fat cell is black. Scale bar = 20 μ m. (b) Vinculin labeling in the adipocyte cytoplasm (arrow). Scale bar = 20 μ m. In all cases, the nuclei have been counterstained blue with DAPI and the illustrations are from 4 month old rats.

was innervated at all ages (Fig. 4a-d). Thus, no nerve fibres (sensory, motor or autonomic) were present in any of the fibrocartilages associated with the Achilles tendon in any animal (Fig. 4f-h). Neither was the acellular bursal lining of the sesamoid and periosteal fibrocartilages positive for PGP 9.5. Blood vessel-associated nerve fibres were, however, present in the paratenon. Some of these nerves labeled with antibodies against substance P and CGRP (indicating that they were nociceptive), others labeled with antibody neurofilament 200 (suggesting mechanoreceptors; Fig 4e). No nerve fibres were present in the region where the Achilles tendon was in contact with plantaris.

The nerve fibres/bundles within the fat pad were more common in the proximal region than at the tip. They

typically lay between adjacent fat cells (Fig. 5), though some were present within and beneath the synovial membrane and where the synovium was reflected onto the tendon or the periosteum. All fibres within the fat pad were immunoreactive to PGP 9.5 (Fig. 4a). Many (but not all) of the nerve fibres innervating the fat pad (both blood-vessel associated and 'free') contained 200 kD neurofilaments (Fig. 4c). A qualitative evaluation suggested that the number of fibres immunoreactive to PGP 9.5 and neurofilament 200 increased with age up to 4 months, but that the number of positive fibres was less in 24 month old animals. Vessel-associated and 'free' nerve fibres immunoreactive to CGRP (Fig. 4d) and substance P (Fig. 4b) were also present in the fat pad at all ages studied and labeling here also increased

Fig. 3 The cell composition of the fat pad (a) CD68 positive cells (arrows) within the fat pad of a 4 month old rat. Scale bar = 20 μ m (b) The abundance of CD68 positive cells (arrows) in the synovial lining of the fat pad in a 4 month old rat, contrasts with the rare finding of these cells in the synovium of neonates (not shown). B – Bursa. Scale bar = 20 μ m. (c) CD68 positive cells (arrows) associated with a bundle of nerves (N) in the fat pad. 4 month old rat. Scale bar = 20 μ m (d) The presumptive fat pad in the neonate. Note the large population of CD68 positive cells (arrows) that are present before pronounced differentiation of the adipocytes themselves. Scale bar = 20 μ m. (e) CD68 positive cells (arrow) on the surface of the sesamoid fibrocartilage (SF) in a 4 month old rat. PF – Periosteal fibrocartilage. (f) Labelling for myeloid-related protein 14 that is associated with blood vessels (BV), is particularly prominent in 24 month old rats. Scale bar = 20 μ m. All sections have been counterstained with Mayer's haematoxylin.

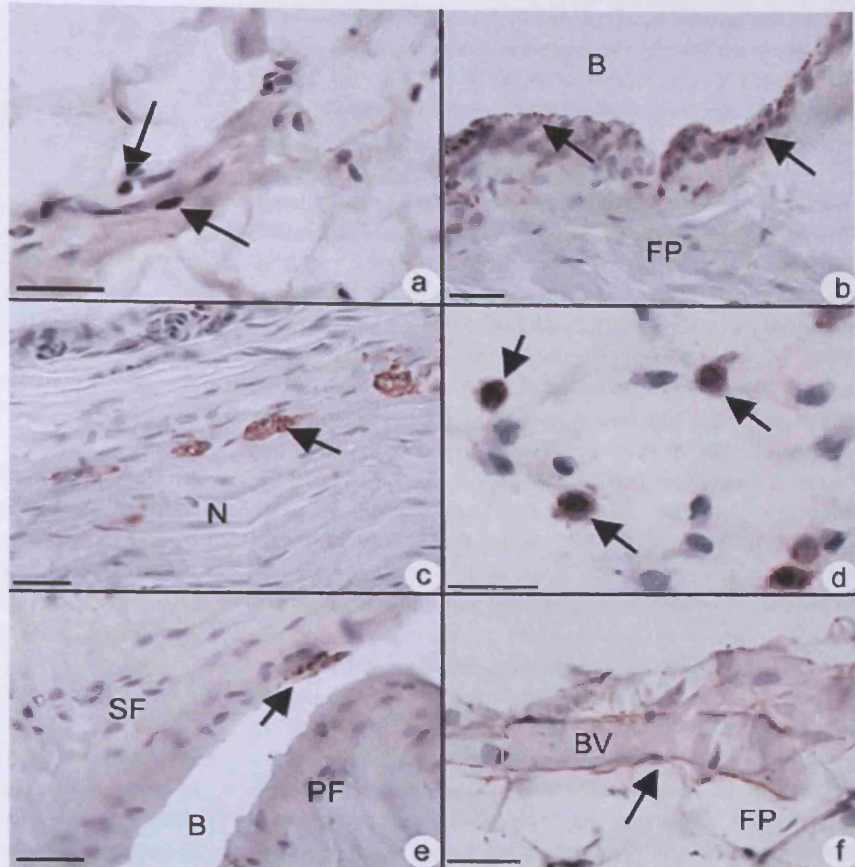
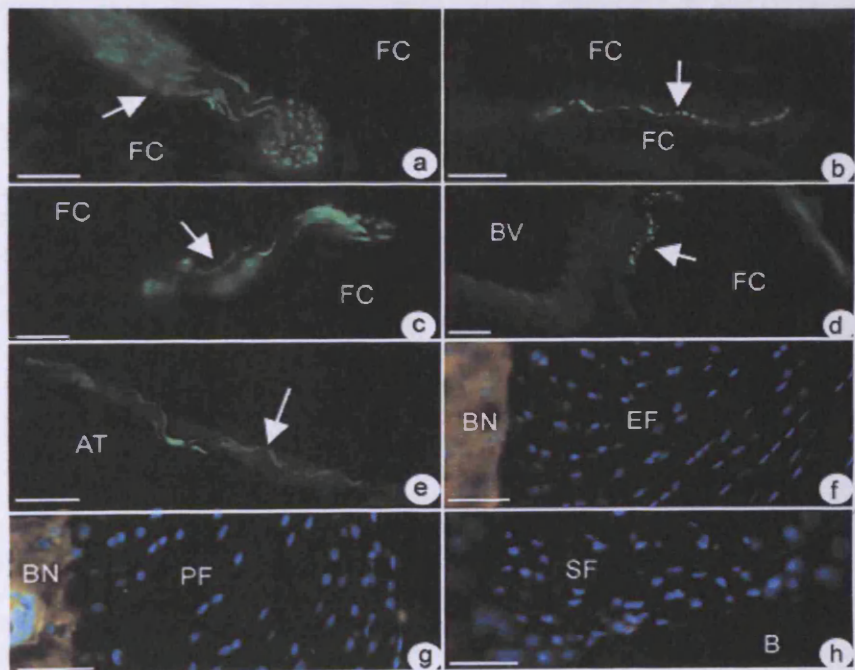


Fig. 4 The innervation of the fat pad (a–d). Nerve fibres are arrowed that are immunoreactive to (a) PGP 9.5 – in a large bundle of nerve fibres within the fat. FC – fat cells. Scale bar = 30 μ m (b) Substance P – in a naked nerve fibre running between adjacent fat cells. Scale bar = 20 μ m (c) Neurofilament 200 in a medium-sized bundle of nerve fibres in the fat. Scale bar = 30 μ m (d) CGRP – in close association with a large blood vessel (BV). Scale bar = 20 μ m (e) Nerve fibres in the epitenon labelled with neurofilament 200. AT – Achilles tendon. Scale bar = 30 μ m. In contrast to the fat pad, the enthesis (f), periosteal (g) and sesamoid (h) fibrocartilages (EF, PF, and SF respectively) are all devoid of nerve fibres and thus all fail to label with the pan neurofilament marker PGP 9.5. In the absence of any neuronal labelling in f–h, the cell nuclei are counterstained blue with DAPI to show the tissue itself. B, bursa; BN, bone. Scale bars for f–h = 50 μ m. All sections were from 4 month old rats.



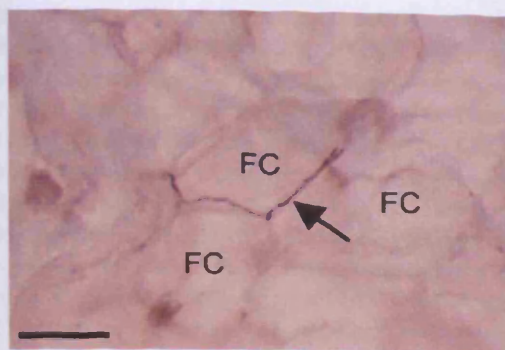


Fig. 5 A CGRP-positive fibre (arrow) running between adjacent fat cells (FC) in a 4 month old rat. Scale bar = 30 μ m. Counterstained with Mayer's haematoxylin.

with development up to 4 months of age. However, peptidergic fibres (i.e. substance P or CGRP-containing fibres) did not become less abundant in aged rats. In all animals, NF200 nerve fibres were more abundant within the fat pad than those immunoreactive to either substance P or CGRP.

Discussion

Previous studies have highlighted the biomechanical importance of Kager's fat pad and particularly its calcaneal bursal wedge (Canoso et al. 1988; Theobald et al. 2006). The bursal wedge fails to move into the retrocalcaneal bursa in patients with SpA (Canoso et al. 1988). Our present results point to further structural features of the fat pad, which not only reflect its mechanical role but also support the hypothesis that it has additional functions. The co-localisation of actin filaments and vinculin in its adipocytes indicates the presence of focal contacts, which mechanically link actin microfilaments in the cell cytoplasm to the extracellular matrix via the transmembrane linkers – integrins. As focal contacts are known to be important in mechanosensitive cell signaling (Bershady et al. 2003; D'Addario et al. 2003), they are likely to link the fibrous components of the fat pad to the adipocytes, thus integrating the fibro-adipose nature of the tissue. The occasional signs of fibrocartilage differentiation suggest that the fat is subject to some degree of compression and the fibrous strands point to a degree of resilience that it must have against tensile loading. Hence, like the fat pad in the heel, Kager's pad could act as a shock absorber (Jahss et al. 1992). We conclude that it is likely that the fat contributes to dissipating stress away from the tendon-bone interface, like other depots of 'insertional angle fat' (Benjamin et al. 2004b). It is thus truly an integral part of the Achilles tendon enthesis organ (Benjamin et al. 2004a).

Our study shows that the normal Achilles enthesis is not innervated. Despite an exhaustive search for nerve fibres in rats of all ages, none was found within the enthesis, sesamoid or periosteal fibrocartilages. This was paralleled

by an absence of blood vessels in these tissues and recalls the avascular and aneural nature of articular cartilage. The lack of nerve fibres is likely to reflect the relatively high levels of compression to which the fibrocartilages are subject, although the factors responsible for this are unknown. However, aggrecan may be important in accounting for the absence of nerves, as one of its major glycosaminoglycans (chondroitin sulphate) is known to act as an axonal growth inhibitor in the central nervous system (Johnson et al. 2002) and it is present in enthesis organ fibrocartilages (Waggett et al. 1998; Milz et al. 2005). It is a key molecule associated with compression-tolerance (Milz et al. 2005) and it also inhibits endothelial cell adhesion and migration (Johnson et al. 2005). Hence, vessel and nerve ingrowth reported previously in the entheses of elderly human Achilles tendons (Benjamin et al. 2007) may follow degenerative changes in the fibrocartilage, which are common in older people (Rufai et al. 1995). However, this does not explain why nerve fibres were also absent at birth, before the fibrocartilage had started to differentiate (Rufai et al. 1992).

In contrast to the aneural nature of enthesis organ fibrocartilages, the fat pad contains a large number of nerve fibres, including putative mechanoreceptors and nociceptors. The former could be important in monitoring movements of the fat pad during plantar and dorsiflexion. Because of the intimate association between fat cells and their nerve fibres, the slightest deformation of the adipose tissue accompanying foot movements could trigger action potentials in the proprioceptive fibres. Equally, nociceptive fibres could be stimulated by any abnormal loading of the tissue. This could occur for example when fluid accumulates in patients with retrocalcaneal bursitis and the fat pad is thus subject to abnormal compression (Canoso, 1998). It is interesting to note that Hoffa's fat pad also contains nociceptive fibres and that an increased number occurs in 'jumper's knee' (Witonski & Wagrowska-Danielewicz, 1999). The number of mechanoreceptive fibres within the Achilles fat pad varies with age – increasing during growth up to sexual maturity, and then decreasing with old age. However, an age-related decrease in peptidergic fibres was not obvious and this is in accordance with the findings of Bergman et al. (1999) that mechanoreceptors are preferentially affected by age in comparison to nociceptive/peptidergic fibres. Finally, the presence of mast cells within the fat pad suggests the possibility of neurogenic inflammation in association with Achilles-related pain (McQueen, 1999). Peptidergic fibres may also play a vasodilatory role, affecting the blood vessels with which they are so closely associated. This can lead to tissue oedema and inflammation under conditions of tissue damage causing pain (McQueen, 1999).

CD68 labeling demonstrated the presence of a striking number of macrophages. These cells may be compared to macrophages demonstrated previously in the greater

omentum. This too is a fatty synovial fold and one which provides a route for macrophages to enter the peritoneal cavity (Krist et al. 1995). If macrophages can pass from Kager's pad into the retrocalcaneal bursa, they could play a role in combating infection and/or removing cell debris. Macrophages that we identified on the surface of the bursal wall fibrocartilages may also be important. In man, we have previously demonstrated that debris is generated as a result of wear and tear of the lining periosteal and sesamoid fibrocartilages (Rufai et al. 1995). Fat at entheses could also be a source of the macrophages present in patients with SpA (McGonagle et al. 2002). It is interesting to note that along with the Achilles tendon, other entheses commonly affected in SpA are also associated with significant quantities of fat at their entheses – e.g. the proximal and distal attachments of the patellar tendon and the calcaneal enthesis of the plantar aponeurosis. Fat may thus be an important immune organ at healthy attachment sites, but also one that may be implicated in autoimmune or autoinflammatory conditions.

In conclusion, our study presents new data relating to the innervation and cellular composition of fat at the attachment of the Achilles tendon, which highlights the possibility of several novel functions of the fat pad. Our findings reinforce the importance of considering fat when trying to make sense of insertional disorders affecting the Achilles tendon.

Acknowledgments

We wish to thank Dr Jim Ralphs for supplying the vinculin and actin antibodies. Hannah Shaw is an Anatomical Society of Great Britain and Ireland studentship holder.

References

- Benjamin MHT, Suzuki D, Redman S, Emery P, McGonagle D (2007) Microdamage and altered vascularity at the enthesis-bone interface provides an anatomic explanation for bone involvement in the HLA-B27 associated spondyloarthritides and allied disorders. *Arthritis Rheum* 56, 224–233.
- Benjamin M, McGonagle D (2001) The anatomical basis for disease localisation in seronegative spondyloarthropathy at entheses and related sites. *J Anat* 199, 503–526.
- Benjamin M, Moriggi B, Brenner E, Emery P, McGonagle D, Redman S (2004a) The 'enthesis organ' concept: Why enthesopathies may not present as focal insertional disorders. *Arthritis Rheum* 50, 3306–3313.
- Benjamin M, Redman S, Milz S, Buttner A, et al. (2004b) Adipose tissue at entheses: the rheumatological implications of its distribution. A potential site of pain and stress dissipation? *Ann Rheum Dis* 63, 1549–1555.
- Bergman E, Fundin BT, Ulfhake B (1999) Effects of aging and axotomy on the expression of neurotrophin receptors in primary sensory neurons. *J Comp Neurol* 410, 368–386.
- Bershadsky AD, Balaban NQ, Geiger B (2003) Adhesion-dependent cell mechanosensitivity. *Annu Rev Cell Dev Biol* 19, 677–695.
- Biewenga J, van der Ende MB, Krist LF, Borst A, Ghufuron M, van Rooijen N (1995) Macrophage depletion in the rat after intraperitoneal administration of liposome-encapsulated clodronate: depletion kinetics and accelerated repopulation of peritoneal and omental macrophages by administration of Freund's adjuvant. *Cell Tissue Res* 280, 189–196.
- Canoso JJ (1998) The premiere enthesis. *J Rheumatol* 25, 1254–1256.
- Canoso JJ, Liu N, Traill MR, Runge VM (1988) Physiology of the retrocalcaneal bursa. *Ann Rheum Dis* 47, 910–912.
- Canoso JJ, Stack MT, Brandt KD (1983) Hyaluronic acid content of deep and subcutaneous bursae of man. *Ann Rheum Dis* 42, 171–175.
- D'Addario M, Arora PD, Ellen RP, McCulloch CA (2003) Regulation of tension-induced mechanotranscriptional signals by the microtubule network in fibroblasts. *J Biol Chem* 278, 53090–53097.
- Damoiseaux JG, Dopp EA, Calame W, Chao D, MacPherson GG, Dijkstra CD (1994) Rat macrophage lysosomal membrane antigen recognized by monoclonal antibody ED1. *Immunology* 83, 140–147.
- Doran JF, Jackson P, Kynoch PA, Thompson RJ (1983) Isolation of PGP 9.5, a new human neurone-specific protein detected by high-resolution two-dimensional electrophoresis. *J Neurochem* 40, 737–742.
- Fantuzzi G (2005) Adipose tissue, adipokines, and inflammation. *J Allergy Clin Immunol* 115, 911–919; quiz 920.
- Goncharova EJ, Kam Z, Geiger B (1992) The involvement of adherens junction components in myofibrillogenesis in cultured cardiac myocytes. *Development* 114, 173–183.
- Hoyle CH, Chakrabarti G, Pendleton NP, Andrews PL (1998) Neuromuscular transmission and innervation in the urinary bladder of the insectivore *Suncus murinus*. *J Auton Nerv Syst* 69, 31–38.
- Jahss MH, Michelson JD, Desai P, et al. (1992) Investigations into the fat pads of the sole of the foot: anatomy and histology. *Foot Ankle* 13, 233–242.
- Johnson WE, Caterson B, Eisenstein SM, Hynds DL, Snow DM, Roberts S (2002) Human intervertebral disc aggrecan inhibits nerve growth in vitro. *Arthritis Rheum* 46, 2658–2664.
- Johnson WE, Caterson B, Eisenstein SM, Roberts S (2005) Human intervertebral disc aggrecan inhibits endothelial cell adhesion and cell migration in vitro. *Spine* 30, 1139–1147.
- Khan MA, Dashwood MR, Thompson CS, Mumtaz FH, Morgan RJ, Mikhailidis DP (1999) Time-dependent up-regulation of neuronal 5-hydroxytryptamine binding sites in the detrusor of a rabbit model of partial bladder outlet obstruction. *World J Urol* 17, 255–260.
- Krist LF, Eestermans IL, Steenbergen JJ (1995) Cellular composition of milky spots in the human greater omentum: an immunohistochemical and ultrastructural study. *Anat Rec* 241, 163–174.
- Lagasse E, Weissman IL (1992) Mouse MRP8 and MRP14, two intracellular calcium-binding proteins associated with the development of the myeloid lineage. *Blood* 79, 1907–1915.
- Ly JQ, Bui-Mansfield LT (2004) Anatomy of and abnormalities associated with Kager's fat Pad. *Am J Roentgenol* 182, 147–154.
- Mayne R (1988) Preparation and applications of monoclonal antibodies to different collagen types. *Clin Biochem* 21, 111–115.
- McGonagle D, Marzo-Ortega H, O'Connor P, et al. (2002) Histological assessment of the early enthesitis lesion in spondyloarthropathy. *Ann Rheum Dis* 61, 534–537.
- McQueen DS (1999) *Inflammatory pain and the joint*. Basel: Birkhauser.

- Milz S, Benjamin M, Putz R (2005) Molecular parameters indicating adaptation to mechanical stress in fibrous connective tissue. *Adv Anat Embryol Cell Biol* **178**, 1–71.
- Nakamura T, Kawahara H, Miyashita H, Watarai K, Takagi M, Tachibana S (1987) Cross reactive identification of types 1 and 2C fibers in human skeletal muscles with monoclonal anti-neurofilament (200 kd) antibody. *Histochemistry* **87**, 39–45.
- Ralphs JR, Waggett AD, Benjamin M (2002) Actin stress fibres and cell-cell adhesion molecules in tendons: organisation in vivo and response to mechanical loading of tendon cells in vitro. *Matrix Biol* **21**, 67–74.
- Rufai A, Benjamin M, Ralphs JR (1992) Development and ageing of phenotypically distinct fibrocartilages associated with the rat Achilles tendon. *Anat Embryol (Berl)* **186**, 611–618.
- Rufai A, Ralphs JR, Benjamin M (1995) Structure and histopathology of the insertional region of the human Achilles tendon. *J Orthop Res* **13**, 585–593.
- Rufai A, Ralphs JR, Benjamin M (1996) Ultrastructure of fibrocartilages at the insertion of the rat Achilles tendon. *J Anat* **185**, 185–191.
- Skofitsch G, Jacobowitz DM (1985) Calcitonin gene-related peptide: detailed immunohistochemical distribution in the central nervous system. *Peptides* **6**, 721–745.
- Theobald P, Bydder G, Dent C, Nokes L, Pugh N, Benjamin M (2006) The functional anatomy of Kager's fat pad in relation to retrocalcaneal problems and other hindfoot disorders. *J Anat* **208**, 91–97.
- Waggett AD, Ralphs JR, Kwan AP, Woodnutt D, Benjamin M (1998) Characterization of collagens and proteoglycans at the insertion of the human Achilles tendon. *Matrix Biol* **16**, 457–470.
- Wakabayashi Y, Maeda T, Tomoyoshi T, Kwok YN (1998) Increase of growth-associated protein-43 immunoreactivity following cyclophosphamide-induced cystitis in rats. *Neurosci Lett* **240**, 89–92.
- Witonski D, Wągrowicka-Danielewska M (1999) Distribution of substance-P nerve fibers in the knee joint in patients with anterior knee pain syndrome. A preliminary report. *Knee Surg Sports Traumatol Arthrosc* **7**, 177–183.
- Yokokawa K, Sakanaka M, Shiosaka S, Tohyama M, Shiotani Y, Sonoda T (1985) Three-dimensional distribution of substance P-like immunoreactivity in the urinary bladder of rat. *J Neural Transm* **63**, 209–222.
- Yokokawa K, Tohyama M, Shiosaka S, et al. (1986) Distribution of calcitonin gene-related peptide-containing fibers in the urinary bladder of the rat and their origin. *Cell Tissue Res* **244**, 271–278.